ISBN 978-608-4723-06-6

SS. CYRIL AND METHODIUS UNIVERSITY IN SKOPJE
FACULTY OF DESIGN AND TECHNOLOGIES OF FURNITURE AND INTERIOR – SKOPJE
REPUBLIC OF NORTH MACEDONIA

INNOVAWOOD

WOOD TECHNOLOGY & PRODUCT DESIGN

7th INTERNATIONAL SCIENTIFIC CONFERENCE

7th INTERNATIONAL SCIENTIFIC CONFERENCE

WOOD TECHNOLOGY & PRODUCT DESIGN PROCEEDINGS

17th-20th SEPTEMBER 2025, OHRID

PROCEEDINGS

7th INTERNATIONAL SCIENTIFIC CONFERENCE

WOOD TECHNOLOGY & PRODUCT DESIGN

17– 20 SEPTEMBER, 2025
UNIVERSITY CONGRESS CENTRE – OHRID
REPUBLIC OF NORTH MACEDONIA

WOOD TECHNOLOGY & PRODUCT DESIGN
Ohrid, North Macedonia, 17–20 September, 2025

PROCEEDINGS

Vol. VII / Pg. 1- 312
Skopje, 2025

UDK 674-045.431(062)
684.4(062)

ISBN 978-608-4723-06-6

Published
Ss. Cyril and Methodius University - Skopje
Faculty of Design and Technologies
of Furniture and Interior – Skopje

Dean
Gjorgi Gruevski, Ph.D.

Organizers:
Ss. Cyril and Methodius University - Skopje
Faculty of Design and Technologies
of Furniture and Interior – Skopje
INNOVAWOOD -Brussels

Publisher address:
Faculty of Design and Technologies of
Furniture and Interior
Ul. 16 Makedonska Brigada br. 3, PO box 223, 1000 Skopje
Republic of North MACEDONIA

CONTENTS

MACHINING ACOUSTICS: SIGNAL PROCESSING AND DEEP LEARNING AS A TOOL FOR PROCESS MONITORING

(Keynote lecture)

Srđan Svrzić[1]

[1]*Associate professor, Department of Wood Technology,*
Faculty of Forestry, Belgrade University, Serbia
e-mail: srdjan.svrzic@sfb.bg.ac.rs

ABSTRACT

The requirements of Industry 4.0 and beyond go hand in hand with adaptive, intelligent process control through the application of some form of AI. To this end, some acoustic phenomena have been observed in this series of research conducted over the last few years. Noise analysis for different working conditions of circular saw blades was investigated in this study. The main objective of this work was to verify the existing relationships between the recorded noise patterns and the corresponding operating conditions of different circular saw blades. This goal was achieved by analyzing noise signals and using different neural network architectures, such as GoogleNet, MobileNetV2, VGG19, Dense-Net, Squeeze-Net, ResNet and InceptionV3. The results obtained in this series of investigations suggest that the noise generated during cutting can be used as a tool for process monitoring with high accuracy. Various cases are presented in this paper, such as determining the speed of the same saw, recognizing different types of saws idling at different speeds, recognizing types of wood being processed with the same saw, and idling the same type of saw at different bluntness and utilization. In all cases presented, the trained neural networks showed a relatively high accuracy in determining the observed output.

Keywords: acoustic signal, Circular saw blade, Wood machining, Process monitoring, Decision making, Deep learning network.

1. INTRODUCTION

When several bodies or media interact with each other, sound is inevitably generated. It is regarded as a mechanical wave that propagates through the surrounding medium such as gas, liquid or solid. By definition, sound is a longitudinal wave that represents fluctuations in pressure or density of the conducting medium. Sound can be defined as a signal, i.e. it carries information, such as speech. It is determined by amplitude, frequency and duration. Sound is often equated with noise, i.e. if a sound has no recognizable pattern, it is classified as noise.

A tool (circular saw blade) behaves like a noise source, either when idling or when cutting. In the first case, it behaves like a vibrating guitar string which, depending on the speed, the number of teeth and the geometry of the teeth, produces a sound that is often referred to as whistling. In the second case, additional noise is generated by the interaction between the tool and the material, which is strongly influenced by the properties of the material itself. The noise generated during woodworking comes from four possible sources: Machine motor, gearbox, whistling of the tool and interaction between tool and material. These noises cannot be observed separately during processing. The interaction between tool and material leads to an increased load on the motor and influences the whistling of the tool, so that a comparison of the noise when idling and the noise during cutting is pointless.

In recent decades, many authors have addressed the possibility of using noise as a means of process monitoring. This is important from the point of view of carrying out the cutting process within the specified optimum parameter limits, the surface quality, the possible exceeding of the power used or the blunt condition of the tool.

Different types of broadband frequency sensors (Nasir et al. 2019, Tanaka et al. 1992, Aguilera et al. 2007) or microphones (Cyra and Tanaka 2000, Iskra and Tanaka 2005, 2006, Iskra and Hernández

2012, Aguilera et al. 2016, Miric-Milosavljevic et al. 2023) were used for sound and acoustic emission (AE) measurements. In addition, the sound recordings were processed using MATLAB software (Nasir et al. 2019, Mandic et al. 2015, Miric-Milosavljevic et al. 2023).

Both power consumption and sound or AE signals provide inputs for process control and monitoring (Goli et al. 2010, Aguilera and Zamora 2007, Aguilera and Barros 2010, 2012, Aguilera 2011a).

While cutting force (Naylor et al. 2012, Porankiewicz et al. 2011, Goli et al. 2018) and power consumption (Kovač et al. 2021) have been evaluated as factors that strongly depend on selected cutting parameters, some authors did not find a strong relationship between noise and other sawing and milling factors (Szwajka et all. 2008) and mostly concluded that AE signals gave worse results than power measurements (Jemielniak et al. 2011), while some others only investigated sound pressure level as an output. It is important to emphasize that most of the work focused on milling.

The progression of tool bluntness during milling was also investigated using sound pressure measurements (Aguilera et al. 2016) and provided satisfactory results.

However, the frequency, time domain and intensity analysis was performed by a few authors (Mohring et al. 2019, Nasir et al. 2019, 2020 and 2021). The noise represents a three-dimensional signal and must therefore be observed in this way. A simple amplitude or sound pressure analysis cannot provide satisfactory input for further processing or relevant considerations. This method provided a comprehensive picture of the sounds generated during cutting with different tools that allow further analysis and the implementation of different artificial neural networks (ANN) to monitor the whole process.

Various signal processing techniques using time and frequency analyses are used to determine the effects of the cutting parameters. The monitoring of the machining process, predictions and decision making can be achieved by some AI technologies such as artificial neural networks (ANN), fuzzy logic and neuro-fuzzy inference systems (Abellan-Nebot and Subirón 2010). The prediction of tool wear (Szwajka et al. 2008, Zbieć 2011, Zafar et al. 2015) and the prediction of parameters (Iskra and Hernández 2012) were achieved using the ANN approach. The modelling and prediction of surface roughness was also performed using ANN (Iskra and Hernández 2009, 2012, Tiryaki et al. 2014, Stanojevic et al. 2017).

Deep learning networks, or more generally, AI approaches in wood research are used for wood identification (Sun et al. 2021, de Geus 2020), wood fiber segmentation (Kibleur et al. 2022), wood processing and tool monitoring (Nasir and Sassani 2021, Jegorowa et al. 2021) and classification of processing parameters (Svrzic et al. 2023). The basic idea of AI implementation is to create a tool that can be used to make decisions that can lead to more efficient production processes. In order to achieve intelligent production, the collected data must be transformed in such a way that it is suitable for the deep learning process. In general, there are some rules for the preparation of raw data: 1) The data must be suitable for the network architecture; 2) The dimensionality must be reduced so that the patterns are more recognizable and 3) The data must be prepared in such a way that it covers the entire solution space.

Regarding the scope of this article, particular attention has been paid to the acquisition and analysis of sound signals (also in terms of measuring cutting performance), especially considering that there is still much room for theoretical, experimental and even more practical applications in the field of woodworking. The global market for woodworking machinery was estimated at $4.72 billion in 2022 and is expected to grow from $4.86 billion in 2023 to $6.80 billion in 2030 (Fortune Business Insight 2023). The proposed approach to process control can increase the applicability and commercial value of the machine and thus contribute to the global market.

2. MATERIALS AND METHODS

The Freud LU1C 0100, Freud LU2B 0500 and Freud LU2C 1200 circular saw blades were used for this study (Fig. 1 a, b and c). The corresponding numbers of teeth were 22, 48 and 80 respectively. The saw blade LU1C 0100 and the other two have a diameter of 250 mm, an inner diameter of 30 mm, a cutting width of 3.2 mm and a body thickness of 2.2 mm. The carbide-tipped tooth form of the LU1C 0100 is ATB with a positive cutting angle of 10° (Table 1). According to the manufacturer, this blade is intended for longitudinal and cross cuts in solid wood. The LU2B 0500 blade has ATB-

shaped carbide teeth with a positive cutting angle of 10° and is intended for cutting solid wood and wood-based materials. The third saw blade is the LU2C 1200 with tungsten carbide (TC), ATB-shaped teeth and a positive cutting angle of 15°. It is designed for rip and cross cuts in softwood, hardwood and wood-based materials.

(a) (b) (c)

Figure 1. *FREUD (a) LU1C 0100; (b) LU2B 0500; (c) LU2C 1200 circular saw blades.*

Table 1. *The tool and cutting conditions.*

Cutting tool	LU1C0100 (Freud)	LU2B 0500	LU2C 1200
Cutting speed	4000 min^{-1}	2000/3000/4000	4000 min^{-1}
Feed rate	10 m/min.	-	-
Tooth shape	ATB	ATB	ATB
Number of tooth	22	48	80
Diameter (mm)	250	250	250
Body thickness b (mm)	2.2	2.2	2.2
Cutting width B (mm)	3.2	3.2	3.2
Rake angle (°)	20	20	18
Clear angle (°)	15	13	5
Inclination angle (°)	10	10	10
Tool override (mm)	10	-	-

Table 2. *Material conditions.*

	Beech	Fir
Moisture content (avg.) (%)	8.16	8.65
St.Dev	0.41	0.14
Wood density air dry (avg.) (g/cm^3)	0.71	0.42
St.Dev	$2.6*10^{-2}$	$3.7*10^{-3}$
Wood density oven dry (avg.) (g/cm^3)	0.69	0.40
St.Dev	$2.5*10^{-2}$	$4.4*10^{-3}$

In one phase of this study, boards of beech (Fagus moesiaca) and fir (Abies alba) measuring 1000 mm × 500 mm × 35 mm were cut. The number of boards was 12 and the total number of cuts was 480 for each species. The cutting tool used was the LU1C 0100 circular saw blade, which is designed for longitudinal and cross cutting of solid wood.

The study was conducted in the Laboratory of Machines and Apparatus at the Faculty of Forestry, University of Belgrade (Beograd, Serbia). The machining system used for this study was a Minimax CU 410K combined machine (SCM, Rimini, Italy) equipped with a 3 kW three-phase asynchronous

motor. The speed of the motor was set by a customized frequency controller to 4000 rpm with a corresponding frequency of 50.5 Hz. The noise occurring when the tool was idling was recorded using a dbx RTA-M measurement microphone with an electret condenser on the back (Fig. 2a). The RTA-M is an omnidirectional, low-profile frequency measurement microphone specifically designed to record all frequencies from 20 Hz to 20 kHz, ensuring accurate "real-time "pinging" analysis of the audio signal. It is operated with phantom power. To reduce the effects of vibration, the microphone is housed in a vibration-damping rack. The Focusrite Scarlet SOLO USB audio interface (Fig. 2b) was connected to a PC. Audacity, a cross-platform open source audio software, was used to record the audio signals. The recordings were sliced and trimmed using the WavePad Sound Editor developed by NCH Software. The measurements were carried out at a sampling rate of 44100 Hz.

Figure 2a. *RTA-M Measurement microphone.*

Figure 2b. *Scarlet SOLO audio interface.*

The microphone was placed 1200 mm away from the rotating tool. The Dino-Lite Edge USB microscope with 470x magnification was used for visual observation of the tool condition in the case of the LU2C 1200 saw (Fig. 3).

Figure 3. *Dino-Lite Edge USB microscope.*

The investigation was divided into the following sections:

1. the idle rotation of the LU2B0500 saw at three different speeds (2000, 3000 and 4000 rpm);
2 the idle rotation of three different saws (LU1C 0100, LU2B 0500 and LU2C 1200) at the same speed (4000 rpm);
3. cutting beech and fir wood with the LU1C 0100 saw at the same speed (4000 rpm);
4. the idle rotation of the LU2C1200 saw with different degrees of bluntness at the same speed (4000 rpm).

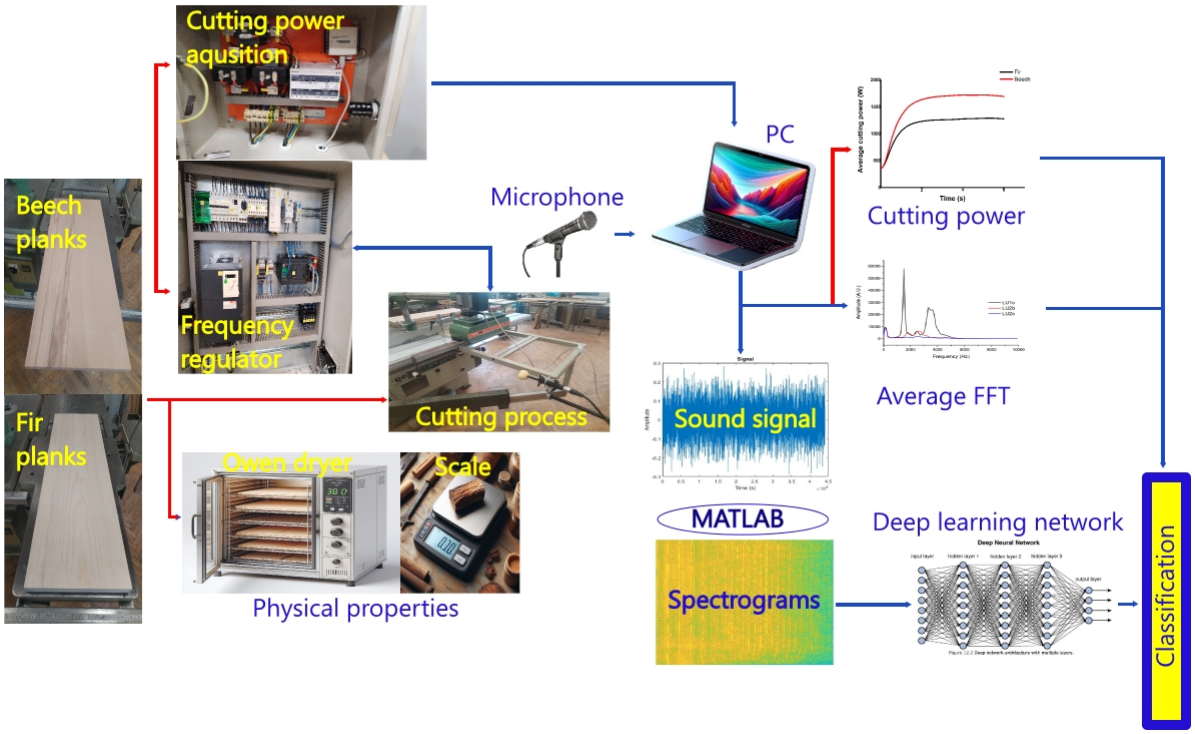

Figure 4. *Experimental flowchart.*

The experimental flow chart of the research carried out is shown in Fig. 4. The blue arrows show the processes in experimental sections 1, 2 and 4, while the red arrows represent section 3.

The device has a Circutor CW-TAN active power transformer for unbalanced three-phase systems with the following characteristics: alternating current 5 A, alternating voltage 230 V, frequency 50 Hz, accuracy 0.5 % and analog voltage output 0-10 V (Mandić et al. 2011). The possible measuring ranges are 5, 10 and 15 kW. The measured cutting power data are given in Watts. The operator selects the expected range for a better resolution of the results. The entire system is based on the Power Expert software platform and the sampling rate has been set to 1000 Hz. The device is also suitable for mobile use. The rotational speed of the saw blade has been set to 4000 rpm with the frequency controller connected to the machine's electric motor. The drive electric motor provides the energy for the interaction between the tool and the wood and for overcoming any friction that occurs between the moving parts of the machine.

$$P_C = P_T - P_I\,(W) \quad (1)$$

Where: P_C - useful power engaged for wood cutting, P_I – machine parts friction overcoming power (idle power), and P_T – total power. The power consumption used in this work was the useful power P_C.

The sounds produced during the experiment came from moving machine parts (electric motor, bearings, spindles, etc.) and from the whistling of the saw blade. These sounds were captured with the microphone and recorded on the PC as wave files. Originally, the length of the wave files were 4 minutes for each saw blade speed. Spectral analysis was performed on these recordings using the fast Fourier transform (FFT) and the short-time Fourier transform (STFT). On these recordings, spectral analysis was performed using FFT and STFT. The following set of equations describes FFT.

$$F_k = \sum_{i=0}^{N/2-1}\left(g_i W^{ik} + h_i W^{(i+N/2)k}\right) \quad (2)$$

$$F_{2k} = \sum_{l=0}^{N/2-1}(g_i + h_i)(W^2)^{lk} \quad (3)$$

$$F_{2k+1} = \sum_{l=0}^{N/2-1}[(g_i - h_i)W^l](W^2)^{lk} \quad (4)$$

In these equations, N is a number of samples, hi and gi equal sets of samples, $W=e^{-j\Omega T}$ and F_k is the Fourier series for discrete Fast Fourier Transformation (FFT). For N/2 even and N/2 odd samples, the expressions in Eqs. 3 and 4 could be regarded as discrete Fourier transformations (DFTs). The number of iterations required for completing the process described in Eq. 3 is Nlog2N. The short-time Fourier transform or short-term Fourier transform (STFT) is a natural extension of the Fourier transform in addressing signal non-stationarity by applying windows for segmented analysis. In practice, the procedure for computing STFTs is to divide a longer time signal into shorter segments of equal length and then compute the Fourier transform separately on each shorter segment. The sound/noise signals thus transformed could present the starting point for alternative machining systems and process monitoring, and introducing smart machining.

The use of just FFT was not enough for detailed analysis because the obtained power spectrum involved lots of noise or parasitic frequencies. Further implementation of wavelet transformation, involving Daubichies wavelet, thus obtaining spectral density graph, significantly smoothened the spectral line thus pointing to which spectral areas are to be carefully observed. This is particularly important for creating inputs to databases for deep learning networks. Wavelet transform could be described by following equations:

$$\Psi_{a,b}(t) = \frac{1}{\sqrt{a}}\Psi\left(\frac{t-b}{a}\right) \quad (5)$$

$$W_\Psi(f)(a,b) = \langle f(t), \Psi_{a,b}(t)\rangle \quad (6)$$

Where: Ψ presents the mother wavelet with its parameters *a* and *b* which present the trimming and sliding of the wavelet, respectively; W is the wavelet transform function, and f is the time domain data function.

A further step was the creation of a database for training deep learning networks. All of the sound signal recordings were transformed into 2D images of 3D spectrograms accomplished by MATLAB R2023 edition. Spectrograms are 3D (frequency-time-power) charts obtained by STFT or wavelet transform of original sound signals. The 2D presentation involves an RGB scale to present the power of certain peaks or spectral areas.

The process of creating spectrograms is known as Gabor transform and it is intended for making time-frequency plots. The main idea is convoluting the window function (Gaussian function of different lengths) with the time series data function:

$$G(f) = \int_{-\infty}^{\infty} f(\tau)e^{-j\omega\tau} \cdot g(t-\tau)d\tau \quad (7)$$

Where: G is the Gabor transform, f(t) is the data function, and g is the window function.

A further step consisted of cutting the entire 4-minute recording into smaller, even parts of 1 second in length, which was done using the WavePad software. Now it was possible to create a database for training the deep learning network. The first step was to import all 240 short-time recordings of the sound signal for each saw blade speed and convert them into 2D images of 3D spectrograms. Spectrograms are 3D plots (frequency-time-power) obtained by STFT or wavelet transform of the original sound signals. In the 2D representation, an RGB scale is used to represent the power of specific peaks or spectral regions. These 2D spectrograms were saved in the JPG format and served as training data for the deep learning networks: GoogleNet, MobileNetV2, VGG19, Dense-Net, Squeeze-Net, ResNet and Inception V3, which were developed specifically for image recognition. All the implementation was done by using the Python 3.7.4 programming language; along with the PyTorch 1.6.0 and Torcvision 0.7.0 libraries with the Cuda 10.2 GPU drivers. All the computations

were done on the workstation with the AMD Threadripper 3970X (32 cores, 3.79 GHz processor), 128GB RAM and two Titan RTX (24GB)+NVLink GPUs.

4. RESULTS AND DISCUSSION

The examples of the recordings in wave format for different phases of the experiment are shown in Fig. 5. They have different shapes, indicating different sound intensities, but do not provide sufficient data for classification or any kind of analysis. These audio files were subjected to an FFT to extract specific frequency ranges that could indicate signal changes in order to distinguish different working conditions. The graphs of the FFT for specific cases show the average values of the signal intensities for specific frequencies, excluding the time domain (Fig.6).

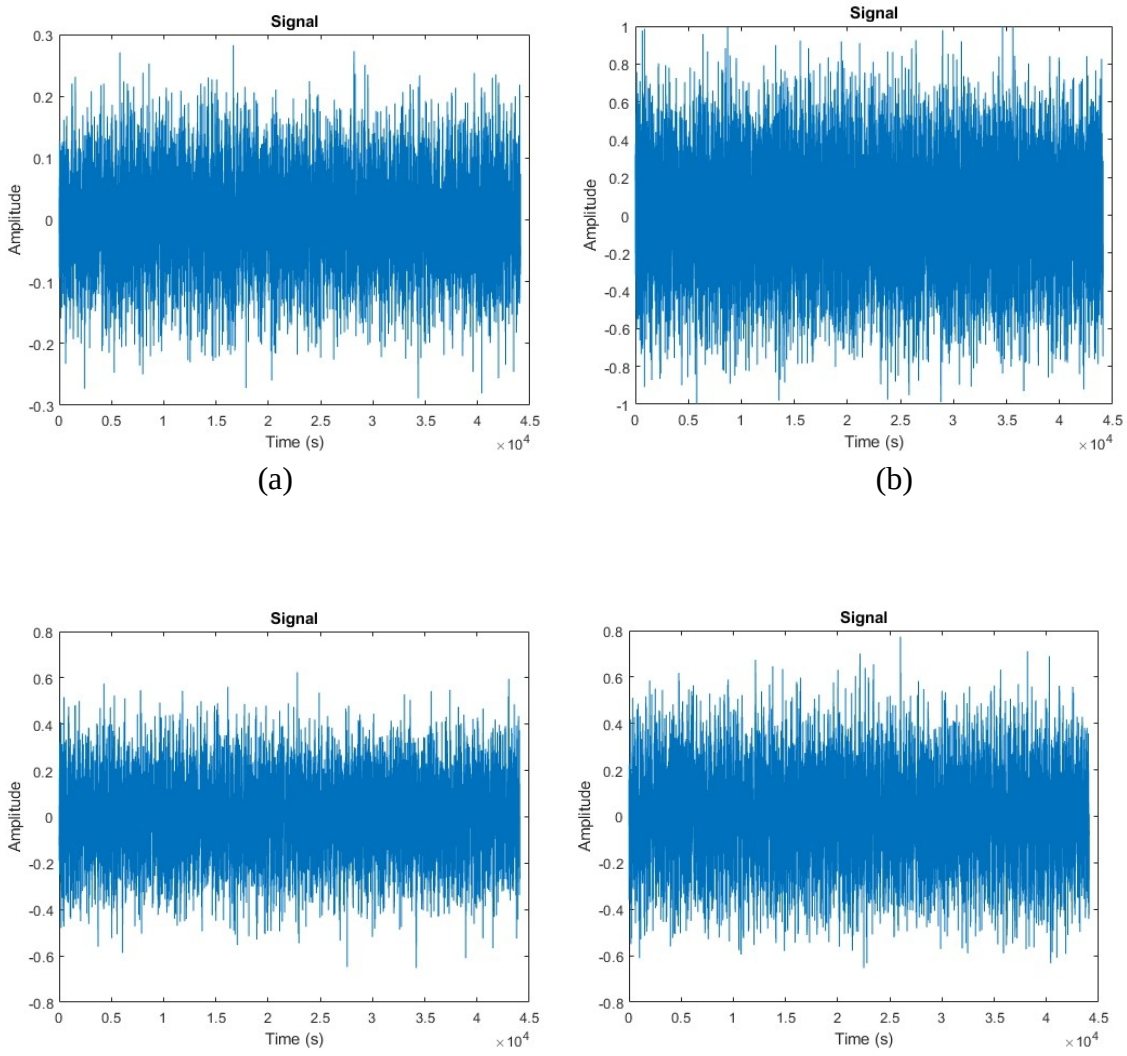

Figure 5. *Example of wav format recordings for: (a) LU1C 0100 at 3000 rpm; (b) LU1C 0100 at 4000 rpm; (c) LU2B 0500 at 4000 rpm and LU2C 1200 at 4000 rpm.*

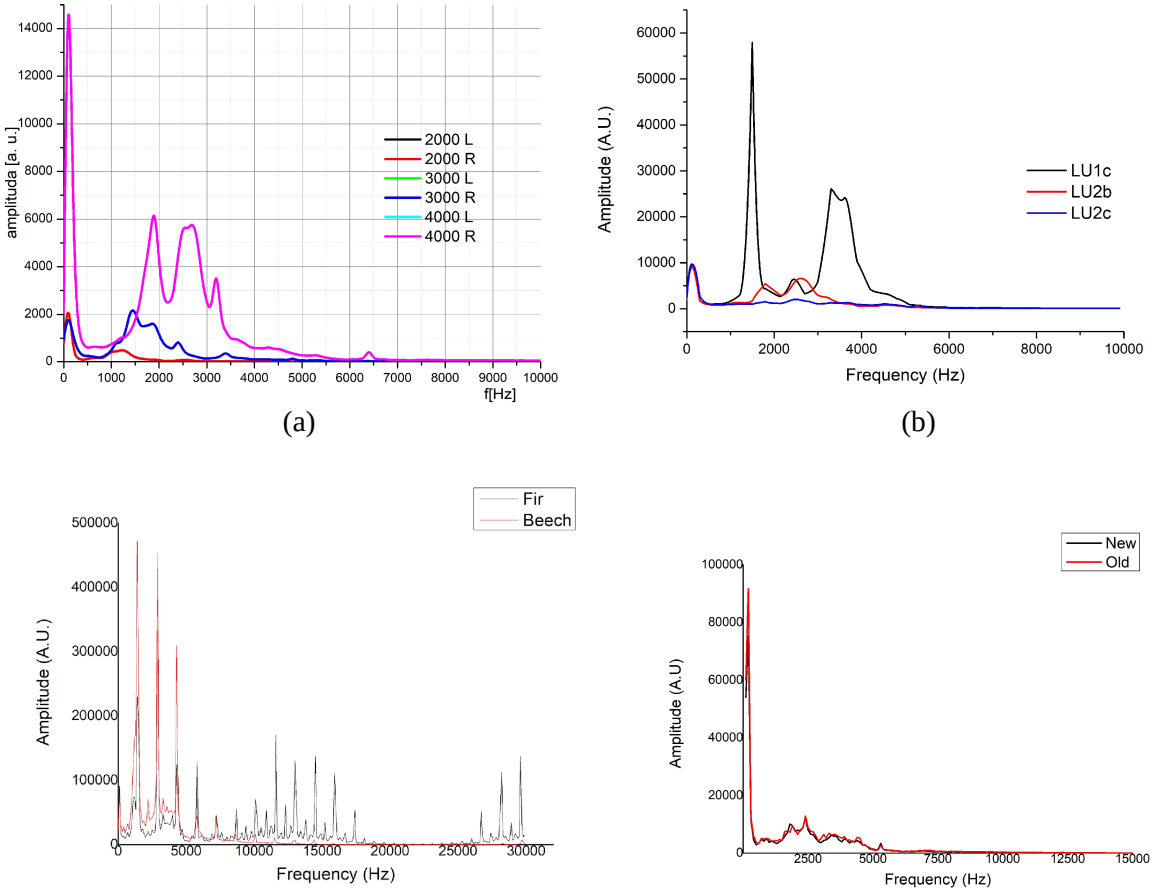

Figure 6. *Average FFT for: (a) LU1C 0100 at three different speeds; (b) LU1C 0100, LU2B 0500 and LU2C 1200 at same speed, (c) LU1C 0100 when cutting beech and fir wood and (d) new and used LU2C 1200.*

In most cases of the average FFT, the graphs behave in very different ways. The most obvious examples are the idling noise of the LU1C 0100 at three given speeds and the idling noise of all saws at the same speed (Fig. 6. a and b). The less noticeable differences are found in the idling noises of the new and the old LU2C 1200 saw (Fig. 6d). The legend in Fig. 6 (a) with the markings L and R stands for the left and right recording channels, which are identical, so that there are only three lines: purple for 4000, blue for 3000 and red for 2000 rpm. The spectral ranges between 0 and 500 Hz show very pronounced peaks at all speeds, which increase as the speed of the processing system increases. These peaks are due to the noise generated by the machine itself – the rotation of the electric motor, spindle and gearbox. Another interesting spectral range is between 1000 and 3500 Hz. At these frequencies, a clear increase in the signal can be recognized, which is due to the rotation of the circular saw blade. This assumption is based on simple maths: 2000 revolutions per minute correspond to approximately 66 revolutions per second, multiplied by 48 saw blades results in a frequency of approximately 1600 Hz, at 3000 revolutions per minute the frequency is 2400 Hz and at 4000 revolutions per minute the frequency value is 3168 Hz.

Taking into account the three-column problem and according to Fig. 6 (b), it was possible to extract two spectral ranges that were of interest for further analysis. The first spectral range extended from 0 to about 700 Hz with a peak at 100 Hz. The curves for all three saw blades observed overlapped in this range. As previously mentioned (Svrzic at al. 2023), this spectral range could be related to the noise generated by the machine itself. Since the speed was the same for all saw blades, the curves overlapped completely. The second spectral range of interest is from about 1000 Hz to about 5000 Hz. The spectral density curves for all three saw blades showed different behavior in this

range and resulted in different peak values, especially in the case of the LU1C saw blade. This spectral range was associated with the noise generated when the observed circular saw blades are idling. As can be seen from Fig. 6 (c), the sound intensities for beech are significantly higher in the spectral range from 0 to about 4500 Hz. This is consistent with previous studies (Miric-Milosavljevic et al. 2024), in which the idling noise of the same circular saw blade was analysed and in which these frequencies were also found, but with an order of magnitude higher intensity. Some of the peaks in the spectral density diagram are particularly interesting. At a frequency of 1400 Hz, the peak for beech is 472000 (A.U.), which is more than twice as high as 230000 (A.U.) for fir. A slightly smaller divergence occurs at 2900 Hz. At this spectral point, the intensity was 453000 (A.U.) for beech and 439000 (A.U.) for fir. The most interesting intensity peak was found at 4300 Hz, where the intensity was 309000 (A.U.) for beech and 124000 (A.U.) for fir, as this peak was completely absent in previous studies (Miric-Milosavljevic et al. 2024). Some high-frequency overtones occurred in fir but not in beech, in the spectral ranges from 7500 to 17500 Hz and from 26000 to 30000 Hz. The reason for this is not entirely clear. One possible explanation lies in the different macroscopic structures of the selected wood species. As a softwood, fir consists mainly of tracheids (91 %), which are considerably longer than the tracheids and libriform fibres of beech. The proportion of cellulose, which has a large proportion of crystalline structure, is also significantly higher in fir wood than in beech wood. In particular, the microfibril angle in the S2 layer of the cell wall is considered an important factor for sound propagation in wood (Brémaud 2012). Compared to most hardwoods, softwoods have a very homogeneous cell structure and uniserised rays. The transition of waves from tracheids to tracheids without the strong influence of vertically orientated rays can be seen as a key factor for wave propagation in fir. This leads to the conclusion that the high-frequency waves in the sound spectrum of fir wood are mainly the result of wave propagation from tracheid to tracheid (Dünisch 2017).

The average FFT for new and used LU2C 1200s is similar, with peaks at low frequencies below 500 Hz and other interesting peaks in the spectral range from 1500 to just above 5000 Hz. In this case, the differences in the waveform are not as obvious as in the previous cases.

However, the average FFT offers no insight into the time scale. As already mentioned, the peaks shown in Fig. 6 (a), (b), (c) and (d) are merely average values at specific points in time. Considering the cyclical nature of the sounds generated during the experiment, the overall picture is somewhat blurred. The STFT is a logical step in visualizing the sound signals obtained.

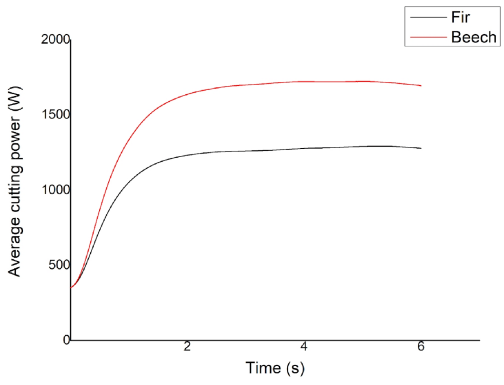

Figure 7. *Average cutting powers for beech and fir wood.*

Power consumption was also measured when cutting beech and fir wood. The average values of the cutting performance for beech and fir wood are shown in Fig. 7. As expected, the average value of the cutting performance for beech is about 50% higher than for fir.

In Fig. 8 (a), the photo under the microscope shows a brand new, unpackaged circular saw blade. It can be seen that the tooth edges and surfaces are in perfect condition, while the same image (b) of a used tool shows cracked edges, traces of corrosion and material deposits on the lateral tooth surfaces.

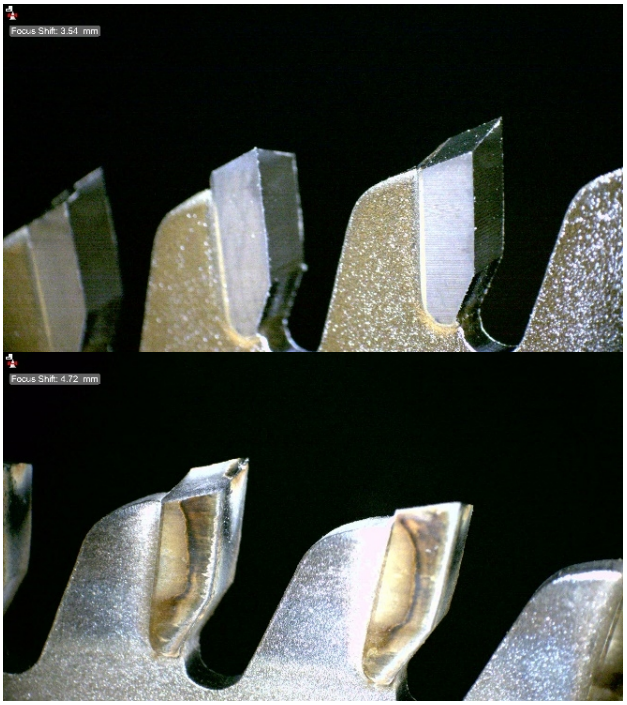

(a) (b)

Figure 8. *Microscopic picture (a) new blade; (b) used blade of LU2C 1200.*

The next step in data processing was to create suitable inputs for ANN. The input data for deep learning networks are spectrograms (see Fig. 9 to 13). The spectrograms were divided into an appropriate number of folders (one for each category according to the number of factors).

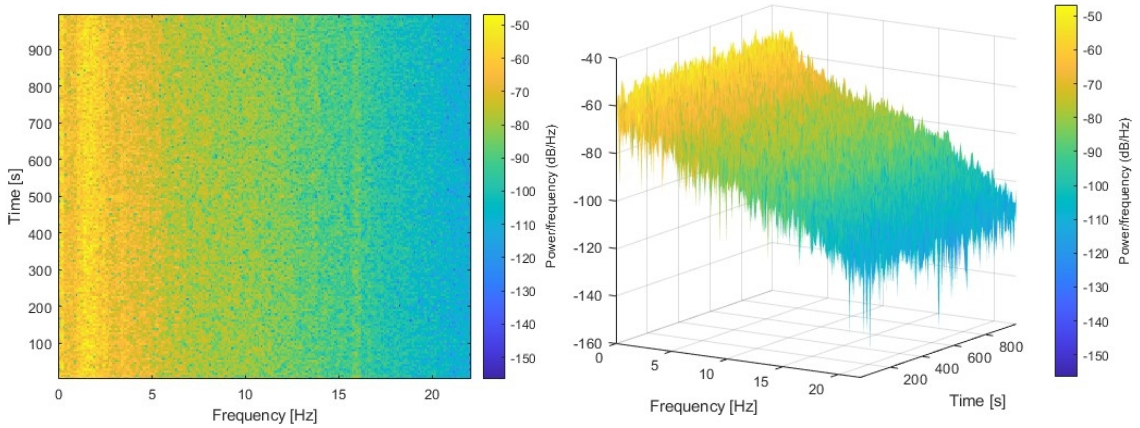

(a) (b)

Figure 9. *Spectrograms presented in (a) 2D and (b) 3D.*

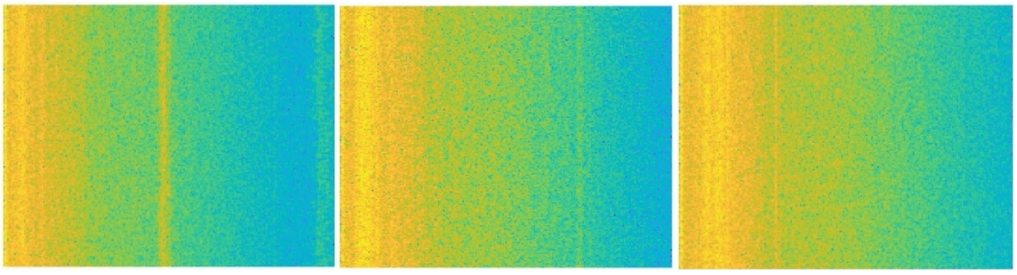

(a) (b) (c)

Figure 10. *Adjusted spectrograms for LU1C 0100 at: (a) 2000 rpm (b) 3000 rpm and (c) 4000 rpm.*

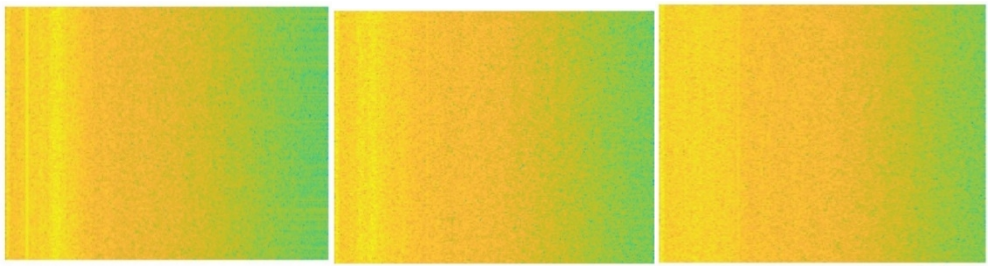

(a) (b) (c)

Figure 11. *(a) Spectrogram without tick and axes for processed sound signal for the LU1C circular saw blade; (b) Spectrogram without tick and axes for processed sound signal for the LU2B circular saw blade; (c) Spectrogram without tick and axes for processed sound signal for the LU2C circular saw blade.*

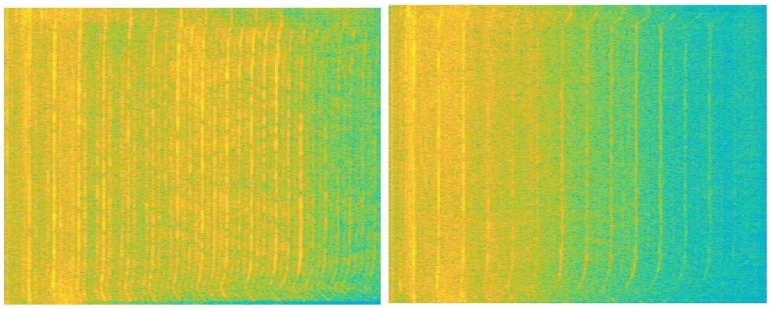

(a) (b)

Figure 12. *Sound spectrograms for: (a) fir and (b) beech wood.*

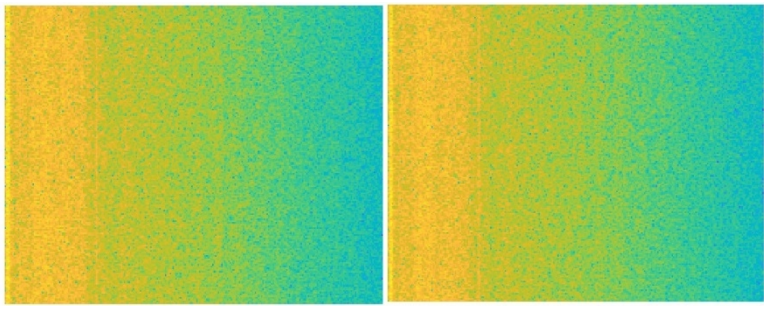

(a) (b)

Figure 13. *Spectrograms for LU2C 1200 (a) new; (b) used circular saw blade.*

The metrics selected for the evaluation and comparison of the developed models included:

$$Accuracy = \frac{T_p + T_n}{T_p + F_p + T_n + F_n} \quad (8)$$

$$Precision = \frac{T_p}{T_p + F_p} \quad (9)$$

$$Recal = \frac{T_p}{T_p + F_n} \quad (10)$$

$$f_1 score = 2\frac{Recal * Precision}{Recal + Precision} \quad (11)$$

where T_p are true positive, T_n are true negative, F_p are false positive, F_n are false negative classifications.

The results for the trained networks are shown in Figs. 14 and 15 and Tables 3 and 4. To analyse the idle noise (research stages one and two), the GoogleNet network was chosen for selected tools,

while six different networks were used for the other stages: MobileNetV2, VGG19, Dense-Net, Squeeze-Net, ResNet and Inception V3.

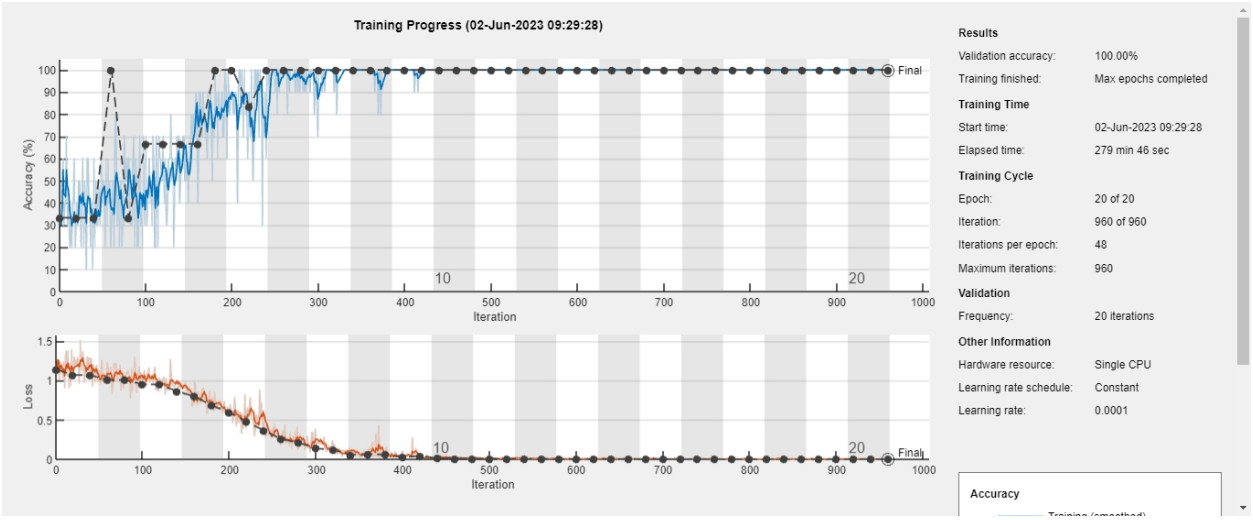

Figure 14. *Deep learning process report (single blade different rotational speeds).*

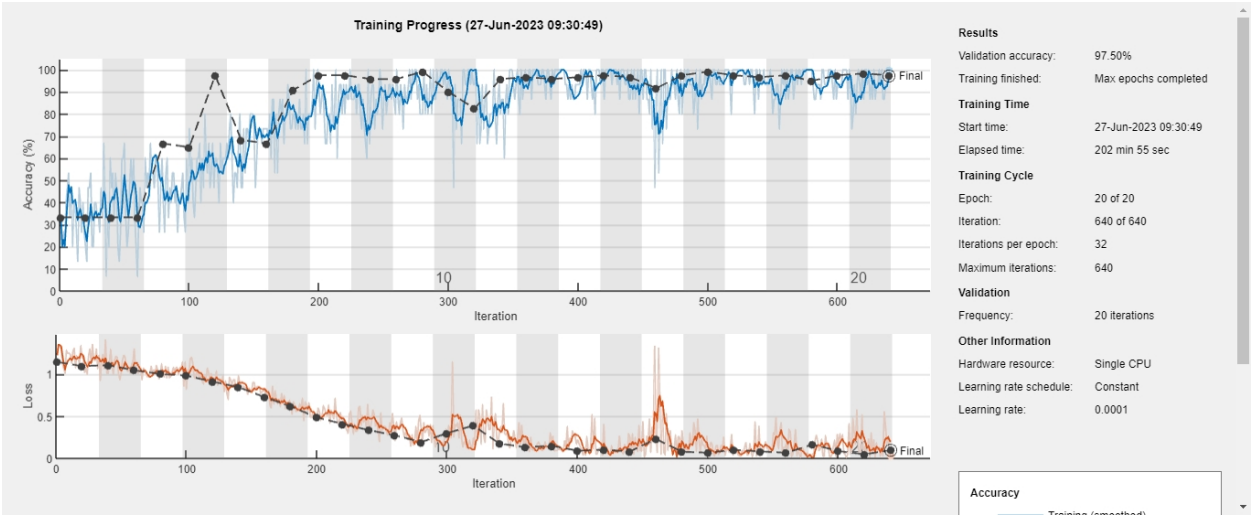

Figure 15*. Deep learning network report (three different blades at same speed).*

The validation accuracy for testing and decision making for a single tool spinning at three different speeds was 100% and for three different tools spinning at the same speed was 97.5%, according to GoogleNet ANN.

Table 3. *Performances of the developed deep learning models for machining sound classification.*

	MobileNetV2	VGG19	Dense-Net	Squeeze-Net	ResNet	Inception_v3
Accuracy	**0.980**	0.960	0.950	0.950	0.970	0.940
Precision	**0.980**	0.942	0.941	0.959	0.980	0.958
Recal	**0.980**	0.980	0.960	0.940	0.960	0.920
f1	**0.980**	0.961	0.950	0.949	0.970	0.939

The results of the deep learning models in the case of cutting different wood species are shown in Table 3. The best performance was achieved by the MobileNetV2 deep learning network with an accuracy of 98%. The second best performance was achieved by the ResNet deep learning network with an accuracy of 97%, followed by VGG 19 (96%), Dense-Net and Squeeze-Net (95%) and finally

Inception-V3 with an accuracy of 94%. The performance results obtained in this work for the developed deep learning models can be considered significantly good in light of other research (Jegorowa et al. 2020, Swidiersky 2022). However, there were no comparable studies involving different wood species. Future research in this direction should include more wood species and more types of tools to substantiate the results presented in this paper. In addition, there is still room for investigation of the tool condition using the applied methodology as well as the sound wave propagation in the wood during cutting.

Table 4. *Performances of the developed deep learning models for different tool condition sound classification.*

	MobileNetV2	VGG19	Dense-Net	Squeeze-Net	ResNet	Inception_v3
Accuracy	**0.930**	0.85	0.9	0.89	0.91	0.87
Precision	**0.921**	0.830189	0.857143	0.882352941	0.886792	0.862745
Recal	**0.940**	0.88	0.96	0.9	0.94	0.88
f1	**0.930**	0.854359	0.90566	0.891089109	0.912621	0.871287

According to Table 4, deep learning models provided satisfactory results in recognizing the tool state. The accuracy of tool wear detection varied from 85% for the Dense-Net network to 93% for MobileNet V2. The values shown in Table 3, especially the accuracy, are slightly lower than the tool type detection (97.5%), but can be considered significant as they are caused by small changes in tooth geometry.

5. CONCLUSION

The methodology presented in this paper offers good prospects for noise detection as a tool for monitoring the machining process, leading to smart machining as part of Industry 4.0 and beyond.
The right choice of frequency range, signal processing and data preparation together with the application of a neural network can provide an answer to the machining process, material and tool.

In this article, it is shown that the noise generated by the use of a circular saw, whether it is interacting with the material or just idling, can provide enough information for process monitoring.

After all that has been said before, one could come to the conclusion:

- The sound signal investigated in this study proves to be a satisfactory data carrier for this type of investigation;
- The processing of the sound signal provided quite good information that is consistent with certain circular saw blades;
- From the average spectral density plots, it was quite clear which spectral regions were of interest for training the deep learning network;
- The spectrograms provided a sufficiently good basis as data for the deep learning process;
- According to the results of the deep learning networks, a validation accuracy of 100, 97.5, 98 and 93% was achieved, proving that this approach can be used for monitoring cutting processes in terms of decision making;
- However, the results presented relate to the particular environmental conditions. No reverberation noise was taken into account;
- Further research in this area will include the interaction of a tool (circular saw blade) with other, more homogeneous materials commonly used in woodworking, with different cutting conditions and different degrees of bluntness of the tool.

Acknowledgement

This research was funded by the Ministry of Science, Technological Development and Innovation of the Republic of Serbia, under registration number 451-03-65/2024-03/200169, dated 05.02.2024.

REFERENCES

1. Abellan-Nebot J. V. Subirón F. R. (2010) “A review of machining monitoring systems based on artificial intelligence process models”, The International Journal of Advanced Manufacturing Technology, 47(1–4), 237–257, DOI: 10.1007/s00170-009-2191-8
2. Aguilera A. (2011) “Cutting energy and surface roughness in medium density fiberboard rip sawing”, *European Journal of Wood and Wood Products*, 69(1), 11-18. DOI: 10.1007/s00107-009-0396-z
3. Aguilera A. (2011a) “Surface roughness evaluation in medium density fibreboard rip sawing”, European Journal of Wood and Wood Products, 69(3), 489-493. DOI:10.1007/s00107-010-0481-3
4. Aguilera A. Barros J. L. (2010) “Sound pressure as a tool in the assessment of the surface roughness on medium density fibreboard rip sawing process”, Maderas. Ciencia y tecnologia, 12(3), 159–169, DOI:10.4067/S0718-221X2010000300001
5. Aguilera A. Rolleri A. Burgos F. (2016) “Cutting distance as factor to evaluate the quality of wood machined surfaces: A preliminary study”, Maderas, Ciencia y tecnologia vol.18 no.1, doi.org/10.4067/S0718-221X2016005000001
6. Aguilera A. Zamora R. (2007) “Wood machining process monitoring of blackwood (Acacia melanoxylon) with acoustic emission technique and his relationship with resulting surface roughness”, Maderas: Ciencia y Technologia, 2007, 9(3), 323-332, doi.org/10.4067/S0718-221X2007000300011
7. Brémaud I. El Kaïm Y. Guibal D. Minato K. Thibaut B. Gril J. (2012) “Characterisation and categorisation of the diversity in viscoelastic vibrational properties between 98 wood types”, Annals of Forest Science 69(3), DOI: 10.1007/s13595-011-0166-z
8. Cyra G. Tanaka C. (2000) “The effects of wood-fiber directions on acoustic emission in routing”, Wood Science and Technology, 34, 237–252.
9. de Geus, A.R., da Silva, S.F., Gontijo, A.B., Silva, F.O., Batista, M.A., Souza, J.R. (2020) “An analysis of timber sections and deep learning for wood species classification”, Multimedia Tools and Applications, 79, 34513–34529, DOI: 10.1007/s11042-020-09212-x
10. Dünisch O. (2017) “Relationship between anatomy and vibration behaviour of softwoods and hardwoods”, IAWA Journal, 38(1), 81-98, DOI: 10.1163/22941932-20170158
11. Goli G. Curti R. Marcon B. Scippa A. Campatelli G. Furferi R. Denaud L. (2018) “Specific Cutting Forces of Isotropic and Orthotropic Engineered Wood Products by Round Shape Machining”, Materials, 11(12): 2575, DOI: 10.3390/ma11122575
12. Goli G. Fioravanti M. Marchal R. Uzielli L. (2010) “Up-milling and down-milling wood with different grain orientations - Theoretical background and general appearance of the chips”, European Journal of Wood and Wood Products, 67(3):257-263, DOI: 10.1007/s00107-009-0323-3
13. Iskra P. Hernández RE. (2009) “The influence of cutting parameters on the surface quality of routed paper birch and surface roughness prediction modeling”, Wood and Fiber Science, 41(1), 28–37.
14. Iskra P. Hernández RE. (2009) “The influence of cutting parameters on the surface quality of routed paper birch and surface roughness prediction modeling”, Wood and Fiber Science, 41(1), 28–37.
15. Iskra P. Hernández RE. (2012) “Toward a process monitoring of CNC wood router. Sensor selection and surface roughness prediction”, Wood Science and Technology, 46(1–3), 115–128, DOI: 10.1007/s00226-010-0378-7
16. Iskra P. Hernández RE. (2012) “Toward a process monitoring of CNC wood router. Sensor selection and surface roughness prediction”, Wood Science and Technology, 46(1–3), 115–128, DOI: 10.1007/s00226-010-0378-7
17. Iskra P. Tanaka C. (2005). “The influence of wood fibre direction, feed rate and cutting width on sound intensity during routing,” Holz als Roh-und Werkstoff 63, 167-172. DOI: 10.1007/s00107-004-0541-7

18. Iskra P. Tanaka C. (2005). “The influence of wood fibre direction, feed rate and cutting width on sound intensity during routing,” Holz als Roh-und Werkstoff 63, 167-172. DOI: 10.1007/s00107-004-0541-7
19. Jegorowa A. Kurek J. Antoniuk I. Dołowa W. Bukowski M. Czarniak P. (2020) “Deep learning methods for drill wear classification based on images of holes drilled in melamine faced chipboard”, Wood Science and Technology 55(1):1-23, DOI: 10.1007/s00226-020-01245-7
20. Jemielniak K. Urbański T. Kossakowska J. Bombiński S.(2011)” Tool condition monitoring based on numerous signal features”, Int J Adv Manuf Technol (2012) 59:73–81, DOI 10.1007/s00170-011-3504-2
21. Kibleur P. Aelterman J. Boone MN. Van den Bulcke J. Van Acker J. (2022) “Deep learning segmentation of wood fiber bundles in fiberboards”, Composites Science and Technology, 221, https://doi.org/10.1016/j.compscitech.2022.109287
22. Kováč J. Harvánek P. Krilek J. Kuvik T. Melicherčík J. (2021) “Analysis of cutting conditions in the process of cross-cutting wood by circular saws”, “Circular saw cross-cutting,” BioResources 16(1), 1029-1041. DOI:10.15376/biores.16.1.1029-1041
23. Mandic M. Svrzic S. Danon G. (2015) “The comparative analysis of two methods for the power consumption measurement in circular saw cutting of laminated particle board”, Wood Research 60 (1), 125-136.
24. Miric-Milosavljevic M. Svrzic S. Nikolić Z. Djurkovic M. Furtula M. Dedic A. (2024)” Signal Processing and Machine Learning as a Tool for Identifying Idling Noises of Different Circular Saw Blades”, BioResources, 2024, 19(1), 1744-1756, 10.15376/biores.19.1.1744-1756
25. Nasir V. Cool J. Sassani F. (2019) “Acoustic emission monitoring of sawing process: Artificial intelligence approach for optimal sensory feature selection”, *The International Journal of Advanced Manufacturing Technology* 102, 4179-4197. DOI:10.1007/s00170-019-03526-3
26. Nasir V. Sassani F. (2021) “A review on deep learning in machining and tool monitoring: methods, opportunities, and challenges”, The International Journal of Advanced Manufacturing Technology 115(2683–2709), DOI:10.1007/s00170-021-07325-7
27. Naylor A. Hackney P. Perera N. Clahr E. (2012) “Mechanical Cutting Force Model,” BioResources 7(3), 2883-2894., ISSN 1930-2126
28. Porankiewicz B. Axelsson B. Grönlund B. Marklund B. (2011) “Main and Normal Cutting forces by Machining Wood of Pinus Sylvestis”, BioResources 6(4), 3687-3713, DOI: 10.15376/BIORES.6.4.3867-3713
29. Stanojevic D. Mandic M. Danon G. Svrzic S. (2017) “Prediction of the surface roughness of wood for machining”, Journal of Forestry Research, 28(3), 1281–1283, DOI: 10.1007/s11676-017-0401-z
30. Sun Y. Lin Q. He X. Zhao Y. Dai F. Qiu J. Cao Y. (2021) “Wood Species Recognition with Small Data: A Deep Learning Approach”, International Journal of Computational Intelligence Systems,14(1),1451 – 1460, DOI: 10.2991/ijcis.d.210423.001
31. Svrzic S. Djurkovic M. Danon G. Furtula M. Stanojevic D. (2021) “On acoustic emission analysis in circular saw cutting beech wood with respect to power consumption and surface roughness,” *BioResources* 16(4), 8239-8257. DOI: 10.15376/biores.16.4.8239-8257
32. Szwajka K. Zielinska-Szwajka J. Gorski J. (2008) “Neural networks based in process tool wear prediction system in milling wood operations”, In International Symposium on Instrumentation Science and Technology (International Society for Optics and Photonics, 713312–713312, DOI: 10.1117/12.812090
33. Tanaka C. Nakao T. Nishino Y. Hamaguchi T. Takahashi A. (1992) “Detection of wear degree of cutting-tool by acoustic-emission signal”, Mokuzai Gakkaishi, 38(9), 841–846.
34. Tiryaki S. Malkoçoğlu A. Özşahin S. (2014) “Using artificial neural networks for modeling surface roughness of wood in machining process”, Construction and Building Materials, 66, 15, 329-335, doi.org/10.1016/j.conbuildmat.2014.05.098
35. Zafar T. Kamal K. Sheikh Z. Mathavan S. Jehanghir A. Ali U. (2015) “Tool health monitoring for wood milling process using airborne acoustic emission”, 2015 IEEE International

Conference on Automation Science and Engineering (CASE), Gothenburg, Sweden,1521–1526, DOI: 10.1109/CoASE.2015.7294315

36. Zbieć M. (2011) “Application of neural network in simple tool wear monitoring and identification system in MDF milling”, Drvna Industrija, 62(1), 43–54, doi.org/10.5552/drind.2011.1020

ANALYSIS OF QUALITY CONTROL METHODS IN THE FURNITURE FACTORY "DIVA DIVANI" VRANJSKA BANJA

Damjan Stanojevic[1], Anastasija Temelkova[2], Elena Jeftoska[2], Zoran Trposki[2]

[1]*Academy of Technical and Educational Vocational Studies, Serbia*
Department of Vranje,
e-mail:damjan.stanojevic@akademijanis.edu.rs
[2]*Ss. Cyril and Methodius University in Skopje, Macedonia,*
Faculty of Design and Technologies of Furniture and Interior-Skopje,
e-mail:temelkova@fdtme.ukim.edu.mk;jeftoska@fdtme.ukim.edu.mk;trposki@fdtme.ukim.edu.mk

ABSTRACT

The goal of the research presented in the paper is the analysis of various quality control procedures in a factory that produces upholstery products. The upholstery industry is very developed in Vranje, the competition is high, so quality control has a huge impact on the company's operations.

Quality control is one of the key elements in the production management system in a furniture factory. Its role is to ensure that each product meets defined technical, aesthetic and functional requirements, as well as the expectations of end users. Establishing systematic quality control — from incoming control of raw materials, through process control at all stages of production, to final control of finished products — enables the detection and elimination of defects at an early stage, thereby significantly reducing the costs of repairs and complaints. This paper presents a complete quality control system in a furniture factory, from start to finish, and presents the conclusions reached, as well as their implementation for the better business of the company.

Keywords: quality system, furniture, wood technology.

1. INTRODUCTION

The furniture factory is a key place where creativity, tradition and modern technology come together to create furniture of the highest quality. With many years of experience in production, the factory emphasizes precision in every step of the process – from the selection of the highest quality materials to the final processing.

Quality control is the foundation of its business, ensuring that each piece of furniture meets the highest standards. Using modern technologies and tools, as well as the dedication of its craftsmen, each product receives attention to the smallest detail. The diverse range of furniture covers all the needs of a modern home – from classic and traditional, to innovative and modern designs. In addition to functionality, the factory strives to bring elegance and a unique aesthetic to each piece of furniture. It proudly offers the possibility of personalization, allowing customers to adapt the design to their wishes and taste. By choosing its products, customers gain durability and comfort that lasts for generations.

Environmental responsibility is a priority – materials that comply with the principles of sustainable development are used. The team of experts is dedicated to innovation, following global trends and constantly improving production processes. It also strives to provide customers with an exceptional user experience, from the initial consultation to the delivery of the product.

Furniture from the factory is not only functional, but also emotionally valuable – it brings warmth and a personal touch to every home. With a wide selection of colors, materials and styles, the factory satisfies the requirements of even the most demanding customers.

If we want to be part of the world, quality control is essential. This means that a manufacturer, if he wants to export his goods to the demanding European market, must control his products, which must be in compliance with the technical and technological standards that prevail there. When it comes to product quality, these standards are clearly defined and they mainly relate to safety, health and consumer protection in general. But it is not enough for a company to achieve that quality just

once, it must also maintain it. Quality is assessed by highly educated people from various fields, technologists, economists, chemists and other experts.

2. MATERIAL AND METHODS

The analysis of quality control methods was carried out at the furniture factory "Diva Divani" in Vranjska Banja. The complete quality control in the production process from start to finish, by stages, as well as the final quality control of the product are presented.

The basics of the quality policy are:

a) "Satisfied customer" is the primary value on which the company's management and production processes are based.

b) Development of a quality culture at all organizational levels.

c) Take into account the characteristics of the product and the products offered.

d) Strive for the optimization of business processes in order to achieve the highest level of efficiency and effectiveness.

e) Adopt a method that will enable timely resolution of customer complaints.

For wood products, it is necessary to have an FCS certificate from the supplier. Wood products, chipboard, plywood, hardboard, MDF, HDF, in addition to the above FCS standard must have the E1 mark with a tendency to achieve a reduction of formaldehyde to the E0 level.

Diva Divani does not require, but strongly recommends obtaining an ISO 9001 certificate, the exception being packaging materials (pallets, boxes, nylon and other raw materials that do not enter the final product). Suppliers of materials that do not have an ISO 9001 certificate for them are subject to a possible audit by Diva Divani. Diva Divani Procurement decides on the execution of the audit. Suppliers are obliged to provide the purchasing office with valid certificates. The purchasing office is obliged to keep a register of all certificates and check their validity. The supplier is required to provide a REACH declaration.

a. RECEIPT OF GOODS FOR STORAGE

✓ Warranty

The manufacturer must guarantee that all raw materials comply with the requirements and regulations of Diva Divani as well as international regulations, for which they must have the appropriate certificates, as well as that they meet the delivery requirements of Diva Divani. For certain materials, Diva Divani may request additional certificates from the supplier, which in this case are delivered as a separate document. The warranty applies to the raw materials presented 24 months from the date of delivery (in other words, from the moment of transport, the liability towards Diva Divani in accordance with the agreed transport clauses comes into force).

The warranty covers all physical defects, functional and aesthetic, all deviations from the reference sample and valid documentation resulting from an inadequate production process, improper handling or transport of the raw materials.

✓ Non-conformity

Products received from suppliers are always controlled, while the operators who perform this work are responsible for the good performance of that work, therefore they perform the check immediately during the process.

Formalization and recording are carried out on special documents with records of non-conformity and are handled accordingly.

The warehouseman performs qualitative and quantitative controls of incoming goods. In the event of non-compliance with the requirements for raw materials, Diva Divani reserves the right to refuse the delivery of goods in part or in full, with the help of a commission, which draws up a report and sends it to the supplier with a request for an analysis of the causes of the complaint submitted, defining corrective and preventive measures.

It is mandatory that all wood raw materials and solid wood comply with the FSC standard. The FSC label indicates that each piece of wood incorporated into the furniture comes from a forest where there is no illegal logging, genetically modified wood, that the logging does not cause landslides in

those areas or leaching of fertile soil or that it has led to the displacement of the population due to deforestation.

Upon receipt, the following checks are performed:

• Checking the dimensions of the material (wood and wood products) based on the dimensions shown on the supplier's invoice - mandatory control for each delivery
• Checking the relative humidity level of the material - mandatory control for each delivery
• Visual inspection of the quality of the material - mandatory control for each delivery.
• Checking the quantity of material received and the quantity specified in the supplier's document - mandatory control for each delivery
• Material storage

Figure 1. *Material to use.*

Figure 1 shows the material (fir sawn timber) used for the production of upholstered furniture. Fir (Spruce) Wood Company Standard

L4000 x P145 x H22 (tolerance ±1mm)
L3500 x P145 x H22 (tolerance±1mm)
L4000 x P175 x H22 (tolerance ±1mm)
L3500 x P175 x H22 (tolerance ±1mm)
L4000 x P200 x H45 (tolerance +1mm)

Figure 2. *Measuring moisture content in wood.*

Figure 2 shows the checking of the relative humidity of the material with an electric moisture meter. An important parameter that directly affects the quality of the structure and the finished product. The control is carried out by the warehouseman, and the control is mandatory for each delivery

The company's standard for wood is 12% (tolerance is ± 2%)

As for the visual inspection of the material quality, it is usually carried out by the technician in charge of the wood together with the head of the department (control is mandatory upon each delivery) Criteria for classifying the external appearance of wood

• dimension of knots and their frequency (position is not important)
• cracks, rings, resin pockets (size and density)
• color, fiber deformation, rot, insects
• deviations due to uneven shrinkage – curvature, distortion, lateral curvature

Figure 3 shows the wood quality classes by appearance

• Class CPC (G4-0 SRPS EN 1611-1) – high resistance (clean wood without knots),
• Class I high resistance (Net surface: 83-100%, knots ≤10 mm),
• Class II (G4-2 SRPS EN 1611-1) – normal (medium) resistance (Net area: 67-83% 10 mm ≤ knots ≤20 mm),
• Class III (G4-3 SRPS EN 1611-1)

Figure 3. *Wood quality classes.*

As for wood panels, incoming quality control is carried out by a technologist with the head of the production unit and the warehouseman - control is mandatory upon each delivery.

- 18mm chipboard, raw or laminate, must be compatible with the standard EN 312 - type 2 or P3, three-layer coating EN 13501-1, class D-s1, d0, formaldehyde class E1 or E0 (must be marked on each package of the material)

- All wood panels (chipboard, hardboard, plywood) must comply with E1 or E0 (standard EN 120), which means that the formaldehyde content must be ≤ 8mg / 100g.

Sadržaj formaldehida Proizvod je dostupan u klasi formaldehida	**E1** EN 120 (U skladu sa D.M. 10/10/08)	**UNI EN 312** **(mg / 100g)**	**≤ 8mg / 100g.**

Figure 4. *Standard for formaldehyde content.*

Their goal is to use all materials with the E0 standard in the future.

The E0 label for HCHO or formaldehyde, according to the European standard, indicates the complete absence of formaldehyde emissions (below 0.5 mg/liter) in products that have this label.

The warehousekeeper is obliged to check the quantity of each delivery and compare it with the quantity in the manufacturer’s invoice

All these checks must be carried out before storing the material in the warehouse. In the event of a discrepancy between the ordered and received material, or in the event of non-conformity of the material, the purchasing office should be informed, which will inform the supplier about the return of the goods.

As for the production unit of cutting sponge and conflin, polyurethane, conflin, pleats, felt and TNT are controlled.

Experimental methods for checking physical and mechanical characteristics can only be performed in an accredited laboratory. It is desirable to perform these tests frequently, but it is not necessary for each delivery. The test consists of density (UNI 6349, DIN53420, ISO 1855), bearing capacity (BS 4443, Pt.1M.5, UNI 6351, DIN 53577, ISO 3386), deterioration (BS 4443, Pt.1M.5, UNI 6351, DIN 53577, ISO 3386), tensile strength (BS 4443, Pt.1M.5, DIN 53577), permanent deformation (BS 4443, Pt.1M.5, UNI 6351, DIN 53577), dynamic resistance (UNI 6356 Pt.2), elastic limits (UNI 6357) and air permeability.

3. RESULTS

The Quality Control Team, in cooperation with the process technologists, is responsible for the detection and assessment of non-conformities found in the material. If a defect is determined, the

quality tool coordinator draws up an official report, which informs the supplier of the defects found.

At the same time, the data is recorded in the DDPR system for further processing and monitoring. The report contains all relevant information, including:

- Invoice number and date
- Date of receipt of the material
- Detailed description of the non-conformity found
- Notes and additional comments related to the defect
- Official response from the supplier
- Defined corrective and preventive measures to be taken

This data is systematically presented in the form of a tabular report, covering a period of one month, enabling trend analysis and decision-making with the aim of improving quality.

ID	Date	Difetto materiale	Fornitore	Materiale In Fornitura	Descrizione Difetto	Stato difetto	ogovor firme	note	AZIONI
135	08.05.2019	MATERIALE NON CONFORME A SPECIFICHE RICHIESTE	VIN PRODUKT	vijak za mehanizam tipa FREEDOM(1364mm)	nisu uradjeni po crtezu (1364mm) 20kom. Umetak je veci a treba da bude 31,5.	CHIUSO		20kom	Zamena izvrsena.
136	08.05.2019	MATERIALE NON CONFORME A SPECIFICHE RICHIESTE	VIN PRODUKT	MN218-SHAINE	na dve metalne nogice rastojanje izmedju rupa je bilo manje treba 167 a njihovo rastojanje je 155 radili smo doradu u nasoj radionici , kao i na pet nogica gde smo malo prosirivali rupe, jer je isti slucaj ali smo u pitanju 5mm razlika.	CHIUSO		pod fakturom dosle 12 komada, dorada je vrsena na 7 u nasoj radionici	kontrolisati sledecu isporuku
137	08.05.2019	MATERIALE NON CONFORME A SPECIFICHE RICHIESTE	TAMI TRADE	SCHIENALI IN METALO per porto	Nemaju cist novoj, odnosno ima farbe na njemu, potrebno je svaku rupu opet urezati.	CHIUSO	U procesu smo resavanja tog problema. Vec smo kupili novu masinu i poceli sa ugradnjom novih (blind zakovica) Ove stare kolicine na zalost mozemo i mi doci kod Vas u fabrici da Vam resimo. Saljem Vam sliku da vidite kako smo resili taj problem.		
138	08.05.2019	MATERIALE NON CONFORME A SPECIFICHE RICHIESTE	A VENTURIN	najlon 1800x0.08gr	NAJLON ZA DRUGO POKRIVANJE SE CEPA.Pri povlacenju on pukne.	CHIUSO		dobavljac ce izvrsiti zamenu. Sve sto nije dobro ostavite sa strane i vratiscemo. Samo me obavestite koja je kolicina u pitanju.	Prijavljeno na 650kg
139	08.05.2019	MATERIALE NON CONFORME A SPECIFICHE RICHIESTE	EURO SPIN	DVONAVOJNI VIJAK M8X120	NEMA NAVOJ CELOM DUZINOM	CHIUSO	poveca najvise po 10mm sa obe strane i deo u sredini bez navoja bi bio 20mm		U razgovoru sa tehnickom pripremom prihvacen je predlog da vijak ima u sredini deo od 20mm bez navoja. Moze i cela duzina vijka da bude u navoju. **Vraceno i nije fakturisano**
140	08.05.2019	MATERIALE NON CONFORME A SPECIFICHE RICHIESTE	FURTECO	mecc. coppia WS 189-5 LISBONA	cevi stizu sa vecom dimenzijom 132(nsama potreno 1168), tockici su veci .(pogledati zapisnik)	CHIUSO			Sledeca isporuka bice sakotrokirana.Trenutno za proizvodnju naruciti kolicine koje su potrebne (tockice, srafove, cevi od dobavljaca VIN PRODUKT-a jer ti delovi mogu da se upotrebe za sklop mehanizma).
141	14.05.2019	MATERIALE NON CONFORME A SPECIFICHE RICHIESTE	VIN PRODUKT	MN220-ORSON	Prema crtezu metalna nogica treba da ima visinu 110mm, nama su stigle sa visinom od 120mm.	CHIUSO		6 metalnih nogica bice vraceno dobavljacu.	**uradioli knjizno odobrenje.**
142	15.05.2019	MATERIALE NON CONFORME A SPECIFICHE RICHIESTE	NAVLAKA ZADUSEK CLIO	Leder Lux	Primetili smo tragove odnosno plave mrlje, smatramo da su presikani tragovi hemijske olovke (slika - imamo trag hemijskom olovkom na naticu). Zelimo da ukazemo da se stavljaju naljepnice(etikete) na zakovanju, a ne ispis markerom.	CHIUSO	Sto se tice obelezavanja dimenzija i br. komada na dzaku ispisano markerom, mozemo pisti na etiketi i tako ce biti za sve sledece isporuke, osim ovih koje su vec zavrsene.Sto se tice hemiske na rajfesluzu, ona mora ostati jer se rajfesluz mora obelezavati u izradi navlake. Da bi resili ovaj problem, koristicemo u buduce dvesnu olovku i videti da li to daje bolje rezultate.	poslati obavesenje dobavljacu	treba kontrolisati
143	20.05.2019	MATERIALE NON CONFORME A SPECIFICHE RICHIESTE	KOSMOPEL L	pelle grigio perla 25	pojava crvenih tacaka.	CHIUSO	Per quanto riguarda pelli già tagliate o salotti già fatti, possiamo inviarti una bottiglia di colore per provare a coprire i piccoli puntini colorati. Penso che una buona parte del problema sia possibile risolvere.	bice stopirana, kolicina u magacinu 154.06	
144	20.05.2019	MATERIALE NON CONFORME A SPECIFICHE RICHIESTE	NISI DREAM	MATERASSO ORIGINE 160X192X13	Imamo dva duseka sa zutim mrljama, ne mozemo ih koristiti u proizvodnji.	CHIUSO			
147	22.05.2019	MATERIALE NON CONFORME A SPECIFICHE RICHIESTE	RENATO NISI	NEW TAORMINA DA 160CM COIN BAIONETE	stigli su mehanizmi na kojima ne postoje rupe na prednjem delu. Sva 10 mehanizama su bez rupa.	CHIUSO	In merito al suo problema con le reti New Taormina le inoltro questa comunicazione inviata in data 8 ottobre 2018 in merito alle modifiche delle reti NEW TAORMINA. Dal 1 Gennaio vengono prodotte senza foro.	Ovaj slucaj resavamo u proizvodnji, a u buduce vise paznje molim.	
148	22.05.2019	MATERIALE NON CONFORME A SPECIFICHE RICHIESTE	VIN PRODUKT	VINKLA OSAKA	Stigle su nam vinkle sa rupama koje nisu uradjene po crtezu. Rupe trebaju biti 67 one su 66.	CHIUSO		Fakturom su stigle 620 vinkli, 20 kom. uzeli za proizvodnju i obradili jer su bile hitne, ostatak vracamo dobavljacu na popravku	vratili i popravka je uradjena

Figure 5. *Display of detected material errors.*

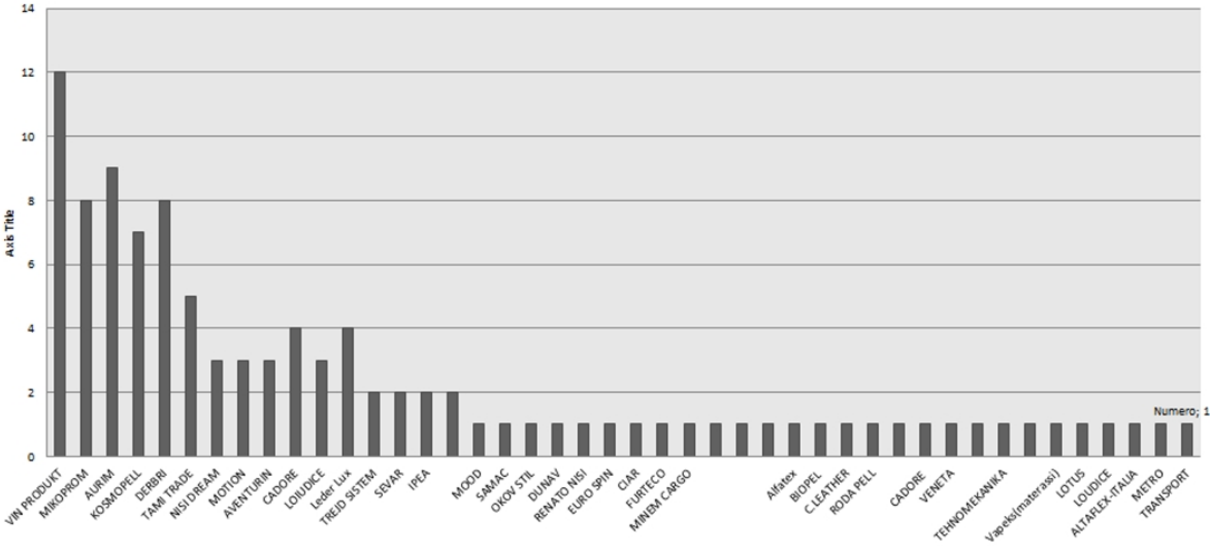

Figure 6. *Graphical representation of recorded non-conformities of raw materials by supplier.*

4. DISCUSSION

Quality control in the assembly process of wooden frame structures plays a crucial role in the production cycle of a furniture factory, as it directly affects the stability, durability and overall quality of the final product. It includes:

- systematic inspection of materials,

• assembly precision,
• quality of joints and
• used adhesives.

Figure 7 shows examples of compliant and non-compliant joints

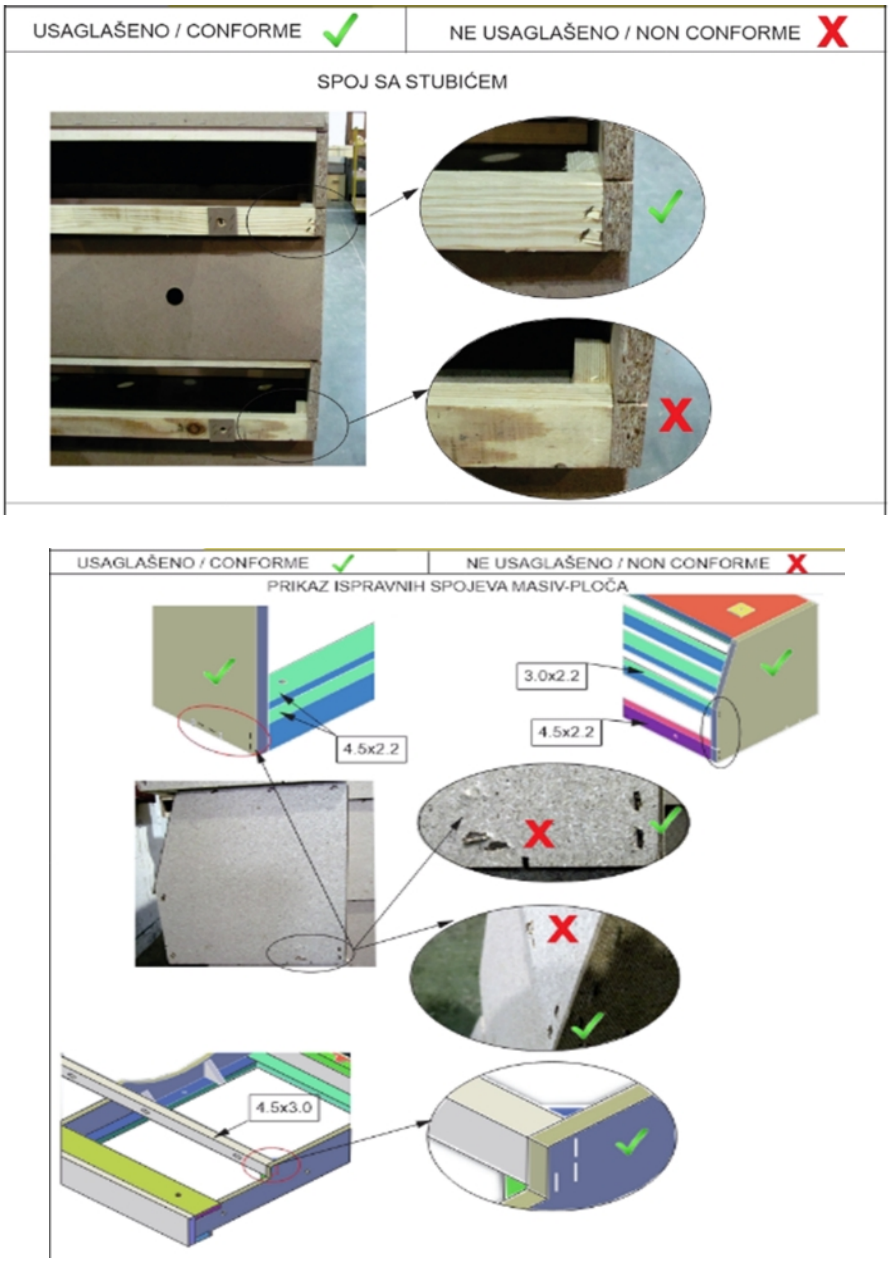

Figure 7. *Display of correct and incorrect connections.*

Figure 8 shows a diagram of the total number of recorded errors in all production processes.

Produzione 2023	Diffeti totale	100%
TAGLIO PELLE	421	29.3%
TAPPEZZERIA	353	24.6%
CUCITO	464	32.3%
TAGLIO TESSUTO	36	2.5%
ASSEMBLAGGIO FUSTI	30	2.1%
TAGLIO FUSTI	20	1.4%
UFFICIO TECNICO	2	0.1%
MESSA IN BIANCO	8	0.6%
CINGHIATURA		0%
MATERIALE PELLE	45	3.1%
MATERIALE TESSUTO	45	3.1%
GOMMA		0.0%
NON DEFINITO	11	0.8%
Totale	1435	

Produzione 2022	Diffeti totale	
TAGLIO PELLE	586	31%
TAPPEZZERIA	411	22%
CUCITO	383	20%
TAGLIO TESSUTO	43	2%
ASSEMBLAGGIO FUSTI	45	2%
TAGLIO FUSTI	35	2%
UFFICIO TECNICO	17	1%
MESSA IN BIANCO	17	1%
CINGHIATURA	1	0%
MATERIALE PELLE	235	12%
MATERIALE TESSUTO	82	4%
GOMMA	5	0%
NON DEFINITO	50	3%
Totale	1910	

Produzione DA APRILE 2021	Diffeti totale	
TAGLIO PELLE	337	28%
TAPPEZZERIA	161	13%
CUCITO	294	24%
TAGLIO TESSUTO	31	3%
ASSEMBLAGGIO FUSTI	43	3%
TAGLIO FUSTI	20	2%
UFFICIO TECNICO	33	3%
MESSA IN BIANCO	11	1%
CINGHIATURA	4	0%
MATERIALE	281	23%
Totale	1225	

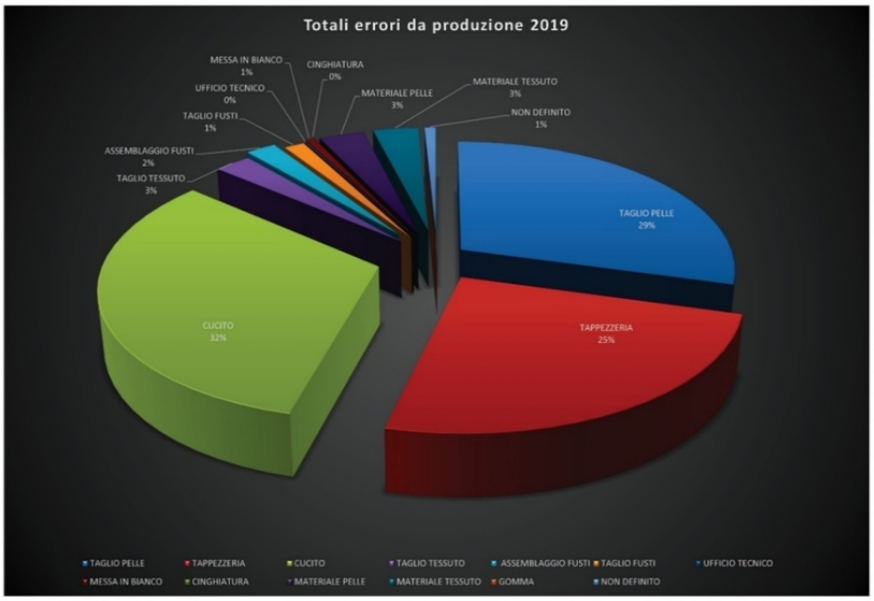

Figure 8. *Diagram of the total number of recorded errors in all production processes.*

Figure 9 shows a graphical representation of total complaints in percentages.

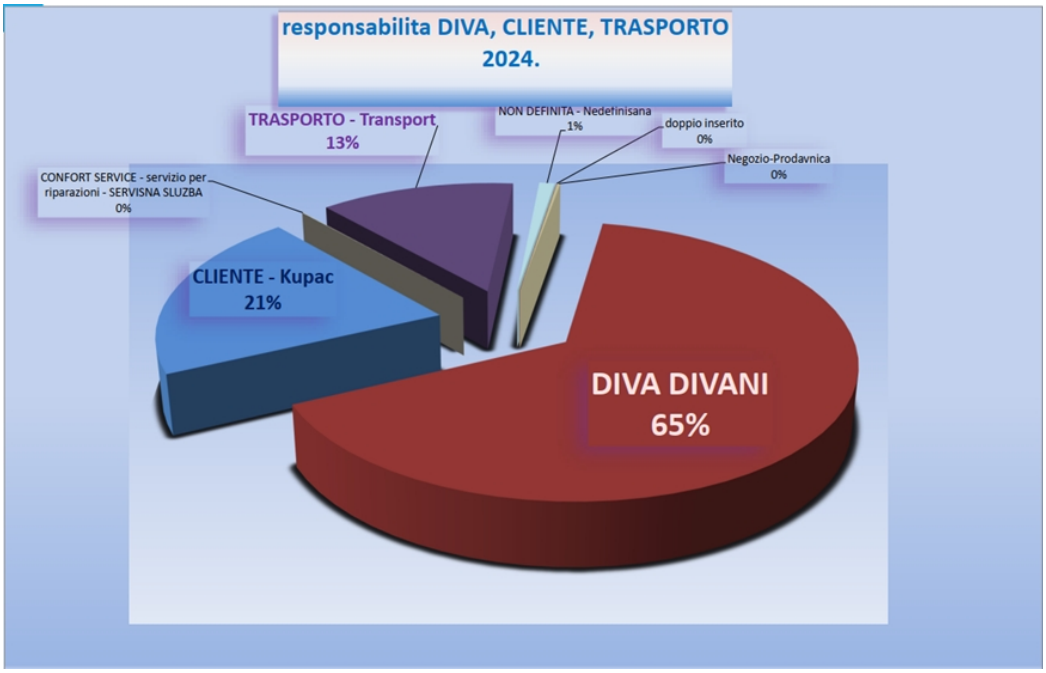

Figure 9. *Graphical representation of total complaints in percentages.*

5. CONCLUSIONS

Once the proposals have been reviewed and approved, a report needs to be prepared and distributed to all stakeholders in the factory, including management, production and quality control teams. This report clearly outlines all the findings of the analysis, the proposed improvement measures and the implementation deadlines.

An annual analysis of recorded operator errors not only helps to resolve problems from the previous year, but also plays a key role in preventing future errors. Correcting the identified errors leads to improved processes and the quality of finished products, as well as higher factory

productivity. Investing in continuous improvement of work processes, operator training and equipment maintenance is the key to the success of any factory that wants to achieve high quality standards.

Quality control is one of the key elements in the production management system in a furniture factory. Its role is to ensure that each product meets defined technical, aesthetic and functional requirements, as well as the expectations of end users. By establishing systematic quality control — from incoming raw material control, through process control in all stages of production, to final control of finished products — it is possible to detect and eliminate defects at an early stage, which significantly reduces the costs of repairs and complaints.

By applying standardized procedures and using adequate measuring tools and methods, uniformity of production and reliability of delivery are achieved. The quality of finished furniture directly affects the image of the company, the level of customer satisfaction and its competitiveness in the market. Therefore, continuous improvement of the quality control system is a prerequisite for sustainable growth and development of the production system.

In conclusion, quality control in furniture production is not just an operational function, but a strategic component of the business that ensures product compliance with technical specifications, safety standards, and customer expectations.

REFERENCES

1. Stanojevic, D. (2008): Quality Management, script, VSPSS, Vranje.
2. Cvijanović J., Klarin M. (1998): Enterprise Organizational Structure and JUS ISO 9000, II International Symposium "Industrial Engineering '98" - SIE'98, Belgrade, pp. 123-127.,
3. Dimitric M., Popovic B., Bukvic N. (1996): Designing Process Control in a Quality System, I International Symposium "Industrial Engineering '96" - SIE'96, Belgrade, pp. 220-223.,
4. Funabaski G. (2012): Production Management and Quality Control, VSPSS, Zajecar,
5. Technical Documentation of the Factory "DIVA DIVANI"

EFFECT OF HOT WATER EXTRACTION ON THE SOLUBILITY OF MILLED AND SOLID OAK WOOD (*QUERCUS ROBUR* L.)

Dario Pervan[1,*], Miljenko Klarić[1], Josip Istvanić[1], Alan Antonović[1]

[1]*University of Zagreb Faculty of Forestry and Wood Technology, Zagreb, Republic of Croatia,*
*e-mail: mklaric@sumfak.unizg.hr; jistvanic@sumfak.unizg.hr; aantonovic@sumfak.unizg.hr; *dpervan@sumfak.unizg.hr*
[*]*Corresponding author*

ABSTRACT

This study investigates the solubility of milled and solid oak wood (*Quercus robur* L.) samples using Method B (hot water extraction) as described in the ASTM D1110-21 standard. Serving as a continuation of previous research employing cold water extraction (Method A), the current work provides a comparative view of how elevated temperatures influence the release of water-soluble extractives, including tannins, gums, sugars, coloring matter and starches found in the wood. Although present in minor quantities, these extractives can significantly impact wood properties during hydrothermal processing, particularly in terms of discoloration and surface chemistry. The study focuses on oak wood (*Quercus robur* L.) due to its high technical and economic value in Croatia.

Keywords: penduculate oak (*Quercus robur* L.), hot water solubility, milled, solid, extraction, wood**.**

1. INTRODUCTION

Although they represent a relatively small proportion of the wood's chemical composition, extractives significantly influence its properties, including natural durability, color changes during hydrothermal treatment, and aroma. The chemical structure of wood is complex and varies considerably among different species. On average, wood contains 46–56 % cellulose, 23–35 % hemicellulose, and 15–35 % lignin. Extractives, non-structural components soluble in neutral solvents, typically constitute 4–10 % of the dry mass of wood from temperate species, but may account for up to 20 % in tropical species. These compounds include a wide range of organic substances such as fats, waxes, alkaloids, proteins, simple and complex phenolics, sugars, pectins, mucilages, gums, resins, terpenes, starches, glycosides, saponins, and essential oils. Many serve as metabolic intermediates, energy reserves, or defense agents against microbial attack. Extractives contribute to various wood characteristics, including color, odor, and resistance to decay (Pettersen, 1984).

Studies on the solubility of wood in organic solvents demonstrate that due to its heterogeneous chemical composition, different solvents are needed to extract specific molecular components. Most extractives can be removed using solvents such as water, benzene, toluene, or acetone. However, no single solvent is capable of extracting all components completely. The most effective extraction results of wood have been achieved using solvent mixtures, including acetone–water (9:1), ethanol–toluene (1:2), acetone–hexane, and ethanol–benzene (1:2) (Horvat, 2005). Water is particularly effective for extracting polar, low-molecular-weight compounds such as tannins, sugars, and certain phenolics. Hot water extraction (HWE) improves the solubility and diffusion of these substances from the wood matrix of some wood species. For instance, Dababi *et al*. (2020) successfully extracted tannins from Aleppo pine bark and sumac root using water medium, confirming its potential for isolating bioactive compounds for applications such as environmentally friendly adhesives

The efficiency of water extraction depends on parameters such as temperature, extraction time, and wood species. Higher temperatures typically increase the yield of extractives, although they can also lead to degradation of heat-sensitive compounds. For example, Fang *et al*. (2013) reported that hot water extraction at 100 °C yielded 20 mg/g of extractives from spruce wood, while increasing the temperature to 140 °C raised the yield to 43 mg/g. Water extraction is considered an environmentally sustainable method, as it eliminates the need for organic solvents, making it particularly suitable for

applications in food, pharmaceuticals, and bio-based materials. However, it is less effective for non-polar compounds such as fats, waxes, and resins, which require non-aqueous solvents, typically organic or certain inorganic solvents, for efficient extraction.

Water was selected as the solvent for this research because wood is frequently exposed to water during industrial processing, particularly during hydrothermal treatment. Additionally, water soluble extractives play a crucial role in the winemaking industry. For example, barrels made from pedunculate oak are prized for their extractives, which dissolve into wine and contribute to its distinctive aroma, flavor, and color.

2. AIM OF RESEARCH

The primary objective of this research was to investigate, through laboratory experimentation and subsequent analysis, the influence of drying and initial moisture content of pedunculate oak (*Quercus robur* L.), in both milled and solid form, on its solubility in hot water. Specifically, the study aimed to quantify the amount of extractive material obtained through hot water extraction (Method B), following the standard procedure outlined in ASTM D1110-21. The experiment was conducted at the Faculty of Forestry and Wood Technology, University of Zagreb. The study aims to determine how particle size and initial moisture content influence the efficiency of hot water extraction of wood extractives from milled and solid oak samples.

3. OBJECTS AND METHODS OF RESEARCH

3.1. Materials

Milled and solid samples of pedunculate oak (*Quercus robur* L.) were used to evaluate water solubility. The extraction was conducted using demineralized water (ASTM Type II), following the hot water extraction procedure (Method B) described in ASTM D1110-21 Standard Test Methods for Water Solubility of Wood. This standardized approach ensures consistency in determining the content of water-soluble constituents. Wood samples were sourced from oak lamellae with dimensions of 1000 × 130 × 7 mm, cut using an Einhell TC-SB 200/1 band saw. For the preparation of material intended for milling, each element was trimmed by 3 cm from both longitudinal edges and 7 cm from the end grain. The remaining central lamella (Figure 1) was further divided into samples weighing approximately 4 g and measuring 31 × 18 mm.

Figure 1. *Central lamella from which samples were made.*

Coarse milling was performed using a Retsch SM400 cutting mill with a 4 mm mesh screen, followed by fine milling with a Retsch SR300 rotor mill using 1 mm and 0.5 mm mesh screens (Figures 2 and 3).

Figure 2. *Retsch SM400 mill.*

Figure 3. *Retsch SR300 mill.*

The resulting material was sieved through laboratory-grade sieves with mesh openings of 425 µm and 250 µm. Only the fraction retained on the 250 µm sieve was used (Figure 4) for further analysis, while coarser and finer particles were excluded. For solid wood testing, elements were similarly trimmed by 3 cm on each lateral side and 7 cm from the end. Additionally, the central lamella was longitudinally reduced by 3 cm. Narrow slats were then cut from the remaining wood and used to prepare intact test specimens (Figures 5) as well as gravimetric samples.

Figure 4. *Milled material used.*

Figure 5. *Example of solid sample used.*

Solid wood specimens were cut to approximate dimensions of 20 × 15 mm to achieve a target mass of approximately 2 g. All samples, milled and solid, were air-dried prior to extraction to standardize moisture content.

3.2 Methods

The initial moisture content of the samples was determined by the gravimetric method using a Sartorius CPA225D analytical scale with a precision of 0.01 mg and a Memmert UF110 Plus laboratory drying oven. For solid wood samples, moisture content was determined using previously prepared samples, which were further cut into smaller specimens. For milled wood, the moisture content was assessed using excess material not required for other experimental procedures. Approximately 1 g of each sample was weighed into pre-dried containers and placed in the oven at 103 ± 2 °C until a constant mass was achieved. After drying, samples were transferred to a desiccator to cool to room temperature, after which they were reweighed. The moisture content of the wood was calculated using the following equation (1):

$$\omega = \frac{(W_1 - W_0)}{W_0} \times 100 \quad (1)$$

ω –moisture content (%)
W_1 – mass of the sample with moisture content (g)
W_0 – mass of the sample in an absolutely dry state (g)

The extraction process involved four sets of samples, each consisting of 6 replicates:

1. Milled samples with a defined moisture content
2. Solid samples with a defined moisture content
3. Milled samples in an absolutely dry state
4. Solid samples in an absolutely dry state

For the determination of hot water solubility, approximately 2 grams of each sample were weighed into a round-bottom flask (Figure 6). Subsequently, 100 mL of distilled water was added to the flask. The flask was then placed in a laboratory water bath equipped with a Liebig condenser (Figure 7). It was positioned such that the contents of the flask remained submerged below the water level in the bath. Extraction was conducted for a duration of 3 hours. After completion, the contents of the flask were filtered using the vacuum filtration system (Figure 8).

Figure 6. *Extraction aparatus.*

Figure 7. *Solid wood samples during extraction.*

Figure 8. *Filtrtation process.*

The residue retained in the crucible was then dried at a temperature of 103 ± 2 °C using a Memmert UF 110 plus drying oven. The drying process lasted 4 hours. Upon drying, the samples were placed in a desiccator to condition at room temperature. Finally, the samples were weighed to determine the mass of the insoluble fraction.

4. RESULTS AND DISCUSSION

Results of descriptive statistics of solubility in hot water are shown in Table 1.

***Table 1**. Descriptive statistics of solubility in hot water [%].*

	Number of observations	Minimum	Maximum	Mean	Std. deviation
Milled samples (MC = 9.8 %)	6	6.49	10.28	7.5367	1.38228
Absolutely dry milled wood samples	6	6.78	8.20	7.5200	0.48683
Solid samples (MC = 11.34 %)	6	14.85	19.17	16.7850	1.57604
Absolutely dry solid samples	6	1.90	2.85	2.3467	0.31935

The descriptive statistical analysis provides insights into how different physical states and moisture levels of wood samples influence their solubility in hot water. Four distinct sample conditions were analyzed: milled samples with 9,8 % moisture content, absolutely dry milled samples, solid samples with 11,34 % moisture content and absolutely dry solid samples.

Among the tested groups, the solid samples with moisture content exhibited the highest mean solubility. This suggests that moisture plays a critical role in facilitating the release of water soluble compounds, particularly in whole wood structures. The presence of moisture likely enhances the swelling of cell walls and increases the mobility of extractives, thus promoting higher solubility during the extraction process. However, this group also demonstrated the greatest variability among replicates, implying that the interaction between natural moisture and intact wood structure may introduce inconsistencies in solubility behavior, possibly due to heterogeneous distribution of extractives or differences in wood density. On the opposite end of the spectrum, absolutely dry solid samples showed the lowest mean solubility and the most consistent results among all sample groups.

The lack of moisture in these samples reduces the swelling capacity of the wood matrix and limits the diffusion of extractable components into the surrounding solvent. The low variability within this group suggests a stable and predictable interaction between the dry solid structure and hot water, likely due to minimal structural changes during the extraction process. Milled samples, both with moisture content and in an absolutely dry state, exhibited intermediate levels of solubility. Interestingly, despite the reduction in particle size, which typically increases surface area and enhances extractability, the differences in solubility between moist and dry milled samples were marginal. This finding implies that while milling facilitates solvent access, moisture still plays a more dominant role in enhancing solubility. However, the milled samples with moisture content displayed greater variability compared to their dry counterparts, indicating that moisture content introduces additional factors affecting extractability, even in finely divided samples. Distribution of results per given sample is presented in Figure 9,10,11 and 12.

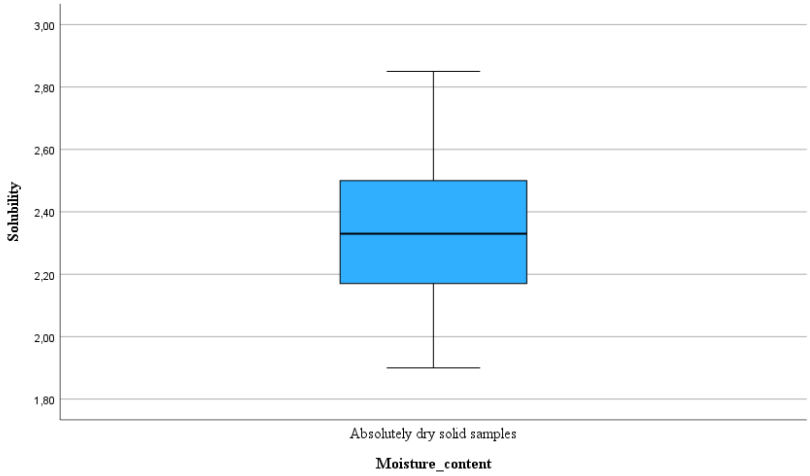

***Figure 9**. Solubility of absolutely dry solid samples [%].*

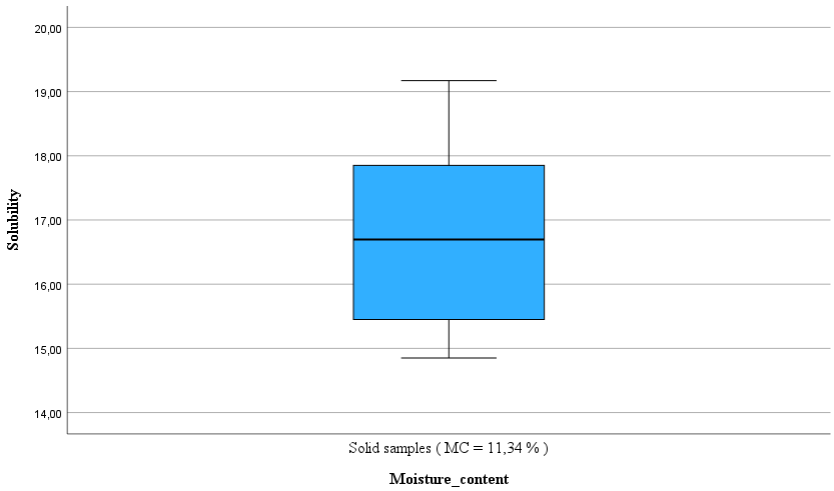

Figure 10. *Solubility of solid samples with moisture content [%].*

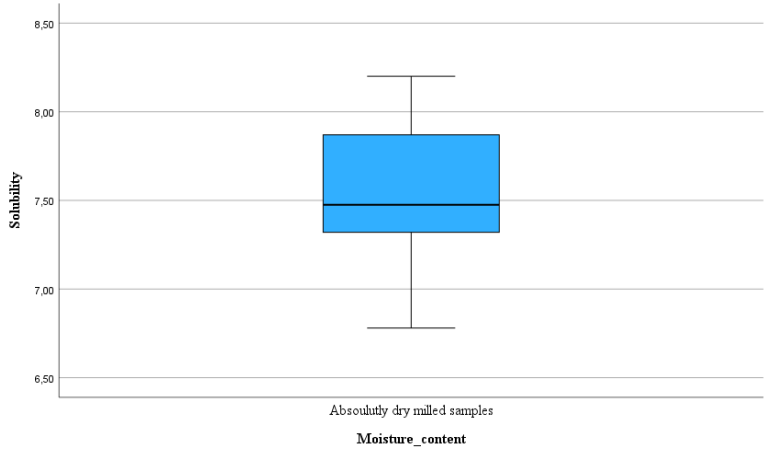

Figure 11. *Solubility of absolutely dry milled samples [%].*

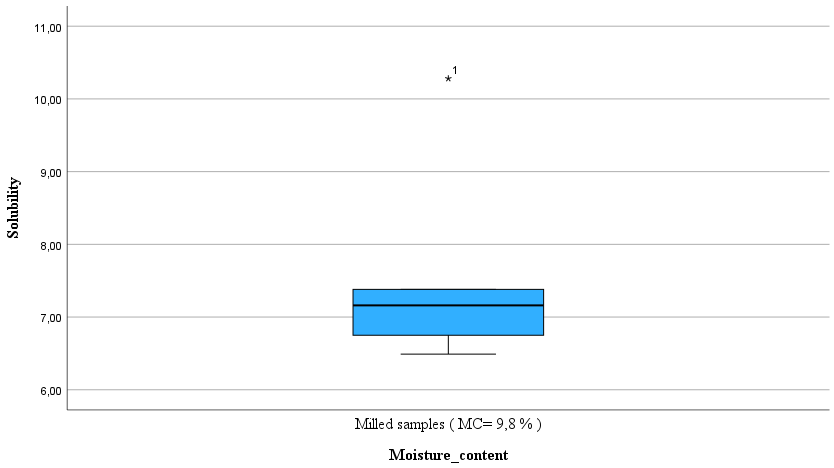

Figure 12. *Solubility of milled samples with moisture content [%].*

Taken together, these results clearly illustrate that both the physical form of the sample and its moisture content significantly influence solubility outcomes. Moisture appears to have a greater overall impact than particle size reduction.

Kruskal-Wallis test was performed to see if there were significant statistical differences between 4 groups of samples. Kruskal-Wallis test showed there were statistical differences ($p < 0,05$) so post

hoc pairwise comparisons of solubility in hot water were performed using the Mann–Whitney U Pairwise Comparisons (this test was chosen because of non-normal distribution of the data and small sample size), with Bonferroni correction applied to account for multiple comparisons. (Table 2).

Table 2. *Mann–Whitney U Pairwise Comparisons between samples*.

Sample Comparison	Test Statistic	Standard Error	Sig. (2-tailed)	Adjusted Sig. (Bonferroni)
Absolutely dry vs. absolutely dry milled samples	10.333	4.082	0.011	0.068
Absolutely dry solid vs. solid samples (MC = 11.34%)	18.000	4.082	<0.001	0.001
Milled samples (MC = 9.8%) vs. absolutely dry milled samples	-2.667	4.082	0.514	1.000
Milled samples (MC = 9.8%) vs. solid samples (MC = 11.34%)	-10.333	4.082	0.011	0.068

Among the six tested sample pairs, a statistically significant difference was observed only between the absolutely dry solid samples and the solid samples with a moisture content of 11.34 % (adjusted $p = 0.001$). This significant increase in solubility suggests that higher moisture content prior to testing or the condition (milled or solid) of the sample during processing, may enhance the leaching of water soluble extractives or thermal degradation products when subjected to hot water.

The result indicates that even moderate increases in pre-conditioning moisture can substantially influence the extractive behavior of wood-based materials under thermal exposure. All other pairwise comparisons, including those between milled and solid samples or between absolutely dry and samples with moisture content, did not yield statistically significant differences following Bonferroni adjustment ($p > 0.05$), although some unadjusted values suggested trends toward significance (*e.g.*, $p = 0.011$). These findings imply that factors such as mechanical processing (milling) or relatively small variations in moisture content (e.g., 9.8 % vs. 11.34 %) do not independently exert a strong enough influence on hot water solubility to be considered statistically meaningful. Overall, the results underscore the pronounced effect of the initial physical and moisture state of wood samples on hot water solubility, a parameter intimately linked to the presence of low-molecular-weight extractives, hemicellulose breakdown products, and residual chemicals from prior processing. In particular, the marked difference in solubility between fully dry and moisture-conditioned solid samples highlights the role of moisture in modulating both structural and chemical behaviors of lignocellulosic materials.

These insights are especially relevant for optimizing hydrothermal processing of wood, where moisture content and its interaction with thermal conditions affect the efficiency of steaming or drying treatments, ultimately influencing wood quality, dimensional stability, and color change.

In comparison to the study conducted by Klarić et al. (2023), which measured the solubility of similar samples in cold water, the solubility of the samples in hot water was on average lower. This difference was more pronounced for milled samples than for solid samples, which exhibited similar average solubility values in cold water. Statistically significant differences in solubility were observed between milled and solid samples, both in the presence of moisture content and in absolutely dry conditions. Additionally, significant differences were found between solid wood samples with moisture content and those that were completely dry. However, when considering solubility in hot water specifically, a significant difference was observed only between absolutely dry solid samples and solid samples with moisture content.

5. CONCLUSION

- Moisture content of wood affects its solubility in hot water
- Samples of solid wood with higher moisture content had higher average solubility than absolutely dry solid wood samples
- In case of milled wood samples, averages of solubility were similar between samples with moisture content and absolutely dry samples

- In case of samples that were absolutely dry, milled samples had higher average solubility than solid samples
- Comparing it with cold water solubility, hot water solubility is in average lower than cold water solubility

REFERENCES

1. Dababi, I., Gimello, O., Elaloui, E., Brosse, N. (2020): Water extraction of tannins from Aleppo pine bark and sumac root for the production of green wood adhesives. Molecules, 25(21), 5041.
2. Fang, W., Yang, W., Ekeberg, D., Jönsson, L. J., Lundqvist, S.-O. (2013): Evaluation of selective extraction methods for recovery of polyphenols from pine. Holzforschung, 67(8), 843–851.
3. Klarić, M., Matišev, B., Španić, N., Barlović, N. (2023): The influence of drying and initial moisture content of milled and solid oak wood (Quercus robur L.) samples on its solubility in cold water. In: 32nd International Conference on Wood Science and Technology – ICWST 2023 "Unleashing the Potential of Wood-Based Materials", 113–120. University of Zagreb Faculty of forestry and wood technology.
4. Pettersen, R. C. (1984): The chemical composition of wood. The Chemistry of Solid Wood, 207, 57–126.
5. **** ASTM D1110-21 : Standard Test Methods for Water Solubility of Wood

The Authors´ Addresses:

* Postgraduate student – project assistant Dario Pervan, mag. ing. techn. lign.; Assistant professor Miljenko Klarić, Ph.D.; Assistant professor Josip Ištvanić, Ph.D.; Associate professor Alan Antonović, Ph.D.
Wood Technology Department, Faculty of Forestry, University of Zagreb, Svetošimunska 23 10000 Zagreb, Republic of Croatia
e-mail: dpervan@sumfak.unizg.hr; mklaric@sumfak.unizg.hr; jistvanic@sumfak.unizg.hr; aantonovic@sumfak.unizg.hr;
*Corresponding author

CHANGE IN pH OF BEECH SAPWOOD AND FALSE HEARTWOOD DURING THE HOMOGENIZATION OF WOOD COLOR BY STEAMING

Michal Dudiak[1], Ladislav Dzurenda[1]

[1]Technical University in Zvolen, Slovakia
Faculty of Wood Sciences and Technology
e-mail: xdudiak@tuzvo.sk; dzurenda@tuzvo.sk

ABSTRACT

The paper presents the results of experimental monitoring of changes in acidity (pH) of beech sapwood and false heartwood during the steaming process using saturated steam at a temperature of 105°C for 18 hours. The aim of the treatment was to eliminate color differences between individual zones of the wood. The results show that due to the partial hydrolysis of hemicelluloses and amorphous cellulose, the pH decreases: in the sapwood from pH = 5.4 to pH = 4.7 and in the heartwood from pH = 5.1 to pH = 4.5. The changes in acidity are not uniform - approximately 70% of the total decrease occurs within the first 6 hours of the process. The research also confirmed that the enzymatic processes associated with the formation of the false heartwood, specifically the activity of peroxidase and polyphenol oxidase, do not affect the course of hydrolysis during steaming. This knowledge can contribute to the optimization of beech wood steaming technologies in order to unify the color of the material.

Keywords: beech wood; sapwood; false heartwood; steaming; moisture content; wood color; total color difference; wood acidity.

1. INTRODUCTION

False heartwood is a growth defect of the European beech tree, which is formed during the growth of the tree in the mature wood zone. Among other things, false heartwood differs in color from the white-gray or pale brown color of beech wood by a range of shades of red-brown. The representation of false heartwood in sawmill-processed wood mass is up to 35%. The color difference of false heartwood from sapwood and mature wood is the reason for the exclusion of sawmill assortments from the production of bent furniture, sports equipment and partly construction and joinery products.
One of the alternatives for eliminating color differences between sapwood and false heartwood while maintaining the original structural and mechanical properties of beech wood is its heat treatment by steaming. At the Faculty of Wood Sciences and Technology, Technical University in Zvolen, the project APVV 21 0051 "*Research on the false heartwood and sapwood of the wood species Beech (Fagus sylvatica L.) for the purpose of eliminating color differences by the process of thermal treatment with saturated steam*"

From a chemical point of view, the false heartwood of beech does not fundamentally differ from sapwood in the proportion of cellulose, lignin and hemicelluloses, but more in the proportion of secondary components, such as tannins, organic acids, pectin, etc. *Nečesaný (1956), Albert et al., (2003), Vek et al., (2015), Gülsoy et al., (2021), Dudiak (2023), Dzurenda et al., (2023)*. There is also a certain difference in the acidity of the wood, while the pH of beech sapwood is pH = 5.13 - 5.59, the acidity of beech heartwood according to the authors: *Gäumann (1949), Nečesaný (1956), Dzurenda et al., (2023)* is pH = 5.06 - 5.32.

The process of steaming wet wood with a moisture content of w ≥ 40% is carried out by extraction of water-soluble substances and partial hydrolysis of hemicelluloses and amorphous cellulose *Fengel and Weneger (1989), Tolvaj and Faix (1996), Kačík (2001), Samešová et al., (2018).* Hydrolysis processes initiate polysaccharide degradation in the form of oxidation of carbohydrates and pectin, dehydration of pentose to 2-furaldehyde, and free radicals and phenolic hydroxyl groups begin to form in lignin, which result in the formation of new chromophoric groups causing a change in the

color of wood *Fengel and Weneger (1989 Hon (2001), Sundqvist et al., (2006), Výbohová et al., (2018).*

The aim of the work is to present the knowledge acquired within the framework of the project APVV 21 0051 on the influence of initial pH differences in beech sapwood and false heartwood on hydrolysis processes and the course of pH changes in beech wood in the steaming process when removing color differences in sapwood and false heartwood.

2. MATERIALS AND WORK METHODS

Based on experimental research aimed at analyzing the influence of temperature and duration of steaming on the unification of the color of beech sapwood and false heartwood presented in the work of Dzurenda and Dudiak (2024), three steaming modes were proposed for unifying the color of sapwood and false heartwood with different degrees of darkening of steamed beech wood.

Figure 1. *Wood color of unsteamed beech wood with false heartwood (native) and steamed.*

With steaming mode at a steaming temperature of t ≈ 105 °C, beech sapwood and false heartwood acquire a pale brown color within τ = 18 hours. The values of the color coordinates of beech sapwood and false heartwood before steaming and the values of the coordinates of steamed color-homogenized beech wood with mode are shown in Table 1.

Table 1. *Values in the CIE L*a*b* color space coordinates of beech sapwood and false heartwood before and after steaming.*

Beech wood		Values in color space coordinates CIE L*a*b*		
		L*	a*	b*
Unsteamed	Sapwood	78.5 ± 2.5	9.2 ± 1.6	19.5 ± 1.8
	False heartwood	63.8 ± 3.6	11.5 ± 1.8	19.9 ± 1.6
Steamed		63.4 ± 2.3	13.0 ± 1.4	19.1 ± 1.6

In a targeted experiment of unifying the white-gray color of sapwood and the red-brown color of false heartwood by steaming with saturated steam at a temperature of t = 105 ± 2.5 °C for 18 hours, the change in acidity of beech sapwood and false heartwood was monitored. Steaming was carried out in a pressure autoclave APDZ 240 in Sundermann s.r.o. Banská Štiavnica. During the wood steaming process, six sets of beech blanks with blanks made from the beech sapwood zone and false heartwood were placed in the pressure autoclave. Each set contained 15 blanks with dimensions of 32 x 50 x 800 mm from sapwood and 15 blanks with dimensions of 32 x 50 x 800 mm from false heartwood. The conditions for steaming beech wood in a saturated water steam environment, including the time intervals for collecting individual sets of steamed blanks, are shown in the diagram in Fig. 2 and Table 2.

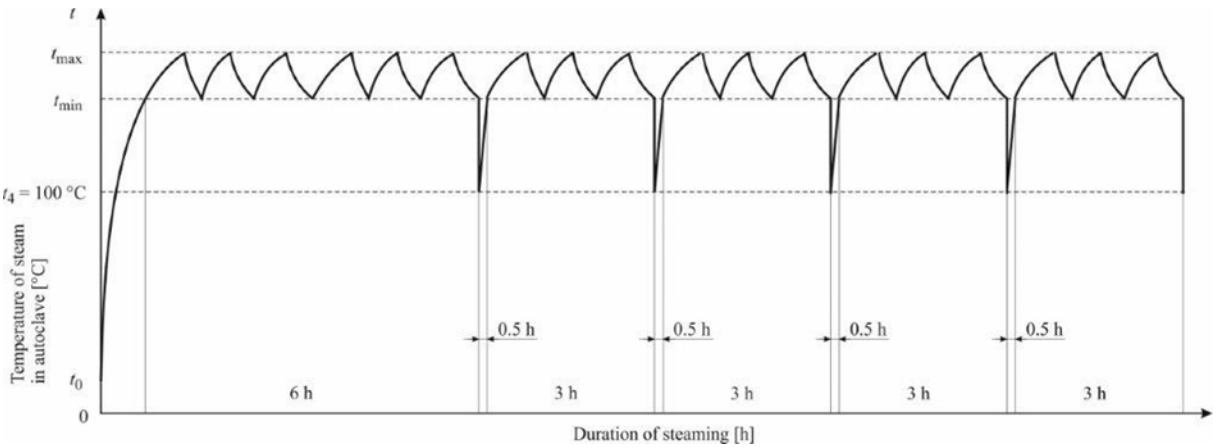

Figure 2. *Diagram of beech wood steaming in the process of removing color differences between the color of sapwood and false heartwood with marked intervals for sampling beech wood for determining the pH of the wood.*

Table 2. *Technological conditions for steaming beech wood.*

Temperature of saturated water steam			Length of time wood is exposed to colour modification				
t_{min}	t_{max}	t_4					
102	108	100	τ_1 = 6 h	τ_2 = 9,5* h	τ_3 = 13* h	τ_4 = 16,5* h	τ_5 = 20* h

*Note: * After 6 hours and subsequent 3 hours steaming intervals, there was a break of 0.5 hours during which, in the case of steaming with saturated water steam, the saturated steam pressure in the autoclave was reduced for safe opening of the autoclave, the planned group of steamed beech wood was selected from the autoclave, and after closing and pressurizing the autoclave with saturated water steam, the steaming process continued for the purpose of modifying the color of the wood.*

For direct measurement of the pH of wet unsteamed and steamed wood with saturated water steam, *Geffert et al., (2019)* proposed an original method for measuring the pH of an aqueous solution in the lumens of wet wood cells with $W > W_{BNV}$, using a SENTRON pH meter of the SI 600 series with a LanceFET+H 22704-010 insertion probe, Fig. 3.

Figure 3. *SENTRON pH meter SI 600 series with LanceFET+H probe 22704-010.*

Since the pH measuring probe has a diameter of d = 10 mm and cannot be immersed (pressed) into a solid material, according to the proposed methodology for measuring the pH of wood, a hole with a diameter of 12 mm was created at the measurement location with a cordless drill, the chips created by drilling were poured into the drilled hole and the LanceFET+H 22704-010 probe of the SENTRON SI 600 pH meter was inserted into the wet chips in the drilled hole. After a while of stabilization ($\tau \approx 30 – 60$ s.), the pH value of the measured wood was read. The actual measurement of the pH of wood is shown in Fig. 4.

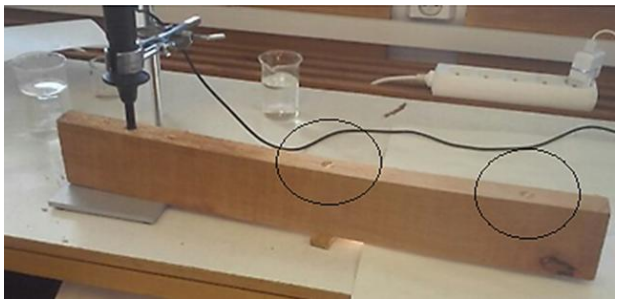

Figure 4. *View of direct measurement in the pH of steamed beech wood.*

3. RESULTS

The measured pH values of wet beech sapwood and false heartwood before steaming, as well as during the steaming process at 6 h, 9 h, 12 h, 15 h and 18 h of the technological steaming process are shown in Fig. 5.

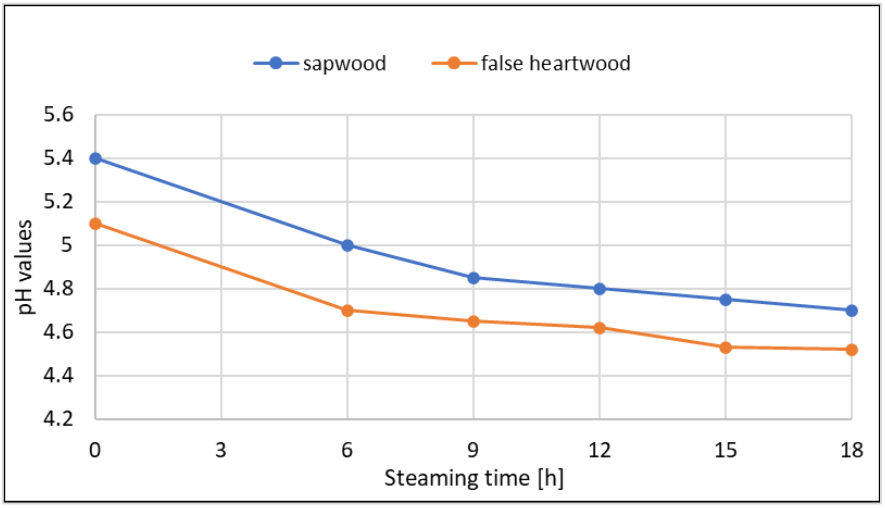

Figure 5*. Changes in acidity of beech sapwood and false heartwood during 18 h of steaming at a steaming temperature of t = 105 °C.*

Table 3 shows the average values and standard deviations of the acidity of the analyzed samples of beech sapwood and false heartwood before steaming and after 18 h of steaming. Changes in the acidity of beech sapwood and false heartwood caused by the steaming process are determined in the form of the difference in ΔpH values of unsteamed beech wood and steamed beech wood at a given temperature after 18 h of steaming:

$$\Delta pH = pH_0 - pH_{18} \quad (1)$$

Where: pH_0 – acidity of beech wood before steaming;
pH_{18} – acidity of beech wood after 18 h of steaming.

Table 3. *Acidity of beech wood before steaming and after 18 hours of steaming.*

Beech wood	Unsteamed	Steamed t = 105 °C, τ =18 h	
	pH [-]	*pH* [-]	Δ *pH* [-]
Sapwood	5.4 ± 0.1	4.7 ± 0.2	0.7
False heartwood	5.1 ± 0.2	4.5 ± 0.2	0.6

The changes in the acidity of beech sapwood and the acidity of the false heartwood caused by the steaming process for a duration of τ = 18 hours are practically the same. The lower acidity value of unsteamed beech false heartwood compared to beech sapwood by ΔpH = 0.3% on the course of wood hydrolysis was not demonstrated.

The analysis of the course of pH changes in the steaming process in Fig. 5 shows the unevenness of changes in wood acidity during 18 hours of steaming. The approximately 60% decrease in wood acidity during the first 6 hours of the steaming process is more pronounced than in the last 12 hours of steaming. This is also numerically proven by the average hourly decrease in ΔpH, while the decrease in acidity of beech sapwood and false heartwood in the first 6 hours is $\Delta pH = 0.066\ pH.h^{-1}$, so the average hourly decrease in acidity in the last 12 hours is $\Delta pH = 0.025\ pH.\ h^{-1}$ which is 2.7 times less. The above statement is in accordance with the work of *Dzurenda et al., (2020)* analyzing the pH change in the process of steaming maple wood and the work of *Dzurenda and Dudiak (2021)* analyzing the pH change in the process of steaming birch wood.

Based on the presented facts, it can also be stated that the chemical changes in beech false heartwood created by the enzymatic processes of peroxidase and polyphenol oxidase, which are responsible for the oxidation of phenolic compounds and the characteristic coloration of false heartwood *Hofmann et al., (2004), Albert et al., (2003), Tolvaj et al., (2009)* during tree growth and the formation of heartwood do not affect the hydrolysis process.

4. CONCLUSION

The paper presents the results of experimental work monitoring the change in acidity of beech sapwood and false heartwood in the process of steaming wood with saturated steam in order to remove color differences at t = 105 °C for τ = 18 hours.

Wet beech wood under the above thermal treatment conditions, due to the partial hydrolysis of hemicelluloses and amorphous cellulose, changes the pH of sapwood from pH = 5.4 to pH = 4.7 and changes the pH of false heartwood from pH = 5.1 to pH = 4.5.

The course of pH changes in the steaming process indicates the uneven decrease in wood acidity during 18 hours of steaming. The approximately 70% decrease in wood acidity during the first 6 hours of the steaming process is more pronounced than in the last 18 hours of steaming.

Based on the presented facts, it can also be stated that the lower acidity of beech false heartwood created by the enzymatic processes of peroxidase and polyphenol oxidase, which are responsible for the oxidation of phenolic compounds and the characteristic coloration of false heartwood during tree growth and false heartwood formation, does not affect the hydrolysis process.

ACKNOWLEDGMENTS

This paper was prepared within the grant projects: APVV 17-0456, APVV 21-0051 and VEGA 1/0256/23 as the result of work of the authors and the considerable assistance of the agencies.

REFERENCES

1. Albert, L.; Hofmann, T.; Németh, Z.S.; Rétfalvi, T.; Koloszár, J.; Varga, S.Z.; Csepregi, I. Radial variation of total phenol content in beech (*Fagus sylvatica* L.) wood with and without red heartwood. Holz als Roh- und Werkst. 2003, 3, 227–230.
2. Dudiak, M. Density of beech (*Fagus sylvatica* L.) wood through a cross-section of the trunk. Acta Facultatis Xylologiae Zvolen. 2023, Vol. 65, no. 2, 5-11.
3. Dzurenda, L.; Geffert, A.; Geffertová, J.; Dudiak, M. Evaluation of the process thermal treatment of maple wood saturated water steam in terms of change of pH and color of wood. BioResources 2020, 15, 2550–2559.
4. Dzurenda, L.; Dudiak, M. Cross-correlation of color and acidity of wet beech wood in the process of thermal treatment with saturated steam. Wood Res. 2021, 66, 105–116.
5. Dzurenda, L.; Dudiak, M.; Kučerová, V. Differences in Some Physical and Chemical Properties of Beechwood with False Heartwood, Mature Wood and Sapwood. Forests 2023, 14, 1123.
6. Dzurenda, L., Dudiak, M. Homogenization of the Color of Beech Sapwood and False Heartwood by the Steaming Process. Forests 2024, 15, 1009. https://doi.org/10.3390/f15061009

7. Fengel, D.; Wegener, G. Wood: Chemistry, ultrastructure, reactions. Walter de Gruyter. Berlin, 1989, 613 pp.
8. Gäumann, F. Über die Pilz Widerstandsfähigkeit des roten Buchenkerdes. Schweiz. Zschr. Forstw. 1946, 97, 22-24.
9. Geffert, A.; Geffertová, J.; Dudiak, M. Direct method of measuring the pH value of wood. Forests 2019, 10(10): 852.
10. Gülsoy, S.K.; Aksoy, H.; Türkmen, H.G.; Çanakçi, G. Fiber Morphology and Chemical Composition of Heartwood and Sapwood of Red Gum, BlackWillow, and Oriental Beech. J. Bartin Fac. For. 2021, 23, 119–124.
11. Hofmann, T.; Albert, L.; Rétfalvi, T.; Bányai, É.; Visiné Rajczi, E.; Börcsök, E.; Németh, Z.S. Quantitative TLC Analysis of (+)-Catechin and (-)-Epicatecin from Fagus sylvatica L. with and without Red Heartwood. J. Planar Chromatogr. 2004, 17, 350–354.
12. Hon, N.S. D., Shiraishi, N. Wood and Cellulosic Chemistry. 2001, p. 928. ISBN 9780824700249.
13. Kačík, F. Vznik a chemické zloženie hydrolyzátov v systéme drevo-voda-teplo [Formation and chemical composition of hydrolysates in the wood-water-heat system]. Technical University in Zvolen. 2001. 75 p. ISBN 80-228-1098-3.
14. Nečesaný, V. Bukové jadro, štruktúra, pôvod a vývoj [Beech Heartwood, Structure, Origin and Development]. Publishing House of the Slovak Academy of Sciences: Bratislava, Slovakia, 1959; 256 p.
15. Samešová, D.; Dzurenda, L.; Jurkovič, P. Contamination of water by hydrolysis products and extraction from the thermal treatment of beech and maple timber during modification the color of wood. Chip and Chipless Woodworking Processes 2018, 11(1): 277–282.
16. Sundqvist, B.; Karlsson, O.; and Westremark, U. Determination of formic-acid and acid concentrations formed during hydrothermal treatment of birch wood and its relation to color, strength and hardness," Wood Science Technology, 2006, 40(7), 549-561.
17. Tolvaj, L., Faix, O., 1996: Modification of wood colour by steaming. Proceeding of ICWSF '96 Conference. 10-12 April. Sopron, Hungary. 1996. pp 10-19.
18. Tolvaj, L.; Nemeth, R.; Varga, D.; Molnar, S. Colour homogenisation of beech wood by steam treatment. Drewno 2009, 52, 5–17.
19. Vek, V.; Oven, P.; Poljanšek, I.; Ters, T. Contribution to Understanding the Occurrence of Extractives in Red Heart of Beech. Bioresources 2015, 10, 970–985.
20. Výbohová, E.; Geffert, A.; Geffertová, J. Impact of steaming on the chemical composition of maple wood. BioResources 2018, 13(3), 5862-5874.

Authors' Address:

Ing. Michal, Dudiak, PhD.
Technical university in Zvolen
T. G. Masaryka 24,
960 01 Zvolen, mail: xdudiak@tuzvo.sk

prof. Ing. Ladislav Dzurenda, PhD.
Technical university in Zvolen
T. G. Masaryka 24,
960 01 Zvolen, mail: dzurenda@tuzvo.sk

NATURAL COLOR VARIABILITY OF PINE WOOD IN THE COLOR SPACE CIE L*a*b*

Michal Dudiak[1], Adrián Banski[1]

[1]*Technical University in Zvolen, Slovakia*
Faculty of Wood Sciences and Technology
e-mail: xdudiak@tuzvo.sk; banski@tuzvo.sk

ABSTRACT

The color of pine wood represents an important aesthetic and technological parameter that influences its use in furniture making and interior applications. The aim of this study was to determine the color of pine sapwood and heartwood in the color space CIE L*a*b* at 10% moisture content and to analyze the natural color variability. Measurements on samples from the Štiavnické vrchy locality showed that the lightness (L*) of sapwood averaged 78.5 ± 2.5, while heartwood had a value of 63.8 ± 3.6. On the red color coordinate (a*), values were 9.2 ± 1.6 for sapwood and 11.5 ± 1.8 for heartwood, while the yellow color (b*) was at levels of 19.5 ± 1.8 and 19.9 ± 1.6, respectively. The total color difference ΔE* was approximately 14.9, confirming a significant color heterogeneity between sapwood and heartwood. These results are crucial for optimizing the processing and application of pine wood in design and manufacturing.

Keywords: pine wood; sapwood; heartwood; wood color; total color difference.

1. INTRODUCTION

Pine wood (genus Pinus) is among the most widely used coniferous woods in Europe and worldwide. It is known for its good technical properties, such as strength, workability, and a favorable price-performance ratio. However, the color of pine wood can vary significantly depending on the age of the tree, the part of the stem (sapwood vs. heartwood), the drying method, as well as the geographical and ecological origin. This color heterogeneity can cause problems in manufacturing processes where uniform appearance is required, such as in furniture, flooring, or panel production.

Wood color is an important aesthetic and technological property that influences its market acceptance, usability in specific applications, and the perceived value of final products. Consumers and designers often prefer materials with uniform color and minimal visual deviations. Consequently, color homogeneity becomes a key criterion when selecting wood species for interior and furniture purposes. Nevertheless, wood as a natural material exhibits significant intra- and interspecies color variability, which results from a combination of anatomical, physiological, and environmental factors. Wood color is one of the main criteria for assessing its quality, affecting how customers perceive wood products, especially in furniture, decorative products, veneers, and flooring; therefore, precise color matching of different samples is necessary (Torres *et al.* 2010). According to Abrahão (2005), color uniformity is extremely important in wood quality assessment because it determines the final appearance of the wooden product.

Color expression often involves a subjective experience dependent on the available light source, surface properties, and the individual observer’s eye. To study color changes, it is necessary to measure color objectively. Objective color measurement is performed instrumentally, corresponding to visual evaluation, using spectrophotometers or colorimeters, and is numerically defined based on a standardized colorimetric calculation developed by the International Commission on Illumination (CIE) (Barański *et al.* 2017, 2020).

During processing, wood undergoes mechanical treatment such as drying or thermal modification, both of which significantly influence changes in its natural color and chemical composition (Gonzalez de Cademartori *et al.* 2013; Gonçalez *et al.* 2014; Barcík *et al.* 2015). Significant changes in wood structure occur when temperatures exceed 180 °C, while carbonization begins at 250 °C (Kačíková and Kačík 2011).

Instrumental methods for determining colorimetric parameters and color differences comply with ISO standards. These standards include definitions of basic terms, requirements for colorimetric systems, fundamentals of colorimetric calculation, and guidelines for proper instrumental color measurement (Kazimierska 2014). Colorimetric measurement is valuable for quality control of wood and for evaluating the color of final wood products (Klement and Huráková 2015). The mechanism of wood color and its changes is a complex process influenced by various factors (Kudra *et al.* 2003; McCurdy *et al.* 2005; McDonald *et al.* 2010).

The aim of this study is to determine the color of dry pine sapwood and heartwood at moisture content w = 10% in the color space CIE L*a*b* and to analyze the natural color variability of pine wood.

2. MATERIALS AND WORK METHODS

The color measurement of pine wood without true heartwood was performed on pine wood from the Štiavnické vrchy locality (N48.40582° E18.85389°). From this locality, 30 pine logs were selected, from which center lumber with dimensions of 50×300×1000 mm was produced in a quantity of 30 pieces.

To preserve the original wood color, the lumber was dried in a climate-controlled room at a temperature of t = 20 °C and relative humidity φ = 60% to a moisture content of w = 10 ± 0.5 %. The bearing surfaces of the dry lumber were machined on a horizontal planar milling machine FS 200.

The color of pine wood in the color space CIE L*a*b* was measured using a Color Reader CR-10 colorimeter (Konica Minolta, Japan). A D65 light source was used, and the diameter of the optical measuring aperture was 8 mm. The colorimeter evaluates the color of pine wood using a three-axis system (Fig. 1), measuring the coordinates of lightness (L*) and chromaticity (a*, b*) in accordance with ISO 11664-2 (2007) and ISO 11664-4 (2008). The CIELAB color system recommended by the CIE consists of two axes with parameters a* and b*, placed at right angles to each other, which define the color shade. The third axis represents the lightness L*, perpendicular to the a* b* plane.

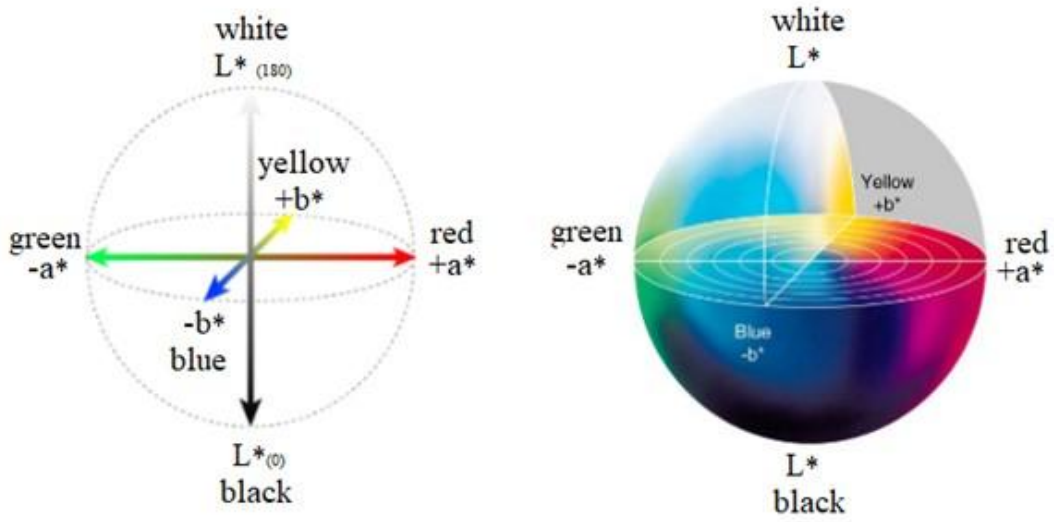

Figure 1. *Schematic of three-axis color change measurement system.*

The results of the measurements of lightness values L* and the values of the basic chromatic coordinates of red color a* and yellow color b* in the color space CIE L*a*b* are presented in the form of the mean value $\bar{x}$ and the standard deviation s_x.

$$x = \bar{x} \pm s_x\,[-] \tag{1}$$

The degree of dispersion of the measured values is assessed (evaluated) by the coefficient of variation:

$$v_x = \frac{s_x}{\bar{x}} \cdot 100 \ [\%] \quad (2)$$

Color differences in the CIE space can be straightforwardly determined by calculating their spatial distance, equal to the square root of the sum of the squares of differences for each of the three coordinates of the two compared colors, according to the relationship (in accordance with ISO 11664-4 (2008) and ISO 11664-6 (2022) standards,

$$\Delta E^* = \sqrt{(L_1 - L_2)^2 + (a_1 - a_2)^2 + (b_1 - b_2)^2} \quad [-] \quad (3)$$

where ΔE* is the parameter determining the overall color change, ΔL* is the difference of the parameter determining the color change in the white-black direction, Δa* is the difference of the parameter determining the color change in the red-green direction, Δb* is the difference of the parameter determining the color change in the yellow-blue direction.

The color of pine wood on the cross-section is shown in Fig. 1a. Figures 1b–d show the color of pine wood on the planed surface of the lumber. According to visual evaluation, the color of pine sapwood is white with a yellowish tint, and the color of the heartwood is red-yellow with a higher resin content, which gives the wood a redder color.

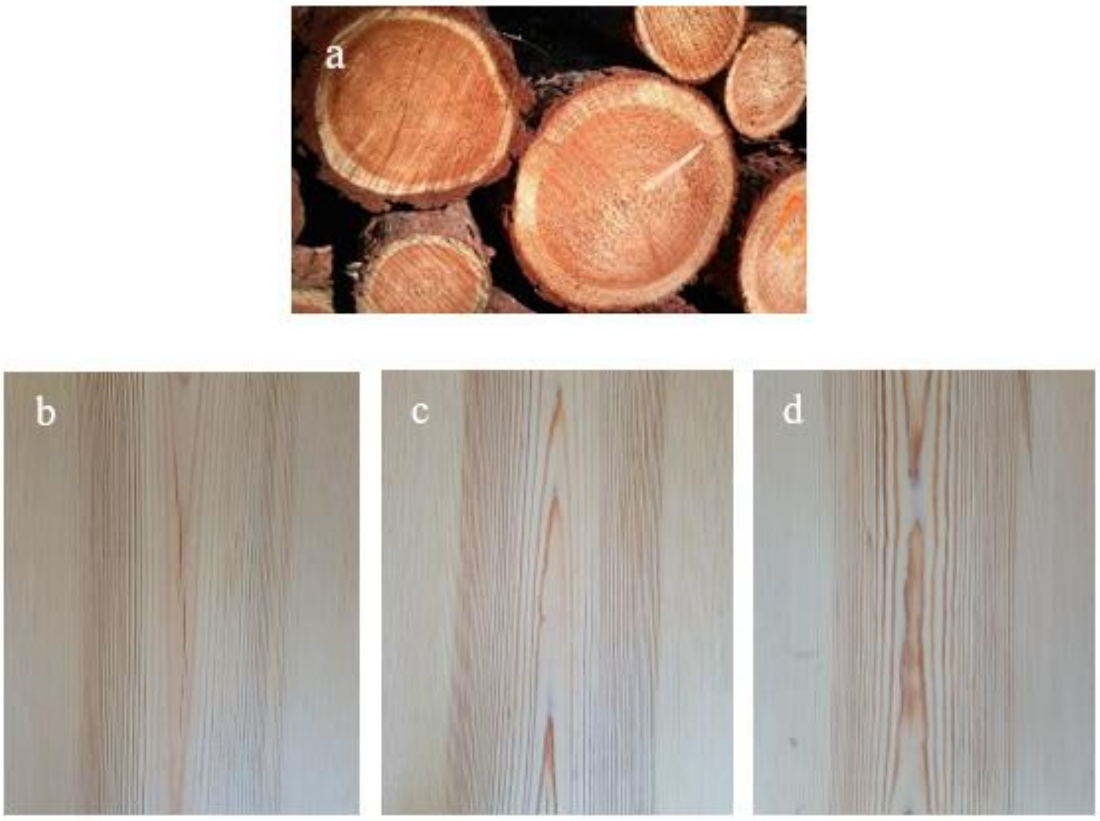

Figure 1. *Color of pine heartwood and sapwood on the cross-section of the log (a); and on the bearing surfaces of the lumber (b, c, d).*

The results of the statistical processing of the measured color values of sapwood and heartwood on the individual coordinates of the CIE Lab* color space are presented in Table 1 and Table 2.

Table 1. *Values in the CIE L*a*b* color space coordinates of pine sapwood.*

Pine sapwood	Color coordinates CIE L*a*b*		
	L*	a*	b*
Number of measurements [-]	150	150	150
Measured value	78.5 ± 2.5	9.2 ± 1.6	19.5 ± 1.8
Standard deviation s_x [-]	2.5	1.6	1.8
Coefficient of variation v_x [%]	3.2	17.4	9.2

Table 2. *Values in the CIE L*a*b* color space coordinates of pine heartwood.*

Pine heartwood	Color coordinates CIE L*a*b*		
	L*	a*	b*
Number of measurements [-]	150	150	150
Measured value	63.8 ± 3.6	11.5 ± 1.8	19.9 ± 1.6
Standard deviation s_x [-]	3.6	1.8	1.6
Coefficient of variation v_x [%]	5.7	15.7	8.0

For the visual evaluation of the results, a graphical representation was created from the measured color values of sapwood and heartwood on the individual coordinates of the CIE Lab* color space, which is shown in Fig. 2.

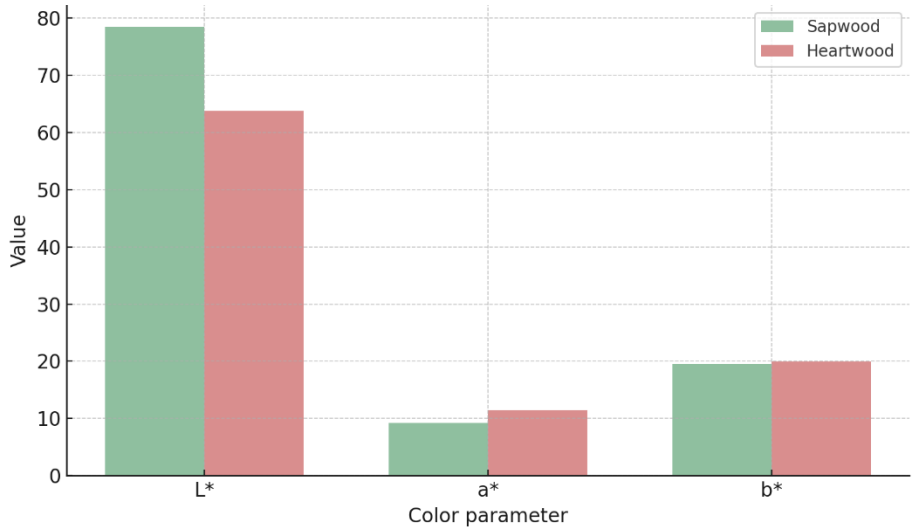

Figure 2. *Graphical representation of the measured color values of sapwood and heartwood pine wood on the coordinates of the color space CIE L*a*b*.*

Measurements showed that there are significant differences in the color parameters between pine heartwood and sapwood in the color space CIE L*a*b*. In lightness (L*), sapwood reached an average value of 78.5 ± 2.5, while heartwood had a value of 63.8 ± 3.6. The difference of 14.7 units means that sapwood appears visually much lighter, which is related to the lower content of colored extractives in the sapwood part.

On the red color coordinate (a*), sapwood had an average value of 9.2 ± 1.6, whereas heartwood reached 11.5 ± 1.8. The difference of 2.3 units shows that heartwood has a warmer, more reddish tone, which may be caused by a higher content of resins and color pigments in the heartwood. This parameter also had the highest relative variability, indicating significant deviations between individual samples.

On the yellow color coordinate (b*), sapwood was at 19.5 ± 1.8 and heartwood at 19.9 ± 1.6. The difference of 0.4 units is minimal and suggests that the yellow component of the color is very similar in both parts of the wood, playing no major role in visual differentiation.

To determine the overall visual distinction between sapwood and heartwood, the total color difference ΔE* was calculated. The resulting value of ΔE* ≈ 14.9 represents a very pronounced color difference, which is clearly recognizable by the naked eye even without direct side-by-side comparison of samples (Cividini *et al.* 2007). The high ΔE* value is mainly contributed by the difference in lightness (L*), to a lesser extent by the red tone (a*), and minimally by the yellow tone (b*).

These results confirm that the visual color heterogeneity between pine sapwood and heartwood is significant. When used in furniture making or interior cladding, these natural color differences must be considered-either avoided by selecting homogeneous material or deliberately used as a design element. It is also possible to eliminate this color heterogeneity to a single color shade by applying appropriate wood thermal modification technologies.

3. CONCLUSION

The study confirmed that the natural color variability of pine wood between sapwood and heartwood is significant and has a crucial impact on the aesthetic appearance and value of the final products. In furniture manufacturing and interior cladding, these differences must be taken into account, as they can either be eliminated by appropriate thermal modification technologies or deliberately used to create attractive designs. Precise colorimetric measurements in the CIE Lab* space represent an effective tool for quantifying and controlling color homogeneity of wood, thereby contributing to higher quality and customer satisfaction. Future research could focus on optimizing processing and surface treatments to minimize color differences or aesthetically utilize them.

ACKNOWLEDGMENTS

This paper was prepared within the grant project: VEGA 1/0423/25 as the result of work of the authors and the considerable assistance of the agencies.

REFERENCES

1. Abrahão, C. P. (2005). Estimation for Some Properties of the Wood of Eucalyptus urophylla by Spectrometry, Ph.D. Dissertation, Federal University of Viçosa, Viçosa, Brazil.
2. Barański, J., Klement, I., Vilkovská, T., and Konopka, A. (2017). “High temperature drying process of beech wood (Fagus sylvatica L.) with different zones of sapwood and red false heartwood,” BioResources 12(1), 1861-1870. DOI: 10.15376/biores.12.1.1861-1870
3. Barański, J., Konopka, A., Vilkovská, T., Klement, I., and Vilkovský, P. (2020). “Deformation and surface color changes of beech and oak wood lamellas resulting from the drying process,” BioResources 15(4), 8965-8980. DOI: 10.15376/biores.15.4.8965-8980
4. Barcík, Š., Gašparík, M., and Razumov, E. Y. (2015). “Effect of temperature on the color changes of wood during thermal modification,” *Cellulose Chemistry and Technology* 49(9-10), 789-798.
5. Cividini, R., Travan, L., and Allegretti, O. (2007). “White beech: A tricky problem in the drying process,” in: ISCHP, Québec City, Canada, pp. 135-140.
6. Gonzalez de Cademartori, P. H., Schneid, E., Gatto, D. A., Stangerlin, D. M., and Beltrame, R. (2013). “Thermal modification of *Eucalyptus grandis* wood: Variation of colorimetric parameters,” *Maderas. Ciencia y Tecnología* 15(1), 57-64. DOI: 10.4067/S0718-221X2013005000005
7. Gonçalez, J. C., Bezerra Marques, M. H., Sousa Karas, M. C., Janin, G., and Gomes Ribeiro, P. (2014). “Effect of drying process on Marupá wood color,” *Maderas. Ciencia y Tecnología* 16(3), 337-342. DOI: 10.4067/S0718-221X2014005000026
8. ISO 11664-2 (2007). “Colorimetry – Part 2: CIE standard illuminants,” International Organization for Standardization, Geneva, Switzerland.
9. ISO 11664-4 (2008). “Colorimetry – Part 4: CIE 1976 L*a*b* Colour space,” International Organization for Standardization, Geneva, Switzerland.
10. ISO 11664-6 (2022). “Colorimetry – Part 6: CIEDE2000 colour-difference formula,” International Organization for Standardization, Geneva, Switzerland.

11. Kacíková, D., and Kacík, F. (2011). *Chemical and Mechanical Changes During Thermal Treatment of Wood*, Technical University in Zvolen, Zvolen, Slovakia.
12. Kazimierska, M. (2014). "Obiektywna ocena barwy wyrobów użytkowych [Objective assessment of the color of consumer products]," Technologia i Jakość Wyrobów 59, 44-47. (In Polish)
13. Klement, I., and Huráková, T. (2015). "High temperature drying of beech wood with content of red heartwood," in: Selected Processes at the Wood Processing, Hokovce, Slovakia.
14. Kudra, V. S., Vitter, R. M., and Gaida, Y. I. (2003). "Effect of false heart on the quality of beech wood," Lesnoe Khozyaistvo 5, 23-24.
15. McCurdy, M. C., Pang, S., and Keey, R. B. (2005). "Measurement of colour development in Pinus radiata sapwood boards during drying at various schedules," Maderas. Ciencia y Technologia 7(2), 79-85. DOI: 10.4067/S0718-221X2005000200002
16. McDonald, A. G., Fernandez, M., Kreber, B., and Laytner, F. (2010). "The chemical nature of kiln brown stain in Radiata pine," Holzforschung 54, 12-22.

Authors' Address:

Ing. Michal Dudiak, PhD.
Technical university in Zvolen
T. G. Masaryka 24,
960 01 Zvolen, mail: xdudiak@tuzvo.sk

Ing. Adrián Banski, PhD.
Technical university in Zvolen
T. G. Masaryka 24,
960 01 Zvolen, mail: banski@tuzvo.sk

EFFECT OF TANNIC ACID (TA) ON INCREASING UREA-FORMALDEHYDE (UF) ADHESIVE PERFORMANCE

Ivana Gavrilović Grmuša[1] , Tamara Tešić[1], Danica Bajuk Bogdanović[2], Milica Rančić[1]

[1]University of Belgrade, Faculty of Forestry, Kneza Višeslava 1, Belgrade, Serbia
[2]University of Belgrade, Faculty of Physical Chemistry, Studentski trg 12-16, Belgrade, Serbia
e-mail: ivana.grmusa@sfb.bg.ac.rs; student.tamaratesic2262002@sfb.bg.ac.rs; danabb@ffh.bg.ac.rs; milica.rancic@sfb.bg.ac.rs

ABSTRACT

The increasing awareness of environmental issues, including fossil fuel depletion and global warming, has positioned wood and novel wood products at the forefront due to their advantageous effects on reducing greenhouse gas (GHG) emissions and carbon footprints. The potential for the wood-based panels to be utilized in innovative and challenging constructions mostly relies on adhesives which are often manufactured from oil-derived basic materials such as petroleum and natural gas. The crucial solution must encompass the transition to eco-friendly adhesives, the reduction of carbon dioxide emissions, and the adoption of more sustainable solutions. In order to create a more sustainable and conscious society, environmental regulations have also drawn attention to the use of green design principles and the production of bio-based adhesives from raw materials. Therefore, the key to satisfying the wood industry's current green expectations is creating an environmentally friendly adhesive using renewable resources. On the other side, making the adhesive bond as strong as or stronger than the wood itself is crucial for structural applications.

Tannic acid (TA), as a natural polyphenolic polymer, has shown great potential to be used as an eco-friendly bio-adhesive and alternative to petroleum-based adhesives, offering sustainability and reduced toxicity. In wood processing, tannic acid adhesives are valued for their strong bonding capabilities and natural origin, reducing dependence on synthetic resins. This study aimed to evaluate the potential of tannic acid application in conventional urea-formaldehyde (UF) wood adhesive formulations. Tannic acid-based UF (TA-UF) resins, with three different concentrations of tannic acid (1, 3, and 5% wt) were prepared, and adhesive properties were tested and compared with properties of pure UF resin. Testing of tensile shear strength showed that the addition of a higher concentration of tannic acid in UF adhesive formulation increases its adhesive and mechanical performances compared to pure UF adhesive which implies that TA-UF resins could be successfully applied as an environmentally friendly, bio-based wood adhesive.

Keywords: tannic acid, UF resin, wood adhesive, biomaterials, bio-adhesive.

1. INTRODUCTION

Urea-formaldehyde (UF) resins are among the most widely used adhesives in the wood-based panel industry due to their low cost, high reactivity, and good bonding performance. However, their primary drawback lies in the emission of free formaldehyde during and after curing, which poses significant health and environmental concerns. In response to increasingly stringent regulations on formaldehyde emissions, recent research efforts have focused on modifying UF resins using bio-based additives that can improve environmental performance without compromising adhesive quality.

One such promising additive is tannic acid, a naturally occurring polyphenolic compound found in various plant sources. Due to its abundance of phenolic hydroxyl and carboxyl groups, tannic acid can potentially react with free formaldehyde and participate in cross-linking reactions within the resin matrix, thereby reducing emissions while enhancing or maintaining mechanical strength. Evaluating the performance of bio-based adhesive systems requires a comprehensive understanding of their interaction with the wood substrate. In addition to assessing tensile shear strength and formaldehyde emission levels, it is essential to analyze the chemical structure of the modified resins (e.g., via FTIR spectroscopy) and to characterize the failure mode after mechanical testing. The type of failure

whether cohesive, adhesive, mixed, or substrate-related—provides important insights into the quality of the adhesive bond and the effectiveness of the modification.

Tannic acid (TA) is a colourless to pale yellow solid with an astringent taste [1]. Due to its wide range of special chemical properties and health benefits, it became one of the most researched substances that serves as a commercial, raw additive in coating, adhesive, health, pharmaceutical and food industry. TA is also known for its antimicrobial, anticancer, antiviral, and anti-inflammatory properties [2].

TA has a promising application as a non-toxic and inexpensive green crosslinking agent for multifunctional bio-materials, especially in industry of wood adhesives [3]. Formaldehyde-based resins are used as binders in the production of wood-based panels thanks to their low cost and high reactivity advantages [4]. Urea formaldehyde (UF) is the dominant type of adhesive in the production of wood-based panels, due to its favorable characteristics, but these resins also have certain disadvantages related, first of all, to poor water resistance and formaldehyde emission (FE) [5]. Tannic acid can be used to fabricate bioadhesives by partial or complete replacement of phenolic substances in conventional wood adhesives [6].

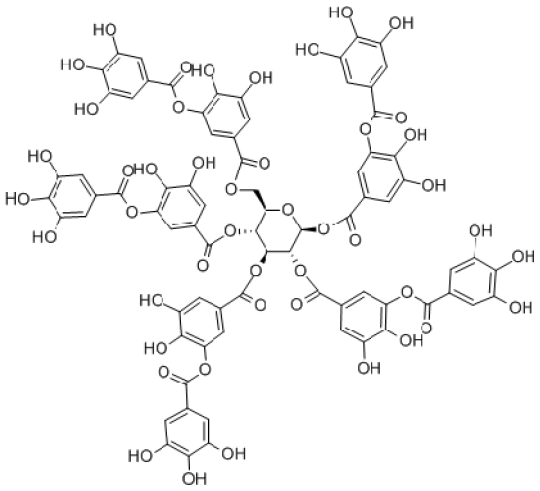

Figure 1. *Tannic acid structure.*

In this study, UF resins were modified with varying concentrations of tannic acid (1%, 3%, and 5%) to investigate its effect on the chemical structure, bonding performance, and failure behavior of adhesive joints. The goal was to assess the feasibility of tannic acid as a formaldehyde-reducing, performance-preserving additive for UF adhesives used in wood composites.Tannic acid (TA) is a natural polyphenol and the most abundant natural compound after cellulose, hemicellulose and lignin [1]. This substace is widely found in plants, including hydrolyzed and condensed tannins. Hydrolyzable tannins consist of gallic or ellagic acid and sugar molecules (e.g., glucose), while tannic acid is composed of polymerized flavonoids with different degrees of polymerization. Tannic acid is the most common hydrolyzable tannin and is composed of a glucose ring esterified with five digallic acid [2,3]. Although TA molecule carries no carboxylic acid group, it is called “acid” due to the presence of numerous phenol groups, which are responsible for its acidic character [3].

2. EXPERIMENTAL SECTION

2.1 Materials

A commercial UF resins (UF) was provided by domestic company (Serbia). Tannic acid was purchased from Sigma Aldrich Chem (Steinheim, Germany). Ammonium chloride was purchased from Centohem (Serbia). Beech (*Fagus sylvatica*) logs were selected from a known locality and growth conditions (mountain Goč, Serbia). Afterward, primary boards with the desired orientation of growth rings were cut.

2.2. Tensile shear strength determination

2.2.1. Preparation of wood samples

The sawn timber was dried in a semi-industrial conventional kiln (Nigos MC 3000, capacity 0.8 m^3). The most homogeneous groups of testing samples were selected for further experiments.

2.2.2. Preparation of UF-tannic acid adhesive

Firstly, the adhesive solid content of UF resin was determined to be used for further adhesive formulations and analyses. Every formulation was prepared in concentration calculated using solid weight relative to UF resin solid content. Ammonium chloride salt solution (concentration of 20%) was used as hardener for all samples in the concentration of 1% w/w. Tannic acid was added to UF adhesive in concentrations of 1%, 3% and 5%, respectively, by weight. One group of samples, with pure UF resin, was used as a control group.

2.2.3. Characterization of UF adhesive

Adhesive obtained in this research was performed according to the following standards: determination of pH (SRPS EN 1245:2012); determination of density (SRPS EN 542:2009); determination of conventional solids content and constant mass solids content (SRPS EN 827:2009); determination of tensile shear strength of lap joints for wood adhesives (SRPS EN 205:2017); and adhesive was classified according to standard for classification of thermosetting wood adhesives (SRPS EN 12765:2017).

The FTIR-ATR spectra were obtained with an FTIR spectrometer (iS20, Thermo Nicolet) with a resolution of 4 cm^{-1} in the wavelength region 4000–525cm^{-1}, using a diamond single reflection attenuated total reflectance (ATR). All spectra were obtained with 32 scans, and the background measurement was made using air.

2.2.4. Determination and optimization of glue-line quality

The adhesive mixes were applied by a rubber roller onto one surface of the two wood specimens to be bonded (200 g/m^2). Assembling was always performed in parallel grain directions. The ply without direct application of the adhesive mix was always in the bottom position to improve the penetration into its structure. Again, a special effort was made to have the taper as low as possible, guaranteeing equal penetration conditions for all samples. Five joint samples were pressed in a hydraulic press at 120°C and 1.5 MPa for 15 minutes. Before testing, the single lap shear test specimens (150 mm × 20 mm × 5 mm) were conditioned at 20 ± 2°C and 65 ± 5% relative humidity for one week. The lap shear test will be conducted according to SRPS EN 205 standard test on a hydraulic test machine (Wood tester WT4) with a measuring scale of 50 kN at a testing speed of 6 mm/min loading rate in tensile mode with the load direction always parallel to the grain in all tested specimens. The failure zone (shear area 20 mm × 10 mm) was examined using a light microscope to determine the proportion of wood failure and the thickness of the wood layer in the wood failure. Five replications were performed for each set of parameters. An analysis of variance (ANOVA) was applied to obtain centralized values and standard errors.

3. RESULTS AND DISCUSSION

For any bio-based wood adhesive, a comprehensive evaluation of its performance in wood composite applications is essential. Understanding the interaction between the adhesive and the wood substrate provides valuable scientific insight that informs the development of adhesives with improved mechanical strength, water resistance, thermal stability, rheological behavior, and penetration capability.

In interpreting the measured bonding strength, it is also critical to consider the failure mode observed during mechanical testing. Four principal failure modes are typically recognized in adhesive-bonded wood composites:

(a) cohesive failure within the adhesive layer,
(b) adhesive failure at the interface,
(c) mixed failure, which combines both cohesive and adhesive elements, and
(d) wood cohesive failure, where the failure occurs within the wood substrate itself.

The identification of failure type provides key information about the bond quality and the relative strength of the adhesive versus the substrate, and should be considered alongside strength data when assessing adhesive performance.UF adhesive is the most important adhesive in the wood industry, especially in the production of wood-based panels, primarily because of its relatively good characteristics and low price. However, considering that it has poor water resistance and high formaldehyde emission, it is necessary to make some modifications to the chemistry of the glue itself in order to make it more environmentally friendly. Herein, we prepared modified adhesive formulations based on commercial UF resins (UF), cured alone (UF) and with tannic acid (UFTA1, UFTA3 and UFTA5) and evaluated their adhesive properties following the change in shear strength of samples with different TA content.

Table 1. *The technical properties of UF resin.*

Sample	Property					
	Solid content (wt%)	Density (g/cm^3)	Gel time (s)	pH	Free-F (wt%)	Viscosity, F^4_{20} (s)
UF	68	1.290	71	8.0	0.14	84

3.1. FTIR analysis

Fourier Transform Infrared (FTIR) spectroscopy was used to analyze the chemical structures of the adhesive resins. The corresponding FTIR spectra are presented in Figure 1, where Figure 1a displays the spectra of the commercial UF adhesive emulsion and its cured form (cUF), while Figure 1b shows the spectra of cured UF adhesives modified with 1%, 3%, and 5% tannic acid (labeled as UFTA1, UFTA3, and UFTA5, respectively).

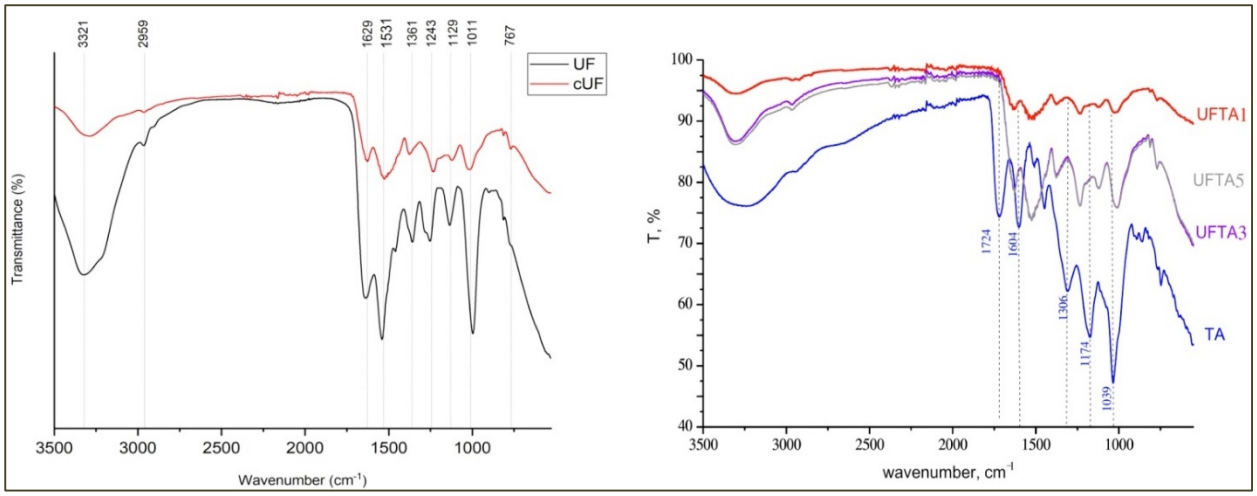

Figure 2. *FTIR spectra of: 1a) pure, commercial UF adhesive emulsion and cured resin (cUF); 1b) cured UF adhesive with different tannic acid concentrations (1%, 3%, 5 %).*

As shown in Figure 1a, both the UF adhesive and its cured form (cUF) exhibit characteristic absorption bands. The broad peak around 3320 cm $^{-1}$ corresponds to O–H and N–H stretching vibrations, while the band near 2969 cm $^{-1}$ is attributed to C–H stretching of methyl and methylene groups. Peaks at 1659 cm $^{-1}$ and 1531 cm $^{-1}$ are assigned to C=O stretching and N–H bending of amide groups, respectively, indicative of urea-formaldehyde network formation. The cured resin (cUF) shows slight shifts and reduced intensity in these regions, suggesting partial reaction and cross-linking during curing.

In Figure 1b, the FTIR spectra of tannic acid-modified resins (UFTA1, UFTA3, and UFTA5) show notable differences compared to the unmodified cured resin. With increasing tannic acid content, a progressive reduction in the intensity of amide-related bands (1650–1530 cm $^{-1}$) is observed, indicating potential interaction between tannic acid and the resin matrix. Furthermore, enhanced absorbance around 1020–1240 cm $^{-1}$ suggests increased C–O and C–N bond formation,

likely due to the incorporation of polyphenolic structures from tannic acid. These spectral changes confirm chemical modification of the UF resin network, which may influence both the reactivity and emission behavior of the adhesive.

The observed FTIR spectral changes are consistent with the expected chemical interactions between tannic acid and the UF resin network. Tannic acid, being rich in phenolic hydroxyl and carboxyl groups, can react with free formaldehyde or participate in the cross-linking process, thereby reducing the amount of unreacted formaldehyde available in the system. This is supported by the diminished intensity of amide bands and the appearance of new C–O and C–N stretching vibrations in the modified samples, particularly in UFTA3 and UFTA5.

3.2. Tensile shear strength determination

The tensile shear strengths of examined adhesives are shown in Figure 2. The tensile test results of the samples demonstrated that the resin mixed with tannic acid (1, 3 and 5% by weight) had very good performance compared to pure UF resin. The effect of tannic acid on the properties of UF adhesive is mainly related to its addition concentration and the crosslinking of tannic acid with polymer. Shear strength was slightly lower in the case with 1% and 3% tannic acid addition but increased with concentration of 5% of tannic acid.

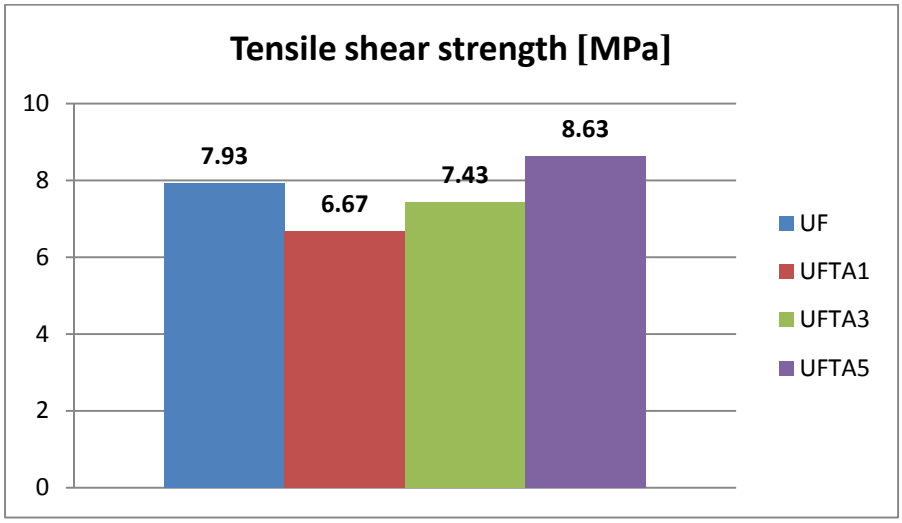

Figure 3. *Shear strength of beech wood samples with cured pure UF adhesive (UF) and samples with tannic acid addition in different concentrations (UFTA).*

The tensile shear strength of the unmodified and tannic acid-modified UF adhesives is presented in Figure 3. The reference UF resin exhibited a strength of 7.93 MPa, serving as the baseline for comparison. The addition of 1% tannic acid (UFTA1) resulted in a decrease to 6.67 MPa, suggesting that low tannic acid content may interfere with optimal polymer network formation or introduce brittleness at the adhesive interface. An increase to 3% tannic acid (UFTA3) led to partial recovery of shear strength (7.43 MPa), while the 5% formulation (UFTA5) outperformed the reference resin, reaching 8.63 MPa. This improvement is likely due to enhanced cross-linking and interaction between the phenolic groups of tannic acid and the resin matrix, which strengthens the adhesive bond.

These findings confirm that while small additions may temporarily weaken bonding, higher tannic acid content improves tensile shear strength, likely through chemical integration into the resin network. Combined with reduced formaldehyde emissions (as indicated by FTIR), the UFTA5 formulation demonstrates potential for more sustainable and high-performance UF adhesives.

The different failure modes observed after the adhesion tests—namely cohesive, adhesive, and substrate failure—were identified through surface analysis of the bonded specimens using high-resolution imaging. Cohesive failure was defined as adhesive remaining on both overlapping surfaces, indicating internal failure within the adhesive layer. Adhesive failure occurred when adhesive was present on only one surface, reflecting poor bonding at the interface. Substrate failure was

characterized by the fracture of the wood substrate itself, with the adhesive bond remaining intact. All tested specimens exhibited 100% substrate failure, regardless of tannic acid concentration. This consistent failure mode strongly suggests that the adhesive bond strength exceeded the internal strength of the wood substrate, and that the bond was not the weakest point in the assembly. From a technical and industrial perspective, this outcome is highly desirable, as it confirms the structural integrity and reliability of the adhesive joint under load.

Moreover, the occurrence of substrate failure even in samples modified with tannic acid (UFTA1, UFTA3, UFTA5) indicates that the incorporation of bio-based additives did not compromise bonding performance. In fact, the enhanced tensile shear strength observed for UFTA5, combined with substrate failure as the dominant fracture mode, highlights the potential of tannic acid-modified UF resins for structural applications where high bond strength and environmental performance are both critical.

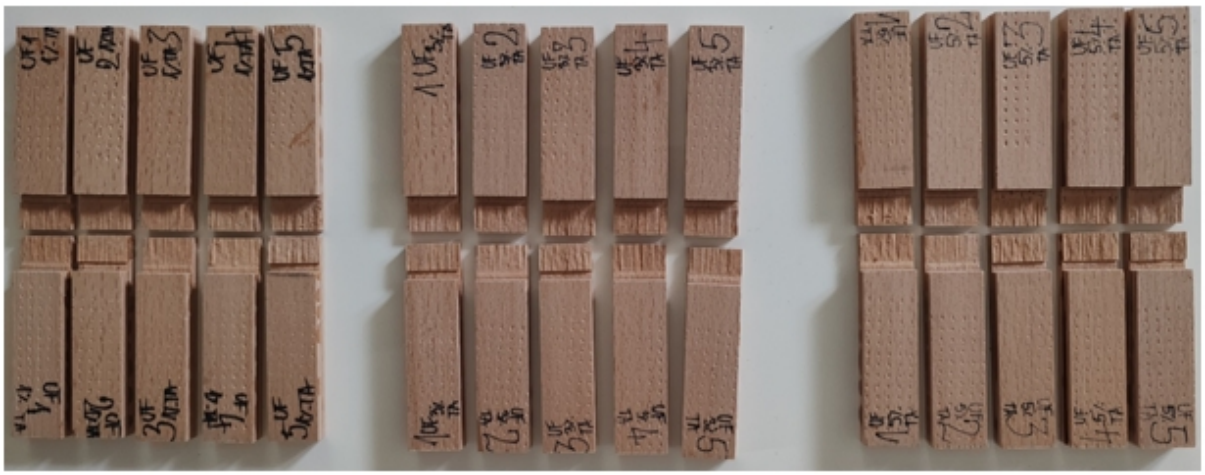

Figure 4. *The joint samples underwent complete (100%) wood fracture following tensile shear testing.*

4. CONCLUSION

Wood adhesives based on UF resin and tannic acid were prepared, characterized and their adhesive and mechanical properties were investigated to determine their potential as wood adhesives in order to reduce formaldehyde emission. This study demonstrated the potential of incorporating tannic acid — a bio-based phenolic compound — into urea-formaldehyde (UF) adhesives to improve both environmental and mechanical performance. FTIR spectroscopy confirmed chemical interactions between tannic acid and the UF resin matrix, evidenced by changes in functional group intensities and the emergence of new bands corresponding to C–O and C–N bonds. These findings indicate partial integration of tannic acid into the polymer network.

The modified adhesives exhibited variable tensile shear strength depending on tannic acid content. While 1% addition (UFTA1) resulted in decreased strength, higher concentrations, particularly 5% (UFTA5), improved mechanical performance beyond that of the unmodified UF resin. Notably, all adhesive formulations — regardless of tannic acid content — resulted in 100% substrate failure, confirming that the bonding strength exceeded the internal strength of the wood substrate.

In addition to mechanical improvements, the presence of tannic acid is known to reduce formaldehyde emissions due to its phenolic and acidic functional groups, which can chemically bind or adsorb free formaldehyde. This dual effect — enhanced bond strength and reduced emissions — positions tannic acid-modified UF resins as a promising and more sustainable alternative for wood-based composite production.

Further research may focus on optimizing the concentration and distribution of tannic acid within industrial formulations, as well as evaluating long-term durability and emission behavior under variable environmental conditions.

ACKNOWLEDGEMENTS

This research was funded by the Ministry of Science, Technological Development and Innovation of the Republic of Serbia, grant number 451-03-137/2025-03/200169.

REFERENCES

1. Chen C., Yang H., Ma Q. (2022): Tannic acid: a crosslinker leading to versatile functional polymeric networks: a review; *RSC Adv.*, 12: 7689–7711.
2. Zhang W., Roy S., Ezati P., Yang DP, Rhim JW (2023): A green crosslinker for biopolymer-based food packaging films, *Trends in Food Science & Technology*, 136: 11-2.
3. Alavarse A.C, Frachini ECG, da Silva RLCG, Hashimoto Lima V., Shavandi A., Petri DFS (2022): Crosslinkers for polysaccharides and proteins: Synthesis conditions, mechanisms, and crosslinking efficiency: a review, *International Journal of Biological Macromolecules*, 202: 558-596.
4. Oktay S., Pizzi A., Köken N., Bengü B. (2024): Tannin-based wood panel adhesives, *International Journal of Adhesion and Adhesives*, 130: 103621.
5. Lubis MAR, Hong MK, Park BD (2018): Hydrolytic removal of cured urea-formaldehyde resins in medium-density fiberboard for recycling, *J Wood Chem Technol*, 38: 1-14.
6. Li J., Lei H., Xi X., Li C., Hou D., Song J., Du G. (2023): A sustainable tannin-citric acid wood adhesive with favorable bonding properties and water resistance, *Industrial Crops and Products*, 201: 116933.

INFLUENCE OF STEAMING ON THE DRYING BEHAVIOR OF BLACK LOCUST SAWN TIMBER

Goran Milić[1], Nebojša Todorović[1], Marko Veizović[1], Ranko Popadić[1]

[1]*University of Belgrade – Faculty of Forestry, Department of Wood Science and Technology, Belgrade, Republic of Serbia*
e-mail: goran.milic@sfb.bg.ac.rs; nebojsa.todorovic@sfb.bg.ac.rs; marko.veizovic@sfb.bg.ac.rs; ranko.popadic@sfb.bg.ac.rs

ABSTRACT

This study investigates the impact of steaming on the conventional drying process of black locust (*Robinia pseudoacacia* L.) sawn timber. Matched samples of steamed and unsteamed boards were dried under identical conditions in a laboratory kiln. Contrary to typical literature findings, the steamed boards had a slightly higher initial moisture content at the start of drying, as they were not fully green when steamed, while the unsteamed boards underwent further air drying during the entire steaming period (approx. 10 days). Moisture content of the boards was monitored using both gravimetric method and in-kiln moisture probes. Moisture profiles across the board thickness were also tracked during drying, while final drying quality indicators – such as case-hardening and moisture gradients – were assessed after the process. The results show that steamed boards exhibited faster moisture loss during the initial drying phase, which can be attributed to their higher initial moisture content and more efficient removal of free water. At the end of drying, steamed boards showed more uniform moisture distribution and lower residual stresses, resulting in improved overall drying quality. These findings confirm that steaming of green timber positively influences drying behavior and quality, supporting its use as a pre-treatment in the industrial drying of black locust timber – not only for colour change, but also for improving drying quality.

Keywords: black locust, steaming, drying, moisture content, drying quality.

1. INTRODUCTION

Black locust (*Robinia pseudoacacia* L.) is increasingly promoted as a sustainable hardwood in Europe and North America because of its fast growth, excellent natural durability and high resistance to decay and insects. The wood is highly valued for outdoor application: garden furniture, decking, fencing and cladding, but it is also used for interior furniture and flooring. In spite of its relatively high density (≈ 730 kg m^{-3} oven-dry), black-locust timber is generally considered easy to dry compared with most ring-porous hardwoods. However, due to the relatively small diameter of logs (20-35 cm), the knot-free portion in timber is rather small. Moreover, its greenish-yellow colour – and the sharp contrast between sapwood and heartwood – restricts its use in high-end interior applications. Although the natural colour is acceptable for many outdoor uses, most interior products require a uniform dark-brown tone. For this reason, black-locust boards are often steamed before kiln drying. Steaming is carried out either in tight-stacked or in stickered stacks and lasts appreciably longer than for other hardwoods in order to achieve a deep, even brown.

Kačík et al. (2023) and Hofmann et al. (2022) showed that the high extractives content of black locust (up to 9 % of oven-dry weight) and their oxidation are responsible for the brown colour formed during steaming. Tolvaj et al. (2010) reported that a similar shade can be produced even in dry wood if temperatures above 95-100 °C are applied, although such high-temperature cycles are rarely used in industry. After steaming, the wood machines more cleanly (less grain tear and splitting) and exhibits reduced photodegradation under UV exposure (Hofmann et al. 2022). Proper steam treatment can also improve adhesion performance, as demonstrated for black-locust bonding by Varga and van der Zee (2008).

In general, beyond colour change, steaming can redistribute bound water, collapse tyloses and relieve growth stresses, thereby reducing moisture gradients during subsequent kiln drying. These

mechanisms can shorten drying times and lower residual stress in beech timber (Milić et al. 2015); however, systematic data for black locust remain scarce and reported effects are sometimes contradictory.

The present study evaluates the influence of a long steaming cycle on the drying behaviour and drying quality of black locust timber.

2. MATERIAL AND METHODS

Approximately 0.8 m³ of black-locust (*Robinia pseudoacacia* L.) boards, sawn from logs grown in northern Serbia, were used. Boards had a nominal thickness of 30 mm, random widths of 120–300 mm, and lengths of 1.0 m or 2.0 m. The material was randomly divided into two equal groups (steamed vs. unsteamed). Steaming was performed in an industrial direct-steam chamber (total volume 20 m^3), in which the steam is produced in steam boiler and injected into the chamber. The timber was stacked without stickers. The cycle lasted 260 h (Table 1).

Table 1. *Steaming schedule (black locust 30 mm).*

Phase	Time (h)	Temperature (°C)
Heating	72	to 100
Active steaming	168	100-103
Cooling	20	-
Total	260	-

Both steamed and unsteamed boards were transported to the Faculty of Forestry (Belgrade). From the delivered material, 126 boards were randomly selected – just enough to fill the conventional laboratory kiln – 63 steamed and 63 unsteamed. Before loading, the boards were stored for four days at 22 °C in the laboratory. Steamed and control boards were stacked in alternate layers in the laboratory kiln (0.8 m³ capacity, axial-flow fans, reversible air circulation). Eight resistance moisture probes (electrode depth 12 mm, spacing 32 mm) were installed – four in steamed and four in unsteamed boards – distributed throughout the stack height.

The medium-intensity drying schedule supplied by the kiln manufacturer (Table 2) was chosen; it begins at 35 °C and equilibrium moisture content (EMC) 16% and ends at 60 °C and EMC 4%. Heating-up was ramped at 3.6 °C h^{-1} to the initial set-point. The conditioning phase lasted for 18 h at 55 °C and EMC 11%.

Table 2. *Drying schedule (black locust 30 mm).*

MC (%)	60	55	50	45	40	35	30	25	20	15	10	5
T (°C)	35	36	36	36	36	37	40	43	47	55	60	60
EMC (%)	16.0	15.5	15.0	14.6	14.1	13.2	12.2	10.3	7.5	5.6	4.7	4.2
Fan Speed (%)	100	100	100	100	100	100	100	96	94	88	84	84

Six control boards (three steamed, three unsteamed) were placed in the top two layers. From each board, paired specimens were excised at nine time points during drying (0, 24, 48, 72, 96, 144, 192, 240, 336 h):

- Sample A – 20 mm long (along the grain), full board width and thickness; used to determine whole-board MC.
- Sample B – central 50 mm segment of the board, also 20 mm long; sliced into five lamellae across thickness with a sliding microtome to obtain MC profiles (Fig. 1).

All specimens were weighed before and after oven-drying at 103 ± 2 °C to calculate moisture content (MC).

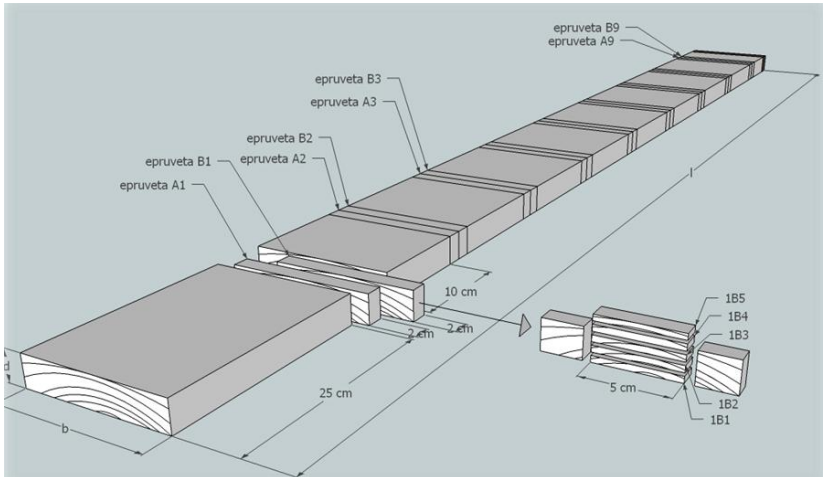

Figure 1. *Test samples for determination of MC and MC profiles (5 lamellae) during drying.*

After kiln-drying, next to determination of MC, a standard prong test (CEN/TS 14464; EN 14298) was performed on seven boards per treatment. The gap was measured with feeler gauge after 48 h equalisation period at room conditions; a gap ≤ 2 mm was classified as “Q-quality” (Welling 1994).

3. RESULTS

Figure 2 shows air parameters in the kiln (dry-bulb temperature and EMC) during drying and the average MC curve derived from the „active“ in-kiln probes (typically 4-5 with highest values). At the beginning of drying average MC of steamed boards (4 probes) was 57%, while for unsteamed (4 probes) it was 50%. A higher initial MC in steamed timber is not unusual, especially when the material enters the steaming chamber partially air-dried; condensation of water vapour on relatively dry surfaces can raise MC slightly. The effect is pronounced in black locust because the steaming cycle is very long (at the same time unsteamed timber continues drying).

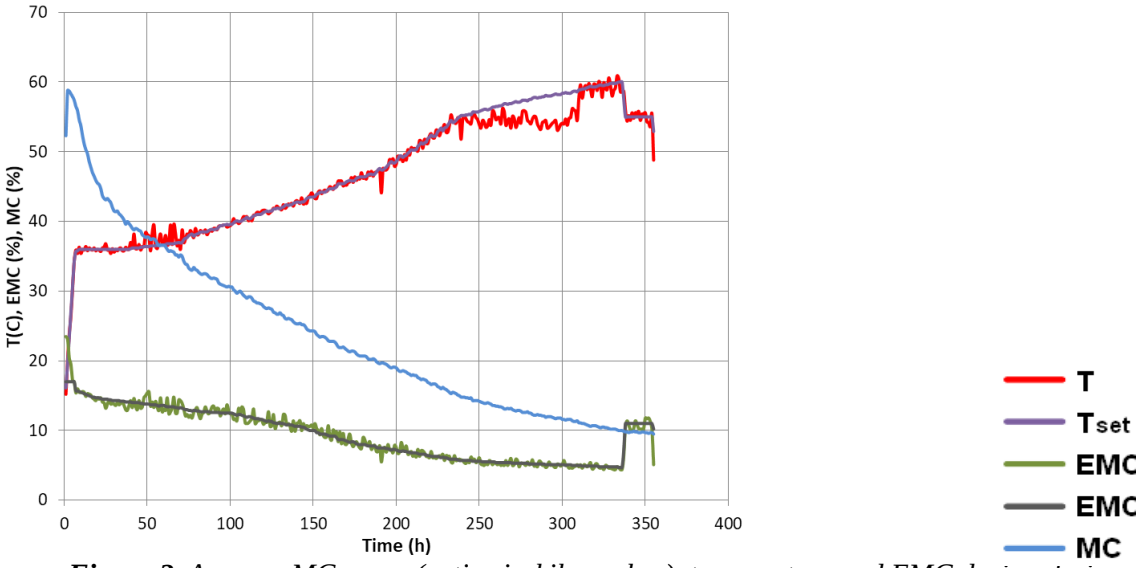

Figure 2. *Average MC curve (active in-kiln probes), temperature and EMC during drying.*

Throughout the first ten days of drying, probe readings in steamed boards were 4–7% higher than in unsteamed boards; after 240 h the difference became negligible. Gravimetric measurements on the control boards from the top layer showed lower absolute MCs (Fig. 3) than the probes, yet still indicated the same trend – steamed boards started about 3.5 % wetter. Although these boards were closest to the heaters and thus subjected to the most severe conditions, the discrepancy between gravimetric and probe values confirms that resistance probes, when factory-calibrated for “group 3” species (oak, ash, most softwoods), do not read black-locust MC accurately.

The difference in MC between steamed and unsteamed boards (determined by oven-dry method) narrowed rapidly and became negligible after day 3; from that point to the end of drying, MC remained uniform across all boards and was even slightly lower in the steamed group. Because the steamed boards started wetter yet reached 10% MC about 20 h sooner than the unsteamed boards (Fig. 3), long-cycle steaming can be expected to yield drying rates that are at least comparable to – and usually somewhat higher than – those of unsteamed black-locust timber.

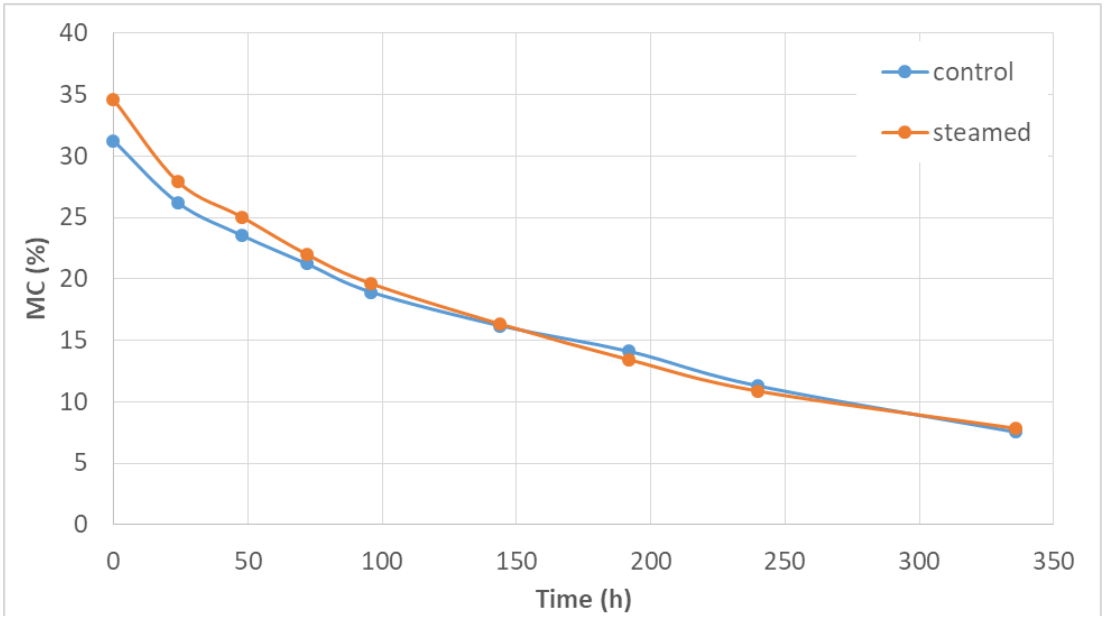

Figure 3. *Average MC curve of steamed and control boards determinated by oven-dry method.*

Initial MC profiles across the thickness also showed slightly higher MC in steamed boards, mainly in the surface zone: average surface MC was 30.1% (steamed) vs. 27.7% (unsteamed), while centre MCs were nearly equal (35.3% vs. 34.7%). As expected, the surface-to-core MC difference increased during the first two–three days, peaking at 10-10.5% after 48–72 h for both groups, then declined steadily. From 96 h onward – when both groups had cca. 10% MC difference – the profiles diverged: steamed boards developed a markedly flatter MC profile. Surface MCs are almost identical, but centre MC in steamed boards dropped faster, indicating more efficient bound-water movement as a result of steaming.

The results obtained at the end of drying (Table 3) also support this assumption. Average final MC was practically identical, yet the MC gradient (core – surface) was significantly lower in steamed boards. The prong-test gap was also significantly smaller, confirming lower residual stress. All steamed boards fell within Q-quality (gap ≤ 2 mm), while two of the seven unsteamed boards exceeded this limit.

Table 3. *Average final MC, MC difference and case-hardening of steamed and unsteamed boards.*

	Final MC (%)	MC_{cen}- MC_{surf}	Gap (mm)
Steamed	7.5	2.1	1.50
Unsteamed	7.7	3.1	1.85

Overall, the long steaming cycle produced measurably flatter moisture-content gradients and significantly lower residual stress in the steamed boards. These findings indicate that long steaming is useful not only for darkening and equalisation the colour of black locust timber, but also as an effective pre-treatment that improves final drying quality.

4. CONCLUSIONS

In this study, the drying behaviour of 30 mm black-locust boards subjected to a 260-hour steaming cycle was investigated. The treatment produced a uniform dark-brown colour and improved kiln-drying performance. Steamed timber reached 10 % moisture content roughly a day sooner than the unsteamed controls and maintained 30–40% flatter through-thickness MC profiles, indicating more efficient bound-water movement. It also exhibited lower residual stresses: every steamed board showed a prong-test gap ≤ 2 mm and qualified for EN 14298 class Q, whereas two of seven unsteamed boards fell into class S.

ACKNOWLEDGEMENTS

This study was financially supported by the Ministry of Science, Technological Development and Innovation of the Republic of Serbia (Grant No. 451-03-137/2025-03/200169).

REFERENCES

1. Hofmann, T., Tolvaj, L., Visi-Rajczi, E. and Varga, D. (2022): Chemical changes of steamed timber during short-term photodegradation monitored by FTIR spectroscopy. Eur. J. Wood Prod. 80, 841–849.
2. Kačík, F., Kubovský, I., Bouček, J., Hrčka, R., Gaff, M., & Kačíková, D. (2023): Colour and Chemical Changes of Black Locust Wood during Heat Treatment. Forests, 14(1), 73.
3. Milić, G., Todorović, N. and Popadić, R. (2015): Influence of steaming on drying quality and colour of beech timber. Glasnik Šumarskog Fakulteta 112, 83–96.
4. Tolvaj, L., Molnar, S., Nemeth, R. and Varga, D. (2010): Color modification of black locust depending on the steaming parameters. Wood Research 55(2), 81-88.
5. Varga, D. and van der Zee, M.E. (2008): Influence of steaming on selected wood properties of four hardwood species. Holz Roh Werkst, 66: 11-18.
6. Welling, J. (1994): European Drying Group (EDG) Recommendation: Assessment of Drying Quality of Timber
7. EN 14298 Sawn timber – Assessment of drying quality
8. CEN/TS 14464 Sawn timber – Method for assessment of case-hardening

Milić Goran, D.Sc., professor
University of Belgrade - Faculty of Forestry
Department of Wood Tecnology
Kneza Višeslava 1
11030 Belgrade, Republic of Serbia

THE EFFECTS OF NATURAL DEGRADATION ON THE CHEMICAL COMPOSITION OF PEDUNCULATE OAK STUMP (*QUERCUS ROBUR* L.)

Jasmina Popović[1], Gordana Petković[1], Miloš Šuljagić[1], Mlađan Popović[1], Milanka Điporović-Momčilović[1], Radoslav Lozjanin[2], Ivana Stojiljković[1*]

[1]University of Belgrade, Faculty of Forestry, Belgrade, Serbia
e-mail: jasmina.popovic@sfb.bg.ac.rs; gordana.petkovic@sfb.bg.ac.rs;
student.milossuljagic1702058@sfb.bg.ac.rs;mladjan.popovic@sfb.bg.ac.rs;
milanka.djiporovic@sfb.bg.ac.rs; ivana.stojiljkovic@sfb.bg.ac.rs
[2]Public Enterprise “Vojvodinašume”, Novi Sad, Serbia
e-mail: radoslav.lozjanin@sgsmitrovica.rs

ABSTRACT

After trees are cut down, the stumps usually remain in the forest. Recently, there has been a growing interest in utilizing stump biomass as an energy resource or alternative raw material to produce various chemicals. However, stumps left in the forest are exposed to various biotic (microorganisms, insects) and abiotic factors (UV radiation, precipitation, low/high temperatures, oxygen from the air, atmospheric pollutants), causing their degradation over time.

This paper investigates the changes in the chemical composition of the xylem of Pedunculate oak stumps (*Quercus robur* L.) after two years of natural degradation. In that aspect, the samples of the freshly cut stump were compared to the samples obtained from the stump that was exposed in the forest environment for two years. During this period, the cellulose and ash content decreased by 3.7% and 30%, respectively, while the lignin content increased by 5%. It was also found that after two years, the content of wood extractives in the oak stump increased by 15%. To detect natural products of stump wood extracts, the High-Performance Thin-Layer Chromatography (HPTLC) technique and post chromatographic derivatization with ASA (*p*-anisaldehyde/sulfuric acid) reagent were used. ASA is a widely used reagent for the detection of terpenoids, steroids, and carbohydrates through color differentiation. The developed colors are indicative of the chemical nature of the compounds. Compounds visualized under white light after derivatization and heating show that extracts from the stump wood, following two years of natural degradation, have more terpenoids, producing blue, purple, or brown zones. A decrease in the intensity of the gray and green spots under white light can also be observed, indicating that the chemical profile of the wood extract is less rich in steroids and allylic alcohols. Terpenoids are not only important for the tree’s defense mechanisms but also for their role in the production of aromatic compounds that contribute to the wood’s uses in industries like winemaking.

Keywords: *Quercus robur* L., natural degradation, stump, chemical composition, HPTLC

1. INTRODUCTION

After tree felling, stumps usually remain in the forest (Walmsley and Godbold, 2010) and represent a potential source of carbon (C) and nutrients such as nitrogen (N), phosphorus (P), potassium (K), calcium (Ca), and magnesium (Mg) (Wang et al, 2022; Palviainen et al, 2015; Sucre and Fox, 2009; Persson, 2013; Lasota, 2018). The degradation of stumps contributes to nutrient cycling within forest ecosystems, enriching forest soils with organic minerals, nitrogen (N), and carbon (C), thereby supplying nutrients essential for the growth of trees in future forest generations (Deng et al, 2018; Sucre and Fox, 2009; Persson, 2013).

The removal of stumps can have negative consequences for soil structure and fertility, increase erosion, and reduce organic carbon stocks (Moffat et al, 2011; Sucre and Fox, 2009; Persson, 2013; Olsson et al, 1996). Moreover, stumps serve as habitats for numerous forest organisms, so their removal may threaten the survival of these populations and negatively impact forest biodiversity (Moffat et al, 2011; Walmsley and Godbold, 2010; Persson, 2013). On the other hand, decaying

stumps increase the risk of pests and diseases (Walmsley and Godbold, 2010; Moffat et al, 2011; Persson, 2013), which is why in some countries such as the United Kingdom, the northwestern United States, and Canada, commercial stump removal is practiced as a method of rot prevention (Cleary et al, 2013; Persson, 2013), while in Finland and Sweden, stumps are utilized for bioenergy production (Hakkila, 2004; Walmsley and Godbold, 2010; Persson, 2013).

In the context of increasing demand for renewable energy sources and the reduction of fossil fuel use, interest in utilizing stumps as a raw material for bioenergy and chemical production is growing (Bjorheden, 2006; Walmsley and Godbold, 2010). Stumps make up the largest portion of coarse woody biomass remaining after tree harvesting and may account for up to 20% of additional biomass (Richardson et al, 2002; Hakkila and Aarniala, 2004; Walmsley and Godbold, 2010). In some European countries, particularly in Scandinavia, stumps and coarse roots are commercially removed for the production of fiber and bioenergy (Moffat et al, 2011; Persson, 2013; Walmsley and Godbold, 2010; Hakkila, 2004; Walmsley and Godbold, 2010). As early as the 17th century, and especially during the 19th century in Sweden and Finland, stumps were used for the production of tar and other wood-derived products (Karlsson, 2007; Walmsley and Godbold, 2010; Persson, 2013). Partially decomposed stumps found in forests are also a potential resource for the production of various wood-based products (Rahmati et al, 2019).

Stump decomposition is a complex and long-term process influenced by numerous biotic and abiotic factors, including climatic conditions, soil properties (Moffat et al, 2011), microbial activity, wood species, and the physico-chemical properties of the stump itself (van Geffen et al, 2010; Moffat et al, 2011; Deng, 2018; Zhu et al, 2017; Lasota, 2018; Erdenebileg et al, 2020). White-rot and brown-rot fungi play a key role in the degradation of cellulose, hemicelluloses, and lignin, leading to progressive mass loss and changes in the density of woody biomass (Rahmati et al, 2019). The decomposition rate is also significantly affected by the C:N ratio, extractive content, and tissue type (heartwood, sapwood, bark) (Moffat et al, 2011; Lasota, 2018; Kanbayashi et al, 2021). Generally, nutrient-rich tissues such as sapwood decompose faster than heartwood, which is rich in extractives with antifungal properties (Moffat et al, 2011). Over time, the proportion of carbohydrates decreases while the lignin-to-nitrogen ratio increases, which slows down the decomposition rate (Moffat et al, 2011).

Pedunculate oak (*Quercus robur* L.) is one of the most abundant and ecologically important hardwood species in Serbia, especially in the floodplain forests of Vojvodina along major rivers such as the Sava and Danube, as well as in regions like Mačva and Pomoravlje (Banković, 2009). This species is valued for its natural durability and high concentration of polyphenolic extractives, which contribute to its resistance to biological degradation and define its potential use in various industries.

Despite its wide distribution and economic importance, changes in the chemical composition occurring during the natural degradation of pedunculate oak stumps have not been sufficiently studied. Considering the increasing demand for sustainable utilization of woody biomass, understanding these changes can contribute to better resource use. This study aims to examine changes in the chemical composition of the xylem of pedunculate oak (*Quercus robur* L.) stumps after two years of natural degradation in forest conditions, to evaluate their potential for industrial or energy purposes.

2. MATERIAL AND METHODS

Samples for chemical composition analysis were taken from pedunculate oak stumps (*Quercus robur* L.) from the same site within the “Morović” forest management unit (Public Enterprise “Vojvodinašume”, Serbia). Two groups of samples were analyzed: stumps from freshly felled trees (Qr) and stumps in the degradation phase, remaining from trees felled two years earlier (DQr). The stumps originated from trees of approximately the same age (around 110 years), eliminating variability related to tree age.

From each stump, discs approximately 3 cm thick were cut and air-dried for three months. After removing the bark, the remaining xylem was ground and sieved. For analysis, the particle fraction of 0.5–1 mm was used, following TAPPI standard T 257 cm-02.

The moisture content of the stump samples was determined gravimetrically by drying to constant mass at 105 ± 2 °C (TAPPI T 264 cm-97), and was 7.77 ± 0.11% for the Qr sample and 7.60 ± 0.10% for the DQr sample.

The chemical characterization of the stumps (Qr and DQr) included the determination of: cellulose content using the Kürschner-Hoffer method (Browning, 1967); extractives soluble in toluene: ethanol (2:1, v/v) after 8 hours of extraction in a Soxhlet apparatus (ASTM D1105-21); extractives soluble in hot water after 3 hours of extraction (TAPPI T 207 cm-99; ASTM D1110-21); ash content at 900 °C (TAPPI T 413 om-22); and lignin content, determined as the sum of acid-insoluble lignin (TAPPI T 222 om-11) and acid-soluble lignin measured at a wavelength of 205 nm using a UV spectrophotometer Vision-600 (TAPPI T UM 250). All analyses were performed in triplicate, and the results are expressed as mean values with standard deviations. The hemicelluloses content was calculated as the difference between the total wood mass (100%) and the sum of the other wood components.

A one-way analysis of variance (ANOVA) with a 95% confidence level was used to determine the significance of differences between fresh and degraded stump samples.

A CAMAG Linomat 5 (Muttenz, Switzerland) was used to apply 20 µL of extracts in 6 mm bands onto 20 cm × 10 cm HPTLC glass silica gel plates. The bands were positioned 8 mm from the plate's lower edge, with a minimum of 13 mm separating them on either side. Using the mobile phase ethyl acetate: *n*-hexane: formic acid: water (11:2:1:0.5 *v/v/v/v*) in a saturated Twin Trough Chamber (20 cm × 10 cm), chromatographic development was performed, and mobile phase to was allowed to migrate a distance of 70 mm. After being taken in TIFF format, the pictures of the acquired HPTLC chromatograms were processed with VideoScan (version 1.02, CAMAG). To identify natural oxidisable molecules, a *p*-anisaldehyde/sulfuric acid (ASA) reagent was used for derivatization. The zones were then visible after 10 minutes of heating on a plate at 110 °C. The ASA reagent was freshly prepared by mixing 10 mL of glacial acetic acid with 85 mL of methanol. To this chilled solution, 5 mL of concentrated sulfuric acid and 0.5 mL of *p*-anisaldehyde were added (Martelanc et al, 2016). All chemicals and reagents for this investigation were purchased from commercial suppliers. Formic acid, sulfuric acid, acetic acid (glacial, 100%), methanol, and HPTLC silica gel 60 (Art. 105461) glass plates were purchased from Merck KGaA (Darmstadt, Germany). Ethyl acetate was supplied by Centrohem (Stara Pazova, Serbia). *n*-Hexane, *p*-anisaldehyde, and standards of rosmarinic acid (96%), *β*-sitosterol (≥95%), and oleanolic acid (≥97%) were bought from Sigma Aldrich Chemie GmbH (Steinheim, Germany).

3. RESULTS AND DISCUSSION

The chemical composition of Qr and DQr pedunculate oak (*Quercus robur* L.) stumps is presented in Figures 1 and 2. The analyzed parameters reveal clear changes in the chemical composition of oak stumps after two years of natural degradation.

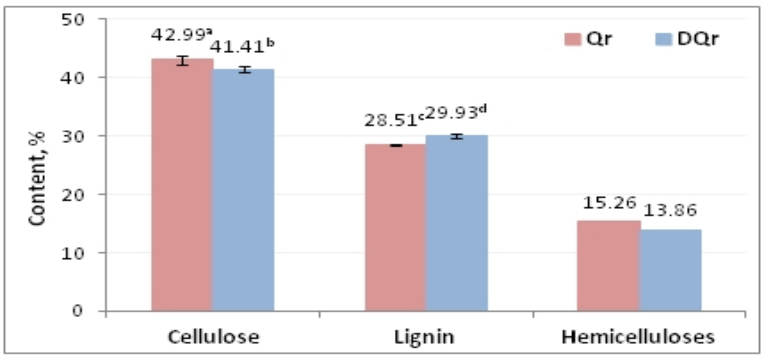

Figure 1. *Content of structural components from a freshly felled tree (Qr) and from a tree felled two years ago (DQr) pedunculate oak stumps (% dry mass). Different letters ($^{a, b, c, d}$) indicate statistically significant differences ($p < 0.05$).*

As shown in Figure 1, the contents of cellulose and hemicelluloses in degraded stump samples (41.44% and 13.86%, respectively) are significantly lower compared to those in fresh stumps (42.99% and 15.26%, respectively). In contrast, the lignin content in DQr samples (29.93%) is significantly

higher compared to Qr samples (28.51%). Rahmati et al (2019) also reported a greater degree of cellulose and hemicelluloses degradation compared to lignin in stumps of Oriental beech (*Fagus orientalis* Lipsky) over a felling period of 2 to 25 years.

The crystalline structure of cellulose contributes to its resistance to enzymatic degradation (Teeri and Henriksson, 2009). Hemicelluloses do not form crystalline structures like cellulose, making them more accessible and sensitive to enzymatic hydrolysis and microbial degradation (Saha, 2003). Additionally, hemicelluloses provide a physical barrier around cellulose microfibrils, thereby protecting them from the action of hydrolytic enzymes of microorganisms (Rahmati et al, 2019). As a result, hemicelluloses are more exposed to microbial attack, especially in the early stages of degradation. This explains the higher degradation rate of hemicelluloses, whose content in DQr samples is approximately 9.4% lower compared to Qr, while cellulose content is about 3.7% lower.

Polysaccharides are embedded in a lignin matrix that protects them from microbial attack (Nilsson, 2009). During natural wood degradation, polysaccharides degrade faster than lignin, which is the most resistant component of the cell wall to biological degradation (Rahmati et al, 2019). Lignin's resistance to enzymatic degradation is due to its complex, highly branched heteropolymeric structure, as well as its pronounced aromatic and hydrophobic nature (Kai et al, 2018; Sánchez and Alméciga-Díaz, 2011; Rahmati et al, 2019). Consequently, the total lignin content in partially degraded stumps is approximately 5% higher than in freshly cut stumps. According to Moffat et al (2011), increased lignin content after partial degradation slows down the rate of further decay.

The observed differences in the content of structural cell wall components between fresh and degraded stump samples indicate more intensive degradation of polysaccharides during natural stump decomposition, which is consistent with known patterns of lignocellulosic biomass decay (Rahmati et al, 2019). Microorganisms involved in lignin degradation include specific fungi and bacteria commonly found in soil and decaying vegetation (Kai et al, 2018; Sánchez et al, 2011).

Cell wall polysaccharides are mostly selectively degraded by brown- and soft-rot fungi, and to a lesser extent by white-rot fungi (Tomak, 2014; Rahmati et al, 2019; Nilsson, 2009), as well as by certain aerobic and anaerobic bacteria (Teeri and Henriksson, 2009). In the early stages of degradation, brown-rot fungi selectively degrade hemicelluloses, which are more sensitive to microbial breakdown, and subsequently degrade cellulose, leaving lignin as a slightly modified residue (Nilsson, 2009; Tomak, 2014; Rahmati et al, 2019; Kai et al, 2018).

The lower content of polysaccharides and higher lignin content in decomposing oak stumps, due to the higher degradation rate of polysaccharides compared to lignin, indicates the action of brown-rot fungi. Brown-rot fungi lead to significant decomposition and mass loss, resulting in reduced density and diminished mechanical properties of the wood (Tomak, 2014; Rahmati et al, 2019).

Figure 2 shows the content of non-structural components (extractives and mineral substances) in freshly cut oak stumps and oak stumps after two years of natural forest degradation.

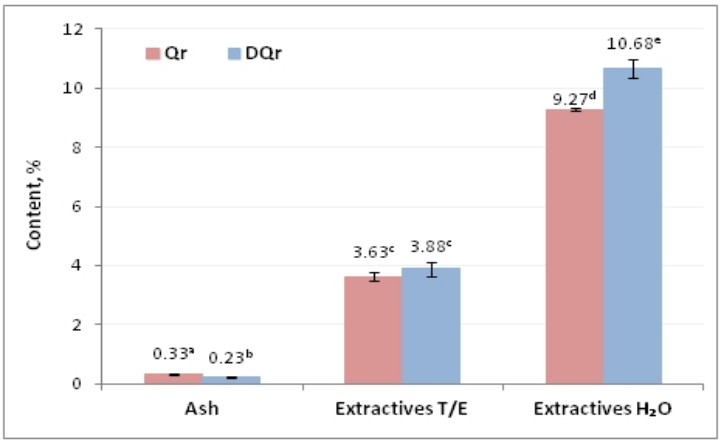

Figure 2. *Content of non-structural components from a freshly felled tree (Qr) and from a tree felled two years ago (DQr) pedunculate oak stumps (% dry mass). Different letters ($^{a, b, c, d, e}$) indicate statistically significant differences ($p < 0.05$).*

Regarding non-structural wood components, *Quercus robur* L. stumps after two years of degradation exhibited higher extractive content and lower ash content compared to fresh stumps (Figure 2). The mineral content was expressed as ash content after complete combustion at 900 °C (TAPPI T 413 om-22). The overall mineral content in wood is generally low, amounting to 0.33% in fresh *Q. robur* L. stumps. During natural stump decomposition, the content of mineral elements decreases further (Xie et al, 2024), resulting in approximately 30% lower ash content in degraded oak stumps compared to fresh ones.

This significantly reduced ash content in degraded samples is the result of a combination of leaching and biological uptake of mineral substances due to atmospheric influences and microbial activity. During the decomposition of stumps, rainwater and groundwater over time wash inorganic ions (such as K^+, Mg^{2+}, Ca^{2+}, and others like phosphate) from the wood and transport them into deeper soil layers. This is one of the main reasons for the reduction of inorganic content and is particularly prominent in the early stages of decomposition (Lasota, 2018; Xie et al, 2024).

In addition, during wood decomposition, minerals are transformed from free inorganic forms into forms that are no longer free inorganic compounds (Lasota, 2018; Filipiak, 2018; Khanina et al, 2024). As the organic matter in wood breaks down into simpler molecules, part of the inorganic content becomes bound into newly formed organic complexes (e.g., humus), which increases soil fertility but reduces the availability of free inorganic ions (Filipiak, 2018; Khanina et al, 2024). Furthermore, surrounding plants and wood-degrading microorganisms, such as fungi and bacteria, absorb and assimilate some of the inorganic ions for their metabolism, thus contributing to the further reduction of free inorganic substances in the wood (Lasota, 2018; Filipiak, 2018; Khanina et al, 2024).

The observed increase in extractives soluble in toluene: ethanol, and hot water in degraded oak stumps by approximately 6.9% and 15%, respectively, indicates the accumulation of low-molecular-weight degradation products such as sugars, phenolics, and organic acids during the degradation process. Onuchin et al (2018) reported that during wood decay, the content of starch and pentosans generally decreases, while the content of extractives soluble in water and benzene increases, which is consistent with the results of these studies.

The content of extractives soluble in toluene: ethanol did not differ significantly between Qr and DQr samples, suggesting that components of this fraction degrade relatively slowly. However, after two years of natural degradation, the content of water-soluble extractives in oak stumps increased by approximately 15%.

Species of the genus *Quercus* are known for their high polyphenol content (Fernandez de Simon et al, 1996), including volatile phenols, phenolic acids, and ellagitannins (Zhang et al, 2015). These polyphenols are water-soluble and play a key role in enhancing the natural durability of wood and preventing its degradation by fungi (Valette et al, 2017; Rahmati et al, 2019; Chang et al, 2010). In addition to the heartwood and bark, stumps are particularly rich in extractives (Stefanescu et al, 2022). Polyphenolic compounds are characterized by high antioxidant, antibacterial, and antifungal activity, which makes them toxic to microorganisms (Agarwal, 2021; Rahmati et al, 2019; N'Guessan et al, 2023), contributing to the wood's resistance to biodegradation (Taylor et al, 2002; Valette et al, 2017; Rahmati et al, 2019). Their biological activity against wood-degrading microorganisms is one of the main reasons for the low degradation rate of these components (Rahmati et al, 2019) and may explain the increased content of water-soluble substances after two years of oak stump degradation (N'Guessan et al, 2023).

The High-Performance Thin-Layer Chromatography method and post-chromatographic derivatization with ASA reagent were employed to identify natural products of stump wood extracts (Jork et al, 1994). Distinct chromatographic profiles of the extracts were obtained using a mobile phase composed of ethyl acetate, *n*-hexane, formic acid, and water (11:2:1:0.5, *v/v/v/v*), optimized to achieve maximum separation of phenolic compounds, terpenoids, and steroids in water extracts from fresh and biodegraded stump wood. The separated compounds were visualized by characteristic colors following derivatization with ASA reagent under white light, which facilitates the detection of diverse organic compounds (Wagner et al, 1984; Agatonovic-Kustrin et al, 2021). Standards of rosmarinic acid, *β*-sitosterol, and oleanolic acid were used for compound identification and color comparison (Figure 4). Following derivatization with ASA reagent, rosmarinic acid, a phenolic compound, exhibited a purple to brownish purple zone. *β*-Sitosterol, a phytosterol, developed a dark violet to purple coloration with greyish hues, reflecting its structural similarity to steroids. Oleanolic acid,

representing triterpenoids, showed purple to violet zones, consistent with the typical responses of this class under the reagent.

HPTLC analysis revealed distinct differences in the chemical profiles of the xylem extracts from fresh and naturally degraded *Quercus robur* L. stumps. The DQr extract exhibited a visibly richer chromatographic profile compared to the Qr extract, particularly under post-derivatization visualization. A prominent purple zone at $R_F \approx 0.73$-0.75 was observed in the DQr extract, less intense in Qr. This zone corresponds in both color and R_F value to the oleanolic acid standard, suggesting a higher content of triterpenoid compounds in the degraded sample. Conversely, a zone at $R_F \approx 0.70$-0.72, corresponding to the *β*-sitosterol standard, indicates a reduction in phytosterol content after two years of natural degradation in forest conditions (Figure 4).

In the R_F range of approximately 0.40 to 0.60, several purple-colored zones were observed in the DQr extract following derivatization with ASA reagent. These zones were either absent or barely visible in the Qr extract, suggesting a degradation-induced accumulation or transformation of specific compounds over time. Based on their R_F values, these zones likely correspond to triterpenoid derivatives or sesquiterpenes, or complex phenolic derivatives such as glycosides, which are known to develop purple to violet coloration under this reagent. The appearance of these compounds exclusively or more prominently in the degraded wood extract may indicate biochemical changes in the xylem matrix during the natural degradation process, possibly due to enzymatic or microbial activity enhancing the release or formation of such semi-polar terpenoid structures.

In the Qr extract, a prominent yellow to ochre-green zone was detected at $R_F \approx 0.02$-0.03 following derivatization. This low-mobility band likely corresponds to highly polar compounds, such as phenolic glycosides or hydrolyzable tannins. The absence of this zone in the DQr extract may suggest degradation or leaching of these compounds during long-term exposure to natural environmental conditions.

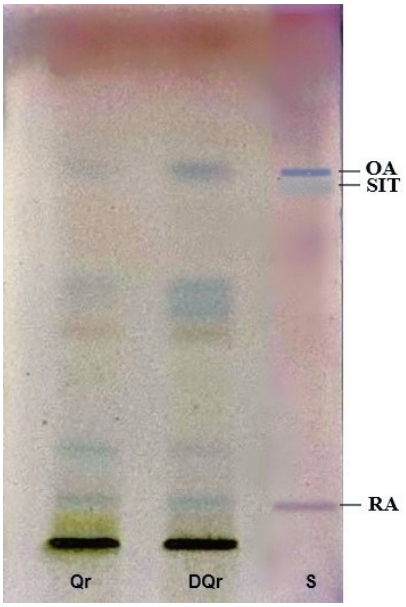

Figure 3. *HPTLC profiles of xylem extracts from fresh (Qr) and naturally degraded (DQr) Quercus robur L. stumps, and standard (S) of rosmaric acid (RA), β-sitosterol (SIT), and oleanolic acid (OA) after derivatization with ASA reagent, white light.*

Based on the obtained chemical composition results, it can be concluded that degraded *Quercus robur* L. stumps still represent a significant source of valuable components, particularly lignin and water-soluble extractives, and have the potential to contribute to sustainable forest resource management and the utilization of residual biomass.

The increased lignin content indicates their suitability as a raw material for the production of bio-based chemicals, such as phenolic derivatives, biopolymers, or components for the industrial production of adhesives and resins.

Given the substantial amount of residual carbon (in the form of cellulose and especially lignin), degraded stumps, following appropriate treatment, may also be used as biofuel (solid biofuel or pellets). This is supported by the increased lignin content, which has a higher heating value (26.7 MJ/kg) (Runge, Wipperfurth and Zhang, 2013) than cellulose and hemicelluloses (17.3 MJ/kg and 16.2 MJ/kg, respectively (Döring, 2013)). Additionally, the lower content of non-combustible inorganic substances, which negatively affect the heating value of wood (Döring, 2013; Runge, Wipperfurth and Zhang, 2013), further supports the increased energy potential of decomposing stumps. Naturally, further research is needed to confirm and quantify this hypothesis and to optimize stump processing methods for bioenergy or biochemical applications.

The increased content of water-soluble extractives, such as tannins and other polyphenols, along with the HPTLC results indicating elevated levels of terpenoids, point to the presence of bioactive compounds in decomposed oak stumps. This opens up the possibility of utilizing decomposed stumps as a source for the extraction of bioactive compounds, with potential applications in phytopharmacy, cosmetics, or wood protection. Accordingly, a comprehensive qualitative and quantitative analysis, including total phenolic content (TPC) and a phenolic profile of the extractives, would be necessary to evaluate their industrial potential.

4. CONCLUSION

The results of this study have shown that significant changes in the chemical composition of *Quercus robur* L. stumps occur over two years of natural degradation. A decrease in the content of cellulose, hemicelluloses, and mineral matter was observed, while the content of lignin and water-soluble extractives increased. These changes reflect the selective degradation of wood components under the influence of microorganisms and abiotic factors.

Despite the degradation, the results of the chemical analysis indicate that decomposed stumps still contain considerable amounts of lignocellulosic material and bioactive compounds, making them suitable for further utilization in various industrial sectors. Their valorization could contribute to reducing forestry waste, increasing the efficiency of biomass utilization, and supporting the development of sustainable technologies based on renewable resources.

REFERENCES

1. Agarwal, C., Hofmann, T., Visi-Rajczi, E., Pásztory, Z. (2021): Low-frequency, green sonoextraction of antioxidants from tree barks of Hungarian woodlands for potential food applications. Chemical Engineering and Processing - Process Intensification, 159, 108221.
2. Agatonovic-Kustrin, S., Balyklova, K.S., Gegechkori, V., Morton, D.W. (2021): HPTLC and ATR/FTIR Characterization of Antioxidants in Different Rosemary Extracts, Molecules 2021, 26(19): 6064.
3. Banković, S. (2009): The National Forest Inventory of the Republic of Serbia: the growing stock of the Republic of Serbia. - Belgrade: Ministry of Agriculture, Forestry and Water Management of the Republic of Serbia, Forest Directorate.
4. Bjorheden, R. (2006): Drivers behind the development of forest energy in Sweden. Biomass and Bioenergy, 30: 289–295.
5. Browning, B.L. (1967): Methods of Wood Chemistry, Vol. II. New York: Interscience Publishers.
6. Chang, H.T., Yeh, T.F., Chiang, C.H. (2010): Influence of extractives on the decay resistance of wood. Wood Science and Technology, 44: 99–110.
7. Cleary, M.R., Arhipova, N., Morrison, D.J., Thomsen, I.M., Sturrock, R.N., Vasaitis, R., Gaitnieks, T., Stenlid, J. (2013): Stump removal to control root disease in Canada and Scandinavia: A synthesis of results from long-term trials, Forest Ecology and Management, 290: 5-14.
8. Deng, X., Ye, L., Liu, Y., Li, Y. (2018): Decay dynamics and carbon release from decomposing coarse roots and stumps of Pinus massoniana. Forest Ecology and Management, 426: 131–140.

9. Döring, S. (2013): Power from Pellets: Technology and Applications, Springer-Verlag Berlin Heidelberg.
10. Erdenebileg, U., Yamamoto, M., Shibata, H. (2020): Wood decomposition rate and fungal colonization of stumps in a natural temperate forest. Journal of Forest Research, 25: 97–107.
11. Fernández de Simón, B., Cadahía, E., Conde, E., García-Vallejo, M.C. (1996): Low Molecular Weight Phenolic Compounds in Spanish Oak Woods. Journal of Agricultural and Food Chemistry, 44(6): 1507–1511.
12. Filipiak, M. (2018): Nutrient dynamics in decomposing dead wood in temperate forests – the role of wood-inhabiting fungi. Fungal Ecology, 35, 168–179.
13. Hakkila, P. (2004): Developing Technology for Large-Scale Production of Forest Chips. Wood Energy Technology Programme, 1999–2003. Helsinki, National Technology Agency.
14. Hakkila, P., Aarniala, M. (2004): Recovery of logging residues and stumps for energy in Finland. International Journal of Forest Engineering, 15(1): 3–8.
15. Jork, H., Funk, W., Fischer, W., Wimmer, H. (1994): Thin-Layer Chromatography: Reagents and Detection Methods, Volume 1b. 1st ed. Hoboken: Wiley-VCH.
16. Kai, D., Chow, L.P., Loh, X.J. (2018): Lignin and its properties. Chapter 1. In: Functional materials from lignin: Methods and advances, N. Gathergood, X. J. Loh, D. Kai, and Z. Li (Eds.). World Scientific: 1-29.
17. Kanbayashi, T., Hatae, J., Matsushita, Y. (2021): Photodegradation of lignin and other wood components under UV radiation. Journal of Wood Scienc*e*, 67: 1–10.
18. Karlsson, M. (2007): History of tar production from pine stumps in Sweden. In Walmsley, J. D., and Godbold, D. (Eds.), Stump Harvesting and Climate Change, Forestry Commission, UK: 23–26.
19. Khanina, L., Bobkova, K., Kobyakov, K., Smirnova, O. (2024): Changes in the concentration of chemical elements during decomposition of coarse woody debris in beech forests. Russian Journal of Ecology, 54(6): 658–665.
20. Lasota, J. (2018): Decomposition of wood residues in forest ecosystems and their influence on soil properties. Sylwan, 162: 131–138.
21. Martelanc, M., Naumoska, K., Vovk, I. (2016): Determination of common triterpenoids and phytosterols in vegetable waxes by HPTLC–densitometry and HPTLC–image analysis. Journal of Liquid Chromatography and Related Technologies, 39(5–6), 312–321.
22. Moffat, A.J., Nisbet, T.R., Nicoll, B.C. (2011): Environmental effects of stump and root harvesting. Forestry Commission Research Note. Edinburgh, UK: Forestry Commission.
23. N'Guessan, J.L.L., Bobelé F.N., N'guessan J.C.Y., Amusant, N. (2023): Wood Extractives: Main Families, Functional Properties, Fields of Application and Interest of Wood Waste. Forest Products Journal, 73(3): 194-208.
24. Nilsson, T. (2009): Fungal decomposition of lignocellulosic materials. International Biodeterioration, 63: 855–861.
25. Olsson, B.A., Staaf, H., Lundkvist, H., Bengtsson, J., Rosén, K. (1996): Carbon and nitrogen in coniferous forest soils after clear-felling and harvest of different intensities. Forest Ecology and Management, 82: 19–32.
26. Onuchin, E., Medyakov, A., Grunin, L., Sidorova, E. (2018): A study of the structure of wood damaged by rot using nuclear magnetic resonance. Journal of Applied Engineering Science, 16(2): 258–262.
27. Palviainen, M., Finér, L., Kurka, A.-M., Mannerkoski, H., Piirainen, S., Starr, M. (2015): Decomposition and nutrient release from logging residues after clear-cutting of mixed boreal forest. Forest Ecology and Management, 220: 155–165.
28. Persson, T. (Ed.) (2013): Environmental effects of stump harvesting. Forest Ecology and Management 290: 1–4.
29. Rahmati, Y., Nourmohammadi, K., Naghdi, R., Kartoolinejad, D. (2019): Effect of fungal degradation on physico-chemical properties of exploited stumps of oriental beech over a 25-year felling period and the obtained Kraft pulp properties. Journal of Forest Science, 65(3): 96–105.
30. Richardson, J., Bjorheden, R., Hakkila, P., Lowe, A.T., Smith, C. T. (2002): Bioenergy from sustainable forestry: guiding principles and practice. Springer Science and Business Media.

31. Runge, T., Wipperfurth, P., Zhang, C. (2013): Improving biomass combustion quality using a liquid hot water treatment, Biofuels, 4(1): 73-83.
32. Saha, B.C. (2003): Hemicellulose Bioconversion. Journal of Industrial Microbiology and Biotechnology, 30: 279-291.
33. Sánchez, O., Sierra, R., Alméciga-Díaz, J.C. (2011): Delignification process of agro-industrial wastes: An alternative to obtain fermentable carbohydrates for producing fuel. In Alternative Fuel. InTech.
34. Ştefănescu, R., Ciurea, C.N., Mare, A.D., Man, A., Nisca, A., Nicolescu, A., Mocan, A., Babotă, M., Coman, N.A., Tanase, C. (2022): *Quercus robur* Older Bark—A Source of Polyphenolic Extracts with Biological Activities. Applied Sciences, 12(22): 11738.
35. Sucre, E.B., Fox, T.R. (2009): Soil nutrient and carbon pools in loblolly pine forests following stump removal and site preparation. Forest Ecology and Management, 258: 1786–1793.
36. Taylor, A.M., Gartner, B.L. Morrell, J.I. (2002): Heartwood Formation And Natural Durability – A Review, Wood and Fiber Science, 34(4): 587-611.
37. Teeri, T., Henriksson G. (2009): Enzymes Degrading Wood Components. Ch 11. In: Wood Chemistry and Biotechnology. M. Ek, G. Gellerstedt, and G. Henriksson (Eds.), Walter de Gruyter GmbH and Co. KG, Berlin: 245-272.
38. Tomak, E.D. (2014): Fungal degradation of lignin in wood. International Biodeterioration and Biodegradation, 90, 142–147.
39. Valette, N., Perrot, T., Sormani, R., Gelhaye, E., Morel-Rouhier, M. (2017): Fungal degradation of wood: From fundamentals to biotechnology. Current Forestry Reports, 3: 29–50.
40. van Geffen, K.G., Berg, M.P., Aerts, R. (2010): Potential role of litter quality in the effects of climate change on decomposition in southeastern Mediterranean ecosystems. Plant and Soil, 334, 365–376.
41. Wagner, H., Bladt, S., Ygainski, E.M. (1984): Plant Drug Analysis. 1st ed. Springer-Verlag GmbH, Heidelberg.
42. Walmsley, J.D., Godbold, D.L. (2010): Stump harvesting for bioenergy – A review of the environmental impacts. Forestry, 83(1): 17–38.
43. Wang, C., Zhang, Q., Wang, Z. (2022): Carbon and nutrient dynamics of decaying tree stumps in forest ecosystems. Science of the Total Environment, 838, 156117.
44. Xie, Z., Liang, X., Liu, H., Deng, X., Cheng, F. (2024): Nutrient Element Stocks and Dynamic Changes in Stump–Root Systems of *Eucalyptus urophylla* × *E. grandis.* Forests 15 (1): 1.
45. Zhang, B., Cai, J., Duan, C.Q., Reeves, M., He, F. (2015): A Review of Polyphenolics in Oak Woods. International Journal of Molecular Sciences, 16(4): 6978–7014.
46. Zhu, W., Liu, W., Chen, H., Jiang, L., Li, H. (2017): Climatic control of wood decomposition rates across forest ecosystems. Global Ecology and Biogeography, 26, 1364–1375.

Acknowledgments

This work was supported by the Ministry of Science, Technological Development and Innovation of the Republic of Serbia, contract numbers: 451-03-137/2025-03/200169.

The Authors' Address:

Dr. **Jasmina Popović**, associate professor; MSc. **Gordana Petković**, PhD candidate; **Miloš Šuljagić**, undergraduate student; Dr. **Mlađan Popović**, full professor; Dr. **Milanka Điporović-Momčilović**, full professor; Dr. **Ivana Stojiljković**, assistant professor; University of Belgrade, Faculty of Forestry, Kneza Višeslava 1, Belgrade, Serbia;

MSc. **Radoslav Lozjanin**, PhD candidate; Public Enterprise "Vojvodinašume", Novi Sad, Serbia

INFLUENCE OF BIOMASS TO GLYCEROL RATIO ON THE LIQUEFACTION OF OAK (*QUERCUS ROBUR*) AND HEMP (*CANNABIS SATIVA*) FOR USE IN FORMALDEHYDE-FREE ADHESIVES

Božidar Matin[1], Ana Matin[2], Ivan Brandić[2], Mario Jurišić[1], Dario Pervan[1], Josip Ištvanić[1], Alan Antonović[1]

[1]*University of Zagreb, Faculty of Forestry and Wood Technology, Zagreb, Croatia, e-mail:bmatin@sumfak.unizg.hr; mjurisic@sumfak.unizg.hr; dpervan@sumfak.unizg.hr; jistvanic@sumfak.unizg.hr; aantonovic@sumfak.unizg.hr*
[2]*University of Zagreb, Faculty of Agriculture, Zagreb, Croatia, e-mail:amatin@agr.hr;* ibrandic@agr.hr

ABSTRACT

The increasing demand for sustainable materials has accelerated efforts to replace formaldehyde-containing adhesives in wood composites with bio-based alternatives. In this study, the liquefaction of oak wood (Quercus robur) and hemp stalks (Cannabis sativa) using glycerol as a solvent and sulphuric acid as a catalyst under controlled conditions (150 °C, 120 min) is investigated. Three ratios of biomass to solvent (1:3, 1:4 and 1:5) were analysed. The oak biomass showed liquefaction percentage of liquefaction of up to 93.88%, with insoluble residues between 6.12 and 14.45% and a dry matter content between 50.13 and 54.78%. The hydroxyl number reached a maximum of 841.43 mg KOH/g, indicating a high density of reactive functional groups. Hemp biomass showed liquefaction percentage of liquefaction of up to 91.64%, insoluble residues of 8.36 to 15.27%, a dry matter content between 57.19 and 63.28% and a hydroxyl number of up to 829.61 mg KOH/g. Optimum results for both biomass types were achieved at a ratio of 1:5. These results emphasise the potential of liquefied oak and hemp as promising candidates for the development of formaldehyde-free adhesives that promote the use of environmentally friendly materials in the production of wood-based materials.

Keywords: oak, hemp, glycerol, liquefaction, hydroxyl number.

1. INTRODUCTION

The increasing global demand for energy and the environmental concerns associated with fossil fuel consumption have fuelled efforts to develop renewable energy sources. Biomass has emerged as a promising alternative due to its renewability, biodegradability and ability to be converted into fuels, chemicals and energy carriers (Chowdhury et al., 2025.). The efficient utilisation of biomass requires an understanding of its chemical composition, especially cellulose, hemicellulose, lignin and minor extractives. Among the thermochemical conversion processes, liquefaction is particularly effective in converting biomass to liquid intermediates using alcohols or phenolic solvents. Process efficiency is influenced by temperature, solvent to biomass ratio, catalyst concentration and reaction time. Lignin is generally easier to liquefy than hemicellulose and cellulose. Liquefied biomass is used in applications such as resin synthesis and the production of composite materials, especially when phenol is used as a solvent (Antonović et al., 2014.; Feng et al., 2018.; Zhou et al., 2023.).

Forest-derived biomass accounts for a significant proportion of the world’s biomass resources, making hardwood species such as oak valuable candidates for the development of bio-based materials due to their favourable composition and structural properties (Parikka, 2004.). In addition to lignocellulosic raw materials from forestry, agricultural crops such as hemp offer high biomass yields and favourable fibre properties. Hemp is one of the fastest growing crops and is known for its strong natural fibres and wide industrial applicability. The chemical composition of hemp fibres includes a high proportion of cellulose, moderate amounts of hemicellulose and a lower proportion of lignin. Possible uses include textiles, paper, composites and thermal insulation, with additional potential for the production of biofuel from stalk residues (Ahmed et al., 2022).

In this study, the liquefaction behaviour of oak and hemp is investigated under identical process conditions (150 °C, 120 min, solvent to biomass ratio 1:3, 1:4 and 1:5) to evaluate their suitability for conversion into precursors for biocomposite materials.

2. MATERIALS AND METHODS

2.1. Raw material collection and sampling

Oak and hemp biomass was used for the research. The hemp biomass came from a private producer in the Zagreb region, while the oak biomass was obtained from the company Bjelin Spačva d.o.o., in Vinkovci, Croatia. The chemical analyses were carried out in the laboratories of the University of Zagreb, Faculty of Forestry and Wood Technology, and Faculty of Agriculture, using standardised methods. Before being analysed, the biomass samples were dried for 48 hours in a Memmert UF 160 laboratory dryer (Memmert GmbH, Germany) at a constant temperature of 60 °C. This drying process ensured moisture equilibrium in the material, and allowed a consistent basis for comparison between the samples under standardised conditions.

2.2. Methods

2.2.1. Preparation of samples for analysis

After the drying process, the biomass was first ground using an SM400 laboratory mill (Retsch GmbH, Germany) equipped with a 6.0 mm round-hole sieve, in accordance with the HRN EN ISO 14780:2017 standard. The material was then further processed using an SR300 hammer mill (Retsch GmbH, Germany) with a 1.0 mm trapezoidal perforated sieve, which also complies with the same standard. The samples were then sieved using a Retsch AS 200 BASIC vibrating sieve shaker (Retsch GmbH, Germany), in accordance with the HRN EN ISO 17827-2:2016 standard. Various mesh sizes were used, in accordance with the ISO 3310-1:2016 specification, in order to achieve the desired particle size distribution. After the grinding and sieving process, particles with a size of 0.50 to 1.00 mm were selected for further analysis, as this size range has been shown in previous studies to be optimal for isolating the desired chemical components. To ensure the reproducibility of the results, each sample was analysed at least three times.

2.2.2. Lignocellulosic composition

The analysis of the lignocellulosic composition, in particular the extractives, cellulose, lignin, and hemicellulose, was carried out according to standardised methods and previous studies (Antonović et al., 2019; Jovičić et al., 2022; Matin et al., 2024). The structural analysis included the determination of the extract content (TAPPI T 204) using a Soxhlet R108S BEHRotest extractor (Behr Labour-Technik GmbH, Germany), with a solvent mixture of methanol (CH_3OH) and benzene (C_6H_6) in a volume ratio of 1:1. The cellulose content was determined by treating the sample with a mixture of nitric acid (HNO_3) and ethanol (C_2H_5OH) in a volume ratio of 1:4 and then boiling in a Hydro H9V Lauda water bath (Lauda GmbH, Germany). The lignin content was analysed according to the TAPPI T 222 standard, using 72% sulphuric acid (H_2SO_4) and heating on an IKA C-MAG HS 7 magnetic stirrer (IKA®-Werke GmbH & Co. KG, Germany). The hemicellulose (HC) content was calculated using the following equation:

$$HC = 100 - (\text{ash\%} + \text{extractives\%} + \text{cellulose\%} + \text{lignin\%})$$

2.2.3. Liquefaction of the biomass samples

The liquefaction process was performed according to previous research (Jovičić et al., 2022.). Glycerol ($C_3H_8O_3$), a type of polyhydric alcohol, was used as the liquefying agent, while 3% sulphuric acid (prepared from 98% H_2SO_4) served as the acid catalyst. Liquefaction was carried out in a 500 mL round bottom flask equipped with a condenser and heated using a magnetic stirrer controlled by a thermostatically controlled hot plate. The process began with the addition of 50 g glycerol and 1.5 g sulphuric acid to the flask. The mixture was stirred and heated until it reached a temperature of 150 °C. Once the target temperature was reached, a measured amount of the biomass sample was added to the flask. The amount of biomass varied depending on the chosen mass ratio between the

sample and the solvent mixture (1:3, 1:4, or 1:5). Liquefaction was then carried out for 120 minutes at 150 °C, with the temperature of the solvent being continuously monitored throughout the process.

2.2.4. Analysis of the liquefied biomass samples

The analysis of liquefied biomass samples in this study was performed according to methods established in previous studies by Antonović et al. (2019) and Matin et al. (2024). These studies provided a comprehensive framework for evaluating the key properties of liquefied lignocellulosic materials, that are critical for assessing the efficiency of the liquefaction process and the potential application of the resulting polyols. By applying and adapting these validated methods, this study ensured consistency with the existing literature while allowing comparison of results for different biomass types and process conditions.

2.2.4.1. Insoluble residue

The insoluble residue (IR) refers to the portion of the biomass that does not dissolve during the liquefaction process and remains as a solid. To determine this proportion, the liquefied samples were treated with a solvent mixture of 1,4-dioxane and water in a volume ratio of 8:2. The liquefied mixture was stirred thoroughly on a magnetic stirrer for 60 minutes, and then filtered through a B2 glass fibre filter. The filtrate was repeatedly washed with the same solvent mixture until a colourless solution was obtained, ensuring complete removal of the soluble components. The remaining dioxane-insoluble fraction was then dried in a laboratory oven at 105 °C until a constant weight was reached. The mass of the dried insoluble residue was recorded and expressed as a percentage of the original mass of the liquefied sample. The percentage of insoluble residue was calculated using the following equation:

$$IR = [m(fp+ds) - m(fp)] / m(s) \times 100 \ (\%)$$

where:
m(fp + ds) - the mass of the filter paper together with the dried sample (g),
m(fp) - the mass of the filter paper (g),
m(s) – the mass of the sample (g).

2.2.4.2. Liquefaction percentage

The liquefaction (LP) indicates the proportion of biomass that has been successfully converted into a liquid state during the liquefaction process. To determine the LP, 1 g of the liquefied biomass sample is weighed into a dry beaker. Subsequently, 100 mL of distilled water and a magnetic stirrer are added. The beaker is then placed on a magnetic stirrer with several positions and stirred for 30 minutes. During this time, the mass of a filter paper is measured. After stirring, the mixture is filtered through the weighed filter paper, which is placed in a glass funnel over an Erlenmeyer flask. The undissolved part of the sample remains on the filter paper, while the dissolved fraction passes into the flask. The filter paper with the solid residue is then dried at 80 °C ± 2 °C for 24 hours until a constant weight is achieved. The liquefaction percentage is calculated using the following equation:

$$LP = 100 - \text{Insoluble residue (IR)} \quad (\%)$$

2.2.4.3. Dry matter

The dry matter content (DM) of liquefied wood indicates the amount of solid substances that remain in the liquid product after the thermochemical liquefaction of wood biomass. To determine the dry matter content, an empty watch glass was first weighed. Then, 1 g of the liquefied sample was placed on the watch glass. The samples were dried in a dryer at 150 ± 2 °C for 24 hours, cooled in a desiccator, and weighed again together with the watch glass. The percentage of dry matter was calculated using the following equation:

$$DM = [m(wg+ds) - m(wg) / m(s)] \times 100 \quad (\%)$$

where:
m(wg+ds) - mass of the watch glass plus dried sample (g),
m(wg) - mass of the empty watch glass (g),
m(s) - mass of the original sample (g).

2.2.4.4. Hydroxyl (OH) number

The hydroxyl number (OH) indicates the amount of potassium hydroxide (KOH), in milligrammes, that is required to neutralise the hydroxyl groups in one gramme of a sample. It serves as a quantitative measure of the content of hydroxyl groups (OH) in chemical compounds and is given in mg KOH/g. This parameter is a key indicator of the hydroxyl group concentration in polyols and plays a crucial role in the formation of urethane bonds, which have a direct impact on the physical and mechanical properties of the resulting polyurethane products. A higher hydroxyl number corresponds to a larger number of reactive hydroxyl groups, which leads to stronger cross-linking and, consequently, to a stiffer and more durable end material. Therefore, monitoring and controlling the hydroxyl number is essential in polyol production.

The OH number was determined according to the methods described in previous studies. A sample weighing between 0.51 and 0.56 g was placed in a beaker, to which 25 mL of an esterification reagent was added. The beaker was then heated in a water bath for 5 to 10 minutes, until the sample separated from the bottom. The beaker was then kept in a water bath at 98 ± 2 °C for 15 minutes, with the water level adjusted so that the part of the beaker containing the sample was submerged.

After heating, the samples were removed from the water bath and allowed to cool. Then, 50 mL of pyridine and 10 mL of hot distilled water were added to each beaker. A magnetic stirrer was introduced, and the beaker was placed on a magnetic stirrer for thorough mixing. A pH metre was introduced into the mixture to monitor the titration process. Instead of flasks, beakers with lids were used to accommodate the pH metre during the titration. Finally, the samples were titrated to the equivalence point using a previously standardised 0.5 M potassium hydroxide (KOH) solution.

The hydroxyl number (OH) of the liquefied biomass sample, expressed in mg KOH/g, was calculated using the following equation:

$$OH = [(B-A)\times N\times 56.1/\ m] \times 100 \quad (\%)$$

where:

B - consumption of KOH (mL),

A - consumption of KOH for the blank test (mL),

N - normality of the solution,

m - mass of the sample (g).

3. RESULTS AND DISCUSSION

In this study, the effect of different biomass-solvent ratios on key liquefaction properties was investigated, including liquefaction percentage, isolable residue, dry matter and hydroxyl value (OH). The results of the lignocellulosic composition are shown in Table 1.

Table1. *Lignocellulose composition of the oak and hemp biomass samples (%).*

Sample	Cellulose	Lignin	Hemicellulose	Extractives
Oak	48,91	25,78	22,01	3,64
Hemp	47,13	21,89	17,10	4,89

Table 2. shows the degree of liquefaction, the isolable residue, the dry matter and the hydroxyl value (OH) of the liquefied biomass samples of oak and hemp.

Table 2. *Percentage of LP, IR, DM (%) and OH number (mg KOH/g) in the liquefied samples of oak and hemp.*

Sample	Ratio	LP	IR	DM	OH
Oak	1/3	85,55	14,45	54,78	639,12
	1/4	89,11	10,89	52,91	742,23
	1/5	93,88	6,12	50,13	841,43
Hemp	1/3	84,73	15,27	63,28	561,68
	1/4	87,45	12,55	58,99	782,38
	1/5	91,64	8,36	57,19	829,61

Since the hydroxyl number (OH number) is the most critical parameter in liquefaction, and provides essential information about the reactivity and binding potential of the liquefied biomass in subsequent syntheses, it is considered more important than other liquefaction properties such as the liquefaction percentage and the dry matter content.

Lignocellulosic composition analysis revealed that oak biomass contains slightly more cellulose (48.91%) and lignin (25.78%) compared to hemp (47.13% and 21.89%, respectively). This indicates that oak has a stiffer structure, which could make it more resistant to chemical degradation during liquefaction. The hemicellulose content was also higher in oak (22.01%) than in hemp (17.10%), indicating a potentially higher reactivity of oak in the early stages of liquefaction, as hemicellulose is more easily degraded than cellulose. On the other hand, hemp showed a higher content of extractives (4.89%) than oak (3.64%). These non-structural compounds can influence the liquefaction process by increasing the reactivity or influencing the composition of the final product.

The lignocellulosic composition of oak wood does not deviate from the literature data, in which Antonović et al. (2019) report 47.23% cellulose and 21.82% lignin, Donata et al. (2010) 46.3 to 48.1% cellulose, 26.5 to 27.1% lignin and 3.8 to 4.2% extractives, and Matin et al. (2025.) 49.11% cellulose, 29.43% lignin, 14.95% hemicellulose and 7.74% extractives.

According to Marrot et al. (2022), the chemical composition of hemp comprises 46.1% cellulose, 22.81% lignin, 24.12% hemicellulose, and 4.14% extractives. Similarly, Danielewicz and Surma-Ślusarska (2010) reported a cellulose content of 36.3 to 46.9%, a lignin content of 18.2 to 27.1%, a hemicellulose content of 21.9 to 34.3%, and an extractives content of about 1.2%. These values show that the results obtained in this study are generally consistent with the values reported in the literature.

The liquefaction results showed that the biomass to solvent ratio had a significant effect on all analysed parameters: liquefaction percentage (LP), insoluble residue (IR), dry matter content (DM), and hydroxyl number (OH), for both oak and hemp samples. As expected, increasing the amount of solvent (i.e., changing from a 1:3 to a 1:5 biomass to solvent ratio) resulted in a higher degree of liquefaction.

For oak, the degree of liquefaction increased from 85.55 (1:3 ratio) to 93.88% (1:5), while for hemp it increased in the same range from 84.73 to 91.64%. Accordingly, the amount of insoluble residue decreased the more biomass was converted into the liquid phase, with a decrease from 14.45 to 6.12%, for oak and from 15.27 to 8.36% for hemp. The dry matter content showed a decreasing trend with higher solvent contents. Oak showed a decrease from 54.78 to 50.13%, while hemp showed a stronger decrease from 63.28 to 57.19%. This trend indicates a dilution effect, as a larger volume of solvent reduces the concentration of solids in the liquefied mixture. The hydroxyl number, which is a key indicator of the reactivity of the liquefied product, increased significantly with higher solvent levels. For oak, the OH number increased from 639.12 (1:3) to 841.43 mg KOH/g (1:5), and for hemp from 561.68 to 829.61 mg KOH/g. This increase is related to the more efficient degradation of biomass components and the release of hydroxyl-rich compounds under higher solvent volumes, making the resulting polyols more suitable for further polyurethane synthesis.

Overall, the oak samples showed a slightly higher liquefaction efficiency and higher OH values compared to hemp under the same conditions, suggesting a greater potential for polyol production. However, the hemp-based liquefied products showed a higher dry matter content at each ratio, which may be advantageous in applications where solids yield is a priority. Comparing the results obtained with previous studies (Antonović et al., 2019; Đurović et al., 2024; Matin et al., 2025), it can be

concluded that both oak and hemp biomass have sufficiently favourable liquefaction properties for further application.

4. CONCLUSION

This study showed that the ratio of biomass to glycerol significantly affects the liquefaction efficiency of oak (Quercus robur) and hemp (Cannabis sativa), and has an impact on key parameters such as liquefaction percentage, insoluble residue, dry matter, and hydroxyl number. Increasing the solvent ratio improved the liquefaction efficiency, with the 1:5 ratio giving the best results for both biomasses. Oak showed slightly better overall performance, but hemp also proved to be a promising alternative for bio-based applications. The hydroxyl number was confirmed as the most important indicator of suitability for further use in formaldehyde-free adhesives. These results underpin the potential of oak and hemp as sustainable raw materials for environmentally friendly adhesive systems, and provide a basis for future research to optimise liquefaction conditions and expand the development of bio-based adhesives.

ACKNOWLEDGEMENT

This research was funded as part of the project “Light massive products - an innovative method of expanding foam in furniture with higher added value”

REFERENCES

1. Ahmed, A. F., Islam, M. Z., Mahmud, M. S., Sarker, M. E., Islam, M. R. (2022): Hemp as a potential raw material toward a sustainable world: A review. Heliyon, 8(1).
2. Antonović, A., Ištvanić, J., Medved, S., Antolović, S., Stanešić, J., Kukuruzović, J., Đurović, A., Španić, N. (2019): Influence of Different Wood Specie Chemical Composition on the Liquefaction Properties. In Proceedings of the 30th International Conference on Wood Science and Technology, Zagreb, Croatia, 12–13 December 2019; Volume 25.
3. Antonović, A., Jambreković, V., Španić, N., Medved, S., Ištvanić, J., Devčić, M. (2014): Influence of pH Value of Liquefied Wood as a Hardener of Urea-Formaldehyde Resin with 4% Melamine Addition in Particleboard Production. In *25th International Scientific Conference-NEW MATERIALS AND TECHNOLOGIES IN THE FUNCTION OF WOODEN PRODUCTS* (pp. 135-144).
4. Chowdhury, P., Mahi, N. A., Yeassin, R., Chowdhury, N. U. R., Farrok, O. (2025): Biomass to biofuel: Impacts and mitigation of environmental, health, and socioeconomic challenges, Energy Conversion and Management: X, Volume 25,100889,
5. Danielewicz, D., Surma-Ślusarska, B. (2010): Processing of industrial hemp into papermaking pulps intended for bleaching. *Fibres Text. East. Eur*, *18*(6), 110-114.
6. Donata, K., Andrzej, R., Janusz, Z., Zielenkiewicz, T., Antczak, A. (2010): Comparison of the chemical composition of the fossil and recent oak wood. Wood Res, 55, 113-120.
7. Đurović, A., Matin, B., Brandić, I., Tomić, I., Matin, A., Antonović, A. (2024): Influence of soybean (Glycine max) and hemp (Cannabis sativa) stalks biomass to glycerol solvent ratio on liquefied properties. In 59th Croatian and 19th International Symposium on Agriculture (pp. 507-513).
8. Feng, S., Wei, R., Leitch, M., Xu, C. C. (2018): Comparative study on lignocellulose liquefaction in water, ethanol, and water/ethanol mixture: Roles of ethanol and water. Energy, 155, 234-241.
9. HRN EN ISO 14780:2017 Solid biofuels – Sample preparation (ISO 14780:2017; EN ISO 14780:2017).
10. HRN EN ISO 17827-1:2024 Solid biofuels -- Determination of particle size distribution for uncompressed fuels -- Part 1: Oscillating screen method using sieves with apertures of 3,15 mm and above (ISO 17827-1:2024; EN ISO 17827-1:2024)
11. Jovičić, N., Antonović, A., Matin, A., Antolović, S., Kalambura, S., Krička, T. (2022): Biomass valorization of walnut shell for liquefaction efficiency. Energies, 15(2), 495.

12. Marrot, L., Candelier, K., Valette, J., Lanvin, C., Horvat, B., Legan, L., DeVallance, D. B. (2022): *Valorization of hemp stalk waste through thermochemical conversion for energy and electrical applications. Waste Biomass Valorization 13: 2267–2285*.
13. Matin, B., Jovičič, N., Krička, T., Jurišić, V., Matin, A., Grubor, M., Bilandžija, N., Đurović, A., Antonović, A. (2024): Comparison of the physico-chemical properties of liquefied biomass from oak (Quercus robur L.) and walnut shell (Juglans regia L.) for the production of biocomposites. In 59th Croatian and 19th International Symposium on Agriculture (pp. 489-493).
14. Matin, B., Mikulić Alilović, I., Brandić, I., Matin, A., Jurišić, V., Špelić, K., Ištvanić, J. Antonović, A. (2025): The polymer properties of liquefied oak biomass (Quercus robur L.) as a potential additive. In *Proceedings of the 50th International Symposium Opatija, Croatia, 11th–13th March 2025* (pp. 399-408). Zagreb: University of Zagreb Faculty of Agriculture.
15. TAPPI – T 204 Solvent Extractives of Wood and Pulp 2007, Technical Association of the Pulp and Paper Industry.
16. TAPPI - T 222 Acid-insoluble lignin in wood and pulp 2002, Technical Association of the Pulp and Paper Industry.
17. Parikka, M. (2004): Global biomass fuel resources. Biomass and bioenergy, 27(6), 613-620.
18. Zhou, Z., Ouyang, D., Liu, D., Zhao, X. (2023): Oxidative pretreatment of lignocellulosic biomass for enzymatic hydrolysis: Progress and challenges. *Bioresource Technology*, *367*, 128208.

The Authors' Address:

Božidar Matin MSc, University of Zagreb Faculty of Forestry and Wood Technology, Svetošimunska cesta 23, Zagreb, Croatia,

Professor PhD Ana Matin, University of Zagreb Faculty of Agriculture, Svetošimunska cesta 25, Zagreb, Croatia,

PhD Ivan Brandić, University of Zagreb Faculty of Agriculture, Svetošimunska cesta 25, Zagreb, Croatia,

Mario Jurišić MSc, University of Zagreb Faculty of Forestry and Wood Technology, Svetošimunska cesta 23, Zagreb, Croatia,

Dario Pervan MSc, University of Zagreb Faculty of Forestry and Wood Technology, Svetošimunska cesta 23, Zagreb, Croatia,

Associate Professor PhD Josip Ištvanić, University of Zagreb Faculty of Forestry and Wood Technology, Svetošimunska cesta 23, Zagreb, Croatia.

Professor PhD Alan Antonović, University of Zagreb Faculty of Forestry and Wood Technology, Svetošimunska cesta 23, Zagreb, Croatia.

THE IMPACT OF BEECH LOG QUALITY ON THE WORKLOAD OF THE PRODUCTION SYSTEM IN THE SAWMILL PROCESSING

Ranko Popadić[1], Goran Milić[1], Nebojša Todorović[1], Marko Veizović[1]

[1]University of Belgrade – Faculty of Forestry, Department of Wood Science and Technology, Belgrade, Republic of Serbia
e-mail: ranko.popadic@sfb.bg.ac.rs; goran.milic@sfb.bg.ac.rs; nebojsa.todorovic@sfb.bg.ac.rs;marko.veizovic@sfb.bg.ac.rs

ABSTRACT

This paper examines the impact of beech log quality on the workload of the production system during sawmill processing. Specifically, it analyzes the extent to which labor and machinery utilization depend on the quality of the processed roundwood. The research was conducted on a sample of 60 beech sawlogs with diameters ranging from 30 to 39 cm and a length of 4 m, which were classified into three quality grades. The logs were sawn using a log band saw and a resaw band saw, applying free sawing methods and quality-based cutting. The resulting sawn timber was then photographed, enabling the use of photogrammetry to determine the exact dimensions of the assortments and the distribution of wood defects. Based on these images, a simulation of the secondary processing of the obtained assortments was conducted to assess the workload on secondary machines. Subsequently, data from primary machines were incorporated into the calculation, and the total workload of the production system was determined. The results indicate that the workload of individual workstations varies significantly, depending on the distribution of wood defects and the decision regarding which machine will be used for defect removal. However, it was established that a decrease in raw material quality leads to an increase in overall system workload.

Keywords: sawmill processing, log quality, production system workload, beech wood.

1. INTRODUCTION

The profitability of processing beech sawlogs depends not only on the prices of raw logs and finished products but also on a range of production-related factors. While raw material and product prices are driven by market forces and are generally beyond direct control, profitability analyses in sawmilling increasingly focus on optimizing raw material yield, selecting appropriate equipment, structuring the workforce efficiently, and managing production parameters.

A number of studies in the field of sawmilling can support such analyses. Ištvanić (2003) and Olufemi et al. (2012) compared yield across different wood species, while the influence of sawing methods, log diameter, and log quality on yield is discussed by Hapla and Ohnesorge (2005), Popadić et al. (2014), and Forghani et al. (2024). The impact of equipment selection and the sequence of technological operations is examined by Shepley et al. (2004), Clement et al. (2006), and Thomas and Buehlmann (2016). Economic aspects of wood processing are addressed by Mandiringana et al. (2022) and Buehlmann and Thomas (2025).

Overall processing costs are also significantly affected by labor utilization and applied technologies. This raises a critical question: to what extent can cost savings from purchasing lower-quality, cheaper raw materials be justified if processing such material leads to higher machine and labor utilization and a reduced overall processing capacity? The answer depends on several factors, including the technological capabilities and value of the installed equipment, current labor costs, raw material prices, and other operational conditions, making it a complex issue.

To contribute to a better understanding of this topic, the primary objective of this paper is to determine how sawlog quality affects the workload and utilization level of the production system during processing.

2. MATERIALS AND METHODS

The cumulative workload associated with processing each log was obtained by summing the time-based workloads of all workstations within the production line. Considering the heterogeneity in machinery—regarding technical parameters, automation, and human labor—the workload at each station was standardized and presented as time per log.

The research was conducted under industrial conditions in a sawmill that processes beech sawlogs into sawn timber for commercial purposes. Prior to analysis, the productivity of each workstation was established. It was acknowledged that the workloads of certain machines are interdependent and influenced by the operator's decisions regarding where specific cuts are performed. For instance, some primary cuts can be made on the log band saw or deferred to the resaw band saw. A similar relationship exists between the edging saw and the saw for flooring elements, as well as between the first and second crosscut saws. Therefore, the productivity of primary machines was determined as a group value, while the productivity of secondary machines was calculated as an average. An exception was made for the crosscut saw used for flooring elements, whose specific design and high operating speed justified a separate analysis.

The combined productivity of the primary machines (log band saw and resaw band saw), expressed in linear meters of cut, was 4.85 m/min. The average productivity of the secondary longitudinal saws was approximately 23 linear meters per minute. For crosscut saws used on sawn timber, the tool travel length is fixed (independent of the width of the processed assortment), so productivity was expressed as the number of crosscuts, which averaged seven per minute. The productivity of the crosscut saw for flooring elements was 20 cuts per minute. Based on these values, the workload norms were established: 0.117 minutes per cut for the timber crosscut saw and 0.05 minutes per cut for the flooring element crosscut saw.

The study utilized 60 logs with diameters ranging from 30 to 39 cm and a length of 4 m, classified into three quality grades according to the standard SRPS D.B4.028. The logs were sawn into timber of 25 mm and 50 mm thickness. Sawing patterns were documented during processing and later used to calculate the workload during the primary sawing stage.

The workload for secondary processing was determined by simulation, as recording each cutting bill under actual production conditions would have been impractical and would have significantly disrupted workflow. A photogrammetric approach was used, and the simulation proceeded as follows: all sawn timber obtained after log breakdown were photographed from both sides, allowing precise visualization of the distribution and size of wood defects. Based on the processed images, a simulation of the production of sawn timber and flooring elements for parquet production was carried out, applying a crosscutting-ripping-crosscutting process order, typical for beech secondary processing.

The resulting cuts were measured, and the workload for each board and log was calculated.

Measurements were conducted using Image Tool software, which, once calibrated to a known reference length, accurately determines real-world dimensions from photographs. All simulated cuts were verified to ensure compliance with dimensional standards. The software automatically transfers the recorded values from the image to a Microsoft Excel-compatible section of the application (Figure 1).

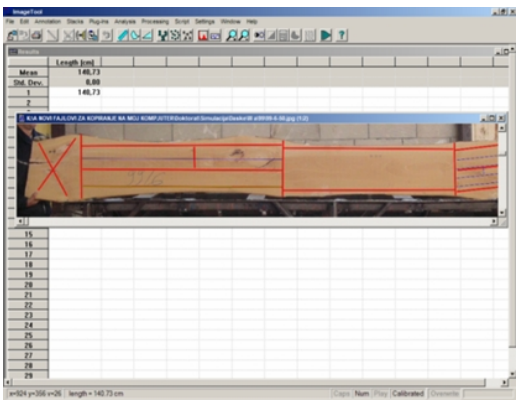

Figure 1. *Measurement of cut length and automatic data entry into the spreadsheet.*

Following the simulation, the calculation of the total workload for each individual log was carried out. The processing time of the primary machines was determined by multiplying the productivity rate of the primary machines (4.85 m/min) by the total length of primary cuts made from the log. The time-related workload associated with edging operations was calculated by dividing the total length of longitudinal cuts (performed on both edgers) by the average productivity rate (23 m/min). The workload associated with crosscutting operations was calculated by multiplying the respective number of cuts by the corresponding workload norms (0.117 or 0.05 minutes per cut). Finally, the total processing workload for each log was obtained by summing the times of all individual operations.

3. RESULTS AND DISCUSSION

The total length of primary cuts per log varied significantly, ranging from approximately 20.5 meters to over 65 meters. This variation is partly attributed to differences in log diameter and shape, as well as to the cutting of different timber thicknesses. However, the primary contributing factor was the presence of false heartwood. When false heartwood occupied a larger portion of the log volume, it was separated into individual assortments during primary cutting. As a result, the primary machines were subjected to increased workload due to a higher number of log rotations. Consequently, some of these logs showed lower workloads on the edging machines during the secondary processing stage.

The total length of cuts on edging machines ranged from approximately 52 to 103 meters per log, with most logs falling between 60 and 80 meters. These differences were primarily the result of variations in the number of assortments subjected to secondary processing and their respective quality.

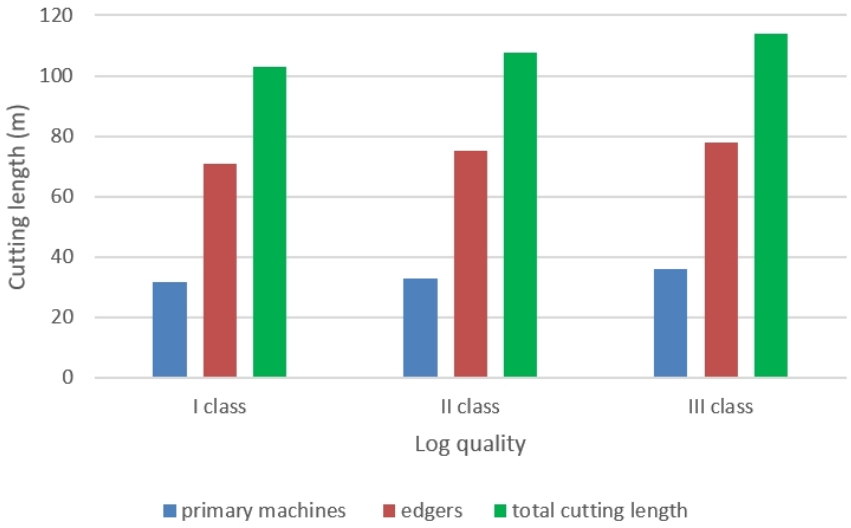

Figure 2. *Average cutting length per log by quality grade.*

As shown in Figure 2, the cutting length on secondary machines was 2-2.5 times greater than on primary machines. This is expected, considering that primary assortments are typically produced from a single primary cut (occasionally two, in the case of forming the opening face), while multiple cuts are necessary during secondary processing – particularly for edging and defect removal. The increase in total cutting length with decreasing log quality can be explained by the need for more log rotations during quality-based sawing, as well as the increased number of cuts required to eliminate wood defects.

The total number of crosscuts per log ranged from 25 to 135. Higher-quality logs, which contain fewer defects, required less crosscutting, whereas lower-quality logs processing resulted in a higher number of flooring elements and, therefore, more intensive crosscutting. Wood quality appears to have the most significant influence on the workload of the crosscutting stations. The average number of crosscuts per log, according to quality grade, is presented in Figure 3.

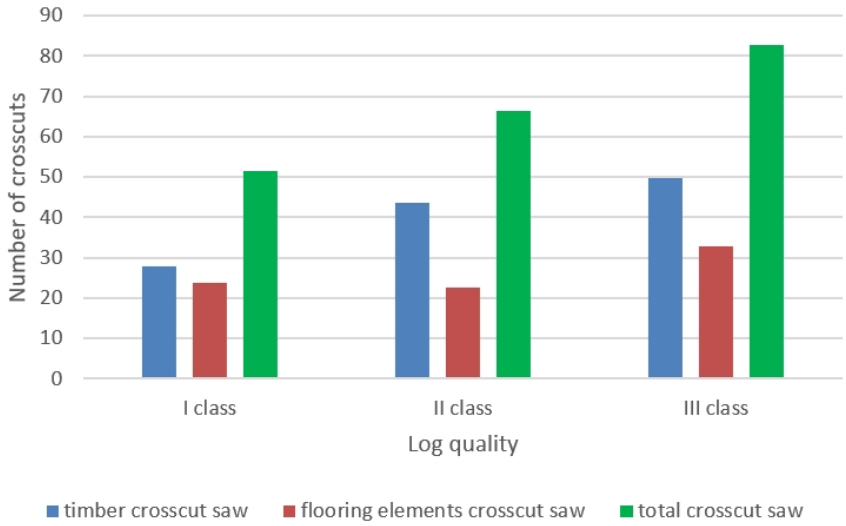

Figure 3. *Average number of crosscuts per log by quality grade.*

While cutting length and number of cuts provide useful insights into individual workstation workloads, the overall production system workload can only be accurately assessed through a common metric – time. Figure 4 shows the workload distribution among different system components, expressed in minutes per log.

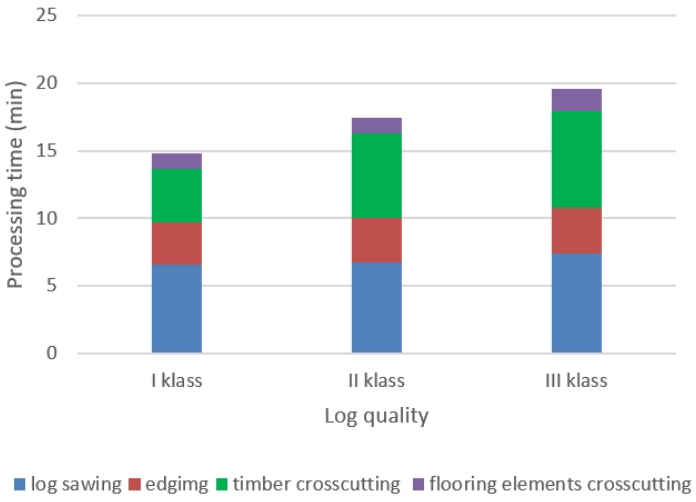

Figure 4. *Production system workload during processing of beech logs by quality grade.*

For the highest-quality logs, primary sawing operations consumed more time than other operations. However, as log quality decreased, crosscutting operations took longer. This is due to the increased number of assortments requiring intervention to remove wood defects, which, in the case of beech processing, is most often done by crosscutting. Longitudinal processing operations had the shortest durations and imposed the least workload on the system, primarily due to the high speed and capacity of edging machines. This also indicates that a relatively small number of defects are removed during longitudinal cutting.

The presented data clearly illustrate the previously discussed trends: system workload increases as log quality decreases, with the most significant rise observed in crosscutting operations of sawn timber and flooring elements. Total processing time depends on the applied technology, average dimensions and quality of the logs, and various other factors. Nonetheless, the results indicate that the workload during the processing of second-grade logs increases by approximately 20%, and for third-grade logs by about 35%, compared to first-grade beech sawlogs.

4. CONCLUSION

Based on the results of the study on the impact of sawlog quality on the workload of the production system during processing, the following conclusions can be drawn:

- The total length of primary cuts depends on the dimensions and shape of the logs, the thickness of the lumber being produced, and the number of log rotations during quality-based cutting – particularly in logs containing false heartwood.
- The cutting length on secondary machines is 2-2.5 times greater than on primary machines. Variations in the workload of edgers when processing individual logs are influenced by both the number and the quality of assortments entering secondary processing.
- Processing higher-quality logs results in a lower workload for crosscutting machines due to the reduced number of wood defects. As log quality decreases, the need for crosscuts increases, particularly with the higher production of flooring elements. Wood quality has the greatest impact on the workload at crosscutting workstations.
- During the processing of the highest-quality logs, primary sawing operations take the most time. However, as log quality decreases, the duration of crosscutting operations increases. Longitudinal processing of sawn timber contributes the least to overall system workload.
- The workload of the production system increases as the quality of sawlogs decreases. The total processing workload for second-grade logs is approximately 20% higher, and for third-grade logs about 35% higher, compared to the processing of first-grade beech sawlogs.

ACKNOWLEDGEMENTS

This study was financially supported by the Ministry of Science, Technological Development and Innovation of the Republic of Serbia (Grant No. 451-03-137/2025-03/200169).

REFERENCES

1. Buehlmann, U., Thomas, E. (2025). The impact of cost and price fluctuations on U.S. hardwood sawmill profit, BioResources, 20 (3):5587–5601.
2. Clement C., Lihra T., Gazo R., Beauregard R. (2006): Maximizing lumber use: The effect of manufacturing defects on yield, a case study, Forest Products Journal, 56 (1):60-65.
3. Forghani K., Carlsson M., Flener P., Fredriksson M., Pearson J., Yuan D. (2024): Maximizing value yield in wood industry through flexible sawing and product grading based on wane and log shape, Computers and Electronics in Agriculture, 216.
4. Hapla F., Ohnesorge D. (2005): Modelling of the sawn timber yield of beech logs with regard to the dimension and red heart proportion, Broad spectrum utilisation of wood, Cost Action E44 Conference in Vienna, 14. – 15. 6. 2005.
5. Ištvanić, J. (2003): Pilanska obradba bukve (Fagus sylvatica L.) u Hrvatskoj, Šumarski list, 7-8: 373-387 (in Croatian).
6. Mandiringana, M., Matakala, M., Mwanabute, N. P., Ngoma, J., Ncube, E. (2022). Analysis of the factors limiting the performance of small-to-medium scale sawmills in the copperbelt of Zambia, BioResources, 17 (1):369-383.
7. Olufemi, B., Akindeni, J.O., Olaniran, S.O. (2012): Lumber Recovery Efficiency among Selected Sawmills in Akure, Nigeria, Drvna industrija, 63 (1):15-18.
8. Popadić, R., Šoškić, B., Milić, G., Todorović, N., Furtula, M. (2014.): Influence of the Sawing Method on Yield of Beech Logs with Red Heartwood, Drvna industrija, 65 (1):35-42.
9. Shepley, B.P., Wiedenbeck, J., Smith, R.L. (2004): Opportunities for expanded and higher value utilization of No. 3A Common hardwood lumber, Forest Products Journal, 54 (9): 77-85.
10. Thomas, E., Buehlmann, U. (2016): Potential for Yield Improvement in Combined Rip-First and Crosscut-First Rough Mill Processing, BioResources, 11 (1):1477–1493.

ANALYSIS OF HEAT CONSUMPTION DURING CONVECTIVE WOOD DRYING OF BEECH SAWN TIMBER OF DIFFERENT THICKNESS

Goran Zlateski[1], Ana Marija Stamenkoska[1], Branko Rabadjiski[1]

[1]Ss. Cyril and Methodius University in Skopje, North Macedonia,
Faculty of design and technologies of furniture and interior-Skopje
e-mail: zlateski@fdtme.ukim.edu.mk; stamenkoska@fdtme.ukim.edu.mk;
rabadziski@fdtme.ukim.edu.mk

ABSTRACT

In the paper, the heat consumption of beech sawn timber with a thickness of 50,0 and 70,0 (mm) are analyzed under conditions of classic convective drying. The drying mode is compiled on the basis of data on the temperature of the drying agent (air), the relative humidity of the air and the speed of air movement in accordance with the current value of moisture in the wood.

The heat consumption is analyzed in all stages of the drying cycle such as heating the wood, active drying of the wood and conditioning, i.e. equalization of the moisture in the cross-section within ± 2.0 (%). The moisture content of sawn timber at the beginning of drying is about 45,0 (%) and at the end of drying is 8,0 (%).

Keywords: beech, sawn timber, convective drying, heat consumption.

1. INTRODUCTION

The research related to energy consumption in the wood industry in general, and especially the research on the calculation of heat consumption for the purposes of wood drying, has always attracted the attention of the scientific public for obtaining results that will open opportunities for increasing energy efficiency.

In every company from the wood industry that is engaged in the production of solid wood products (chairs, tables ...), it is necessary to have installed a dryer for artificial drying of the wood.

The convective drying method is the most widely accepted method in wood drying technology, which uses hot air of certain thermodynamic parameters in order to evaporate moisture from the wood. It's the method of modern operation (drying) and timely delivery of quality dry wood with a final percentage of moisture suitable for the production of solid wood product.

These wood drying facilities are made with the most modern materials to prevent corrosion and equipped with modern devices for tracking, controlling and realizing the drying cycle defined by an appropriate schedule for drying the sawmill assortments.

The drying regime is composed of the values of the temperature and relative humidity of the drying agent (atmospheric air) matched with the values of moisture in the wood at the beginning, during and at the end of the drying process.

Several authors like Vengert and Meyer (1993), Denig et al (1996), Seeger (1989), Kolin (2000), Barišić (1957), Milić (2020), Zlateski et al (2023) and FAO organization (1990) as well reported energy consumption for hardwood species from 2,15 to 3,5 (GJ/m^3) depending on the construction of dry kiln, wood species, wood thickness and initial moisture content of wood.

Taking into account that the largest part of the total energy consumption in the wood industry belongs to the consumption of heat energy for the purposes of artificial drying of the wood, we decided to make a detailed analysis (calculation) of total heat quantity for one drying cycle of beech sawn timber with thickness of 50,0 (mm) and 70,0 (mm) as well.

We believe that the obtained results will contribute to the improvement and rationalization of the processes of wood drying and thus the realization of an economic benefit to the overall operation of the companies from the wood industry.

2. MATERIALS AND METHODS

The drying of sawn timber of beech (*Fagus Sylvatica* L) was carried out in a dryer for artificial convective drying equipped with a device for automatic drying management. Sawn timber with a thickness of 50,0 (mm) are dried separately from those with a thickness of 70,0 (mm). Characteristics of the material as well as the dryer are shown in table 1, table 2 and table 3 as well.

Table 1. *Material properties of wood with 50,0 mm in thickness.*

Wood species	beech
Specific density	0,68 (g/cm^3)
Thickness of wood	50,0 (mm)
Initial wood moisture content	45,0 (%)
Final wood moisture content	8,0 (%)
Wood saturation point	31,0 (%)
Specific heat of dry wood	1,3563 (kJ/(kg℃)
Length of the stack	10,5 (m)
Width of the stack	6,5 (m)
Height of the stack	4,1 (m)
Volume of the wood	187,41 (m^3)
Thickness of the stickers	25,0 (mm)

Table 2. *Material properties of wood with 70,0 mm in thickness.*

Wood species	beech
Specific density	0,68 (g/cm^3)
Thickness of wood	70,0 (mm)
Initial wood moisture content	48,0 (%)
Final wood moisture content	8,0 (%)
Wood saturation point	31,0 (%)
Specific heat of dry wood	1,3563 (kJ/(kg℃)
Length of the stack	10,5 (m)
Width of the stack	6,5 (m)
Height of the stack	4,1 (m)
Volume of the wood	196,78 (m^3)
Thickness of the stickers	30,0 (mm)

Table 3. *Dry kiln properties.*

Drying method	convective
Construction	metal
Control of drying process	automatic
Length	l_s=8,5 (m)
Width	S_s=10,6 (m)
Height	h_s=5,26 (m)
Volume	V_s=468,52 (m^3)
Thickness of floor	d_p=200,0 (mm)
Thickness of wall	d_z=100,0 (mm)
Thickness of ceiling	d_t=100,0 (mm)
Thickness of door	d_v=100,0 (mm)
Duration of the drying cycle of wood- 25,0 in thickness	360,0 (h)
Duration of the drying cycle of wood- 50,0 in thickness	600,0 (h)
Working hours per year	6000 (h),
Air movement speed in the dryer	V_{vozduh}=2,5 (m/s)
Specific gravity of dry air	$\gamma_{suv\ vozduh}$=0,87 (kg/m^3)
Specific weight of the wall construction material	γ_{zid}=2900(kg/ m^3)

Specific gravity of the ceiling construction material	γ_{tavan}=2900(kg/ m^3)
Specific gravity of the floor construction material	γ_{pod}=2400(kg/ m^3)
Specific gravity of the door construction material	γ_{vrata}=2900(kg/ m^3)
Specific heat of the wall construction material	c_{zid}=0,85(kJ/(kg°C)
Specific heat of ceiling construction material	c_{tavan}=0,85(kJ/(kg°C)
Specific heat of the floor construction material	c_{pod}=0,922(kJ/(kg°C)
Specific heat of the door construction material	c_{vrata}=0,85(kJ/(kg°C)
Specific heat for other equipment (average)	$c_{ostanato}$=0,551(kJ/(kg°C)
Specific heat for dry air	$c_{suv\ vozduh=}$1,003(kJ/(kg°C)
Maximum temperature on the inside of the walls ie. temperature of the medium in the chamber	$t_{sredina}$=70,0 (°C)
Outside air temperature	$t_{nad.vozduh=}$20,0 (°C)
Average wall temperature	t_{zid}= 45,0 (°C)
Average ceiling temperature	t_{tavan}=45,0 (°C)
Average floor temperature	t_{pod}= 45,0 (°C)
Average door temperature	t_{vrata}=45,0 (°C)
Average temperature of the rest	$t_{ostanato}$= 45,0 (°C)
Coefficient of heat transfer - floor	k_{pod}= 13,84 (kJ/(m^2 h°C)

The total amount of heat for one drying cycle:
a) heating the dryer,
b) heating the wood and stickers to a drying temperature,
c) heat loss during drying,
d) heating the air in the dryer,
e) heating and evaporation of moisture from the wood and
f) heating the air in the dryer.

$$\sum Q = \left(Q_{komora} + Q_{drvo+letvi} + Q_{zaguba} + Q_{vozduh} + Q_{isparuvanje}\right)\ (kJ)$$

a) The amount of heat for heating the dryer is calculated as the sum of the amount of heat for heating the walls, ceiling, floor, door and other equipment of the dryer.

$$Q_{komora} = Q_{zid} + Q_{tavan} + Q_{pod} + Q_{vrata} + Q_{ostanato}$$

- wall

$$Q_{zid} = V_{zid} \times \gamma_{zid} \times c_{zid} \times (t_{zid} - t_{nad.vozuduh})(kJ)$$

where:
V_{zid} - volume of the walls (m^3)
γ_{zid} - specific weight of the material from which the wall is made (kg/m^3)
c_{zid} - specific heat of the material of the wall (kJ/kg ^{0}C)
t_{zid} - wall temperature (^{o}C)
$t_{nad.vozuduh}$ - outdoor air temperature (^{o}C)

- ceiling

$$Q_{tavan} = V_{tavan} \times \gamma_{tavan} \times c_{tavan} \times (t_{tavan} - t_{nad.vozuduh})(kJ)$$

where:
V_{tavan} - volume of the ceiling (m^3)
γ_{tavan} - specific weight of the material from which the ceiling is made (kg/m^3)
c_{tavan} - specific heat of the material from which the ceiling is made (kJ/kg ^{0}C)
t_{tavan} - temperature of the ceiling (^{o}C)
$t_{nad.vozuduh}$ - outdoor air temperature (^{o}C)

- floor

$$Q_{pod} = V_{pod} \times \gamma_{pod} \times c_{pod} \times (t_{pod} - t_{nad.vozuduh})(kJ)$$

where:
V_{pod} - floor volume (m^3)
γ_{pod} - specific weight of the material from which the floor is made (kg/m^3)
c_{pod} - specific heat of the material from which the floor is made (kJ/kg ^{0}C)
t_{pod} - floor temperature (^{o}C)
$t_{nad.vozuduh}$ - outdoor air temperature (^{o}C)

- door

$$Q_{vrata} = V_{vrata} \times \gamma_{vrata} \times c_{vrata} \times (t_{vrata} - t_{nad.vozudh})(kJ)$$

where:
V_{vrata} - door volume (m^3)
γ_{vrata} - specific weight of the material from which the door is made (kg/m^3)
c_{vrata} - specific heat of the material from which the door is made (kJ/kg ^{0}C)
t_{vrata} - door temperature (^{o}C)
$t_{nad.vozuduh}$ - outdoor air temperature (^{o}C)

- rest of the dryer's equipment

$$Q_{ostanato} = 2000 \times c_{ostanato} \times (t_{ostanato} - t_{nad.vozuduh})(kJ)$$

where:
$c_{ostanato}$ - specific heat of the material from which the rest of the equipment is made (kJ/kg ^{o}C)
$t_{ostanato}$ - temperature of the rest of the equipment (^{o}C)
$t_{nad.vozuduh}$ - outdoor air temperature (^{o}C)

b) the amount of heat to heat wood and stickers to drying temperature

$$Q_{drvo} = V_{drvo} \times \gamma_{drvo} \times c_{drvo} \times (t_{sredina} - t_{nad.vozudh})(kJ)$$

where:
V_{drvo}- volume of wood in the chamber (m^3)
γ_{drvo}- specific weight of wood (kg/m^3)
c_{drvo} - specific heat of wood (kJ/kg ^{o}C)
t_{zid} - ambient temperature (^{o}C)
$t_{nad.vozuduh}$ - outdoor air temperature (^{o}C)

The amount of heat for heating the stickers is calculated according to the formula:

$$Q_{letvi} = V_{letvi} \times \gamma_{letvi} \times c_{letvi} \times (t_{sredina} - t_{nad.vozuduh})(kJ)$$

where:
V_{letvi}- volume of the stickers in the chamber (m^3)
γ_{letvi}- specific weight of the wood from which the stickers are made (kg/m^3)
c_{letvi} - specific heat of the wood from which the stickers are made (kJ/kg ^{o}C)
$t_{sredina}$ - middle temperature (^{o}C)
$t_{nad.vozuduh}$ - outdoor air temperature (^{o}C)

$$Q_{drvo+letvi} = Q_{drvo} + Q_{letvi}$$

c) Heat loss through the walls, doors, ceiling and others during drying

The insulating materials from which the metal dryer is made - a combination of Al-sheet and mineral wool as an insulator give the right to not take heat energy losses through the walls, ceiling, door into account in the design task.

- heat loss through the dryer floor

$$Q_{zagubi} = F \times k \times Z_{25/50mm} \times (t_{sredina} - t_{pocva})(kJ)$$

where:
F- surface through which the heat passes (m^2)
k- heat transfer coefficient
$Z_{25/\ 50\ mm}$ - duration of drying according to Sokolov (h)
$t_{sredina}$ - middle temperature (^oC)
t_{pocva} - soil temperature (^oC)

d) The heat for heating the air in the dryer

$$Q_{vozduh} = L \times c_{vozduh} \times (t_{sredina} - t_{nad.vozduh})(kJ)$$

L- amount of air (kg vozduh)

$$L = \frac{W_{polnenje}}{0,039} \text{ (kg vozduh)}$$

where:
c_{vozduh}- specific heat of dry air (kJ/kg ^oC)
$t_{sredina}$ - middle temperature (^oC)
$t_{nad.vozduh}$ - outdoor air temperature (^oC)

e) The total heat for evaporation of moisture from the wood for the entire drying cycle is a sum of the heat required for: breaking the hygroscopic bond, for heating and evaporating the moisture from the assortments and for heating and evaporating the moisture remaining in the wood after drying.

$$Q_{vkupno\ isparuvanje} = Q_{hig.vlaga} + Q_{drvo\ vlaga} + Q_{ostanata\ vlaga}\ (kJ)$$

where:
$Q_{hig.vlaga}$- heat to break the hygroscopic bond (kJ)
$Q_{drvo\ vlaga}$ - for heating and evaporation of moisture from the assortments (kJ)
$Q_{ostanata\ vlaga}$- heating and evaporation of the moisture remaining in the wood after drying (kJ)

$$Q_{hig.vlaga} = \left[\left(18 - \frac{22 \times W_k}{B + W_k}\right) \times r_0 \times V_{drvo}\right] \times 4,18(kJ)$$

where:
r_0 - density of wood (kg/m^3)
W_k - final wood moisture
$V_{\_drvo}$- useful capacity of the dryer (m^3)

$$Q_{drvo\ vlaga} = r_0 \times V_{drvo} \times \frac{W_{p-}W_k}{100} \times (608 + 0,311 \times t_{sredina}) \times 4,18\ (kJ)$$

$$Q_{ostanata\ vlaga} = V_{drvo} \times r_0 \times W_k \times (t_{sredina} - t_{nad.vozduh}) \times 4,18(kJ)$$

f) The coefficient of useful heat

$$K_{toplina} = \frac{Q_{drvo\ vlaga}}{\sum Q} \times 100\ (\%)$$

where:
$Q_{drvo\ vlaga}$ - for heating and evaporation of moisture from the assortments (kJ)
$\sum Q$- total amount of heat in one drying cycle (kJ)

The following formula is used to calculate the amount of heat for evaporation of 1,0 (kg) of wood moisture for one filling of the chamber:

$$q_{1kgvlaga} = \frac{\sum Q}{W_{polnenje}} (\frac{kJ}{kg})$$

where:
$\sum Q$- total amount of heat for one drying cycle (kJ)
$W_{polnenje}$ - the amount of evaporated moisture from the entire amount of wood from one filling of the chamber (kg moisture)

For the calculation of the amount of heat for moisture evaporation of 1,0 (m^3) for one filling of the chamber for one cycle, the following formula is applied:

$$q_{1m3} = \frac{\sum Q}{V_{drvo}} (\frac{kJ}{m^3})$$

where:
$\sum Q$- total amount of heat for one drying cycle (kJ)
V_{drvo} - useful volume of the dryer (m^3)

To calculate the amount of heat for 1,0 (h) drying, the following formula is applied:

$$q_{1h} = \frac{Q_{vkupno\ isparuvanje}}{Z_{25/50mm}} (\frac{kJ}{h})$$

where:
$Q_{vkupno\ isparuvanje}$ - total heat for evaporation of moisture from wood for the entire drying cycle (kJ)
$Z_{25/50mm}$- duration of drying according to Sokolov (h)

3. RESULTS AND DISCUSSION

As we mentioned before, the consumption of heat and water vapor for the purposes of artificial drying of beech sawn timber with two thicknesses of 50,0 and 70,0 (mm) was investigated. The results are shown in tables 4,5,6,7,8 and 9 respectively.

Table 4. *Heat required to heat the dryer.*

Heat	kJ (GJ)
Heat for heating the longitudinal walls	544765,00
Heat for heating the transverse wall	339677,00
Heat for heating the longitudinal walls and the transverse wall	884442,00
Heat to heat the ceiling	555241,25
Heat for floor heating	996866,40
Heat to warm the door	339677,00
Heat - the rest	27550,00
Total heat for heating the dryer	**2803776,65 (2,80)**

Table 5. *Heat required to heat wood and stickers to drying temperature.*

Wood thickness	**50,0 (mm)**	**70,0 (mm)**
	kJ (GJ)	kJ (GJ)
Total heat for heating wood and stickers	8946523,71 **(8,94)**	9392466,47 **(9,39)**

Table 6. *Heat required to heat the air in the dryer*

Wood thickness	**50,0 (mm)**	**70,0 (mm)**
	kJ (GJ)	kJ (GJ)
Heat to heat the air in the dryer	60632446,61 **(60,63)**	68826020,48 **(68,82)**

Table 7. *Heat required to heat and evaporate the moisture from the wood.*

Wood thickness	**50,0 (mm)**	**70,0 (mm)**
	kJ (GJ)	kJ (GJ)
Heat to break up hygroscopic moisture	3338181,262	3505090,325
Heat to heat and evaporate the moisture from the wood	150962056,3	169077503
Heat to heat the moisture that remains in the wood after drying	2130753,997	2237291,697
Total heat of evaporation of moisture from wood	156430991,5 **(156,42)**	174819885 (**174,81)**

Table 8. *Total heat for drying of beech with 50,0 mm in thickness.*

Heat	kJ/GJ/kWh
Total required drying heat for one drying cycle	281898143,3 (281,8)
Total required heat for drying with coefficient of safety of 1,20	338277772 (338,2)
Heat to evaporate moisture from 1,0 m^3 of wood for one cycle	**1504194,823 (1,50) (416,66)**
Heat to evaporate moisture from 1,0 kg of wood moisture for one charge	5978,516783 (0,0059)
Heat for 1h active drying	783050,3981 (0,78)

Table 9. *Total heat for drying of beech with 70,0 mm in thickness.*

Heat	kJ/GJ/kWh
Total required drying heat for one drying cycle	344316156,6 (344,31)
Total required heat for drying with coefficient of safety	413179388 (413,17)
Heat to evaporate moisture from 1,0 m^3 of wood for one cycle	**1749766,014 (1,74) (483,33)**
Heat to evaporate moisture from 1,0 kg of wood moisture for one charge	6432,963287 (0,0064)
Heat for 1h active drying	573860,2611 (0,57)

The results presented in tables above show that the drying process requires very high energy heat consumption compared to other energy needs for wood processing. As we can see from the Table 8 the total consumption of the total heat energy necessary to evaporate moisture from 1,0 (m^3) of sawn timber 50,0 (mm) in thickness for one drying cycle is 1,50 (GJ/m^3) or 416,66 (kWh/m^3). From the table 9 we can notice that total consumption of the total heat energy necessary to evaporate moisture from 1,0 (m^3) of sawn timber 70,0 (mm) in thickness for one drying cycle is 1,74 (GJ/m^3) or 483,66 (kWh/m^3). The results in our research are similar to those achieved Vengert and Meyer (1993), Seeger (1989), Denig et al (1996), Milić (2020), Zlateski et al (2023) and FAO (1990).

4. CONCLUSIONS

The analysis of heat consumption for convective drying of beech sawn timber with different thickness of 50,0 and 70,0 (mm) with initial moisture content of about 45,0 (%) and final moisture content of 8,0 (%) showed:

- Total heat for heating the dryer is 2,80 (GJ).
- Heat required to heat wood and stickers to drying temperature varies from 8,94 (GJ) for sawn timber 50,0 (mm) in thickness to 9,39 (GJ) for sawn timber 70,0 (mm) in thickness.
- Heat required to heat the air in the dryer varies from 60,63 to 68,82 (GJ) depending to wood thickness.
- Heat required to heat and evaporate the moisture from the wood varies between 156,42(GJ) for wood 50,0 mm in thickness and 178,70 (GJ) for wood 70,0 mm in thickness.
- Heat to evaporate moisture from 1,0 (m^3) of wood for one cycle is between 1,50 GJ (416,66 kWh) for wood 50,0 mm in thickness and 1,74 GJ (483,33 kWh) for wood 70,0 mm in thickness.
- Total heat for 1,0 h active drying of wood is from 0,78 (GJ) for wood 50,0 mm in thickness and 0,57(GJ) for wood 70,0 mm in thickness.

REFERENCES

1. Barišić, T. (1957): Umjetno sušenje drveta, Beograd.
2. Danon., G. (2003): Energy efficiency of artificial wood drying, Prerada drveta, p. 23-31.
3. Dening., Wengert, E., Simpson, W. (1996): Drying Hardwood Lumber, United States Department of Agiculture, Forest Service, Forest Products Laboratory General Technical Report FPL - GTR-118, p 186.
4. Dulău, M., Madaras, I., (2019): The 12th International Conference Interdisciplinarity in Engineering,, Development of a monitoring and Control System for Timer’s Drying Process, Procedia manufacturing 32, p. 545- 552.
5. FAO Energy Conservation in Mechanical Forest Industries (1990), Forestry paper No. 93, Rome, Italy, p.72-73.
6. Gorišek Z., Pervan, S., Straţe, A. (2008): Kakovostno izvajanje sušenja lesa – prvi korak za optimalno izkoriščanje lesne surovine. Ljubljana 25 Septemvri, p.26.
7. Jorgensen, N. (2000): How to Improve Drying Quality while Lowering Energy Consumption European COST Action E15 Workshop, Sopron, p.4.
8. Kolin, B. (2000): Hidrotermička obrada drveta, Jugoslavijapublik, Beograd p.214.
9. Krpan, J. (1965): Sušenje i parenje drva. Drugo izdanje, Sveučilište u Zagrebu.
10. Milić, G. (2020): Hidrotermička obrada drveta, Šumarski fakultet, Beograd.
11. Pervan, S. (2000): Priručnik za tehničko sušenje drva. Sand d.o.o., Zagreb, 1, 1-272.
12. Rabadjiski, B., Zlateski, G.: (2007): Hudrotermička obrabotka na drvoto I del- Sušenje na masivno drvo, UKIM - Šumarski fakultet, Skopje
13. Seeger, K. (1989): Energietechnik in der Holzverarbeitung, DRW - Verlag Wienbrener GmbH, p.120.
14. Simpson,W.T. (1989): Drying wood: a review. Drying technology. An International journal.
15. Vengert, G (2003): Kiln insulation, Wood dryig Forum, WoodWEB, Inc.
16. Vengert, G., Mayer, D. (1993): Energy in the Sawmills - Conservation and Cost Reduction. Forestry Facts, School of Natural Resources, Department of Forestry, No. 61, p.8.
17. Zlateski, G. (1999): Proučuvanje na režimite na konvektivno sušenje na bičena gragja od ela i buka so različni dimenzii, Magisterski trud, Skopje.
18. Zlateski, G., Stamenkoska, A.M, Trposki, Z., Koljozov, V., Rabadjiski, B. (2023): Proceeding of 6th International Scientific Conference Wood Technology and Product Design, Ohrid, North Macedonia, p. 210-218.

VOLUME, QUALITATIVE AND VALUE LUMBER YIELD FROM LINDEN LOGS (*TILIA* SPP.)

Josip Ištvanić[1], Alan Antonović[1], Marinko Jaklić[2], *Dario Pervan[1], Karla Vukman[1], Božidar Matin[1], Miljenko Klarić[1]

[1]University of Zagreb Faculty of Forestry and Wood Technology, Zagreb, Republic of Croatia,
e-mail: jistvanic@sumfak.unizg.hr; aantonovic@sumfak.unizg.hr;
kkremenj1@sumfak.unizg.hr;bmatin@sumfak.unizg.hr; mklaric@sumfak.unizg.hr
[2]Joinery and sawmill Pilana Jaklić Ltd.
e-mail: marinko.jakli97@gmail.com
**dpervan@sumfak.unizg.hr*
**Corresponding author*

ABSTRACT

This study compares the volume, qualitative, and value yield of linden logs (*Tilia* spp.) during their processing into sawn boards at the sawmill. A total of 48 logs were selected, divided into four categories: 12 veneer logs for sliced veneer (F class), 12 veneer logs for rotary-cut veneer (L class), 12 sawmill logs of 1st. quality class and 12 sawmill logs of 2nd quality class. The logs were processed using the live sawing method on a log band saw. The resulting sawn boards were categorized by thickness into six groups and assessed for quality across two grades. The highest yield in terms of volume, quality, and value was achieved with veneer logs intended for sliced veneer, while the lowest yield efficiency was recorded for sawmill logs of 2nd quality class.

Keywords: Linden (*Tilia* spp.), veneer logs, sawmilling logs, sawmilling, sawnwood, volume yield, qualitative and value lumber yield.

1. INTRODUCTION

Linden trees (*Tilia cordata* and *Tilia platyphyllos*) are both indigenous to large parts of Europe. The distribution of *T. cordata* primarily spans central and eastern regions, where it is more commonly found. Its range stretches northward to southern areas of Norway and Finland and reaches elevations of up to 1,500 meters in the central Alps. In contrast, *T. platyphyllos* occupies a more limited and fragmented range. Although it extends slightly further south than *T. cordata*, its northern presence only reaches southern Sweden, and it is less frequently encountered in the northern parts of central Europe (Eaton, Caudullo, De Rigo, 2016). Linden trees are typically associated with lowland areas and the lower foothills, rather than mountainous or high-altitude regions. These species have been a consistent part of European woodland ecosystems for over 10,000 years (Lang, 1994). They are commonly found in association with oak and beech forests, and their occurrence is frequently regarded as a sign of ancient woodland areas that have existed continuously since before 1600 CE (Savill, 2013).

In Croatia, the linden tree (*Tilia* spp.) primarily grows in mixed forest stands alongside European beech (*Fagus sylvatica* L.), oak (*Quercus* spp.), and hornbeam (*Carpinus betulus* L.).

Mature specimens typically reach heights of 25–35 m (rarely up to 40 m), with trunk diameters averaging 60–100 cm. It is characterized by a broad, densely branched, elongated-oval crown, with lower branches that usually hang downward. The bole is generally straight and cylindrical, featuring a branch-free section of 10–15 m in length. Linden trees exhibit slow growth rates but are remarkably long-lived, with some individuals surviving up to 1,000 years. The bark undergoes distinct ontogenetic changes: in juvenile trees, it appears greenish-gray, while mature specimens develop darker, deeply fissured bark. Bark constitutes approximately 14% of the tree's volume, with a density of around 340 kg/m³. In mature trees, the bark of the trunk and main branches can reach a thickness of up to 2 cm. Initially smooth and brown, the bark darkens over time to a blackish-gray hue and develops long, irregular, longitudinal cracks with narrow and short transverse fissures along the edges.

Anatomically (Figure 1), growth rings are distinctly visible, whereas tracheids and wood rays are not discernible to the naked eye. Linden wood is a diffuse-porous species with tracheids of medium diameter (30–90 μm), which are indistinguishable to the naked eye. These vessels are distributed diffusely, either solitarily or in small radial clusters (typically 2–3, rarely 4), with a vessel density of 70–130 per mm². Tile cells are absent. The wood rays are heterocellular (composed of both uniseriate and multiseriate structures), predominantly under 1 mm in height, though some multiseriate rays may reach 1–5 mm. Ray frequency ranges from 5 to 12 rays per millimeter. Axial parenchyma is apotracheal-diffuse, scarcely visible even under magnification. The mechanical tissue consists of libriform fibers and fiber-tracheids as transitional forms. The fibers exhibit a polygonal cross-section with tapered ends and slit-like pits.

Linden wood is lightweight and soft, with a pale coloration ranging from whitish to yellowish, often exhibiting reddish tones and occasionally featuring subtle brownish or greenish streaks or blotches. When straight-grained and free of defects, the wood appears smooth, soft, and possesses a fine, uniform texture. Growth rings are poorly visible, pores are invisible to the naked eye, and wood rays are barely distinguishable without magnification. The wood contains numerous, small tracheae arranged singly, in pairs, in short radial chains, or in groups, often exhibiting spiral thickenings. Linden wood is easy to work with, particularly in cutting and turning operations. It splits easily, nails and screws well, adheres effectively with adhesives, accepts staining and surface treatments successfully, and dries with minimal risk of deformation. However, it has low bending strength and is prone to discoloration and cracking, especially when steamed.

Despite its favorable physico-mechanical properties, linden wood is classified as non-durable under atmospheric exposure and is highly susceptible to attacks by xylophagous fungi and, in particular, insects. Consequently, it is not suitable for outdoor use unless protected from moisture or treated with appropriate preservatives. Fortunately, it responds well to impregnation treatments., rendering it suitable for interior applications but unsuitable for exterior use. It is easily treatable and exhibits excellent flexibility.

Due to its relatively low density, softness, and clean appearance, linden wood was historically used in a wide range of applications. In Europe, linden wood, valued for its light color and softness, is primarily used in sculpture, carving, and turning, as its soft texture allows for clean and smooth cuts in all directions relative to the grain.. In contrast, Asian industries prioritize its utilization in plywood and toy manufacturing. Commercially, it is sold as sawn boards and occasionally as peeled veneer, with applications including production of pulp, fiberboard, plywood, sliced veneer, furniture, toys, clogs, molds, pencils, boxes, drawing tools, and musical instruments (Todorović, 2023).

Marenče et al. (2020) studied the relationship between standing beech tree quality and the quality of sawmill products. They found that better quality trees produced more high-grade sawlogs and sawn boards, while defects like covered knots and heart defects were key factors lowering quality. Their methods involved full traceability from tree to board using European standards. Although the sample size was small, the study confirmed that early tree assessment can predict final product value. The authors suggest their approach could be applied to other tree species with minor adjustments.

Vilkovský et al. (2023) examined the effects of three log-sawing patterns live sawing, cant, and quarter sawing, on the quantitative and qualitative yield of beech sawn boards. Using six beech logs processed with a horizontal band saw, the study assessed volumetric yield and the proportion of radial lumber, the latter being an indicator of higher quality due to its dimensional stability. Results showed that cant sawing achieved the highest quantitative yield (up to 84%), while quarter sawing provided the highest qualitative yield (up to 62.7% radial wood).

Prka et al. (2001) and Ištvanić at al. (2011) have studied the volume yield of logs of common walnut (*Juglans regia* L.) at certain stages of sawmill processing. The results have shown that the volume yield of 1st class sawlogs when making sawn boards is around 72%, and for the 2nd class sawlogs 69%.

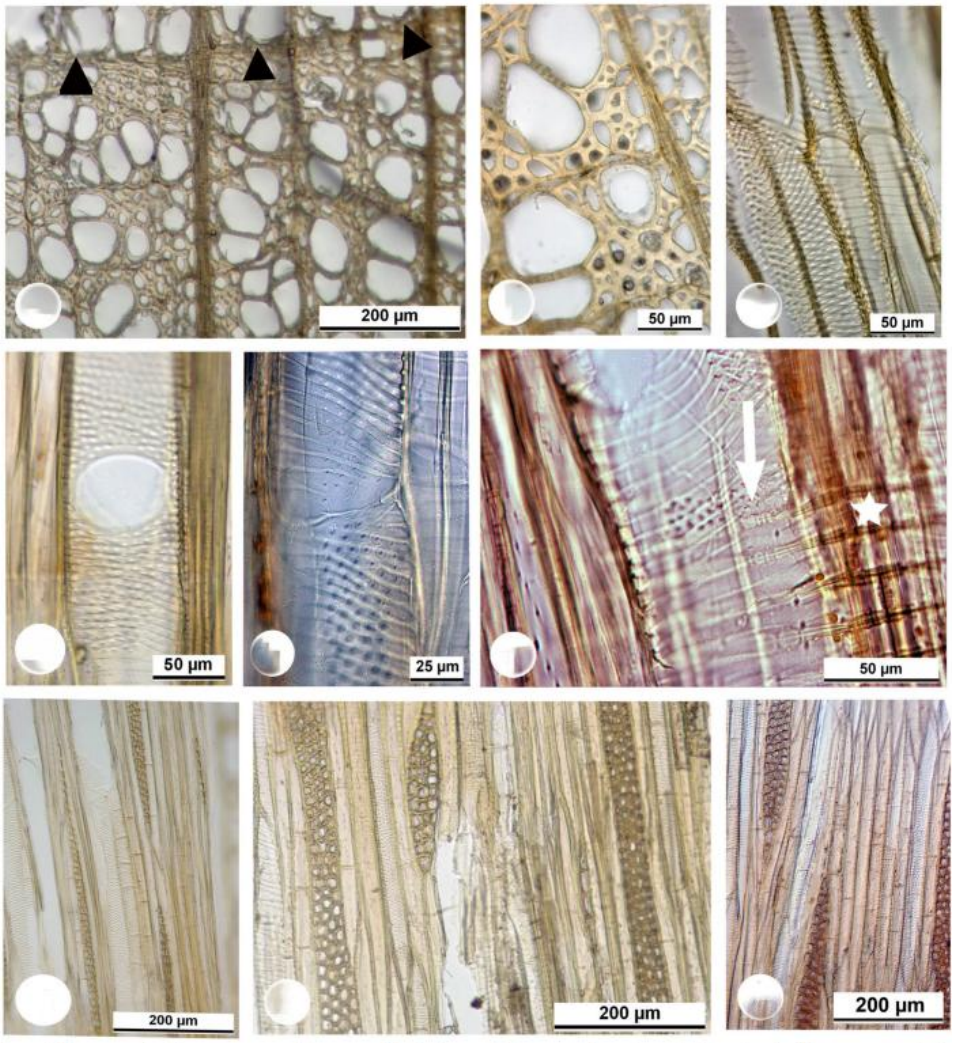

Figure 1. *Anatomical characteristics of linden wood (Gavrilović et al,2024).*

Ištvanić et al. (2016) have studied the volume yield of small-sized round wood of common walnut in Croatia. The results have shown that the volume yield of round wood during its processing into sawn boards ranged from 54.34% to 88.83%.

Rabadjiski et al. (2015) researched the impact of quality, diameter and length of common walnut logs on volume yield in the production of unedged, halfedged and edged boards. They were logs from 36 to 55 cm diameter. These results showed volume yield of round wood was 61.24 to 68.10 %.

Smajić et al. (2021) had examined the performance indicators of sawmilling Pedunculate oak (*Quercus robur* L.) through both theoretical and experimental approaches. Study focused on logs classified as second and third quality classes according to Croatian standard HRN D.B4.028, with diameters ranging from 30 to 39 cm and a length of 4 m. The logs were sawn into boards of 25 mm and 50 mm nominal thickness using an automated primary sawing line equipped with a vertical log band saw and hydraulic carriage. The study reported a quantity yield of 57.29%, a quality yield of 87.89%, and a value yield of 50.35%, providing a benchmark for the efficiency of sawmill processing in this oak species.

Popadić et al. (2014) have explored the impact of different sawing methods on the quantitative and value yields of beech logs containing red heartwood. Study examined 45 logs, evenly divided and processed using round, cant, and live sawing techniques. The findings showed that round and cant sawing produced similar quantitative yields (60.63% and 60.52%, respectively), while live sawing yielded a lower percentage (56.79%). Moreover, live sawing resulted in a reduced proportion of edged boards and red heartwood timber, as well as fewer small products, ultimately leading to a lower value yield compared to the other two methods.

2. AIM OF RESEARCH

Although linden possesses valuable properties, it remains significantly underutilized in industrial wood processing, especially when compared to more dominant hardwood species such as oak and beech. This underrepresentation is particularly evident in Croatia, where linden is rarely processed on a large scale and is often overlooked in both industry and academic research, especially regarding sawmilling practices.

In light of this context, linden (*Tilia* spp.) represents a promising subject for further scientific investigation. The specific focus of this research is to evaluate the sawing performance of linden veneer logs (intended for sliced and rotary-cut veneer), as well as sawlogs from 1st and 2nd quality classes. The processing will be conducted using the live sawing method on a vertical band sawmill.

The efficiency of the sawing process will be measured using the following key indicators:

- **Volume yield,** expressed as the proportion of log volume converted into sawn boards,
- **Qualitative yield,** assessing the quality of the resulting sawn boards, and
- **Value yield,** which considers the economic efficiency of the process based on the market value of the sawn output.

Linden is typically grouped with other broadleaved trees such as alder, poplar, and birch, which collectively account for only 5.1% of Croatia's total forest area. Nevertheless, rising demand for wood raw material is sparking increased interest in the utilization of lesser-used species. In this context, linden is emerging as a potentially valuable and underexploited resource for the Croatian wood processing industry. The results of this study are expected to support the development of higher value-added wood products from linden, thereby encouraging its broader application within the wood processing industry.

3. OBJECTS AND METHODS OF RESEARCH

3.1. Log selection and measurement

For this research, linden (*Tilia* spp.) veneer and saw logs were used. A total of 48 logs were procured, with 12 logs from each quality class. The minimum log length was 2.4 meters. The minimum mid-diameter of logs was 32 cm. All logs originated from the Forest Administration Slatina, Slatina Forest Office, and were classified according to Croatian standards (HRN EN). Veneer logs for slicing (Class "F") were classified according to HRN EN D.B4.020, requiring a minimum length of 2.0 m and mid-diameter of at least 35 cm. Logs had to be healthy, straight, with centered pith and uniform grain, and largely free from visual defects. Minor deviations such as small healthy knots and slight internal discoloration were permitted within specified limits. Veneer logs for rotary-cut (Class "L"), classified under HRN EN D.B4.022, required a minimum length of 2.0 m and mid-diameter of 30 cm. Similar to Class F, they had to be sound and defect-free, with limited tolerance for small healthy knots and internal heart defects not affecting processing.

Saw logs were classified as 1st and 2nd Class according to HRN EN D.B4.028. 1st Class logs had to be straight, healthy, and mostly free of defects, allowing minor imperfections such as small knots, light curvature, and slight end checks. 2nd Class logs permitted a broader range of defects, including medium knots, end cracks, and mechanical damage, within defined limits (Figure 2).

All sample logs were measured without bark for both length and mid-diameter. Descriptive statistical analysis was performed for all examined variables, including mean, standard deviation, minimum, median, and maximum values. Differences in mean values and data groupings for log length and mid-diameter were statistically evaluated to assess significance. These parameters facilitated the analysis of the raw material structure used for experimental sawing. The volume of each individual log was calculated using equation (1). For statistical data analysis on the volume yield IBM SPSS software was used.

$$V_{log} = \frac{D_{mid}^2 * \pi}{4} * L_{log} \quad (1)$$

where: V_{log} – log volume, m^3; D_{mid} – mid diameter of the log, m; L_{log} – log length, m

3.2. Processing logs in the primary sawmill

The primary sawmill, where this study was conducted, was located in Čačinci, Croatia. Mill equipment included a 1600 mm log band saw headrig, with automatic hydraulic-operated carriage, an edger and a cross-cut circular saw.

All logs were sawn using a band saw according to the specified work order, employing the full log sawing method. Multiple nominal thicknesses were cut from the logs, with the actual thickness of the boards depending on the quality and diameter of each log. Logs of higher quality and greater diameter were used to produce boards of larger thickness, while thinner logs were used for smaller thicknesses. From all logs, unedged sawn boards of nominal thicknesses 29, 33, 55, 66, 110, and 120 mm were produced. Each log was processed individually with the aim of maximizing the yield of the thickest boards, as these have the highest market value. The sawn boards were classified into two quality grades: commercial and sawn boards for further processing according HRN EN D.C1.031. All boards had to meet minimum dimensions of 14 cm in width and 2 m in length. After sawing, the boards were measured and sorted according to quality class, length, and thickness. The ends of the boards were treated with a protective coating, bark was removed, and the boards were stacked into piles. These piles were then prepared for dispatch to the customer (figure 1).

All sawn boards produced from the sample logs were measured for thickness, width, and length according to HRN EN 1309-1 and sawn board volume was calculated based on these parameters. The amount of coarse saw residue (slabs, log end off-cuts, edgings, trimmings etc.) and sawdust were not measured and were not included in the research.

In a primary sawmill, lumber volume yield is defined as the ratio of the sawn board volume and log volume according to equation (2):

$$Y_{vol.y} = \frac{V_{c.board} + V_{f.p.board}}{V_{log}} * 100 \quad (2)$$

where: $Y_{\text{vol.y.}}$ – volume yield, %; V_{log} – log volume, m^3; $V_{\text{c.board}}$ – commercial class sawn boards volume, m^3; $V_{\text{f.p.board}}$ – sawn boards for further processing, m^3.

The goal of any efficient sawmilling process is not only to maximize the quantitative yield of logs but also to produce boards of the highest possible quality. Efforts should be directed toward obtaining the greatest possible volume of high-value assortments in the best quality grades from each log.

The qualitative yield of logs is expressed through the average quality coefficient of all boards produced from a given log or batch of logs, calculated using the following equation (3):

$$Y_{q.y.} = \frac{V_{c.board} * k_1 + V_{f.p.board} * k_2}{V_{c.board} + V_{f.p.board}} * 100 \quad (3)$$

where: $Y_{\text{q.y.}}$ – qualitative yield; k_1 – quality index of commercial sawn boards; k_2 – quality index of sawn boards for further processing; $V_{\text{c.board}}$ – commercial class boards volume, m^3; $V_{\text{f.p.board}}$ – sawn boards for further processing volume, m^3.

Commercial grade boards were assigned a quality index of 1, while sawn boards for further processing were assigned a quality index of 0.5.

Considering only the average quantitative or only the qualitative yield of logs does not always provide a reliable assessment of the efficiency of a specific sawing method from the perspective of sawmill processing. This is due to the inherently antagonistic nature of quantitative and qualitative yield categories.

An indicator that simultaneously accounts for both quantitative and qualitative utilization of logs is the value yield coefficient. It can be calculated as the product of the average quantitative and qualitative yield of a log, as defined by equation (5):

$$Y_{val.y.} = Y_{q.y.} * Y_{vol.y.} \quad (4)$$

where: $Y_{val.y.}$ – value yield, $Y_{q.y.}$ – qualitative yield; $Y_{vol.y.}$ – volume yield

For the statistical analysis of volume, qualitative and value yield Microsoft Excel and IBM SPSS software were used.

Figure 2. *Linden logs and sawn boards.*

4. RESULTS AND DISCUSSION

The total of 6.405 m^3 of veneer logs for sliced veneer were sawn into 5.115 m^3 sawn boards, 5.286 m^3 of veneer logs for rotary-cut veneer were sawn into 3.946 m^3 sawn boards, 3.875 m^3 of 1st class sawmill logs were sawn into 2.624 m^3 sawn boards and 5.794 m^3 of 2nd class sawmill logs was sawn into 3.967 m^3 sawn boards.

The distribution of log dimensions by log class are shown in Figure 4 and Figure 5. Descriptive statistical analysis of log dimension data are presented in Table 1., with each log quality group shown separately. A comparison of log diameters and lengths across quality classes is illustrated in Figures 3. and 4.

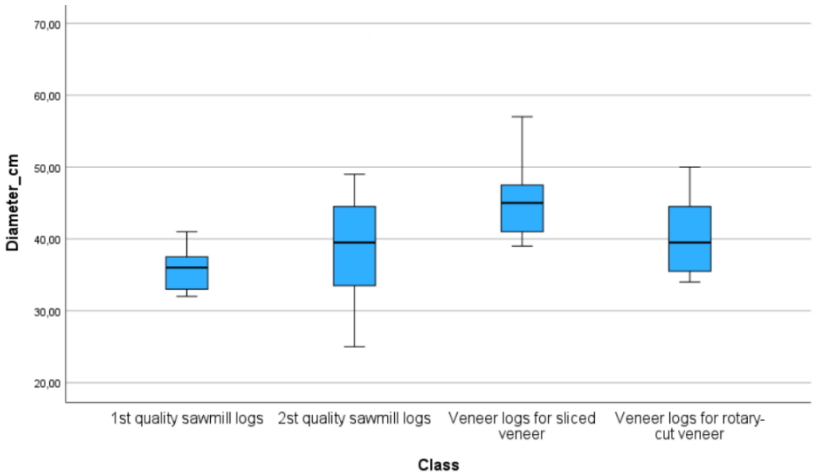

Figure 3. *The distribution of diameters by log class.*

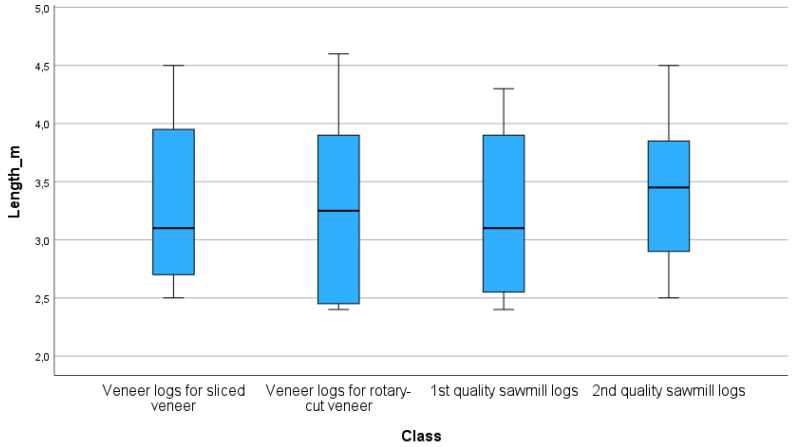

Figure 4. *The distribution of the length of logs by class.*

Table 1. *Descriptive statistics for log diameter and log length by class.*

Class	Variable	N	Minimum	Maximum	Mean	Std. Deviation
Veneer logs for sliced veneer	Diameter, cm	12	39.00	57.00	45.1667	5.28864
	Length, m	12	2.5	4.5	3.325	0.7350
Veneer logs for rotary-cut veneer	Diameter, cm	12	34.00	50.00	40.5000	5.36826
	Length, m	12	2.4	4.6	3.300	0.7544
1st quality sawmill logs	Diameter, cm	12	32.00	41.00	35.7500	2.95804
	Length, m	12	2.4	4.3	3.225	0.6969
2nd quality sawmill logs	Diameter, cm	12	25.00	66.00	40.2500	10.44575
	Length, m	12	2.5	4.5	3.442	0.625

The highest average log diameter was recorded in veneer logs intended for sliced veneer, which was expected given that logs designated for this purpose are selected based on the highest quality requirements for the final product. Veneer logs for rotary-cut veneer and 2nd class sawmill logs had similar average diameters. Lowest average diameter was recorded in 1st class sawmill logs. Average log lengths of each class were similar. The distributions of value yield, qualitative yield, and volume yield across different log classes are presented in Figures 5, 6, and 7, respectively. The shares of commercial-grade sawn boards within each log class are illustrated in Figure 8.

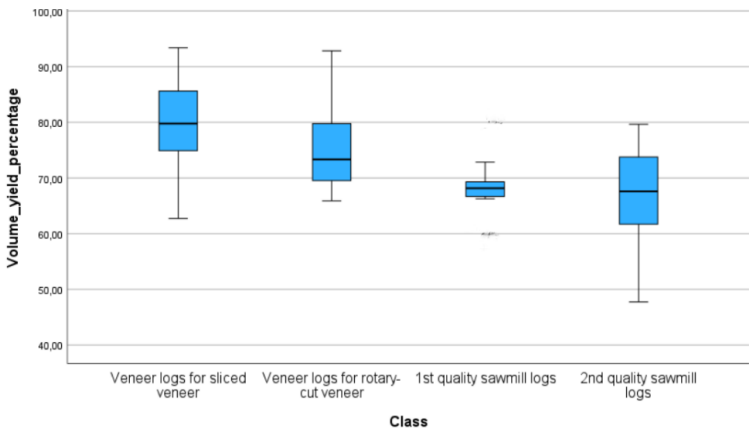

Figure 5. *The distribution of volume yield by log class.*

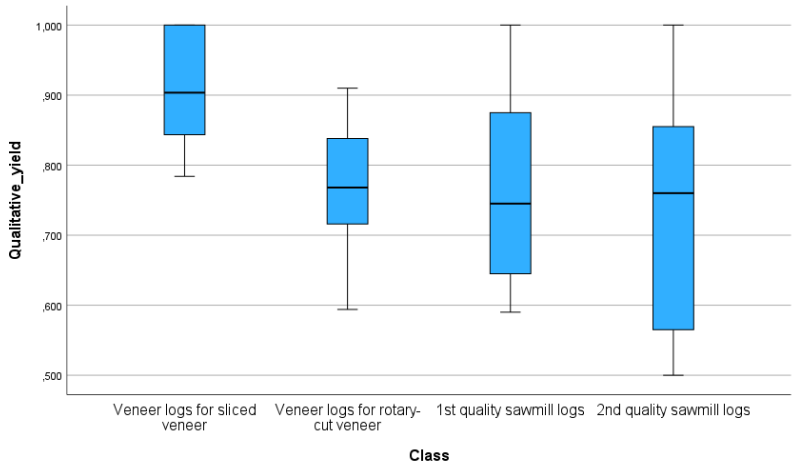

Figure 6. *The distribution of qualitative yield by log class.*

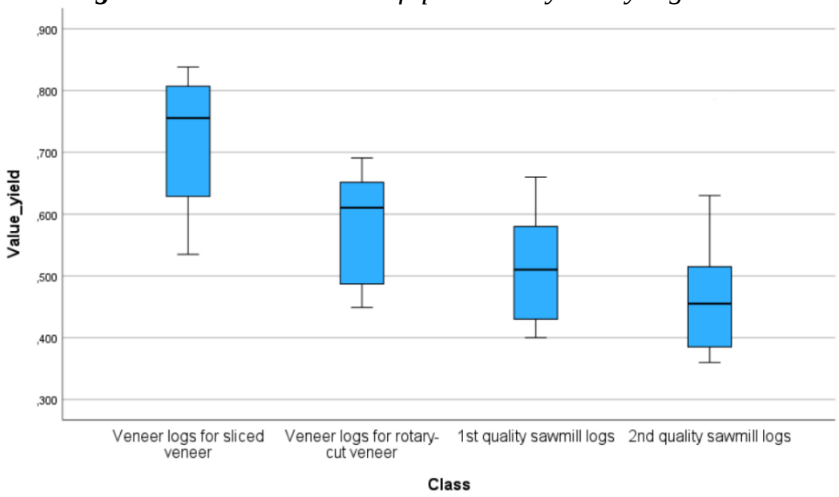

Figure 7. *The distribution of value yield by log class.*

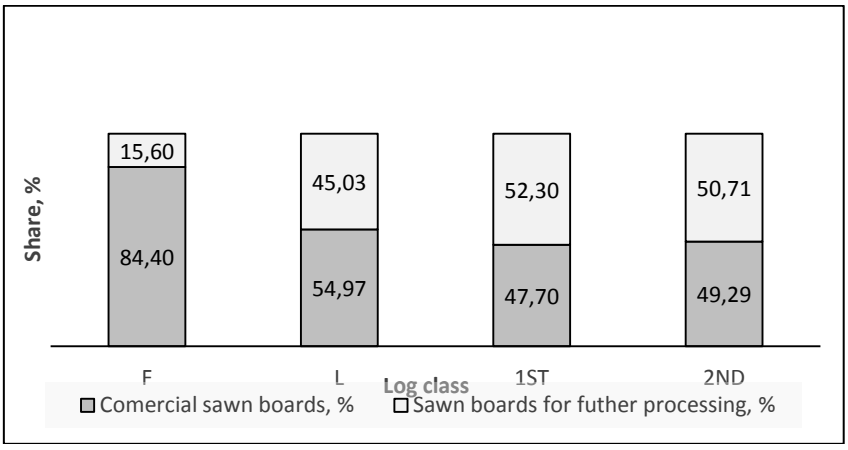

Figure 8. *The distribution of sawn board quality groups by log class.*

In the analysis of lumber volume, qualitative, and value yields, the highest average yields were obtained from veneer logs intended for sliced veneer, followed by veneer logs for rotary-cut veneer, and then by 1st and 2nd class sawmill logs. The qualitative yields of veneer logs for rotary-cut veneer and sawmill logs of the 1st and 2nd classes were comparable. These results appear to be closely associated with the quality and dimensional characteristics of the logs being processed.

The highest share of commercial-grade sawn boards was derived from veneer logs intended for sliced veneer, followed by those for rotary-cut veneer, and lastly by sawmill grade logs. The shares of

commercial boards between 1st and 2nd class sawmill logs were also similar. As indicated in the previous statistical analyses, both classes of veneer logs exhibited slightly greater average diameters and lengths. These dimensional advantages significantly influence volume yield in the production of unedged sawn boards, which was evident in the performance of the veneer logs

A one-way ANOVA was conducted to assess whether statistically significant differences existed in volume yield, qualitative yield, and value yield among the examined log classes. The results of this analysis are presented in Tables 2, 3, and 4. Subsequently, a Tukey HSD post hoc test was performed to identify between which log classes the observed differences occurred. The results of the post hoc analysis are shown in Tables 5.,6. And 7.

Table 2. *Results of ANOVA for volume yield.*

Source	Sum of Squares	df	Mean Square	F	Sig.
Between Groups	1243.136	3	414.379	5.991	0.002
Within Groups	3043.397	44	69.168		
Total	4286.534	47			

Table 3. *Results of ANOVA for qualitative yield.*

Source	Sum of Squares	df	Mean Square	F	Sig.
Between Groups	0.257	3	0.086	5.399	0.003
Within Groups	0.697	44	0.016		
Total	0.953	47			

Table 4. *Results of ANOVA for value yield.*

Source	Sum of Squares	df	Mean Square	F	Sig.
Between Groups	0.422	3	0.141	13,370	<0.001
Within Groups	0.463	44	0.011		
Total	0.885	47			

Table 5. *Results of Tukey HSD post hoc test for volume yield.*

Class	Class	Mean Difference	Std. Error	Sig.	95% CI Lower Bound	95% CI Upper Bound
Veneer logs for sliced veneer	Veneer logs for rotary-cut veneer	3.74412	3.39529	0.690	-5.3213	12.8096
	1st quality sawmill logs	11.13776	3.39529	0.011	2.0723	20.2032
	2nd quality sawmill logs	12.20401	3.39529	0.004	3.1386	21.2695
Veneer logs for rotary-cut veneer	Veneer logs for sliced veneer	-3.74412	3.39529	0.690	-12.8096	5.3213
	1st quality sawmill logs	7.39364	3.39529	0.145	-1.6718	16.4591
	2nd quality sawmill logs	8.45990	3.39529	0.075	-0.6056	17.5253
1st quality sawmill logs	Veneer logs for sliced veneer	-11.13776	3.39529	0.011	-20.2032	-2.0723
	Veneer logs for rotary-cut veneer	-7.39364	3.39529	0.145	-16.4591	1.6718
	2nd quality sawmill logs	1.06625	3.39529	0.989	-7.9992	10.1317
2nd quality sawmill logs	Veneer logs for sliced veneer	-12.20401	3.39529	0.004	-21.2695	-3.1386
	Veneer logs for rotary-cut veneer	-8.45990	3.39529	0.075	-17.5253	0.6056
	1st quality sawmill logs	-1.06625	3.39529	0.989	-10.1317	7.9992

Table 6. *Results of Tukey HSD post hoc test for qualitative yield.*

Class	Class	Mean Difference	Std. Error	Sig.	95% CI Lower Bound	95% CI Upper Bound
Veneer logs for sliced veneer	Veneer logs for rotary-cut veneer	0.143750	0.051380	0.037	0.00656	0.28094
	1st quality sawmill logs	0.154833	0.051380	0.021	0.01765	0.29202
	2nd quality sawmill logs	0.192333	0.051380	0.003	0.05515	0.32952
Veneer logs for rotary-cut veneer	Veneer logs for sliced veneer	-0.143750	0.051380	0.037	-0.28094	-0.00656
	1st quality sawmill logs	0.011083	0.051380	0.996	-0.12610	0.14827
	2nd quality sawmill logs	0.048583	0.051380	0.781	-0.08860	0.18577
1st quality sawmill logs	Veneer logs for sliced veneer	-0.154833	0.051380	0.021	-0.29202	-0.01765
	Veneer logs for rotary-cut veneer	-0.011083	0.051380	0.996	-0.14827	0.12610
	2nd quality sawmill logs	0.037500	0.051380	0.885	-0.09969	0.17469
2nd quality sawmill logs	Veneer logs for sliced veneer	-0.192333	0.051380	0.003	-0.32952	-0.05515
	Veneer logs for rotary-cut veneer	-0.048583	0.051380	0.781	-0.18577	0.08860
	1st quality sawmill logs	-0.037500	0.051380	0.885	-0.17469	0.09969

Table 7. *Results of Tukey HSD post hoc test for value yield.*

Class	Class	Mean Difference	Std. Error	Sig.	95% CI Lower Bound	95% CI Upper Bound
Veneer logs for sliced veneer	Veneer logs for rotary-cut veneer	0.141833	0.041888	0.008	0.02999	0.25367
	1st quality sawmill logs	0.207417	0.041888	<0.001	0.09558	0.31926
	2nd quality sawmill logs	0.246583	0.041888	<0.001	0.13474	0.35842
Veneer logs for rotary-cut veneer	Veneer logs for sliced veneer	-0.141833	0.041888	0.008	-0.25367	-0.02999
	1st quality sawmill logs	0.065583	0.041888	0.408	-0.04626	0.17742
	2nd quality sawmill logs	0.104750	0.041888	0.074	-0.00709	0.21659
1st quality sawmill logs	Veneer logs for sliced veneer	-0.207417	0.041888	<0.001	-0.31926	-0.09558
	Veneer logs for rotary-cut veneer	-0.065583	0.041888	0.408	-0.17742	0.04626
	2nd quality sawmill logs	0.039167	0.041888	0.786	-0.07267	0.15101
2nd quality sawmill logs	Veneer logs for sliced veneer	-0.246583	0.041888	<0.001	-0.35842	-0.13474
	Veneer logs for rotary-cut veneer	-0.104750	0.041888	0.074	-0.21659	0.00709
	1st quality sawmill logs	-0.039167	0.041888	0.786	-0.15101	0.07267

The ANOVA results for volume yield, qualitative yield, and value yield revealed statistically significant differences among the examined log classes. The post hoc Tukey HSD test indicated that the differences in volume and qualitative yields were statistically significant between veneer logs intended for sliced veneer and 2nd quality sawmill logs. Regarding value yield, the post hoc analysis confirmed statistically significant differences between veneer logs for sliced veneer and both sawmill

quality classes, which was expected based on the superior quality and dimensional characteristics of the veneer logs.

Due to the lack of previous studies specifically focused on linden (Tilia spp.), direct comparison with existing research was not possible. However, the results obtained in this study are consistent with findings from research on wood species exhibiting similar sawing characteristics, such as beech. For example, the value yield obtained from live sawing of beech logs of comparable quality to the veneer logs for sliced veneer in this study, as reported by Popadić et al. (2014), demonstrated similar outcomes. Additionally, as observed by Istvanić (2003), volume yield of beech wood increases with larger log diameters, a trend that aligns with the results of this study. The volume yield values for different diameter classes of beech presented by Istvanić (2003) also closely correspond to those recorded in this research. When compared to the qualitative yield values of pedunculate oak reported by Smajić et al. (2023), linden exhibited lower values, which was expected given its anatomical structure and lower wood density. Given the limited representation of linden wood and its sawmill products in current literature, greater attention should be directed toward the economic indicators of efficiency and profitability in the sawmill processing of this species.

5. CONCLUSION

- Linden tree is a poorly represented in wood species in Croatia, and grows together with beech and oak trees,
- Research on the success of sawmill processing of linden in these areas is very rare,
- Average volume yield of the veneer logs for sliced veneer was 79,76 %, the veneer logs for rotary-cut veneer were 75,20 %, the 1st class saw logs were 67,81 %, and the 2nd class saw logs were 66,74 %,
- The veneer logs for sliced veneer proved to produce the best lumber volume yield results. The 2nd class sawmilling logs proved to produce the worst volume yield results,
- Average qualitative yield of the veneer logs for sliced veneer was 0,914, the veneer logs for rotary-cut veneer were 0,770, the 1st class saw logs were 0,759, and the 2nd class saw logs were 0,721,
- Average value yield of the veneer logs for sliced veneer was 0,729, the veneer logs for rotary-cut veneer were 0,580, the 1st class saw logs were 0,514, and the 2nd class saw logs were 0,475,
- Overall, the research results confirm increased volume yield with better logs quality and diameter. The results indicate a possibility of rational processing of the researched linden logs in sawmills,
- Statistical analysis showed that there is significant statistical differences between different log classes regarding measured yields,
- Considering the volume yield there was significant statistical difference between veneer logs for sliced veneer and 2nd class sawmill logs,
- Considering the qualitative yield there was significant statistical difference between veneer logs for sliced veneer and 2nd class sawmill logs,
- Considering the value yield there was significant statistical difference between veneer logs for sliced veneer and all the other log classes,
- It would be interesting to conduct a further research of linden sawn boards, first in elements, then in glued massive wood panels.

REFERENCES

1. Câmpu, R. V., Derczeni, R. A. (2023): European Beech Log Sawing Using the Small-Capacity Band Saw: A Case Study on Time Consumption, Productivity and Recovery Rate, Forests, 14(6), 1137.
2. Eaton, E., Caudullo, G., De Rigo, D. (2016): Tilia cordata, Tilia platyphyllos and other limes in Europe: distribution, habitat, usage and threats. European atlas of forest tree species, Publication office of European union, Luxembourg.
3. Gavrilović, M., Rančić, D., Oskolski, A., Matić, M., Kocev, M., Jelikić, A., Janaćković, P. (2024): The coffin-reliquary of the holy Serbian king Stefan of Dečani (fourteenth century): wood, pigments and metal surfaces, Journal of Wood Science, 70(1), 37.

4. Ištvanić, J., Antonović, A., Čunčić Zorić, A. (2016): The Successfulness Of Sawmilling Small-Sized Roundwood In Croatia Part II - Common Walnut (*Juglans regia* L.); Proceedings of 27th International Conference on Wood Science and Technology (ICWST) Zagreb: University of Zagreb Faculty of Forestry: 1-16.
5. Ištvanić, J., Moro, M., Antonović, A., Beljo Lučić, R., Jambreković, V., Pervan, S. (2011): Lumber yield from European walnut *(Juglans regia* L.) and wild cherry (*Prunus avium* L.) sawlogs; Wood research (Bratislava), 56, 2: 267-276.
6. Ištvanić, J. (2003): Beech (*Fagus Sylvatica* L.) Sawmill processing in Croatia, 77(7-8), 373-387. (in Croatian).
7. Lang, G. (1994): Quaternary vegetation history of Europe: methods and results Gustav Fischer publication, Germany (in German).
8. Marenče, J., Šega, B., Gornik Bučar, D. (2020): Monitoring the quality and quantity of beechwood from tree to sawmill product. Croatian Journal of Forest Engineering: Journal for Theory and Application of Forestry Engineering, 41(1), 119-128.
9. Popadić, R., Šoškić, B., Milić, G., Todorović, N., Furtula, M. (2014): Influence of the Sawing Method on Yield of Beech Logs with Red Heartwood, Drvna industrija, 65, (1), 35-42.
10. Prka, T.; Ištvanić, J.; Trušček, A. (2001): Kvantitativno iskorištenje trupaca običnog oraha (Juglans regia L.) u pojedinim fazama pilanske obradbe. Drvna industrija, 52, (4), 161-172.
11. Rabadjiski, B.; Zlateski, G.; Trichkov, N.; Milchovski, Z. (2015): Quantitative Yield Of Walnut (*Juglans Regia* L.) Sawlogs, II-Nd Class Of Quality During One Phase Sawmill Conversion. Second international scientific conference „Wood technology & product design“, Ohrid, Republic of Macedonia: 226-231.
12. Savill, P.S. (2013): The silviculture of trees used in British forestry. University of Oxford, United Kingdom.
13. Smajić, S., Obućina, M., Antonović, A., Istvanić, J., Jovanović, J. (2023): Analysis of Yield and Sawing Methods During Processing Low Value Pedunculate Oak (*Quercus robur* L.) Logs to Sawmill Products, 32nd International Conference on Wood Science and Technology - ICWST 2023, University of Zagreb Faculty of forestry and wood technology, 180-185.
14. Smajić, S., Ištvanić, J., Obućina, M., Jovanović, J. (2021): Determination of Success Sawmill Processing of Pedunculate Oak (Quercus robur L.) Logs by Live Sawing Method, 14th International Scientific Conference: The Response of the Forest-Based Sector to Changes in the Global Economy – WoodEMA 2021, 363–368.
15. Todorović, N. (2023): Anatomy of wood. University of Belgrade Faculty of forestry, Serbia (in Serbian).
16. Vilkovský, P., Klement, I., Vilkovská, T. (2023): The impact of the log-sawing patterns on the quantitative and qualitative yield of beech timber (Fagus sylvatica L.). Applied Sciences, 13(14), 8262.
17. **** HRN EN D.B4.020 Products of forest utilization. Broadleaved veneer logs.
18. **** HRN EN D.B4.022 Products of forest utilization. Broadleaved logs for rotary cutting
19. **** HRN EN D. B4. 028 Products of forest utilization. Broadleaved sawlogs.
20. **** HRN EN D.C1.031 Sawn linden timber
21. **** HRN EN 1309-1 Round and sawn timber, method of measurement of dimensions - Part 1: Sawn timber.

The Authors´ Addresses:

Assistant professor Josip Ištvanić, Ph.D.; Assistant professor Miljenko Klarić, Ph.D.; Associate professor Alan Antonović, Ph.D.; *Postgraduate student – project assistant Dario Pervan, mag. ing. techn. lign.; Postgraduate student – assistant Karla Vukman, mag. ing. techn. lign.; Postgraduate student – project assistant Božidar Matin, mag. ing. agr.

Wood Technology Department, Faculty of Forestry, University of Zagreb, Svetošimunska 23, 10000 Zagreb, Republic of Croatia

e-mail: jistvanic@sumfak.unizg.hr; aantonovic@sumfak.unizg.hr; mklaric@sumfak.unizg.hr; dpervan@sumfak.unizg.hr; kvukman@sumfak.unizg.hr; bmatin@sumfak.unizg.hr

Marinko Jaklić, mag. ing. techn. lign.

Joinery and sawmill Jaklić Ltd., Četekovac 77, 33514 Čačinci, Republic of Croatia; e-mail: marinko.jakli97@gmail.com

*Corresponding author

EFFECT OF ULTRASOUND PRETREATMENT ON SPRING-BACK AND MOISTURE BEHAVIOR IN DENSIFIED POPLAR WOOD

Marko Veizović[1], Nebojša Todorović[1], Ranko Popadić[1], Goran Milić[1]

[1]University of Belgrade – Faculty of Forestry,
Department of Wood Science and Technology,
Belgrade, Republic of Serbia
e-mail: marko.veizovic@sfb.bg.ac.rs; nebojsa.todorovic@sfb.bg.ac.rs;
ranko.popadic@sfb.bg.ac.rs; goran.milic@sfb.bg.ac.rs

ABSTRACT

This study explores the effects of ultrasound pretreatment on the densification behavior of poplar wood (*Populus* × *euramericana*, cv. "Robusta"). Matched sample pairs were used to form two groups: one underwent ultrasound pretreatment, while the other served as control. The ultrasound pre-treatment was conducted in a water bath at a frequency of 28 kHz, temperature of 30 °C, and duration of 45 minutes. Densification was carried out at a pressing temperature of 200 °C, followed by cooling under pressure to 60 °C to stabilize the compressed structure. The target compression was 50%, reducing the sample thickness from 20 mm to 10 mm. The average compression rate was 49% in the control group and 51% in the ultrasound-pretreated group. After densification, the samples were evaluated for spring-back effect, moisture content after compression, and relative moisture content loss. A statistically significant difference in spring-back was observed between the groups, with the ultrasound pre-treated group showing a mean value of -1.55% compared to 1.4% in the control group, indicating enhanced thickness stabilization. In contrast, no statistically significant differences were found between the groups in post-densification moisture content or relative moisture content loss. These results suggest that ultrasound pretreatment can improve the compressibility and shape retention of poplar wood during densification, likely through cavitation effect which improves moisture flow, without substantially affecting moisture content of densified wood.

Keywords: poplar, densification, ultrasound, spring-back, moisture content.

1. INTRODUCTION

The growing scarcity of wood resources, coupled with rising global demand, has intensified interest in establishing fast-growing plantations worldwide. Populus × euramericana cv. “Robusta” is a hybrid poplar obtained by crossing *Populus deltoides* and *Populus nigra*. As other poplar species, this clone is widely used in veneer, plywood, pulp, packaging, and non-structural furniture components, owing to its workability and uniform texture. Despite these advantages, poplar wood is characterized by low density, modest mechanical strength, and low natural durability, which limit its application in load-bearing or high-wear contexts (Shao et al., 2020). These shortcomings have motivated research into various wood modification methods aimed at improving its performance, including thermal, chemical, and mechanical treatments (Bao et al., 2017). Among these, thermo-hydro-mechanical (THM) densification has gained attention as an environmentally friendly approach to enhance strength and hardness without the use of synthetic chemicals.

Densification is based on the principle of compressing wood in a plasticized state – typically achieved through heat and steam – thereby increasing its density and improving mechanical properties such as hardness, stiffness, and wear resistance. One of the challenges in wood densification is spring-back, the partial recovery of thickness after the pressing pressure is released. Various pre-treatments have been explored to address this issue, including chemical impregnation, enzymatic modification, and physical treatments (Cabral et al., 2022). Ultrasound pretreatment has recently emerged as a promising physical method, utilizing acoustic cavitation to enhance mass transfer, disrupt microstructural barriers, and improve moisture mobility within the wood matrix (He et al., 2014). In the context of densification, improved moisture movement and softening may facilitate greater

compressibility and more stable deformation, potentially reducing spring-back. The present study was therefore designed to evaluate whether ultrasound pretreatment can improve the densification behavior of Populus × euramericana cv. “Robusta” with a particular focus on its effect on the spring-back phenomenon.

2. MATERIAL AND METHODS

From five logs sourced from a commercial plantation in central-eastern Serbia (15-20-year-old), four tangentially sawn boards were prepared per log (n = 20 boards), ensuring growth rings were oriented parallel to the wide face (tangential plane). Boards were kiln-dried to a target moisture content of 12%. Clear, defect-free specimens were subsequently cut for testing. The nominal specimen dimensions before densification were 400 × 30 × 20 mm (L × T × R), where thickness (20 mm) corresponds to the radial direction.

Specimens were prepared as matched pairs cut adjacently from the same board position and with identical growth-ring orientation to minimize variability between groups. Within each pair, one specimen was assigned to ultrasound pre-treatment followed by densification, and the other served as the control (no pre-treatment) and was densified under identical THM conditions. All specimens were labeled to preserve pair identity throughout processing and testing.

Ultrasound pretreatment was carried out in a stainless-steel ultrasonic bath operating at 28 kHz. Specimens were fully submerged in tap water at 25 °C and sonicated for 45 min during which the water temperature increased to 35 °C. To ensure uniform exposure, specimens were placed in custom holders that maintained spacing between them and were weighted to remain fully submerged (Figure 1). After treatment, specimens were reconditioned to 12% moisture content, and prepared for the subsequent densification phase.

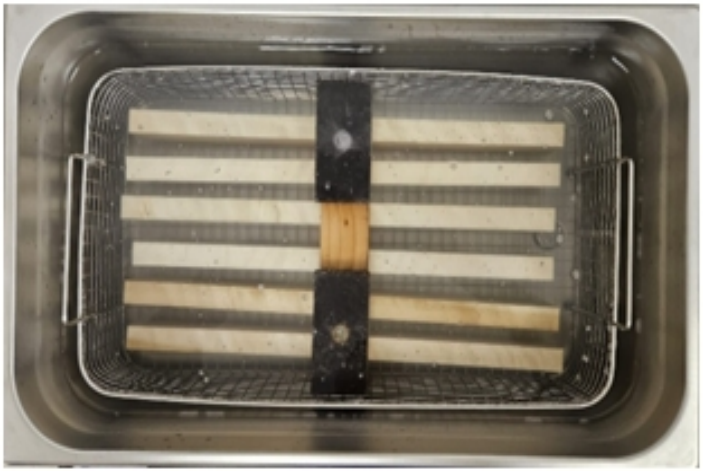

Figure 1. *Wood samples submerged in ultrasonic bath.*

An open-system hydraulic hot-press (Langzauner “Perfect” LZT-UK-30-L, Lambrechten, Austria) equipped with a water-cooling system was used for THM densification of both pre-treated and control groups. Specimens were compressed in the radial direction from 20 mm to 10 mm thickness (50% target compression ratio); a 10 mm metal stop defined the end position.

The THM cycle (Figure 2) comprised the following stages: (a) Pre-heating: Upper and lower platens pre-heated to 170 °C; (b) Loading and closing: Specimens placed in the press; pressure of 4 MPa applied in the radial direction with a closing speed of 3 mm s^{-1} until the metal stop was reached; (c) Primary hold: Conditions held for 3 min after the press platen contacted the stop; (d) High-temperature phase: Platen temperatures raised to 200 °C and maintained for 2 min; (e) Cooling under load: Platens cooled to 60 °C while specimens remained under compression, as in (Han et al., 2022).

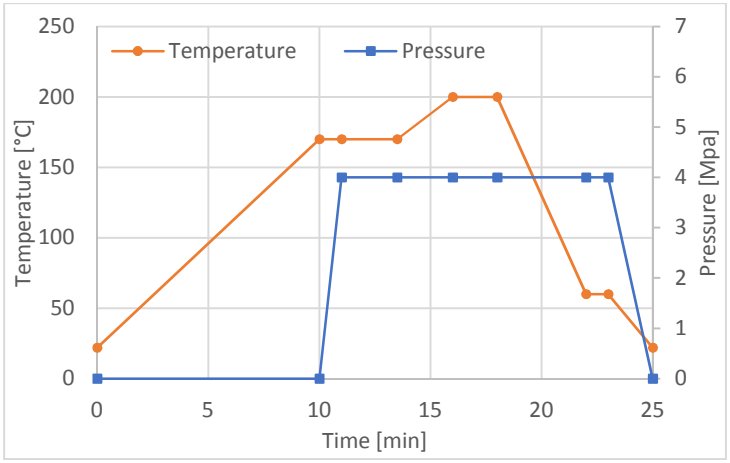

***Figure 2**. Scedule of thermo-hydro-mechanical (THM) treatment, closing speed 3 mm s^{-1}.*

Immediately after the press was opened, the specimens were measured with a digital calliper with a precision of ±0.03 mm. Based on the measurements before and after pressing, the actual compression rate (CR) and spring-back (SB) were calculated using the following equations:

$$CR = \left(\frac{t_0 - t_d}{t_0}\right) \times 100\ [\%]$$

Where:
t_0 - the initial thickness of the specimen before compression;
t_d - the thickness of the specimen after densification

$$SB = \left(\frac{t_d - t_t}{t_0 - t_t}\right) \times 100\ [\%]$$

Where:
t_0 - the initial thickness of the specimen before compression;
t_d - the thickness of the specimen after densification
t_t - the target thickness (10 mm stop plates)

Based on the known moisture content of the specimens prior to densification and the mass measurements taken before and after pressing, the moisture loss during the pressing process was calculated according to EN 13183-1:2002.

3. RESULTS

The measured compression rates indicate a modest yet statistically significant difference between the control and ultrasound-pretreated groups. The average compression rate in the control group was 49.49% (SD = 1.12%), while the pretreated group reached 51.28% (SD = 0.38%). A paired t-test confirmed the statistical significance of this difference ($t = 6.05$, $p < 0.001$), suggesting that ultrasound pretreatment led to a slightly higher degree of compressibility under identical THM conditions. Although the absolute difference in mean values is relatively small (approximately 1.8 percentage points), the consistently higher compression rates and reduced variability in the pre-treated group imply that ultrasound treatment may enhance the uniformity and effectiveness of the densification process.

The control group exhibited a mean spring-back of 1.40% (Figure 3) with a high standard deviation of 2.14%, indicating substantial variability in the dimensional recovery behavior after densification. In contrast, the ultrasound pre-treated specimens showed consistently lower and more uniform spring-back values, with a mean of -1.55% and a standard deviation of only 0.60%. The negative values observed in the treated group, and some specimens in control group, suggest a slight continued shrinkage during the cooling phase of pressing cycle. A paired t-test confirmed that the difference between the groups was statistically significant ($t = -5.51$, $p < 0.001$).

The reduced spring-back effect observed in specimens pretreated with ultrasound can be attributed to several mechanisms induced by ultrasonic action on wood. Ultrasonic treatment in a water bath generates acoustic cavitation, leading to the damage or degradation of pit membranes and the formation of microcracks within cell walls, which enhances the mobility of bound water through the wood (Rudak et al., 2021).The same authors also reported structural modifications of lignin, namely a reduction in the proportion of high-molecular-weight fractions and a corresponding increase in low-molecular-weight components. This alteration likely facilitates the viscous flow of lignin during densification and promotes the formation of new intermolecular bonds during the cooling phase of the process.

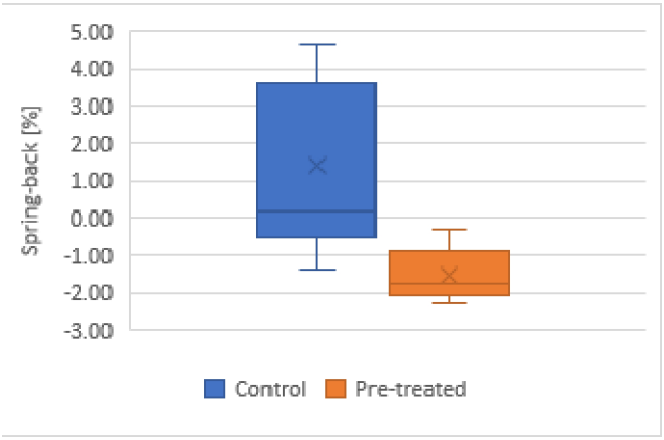

Figure 3. *Spring-back of densified control and ultrasound pre-treated specimens.*

The relative moisture content (MC) loss during densification was similar between the control and ultrasound pre-treated groups. The control group had an average MC loss of 7.73% (SD = 1.07%), while the pretreated group averaged 8.06% (SD = 1.52%). Although the pretreated group showed slightly higher mean values, the difference was not statistically significant ($p = 0.189$).

This suggests that ultrasound pretreatment did not fundamentally alter the overall moisture loss during pressing, aligning with findings that ultrasound primarily improves moisture mobility rather than increasing total water removal (He et al., 2016). This is consistent with the observed compression rate (CR) and spring-back (SB) results (where significant differences were recorded), indicating that the improved densification and dimensional stability in the pretreated group are more likely linked to microstructural changes and enhanced stress relaxation, rather than to greater dehydration during the THM process.

4. CONCLUSIONS

This study examined the effect of ultrasonic pretreatment on the spring-back behavior of densified poplar wood. The ultrasonically pretreated specimens exhibited a more uniform and significantly lower spring-back (mean −1.55%) compared to the control group (mean 1.40%), with negative values recorded in all pretreated specimens and in a few control specimens, indicating slight shrinkage during the cooling stage. As both groups experienced similar moisture loss during pressing, the reduction in spring-back is likely related to ultrasound-induced microstructural changes that enhance deformation stability. These results suggest that ultrasonic pretreatment can be an effective approach for reducing spring-back in densified poplar wood.

ACKNOWLEDGEMENTS

This study was financially supported by the Ministry of Science, Technological Development and Innovation of the Republic of Serbia (Grant No. 451-03-137/2025-03/200169).

REFERENCES

1. Bao, M., Huang, X., Jiang, M., Yu, W., & Yu, Y. (2017). Effect of thermo-hydro-mechanical densification on microstructure and properties of poplar wood (Populus tomentosa). *Journal of Wood Science*, *63*(6), 591–605. https://doi.org/10.1007/s10086-017-1661-0
2. Cabral, J. P., Kafle, B., Subhani, M., Reiner, J., & Ashraf, M. (2022). Densification of timber: a review on the process, material properties, and application. In *Journal of Wood Science* (Vol. 68, Issue 1). Springer. https://doi.org/10.1186/s10086-022-02028-3
3. Han, L., Kutnar, A., Couceiro, J., & Sandberg, D. (2022). Creep Properties of Densified Wood in Bending. *Forests*, *13*(5). https://doi.org/10.3390/f13050757
4. He, Z., Zhang, Y., Wang, Z., Zhao, Z., & Yi, S. (2016). Reducing wood drying time by application of ultrasound pretreatment. *Drying Technology*, *34*(10), 1141–1146. https://doi.org/10.1080/07373937.2015.1099107
5. He, Z., Zhao, Z., Yang, F., & Yi, S. (2014). Effect of ultrasound pretreatment on wood prior to vacuum drying. *Maderas. Ciencia y Tecnología*, *16*(4), 395–402. https://doi.org/10.4067/S0718-221X2014005000031
6. Rudak, O., Barcik, S., Rudak, P., Chayeuski, V., & Koleda, P. (2021). Densification of wood – Chemical and structural changes due to ultrasonic and mechanical treatment. *BioResources*, *16*(4), 8379–8393. https://doi.org/10.15376/biores.16.4.8379-8393
7. Shao, Y., Li, L., Chen, Z., Wang, S., & Wang, X. (2020). Effects of Thermo-Hydro-Mechanical Treatments on Various Physical and Mechanical Properties of Poplar (Populus) Wood. *BioResources*, *15*(4), 9596–9610. https://doi.org/10.15376/biores.15.4.9596-9610

BIOLOGICAL – PSYCHOPHYSICAL AND AESTHETIC CATEGORIES FOR SPACE MODELING

Elena Nikoljski Panevski [1], Umnije Aziri[2], Zejnelabedin Aziri[3], Edona Arifi Sadiku[4]

[1]Professor, Faculty of Design and Technologies of Furniture and Interior,
Ss. Cyril and Methodius University in Skopje
[2]PhD candidate, Faculty of Design and Technologies of Furniture and Interior,
Ss. Cyril and Methodius University in Skopje
[3]Assistant Professor, Faculty of Technological Sciences at "Mother Teresa" University in Skopje
[4]PhD candidate, Faculty of Design and Technologies of Furniture and Interior,
Ss. Cyril and Methodius University in Skopje
e-mail: nikoljski@fdtme.ukim.edu.mk

ABSTRACT

The aim of this paper is to explain the role of the biological - psychophysical and aesthetic in the conceptualization of the architectural space. Research in this direction has been and still is a constant focus of researchers, and in this way, it grows from an initiation into a basis for application in everyday architectural practice. The only possible orientation in this case is interdisciplinary – the use of fundamental knowledge and new research from the fields of human sciences, such as psychology, aesthetics and others. Exploring the architectural space modeling categories, we examine all scientific disciplines that directly and indirectly influence design, planning, design, but also the experience of space as essential parameters in architectural theory and practice.

The goal set in the project consists in the possibility of establishing project parameters that should help us in better solving the interiors. The projects are only abstract projections of the walls of the building, which have reality only on paper, and are justified by the necessity of measuring the distances between the elements of the construction for their practical implementation.

The subject of research in the project is the study of architectural space modeling categories that are equally important as understanding the space as a whole.In a perceptual or three-dimensional sense, the categories add a new dimension and truly define the totality of the interior.The research gives freedom to explore deeper into the history of architecture, to emphasize the forms that are exclusively derived from the relationship between man and nature, namely nature and the biological-psychophysical traits of man.

Keywords: architectural space, interiors, modeling levels, biological level, psychophysical level, aesthetic categories.

1. INTRODUCTION

The goal set in the project consists in the possibility of establishing project parameters that should help us in better solving the interiors. The projects are only abstract projections of the walls of the building, which have reality only on paper, and are justified by the necessity of measuring the distances between the elements of the construction for their practical implementation.

The facades and sections of a building help determine its height. However, architecture does not consist only of the width, length and size of the structural elements that surround the space in which man lives and moves. The key to understanding a building is to understand its interior space. No matter how beautiful, a house, church or palace they are only "boxes" formed by the walls - the content is the space inside. For the realization of the set goal, all categories that model the space are examined.

Table 1. *Overview of the implemented activities that achieved the goals and the indicators that monitored the realization of the goals and the achievement of the results.*

Objectives / activities Time frame for the realization of the project (months)	Objectives / activities Time frame for the realization of the project (months)											
Objectives / activities	1	2	3	4	5	6	7	8	9	10	11	12
1. Investigation of biological parameters for space modeling		R1										
1.1. Anthropometric research on space	I1											
1.2. Ergonomics of the space	I2											
2.0 Psychophysical parameters for space modeling	I3											
2.1 Psychological perception of space		I4										
3.0 Aesthetic categories for modeling the architectural space	I5											
3.1 Perceptual – mental mechanism		I6										
3.1 Elementary perception of the aesthetic		I7										
3.2 Structural perception of the aesthetic									R2			
3.3 Formal perception of the aesthetic			I8							I12	I12	

*I – filled indicator
*R – delivered result

The subject of research in the project is the study of architectural space modeling categories that are equally important as understanding the space as a whole.In a perceptual or three-dimensional sense, the categories add a new dimension and truly define the totality of the interior.

The research gives freedom to explore deeper into the history of architecture, to emphasize the forms that are exclusively derived from the relationship between man and nature, namely nature and the biological-psychophysical traits of man.

Primitive objects were certainly not burdened with an enormous number of requirements and categories, as they are today. They were only supposed to provide biological and psychophysical protection to primitive man. However, the need and the way to their fulfillment were so immediate, that forms instinctively arose that even modern architects find it difficult to discover.

The same applies to the more recent history of man, that is, to traditional architecture, where the relationship between nature and the biological - psychophysical characteristics of man were precisely the objects for living. Modern architecture hardly achieves this kind of synthesis. Because of that, interiors move away from the real needs of people, that is, from the functional level of space modeling. Any disproportion in this segment as a result brings disproportion in the immanent structure of the interior. For that reason, these researches should make a contribution in the direction of confirming the theoretical assumptions.

Table 2. *Detailed review of the realization of the research and the achieved results.*

Goals / activities for the realization of the goal	Indicator for monitoring the realization (I)
1. Research of biological parameters for space modeling	
1.1. Categorization of space	Obtained data and parameters for the space in which the person lives/works
1.2. Biological level of space modeling	Obtained data on the biological parameters of the space in which the person lives/works
2.0 Psychophysical parameters for space modeling	Obtained data on the relationship of man to his environment and vice versa
2.1 Psychological perception of space	Obtained data on the psychology of
3.0 Aesthetic categories for modeling the architectural space	Man in space, environment

3.1 Perceptual – mental mechanism	Obtained analyzes of the aesthetic levels that help the modeling of the space
3.2 Elementary perception of the aesthetic	Obtained data from the perceptual-mental mechanism
3.3 Structural perception of the aesthetic	Obtained data on aesthetic perception
3.4 Formal perception of the aesthetic	Obtained data on structural perception
3.5 Perception of beauty	Received-data on formal perception

Environment - living space

Despite the fact that in further considerations about space we will come to its abstract dimensions in this research, the competencies of this topic remain within the framework of the human environment. The problem of the environment integrally covers: spatial planning, the shaping of the city landscape, architecture, industrial design and visual communications. What is significant in this definition is that environmental issues are complex. The study of environmental problems aims to indicate their interdependence, expansion and negative consequences if they are not taken on time. Human life and society depend on the natural and artificial world and its increasingly intense transformation, which is the result of human intervention in the biological world. This transformation therefore contradicts itself because instead of improving people’s environment, they find themselves in constant danger of losing balance and destruction, living in fear of a dystopian future.Hence, the most important parameters of the targeted and stable organization of the environment are: planning, shaping and control. In the context of such considerations, it is important to highlight the aspiration for the architectural totality of the artificial world, namely the orientation towards interdisciplinarity along the lines of urbanism, architecture, design.

In the process of establishing balance, a detailed acquaintance with the peculiarities of the living space helps us the most, because it enables an accurate approach during its planning and design, in which the biological, psychophysical and aesthetic parameters occupy the most important place. The organization of the living space established in this way is a condition for the biological and social existence of man.People’s interest in space has a vital significance, it extends into the deep past, where together with consciousness it has its roots. It stems from the need to understand the life processes in the environment, with the understanding of natural laws to design it.By his nature, man is adaptable to his environment as much as his biological and psychophysical being arises from the general biology and physics of the environment. His attitude towards the objects that surround him can be: cognitive, active and creative. In all cases, the relationship of man to the environment should be oriented towards creating a dynamic balance between these entities.

Table 3. *This graph shows the percentage of total green infrastructure, green urban areas and tree cover of 37 capital cities (EEA-38, excluding Liechtenstein) as a percentage of their total area. It further shows the processes for all the cities included in the Urban Atlas 2018 database as well as for the corresponding 37 capital cities.*

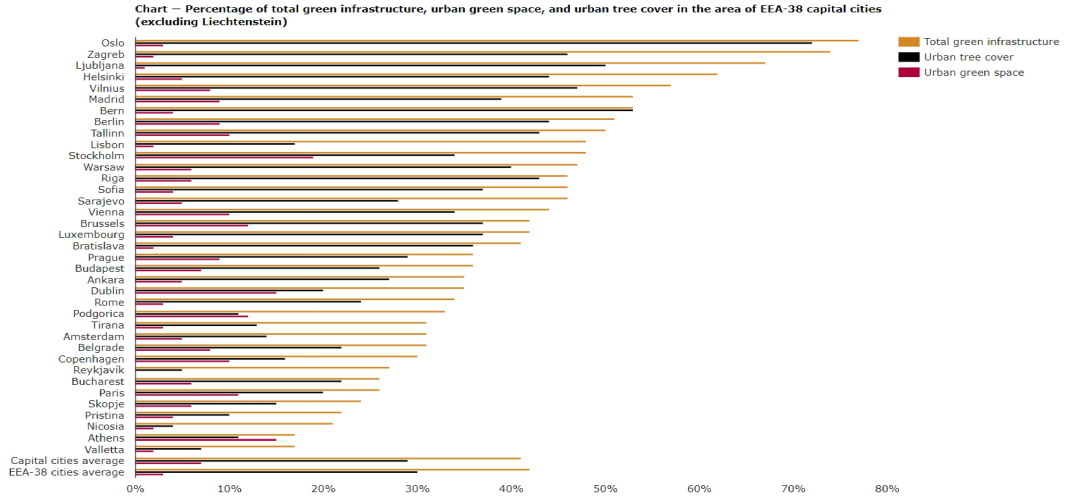

Most human actions also have their own spatial aspect, in the sense that objects of orientation are categorized by relationships, for example: "inside" and "outside", "far" and "close", "together" and "separate". , "continuous" and "dashed".

2. RESEARCH MATERIALS AND METHODS

According to what was stated in the introductory part, space is not only a separate category of orientation, but one of the aspects of any orientation - people spatially orient themselves. In order to be able to realize his intentions, man must understand spatial relations, and then unite them into a single spatial concept. For a better understanding of spatial relations and space in general, there are a number of theories that have been historically analyzed since the old century. According to the theories of the Greek philosophers, the entire space is unique, geometric and measurable. With Einstein's teaching, knowledge of space takes on new dimensions, so that today we can make a global division:
- concrete physical space (micro, everyday and macro) and
- an abstract mathematical space that is assumed in science to describe the physical space with a certain degree of approximation.

Writing about the living space, certain authors insist on the division of the existential space in order to highlight and free its details for study (Georges Patrix, Design et environment, 1975), so for example Patrick divides the living space into:
- space for current life;
- space for research;
- travel space.

The first is a space that people regularly use and whose boundaries are mobile and changeable (apartment, house, office, places to rest, places to socialize, places of one's own choice). These are spaces in which man navigates with his eyes closed (Georges Patrix, Design et environment, 1975). The second, exploration space, is unpopulated space. A place where you can't go at the moment, but a space that can become a living, working or resting place. For example, when we change the place of residence, work, etc. Without definite boundaries or determinate dimensions, this space creates the impression of spatial freedom. The third, travel space, is manifested through the desire to leave the space of everyday life and does not touch the everyday space.

The psychology of space can be explained by introducing a system of abstract concepts (Schulz, Existence, space and architecture, 1999). Taking into account the human experience in relation to its environment, we can say that the perception of space is a complex process because we do not see the world as the same and unique for all of us, but we perceive different worlds, which are the product of special motivations and accumulated experience. Thus, in Schulz's theory, the term "scheme" defines attitudes, behavior, noticing events in the four-dimensional space-time. Spatial "patterns" are composed of elements that have a certain immutability, such as universal elementary structures and certain personal idiosyncrasies. All of this together composes the image of man about his environment as a stable system of three-dimensional relations between objects of different importance. Accordingly we unite these patterns in our concept of existential space.

Such reactions are formed together with the mental development of the individual and with the interaction between the individual and the environment. This is how the process of assimilation and accommodation, i.e. absorption and adjustment, occurs. Opposing the passive subjugation of the environment, man changes it to his liking, imposing a certain structure. the adaptation of man in the world that surrounds him could be defined as a balance between assimilation and accommodation (Schulz, Existence, space and architecture, 1999). There is no pre-defined complete perception of space at the very beginning of the mental development of man, but noticing the space is a gradual and constructive reaction. It is a normal process of behavior that means acceptance of the three-dimensional world. So the awareness of the space results from the experiences and connections made with the surrounding world.

The research methodology in this paper was carried out by applying the adequate methodological approach suitable for this type of research. Basically, the research was divided into three phases, that is:

a. research on the biological level of space modeling;
b. research on the psychophysical level of space modeling;

c. research of aesthetic categories for space modeling.
The methods used were: historical analytical; comparative method; measurement method.

3. RESULTS AND DISSCUSION

3.1. Biological level of space modeling

Modeling the architectural space is the most sensitive of all the tasks that are set before the architects. Its complexity stems from the obligation to study all the factors of the human environment beforehand, especially those that are decisive for the life and health of people – the biological modeling of space. The built architectural space appears as a regulator of external influences on the biological constitution of man. In the basic structure of the interior, the elements for realizing the regulation are incorporated.

It would be most natural for the biological and the psychophysical in man to go together. We take the biological characteristics of man as biological factors for modeling the space. One of the most pressing problems of all humanity today is the relationship of man to the environment; how to keep the earth's biosphere functioning; how to save from overpopulation and hunger; how to protect against extreme pollution/ecosystem destruction. Today, these basically ecological preoccupations take on a dramatic form as a result of environmental pollution and the danger to human life.
Sticking to the line of ecology, we would say that building an object in the natural environment also means taking away from nature itself, that is, usurping the ecosystem.

Environmental Quality Monitors AQI (a unit of measure for measuring the effect of pollution – the amount of pollution divided by the material standard of living and all multiplied by one hundred to get the amount of pollution in percent) doubles every 13.5 years . if this rate of growth continues, the total ecological demand will increase by 32 times in 66 years - this means the destruction of the ecosystem.

The factors of the natural environment do not derive solely from the biology of nature, but have a decisive influence on the biology of man. In all the histories of architecture, it is stated that the first buildings that man made were the result of his opposition to nature, that is, as a result of protection from natural phenomena. Their elementary explanation should not take up more space in this research, some of them are: air, water, insolation, vegetation, heat, relief, earthquake and other weather disasters.The factors of the built environment are the result of natural and human intervention in nature, such as: temperature, humidity, microclimate, aeration, insolation, greenery, noise, vibrations, pollution.

Factors arising from the biological psychophysical characteristics of a person are difficult to consider in isolation because they are causally related. Today, more than ever, it is clear to everyone that architecture is much more than modern construction technologies. The motto "man is the measure of all things" has long been incorporated into architectural theory and practice, which means that everything that is built is built for man and that his measures should be an integral part of architecture. In the world of design, it has long been clear that ergonomics, meaning again the human relationship with objects of daily use, is a driver of design. So first the human needs for greater comfort when using the object, then how to achieve them with which technologies and from which materials - there is no doubt here. It's just that all disciplines on the way of design are intertwined (interdisciplinary approach).

Table 4. *This table shows the basic human needs from the environment, and therefore also from the architecture.*

Table of basic biological needs of man
Conditions in the working and living environment - this includes:
Lighting, air conditioning, ventilation, heating, cooling, radiation, plumbing, cleaning, maintenance
Nutrition – food preparation, food preservation, serving, serving, eating, accommodation and storage of food.
Hygiene – washing, cleaning, cosmetics, massage, gymnastics.
Care – first aid, treatment, therapy

3.2. Biological Anthropology

Physical anthropology or the biology of man is a science that studies the biological properties of man, issues related to the growth and development of the human population and its structures in space and time. The research of this scientific discipline is dedicated to man and his adaptability under the influence of the environment – all the morphological features of the human body are the result of the interactive action of genetic factors and the environment. One of the branches of human biology is anthropometry and ergonomics. The first deals with the measurements of the human body and the second with the relationship between the human body and the objects it uses. The results of research in these disciplines have a direct impact on space modeling and furniture design.

The term anthropomorphism in architecture and planning is the identification of human peculiarities and characteristics with those of the objects in the city. In the field of design, anthropomorphism means taking into account human psychological reactions and ways of use when designing objects or space. It means creating an atmosphere that can be unique for the entire city, settlement or village.

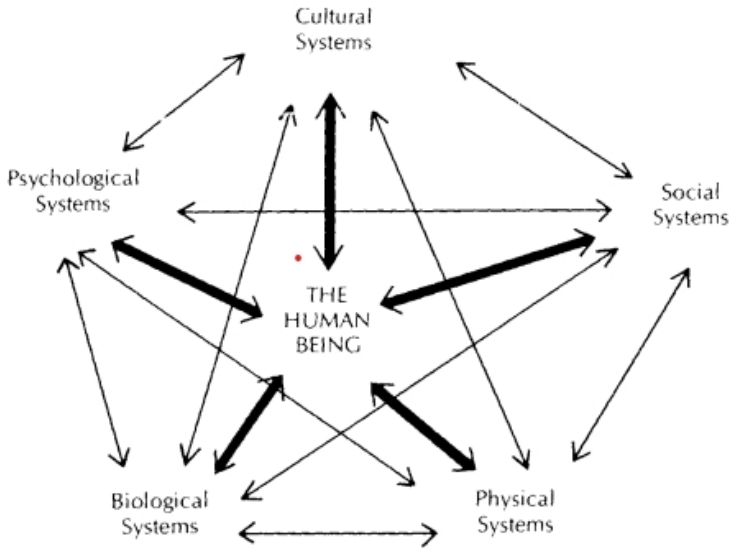

Figure 1. The graph shows the interrelationships between scientific disciplines and man.[1]

3.3. Psychophysical level of architectural space modeling

All construction interventions essentially always have a single goal, and that is the need of man to adapt to the environment. On one side is man with his biological, psychophysical, intellectual, emotional and other needs, on the other side is the environment with its natural characteristics, but also with its social, political, cultural and economic orientation. Architecture is one of the possibilities of adaptation to these needs. This means that the architectural space should be designed in such a way that it satisfies human biological and psychophysical needs together with the natural and social needs of the environment in which we intervene.

Modern psychology has the same views as architecture regarding the need to help man adapt to the environment. The real purpose of psychology is to help man to know himself better, how he could achieve a harmonious balance between his personality and society. The questions that psychologists try to answer are reminiscent of those that architects ask themselves: what do we know about man, what are the possibilities for expressing that knowledge, what inspires man towards creativity, in what kind of interaction does man have with objects, what should be the objective world so that man feels satisfied and secure in it?

Psychophysical as a phenomenology in itself and put in the title of this research refers to the sensitive processes in the human psyche during its interaction with the outside world. We perceive a number of

[1] the interrelationships of man and the mutual action between separate scientific disciplines as well as human interaction with them can be better understood as a set of disciplines - systems.
https://home.snu.edu/~hculbert/points.htm. Accessed 11 February 2024

complex sensory impressions of colors and shapes, light and darkness, speech, music, taste and others – based on sensitive, sensory perception.

3.4. Psychology and architectural space

Architectural space from the perspective of architectural theory has long been analyzed not only on the basis of spatial geometry. Contemporary studies on the conception of architectural space tend to bring man into the center of research and not only because of the "psychological dimensions of space", the impressions, feelings or effects that space leaves on the human user. Deeper than that, the researches in psychology itself are carefully followed, and the conclusions of these researches complement the architectural science (Lynch, City sense and city design, 1995).

For the basis of their architectural content, scientists use current philosophical and psychological studies (Schulz, Existence, space and architecture, 1999). More specifically, the studies are based on Gestalt - psychology and behaviorism. Gestalt-psychology - explains the phenomena in their entirety, without trying to separate them from the whole which they are integrated and outside of which they mean nothing. Gestalt psychologists emphasized that people notice complete patterns or configurations, not individual components, in other words - the Whole is more than the sum of its parts.

Behavioral theory studies the reactions of humans/organisms that can be objectively observed and measured in response to stimuli originating from the environment that surrounds them. In other words, it is behavioral science.

Psychology has always been contained in architectural theory, regardless of the messages of architecture throughout history, successive psychological interpretations have been observed. For example: Egypt - the age of fear, during which man devoted himself to the preservation of the body without which he could not be reincarnated. Antic Greece period was a century of beauty, a symbol of contemplative rest in the game of passions. Antic Rome period was the age of power and its symbols and pomp. Gothic period was the age of mystical aspirations. Christian era period was the age of piety and love. Renaissance period was the age of elegance. Baroque period was a century of predominant power over elegance and styles... (Zevi, Architecture as Space: How to Look at Architecture, 1993).
For researching the psychophysical level of architectural space modeling, it is best to examine what kind of interaction relationships exist between man and space. The dialectical explanation in this case would be that the space is shaped according to the psychology of the people, but also vice versa, the psychology of the people is formed depending on the environment.

The analytical approach could be considered in the following ways:
- Man’s attitude towards certain spatial situations, using the knowledge of behavioral psychology (plurality).
- Through the analysis of the spatial structures and situations to single out constants suitable for separate study, we want to analyze the psychological aspect of the elements that participate in the architectural totality (shape, material, color and others).

The issue of human behavior towards certain spatial situations is two-way – how the spatial structure of the architectural space affects the psychophysical constitution of the human being. In the scientific sphere of psychology, the behavioral approach is perhaps with the answer, while simultaneously researching what is common in people’s demands as well as what is common in different spatial situations.

The psychological constitution of a person often goes back to the memories of the earliest childhood, which further creates predispositions in a person, that is, sympathy or antipathy towards certain values. The difficult establishment of contact between today’s man and the new architecture mostly stems from the relationship between man and matter. People really instinctively love old materials (stone, wood) old styles and constructions, maybe due to the fact that when they were near these objects, they felt safe. On the contrary, in modern architecture materials (concrete, steel, glass, aluminum, plastic, and composites) are products of industrial processing. Therefore, contemporary architecture creates forms that compete with nature. In this way, the old clash of abstraction and naturalism is repeated; in which things that are easier and faster to understand prevail.

3.5. Aesthetic categories of architectural space modeling

Common to the categories of space modeling (biological, psychophysical and aesthetic) is that they are regulators of the relations between man and his environment, between the person and the outside world.

The aesthetic category is realized through the usual instruments: composition, proportion, rhythm, ornament, texture, color, etc. Architects under the pressure of the aesthetic category are constantly in a situation to decide between the useful and the beautiful, actually towards the efforts of balance between their joint actions. if the final modeling of the space contains less aesthetic value, we are immediately ready to claim that the appearance was not taken into account. But a careful analysis will show us that it is not only about aesthetic values, the modeling has failed on many other levels (for example, we say that a dark space is not beautiful because it is dark - biological level).

Unlike other fine-spatial arts, architecture and design realize their primary meaning through their utility. Sometimes we declare the useful, the honest, the thought-out, the real as beautiful. The mentioned attributes refer to the architectural space that man experiences through the mental mechanism of perception; hence the aesthetic properties of the space have primarily a psychological impact on the observer.

3.6. Beauty and science

Theoretically, an answer is still being sought as to whether aesthetics (beauty) is an objective or subjective category. Namely, does it exist objectively or is it inside the person observing the work of art or nature. According to the first assumption, the aesthetics of nature or of a work derives from their properties; the same are imposed on the observer as an objective reality. This attitude is known in philosophy and aesthetics – the attitude that the aesthetic exists in the objective world, outside and independent of us.

If we are looking for a pragmatic scientific confirmation of this fact, then the stated formula is the basic mathematical formula for designing in the golden section or in the proportions of the golden section. Man recognizes and chooses proportions in the golden ratio over others because he perceives them as beautiful, and he perceives them as beautiful because the entire structure of the human body, at the cellular level, is in the golden ratio. All nature that surrounds us, all plants and animals are built in the golden ratio.

Subjective aesthetics disputes the existence of external beauty independent of the organic and thinking nature of man. In subjective aesthetics it is claimed that the only aesthetics we can talk about exists in us, passes through us and for us. The beauty of objects and organisms is not only created by their existence outside of us, but it is our way of thinking about their qualities. According to subjective aesthetics, objects cannot be beautiful or ugly on their own - they are what they are, and their perception of beauty comes from us, the observers, that is, from outside them. Therefore, the beauty of an object does not depend on the nature of the object but on the thought process of experiencing the object by the observer. Hence, the same object evokes different feelings in different people.

From the complexity of the relationship to beauty in subjective aesthetics, we can say that it is only one chapter in psychology. Such a dual concept when we have an object that is the object of observation and an observer who evaluates the aesthetics of the object cannot give an answer to what beauty is, because the answer is found in their union.

Aesthetics should be inseparable; it should be both objective and subjective. The laws of beauty are not found in the objects that are observed, nor in the subject that is the observer, but in their mutual relations represented as one of their many reactions.

Of particular interest to architects is the question of the relationship between the beauty of nature and the beauty of the artificial environment, as they work under pressure not to degrade natural beauty with their creation. And this problem creates really very complex and problematic relationships. In addition to the many ways of adapting the object to nature, they are constantly under pressure to seek balance in an aesthetic sense. Even when we succeed in our effort and the object fits perfectly into the environment and perfectly fulfills the requirements and functions there are still aspects of communication between the natural and the artificial world. The attitude of the observers of the people who only see the work is very important here.

Mixing these two types of beauty is one of the most widespread and harmful illusions. The value of a picture is appreciated simultaneously because of the colors or the ratio of the volumes, but also

because of the youth and pleasant face of the model who posed in the studio. In a novel, style, composition, and the presence or absences of lovable and brave heroes are placed in the same plane. Namely, the wide audience of a work wants to find the same persons orobjects that are used in everyday life. It does not know or does not want to have two types of admiration for two identical values, which cannot be compared (C. Lalo, Introduction a LEstetique).

Transferred to the spheres of architecture, this would mean that the adoption of certain situations from nature (bionic) and certain materials, automatically makes the work palatable to a wider audience. People like and love more what they can understand, that is, what does not require much intellectual effort to understand.

Table 5. *This graph shows us which values are most important to people in developed countries.*[2]

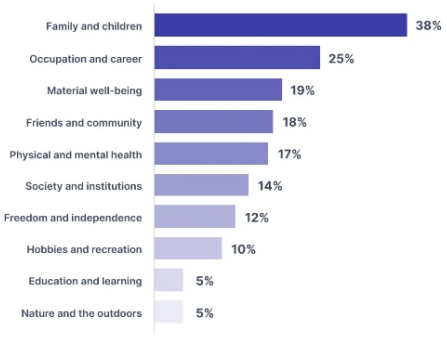

The aesthetic category in the architectural work can be analyzed at: elementary, structural and formal level:

- It basically contains the aesthetics of pure "architectural" instruments: composition, proportion, harmony, color, texture, etc.
- It is structural in the beauty of the union of spatial values with the values of architectural space modeling and
- Formally, it is the aesthetics of the overall undertaking and its relationship to the environment in the broadest sense of time and space.

3.7. An illustration of the psychological experience of beauty

From a psychological point of view, beauty can be an instrument for discovering the higher level of reality or the depth of life. Our feelings become aesthetic if they reveal the deep essence better than the nature of things. The first step in the analysis of any phenomenon/thing is to come to an understanding of the main problems. since we are studying beauty here, we will try to give some definition. The word beauty, which means so much to all of us and which we use so often, is difficult to define, it is easier to describe the feelings about something we call beautiful. We treat what is beautiful with an emphatic, pleasant and long-lasting interest. such a balance is of great importance for our physical constitution, because if it were not so, the world would seem tasteless and boring to us (V.K.Bal, The art of interior design, 1982). To better understand the interplay/dependence between an object/object and the person/observer who likes that object it is desirable to study the sequence that psychologists use to illustrate the human experience.

Table 6. *Interaction between the subject / object and the person / observer.*

W	World, environment, surroundings,
S	Stimulus
O	Our organism with its receptors – brain and muscles
R	Answer
W	World, environment, surroundings

[2] https://miro.medium.com/v2/resize:fit:1400/format:webp/1*h95DrX_hfPo7l7bQNsNx7g.pngPew Research Center, What Makes Life Meaningful? Views From 17 Advanced Economies, 2021

If the bell rings, it happens because someone in the neighborhood pressed it. This stimulus is received by our ears. then through the nervous system the impulse goes to our brain. The brain is able to give a physical response to the stimulus transmitted through the muscles. This is the simplest experiential reaction to external impulses, if we only replace the stimulus of ringing a bell with the beauty of an object we observe, we will get the same chain reactions.

In the experiential experience of beauty, the world (W) may or may not be physically present as the source of the stimulus or stimulus (S). In the completely imaginary experience of beauty, the world is far away. we call upon beautiful thoughts and representations from the rich archive of our consciousness. In experience, the response to beauty (R) is not always the result of visible action. Such action is an indirect result of experience. The whole cycle of experiencing the beautiful can begin and end in consciousness.

The simplest response to beauty is often much more than mere sensitivity, as it requires mental activity. Enjoying beauty does not cause bad consequences and has no repercussions on the object of our interest, nor does it mean depriving the pleasure of other observers. reactions to beauty are irrational and emotional, always completely personal, corresponding to the quantum of experience contained in the consciousness of each individual. It is often difficult to understand the reasons why we find things beautiful. It is equally difficult to convince someone to see beauty where we see it.

Of course, as architects, interior designers, we should orientate ourselves towards that beauty that is affirmed by consumers around the world. The designer should create to his satisfaction but also to the satisfaction of the client. This process is not simple. Despite the fact that the experience of beauty does not require greater intellectual activity, the perception of beauty is not as simple as delighting in it. In fact, we are often more sensitive for simpler reasons than for complex ones that are harder to understand. Analyzing the complex nature of beauty should help us create an environment that will reflect our ideas, but which, in addition to the rest, should satisfy the aesthetic needs of its users.

Although beauty is felt quickly, the response to the initial impulse arises from other responses. reactions are basic or primary depending on the source of the impulse for the beautiful.

Whether we like it or not, interiors attract our attention. The design of furniture and everyday objects as well. For example, after seeing a color in it, we can say that it makes us feel happy. The perception of color is primary, and the evoking of joyful feelings is a secondary response or reaction to the impulse of beauty through the color element. If we appreciate a color as harmonious with its surroundings, we react in a more complex way. If we say that a color is beautiful, we value the color, but this depends on a number of other factors. But can we be sure that someone else will find the color beautiful? No, if we don't know in advance how that person reacts to the given color in other situations. And so a single small component of the complex puzzle called the interior entails a lot of thought.

The idea that beauty is caused by stimulation alone can mislead us and call into question all previous analyses. The experience of beauty, although it does not require the conscious use of higher brain centers, can result from the stimulation of only a certain part of the brain.Our analysis of beauty indicates that the same object is not equally beautiful to everyone, referring to the organism (O) factor. In the physical sense, based on the accumulated experience, no two persons are the same. At any moment the physical, mental and emotional status of two different individuals looking at the same object can be completely different. The individual is influenced by the environment and changes over time. Hence it can be said that the experience of beauty is more a dynamic than a static phenomenon.

4. CONCLUSION

The dimensions of architecture expanded through the discovery of perspective and the graphical representation of height, width, and depth as applied to architecture. Time has thus become four-dimensional which imposes images on objects viewed from different perspectives – again due to the needs of the users, of man.

The experience of space, which we have indicated is characteristic of architecture, is also typical of the city, of streets, squares, alleys and parks, in playgrounds and gardens, wherever man has enclosed space by delineating or limiting the void. If in a building space is limited by six planes (floor, ceiling, four walls), this does not mean that five planes instead of six determine it, because, for example, a courtyard (without a roof) or a public square cannot be considered equal to the inside of the

building – the treatment and experiences in that space are different. Each architectural volume, each partition, represents a boundary between space and its environment, that each building is a machine that creates two types of freedom: its internal space, which is completely determined by the building itself, and the external or urban area, which is determined by the building and its environment.

Constant scientific and technological progress has enabled the dissemination of poetry and literature, paintings, sculptures and music on a vast scale, enriching the spiritual heritage of an ever-increasing number of people. While sound reproduction has almost reached perfection, the progress of color photography indicates that the next few years will see a distinct evolution of general education in chromatic values, an area of visual experience in which the average level of understanding is still below that of with the drawing and the composition.

The projects are only abstract projections of the walls of the building, which have reality only on paper, and are justified by the necessity of measuring the distances between the elements of the construction for their practical implementation. The facades and sections of a building help determine its height. However, architecture does not consist only of the width, length and size of the structural elements that surround the space in which man lives and moves. The key to understanding a building is to understand its interior space. No matter how beautiful they are, a house, church or palace is just a box formed by the walls - the content is the space inside.However, architecture remains isolated and alone. The problem with the representation of space is not even stated yet, far from being solved. The concept of architectural space is not clearly defined or conceptually marked/named. The most common methods of representing buildings in art and architecture histories are plans, facades, elevations, and photographs.

4.1. SUMARY OF THE RESULTS

From the proposed research, it is expected to obtain basic knowledge about the quality of the living space, the architectural space, and considering that, the space of the interior. Based on the research results, the modeling levels of the architectural space will be defined in accordance with national standards and European norms for this matter. Research in the direction of the biological level of space modeling will provide information for better use of space.

These researches are expected to cover an important segment in the field of contemporary researches on the architectural space – especially the interiors. The expected positive results from the research will be the basis for a better understanding of the interior, gaining greater knowledge about the way of designing, planning and realizing it.

The project can be drawn and interpreted in a hundred different ways, it changes the way the individual looks at the space, the procedure and its purpose to show an abstract concept of space, essentially greatly affects the user - the person. It seems that only the human scale has been overlooked in order to feel that space – the outside and the inside. A person’s area in relation to space is determined by their dimensions. Man in reality sees and experiences much more than space, for example a photograph of a building captures only its volume and appearance, which completely excludes the perspective of man as he moves inside and around the building. The key to understanding the complex relationship between man and architecture is precisely the interiors. The essence of human desires and needs from architecture today is determined by interiors.

From the point of view of evolutionary psychology, beauty is not a cultural construct and the appreciation of beauty is not learned, but rather a biological adaptation, part of universal human nature.

That beauty is a biological adaptation is shown by numerous examples from nature, even more than that, but that innate sense of beauty can become an engine of evolution, pushing animals to aesthetic extremes. In other cases, certain environmental or physiological constraints direct the animal to an aesthetic preference that has nothing to do with survival. So if beauty has nothing to do with survival, then it is a biological category and a biological adaptation(Prum, The Evolution of Beauty: How Darwin’s Forgotten Theory of Mate Choice Shapes the Animal World - and Us, 2017).

REFERENCES

1. Ball, V.K. The art of interior design, John Wiley & Sons, Inc.; 2nd edition, 1982.
2. Gideon, S. Space, time, architecture: The Growth of a New Tradition Harvard University Press, 1941
3. Kuhn, Helmut, Gilbert, Katharine Everett, A History of Esthetics, Dover Publications, Incorporated, 1972
4. Herbert, Paul, and Howard Culbertson. Cultural anthropological points of view, 2024.
5. Lynch, K. The image of a City, 1960, Boston.
6. Lalo, Sh. Basic of the aesthetics, 1954, Athens
7. Mark, O. Psychanalyse de la maison, Editions du Seuil, 1972, Paris.
8. Moles, A.,Romer,E. Psychologie de l‘ espace,1973, Paris
9. Nikoljski, A.Biolosko-psihofizicki I estetski kategorii so koi se modelira prostorot, 1979, Skopje
10. Papanek, V. Dizajn za stvarni svet, 1973, Split.
11. Patrix, G. Design et environment, Casterman, 1971, Belgique
12. Patrix, G. Beaute ou laideur,vers un esthetique industriel, Broche, 1967
13. Prum, The Evolution of Beauty: How Darwin’s Forgotten Theory of Mate Choice Shapes the Animal World - and Us, 2017
14. Ragon, M. L’urbanisme et la cite, Broche, 1964.
15. Ragon, M. L’art: pour quoi fair, Casterman, 1971, Belgique
16. Rot, N. Psihologija licnosti, 1975, Zagreb
17. Radonjic, S. Uvod u psihologiju, 1967, Belgrade.
18. Reekie, F.R. Design in the Built Environment, 1972, England
19. Pevsner, N. Izvori moderne arhitecture I dizajna, 2005, Belgrade.
20. Saarinen, E. The City: Its Growt, Its Decay, Its Future, Mitpress, 1965
21. Schulc, Ch.N. Egzistencija, prostor i arhitektura, 1975, Belgrade.

INNOVATION AS A SIGNIFICANT FACTOR IN ENTREPRENEURSHIP WITH AN EMPHASIS ON DIGITALISATION

Mira Stankevikj Shumanska[1], Angela Nikolovska[2], Ivana Antovska[1]

[1]Ss Cyril and Methodius University in Skopje, North Macedonia
Faculty of Design and Technologies of Furniture and Interior – Skopje
[2]KAPA5 ENTERTEJMENT DOOEL Skopje
e-mail:stankevik@fdtme.ukim.edu.mk, angelanikolovska10@gmail.com, antovska@fdtme.ukim.edu.mk

ABSTRACT

Innovation plays a fundamental role in entrepreneurship and significantly contributes to economic growth, as well as to securing a competitive advantage in a rapidly changing global market. Particular emphasis is placed on digitalisation as a radical and transformative form of innovation. This scientific paper explores the role of digitalisation in transforming traditional business models and optimising operational efficiency, as well as in creating new opportunities for value enhancement. Additionally, the paper examines the importance of applying digital technologies, highlighting their potential to increase productivity and support the development of new business models. The research identifies key obstacles to the implementation of innovative practices, especially among small and medium-sized enterprises, such as financial constraints, lack of digital skills, and resistance to change.

Keywords: innovation, digitalisation, Industry 4.0, digital transformation, competitive advantage, operational efficiency.

1. INTRODUCTION

Innovation is a key driver of entrepreneurship and plays a significant role in fostering economic growth and enhancing competitiveness in a constantly evolving global market. Companies that embrace innovation are better positioned to anticipate market trends, respond to consumer needs, and create new value through the development of new or improved products and services.

Innovation is not defined solely by the creation of new products or services, but also by the implementation of improved processes, marketing strategies, and organisational practices. These improvements enable enterprises to enhance their operational capabilities, enter new markets, and meet customer demands more effectively.

In this context, digitalisation emerges as a transformative form of innovation. It introduces radical changes in how companies operate, manage resources, and engage with stakeholders. Digitalisation acts as a catalyst for new innovations and enables the development of new business models, automation of processes, and improved decision-making through the use of data. This scientific paper analyses the impact of digitalisation on entrepreneurship and highlights its potential to reshape traditional practices and stimulate growth through enhanced efficiency and increased adaptability.

The integration of digital technologies has become essential in today’s digital economy, where the rapid adoption of digital tools is synonymous with innovation. This scientific paper explores the complexity and opportunities arising from digitalisation, positioning it as a key strategy for enterprises aiming to achieve long-term success in a competitive business environment.

2. SCOPE AND OBJECTIVES

This scientific paper places particular emphasis on digitalisation and its potential to transform the ways in which entrepreneurs manage resources, generate value, and achieve competitive advantage. It further explores methods for implementing digital technologies across key business processes, including production, marketing, and service delivery, highlighting their contributions to the growth of small and medium-sized enterprises, as well as the challenges these enterprises face.

By integrating a theoretical framework with practical examples, the paper seeks to offer a deeper understanding of how innovation, particularly through digital transformation, drives entrepreneurial activity and supports sustainable business success.

3. DIGITALISATION AS INNOVATION

Digitalisation refers to the enabling, enhancement, or transformation of business operations and activities through the use of digital technologies and a broader range of digitised data. It is more than merely converting analogue information into a digital format, digitalisation fundamentally alters how companies operate and communicate with customers. By implementing digital tools, businesses improve efficiency and ensure seamless functioning across all sectors. With its ability to streamline processes and enhance decision-making, digitalisation transforms industries and opens up new opportunities for growth.

Digitalisation is closely linked to a wide range of economic and business trends. Its capacity to create new business models, such as the platform economy (e.g. Uber, Airbnb, Amazon), demonstrates its transformative potential. Moreover, digitalisation enables greater flexibility, allowing businesses to expand more easily, enter new markets, and respond more rapidly to change.

3.1 Digitalisation or Digitisation?

Although often used interchangeably, *digitalisation* and *digitisation* are distinct terms. Understanding the difference between them is critical to fully grasp the impact of digital innovation.

Digitisation: Refers to the process of converting analogue information into a digital format. For example, scanning paper documents to create digital copies or turning physical materials into digital files represents digitisation. While this is an important step towards modernisation, digitisation amounts to only a small part of the broader process of digital transformation. It simply replaces physical formats with digital ones without altering the underlying processes.

Digitalisation, on the other hand, involves the integration of digital technologies into core business processes, leading to changes in how organisations operate and create value. It uses digital tools to optimise operations, enhance customer experience, and introduce new ways of generating revenue. A key aspect of digitalisation is how it transforms business strategy.

Moving towards full digitalisation equips businesses with the tools to respond more effectively to market demands and build stronger, more adaptable customer relationships.

3.1.1 Digital transformation in business

Digital transformation is a comprehensive process through which businesses redesign their operations, strategies, and organisational culture by adopting digital technologies. It affects all levels of the organisation, from marketing and sales, customer support, to back-end operations such as supply chain and production management. The main objectives of digital transformation include:

- Improving efficiency through process automation, reducing manual errors, and optimising resource use.
- Enhancing the customer experience by using data to create personalised services, enabling easier communication, and improving brand accessibility.
- Driving innovation by creating new business models that can unlock additional revenue streams and market opportunities.

Successful examples of digital transformation can be observed in companies such as Amazon, which evolved from an online bookstore into a global leader in e-commerce, cloud computing, and digital media through continuous innovation. Netflix is another notable example, having transformed its business model from DVD rentals to a subscription-based streaming service, leveraging data to deliver personalised recommendations.

Digital transformation is essential for companies to remain competitive in an era where technology is reshaping industries at an unprecedented pace. According to a report by PwC, the majority of chief executives believe that investments in digital technologies have created value for their business, and around 80% state that mobile technologies and data analytics are key aspects of their strategy. (18th Annual Global CEO Survey — PwC) Effective digital transformation strengthens a company’s ability to adapt, differentiate, and sustain growth in dynamic market

conditions.

3.2 The pace of digital adoption in Europe and worldwide

The implementation of digital technologies is advancing at an unprecedented pace across the globe, driven by the increasing use of the internet and mobile devices. According to the International Telecommunication Union (ITU), global internet usage reached over 68% in 2024, or approximately 5.5 billion people, with the fastest growth occurring in developing regions. (Analysis on Internet traffic and 5G network coverage 2023 — ITU)

In the context of our country, data from the State Statistical Office shows that in the first quarter of 2024, 90.8% of households had internet access at home. During the same period, 91.2% of the population aged 15 to 74 used the internet, and 76.4% reported using it several times per day. Furthermore, 63.5% of individuals ordered or purchased goods or services online in the previous 12 months. (Usage of information and communication technologies in households and by individuals, 2024 — State Statistical Office)

The widespread availability of the internet has accelerated the integration of digital tools into businesses across various industries, establishing digitalisation as a global phenomenon. A key objective of the European Union’s Digital Decade strategy is for more than 90 percent of small and medium-sized enterprises (SMEs) to achieve at least a basic level of digital knowledge. As of 2024, 72.9% of SMEs had reached this threshold. Progress remains uneven across Member States and economic sectors. While countries such as Finland and Denmark have already surpassed the target, others remain well below the EU average. (2025 State Digital Decade — DESI)

In Finland, 92.5% of SMEs have attained at least a basic level of digital intensity. Citizens also demonstrate high levels of digital competence, with 82% possessing at least basic digital skills. Despite existing differences between rural and older populations, Finland’s overall performance reflects broad and inclusive digital progress.

Industry 4.0, a strategic initiative for the comprehensive digitalisation of industrial production, has been widely implemented in Germany, a leading industrial economy. In 2024, 62% of German companies reported using Industry 4.0 technologies and solutions, including software, IT services, and hardware. (Germany - The World’s Leading Industrie 4.0 Nation — GTAI)

However, significant differences continue to exist between European countries. Southern and Eastern Member States, such as Bulgaria and Greece, continue to lag in terms of digital infrastructure and workforce skills. These gaps highlight the need for greater investment in digital tools and training programmes.

At a global level, the COVID-19 pandemic significantly influenced the adoption of digital technologies. Many businesses introduced remote work solutions, digital collaboration tools, and e-commerce platforms. These changes have initiated long-term shifts in business operations, making digitalisation an essential element for resilience and competitiveness in the modern economy.

3.2.1 The impact of digitalisation on industries

The transformative impact of digitalisation is evident across all industries, from manufacturing to finance, healthcare, and retail. The integration of digital tools enables industries to optimise processes, reduce costs, and deliver more personalised and efficient services.

Manufacturing: The rise of Industry 4.0 has fundamentally changed manufacturing by integrating automation, the Internet of Things (IoT), and artificial intelligence to create so-called smart factories. These factories use interconnected systems to monitor production in real time, predict maintenance needs, and reduce downtime. By implementing digital technologies, manufacturers can increase productivity, enhance flexibility, and minimise waste.

Finance: The financial sector has long been undergoing transformation through digitalisation, with the rise of fintech companies replacing traditional banking models. Mobile banking, digital wallets, and blockchain technology have redefined financial services, making them more accessible and secure. Digitalisation has also improved fraud detection through AI-driven risk analysis and enhanced customer service through automated chatbots.

Retail: E-commerce has reshaped the retail industry, with companies like Amazon and Alibaba demonstrating the potential of digital platforms to offer seamless customer experiences. Retailers use big data to forecast demand, deliver personalised recommendations, and optimise supply chains. Mobile commerce (mCommerce) has become a vital channel for businesses, as more consumers shop

via their smartphones.

Healthcare: Digital technologies in healthcare, such as telemedicine and wearable devices, are revolutionising patient care. Real-time health monitoring, AI-assisted diagnostics, and electronic health records (EHRs) are improving patient outcomes while reducing healthcare costs. Digital tools support better chronic disease management, early diagnosis, and broader access to healthcare services. Across all industries, digitalisation enables greater efficiency, cost savings, and enhanced user experiences. It plays a central role in reshaping operational models and aligning business practices with the demands of a digitally connected environment.

3.3 The importance of digitalisation

3.3.1 Enhancing operational efficiency

One of the most significant advantages of digitalisation is its ability to improve the operational efficiency of business processes. By automating repetitive tasks, increasing data accuracy, and enabling real-time decision-making, digital tools streamline workflows and reduce operational costs.

- **Automation:** Digital tools such as robotic process automation (RPA) automate routine tasks such as data entry, invoicing, and customer support queries. Automation reduces the risk of human error, lowers labour costs, and allows employees to focus on higher-value tasks that contribute more directly to business success.
- **Data-driven decision-making:** Digital tools enable companies to collect and analyse vast volumes of data in real time, resulting in more informed decision-making. By using data analytics, businesses gain insights into consumer behaviour, market trends, and operational performance.
- **Resource optimisation:** Digital tools, such as IoT sensors, can monitor equipment and machinery in real time, enabling predictive maintenance and minimising downtime. This helps prevent costly breakdowns, reduces operational expenses, and extends the lifespan of equipment.

3.3.2 Innovation and the creation of new business models

Digitalisation not only improves existing processes but also enables the creation of entirely new business models, fostering innovation across industries.

- **Platform-based business model:** Digitalisation has led to the emergence of platform-based business models, where consumers are directly connected with service providers. Examples include Uber, Airbnb, and Amazon, which have revolutionised traditional industries by enabling peer-to-peer transactions and offering scalable, cost-effective platforms.
- **Subscription-based services:** An increasing number of companies are using digital platforms to offer their products or services via subscription, providing customers with continuous access. Companies such as Spotify and Netflix apply this model to deliver digital content via cloud platforms, offering convenience and personalised user experiences.
- **Customisation and personalisation:** Companies can leverage digital tools to tailor products and services to specific customer needs. E-commerce platforms, for instance, use AI-powered recommendation systems to provide a personalised shopping experience, thereby increasing customer loyalty and boosting sales.

3.4 Tools and technologies in digitalisation

Digitalisation is transforming industries through the integration of advanced technologies that automate processes, enhance data utilisation, and drive innovation. These tools enable businesses to optimise operations, develop new business models, and deliver greater value.

3.4.1 Industry 4.0 technologies

Industry 4.0, often referred to as the fourth industrial revolution, involves the integration of digital technologies into manufacturing and industrial processes to create smart factories. This fundamental shift increases efficiency, flexibility, and responsiveness to market changes.

Key technologies and their impact:

1. Internet of Things (IoT): The Internet of Things refers to the integration of internet connectivity into everyday devices and appliances that traditionally did not have such capabilities. Examples of these devices range from thermostats and energy meters to vehicles and large industrial

machines. Essentially, IoT can turn these devices into "smart" devices, capable of sending and receiving data and communicating with one another. In 2021, just over one-quarter (26%) of small enterprises were using IoT, while large enterprises adopted it at nearly double the rate (48%). Among medium-sized enterprises, nearly 2 in 5 (37%) were using IoT. (Use of Internet of Things in enterprises — Eurostat) The number of IoT devices worldwide is projected to almost double, from 15.9 billion in 2023 to more than 32.1 billion by 2030. (Number of Internet of Things (IoT) connections worldwide from 2022 to 2023, with forecasts from 2024 to 2033 — Statista)

2. Cyber-Physical Systems (CPS: These systems combine physical machines with digital processes, enabling manufacturing operations to be driven by real-time data. According to the latest research, the global market for cyber-physical systems was valued at USD 120.84 billion in 2024 and is projected to reach USD 472.97 billion by 2034, growing at a compound annual growth rate (CAGR) of 14.62% over the forecast period. This rapid growth is driven by the increasing adoption of CPS in sectors such as manufacturing, energy, and healthcare, where CPS enhances productivity, enables automation, and optimizes operational processes through seamless integration of sensors, software, and intelligent control systems. (Cyber-Physical Systems (CPS) Market Size, Share, Trends & Research 2030 — Zion Market Research)

3. Big Data Analytics: The processing of large volumes of data enables companies to gain insights into operations, customer behaviour, and market trends. According to Statista, Big Data was the second most widely adopted technology, with approximately 61% of surveyed companies reporting its use. (Adoption rate of emerging technologies in organizations worldwide in 2023 — Statista)

4. Artificial Intelligence (AI) and Machine Learning (ML): Artificial intelligence is a broad term used to describe machines, most commonly computers, that can simulate human intelligence. AI systems can take various forms, ranging from simple chatbots and calculators to complex systems used in autonomous vehicles. According to McKinsey's Global Survey (2025), 78% of respondents said their organizations are using AI in at least one business function, up from 55% a year earlier, while 71% reported using generative AI. (The State of AI — McKinsey & Company)

Machine learning, which represents the largest segment of the artificial intelligence market, is projected to grow in Europe by a total of USD 106.9 billion (an increase of 431.05%) between 2025 and 2031. (Machine learning market size in Europe — Statist) The artificial intelligence market in Europe is experiencing rapid growth, driven by the increasing adoption of digital technologies, rising awareness of AI's potential, and the opportunities offered by online services. The AI market size in Europe is projected to reach USD 58.10 billion in 2025. According to Statista, the market is expected to grow at an annual rate of 26.27% between 2025 and 2031, reaching a total market volume of USD 235.50 billion by 2031. (Artificial Intelligence - Europe — Statista)

In Eastern Europe, the artificial intelligence market is experiencing a sharp increase in demand for chatbot and virtual assistant technologies, as companies aim to improve customer service and optimise operations. This trend is expected to continue as AI technology becomes more advanced and accessible.

5. Augmented Reality (AR) and Virtual Reality (VR): Augmented Reality (AR) refers to the integration of digital information with the user's environment in real time, in contrast to Virtual Reality (VR), which creates a completely artificial environment. Revenues in the AR and VR market in Europe are projected to reach USD 11.7 billion in 2025. According to Statista, this technology is expected to show an annual growth rate (CAGR) of 7.73% between 2025 and 2029, resulting in a projected market volume of USD 15.8 billion by 2029. In Europe, the number of AR and VR users is expected to reach 486.5 million by 2029. (AR & VR - Europe — Statista)

6. Additive Manufacturing and 3D Printing: 3D printing is a manufacturing process through which computer-generated 3D models are transformed into physical objects by printing in layers. This means that an object is formed by stacking one layer on top of another until a complete three-dimensional item is produced. According to Statista, the number of additive manufacturing and 3D printing devices worldwide is expected to reach 2.8 million by 2030, while the global 3D printing market is projected to reach USD 37.2 billion by 2026. (Additive manufacturing and 3D printing - statistics & facts — Statista)

7. Cloud Computing: is a way of using computing resources such as data storage, software, and processing power via the internet, without the need for owning or maintaining physical infrastructure.

Just like electricity is supplied on demand, cloud services allow users to access as many technological resources as they need, exactly when they need them. According to McKinsey, cloud adoption has become nearly universal, and the global economic potential of cloud computing could reach USD 3 trillion by 2030. (What is cloud computing? — McKinsey & Company)

The significant growth of the Industry 4.0 market confirms its profound impact on global industries. According to the IMARC Group, the global market size for Industry 4.0 reached USD 164.7 billion in 2024, with projections indicating it will reach USD 570.5 billion by 2033, growing at a compound annual growth rate (CAGR) of 14.44% from 2025 to 2033. Europe currently leads with over 35.8% market share. (Industry 4.0 Market Size — Statista IMarc Group) This significant growth is driven by several factors:

- **Pursuit of operational efficiency and productivity improvement:** Companies are leveraging Industry 4.0 technologies such as automation, IoT sensors, AI, and advanced analytics to streamline processes, reduce waste, and optimise resource utilisation. This leads to significant cost savings, increased output, and improved competitiveness.
- **Demand for customisation and personalisation:** The ability to customise products at scale allows manufacturers to tailor production precisely to individual customer requirements, effectively meeting diverse consumer needs.
- **Complexity of modern supply chains:** Industry 4.0 technologies provide real-time visibility into supply chain operations, improving transparency, traceability, and responsiveness. These capabilities are invaluable for mitigating risks, ensuring quality control, and meeting regulatory requirements.

Despite the promising growth, the Industry 4.0 market faces challenges, particularly regarding complexity and integration issues. The diverse nature of Industry 4.0 technologies means that implementation processes can be complex, especially when integrating with existing systems that are often not easily compatible with modern technologies. This can result in costly and time-consuming adaptations, requiring specialised expertise and careful planning to minimise potential disruptions.

The COVID-19 pandemic accelerated the adoption of Industry 4.0 technologies. As global supply chains faced labour shortages and disruptions, businesses turned to automation, IoT, and AI-driven solutions to maintain production levels.

3.4.2 Enterprise Resource Planning (ERP) Systems

ERP systems are integrated software platforms that manage nearly all business processes within a company, including finance, procurement, human resources, and production. Key benefits of using ERP systems include:

- **Centralised data management:** ERP systems provide a comprehensive overview of operations, improving efficiency and interconnectivity across departments. The ERP market in Europe is projected to generate revenues of USD 12.67 billion in 2025. According to Statista, the market is expected to grow at an annual rate of 3.76% over the next five years, reaching a value of USD 15.24 billion by 2030. (Enterprise Resource Planning Software - Europe — Statista)
- **Process automation:** Automating routine tasks reduces manual errors and increases productivity.

In 2023, the share of EU enterprises using ERP software was 43.3% overall, with adoption ranging from 37.9% among small enterprises to 86.3% among large enterprises. (Enterprises in Europe using ERP — Eurostat)

This steady expansion highlights the growing adoption of ERP solutions, as businesses across Europe prioritise operational efficiency, streamlined processes, and increased productivity. ERP systems, which offer centralised data management and integration of business processes, are essential for companies with complex supply chains or operations spread across multiple locations. Customer preferences, market trends, and macroeconomic factors play a significant role in driving ERP implementation in Europe. Countries such as Germany and France are leading the way, driven by a high concentration of manufacturing enterprises. At the same time, Eastern Europe is experiencing growth fuelled by demand for cloud-based, adaptable, and mobile ERP solutions.

3.4.3 Customer Relationship Management (CRM) Software

CRM is software used to manage all interactions with a business’s current and potential customers. The primary goal of a customer relationship management system is to reduce costs and increase profitability by improving customer satisfaction, loyalty, and advocacy. The CRM system

stores customer information across all stages of interaction with the company. According to Statista, projected revenues in the European CRM software market are expected to reach USD 21.71 billion by the end of 2025. This market segment is forecast to grow at an annual rate of 7.73% between 2025 and 2030, resulting in a projected market volume of USD 31.51 billion by 2030. (Customer Relationship Management Software - Europe — Statista) Key features and their impact:

- **Data analytics and personalisation:** The CRM systems enable organisation and analysis of customer data. They also allow businesses to compare this data with historical information and provide clearly structured dashboards that present insights quickly and efficiently.
- **Automation of routine tasks:** Automating everyday tasks, such as calendar management, updating customer information, and data entry, helps employees focus on work that adds greater value to the business. CRM automation simplifies the entire process from marketing to sales through a sequence of coordinated workflows. In 2023, 25.8% of enterprises in Europe were using customer relationship management (CRM) software.

Implementing a centralised system allows businesses to stay organised and concentrate on revenue-generating activities. Using CRM software reduces administrative tasks and allows more time to focus on sales and a positive customer experience.

3.4.4 E-commerce

E-commerce, defined as the trade of goods and services over the internet, is revolutionising the way individuals and businesses conduct transactions on a global scale. The rapid expansion of internet access and digital infrastructure has fuelled the growth of e-commerce, with global retail e-commerce expected to exceed USD 4.3 trillion in 2025. (E-commerce worldwide - statistics & facts — Statista)

This growth is driven by the convenience and efficiency offered by online platforms, allowing businesses to operate entirely online or to complement their traditional sales channels.

The rise of e-commerce is reshaping consumer behaviour and expectations. Online platforms such as Amazon dominate this space by offering a wide range of products and services, easy access, price comparison, and the convenience of shopping from home.

Mobile commerce (m-commerce): Mobile commerce is an integral part of the digital retail transformation, with smartphones accounting for nearly 80% of all retail website visits worldwide in 2025. This trend is particularly strong in regions like Asia, where countries such as China and South Korea generate over 70% of their total online sales via mobile devices, driven by high smartphone penetration and the widespread use of shopping apps like Temu and Shein. (E-commerce worldwide - statistics & facts — Statista)

In Europe, e-commerce continues its strong growth trajectory. In 2025, the European e-commerce market is projected to generate USD 707.9 billion in revenue, with an annual growth rate (CAGR) of 7.95% expected through 2029, reaching approximately USD 961.27 billion by the end of the period. The number of users is projected to reach over 446 million by 2029, with a user penetration rate increasing from 47.6% in 2025 to 55.8% by 2029. (eCommerce - Europe — Statista) Growth is driven by increasing digitalisation, greater mobile usage, and evolving consumer preferences particularly among younger demographics. Clothing, footwear, and fashion accessories remain the most popular online purchase categories, while sustainability and mobile-first shopping trends continue to reshape buying behavior.

In North Macedonia, the e-commerce market is also showing strong growth, with an annual growth rate of 16% projected for the period from 2024 to 2029. (Overview of E-commerce in the Republic of North Macedonia and Comparison with Western Balkan and European Countries, 2024 — E-commerce Association of North Macedonia) However, the market remains relatively small, with the majority of online sales coming from foreign platforms such as AliExpress. Domestic businesses in North Macedonia face challenges such as low levels of digital literacy and limited access to advanced payment technologies, but there is strong potential for growth.

This integration of e-commerce into the broader context of digital transformation highlights its role as a key driver of economic activity in the digital era, offering businesses the opportunity to expand globally and meet the evolving demands of consumers.

4. CONCLUSION

Digitalisation represents a significant form of innovation and has the potential to transform traditional business operations. By adopting digital technologies and automation, companies can improve productivity, increase operational efficiency, and develop new business models. Digital technologies enable more effective resource management, reduce waste, and provide more efficient customer service.

Despite these advantages, small and medium-sized enterprises, especially those in developing countries, often face challenges in implementing digitalisation. These challenges include financial limitations, a lack of digital skills among the workforce, and resistance to change. Addressing these barriers requires a systematic and gradual approach, including investment in employee training and the phased introduction of new technologies.

Digitalisation is not simply a technological upgrade but a strategic necessity that redefines traditional business operations. Companies that prioritise innovation and adopt digital technologies in a structured way will be better prepared to respond to market changes, meet customer expectations, and achieve long-term success.

REFERENCES

1. 18th Annual Global CEO Survey — PwC, https://www.pwc.com/gx/en/ceo-survey/2015/assets/pwc-18th-annual-global-ceo-survey-jan-2015.pdf
2. Analysis on Internet traffic and 5G network coverage 2024 — ITU, https://www.itu.int/en/mediacentre/Pages/PR-2024-11-27-facts-and-figures.aspx
3. Usage of information and communication technologies in households and by individuals, 2024 — State Statistical Office, https://www.stat.gov.mk/pdf/2024/8.1.24.32_mk.pdf
4. 2025 State Digital Decade — DESI, https://digital-strategy.ec.europa.eu/en/library/state-digital-decade-2025-report
5. Germany - The World’s Leading Industrie 4.0 Nation — GTAI, https://www.gtai.de/en/invest/industries/industrial-production/industrie-4-0#:~:text=Germany%20is%20the%20world’s%20automotive,the%20country’s%20industry%20R%26D%20spending.
6. Use of Internet of Things in enterprises — Eurostat, https://ec.europa.eu/eurostat/statistics-explained/index.php?title=Use_of_Internet_of_Things_in_enterprises#:~:text=Highlights&text=In%202021%2C%2029%20%25%20of%20EU,for%20keeping%20their%20premises%20secure.&text=In%202021%2C%20the%20percentage%20of,with%2026%25%20for%20small%20enterprises.
7. Number of Internet of Things (IoT) connections worldwide from 2022 to 2023, with forecasts from 2024 to 2033 — Statista, https://www.statista.com/statistics/1183457/iot-connected-devices-worldwide/
8. Cyber-Physical Systems (CPS) Market Size, Share, Trends & Research 2030 — Zion Market Research, https://www.zionmarketresearch.com/report/cyber-physical-systems-market
9. Adoption rate of emerging technologies in organizations worldwide in 2023 — Statista, https://www.statista.com/statistics/661164/worldwide-cio-survey-operational-priorities/#:~:text=Implementation%20of%20emerging%20technologies%20in%20companies%20worldwide%202023&text=As%20of%202023%2C%20nearly%2092,on%20small%20or%20large%20scale.
10. The State of AI — McKinsey & Company https://www.mckinsey.com/capabilities/quantumblack/our-insights/the-state-of-ai
11. Machine learning market size in Europe — Statista https://www.statista.com/forecasts/1449857/machine-learning-market-size-europe#:~:text=Machine%20learning%20market%20size%20in%20Europe%20from%202021%2D2031&text=The%20market%20size%20in%20the,U.S.%20dollars%20(%2B431.05%20percent).
12. Artificial Intelligence - Europe — Statista https://www.statista.com/outlook/amo/ar-vr/europe

13. AR & VR - Europe — Statista, https://www.statista.com/outlook/amo/ar-vr/europe#:~:text=The%20revenue%20in%20the%20AR,US%243.2bn%20in%202024.
14. Additive manufacturing and 3D printing - statistics & facts — Statista, https://www.statista.com/topics/1969/additive-manufacturing-and-3d-printing/
15. What is cloud computing? — McKinsey & Company https://www.mckinsey.com/featured-insights/mckinsey-explainers/what-is-cloud-computing
16. Industry 4.0 Market Size — Statista IMarc Group https://www.imarcgroup.com/industry-4-0-market
17. Enterprise Resource Planning Software - Europe — Statista, https://www.statista.com/outlook/tmo/software/enterprise-software/enterprise-resource-planning-software/europe
18. Enterprises in Europe using ERP — Eurostat https://ec.europa.eu/eurostat/web/products-eurostat-news/w/ddn-20240516-2
19. Customer Relationship Management Software - Europe — Statista, https://www.statista.com/outlook/tmo/software/enterprise-software/customer-relationship-management-software/europe
20. E-commerce worldwide - statistics & facts — Statista, https://www.statista.com/topics/871/online-shopping/
21. E-commerce worldwide - statistics & facts — Statista, https://www.statista.com/topics/871/online-shopping/
22. eCommerce - Europe https://www.statista.com/outlook/emo/ecommerce/europe
23. Overview of E-commerce in the Republic of North Macedonia and Comparison with Western Balkan and European Countries, 2024 — E-commerce Association of North Macedonia, https://heyzine.com/flip-book/0dee426197.html

DIGITALISATION OF THE WOOD PROCESSING AND FURNITURE MANUFACTURING INDUSTRY

Mira Stankevikj Shumanska[1], Angela Nikolovska[2], Ivana Antovska[1]

[1]Ss Cyril and Methodius University in Skopje, North Macedonia
Faculty of Design and Technologies of Furniture and Interior – Skopje
[2]KAPA5 ENTERTEJMENT DOOEL Skopje
e-mail:stankevik@fdtme.ukim.edu.mk, angelanikolovska10@gmail.com, antovska@fdtme.ukim.edu.mk

ABSTRACT

The potential for digital transformation in industries such as wood processing and furniture manufacturing highlights the vital role of innovation in driving entrepreneurial growth and the evolution of these sectors. Analyses show that while the adoption of innovative practices is essential for all enterprises, a structured and strategic approach is needed to overcome the challenges associated with digitalisation. The scientific paper indicates that innovation, particularly digital innovation, forms the foundation for businesses aiming to maintain their competitive advantage, adapt to market dynamics, and ensure long-term success in a digitalised economy.

Keywords: innovation, digitalisation, digital transformation, wood processing industry, furniture manufacturing, operational efficiency.

1. INTRODUCTION

The wood processing and furniture manufacturing industries have long been rooted in tradition, with production largely based on manual craftsmanship, artisanal skills, and labour-intensive processes. However, the global market and customer demands are evolving rapidly, pushing these industries towards modernisation and the adoption of digital tools. While traditional practices still hold significant value, digitalisation offers an opportunity for progress and has become the only viable path to maintaining competitiveness among manufacturers.

Digitalisation has rapidly emerged as a transformative force across industries, and the wood sector is no exception. As industrial sectors worldwide implement digital innovations to enhance efficiency, optimise production, and boost competitiveness, the wood processing and furniture manufacturing industries face similar pressures. The need to adapt to digital technologies is driven by several factors, including shifts in market dynamics, heightened competition, the rise of Industry 4.0, and the demand for improved resource management and sustainability.

In the wood and furniture industries, digitalisation refers to the integration of digital technologies into business operations and manufacturing processes. These technologies include automation, data analytics, the Internet of Things (IoT), and other advanced tools that enable companies to improve efficiency, monitor operations in real time, and reduce waste. By adopting these technologies, businesses can streamline operations, minimise human error, and make informed decisions based on real-time data.

Nevertheless, despite its benefits, the wood processing and furniture sectors have been slower to embrace digitalisation compared to other industries. The traditional nature of the sector, reliance on manual labour, and insufficient workforce education contribute to this lag. In regions such as the Balkans, companies are still in the early stages of digital implementation. Research shows that while many wood processing companies recognise the potential advantages of digital technologies, the majority lack a systematic or strategic approach to implementing these innovations. (Digitalization in wood processing companies - Managers Perspective — Dražena Gašpar, Mirela Mabić, Ivica Ćorić).

2. POTENTIAL FOR DIGITALISATION

Digitalisation represents a transformative opportunity for the wood processing and furniture manufacturing industries. By integrating digital tools into various aspects of production, supply chain management, and customer communication, businesses can achieve greater efficiency, scalability, and innovation.

2.1 Production Processes

The production process within wood processing and furniture manufacturing is the area where digitalisation can have the most significant impact. Computer-Aided Design (CAD) and Computer-Aided Manufacturing (CAM) form the foundation of this transformation, offering new ways to design, prototype, and manufacture products.

Computer-Aided Design (CAD): The CAD software enables designers to create precise, three-dimensional models of furniture, which can be easily modified, shared, and optimised before production begins. This software eliminates the need for manual drafting and speeds up the design process, while also allowing designers to visualise complex furniture pieces with greater accuracy. The global CAD market is expected to grow from USD 10.11 billion in 2024 to USD 15.77 billion by 2032, showing an annual growth rate of 5.7%. With the introduction of new software packages, the efficiency of production processes and modelling has significantly improved. This has also led to increased creativity in designs across different engineering disciplines. (Computer Aided Design Market Share, Size, Trends, Industry Analysis Report – Polaris)

Computer-Aided Manufacturing (CAM): The CAM software takes CAD designs and translates them into instructions for automated machines such as CNC (Computer Numerical Control) systems. CNC machines can cut, shape, and assemble components with extreme precision, ensuring consistent quality across production batches. These machines can handle complex designs that would be either impossible or financially unfeasible to produce using manual methods. The market for computer-aided manufacturing in Europe is projected to reach USD 1,659.1 million by 2030. It is expected to grow at an annual rate of 8.3% over the period from 2024 to 2030. (Europe Computer Aided Manufacturing Market Size & Outlook – Horizon)

Automation and robotics: In automated production facilities, machines carry out tasks that were previously done by workers. These machines range from basic systems, such as Computer Numerical Control (CNC) machines, to more complex robots that can be programmed for various functions. Robots are typically assigned tasks that are monotonous, dirty, dangerous, or physically demanding. These types of tasks are often referred to as the "4Ds of robotics" and are generally better suited for machines than for people. However, not all workers readily accept the increased use of robots in the workplace. Many are understandably concerned about being replaced. While some low-skilled jobs may be lost as a result, the introduction of robotics can also lead to the creation of new employment opportunities. Despite increasing capabilities, robots still cannot perform every task that humans can. The most effective approach is to combine the strengths of robots and human workers and create environments that support collaboration. The global industrial automation market is valued at 190 billion USD, with process automation being the largest segment. (Unlocking the industrial potential of robotics and automation – McKinsey)

Additive manufacturing (3D printing): 3D printing was previously mentioned in the chapter on digital technologies, but it holds particular significance for manufacturing processes in furniture production. This emerging technology is especially valuable for prototyping and small-scale production. It allows manufacturers to experiment with complex shapes, textures, and materials, enabling innovative furniture designs that go beyond the limitations of traditional woodworking. Additive manufacturing can also shorten production timelines by supporting rapid prototyping and faster product launches.

The digitalisation of manufacturing processes brings notable advantages in terms of flexibility, allowing producers to offer customised designs. The integration of smart technologies, such as IoT sensors in machinery, enables real-time monitoring of equipment performance, predictive maintenance, and greater control over production parameters.

2.2 Supply Chain and Logistics

In the furniture industry, efficient supply chain management is critical due to the high volume of raw materials required, complex logistics, and the global nature of the market. Digitalisation can significantly improve supply chain and logistics operations.

Greater transparency in the supply chain: Enterprise Resource Planning (ERP) systems provide complete visibility across the entire supply chain. From procurement to production and delivery, ERP systems consolidate data into a single platform, offering real-time insights into inventory levels, supplier performance, and shipment status. This visibility supports better and more streamlined decision-making, helping manufacturers manage inventory more effectively and avoid disruptions.

Automated warehousing: Warehouse automation involves optimising repetitive and time-consuming operations traditionally performed manually by workers. In digitised supply chains, automated storage systems use robots and IoT devices to manage the storage and distribution of products. Smart sensors and RFID (Radio-Frequency Identification) can track inventory in real time, reducing the risk of overstocking or stockouts. Warehouse automation also lowers labour costs and improves order accuracy.

According to Statista, the global warehouse automation market was valued at over USD 23 billion in 2023 and is expected to grow at an annual growth rate of around 15%, reaching approximately USD 41 billion by 2027. (Size of the warehouse automation market worldwide from 2023 to 2027 – Statista)

Logistics optimisation: Logistics automation encompasses both hardware and software solutions designed to optimise logistics processes, including transportation, warehousing, and data management. Automating these operations increases efficiency, reduces errors, and shortens execution times. Digital tools can streamline logistics by using data to optimise delivery routes, reduce fuel consumption, and minimise delivery times. For example, GPS tracking and delivery route optimisation algorithms ensure that products are delivered to customers efficiently, lowering delivery costs and increasing customer satisfaction. The global logistics automation market was valued at USD 38.76 billion in 2023 and is expected to grow at an annual rate of 15.90% through 2032. (Logistics Automation Market Share, Size, Trends, Industry Analysis Report – Polaris) Automation plays a key role in enabling business expansion by allowing efficient management of larger workloads through the use of autonomous robots, transport systems, and automated warehouse solutions.

Sustainability: The integration of digital tools can also contribute to sustainability in supply chain management. By optimising resource usage, manufacturers can reduce waste, minimise their carbon footprint, and ensure a more sustainable supply of raw materials.

2.3 Sales, Marketing, and Customer Communication

Digitalisation is transforming how furniture manufacturers and entrepreneurs interact with their customers. E-commerce, digital marketing, and customer data analytics open new opportunities for growth.

E-commerce and Online Sales: The rise of e-commerce platforms enables furniture manufacturers to present their products to a global audience without the need for physical stores. Selling directly to consumers helps reduce overhead costs and increase profit margins. A key advantage is the way these platforms function. For example, online configurators let customers personalise products by selecting materials, colours or dimensions before placing an order, improving the overall shopping experience.

Augmented Reality (AR): Augmented Reality (AR) which refers to the integration of digital information with the user’s environment in real time, plays a key role in the digitalisation of the furniture industry and enhances the sales process. AR is reshaping the way people buy furniture. With AR applications, customers can preview how a piece of furniture will look in their home before purchasing. The IKEA Place app, for instance, allows users to see 3D models of IKEA products in their own rooms, helping to reduce uncertainty and improve satisfaction.

Digital Marketing and Analytics: Modern CRM systems and data analytics tools help manufacturers and retailers segment customer bases, track buying patterns and improve the targeting of marketing campaigns. By understanding customer preferences, companies can offer tailored recommendations, launch focused promotions and build long-term customer loyalty.

3. IMPLEMENTATION OF DIGITAL TECHNOLOGIES

Digital transformation is a complex process that requires careful planning, strategic investment, and adequate technological infrastructure. While the potential benefits of digitalisation are significant, the path to full implementation involves several critical steps.

To successfully implement digital technologies in the wood processing and furniture manufacturing industries, companies should follow a structured approach:

Assessment of existing capacities: The first step in digital transformation is analysing the current state of the business. This involves conducting a digital audit of existing processes, identifying bottlenecks, and determining where digital tools can create the greatest value. This may include evaluating manual tasks, outdated machinery, or inefficient supply chain practices.

Developing a digital strategy: After the assessment, companies need to create a long-term digital strategy aligned with their business objectives. This strategy should define which technologies will be implemented, the desired outcomes (such as cost reduction or improved customer communication), and an implementation roadmap. The strategy should also allow for scalability so that today’s digital solutions can grow alongside the business.

Investing in technology: Once the strategy is in place, the next step is investing in the appropriate technologies. This includes selecting a suitable ERP system, CNC machinery, or implementing IoT devices. Companies should prioritise technologies that offer flexibility, integration capabilities, and real-time data analytics.

Change management and workforce training: A crucial aspect of digital transformation is managing the organisational changes that come with implementing new technologies. This includes preparing employees for the changes, providing thorough training, and fostering a company culture that embraces innovation. Upskilling the workforce is essential, as employees must be able to operate new machinery, interpret data, and manage digital platforms.

Monitoring and continuous improvement: Digital transformation is an ongoing process that requires regular evaluation of the technologies in use. Companies should establish key performance indicators (KPIs) to measure the success of their digital initiatives and identify areas for improvement. As new technologies and innovations emerge, manufacturers must be prepared to adapt and optimise their operations accordingly.

4. CHALLENGES IN IMPLEMENTING DIGITALISATION

Despite the numerous opportunities that digitalisation offers to the wood processing and furniture manufacturing industry, the process of full digital transformation presents numerous challenges. Research highlights several key obstacles that companies in this sector face when attempting to implement digital technologies.

One of the most significant challenges is the financial barrier related to digitalisation. Moving from traditional methods to digital tools requires substantial investment in new equipment, software, and infrastructure. Many wood processing companies, particularly small and medium-sized enterprises, operate with limited budgets. This makes it difficult to justify the costs of these technologies without immediate returns. The lack of financial resources is aggravated by the absence of strategic planning, since most companies do not have an annual digitalisation plan or a dedicated budget for such initiatives.

Another key barrier is the lack of digital skills among the workforce. Many employees in the wood processing industry do not possess the digital literacy or technical knowledge needed to work with advanced technologies such as IoT, automation, and data analytics. This gap in skills presents a serious challenge to the effective implementation of digital solutions. In addition, companies face high staff turnover, which further complicates efforts to develop a digitally capable workforce. Training and upskilling employees require both time and resources. Without a systematic approach to workforce development, companies struggle to keep pace with technological progress.

Resistance to change at various organisational levels is also a major barrier. Middle management and employees, particularly those who have long relied on traditional methods, often resist adopting new technologies. This cultural resistance can slow the pace of digital transformation, as employees may see digitalisation as a threat to their jobs or as an unnecessary disruption to established practices.

On the technological side, the lack of integration between different digital systems creates further challenges. Many companies do not use a unified data system, which means data from various devices and software programmes is inconsistent. This lack of standardisation makes it difficult to obtain a complete overview of operations. The fragmentation of data prevents companies from fully taking advantage of digital technologies for decision-making and process optimisation. (Digitalisation in the Construction and Woodwork sectors – Nicole Oertwig, Konstantin Neumann and Holger Kohl)

Although many wood processing and furniture manufacturing companies recognise the need for digitalisation, they must overcome serious barriers related to finance, employee skills, organisational culture, and technology integration in order to fully implement digital transformation.

4.1 Practices and Strategies

Research highlights several practices that can support the successful implementation of digital technologies in the wood processing and furniture industries:

- **Phased Implementation:** Introducing digitalisation in phases is often the most effective approach. Rather than overhauling all business operations at once, companies should begin by implementing digital tools in specific areas, such as automating a single production line or integrating an ERP system for inventory management. This allows them to assess the impact of digitalisation and make adjustments before scaling the initiative across the entire organisation.
- **Engaging a Technology Consultant:** In many cases, furniture manufacturing companies lack the in-house expertise needed to implement complex digital solutions. Engaging external firms or consultants can help address this issue. These consultants can provide technical support, deliver training, and guide companies through the complexities of digital transformation.
- **Customer-Oriented Digitalisation:** Successful digital transformations often prioritise the customer experience. This includes using digital tools to improve services, personalise marketing efforts, and enhance the online sales experience.
- **Data-Driven Focus:** Digitalisation generates large volumes of data. Businesses must focus on data management and analytics in order to turn this data into actionable insights. Leveraging data to improve decision-making, optimise operations, and predict trends is essential for maximising the benefits of digital transformation.

5. ANALYSIS OF IKEA’S INNOVATION AND DIGITALISATION STRATEGY

Founded in 1943 in Älmhult, Sweden, IKEA has evolved from a small mail-order business into the world’s largest furniture retail company. Known for its flat-pack furniture and Scandinavian style, IKEA operates 486 stores worldwide, with a revenue of nearly 45.1 billion euros in 2024. (FY24 Year in Review – IKEA) The company closely follows customer demands and continuously develops its business model to meet their changing needs.

5.1 IKEA’s Approach to Innovation

- **Stylish and Affordable Products with Scandinavian Design:** IKEA’s business model focuses on producing stylish, functional, and affordable furniture. The products are designed for easy assembly and transport, which optimises logistics and reduces costs. Through in-house production and the establishment of regional manufacturing centres, IKEA maintains strong control over quality and expenses.
- **Omnichannel Experience:** IKEA integrates physical and digital channels to enhance the customer experience and simplify the purchasing process. This approach allows customers to shop online, use 3D visualisation tools to plan their homes, and access fast and secure home delivery. Approximately 899 million customers visited IKEA stores in 2024, while digital sales accounted for 26% of total revenue. (Inter IKEA Group Financial Summary FY24)
- **Sustainability and the Circular Economy:** IKEA is committed to sustainable practices. This includes a focus on renewable energy in its stores, sustainable sourcing of materials, and initiatives such as furniture recycling and buy-back programmes for used products. The company aims to become climate-positive by 2030.

5.2 Digital Transformation Strategy

- **Expansion of E-Commerce:** IKEA has increased its online sales by creating in-store collection points for online orders. This transformation has helped the company adapt to the shift towards online shopping. According to company reports, IKEA's online platform received as many as 4.6 billion visits in 2024. (Inter IKEA Group Financial Summary FY24)
- **Integration of AR and VR:** IKEA's augmented reality (AR) app, IKEA Place, allows customers to visualise furniture in their homes before making a purchase. Virtual reality (VR) is also used in stores to simulate product placement, enhancing the customer experience.
- **Generative AI Shopping Assistant:** In 2023, IKEA introduced a generative AI shopping assistant that enables customers to receive real-time product recommendations and inventory information. This technology has improved the user experience, simplified the purchasing process and increased online conversion rates.

IKEA's ongoing innovations are driven by the need to remain competitive in a rapidly evolving market. The company focuses on understanding customer needs, improving accessibility, and staying true to its core values of sustainability and design. Every innovation is aligned with IKEA's vision to create a better everyday life for its customers and make a positive contribution to society.

6. CONCLUSION

Digitalisation represents a significant form of innovation. By adopting digital technologies and automation, companies in the wood processing and furniture manufacturing industries can improve productivity, increase operational efficiency, and develop new business models. Digital technologies also enable better resource management, reduced waste, and more efficient customer service. The example of IKEA demonstrates how digitalisation can redefine traditional practices and lead to sustainable growth.

The implementation of digital technologies is of great importance for the wood and furniture industries to maintain their competitiveness and meet growing demands for personalised products, faster production times, and sustainability. Digital transformation will require significant investment not only in technology but also in workforce training, as companies must equip their employees with the necessary skills to operate advanced digital tools. The pressure to digitalise is not only about improving efficiency, but also about building more resilient and flexible operations that can adapt to future market changes and innovation.

REFERENCES

1. Digitalization in wood processing companies - Managers Perspective — Dražena Gašpar, Mirela Mabić, Ivica Ćorić, https://sm.ef.uns.ac.rs/index.php/proceedings/article/view/292/413
2. Computer Aided Design Market Share, Size, Trends, Industry Analysis Report – Polaris, https://www.polarismarketresearch.com/press-releases/computer-aided-design-cad-market
3. Europe Computer Aided Manufacturing Market Size & Outlook – Horizon, https://www.grandviewresearch.com/horizon/outlook/computer-aided-manufacturing-market/europe
4. Unlocking the industrial potential of robotics and automation – McKinsey, https://www.mckinsey.com/~/media/mckinsey/industries/advanced%20electronics/our%20insights/unlocking%20the%20industrial%20potential%20of%20robotics%20and%20automation/unlocking-the-industrial-potential-of-robotics-and-automation-final.pdf
5. Size of the warehouse automation market worldwide from 2023 to 2027 – Statista, https://www.statista.com/statistics/1094202/global-warehouse-automation-market-size/#:~:text=The%20global%20warehouse%20automation%20market,billion%20U.S.%20dollars%20in%202027
6. Logistics Automation Market Share, Size, Trends, Industry Analysis Report – Polaris, https://www.polarismarketresearch.com/industry-analysis/logistics-automation-market
7. Digitalisation in the Construction and Woodwork sectors – Nicole Oertwig, Konstantin Neumann and Holger Kohl, https://library.fes.de/pdf-files/bueros/bruessel/20331-20230530.pdf

8. FY24 Year in Review - IKEA, https://www.ikea.com/global/en/our-business/how-we-work/year-in-review-fy24/
9. Inter IKEA Group Financial Summary FY24 - https://www.inter.ikea.com/-/media/interikea/igi/financial-reports/fy24-financial-reports/inter_ikea_group_financial_summary_fy24.pdf?rev=76f8481fd2e14a63a8359eeda8eefdbd&sc_lang=en
10. IKEA - Statistics & Facts - Statista, https://www.statista.com/topics/1961/ikea/

LEAN LOGISTIC - IMPLEMENTATION OF LEAN METHODOLOGY IN MANUFACTURING PROCES ON LATTOFLEX

Ivana Antovska[1], Mira Stankevikj Shumanska[1]

[1]Ss.Cyril and Methodius University, Skopje, Republic of North Macedonia,
Faculty of Design and Technologies of Furniture and Interior
e-mail: antovska@fdtme.ukim.edu.mk; stankevik@fdtme.ukim.edu.mk

ABSTRACT

LEAN methodology focuses on optimizing processes, reducing costs, and increasing quality by identifying and eliminating activities that do not add value to the product or service. It is a systematic approach to eliminating waste in a manufacturing process to create more value for the customer and also jointly shifting the mindset and behavior among those involved in the production process, not just enforcing rules.

This study focuses at implementing the LEAN methodology in the manufacturing processes of the wood processing industry in Macedonia production on lattoflex. The benefits have been identified and a comparison has been made of the quality and quantity of the products before and after the implementation of the LEAN methodology, including added value of the production process itself.

Emphasis is also placed on the involvement of all employees, encouraging them to make suggestions that can facilitate and improve daily operations, thereby increasing motivation.

Keywords : LEAN methodology, Value Stream Mapping , Kaizen, Eliminating Waste, Lattoflex.

1. INTRODUCTION

The main and only request from the company was not to publish its name. The company was established in 2004. Just from the beginning, specialized itself in producing high quality molded plywood parts for chairs, like seats, backrests, shells, armrests and legs. The company has its own beech veneer production and is the main chairs and plywood chair components supplier of almost all national chair manufacturers and resellers, and with its around 90% export orientation is one of the biggest plywood chair components supplier in the Balkans, Western Europe and Scandinavia. It’s very well structured and organized manufacturing, but they are always focused on continuous improvement and waste reduction in production processes – kaizen.

As the subject of interestis is improvement – the kaizen, of manufacturing processes of lattoflex through the implementation of LEAN tools. Lattoflex is produce in different dimensions according to the client's requirements. The process begins with sorting the veneer sheets into 4 classes, from A to D class. The first three classes are used for this product. Next is the gluing phase, the formation of the veneer boards of 7 sheets. Glue is applied with an automatic gluer. Then comes the stacking of the sheets - their preparation for gluing in a high-frequency press. Depending on the number of sheets, drying and forming the impression is from 3 to 7 minutes. Each of the boards must stand and cool for 24 hours.

The next three phases are mechanical processing of the boards - first they are dimensioned along the length of a formatizer, which cuts to the exact length. Next is the operation of a circular saw, which cuts the sheet to the required width of the latoflex. And the last processing is on a milling machine that processes the edges of the latoflex itself, so that they are not sharp. After the milling machine, each latoflex slat is taken by the worker and checked to see if additional manual processing is needed or if there are any other damages and arranged on the appropriate pallet.

The focus is on the last three operations, for which our goal is to synchronize them to work with the same tact time, to reduce the number of employees who will work on this production line and to reduce waste. The cycle time of all three machines is different.

2. METHODOLOGY

Value-stream mapping (VSM) is *diagraming every step involved in the material and information flows needed* to bring a product from order to delivery. It helps us to see and also understand the flow of materials and information as a product goes through the value stream. In LEAN bought materials and information, are with same importance. A value stream is all the actions (both value-creating and non value-creating) required to bring a product from raw material to the arms of the customer. Value stream mapping typically begins with a team creating a **current state map**. This means capturing the actual condition of a value stream's material and information flow. Subsequently, the team draws **a future state map**. That is to say a target image of how material and information *should* flow through the value stream.

3. RESULTS AND DISCUSSION

Developing a future state begins with an analysis of the current situation. We began with quick walk along production process, after that from the shipping end and work upstream. Drawing by hand means we are focusing on understanding the flow of information and materials.

- Drawing the Current-State Map

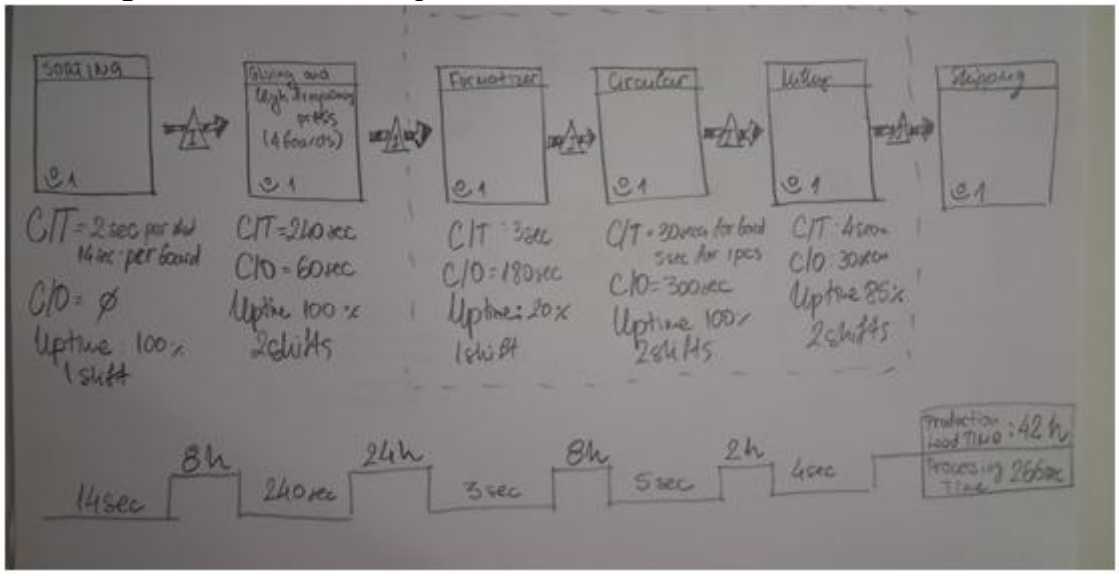

Figure 1. *Current-State Map.*

C/T – cycle time – time elapses between one part coming off the process to the next part coming off
C/O – changeover time – switch from producing one product time to another
Uptime – on-demand machine uptime

We are focusing on the last three operations. Each process is an isolated island and produced and pushed products forward according to schedules instead of the actual needs of the next process. Produced material is not yet needed, and need to be handled, stored… - muda. Also defects stay hidden until the next process finally use the parts and find the problem. It was very often situation, and the waste was around 35%. Overproduction is source of all kind of waste/muda – extra operators, equipment capacity, storage…

- Drawing the Future-State Map

All this problems lead us to find solution – shorter lead time, higher quality, lower costs and to implement LEAN manufacturing with linking this three process. Main characteristic of a LEAN Value Stream is to get one process to produced only what next one needs when it needs it.

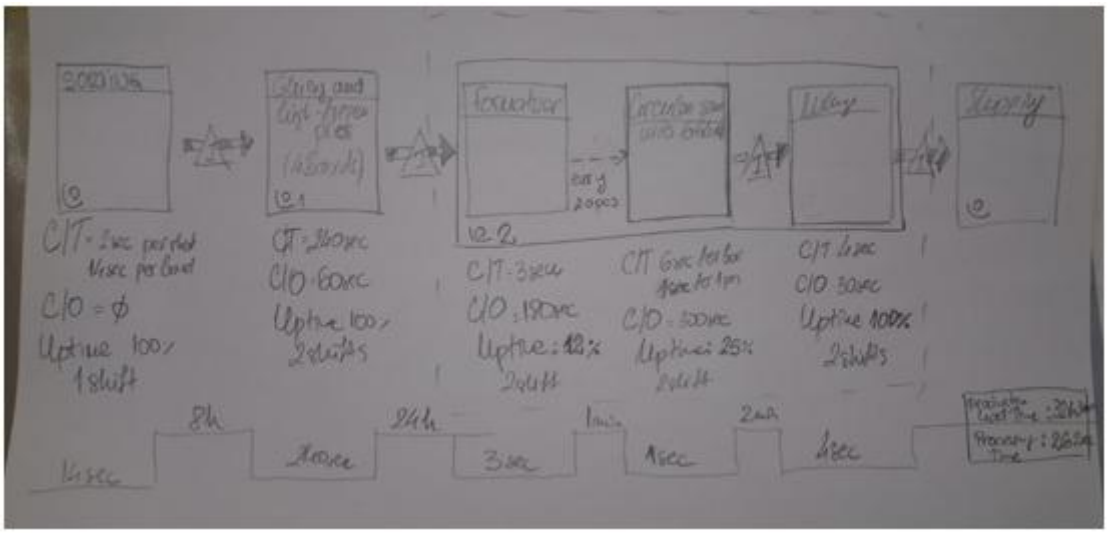

Figure 2. *Future-State Map.*

This Future – State map was implemented in this manufactured process. The first thing was changed the regular circular saw with 6 blades circular saw. The process was designed to operate very slow cycle time. Cycle time reduced from 30seconds to only 6 seconds for 6pcs of lattoflex. We link this process with the pervious one, formatizer, by adding automatic line and got continuous flow by FIFO Lane (first in, first out). Think of FIFO lane like a chute that can hold only certain number of pieces, in this case 20pcs.

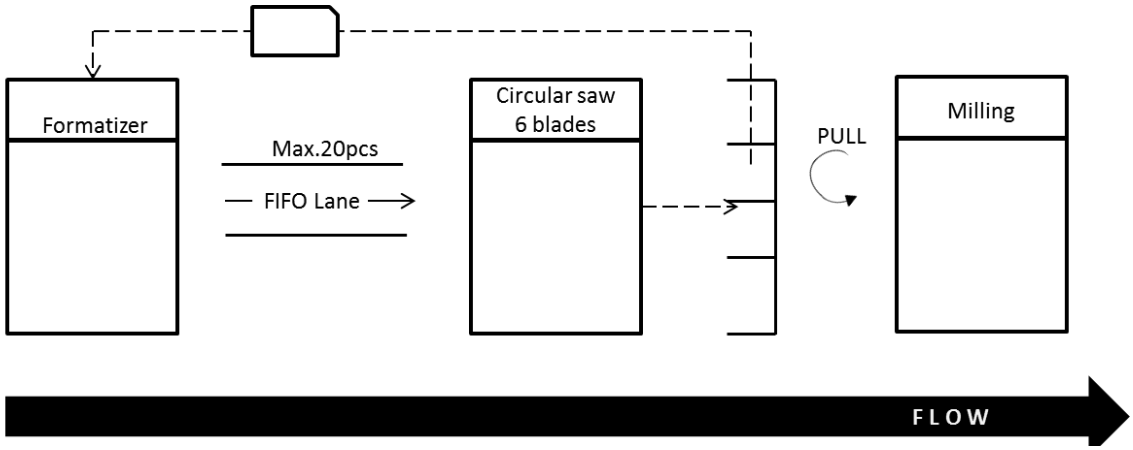

Figure 3. *FIFO lane.*

We reduced the number of workers from 6 to 5 and increase the Uptime to last operation from 85% to 100%. It is very important for adding value to the final product. Defects didn't stay hidden until the next process but will be found after few pieces. By that, the waste is eliminated up to 5%. There is a big difference between Production lead time from 42hours at almost 32hours and only 4seconds in Processing time. With all this benefits fulfill the main point of kaizen - aims to make small, incremental improvements in processes and systems, leading to significant long.

4. CONCLUSIONS

There are a lot of benefits by implementation of LEAN in manufacturing process in production on lattoflex**.** All this changes was made and we got the measurable results. This company has a huge potential for implementation of different parts from LEAN. Some of them are already implemented in other manufacturing processes with excellent results, but always have possibilities for improvements.

By systematic support and a long term vision this kind of implementation is possible in other wood companies in Macedonia.

REFERENCES

1. Rother, M., Shook, J. (2009). Learning to see: value stream mapping to add value and eliminate muda. Cambridge: Lean Enterprise Institute
2. Liker, J. (2004). The Toyota Way: 14 Management Principles from the World's Greatest Manufacturer.McGraw-Hill
3. Официјална интернет страница на LEAN. Достапна на www.lean.org [Пристапено на 01.08.2025.]
4. Зголемување на компетитивноста на компаниите со прмена на актуелни производи пристапи: Студии на случаи (2019). Машински факултет при универзитетот Св.Кирил и Методиј во Скопје

STATISTICAL MODELING OF SURFACE ROUGHNESS IN WOOD BANDSAWING FOR DESIGN, PROCESS MONITORING AND PRODUCT QUALITY OPTIMIZATION

Bujar Selimi

[1] Interior Design and Graphic Design Programs,
Universum International College,
Pristina, Kosovo
e-mail: bujar.selimi@universum-ks.org

ABSTRACT

This study investigates progressive surface degradation during longitudinal wood bandsawing using maximum surface roughness (R_{max}) as a dynamic quality indicator. Measurements were collected at three operational phases on both sides of beech boards under controlled machining conditions. A fixed effects Ordinary Least Squares (OLS) regression model with a phase × side interaction was applied to capture temporal and spatial variation. Phase emerged as the only significant predictor, while side and the interaction were non-significant, indicating machining symmetry. A Linear Mixed effects Model (LMM) with board as a random intercept produced identical fixed effect estimates and negligible between-board variance, confirming overparameterisation and supporting OLS retention. The proposed modelling approach offers an interpretable, statistically robust basis for monitoring surface quality in industrial settings, with potential applications in process stabilization, quality optimization, and predictive tool maintenance.

Keywords: surface roughness, wood sawing, OLS regression, mixed effects model, quality monitoring, longitudinal cutting.

1. INTRODUCTION

Maximum surface roughness (R_{max}) is a sensitive indicator of tool condition in industrial wood machining because it captures localized irregularities that mean parameters such as R_a may overlook (Csanády, Magoss, Tolvaj, 2015). In longitudinal band sawing, R_{max} reflects the combined influence of cutting-edge sharpness, feed-rate stability, and wood heterogeneity (Kminiak, Gašparík, Kvietková, 2015).

Prior studies have applied statistical and computational models to optimize cutting parameters with respect to surface quality, most often targeting R_a (Zhu et al., 2022; Talić & Hodžić, 2024; Bendikienė & Keturakis, 2016). Research on transversal cutting (Kminiak et al., 2015) and up-milling across wood densities (Pinkowski, Piernik, Krauss, 2024) confirms the role of operational phase and feed conditions. In beech up-milling, increases in chip thickness and feed speed raise both roughness and cutting power, with cross-section orientation also affecting outcomes (Piernik, Pinkowski, Krauss, 2023). Demonstrations of on-line sensing and tool-condition regression underline the industrial relevance of roughness monitoring (Sandak et al., 2020; Górski et al., 2019).

Phase‐indexed designs—where the process is sampled at multiple cumulative wear phases—are less common in longitudinal band sawing; compared with unrelated samples, phase indexing reduces between‐run variability and can increase statistical power (Siklienka et al., 2015). Moreover, much of the literature emphasizes R_a, while interpretable R_{max}-based models suitable for shop-floor deployment remain limited.

This study models phase-resolved progression of R_{max} under controlled longitudinal band sawing using a fixed effects Ordinary Least Squares (OLS) regression with a Phase × Side interaction. Measurements were taken at three predefined phases (A, B, C) on both board sides (L, R), enabling assessment of temporal trends and spatial symmetry under stable operating conditions. A Linear

Mixed effects Model (LMM) with Board as a random intercept was fitted as a robustness check to probe potential between-board variance (Gelman & Hill, 2007).

Research question

- Does R_{max} increase across phases (A→B→C) under constant cutting conditions?
- Is there a systematic difference between sides (L vs. R) or a Phase × Side interaction?
- Does an LMM reveal material between-board variance that would alter fixed effects inferen.

Study aims

1. Quantify: Phase-resolved progression of R_{max} under constant operating conditions (A→B→C).
2. Test: Side differences and a Phase×Side interaction (L vs R).
3. Model: Fit a parsimonious OLS model, report R^2, RMSE, and MAPE, and verify assumptions; assess between-board clustering via an LMM (ICC) as a robustness check.

This approach supports reproducible modelling of surface degradation in beech machining and may inform predictive maintenance strategies in sensor-assisted production (Lee et al., 2020; García Plaza, Núñez López, Beamud González, 2018; Achouch, Moussaoui, Zerhouni, 2022). To address these aims, Section 2 details a controlled protocol that combines phase-resolved sampling with profilometric measurements under constant conditions.

2. MATERIALS AND METHODS

2.1 Material specification

European beech (Fagus sylvatica L.) was used for its anatomical uniformity and relevance to surface-roughness studies. All nine boards were sequentially sawn from a single beech log to eliminate inter-log variability and were dimensionally matched (length ≈ 480 cm; thickness ≈ 2.5 cm). Three boards were sampled at each phase of the cutting timeline: A→D1–D3 (≈0 min), B→D4–D6 (≈60 min), C→D7–D9 (≈120 min).

Moisture content (u) was measured with a capacitive meter (GMK 100, GHM-Greisinger, Germany; density curve d.65 ≈ 650 kg·m^{-3}) and expressed on a dry-mass basis according to:

$$u = \frac{m_{wet} - m_{dry}}{m_{dry}} \times 100\ [\%]$$

where:

m_{wet} is the wet mass and m_{dry} is the oven-dry mass of the sample. The moisture content ranged from 45% to 50%.

2.2 Cutting procedure and operating conditions

Longitudinal sawing was performed on an industrial band saw (Braun Canali, TYP HBSG 1100). The machine operated continuously without stoppage throughout the 120 min run; phases A, B, and C mark time stamps along this uninterrupted process and index cumulative tool wear. Operating parameters were held constant to isolate tool–material interaction: feed rate, cutting speed, standardized tooth geometry (tangential cutting), manually regulated blade tension (to minimize vibration), cutting depth, and ambient temperature (18–22 °C).

2.3 Experimental design and sampling

Each board was measured at ten longitudinal positions (P0–P9) spaced 40 cm along ≈ 400 cm of usable length; the first and last 40 cm were excluded to minimize edge effects. Both left and right sides were scanned to capture spatial variation. The design yields 3×3×2×10=180 observations. Inference treats Phase (A–C) and Side (L/R) as fixed factors; Board (D1–D9) is nested within Phase.

2.4 Surface profilometry

R_{max} [μm] was measured immediately after each phase using a contact profilometer (SHAHE GS5337; range 0–6.5 mm; resolution 1 μm; accuracy ±3 μm). Measurements were acquired in raw-acquisition mode after calibration on the manufacturer's reference specimen and recorded with synchronized software.

Figure 1. *Overview of materials and instruments used in the experimental setup. From left to right: (1) beech log/boards from a single source, (2) industrial band saw (Braun Canali – TYP HBSG 1100), (3) processed boards, (4) capacitive moisture meter (GMK 100), and (5) contact profilometer (SHAHE GS5337).*

2.5 Data structure and descriptive summaries

The response variable was R_{max}. Fixed factors were Phase (proxy for cumulative cutting time) and Side. Board (nested in Phase) and Position (nested in Board) were design identifiers. One profile (single trace) was recorded per position and phase.

For each Phase–Side cell, the sample mean $\overline{x}$ and standard deviation s were computed as:

$$\overline{x} = \left(\frac{1}{n}\right)\sum_{i=1}^{n} x_i \qquad s = \sqrt{\frac{1}{n-1}\sum_{i=1}^{n}(x_i - \overline{x})^2}$$

When collapsing across sides with equal per-side sample sizes n

$$\bar{x}_{coll} = \frac{2\overline{x}_L + \overline{x}_R}{2},$$

$$s^2_{coll} = \frac{(n-1)s_L^2 + (n-1)s_R^2 + n(\overline{x}_L - \overline{x}_{coll})^2 + n(\overline{x}_R - \overline{x}_{coll})^2}{2n-1}$$

2.6 Model specification and estimation

We fitted a fixed effects ordinary least squares (OLS) model with Phase (A, B, C) and Side (L, R) as categorical predictors, including their interaction:

$$y_{ij} = \beta_0 + \beta_B I_B + \beta_C I_C + \beta_R I_R + \beta_{B\times R} I_B I_R + \beta_{C\times R} I_C I_R + \epsilon_{ij}$$

where:

- Response: $y_{ij} = R_{max}$
- Indicators: $I_{B,i}$ = indicator variables (1 if true, 0 otherwise)
- Reference: β_0 = intercept for Phase A, Side L
- Errors: $\epsilon_{ij} \sim N(0, \sigma^2)$ i.i.d.

Estimation used the closed-form OLS estimator:

$$\hat{\beta} = (X^T X)^{-1} X^T y,$$

With fitted values $\hat{y}_i = x_i^T \hat{\beta}$ and residuals

$$e_i = y_i - \hat{y}_i$$

2.7 Performance metrics and significance testing

Model fit was evaluated over nn observations using:

- **Root mean square error (RMSE):**

$$RMSE = \sqrt{\frac{1}{N}\sum_{\{i=1\}}^{N} e_i^2}$$

- **Coefficient of determination (R^2):**

$$R^2 = 1 - \frac{\sum_{i=1}^{N} e_i^2}{\sum_{i=1}^{N}(y_i - \bar{y})^2}$$

$$\bar{y} = \frac{1}{N}\sum_{\{i=1\}}^{N} y_i$$

- **Mean absolute percentage error (MAPE):**

$$MAPE = \frac{100\%}{N}\sum_{i=1}^{N}\left|\frac{e_i}{y_i}\right|$$

Type II ANOVA was used, and results were reported as $F(df_1, df_2)$ for each effect. Test statistics:

$$F_{effect} = \frac{MS_{effect}}{MS_{error}}, \quad \text{with.} \quad MS_{effect} = \frac{SS_{effect}}{df_{effect}}, \quad \text{and} \quad MS_{error} = \frac{SS_{error}}{df_{error}}.$$

For the balanced 3×2 design (Phase: 3 levels; Side: 2 levels; N=180), the degrees of freedom were $df_{1,Phase} = 2$, $df_{1,Side} = 1$, $df_{1,Phase\times Side} = 2$, and $df_2 = 174$ (p=6 model parameters).

Coefficient 95% confidence intervals were computed as $\hat{\beta} \pm t_{0.975,df_2} SE(\hat{\beta})$. Interpretation followed standard guidance on statistical power and effect size (Cohen, 1988).

2.8 Assumption checks

Normality (Shapiro–Wilk), homoscedasticity (Breusch–Pagan), and independence (Durbin–Watson) were assessed; Q–Q plots and residuals vs fitted plots were inspected for deviations.

2.9 Robustness check: Linear Mixed effects Model (LMM)

To assess robustness under grouped data conditions, we fitted a Linear Mixed effects Model (LMM) with a random intercept for Board (k=1…9):

$$R_{max,ijk} = \beta_0 + \beta_B I_{B,ij} + \beta_C I_{C,ij} + \beta_R I_{R,ij} + \beta_{B\times R} I_{Rij} + \beta_{C\times R} I_{R,ij} + u_{0k} + \varepsilon_{ijk}$$

Where I_B, I_C and I_R are indicator variables for Phase B, Phase C, and Side R, respectively. The random intercept term $u_{0k} \sim \mathcal{N}(0, \sigma_u^2)$ captures between-board variance, and $\varepsilon_{ijk} \sim \mathcal{N}(0, \sigma^2)$ is the residual error.

Estimation used restricted maximum likelihood (REML) via the MixedLM procedure in *statsmodels* (Python). Random slopes were considered but not included due to non-identifiability; the final model retained a random intercept only. The intraclass correlation coefficient (ICC) was computed as:

$$ICC = \frac{\sigma_u^2}{\sigma_u^2 + \sigma^2}$$

and was approximately 3.7×10^{-5} . Given the negligible ICC and identical fixed effects to OLS, we retained OLS for primary inference.

2.10 Software and reproducibility

All analyses were conducted in Python using statsmodels, scikit-learn, pandas, and numpy. Observations were treated as independent, consistent with the fixed effects design (Field, 2013;

James et al., 2021) and reliability assessment principles for repeated measurements (Atkinson & Nevill, 1998). Full R_{max} data (N = 180) and reproducible scripts are provided in Appendices A–B.

3. RESULTS

3.1 Phase-wise trend of R_{max}

Surface roughness (R_{max}) increased monotonically from Phase A to Phase C (Table 1). Collapsing across sides, the means were 603.5 µm (A), 777.2 µm (B), and 1181.7 µm (C), corresponding to increases of 28.78% (B vs. A) and 95.81% (C vs. A). The C–B difference was 52.05%. These differences were statistically significant (Type II ANOVA; Section 3.3).

Table 1. *Mean R_{max} [µm] and SD by Phase and Side (n_{cell}=30).*

Phase	Side	n	Mean [µm]	SD [µm]
A	L	30	601.9	24.4
A	R	30	605.1	14.8
B	L	30	776.2	18.2
B	R	30	778.1	16.8
C	L	30	1181.2	20.9
C	R	30	1182.1	19.5

Table 2. *Phase-level R_{max} [µm] and SD collapsed across sides (n_{phase}=60).*

Phase	n	Mean [µm]	SD [µm]
A	60	603.5	20.1
B	60	777.2	17.4
C	60	1181.7	20.0

Note: Collapsed mean = $(\bar{x}_L + \bar{x}_R)/2$; collapsed variance

3.2. OLS coefficient estimates

Reference levels: Phase = A, Side = L. Model fit:

Model fit: **R^2 = 0.9939, RMSE = 19.03 µm, MAPE = 1.92%**

Coefficients (β) with standard errors (SE), 95% confidence intervals (CI), and p-values are given in Table 3. Phase B and Phase C show large, statistically significant increases relative to Phase A, whereas the side effect (R vs. L) and its interactions are not statistically significant.

Table 3. *OLS coefficients.*

Term	β	SE	95% CI	p
Intercept (A, L)	601.87	3.53	[594.89, 608.84]	<0.001
Phase = B	174.33	5.00	[164.47, 184.20]	<0.001
Phase = C	579.33	5.00	[569.47, 589.20]	<0.001
Side = R	3.27	5.00	[−6.60, 13.13]	0.514
B×R	−1.37	7.07	[−15.31, 12.58]	0.847
C×R	−2.33	7.07	[−16.28, 11.61]	0.742

3.3. Factor significance (Type II ANOVA)

Reference levels: Phase = A, Side = L. A Type II ANOVA (balanced 3 × 2 design; N = 180) identified a highly significant main effect of Phase ($p < 0.001$), while the main effect of Side and the Phase × Side interaction were not statistically significant. Results are summarized in Table 4.

Table 4. *Type II ANOVA results (df_2=174).*

Effect	df_1	df_2	F	p
Phase	2	174	14098.43	<0.001
Side	1	174	0.50	0.482
Phase × Side	2	174	0.06	0.946

3.4. Assumption verification

Model assumptions were satisfied: Shapiro–Wilk W = 0.989 (p = 0.198), Breusch–Pagan LM = 8.31 (p = 0.140), Durbin–Watson = 1.96. No significant deviations were detected, confirming the validity of the OLS results (Figure 2(b–c)).

3.5. Robustness check – LMM

The LMM (random intercept for Board, REML via *statsmodels*) yielded negligible between-board variance ($\hat{\sigma}_u^2 = 0.014\ \mu m^2;\ ICC \approx 3.7 \times 10^{-5}$). Fixed-effect coefficients and fit metrics matched those of the OLS; OLS was therefore retained for inference.

3.6. Diagnostic plots

Figure 2(a) shows R_{max} distributions per Phase, highlighting the monotonic increase. Figures 2(b–c) show that residuals were normally distributed and exhibited no heteroscedasticity or autocorrelation patterns.

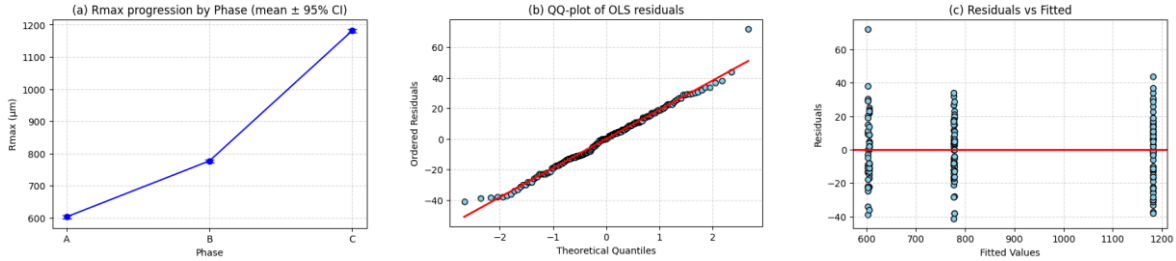

Figure 2. *(a) R_{max} by Phase (mean ± 95% CI; n=60 per phase). (b) Q–Q plot of standardized residuals with 45° reference. (c) Standardized residuals vs fitted with reference line at 0. Axes in µm where applicable.*

Figure 2(a) summarizes phase-wise means with 95% CIs (n=60 per phase). Figures 2(b–c) use standardized residuals and show no material deviations from normality or homoscedasticity.

4. DISCUSSION

4.1 Progressive surface degradation and symmetry

The results show a clear, monotonic increase in R_{max} from Phase A to Phase C (+28.78%, +95.81%, +52.05%), confirming progressive tool wear under controlled operating conditions. This pattern aligns with earlier findings for longitudinal bandsawing of beech, where cutting edge degradation accelerates in later stages of the cycle (Kminiak et al., 2015; Siklienka et al., 2015). The absence of both a Side effect (p=0.482) and a Phase × Side interaction (p=0.946) indicates high machining symmetry, suggesting that side specific calibration is unnecessary for the tested setup.

4.2 Model adequacy and parsimony

The fixed effects OLS explained 99.39% of variance (R^2 = 0.9939, RMSE = 19.03 µm, MAPE = 1.92%), with Phase as the sole significant predictor. This parsimonious specification is well suited to industrial deployment, offering full fit diagnostics while remaining simple to interpret. The LMM robustness check produced identical fixed effects and negligible between board variance (ICC ≈ 3.7×10^{-5}), confirming that additional hierarchical terms do not improve explanatory power for these data.

4.3 Practical relevance, limits, and extensions

Contact profilometry of R_{max} supports low-complexity monitoring strategies consistent with predictive maintenance workflows. Integration with on-line sensing or multi-sensor tool-wear data could enhance forecasting (Sandak et al., 2020; Górski et al., 2019).

Limits – Key constraints to consider when interpreting the results:

- **Sample scope:** All boards were cut from a single European beech log, on a single bandsaw, under one set of operating parameters.
- **Design scope:** Different boards were used at each phase (cross-sectional by phase), with only three cumulative-wear phases per run; this limits temporal resolution.

- **Measurement scope:** No direct measurements of cutting forces, tool–workpiece temperature, or quantitative wear progression were taken.
- **Generalisability:** Findings are specific to the tested configuration; validation is needed for other wood species, moisture contents, tooling geometries, and machine types.

Potential extensions – Denser temporal sampling could support spline-based or segmented models, and combining R_{max} with additional process process monitoring sensors may strengthen predictive maintenance performance.

5. CONCLUSIONS

Phase-based monitoring of R_{max} effectively captured progressive surface deterioration during longitudinal bandsawing of European beech. A simple, interpretable OLS framework—with assumptions met and LMM confirmation of negligible clustering—provides a robust basis for real time quality control and predictive maintenance.

Answers to the study aims:

1. R_{max} increased across phases A→B→C (603.5→777.2→1181.7 μm; $F(2,174)=14098.43$, $p<0.001$).
2. No systematic side effect or Phase×Side interaction (Side $p=0.514$; Phase×Side $p=0.946$); aggregation across sides is justified under the present symmetric setup.
3. A parsimonious OLS achieved excellent fit ($R^2=0.9939$; RMSE=19.03 μm; MAPE=1.92%) with satisfied assumptions; a random-intercept LMM showed negligible between-board variance (ICC $\approx 3.7\times10^{-5}$), confirming OLS for inference.

REFERENCES

1. Achouch, M., Moussaoui, A., & Zerhouni, N. (2022). On predictive maintenance in Industry 4.0: Overview, trends, challenges and opportunities. Applied Sciences, 12(16), 8081.
2. Atkinson, G., Nevill, A. M. (1998): Statistical methods for assessing measurement error (reliability) in variables relevant to sports medicine. Sports Medicine, 26(4): 217–238.
3. Bates, D., Mächler, M., Bolker, B., Walker, S. (2015): Fitting Linear Mixed effects Models Using lme4. Journal of Statistical Software, 67(1): 1–48.
4. Bendikienė, R., & Keturakis, G. (2016). The effect of tool wear and planing parameters on birch wood surface roughness. Wood Research, 61(5), 791–798.
5. Cohen, J. (1988): Statistical power analysis for the behavioral sciences (2nd ed.). Lawrence Erlbaum Associates.
6. Csanády, E., Magoss, E., Tolvaj, L. (2015): Quality of Machined Wood Surfaces. Springer, Cham.
7. Field, A. (2013): Discovering Statistics Using IBM SPSS Statistics (4th ed.). Sage.
8. García Plaza, E., Núñez López, P. J., Beamud González, E. M. (2018): Multi-sensor data fusion for real-time surface quality control in automated machining systems. Sensors, 18(12): 4381.
9. Gelman, A., Hill, J. (2007): Data analysis using regression and multilevel/hierarchical models. Cambridge University Press.
10. Górski, J., Szymanowski, K., Podziewski, P., Śmietańska, K., Czarniak, P., & Cyrankowski, M. (2019). Use of cutting force and vibro-acoustic signals in tool wear monitoring based on multiple regression technique for compreg milling. BioResources, 14(2), 3379–3388.
11. Harrison, X. A., Donaldson, L., Correa-Cano, M. E., Evans, J., Fisher, D. N., Goodwin, C. E. D., … & Inger, R. (2018). “A brief introduction to mixed effects modelling and multi-model inference in ecology.” PeerJ, 6, e4794.
12. James, G., Witten, D., Hastie, T., Tibshirani, R. (2021): An Introduction to Statistical Learning with Applications in R (2nd ed.). Springer.
13. Kminiak, R., Gašparík, M., Kvietková, M. (2015): The dependence of surface quality on tool wear of circular saw blades during transversal sawing of beech wood. BioResources, 10(4): 7123–7135.

14. Lee, J., Ni, J., Singh, J., Jiang, B., Azamfar, M., Feng, J. (2020): Intelligent maintenance systems and predictive manufacturing. Journal of Manufacturing Science and Engineering, 142(11): 1–40.
15. Piernik, M., Pinkowski, G., Krauss, A. (2023): Effect of chip thickness, wood cross sections, and cutting speed on surface roughness and cutting power during up milling of beech wood. BioResources, 18(4): 6784-6801.
16. Pinheiro, J. C., Bates, D. M. (2000): Mixed effects models in S and S-PLUS. Springer.
17. Pinkowski, G., Piernik, M., Krauss, D. (2024): Effect of chip thickness and tool wear on surface roughness and cutting power during up milling wood of different density. BioResources, 19(2): 3112-3127.
18. Sandak, J., Orlowski, K. A., Sandak, A., Chuchala, D., & Taube, P. (2020). On-line measurement of wood surface smoothness. Drvna Industrija, 71(2), 193–200.
19. Siklienka, M., Gašparík, M., Kminiak, R., Dzurenda, L. (2015): Process characteristics of horizontal log band saw in cutting beech logs. Drvna Industrija, 66(2): 129–136.
20. Talić, H., Hodžić, A. (2024): Influence of feed speed and cutting depth during planing on surface roughness of fir, poplar and beech wood. Drvna Industrija, 75(1): 79–85.
21. Zhu, Z., Jin, D., Wu, Z., Xu, W., Yu, Y., Guo, X., & Wang, X. (2022). Assessment of surface roughness in milling of beech using a response surface methodology and an adaptive network-based fuzzy inference system. Machines, 10(7), 567.
22. Zuur, A. F., Ieno, E. N., Walker, N. J., Saveliev, A. A., Smith, G. M. (2009): Mixed Effects Models and Extensions in Ecology with R. Springer, New York.

Appendix A

Table A1. *Individual R_{max} measurements (µm) for all boards, phases, sides, and positions (P0–P9).*

Board	Phase	Side	P0 (µm)	P1 (µm)	P2 (µm)	P3 (µm)	P4 (µm)	P5 (µm)	P6 (µm)	P7 (µm)	P8 (µm)	P9 (µm)
D1	**A**	**L**	593	612	632	579	611	588	589	602	563	599
D1	**A**	**R**	630	610	594	605	627	596	593	614	597	583
D2	**A**	**L**	617	589	631	612	591	568	580	579	631	613
D2	**A**	**R**	590	607	619	592	610	608	594	609	588	609
D3	**A**	**L**	592	640	622	591	577	579	584	597	674	621
D3	**A**	**R**	569	614	594	597	607	629	628	606	628	607
D4	**B**	**L**	782	788	767	755	767	769	771	758	776	803
D4	**B**	**R**	801	797	799	766	759	773	768	789	781	774
D5	**B**	**L**	780	793	759	764	778	760	808	803	762	776
D5	**B**	**R**	789	740	770	783	789	750	762	793	778	798
D6	**B**	**L**	794	810	735	791	768	793	780	748	784	764
D6	**B**	**R**	784	782	778	765	774	787	784	807	740	783
D7	**C**	**L**	1195	1178	1196	1148	1150	1204	1197	1225	1192	1180
D7	**C**	**R**	1145	1182	1212	1160	1213	1199	1216	1172	1152	1169
D8	**C**	**L**	1180	1156	1191	1207	1188	1164	1210	1171	1162	1169
D8	**C**	**R**	1201	1196	1152	1185	1189	1188	1159	1156	1199	1201
D9	**C**	**L**	1218	1170	1143	1179	1190	1181	1166	1193	1153	1180
D9	**C**	**R**	1188	1159	1196	1176	1179	1190	1184	1187	1166	1193

Appendix B – Model Outputs and Reproducibility Details

Table B1*. Example of Predicted Values and Residuals.*

Board	Phase	Side	Position	y (µm)	ŷ (µm)	e (µm)	Relative Error (%)
D1	**A**	**L**	P0	593	601.87	-8.87	-1.49
D1	**A**	**L**	P1	612	601.87	10.13	1.65
D1	**A**	**R**	P0	630	605.13	24.87	3.94
D1	**A**	**R**	P1	610	605.13	4.87	0.80
D4	**B**	**L**	P0	782	776.20	5.80	0.74
D4	**B**	**L**	P1	788	776.20	11.80	1.52
D4	**B**	**R**	P0	801	778.10	22.90	2.94
D4	**B**	**R**	P1	797	778.10	18.90	2.37
D7	**C**	**L**	P0	1195	1181.20	13.80	1.17
D7	**C**	**L**	P1	1178	1181.20	-3.20	-0.27
D7	**C**	**R**	P0	1145	1182.13	-37.13	-3.14
D7	**C**	**R**	P1	1182	1182.13	-0.13	-0.01

Note: Relative Error = 100 × e / y.

B2. Reproduction of Model Performance Metrics

Using all N=180 observations.

Residual definition. $e_i = y_i - \hat{y}_i$, where $\hat{y}_i$ denotes the model-predicted value and \bar{y} is the sample mean.

$$RMSE = \sqrt{\frac{1}{N}\sum e_i^2} = 19.03\ \mu m, \quad R^2 = 1 - \frac{\sum e_i^2}{\sum (y_i - \bar{y})^2} = 0.9939, \quad MAPE = \frac{100}{N}\sum \left|\frac{e_i}{y_i}\right| = 1.92\%$$

B3. Software and Code for Model Reproduction

Below is an example of the Python code used to fit the OLS and LMM models and calculate key metrics.

```
import pandas as pd
import statsmodels.formula.api as smf
from sklearn.metrics import mean_squared_error, r2_score

# Load dataset (Appendix A table)
df = pd.read_csv('Rmax_data.csv')

# Fit OLS model
ols_model = smf.ols('Rmax ~ C(Phase) * C(Side)', data=df).fit()

# Predictions and residuals
df['y_hat'] = ols_model.fittedvalues
df['residual'] = ols_model.resid

# Metrics
rmse = mean_squared_error(df['Rmax'], df['y_hat'], squared=False)
r2 = r2_score(df['Rmax'], df['y_hat'])
mape = (abs(df['residual'] / df['Rmax']).mean()) * 100

print('RMSE:', rmse)
print('R²:', r2)
print('MAPE:', mape)

# Fit Linear Mixed effects Model (board as random intercept)
import statsmodels.api as sm
md = sm.MixedLM.from_formula('Rmax ~ C(Phase) * C(Side)', groups='Board', data=df)
lmm = md.fit(reml=True)
print(lmm.summary())
```

B4. Interpretation Note

- Including predicted values and residuals in the Appendix allows readers to verify calculations for RMSE, R^2, and MAPE.
- Providing executable code ensures full reproducibility of the analysis.

MONITORING SURFACE STABILITY IN WOOD SAWING USING CV–SPC INTEGRATION FOR PREDICTIVE QUALITY CONTROL AND PROCESS DESIGN

Bujar Selimi

[1] Interior Design and Graphic Design Programs,
Universum International College,
Pristina, Kosovo
e-mail: bujar.selimi@universum-ks.org

ABSTRACT

This study tests whether the coefficient of variation (CV) of maximum surface roughness (R_{max}) serves as a statistically reliable and operationally applicable indicator of surface degradation during continuous longitudinal bandsawing of European beech (*Fagus sylvatica* L.). Surface roughness was measured at multiple positions on both faces of boards across three cutting phases. While absolute roughness increased with cutting time, CV decreased and remained within statistical control limits, indicating stable relative variability rather than a self-correcting process. Statistical process control (SPC) tools and linear regression were used to assess trends, process stability, and operational thresholds. CV alone did not function as a sensitive early-warning signal under stable conditions, but combined with absolute roughness monitoring and SPC diagnostics, it contributed to a more robust predictive maintenance framework. Although primarily technical in scope, the observed decrease in CV alongside rising R_{max} may also indicate improved visual uniformity—a potential aesthetic benefit that warrants targeted perceptual validation. The approach is low-complexity, non-invasive, and suitable for integration into automated quality-control systems in industrial wood machining.

Keywords: surface uniformity; industrial wood machining; statistical process control (SPC); coefficient of variation (CV); maximum surface roughness (R_{max}); predictive maintenance.

1. INTRODUCTION

Surface quality plays a critical role in industrial wood cutting, influencing downstream processing, functional performance, and aesthetic outcomes. In particular, surface uniformity can influence the visual coherence of final products, linking process performance to perceived quality in industrial and interior design contexts. Key machining parameters — including feed rate and fiber direction — can significantly affect roughness in beech wood (Sejdiu, Osmani, Sögütlü, 2024). Accordingly, we held feed rate and cutting orientation constant to isolate the effect of progressive blade wear on surface roughness. Fagus sylvatica exhibits favorable machinability and stable roughness behavior, making it a preferred species for longitudinal sawing operations (Aguilera and Martin, 2001). Among surface metrics, R_{max} is widely used to assess tool–material interaction.

Beyond absolute roughness values, the relative consistency of surface finish — expressed via the CV — offers insight into process stability. As the ratio of standard deviation to mean, CV can detect latent irregularities and internal inconsistency during wood machining (Hunter, Schultz, Smith, 2022; Korkmaz, Budakçı, Kılınç, 2024). This makes CV relevant not only for statistical evaluation but also for operational decision-making: in an industrial context, changes in CV can be translated into maintenance triggers, threshold alarms, and adjustments to process parameters before visible quality loss occurs.

Cutting duration has been validated in earlier research as a surrogate indicator for progressive tool wear, especially where direct instrumentation is unavailable or impractical (Trposki, 1993; Kminiak, Gašparík, Kvietková, 2015). Recent studies have reinforced this connection, showing how extended cutting time correlates with increased chip thickness, elevated roughness, and material-dependent changes in cutting power (Pinkowski, Piernik, Krauss, 2024; Sykacek et al., 2023). These trends

highlight the need for diagnostic approaches that capture wear effects indirectly but reliably, and that can be embedded into automated production workflows for real-time quality assurance.

Recent SPC work in wood processing combines variability metrics with multivariate monitoring and mechanistic insight. Industrial resawing, MSPC applications, and narrow-kerf analyses jointly motivate coupling CV with simple control-chart logic and operational roughness thresholds (Orlowski, Sandak, Chuchala, 2020; Mysyk et al., 2017; Moreira et al., 2021; Orlowski et al., 2022).

This study investigates whether CV — modeled through SPC and linear regression over cutting time — can serve as a practical, automation-ready signal for surface degradation during longitudinal beech wood sawing. In parallel, absolute R_{max} thresholds are evaluated to establish operational benchmarks for maintenance intervention. SPC offers real-time diagnostic capability, compatibility with programmable control systems, and does not rely on inferential significance alone. The proposed framework explores CV's potential as a low-complexity indicator for predictive maintenance and surface integrity tracking in environments without invasive wear monitoring.

Previous operational expectations assumed that CV would increase toward the end of the cutting cycle (F3) compared to its start (F1), reflecting greater variability due to progressive blade wear.

The central research question is: **Can the coefficient of variation (CV) function as a statistically reliable and operationally applicable metric for surface degradation when modeled across cutting time using SPC and regression analysis?**

1.1. Aim of the Study

The aim of this study is to:

- **Statistical Objective:** Determine whether the CV of R_{max} responds significantly to progressive blade wear under stable cutting parameters, using SPC charts and time-trend regression.
- **Operational Objective:** Compare CV's diagnostic performance with absolute R_{max} threshold monitoring, and assess its feasibility as a low-complexity, non-invasive indicator for integration into industrial quality control systems.

The ultimate goal is to inform the development of a predictive maintenance framework that links statistical monitoring outputs to actionable operational thresholds, enabling earlier intervention, reduced downtime, and consistent surface integrity in high-throughput wood machining.

2. MATERIALS AND METHODS

2.1. Wood material and equipment

European beech (*Fagus sylvatica* L.) boards were processed. To limit anatomical variability, boards within each phase were taken from a single log, while different logs were used across phases to reflect routine production. Cutting was performed on a Braun Canali bandsaw (TYP HBSG-1100) under fixed machine settings (feed rate, blade tension, and cutting depth).

To reduce moisture-related variability, field moisture was screened with a GMK-100 meter (GHM-Greisinger, Germany; calibration curve d.65 for medium-density hardwoods) at three longitudinal positions (start, mid, end) and two depths (10 mm, 25 mm) on each face. Moisture readings were used only to verify sampling consistency and were not included in the statistical analyses.

2.2. Experimental design and sampling

The cutting process ran continuously for 60 min with three independent sampling phases:

- **F1 (≈ 0 min):** boards B1–B3, freshly sharpened blade;
- **F2 (≈ 30 min):** boards B4–B6;
- **F3 (≈ 60 min):** boards B7–B9.

In each phase, three boards (thickness ≈ 25 mm; length ≈ 4.8 m) were cut. On each board, both faces (Left, Right) were measured at 10 equidistant positions over a 4.0 m gauge length, excluding 0.4 m at each end (spacing ≈ 40 cm). This yielded 180 surface-roughness observations (3 phases × 3 boards × 2 sides × 10 points). The sampling layout and board–face orientation are illustrated in Figure 1.

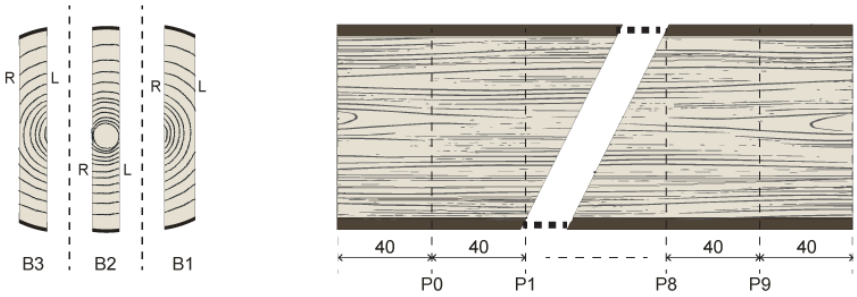

Figure 1. *Layout of board selection (B1–B3) and measurement positions (P0–P9) for R□ax on the left (L) and right (R) faces along the board length.*

The data structure followed a nested hierarchy: Phase → Board → Side → Position. For inferential analyses, observations were aggregated to board–side–phase units (n = 18; 6 per phase).

2.3. Surface roughness measurement protocol

R_{max} was acquired with a SHAHE GS5337 contact profilometer (range 0–6.5 mm; resolution 1 μm; accuracy ±3 μm). Measurements were taken immediately after each phase using identical instrument settings. Parameter definitions followed ISO GPS profile standards (ISO 21920-2), including standardized definitions for Rt, Rz, Ra, Rq, and Rsk.

2.4. Data processing and variability indicators

For each board–side–phase unit, the following were computed from the 10 positions:

- mean roughness $\bar{R}_{max}$
- standard deviation (SD)
- coefficient of variation (CV), calculated as:

$$CV(\%) = \frac{SD}{\bar{R}_{max}} \times 100$$

CV was selected as the variability metric following Atkinson and Nevill (1998), who emphasize its usefulness for expressing absolute reliability and detecting relative differences in measurement consistency. In addition to its statistical role, CV was also interpreted as a potential indicator of visual surface uniformity, allowing parallel consideration of aesthetic coherence in the processed boards alongside process stability.

Time was coded as t = {0,30,60} min for F1, F2, and F3, respectively.

2.5. Statistical analysis

The statistical workflow was pre-specified to address the primary question: whether CV changes across cutting time and whether the process remains in statistical control.

(a) Group contrast (F1 vs F3)

Since phases used different boards (independent groups), CV values from F1 and F3 were compared using Welch's t-test (one-sided, H_1: CV$F3$ > CV$F1$, expecting higher variability with blade wear). Effect size was reported as Hedges' g, and the mean difference (percentage points, pp) with 95 % confidence intervals (CI) was calculated.

(b) Time trend

A simple linear model was fitted,

$CV(t) = \beta_0 + \beta_1 t$,

Parameters were estimated using ordinary least squares (OLS), with model adequacy summarised by R^2. Robust (HC1) standard errors were applied for inference on β_1.

(c) Process stability analysis (SPC and EWMA)

Shewhart I-chart. CV values for the 18 units were plotted as an Individuals chart with control limits: $UCL = \overline{CV} + 3s_{CV}$, where $\overline{CV}$ and s_{CV} denote the mean and the sample standard deviation of unit-

level CV values (baseline). Western Electric run rules were applied (Leavengood & Reeb, 2015; Montgomery, 2009).

EWMA chart. The statistic was defined as $Z_0 = \mu_0$ and $Z_t = \lambda X_1 + (1-\lambda)Z_{t-1}$, where $X_t = CV_t$ and $\mu_0 = \overline{CV}$. We used $\lambda = 0.2$ and $L \approx 2.7$ to target $ARL_0 \approx 370$; σ was estimated by s_{CV} from the baseline set for consistency with the Individuals chart. Control limits at time *t* were

$$UCL_t = \mu_0 + L\sigma\sqrt{\frac{\lambda}{2-\lambda}(1-(1-\lambda)^{2t})}\,,\ LCL_t = \mu_0 - L\sigma\sqrt{\frac{\lambda}{2-\lambda}(1-(1-\lambda)^{2t})}$$

And at steady state:

$$UCL = \mu_0 + L\sigma\sqrt{\frac{\lambda}{2-\lambda}},\ \ LCL = \mu_0 - L\sigma\sqrt{\frac{\lambda}{2-\lambda}}$$

(d) Sensitivity check

The monotonic association between unit-level CV and unit-level $\bar{R}_{max}^{unit}$ was examined using Spearman's ρ to verify that CV patterns were not solely driven by changes in roughness.

(e) Operational threshold and time-to-alarm (*T)**

To define an actionable maintenance trigger, we fixed the data level at points (all 60 positions in F1). The point-level control limit was:

$$UCL_{points} = \bar{R}_{max}^{F1} + 3s_{points}$$

Where $\bar{R}_{max}^{F1}$ is the baseline mean of point-level roughness and s_{points} is the corresponding sample standard deviation computed from all 60 point measurements in F1. The threshold-crossing time was:

$$T^* = \frac{UCL_{points} - \bar{R}_{max}^{F1}}{\hat{\beta}}$$

where $\hat{\beta}$ is the slope (μm/min) from the linear regression of $\bar{R}_{max}$ on time. This points level is kept fixed for all $\bar{R}_{max}$ -based diagnostics; CV-SPC remains at the unit level (18 unit CVs) as a complementary variability monitor.

2.6. Quality control and reproducibility

All data processing (aggregation, CV computation, and statistical tests) was scripted for traceability. Instrument settings, sampling distances, and environmental conditions were kept constant. Raw R_{max} data and threshold calculations are in Appendix A, while worked examples for CV and control limits (Shewhart, EWMA) are in Appendix B to enable independent verification.

3. RESULTS

3.1. Descriptive Statistics

Table 1 presents the main surface roughness indicators (R_{max}) across the three operational phases. Mean $\bar{R}_{max}$ increased from F1 to F3, while mean CV decreased. This reduction in CV indicates increased relative uniformity, which in design-oriented contexts may correspond to a more visually consistent surface, although this was not directly tested.

Table 1. *Descriptive statistics for CV and $\bar{R}_{max}$ by phase.*

Phase	Mean CV (%)	SD CV (%)	Mean R_{max} (μm)
F1	3.24	1.15	603.5
F2	2.50	0.59	674.7
F3	2.29	0.40	777.2

3.2. Group Contrast (F1 vs F3)

Welch's *t*-test (H_1: ($CV_{F3} > CV_{F1}$) results:

- Mean difference (F3–F1): -0.95 pp
- 95 %CI: [−2.16, 0.25]
- t(6.21) = -1.92, $p_{one\text{-}sided}$ = 0.949
- Hedges' g = -1.02

The large one-sided p-value reflects that the observed effect was opposite to the specified hypothesis. For completeness, the two-sided p-value was approximately 0.10, confirming no statistically significant difference in either direction (see Figure 2, left panel).

3.3. CV Time-Trend Analysis

OLS model:

$CV(t) = \beta_0 + \beta_1 t$

- $\hat{\beta}_1 = -0.0159$ pp/min
- 95 %CI [−0.0330, 0.0012] (robust HC1 SEs)
- R^2 = 0.224

The estimated slope was negative and not statistically different from zero at α = 0.05 (see Figure 3, left panel).

3.4. Process Stability Analysis – Shewhart I-Chart

- $\overline{CV} = 2.68\%$
- UCL = 5.21 %, LCL = 0.14 %
- No points exceeded control limits
- Longest run above mean = 3; longest run below mean = 4
- No Western Electric run-rule violations detected

(see Figure 2, right panel).

3.5. Sensitivity Check (CV vs Mean roughness $\bar{R}_{max}$)

Spearman's ρ = -0.455, p = 0.0577 (see Figure 3, left panel).

3.6. Operational Threshold and Time-to-alarm (T^*)

We fixed the data level at points (all 60 positions in F1). The point-level limit defined in Methods is:

$$UCL_{points} = \bar{R}_{max}^{F1} + 3s_{points} = 603.5 + 3 \times 20.10 = 663.8\ \mu m$$

Given the phase-level slope $\hat{\beta} = 2.894 \mu m/min$, the time-to-alarm is:

$$T^* = \frac{663.5 - 603.5}{2.894} \approx 20.8\ min$$

This threshold is reached well before the midpoint of the 60-min cycle (≈39 min remaining). A dashed line at 663.8µm and a dotted vertical at T are shown in Figure 3 (right panel).

3.7. Process Stability Analysis – EWMA Monitoring

The EWMA chart (λ = 0.2, L ≈ 2.7) showed no points outside the control limits and no sustained patterns (see Figure 2, right panel).

3.8. Visual Summary of Statistical Results

Figures 2–3 summarize the group comparison (F1 vs F3), time-trend analysis, and process stability diagnostics (Shewhart and EWMA). Together, these visuals complement the numerical results in Sections 3.2–3.4, enabling direct inspection of variability patterns, temporal trends, and control-limit adherence.

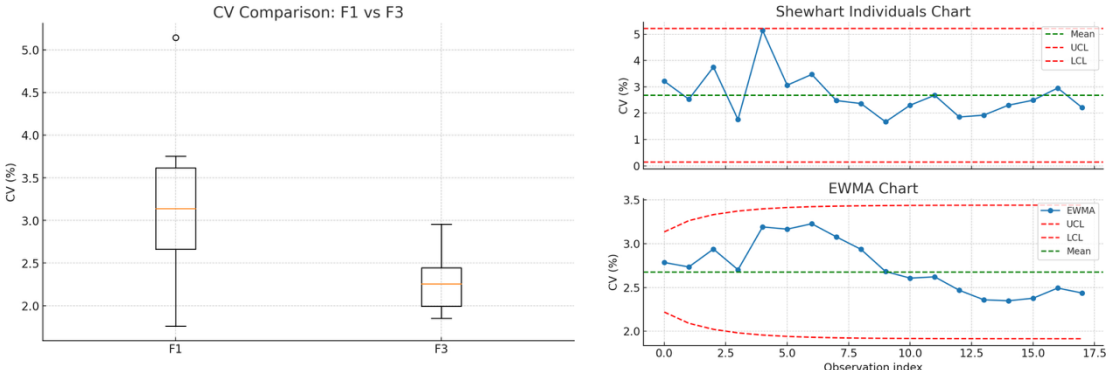

Figure 2. *(left) Boxplot of CV (%) for phases F1 and F3; (right) Shewhart Individuals Chart and EWMA Chart for CV (%).*

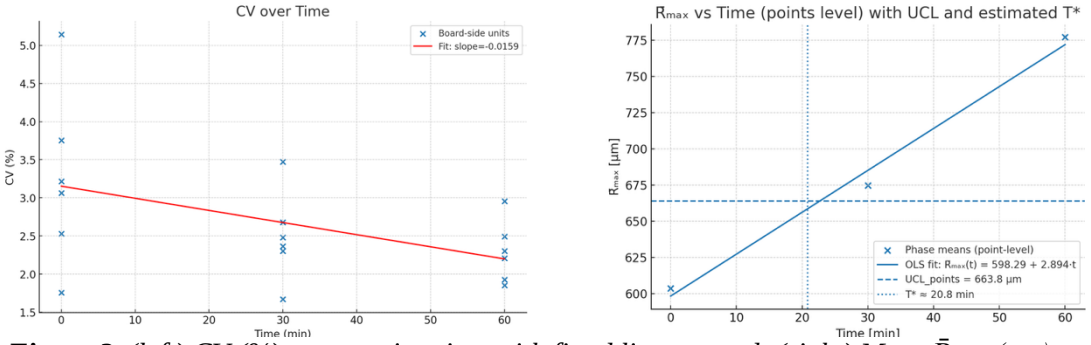

Figure 3. *(left) CV (%) over cutting time with fitted linear trend; (right) Mean* $\bar{R}_{max}$ *(µm) over cutting time with operational threshold (*$\bar{R}_{max}{}^{*}$ *and predicted alarm time (T*).*

4. DISCUSSION

4.1. Statistical Findings vs. Hypothesis

The initial hypothesis was that the CV of R_{max} would increase as blade wear progressed, indicating rising variability in surface quality. However, results showed the opposite trend: mean CV decreased from 3.24 % in Phase F1 to 2.29 % in Phase F3, with no statistically significant increase detected ($t = -1.92$, $p_{one\text{-}sided} = 0.949$; slope = −0.0159 pp/min, 95 %CI [−0.0330, 0.0012]). Shewhart control limits ($\overline{CV} = 2.68\%$, UCL = 5.21 %, LCL = 0.14 %) and EWMA monitoring revealed no special-cause variation. Under stable operating parameters, this pattern suggests that progressive blade wear produces uniformly rougher surfaces rather than greater variability — a finding consistent with controlled hardwood machining trials reporting uniform wear patterns over irregular damage modes. Similar trends have been documented in planed and heat-treated beech, where roughness parameters increased systematically while relative variability remained stable (Gurau, Irle, Buchner, 2017). This stability of CV is consistent with its role as a standardized measure of relative variation that is less sensitive to uniform mean shifts than absolute metrics (Atkinson and Nevill, 1998).

4.2. Operational Implications

While CV remained statistically stable, absolute $\bar{R}_{max}$ increased from 603.5 µm to 777.2 µm over the 60-minute cutting period. Using the point-level F1 threshold $UCL_{points} = 663.8\ \mu m$, the estimated time-to-alarm was $T^* \approx 20.8\ min$. This point would be reached well before the midpoint of the run, indicating that absolute roughness monitoring provides an earlier and actionable maintenance signal.

From a process control perspective, these findings suggest that CV may still be valuable as a complementary indicator — particularly for detecting abnormal variability caused by factors such as machine misalignment, vibration, or feed rate fluctuations. Integration of CV and absolute roughness thresholds into SPC systems could support predictive maintenance in industrial wood machining without direct tool-wear measurement.

4.3. Limitations and Further Research

The study was conducted under fixed feed rate, blade tension, and cutting depth — conditions that may not fully reflect variability in industrial environments where operational parameters fluctuate. The sensitivity of CV to abrupt process disturbances remains to be tested. More advanced monitoring strategies, such as one-sided run-rules control charts accounting for measurement error when tracking CV, could improve detection sensitivity (Tran, Heuchenne, Nguyen, 2020).

Future work should:

- Assess CV behavior under variable cutting parameters.
- Compare the predictive value of CV and $\bar{R}_{max}$ across different wood species and tool geometries.
- Explore adaptive control limit strategies to improve early-warning capability.

4.4. Practical Implementation

The monitoring framework tested here—integrating $\bar{R}_{max}$ thresholds with SPC tools — can be implemented in industrial sawing without direct tool-wear measurement. Implementation requires only routine surface sampling with a profilometer or equivalent sensor, coupled with automated data-processing software capable of computing both $\bar{R}_{max}$ and CV.

Time-to-alarm estimation, as demonstrated $T^* \approx 20.8\,min$, enables maintenance scheduling before critical degradation. CV, while not a strong standalone predictor under stable parameters, can complement roughness monitoring by flagging abnormal variability.

Integration into programmable logic controllers (PLC) or manufacturing execution systems (MES) would allow continuous monitoring, automated alerts, and minimal operator intervention. This approach offers a low-complexity, cost-effective route to predictive maintenance, reduced unplanned downtime, and consistent product quality. The methodological clarifications and worked examples provided in the appendices are intended to facilitate replication and adaptation of this SPC approach in industrial settings.

5. CONCLUSIONS

This study tested whether the CV of (R_{max}) is a reliable, operational indicator of surface degradation in continuous longitudinal sawing of European beech. Absolute roughness increased substantially across the 60-min run ($\bar{R}_{max}$: 603.5 → 777.2 µm), whereas CV declined (3.24% → 2.29%) with no evidence of increase over time (t = −1.92, $p_{one\text{-}sided}$ = 0.949; slope = −0.0159 pp/min; 95%CI [−0.0330, 0.0012]).

Shewhart Individuals $\overline{CV} = 2.68\%$, UCL = 5.21%, LCL = 0.14%) and EWMA charts showed no special-cause variation in CV.The borderline negative correlation between unit-level CV and unit-level $\bar{R}_{max}$ (ρ = −0.455, p = 0.0577) supports the view that wear progression under stable conditions yields uniformly rougher—rather than more variable—surfaces.

Using a point-level threshold from the F1 baseline ($UCL_{points} = 663.8\,\mu m$), the time-to-alarm was $T^* \approx 20.8\,min$—about 39 min before the end of the 60-min cycle. Thus, thresholding absolute roughness enables earlier and more actionable maintenance scheduling than periodic checks. CV alone is unlikely to be a sensitive early-warning metric in well-controlled settings; integrated with absolute thresholds and SPC tools, it remains a useful complementary indicator for abnormal variability.

To our knowledge, this is the first controlled sawing trial to combine CV-based SPC with absolute roughness thresholds for operational diagnostics in European beech. The framework is low-complexity, non-invasive, and suitable for integration into automated quality-control systems. Potential aesthetic implications were not evaluated and should be examined in future work. Further research should test generalizability across species, tooling, and variable operating conditions to refine predictive maintenance strategies in wood machining.

REFERENCES

1. Aguilera, A., Martin, P. (2001): Machining qualification of solid wood of Fagus sylvatica L. and Picea excelsa L.: Cutting forces, power requirements and surface roughness. Holz als Roh- und Werkstoff, 59 (6): 483–488.

2. Atkinson, G., Nevill, A.M. (1998): Statistical methods for assessing measurement error (reliability) in variables relevant to sports medicine. Sports Medicine, 26 (4): 217–238.
3. Gurau, L., Irle, M., Buchner, J. (2017): Surface roughness of heat treated and untreated beech (Fagus sylvatica L.) wood after sanding. BioResources, 12 (3): 6401–6415.
4. Hunter, T.A., Schultz, K., Smith, J. (2022): Testing the processing-induced roughness of sanded wood surfaces separated from wood anatomical structure. Forests, 13 (2): 331.
5. ISO (2021): ISO 21920-2: Geometrical product specifications (GPS) — Surface texture: Profile — Part 2: Terms, definitions and surface texture parameters. International Organization for Standardization
6. Kminiak, R., Gašparík, M., Kvietková, M. (2015): The dependence of surface quality on tool wear of circular saw blades during transversal sawing of beech wood. BioResources, 10 (4): 7123–7135.
7. Korkmaz, M., Budakçı, M., Kılınç, İ. (2024): Assessment of surface roughness in milling of wood with different material temperature and cutting parameters. BioResources, 19 (4): 9343–9357.
8. Leavengood, S., Reeb, J.E. (2015): Statistical process control: Part 8, attributes control charts (EM 9110). Oregon State University Extension Service.
9. Montgomery, D.C. (2009): Introduction to statistical quality control (6th ed.). John Wiley & Sons.
10. Moreira, B.R. de A., Cruz, V.H., Cunha, M.L.O., Viana, R. da S. (2021): Full-scale production of high-quality wood pellets assisted by multivariate statistical process control. Biomass and Bioenergy, 151: 106159.
11. Mysyk, M., Matsyshyn, Y., Mayevskyy, V., Ray, C.D., Kurka, R., Sopushynskyy, I. (2017): Identification of the length distribution of lumber defect-free areas. Wood and Fiber Science, 49 (4): 396–406.
12. Orlowski, K.A., Chuchala, D., Szczepański, M., Migda, W., Wojnicz, W., Sandak, J. (2022): Lateral forces determine dimensional accuracy of the narrow-kerf sawing of wood. Scientific Reports, 12 (1): 86.
13. Orlowski, K.A., Sandak, J., Chuchala, D. (2020): Thickness accuracy of sash gang sawing. BioResources, 15 (4): 9362–9374.
14. Pinkowski, G., Piernik, M., Krauss, D. (2024): Effect of chip thickness and tool wear on surface roughness and cutting power during up milling wood of different density. BioResources, 19 (2): 3112–3127.
15. Sejdiu, R., Osmani, H., Sögütlü, C. (2024): The influence of machining parameters on the surface roughness quality of beech wood (Fagus sylvatica L.) – A comprehensive study. Journal of Engineering Science and Technology, 19 (3): 853–868.
16. Sykacek, T., Kminiak, R., Gaff, M., Klement, I., Barcík, Š., Réh, R. (2023): Influence of tool wear on surface roughness and cutting force in wood milling. Materials, 18 (1): 193.
17. Tran, P.H., Heuchenne, C., Nguyen, H.D. (2020): Monitoring coefficient of variation using one-sided run rules control charts in the presence of measurement errors. arXiv, arXiv:2001.01821.
18. Trposki, Z. (1993): Zgolemuvanje na randemanot so kontrola na maksimalnite vibracii kaj lentovidnata pila-trupčara. In Sovetuvanje za racionalno iskoristuvawe na šumite i iskoristuvawe na drvnata masa vo Republika Makedonija, Skopje, pp. 11–16.

Appendix A – Raw R_{max} Measurements (µm)

Raw R_{max} values for each board–side–phase unit (positions P0–P9).

Board	Phase	Side	P0	P1	P2	P3	P4	P5	P6	P7	P8	P9
B1	**F1**	**L**	593	612	632	579	611	588	589	602	563	599
B1	**F1**	**R**	630	610	594	605	627	596	593	614	597	583
B2	**F1**	**L**	617	589	631	612	591	568	580	579	631	613
B2	**F1**	**R**	590	607	619	592	610	608	594	609	588	609
B3	**F1**	**L**	592	640	622	591	577	579	584	597	674	621
B3	**F1**	**R**	569	614	594	597	607	629	628	606	628	607
B4	**F2**	**L**	648	701	697	682	687	638	649	657	678	697
B4	**F2**	**R**	670	684	637	698	689	678	690	681	689	681
B5	**F2**	**L**	678	668	682	708	692	677	653	657	684	678
B5	**F2**	**R**	676	672	662	690	681	664	664	677	693	688
B6	**F2**	**L**	671	667	673	687	673	670	696	655	640	665
B6	**F2**	**R**	697	661	678	684	689	647	649	686	656	662
B7	**F3**	**L**	782	788	767	755	767	769	771	758	776	803
B7	**F3**	**R**	801	797	799	766	759	773	768	789	781	774
B8	**F3**	**L**	780	793	759	764	778	760	808	803	762	776
B8	**F3**	**R**	789	740	770	783	789	750	762	793	778	798
B9	**F3**	**L**	794	810	735	791	768	793	780	748	784	764
B9	**F3**	**R**	784	782	778	765	774	787	784	807	740	783

WHEN ACOUSTIC TOMOGRAPHY MEETS RESISTOGRAPH

Robert Mařík[1], Valentino Cristini[1]

Mendel University, Brno, Czech Republic,
Faculty of Forestry and Wood Technology,
e-mail: robert.marik@mendelu.cz; valentino.cristini@mendelu.cz

ABSTRACT

The paper presents an integrated approach to assessing the health and structural integrity of trees and wooden logs by combining acoustic tomography with resistograph measurements. Traditional methods are extended through the fusion of data from two complementary diagnostic tools. The first, an acoustic tomograph, detects internal decay and structural anomalies by measuring the propagation delay of elastic waves through wood. The second, a resistograph, assesses the mechanical properties of wood by recording the force required to drill into the material. A set of custom Python scripts has been developed to synchronize and merge data from both devices, enabling a more comprehensive and precise interpretation of internal wood conditions. This combined methodology offers improved diagnostic accuracy and has potential for application in forestry, arboriculture, and wood quality assessment.

Keywords: acoustic tomography, resistograph, wood quality assessment.

1. INTRODUCTION

Tree safety and mechanical stability are a crucial part of greenery management in cities. To ensure the structural stability of trees and reduce the risk of failure, several methods have been developed and implemented by cooperation between scientists, arborists, and wood researchers. The primary interest of these methods is to detect decay, cavities, cracks, ring-shakes and other types of wood damage, (Soge et al., 2021), (Proto et al., 2020). Note also that the methods developed for tree inspection can be used generally to evaluate the wooden logs or parts of wooden constructions.

A couple of scientific devices are available for both noninvasive and invasive tree or wood inspection. Especially acoustic tomography and microdrilling are well known methods which are supported by commercial devices. However, a single method is usually not capable of giving full details of the status of the tree or the log. For this reason, it is suggested to combine more methods (Papandrea et al., 2022).

In order to make accurate predictions, it is necessary to understand the background of the methods and measuring devices.

For an acoustic tomograph, a set of sensors is attached to the tree and the time of flight of the acoustic signal is measured between each pair of the sensors. This time of flight (TOF) and the distance between sensors are used to estimate the speed of sound wave propagation in the cross section. The sound speed is related to the mechanical properties of the material. This method gives usually a good estimate of the health status of the cross section even though it does not reflect the physical background of the wave propagation. Really, as a consequence of the Huygens and Fermat principles, the medium with higher speed of propagation is preferred by the sound ray and thus the travel path of the sound is not geometrically straight line. The real sound propagation path avoids material imperfections. However, this effect can be interpreted equivalently as a slowdown of direct rays on defects. Consequently, linear defects such as cracks or ring-shakes near the center appear as central decay or a cavity on tomogram (Rinn, 2015). Thus, the acoustic tomogram does not represent the local properties of the wood but rather detects the parts of the cross section which are mechanically interconnected and therefore increase the mechanical stability of the whole structure (Rinn, 2015). It is also confirmed by experiments, that cracks may in tomogram appear as big “fat” decayed zone even if only sound wood is present next to these cracks (Wang et al., 2023). Another issue is that certain fungi species may influence the mechanical properties of the wood without affecting acoustic properties.

Such behavior has been confirmed for *Kretschmeria deusta* (Cristini et al., 2022), (Schwarze et al., 1995).

The microdrilling is typically performed by resistograph device. A long thin shaft is used to drill the hole into the material, and the drilling resistance is recorded as a function of the length of the drill hole. The sensitivity of the device even allows dendrochronological tree age estimation for certain species with wide tree rings (Szewczyk et al., 2018).

The combination of an acoustic tomograph and a resistograph offers an integrated approach that helps overcome the limitations of each individual method, enabling a more accurate assessment of the condition of the examined object, such as a tree or wooden log. This method was employed by (Rinn, 2015) to highlight that ring-shakes, which separate the central part of the tree from the outer wood, can be misinterpreted in tomographic images. Similarly, cracks may produce distortions of the same type (Wang et al., 2023).

The output of the resistograph is typically in the form of a data chart with depth on a horizontal axis and drill resistance on the vertical axis. From the local decrease of the resistance it is possible to judge the presence of a defect. However, the graphical representation in the depth-resistance coordinate system does not reflect the geometry of the cross section and makes it difficult to determine the defect location.

The aim of this work is to enable synchronized interpretation of the data from acoustic tomograph and resistograph and provide a tool which allows to merge data from both devices for better and more accurate interpretation. The basic idea will be to visualize both data in one unified geometry which corresponds to the cross-section plane. A set of tools for creating such a visual representation has been developed in Python, which is nowadays a standard for scientific data processing.

Methods

The wave propagations in standing trees and in stem sections with artificial cavities differ (Strobel et al., 2018). In order to get the results as representative as possible, the data have been collected on standing trees which have been intended for felling. Six *Tillia cordata Mill* trees have been selected in Valdštejnova alej (Linden alley) in Jičín, Czech Republic (50.4465947N, 15.3724022E). These mature trees have been historically damaged by severe pruning (topping), with varying extents of internal defects in the trunk. Individuals were selected from the row adjacent to the road. Their habitat conditions in terms of stress load are therefore comparable. Dendrometric parameters differed significantly, especially in trunk diameter, with height varying around 8 m for all individuals.

The acoustic tomograph Fakopp ArborSonic 3D with 12 sensors has been used for acoustic method. Each TOF has been established as the mean value of five measurements. The device RESISTOGRAPH® 4453 with 0.01mm resolution has been used for microdrilling. Drilling was performed midway between each pair of adjacent sensors in a radial direction.

The data from the acoustic tomograph have been processed by the dedicated software ArborSonic 3D v 5.3.162 and with a custom Python library (Mařík et al., 2024) based on EBSI and RSEN+SISE methods described in (Du et al., 2015) and (Du et al., 2018), respectively. Note that both approaches produce comparable outputs and the only quotable difference was in the output format. In the first case the tomogram is obtained as a PNG file and thus the coordinates in the image are in pixels and do not correspond to the coordinates associated with the cross-section and with sensor positions. In contrast, the second method utilizes the coordinates of the cross-section and produces the sound speed as a value rather than just as a color on a color scale. The second option has been used as a more comfortable one for data processing. However, the PNG option is also possible and has been used to merge the resistograph data with the cross-section photo (Mařík & Cristini, 2025).

The following algorithm has been used to convert data recorded by the resistograph to data visually represented by the colored bars in a 2D plane.

Input:

- Node coordinates u_i, $i \in \{1,\ 2,\ \ldots,\ n\}$ centered at the origin, i.e. $\sum_{i=1}^{n} u_i = 0$.
- Drilling resistance $f_i(t)$ on the path from the middle point of the segment $u_i u_{i+1}$ to the tree center as a function of drilling depth t .
- An interval for .

Output:

- Colored bars in 2D plane. Each bar is at the position of drilling, and the color corresponds to the drilling resistance.

Notation:

- Let $u_{n+1} = u_1$ to simplify the notation and unify the formula for all indices.

Algorithm body:

- **Step 1.** The middle point m_i of the segment $u_i u_{i+1}$ is $m_i = (u_i + u_{i+1})/2$.
- **Step 2.** The unit vector e_i from the middle point to the center is $e_i = -m_i/|m_i|$, where $|m_i|$ is the Euclidean norm of the vector m_i. (Note that it is possible to treat the point as a vector and thus a norm makes sense here.)
- **Step 3.** The drilling resistance $f_i(t)$ belongs to the point $m_i + t \cdot e_i$. For all values of t under consideration, draw a corresponding mark to the 2D plane.
- **Step 4.** Repeat from Step 1 to Step 3 for all values of i .

Algorithm has been realized in Python with common libraries for data and image processing, such as NumPy, Pandas, SciPy and Matplotlib. For a practical implementation, the drilling resistances have been visualized as short line segments perpendicular to the drilling path with color corresponding to the resistance values. For convenience, a scale can be drawn along the drilling path. Red-black code has been used for this purpose.

The resistograph data are highly variable curves and smoothing and downsampling is necessary for a reasonable visualisation. The Savitzky-Golay filter has been used for data smoothing, since it preserves peaks of the data and allows fast and reliable signal processing. See also Figure 1.

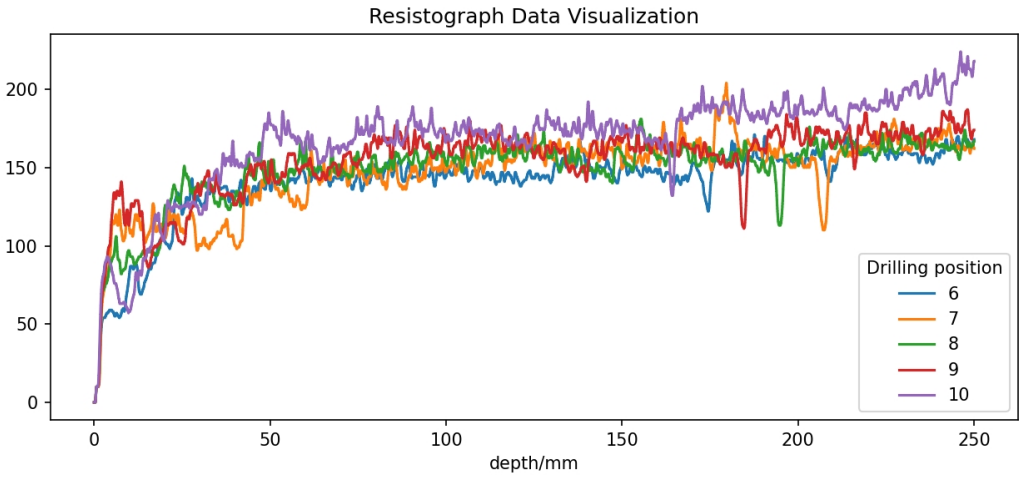

Figure 1. *The resistograph data along five drilling paths. Each of the curves has a short dropdown between 150 and 220 mm. This is an indication of damage at the corresponding position. The position is numbered according to the smaller sensor number. Drilling position 7 is between sensors 7 and 8.*

The trees have been felled, and the stem discs have been transported to the laboratory. Among others, the photographs of the discs have been used as a background image for the resistograph data to compare visually the correspondence of the drilling resistance with the stem condition.

2. RESULTS

The final code which allows to read resistograph files, draw the data in the stem cross-section plane and optionally use a PNG image as a background has been published on GitHub (Mařík & Cristini, 2025). The code is written in a modular way. It can be used to read the data in the native form saved by the resistograph, filter the data, and draw in the cross-section plane. The script may run from a command line or as a library.

An application of the scripts to tree number 5 is in Figure 2 on the left and shows the plane of the cross section with resistograph data visualized as colored bars. The columns (roughly) correspond to the drilling holes, and the colors correspond to the drilling resistance. Dark and white colors correspond to low and high drilling resistance, respectively. Consequently, a dark strip in the column indicates a short local decrease of the mechanical properties (could be a crack or ring shake) whereas the wide dark region would correspond to the cavity or degraded wood. Note also that the resistance typically increases from the boundary to the center and thus we explore the local trend (local increase and decrease) rather than the global trend and actual resistance values.

The right part of Figure 2 shows a combined image with tomogram and selected resistograph data. The columns with drilling resistance have clear black strips which reveal a decrease of mechanical properties. Despite the fact that the tomogram suggests a cavity in the center, the resistograph does not detect anything else than just a short local drilling resistance decrease. Thus, the defect in the stem is located along a narrow region and does not spread out in a large area.

3. DISCUSSION

It is well known that for any device used to evaluate trees of wooden logs, a skilled operator is required to interpret the results of the device correctly. Two or more methods are typically used to determine the health condition of the wood (Soge et al., 2021). The toolkit presented in the paper simplifies simultaneous combined interpretation of the tomographic and resistographic tests and makes the health status prediction more accurate.

Among others, the method allows to distinguish between central cavities-like damage shown on acoustic tomograph and linear damages such as cracks or ring shakes. This allows to confirm or reject the presence of hidden central damage which spreads out on the larger area of the tomogram but allows an alternative interpretation as a linear crack.

Note that coding the values of drilling resistance as colors along a line yields less precise information than the visualization using 2D curves in depth-resistance space. Thus, a careful smoothing and downsamplig is necessary. Since we are interested in the peaks (mostly peaks down corresponding to thin cracks), a filter which preserves these peaks is required. The Savitzky-Gollay filter is a tool which has been used successfully in similar situations.

Even in the case of combined results from two methods, some skills and knowledge of the background are necessary for correct and precise interpretation of the results. As an example, note that the black strips corresponding to the ring shake (which has been confirmed by physical inspection after felling) are not all aligned together (see Figure 2). The dropdown of the resistance on the drilling path between sensors 7 and 8 is shifted with respect to its actual position. For an explanation note the white strip on the same drilling path. This could indicate the presence of a knot which slightly influenced the drilling direction. As a consequence, the position of the drilling path in the cross-section plane does not correspond completely with the actual position of drilling. For this reason, a general trend in the curves is in some sense more important than the exact position of the characteristic signs of the curve.

Because Python is a widely accepted data processing tool, many libraries are available for further data preprocessing or postprocessing. As one particular example it is possible to blend two or more images in a Jupyter notebook using the tool (Octoframes, 2025). An example with mutual comparison of four images is shown in Figure 3. Other possible extensions include various GUI-like interfaces which can be used to develop a user-friendly interface to the toolkit. Thanks to the modularity of the toolkit and the wide spreadout of the Python language, it is even possible to use LLM for certain programming tasks, the approach referred to as *vibe coding*.

4. CONCLUSIONS

It is well known that in order to get more precise predictions on the health status of trees or wooden logs, a combination of more methods is desired (Soge et al., 2021). A toolkit in the form of Python scripts has been created to simplify a simultaneous visualization of data from tomograph and resistograph. Visualization created by this toolkit allows to merge data from two devices to a common

geometry in the plane of the cross-section and allows to distinguish linear defects, such as cracks or ring-shakes, from cavities or decay areas.

Data availability

The Python code and the source data (node positions and resistograph data) are available on GitHub (Mařík & Cristini, 2025).

Acknowledgements

Supported by the Ministry of Education, Youth and Sports of the Czech Republic, project ERC CZ no. LL1909 “Tree Dynamics: Understanding of Mechanical Response to Loading” and MSCA FELLOWSHIPS CZ MENDELU, project CZ.02.01.01/00/22_010/0008893 “Wood Degradation in the Urban Environment”.

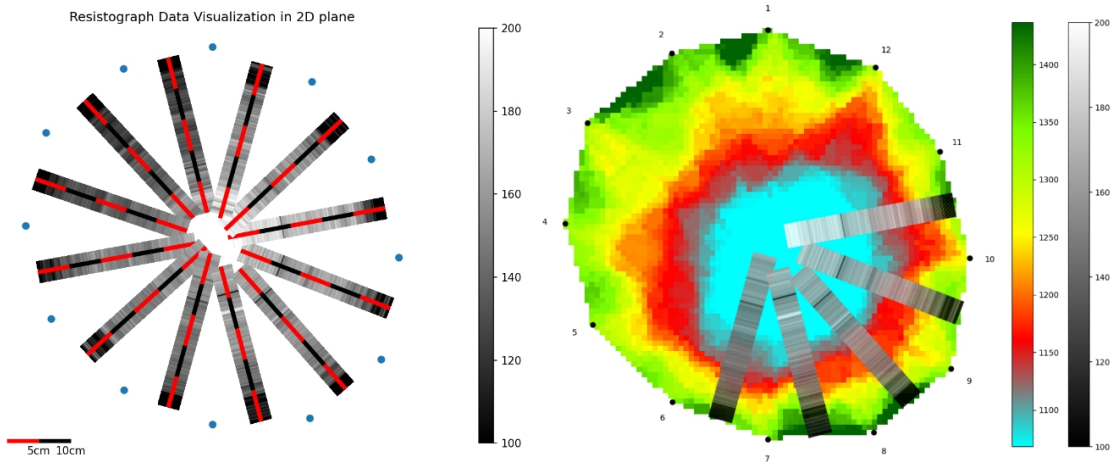

Figure 2. *Resistograph data projected to the 2D cross section of the stem on the left. The same data with tomogram background on the right. Note that the tomogram suggests a central cavity which contradicts the resistograph data showing just narrow region with degraded of mechanical properties (the black strips across selected bars near the end).*

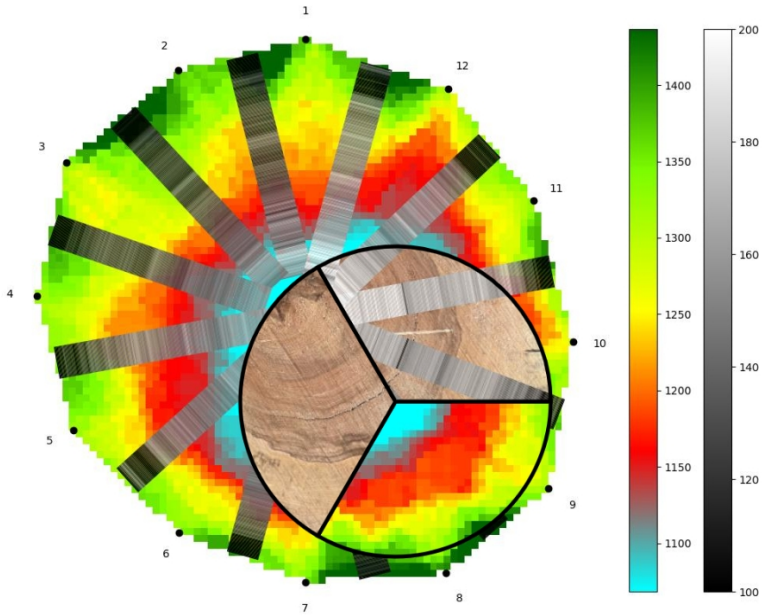

Figure 3. *An example of postprocessing. A swipe comparison of four images (photo of the cross-section and tomogram, both with and without the resistograph data) which allows to explore the output of measurement devices and compare with the actual state of the tree. Live version is available on* https://arborist-mendelu.github.io/resistograph_meets_tomograph *. The colored scale is the speed of the sound; the monochromatic scale is the drilling resistivity.*

REFERENCES

1. Cristini, V., Tippner, J., Tomšovský, M., Zlámal, J., & Mařík, R. (2022). Acoustic tomography outputs in comparison to the properties of degraded wood in beech trees. European Journal of Wood and Wood Products, 80(6), 1377–1387. https://doi.org/10.1007/S00107-022-01872-W
2. Du, X., Li, J., Feng, H., & Chen, S. (2018). Image Reconstruction of Internal Defects in Wood Based on Segmented Propagation Rays of Stress Waves. Applied Sciences 2018, Vol. 8, Page 1778, 8(10), 1778. https://doi.org/10.3390/APP8101778
3. Du, X., Li, S., Li, G., Feng, H., & Chen, S. (2015). Stress Wave Tomography of Wood Internal Defects using Ellipse-Based Spatial Interpolation and Velocity Compensation. BioResources, 10(3), 3948–3962. https://doi.org/10.15376/biores.10.3.3948-3962
4. Mařík, R., & Cristini, V. (2025, July 22). Resistograph data processing toolkit. https://github.com/arborist-mendelu/resistograph_meets_tomograph
5. Mařík, R., Cristini, V., Semík, V., & Zlámal, J. (2024). Acoustic tomography for standing trees. Proceedings of the 67th SWST International Convention: Advancing Regenerative Sustainability with Wood Science, 2–7.
6. Octoframes. (2025). jupyter_compare_view: Blend Between Multiple Images in JupyterLab. https://github.com/Octoframes/jupyter_compare_view
7. Papandrea, S. F., Cataldo, M. F., Zimbalatti, G., & Proto, A. R. (2022). Comparative evaluation of inspection techniques for decay detection in urban trees. Sensors and Actuators A: Physical, 340, 113544. https://doi.org/10.1016/J.SNA.2022.113544
8. Proto, A. R., Cataldo, M. F., Costa, C., Papandrea, S. F., & Zimbalatti, G. (2020). A tomographic approach to assessing the possibility of ring shake presence in standing chestnut trees. European Journal of Wood and Wood Products, 78(6), 1137–1148. https://doi.org/10.1007/S00107-020-01591-0/FIGURES/6
9. Rinn, F. (2015). Central defects in sonic tree tomography. West. Arborist, 20, 38–41. https://download.rinntech.com/RINN_CentralDefectsInSonicTreeTomography_WesternArborist_Spring_2015.pdf
10. Schwarze, F. W. M. R., Lonsdale, D., & Mattheck, C. (1995). Detectability of wood decay caused by Ustulina deusta in comparison with other tree-decay fungi. European Journal of Forest Pathology, 25(6–7), 327–341. https://doi.org/10.1111/J.1439-0329.1995.TB01348.X
11. Soge, A. O., Popoola, O. I., & Adetoyinbo, A. A. (2021). Detection of wood decay and cavities in living trees: A review. Canadian Journal of Forest Research, 51(7), 937–947. https://doi.org/10.1139/CJFR-2020-0340/ASSET/IMAGES/CJFR-2020-0340TAB1.GIF
12. Strobel, J. R. A., de Carvalho, M. A. G., Gonçalves, R., Pedroso, C. B., dos Reis, M. N., & Martins, P. S. (2018). Quantitative image analysis of acoustic tomography in woods. European Journal of Wood and Wood Products, 76(5), 1379–1389. https://doi.org/10.1007/S00107-018-1323-Y/TABLES/5
13. Szewczyk, G., Wąsik, R., Leszczyński, K., & Podlaski, R. (2018). Age estimation of different tree species using a special kind of an electrically recording resistance drill. Urban Forestry & Urban Greening, 34, 249–253. https://doi.org/10.1016/J.UFUG.2018.07.010
14. Wang, X., Allison, R. B., Wang, L., & Ross, R. J. (2023). Acoustic tomography for decay detection in red oak trees. https://doi.org/10.2737/FPL-RP-642
15. Authors address: Mendel University in Brno, Zemědělská 1, 613 00 Brno, Czech Rebublic

THE IMPACT OF TOOL HEIGHT ON THE WORKPIECE IN WOOD CUTTING WITH CIRCULAR SAWS

Mladen Furtula[1], Marija Đurković[1], Srđan Svrzić[1]

[1]*University of Belgrade – Faculty of Forestry, Serbia,*
e-mail: mladen.furtula@sfb.bg.ac.rs

ABSTRACT

The tool height influences the cutting force by changing the angle at which the blade penetrates the wood. This parameter was analyzed at two different heights. In the first set of measurements, previously used to assess the bluntness of the tool, a sharp saw was positioned 3 mm above the workpiece. The second set was also carried out with a sharp saw, but the height of the tool was set to 15 mm above the workpiece. In both cases, all other parameters were kept constant, so it was not necessary to introduce the concept of specific cutting resistance.

By analyzing the average cutting forces, basic data was obtained showing that changing the saw height changes the average fiber cutting angle. When the saw projected 3 mm beyond the workpiece, the average cutting angle Φ_m was 21.25°; with a projection of 15 mm, Φ_m increased to 27.87°. A significant difference is observed between these two configurations, with an average cutting angle difference of 6.62º. The rake angle of the saw used in the analysis was 20º. This change in the average fiber cutting angle explains the variation in the required cutting force under otherwise identical conditions.

1. INTRODUCTION

The reliability and accuracy of machines and tools in the wood industry have a major impact on the final product. This problem is even more noticeable in mass production. In addition to the amortization costs caused by replacements and/or repairs, there is also more scrap in the workpieces and a higher use of service time and therefore less production time. All of this can be seen most easily in the price of the machining costs per product quantity. The right choice of parameters for sharpening tools offers the opportunity to maximize the resources of these tools. In addition to the tool height, tool wear is also influenced by a number of other parameters: the tool material (e.g. HSS, carbide tools, nano-coatings) significantly determines its resistance to wear and impact loads, the temperature in the cutting zone, which depends on the type of machining, the properties of the processed wood such as density, hardness, moisture content and the presence of mineral inclusions also contribute to abrasive wear. The machining modes - including cutting speed, tooth feed, cutting depth and cutting angle - have a direct effect on the mechanical and thermal load of the tool, the duration and continuity of work without interruption increases the thermal load and accelerates material fatigue, maintenance and sharpening of the tool, i.e. regular removal of gumming and deposits and correct sharpening are the key to extending the service life, the stability of the settings and the precision of the machine (centring, vibration, condition of the bearings) also have a major influence on the even wear and reliable operation of the tool. The question arises as to which working procedure should be applied to the tool so that it is utilised optimally and functions smoothly. Cutting power is one of the methods used to determine the dullness or poor power of a tool. Checking the wear and selecting the blunt tool change mode can provide some answers as to what influences tool wear. One of the factors that influence the quality of machining and tool wear, and therefore cutting power, is the height of the tool in relation to the workpiece.

2. THEORETICAL BACKGROUND

The mechanical processing of wood is a complex process. Monitoring and controlling the machining processes requires a good knowledge of the phenomena that can influence the final machining result. From a technical point of view, the processing results can be divided into expected

(desired) and unexpected, i.e. undesired and in many cases unavoidable results. The desired results of wood processing would be the removal of excess material and the achievement of a finished piece with certain dimensions and a certain surface quality. Undesirable side effects of processing are released heat, which leads to increased temperature of tools and work objects, noise, vibrations and more (see Figure 1).

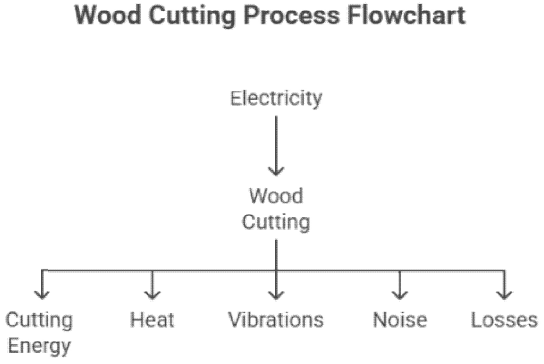

Figure 1. *Energy balance of cutting process.*

Input for the process of cutting wood is electricity, and output is cutting energy, heat, vibrations, noise, and other losses.

A large number of studies have focussed on the determination of cutting forces (Ko et al., 1999, Vazquez-Cooz et al., 2003) or noise or vibration (Lemaster et al., 1985) that occur during processing. However, only a few of them have considered the overall energy balance during the processing of wood or wood-based materials (Iskra et al., 2005). This complex type of research requires suitable equipment to measure the total, active and reactive power of the electric drive motor, cutting forces, heat released during cutting, noise and vibrations. With such equipment, it would be possible to determine the balance of energy consumed during cutting and the factors influencing energy consumption, such as the stability of the tool, the machining time of the machine and the quality of the machined surface (Iskra et al., 2005). The Faculty of Forestry has measuring devices for measuring, monitoring and displaying the power used by the SRD1 and SRD2 electric motors, which can also be used to determine the power required for cutting wood.

Heat losses are the next largest component in the balance of total losses. This is the heat released during friction between the wood and the front surface and possibly the sides of the tool. They are more difficult to measure when you consider that some of the heat released during cutting accumulates in the tool, some in the work object and crisps and some in the ambient air. In well-chosen woodworking regimes (for cutting speeds above 10 m/s), after a rapid initial rise, the temperature of the tool reaches a certain equilibrium temperature at which the heat generated during cutting is approximately equal to the heat released into the environment (Iskra et al., 2005). This could mean that the total increase in active energy during cutting, which occurs when the cutting speed is increased above 10 m/s, is converted into heat loss under the same other cutting conditions.

Vibration can have a major impact on machining results and the service life of tools and machines. The energy consumption of noise and vibration is not large, so it is not a big mistake if they are not taken into account.

As already mentioned, cutting power is influenced by cutting speed, feed rate and cutting angles (Kovač, Mikleš, 2010). According to their measurements, there are optimal tool geometries that reduce the cutting force. The article presents the results when using a saw with a breast angle γ of -10º to 20º, depending on the type of cutting material used. Positive breast angles consume less cutting force than saws without an angle or with a negative angle. This can be explained by the fact that the breast angle γ has an influence on the entry and exit angle of the saw as well as on the mean angle of the fiber cut, as can be seen in Figure 2.

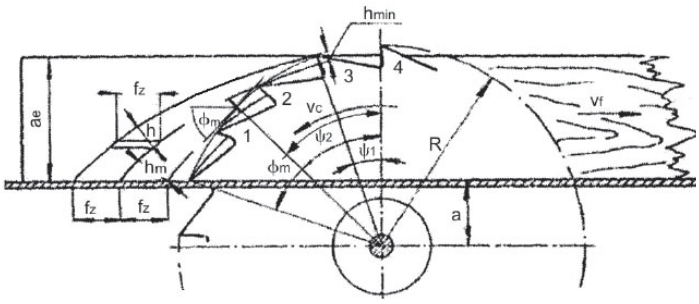

Figure 2. *Cutting process geometry*
f_z – feed per tooth [m/s]; a_e – cutting depth [m]; v_f - feed rate [m/s]; v_c – cutting speed [m/s]; ψ_1 – input angle of the teeth [º]; ψ_2 – output angle of the teeth [º]; Φ_m – average fibre cutting angle [º]; h_m – maximum chip thickness [mm].

Average fibre cutting angle could be calculated as folow:

$$¤_m = \arccos \frac{a + (\frac{a_e}{2})}{R}$$

3. MATERIALS AND METHODS

SRD 1

The UNO-LUX NS measuring and recording device is used to measure, monitor and display the power of the wood cutting machine. The system also analyses and processes the data obtained, stores it and has the option of displaying it later. The system is based on the ULNS Power Expert software package, version 2.0, and functions as a combination of the fixed cable connection of the wood cutting machine with the power measurement system. The ULNS Power Expert software package is used to measure, record, display and calculate characteristic power parameters during woodworking using an NI USB-6008 acquisition card and a suitable wattmeter with an industrial current signal of 0-20mA. The programme corresponds to the Windows platform and is optimised for a resolution of 1024x768.

The analogue signal measurement is based on a Hartmann & Brown wattmeter with a continuous current output of 0-20 mA. Using the switch on the housing, the measuring range can be selected between values of 5 KW, 10 KW and 15 KW, depending on the expected load. The maximum current signal of 20 mA always corresponds to the selected measuring range. The current signal is forwarded from the control cabinet to the subsystem of the recording computer. The signal is sampled and converted using the USB 6008 acquisition card from National Instruments, which is shown in figure no. 4. The NI USB-6008 acquisition card is connected to a PC via a USB port. The measuring system, i.e. a wattmeter with a current output, is connected to the acquisition card at ports 1 and 2, namely AI0+ and AI0-. This card model is intended for voltage measurement, so the current signal is converted into a voltage signal via a high-precision resistor (1% tolerance) of 199 ohms.

Figure 3. *Acquisition card USB 6008.*

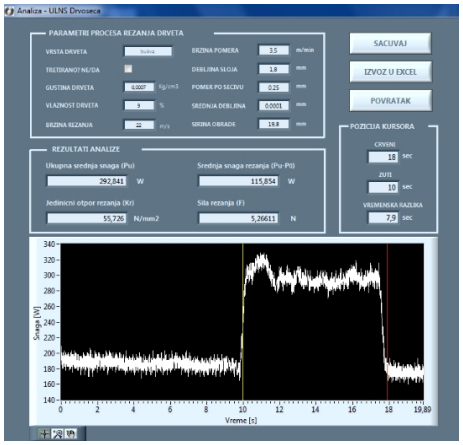

Figure 4. *Screenshots of cutting power. acquisition software.*

The measurement results are recorded, displayed and processed using the software described in this article. All signals are scaled by software and converted into real values with corresponding units of measurement. It is important to mention that this measuring device is portable and can be connected to various machines with the limitation of the maximum permissible power (up to 15 KW), thus enabling the measurement of cutting power in various machining operations.
The recorded data is displayed in the data analysis window (Figure 4) and all recorded parameters can also be saved in the Excel program package.

SRD 2

The SRD2 device is suitable for laboratory and industrial measurement of the cutting power of machines with a three-phase electric motor for processing wood and wood-based materials. The device is also able to monitor the power consumption of three-phase motors over a period of time and record the data of the voltages and currents per phase, the active and reactive energy, the power factor and the harmonics occurring in the power grid. It consists of a PowerLogic PM710 multimeter (Figure 5) from Schneider Electric, which is attached to the door of the enclosure in which the device is installed (Figure 6). The device has an RS232 port for connection to a computer, which enables remote monitoring and recording of the data obtained.

Figure 5: *PowerLogic PM 710.*

Figure 6: *SRD 2 installation setup.*

With the help of the computer software "Power View", the power of a three-phase motor can be measured and recorded in a relatively simple way at no load and under load, i.e. in our case during machining. On the basis of the values obtained, it is possible to calculate the average power during cutting, but also to determine the current and average cutting forces and the specific cutting resistance. The PowerLogic PM710 multimeter is connected to a computer on which the data obtained from the measurement can be recorded and processed via the RS232 and USB interfaces. The Power View software makes it possible to monitor and record the values of the current parameters over a longer period of time. The recorded data is saved in an Excel file and a diagram is created for the recorded values.

Figure 7 shows the part of the software package where the data to be monitored is selected. The software consists of 6 steps to define the type of measurement, the period to be analyzed, the device from which the data is recorded (the sofware can monitor several devices simultaneously) and the parameters to be analyzed. The ModbusReader PM710 SCADA software environment is also available. It enables laboratory and industrial measurements with a precise range and shorter time intervals. The software records the same parameters and displays them in real time.

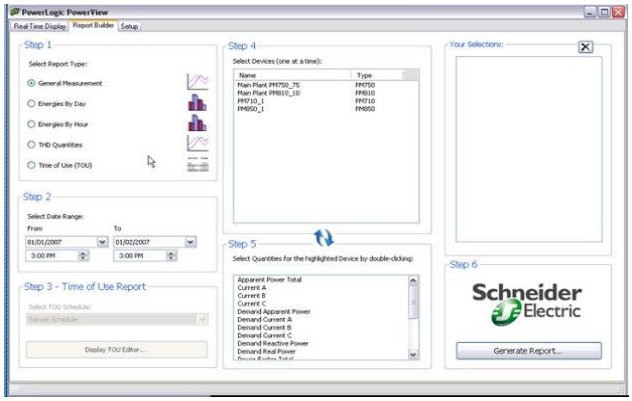

Fugure 7. *Screenshot of Power View cutting power measurement window.*

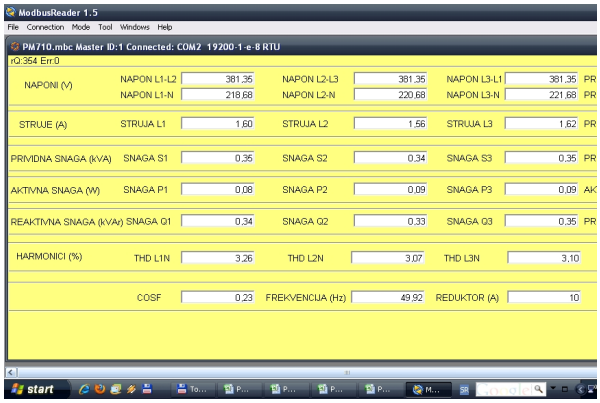

Figure 8. *Screenshot of ModbusReader PM710 software package.*

Figure 8 presents software during process parameter monitoring in real time. After finished recording the data obtained are stored in appropriate previously determined directory.

To verify the method of determining the accuracy and bluntness of the tool, an example of the production of three-layer parquet in the Tarkett Company from Bačka Palanka was taken. All layers are made of wood: the top layer is made of hardwood, the middle layer is made of fir or spruce, while the bottom, levelling layer is made of spruce veneer. After calculating the cost price and the quantity share, the middle layer of slats has the highest cost price. The slats form the middle layer with their geometry and qualitative correctness, and any deviation can have a negative effect on the quality of the end product. Deviations from the established quality standard are due to the poor performance of the tools used to process the slats and the quality of the wood, which affect the quality of the end product.

Materials used during the experiment were fir (Abies Alba) and spruce (Picea Abies) planks. Experimental plan consisted of the following:

- workpieces were cut with new (unused) circular saw blade,
- 4 workpieces were cut with 3 mm tool override (of which 2 were measured by SRD1 and remaining two by SRD2 acquisition system),
- 2 workpieces were cut with 15 mm tool override (measured by SRD1).

Table 1. *Dimensions of workpieces and leftover battens.*

Workpieces dimensions: length: 434 mm width: 147 mm thickness: 28 mm Moisture content 7,5 % ± 0,1	Leftover battens dimensions: length: 434 mm width: 9 mm thickness: 28 mm

The tool specifications are as follows:
Manufacturer: Ake
Type: Mustang*
Teeth material: HSS
Diameter: 250 mm
Kerf: 2.0 mm
Body thickness: 1,4 mm
Number of teeth: 30+2
Tooth shape: MA with edged back side and BG tested
* The saw is coated with an oxide layer that prevents resin contamination

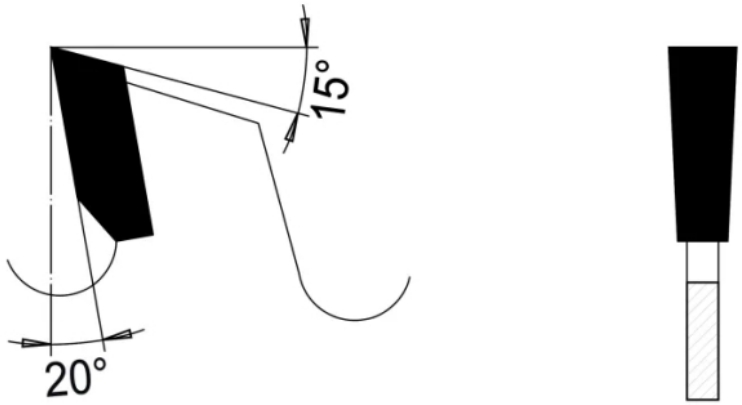

Figure 9. *Saw tooth geometry.*

Cutting operation was performed on Minimax CU410K (figure 11) combined machining center at Laboratory for Machines and apparatus, Faculty of Forestry, Belgrade Universuty.
Cutting parameters: rotational speed ~ 4.000 o/min; feed rate ~ 15 m/min

Figure 10. AKE *Mustang circular saw.*

Figure 11. *Minimax CU410K.*

The statistical analysis, i.e. the hypothesis test to test the cutting forces, was carried out using descriptive statistics to check the regularity of the distribution of the results, and the relationship between the data groups was determined using analysis of variance. The measurements of the two cutting force monitoring devices can be recorded and processed in the MS Excel programme. This is an essential part of processing the results so that only the essential parts of the measurements to be compared can be recorded. Since one measurement included all the cuts of a board (15÷17 cuts), it was necessary to separate the results of the individual cuts. Furthermore, for the results obtained with the SRD1 device, the determination of the average values of the cutting performance by the Power Expert software was used. The data on the mean values were then entered into an Excel document. The statistical analyses were carried out in statistical software package.

4. RESULTS AND DISCUSSION

When checking all the results obtained and recorded on both devices, it was found that the results of the SRD1 and SRD2 devices do not match. There are two deviations that have occurred. The first deviation is in the measured values, i.e. SRD2 shows a higher cutting power than SRD1. This can be explained by the fact that when measuring with the SRD1 device, the voltage and current are only measured on one phase and this result is multiplied by three in the calculation to obtain the final result. The SRD2 device, on the other hand, measures all three phases simultaneously and obtains the total active power consumed from these results. Another discrepancy in the results lies in the time intervals at which these two devices measure. The measurement protocol of the SRD1 device is

constant and has an interval of 0.01 seconds, while this interval is not constant for the SRD2 device and is between 0.25 and 0.28 seconds. This inadequacy of the SRD2 device can be explained by the fact that the PM710 meter, which forms the basis of the device, is intended for continuous monitoring of electricity utilization parameters and is not designed for such rapid measurements.

Both devices had shortcomings that should be eliminated in the future. Due to the precision of the time intervals and the time measurement range, the data recorded by the SRD1 device was processed. The effect of tool override was also determined using two groups of measurements. In the first set of measurements, a saw with a tool height above the workpiece of 3 mm was used, while in the second set, a tool height above the workpiece of 15 mm was used. In this analysis, all other parameters remained the same, so it was not necessary to introduce a specific cutting resistance, but all analyses were carried out using the cutting power of the saw

By analyzing the results of the mean values of the cutting forces, basic data were obtained, which are shown in Tables 2 and 3, while Table 3 shows the data from the analysis of variance between these two types of cutting.

Table 2. *Main statistical values for 3 mm tool override power measurements.*

Alpha value (for confidence interval)	0,05		
Oštra testera 3 mm (Average cutting power [W])			
Count	34	*Skewness*	-0,7066
Mean	564,9559	*Skewness Standard Error*	0,391
Mean LCL	551,2792	*Kurtosis*	2,9905
Mean UCL	578,6326	*Kurtosis Standard Error*	0,7177
Variance	1.536,4514	*Alternative Skewness (Fisher's)*	-0,7397
Standard Deviation	39,1976	*Alternative Kurtosis (Fisher's)*	0,1885
Mean Standard Error	6,7223	*Coefficient of Variation*	0,0694
Minimum	464,83	*Mean Deviation*	31,1857
Maximum	640,74	*Second Moment*	1.491,2617
Range	175,91	*Third Moment*	-40.692,3056
Sum	19.208,5	*Fourth Moment*	6.650.431,84
Sum Standard Error	228,5593	*Median*	577,72
Total Sum Squares	10.902.657,9636	*Median Error*	1,4449
Adjusted Sum Squares	50.702,8974	*Percentile 25% (Q1)*	545,31
Geometric Mean	563,5852	*Percentile 75% (Q2)*	588,555
Harmonic Mean	562,1615	*IQR*	43,245
Mode	#N/A	*MAD (Median Absolute Deviation)*	20,685
		Coefficient of Dispersion (COD)	0,0509

According to results from table 2 it is possible to notice that the average value of cutting force 565 W with minimal and maximal values of 465 and 641 W, respectively.

Table 3. *Main statistical values for 15 mm tool override power measurements.*

Alpha value (for confidence interval)	0,05		
Sharp saw 15 mm (Average cutting power [W])			
Count	34	*Skewness*	0,7683
Mean	530,2482	*Skewness Standard Error*	0,391
Mean LCL	518,7874	*Kurtosis*	4,3601
Mean UCL	541,7091	*Kurtosis Standard Error*	0,7177

Variance	1.078,921	*Alternative Skewness (Fisher's)*	0,8042
Standard Deviation	32,8469	*Alternative Kurtosis (Fisher's)*	1,7832
Mean Standard Error	5,6332	*Coefficient of Variation*	0,0619
Minimum	475,93	*Mean Deviation*	24,9321
Maximum	634,79	*Second Moment*	1.047,188
Range	158,86	*Third Moment*	26.034,1341
Sum	18.028,44	*Fourth Moment*	4.781.275,0323
Sum Standard Error	191,5289	*Median*	526,925
Total Sum Squares	9.595.152,887	*Median Error*	1,2108
Adjusted Sum Squares	35.604,3919	*Percentile 25% (Q1)*	508,99
Geometric Mean	529,2852	*Percentile 75% (Q2)*	550,565
Harmonic Mean	528,3443	*IQR*	41,575
Mode	#N/A	*MAD (Median Absolute Deviation)*	22,26
		Coefficient of Dispersion (COD)	0,0467

Table 3 shows that the average value of the cutting power is 530 W, the minimum power is 476 W and the maximum power is 635 W. Comparing this with the results from Table 2, it can be seen that the minimum and maximum values are similar, but that the average values are still different, as shown in Table 4.

Table 4. *Variance analysis for different tool overrides.*

Analysis of Variance (One-Way)							
Descriptive Statistics							
Groups	*Sample size*	*Sum*	*Mean*	*Variance*			
3	34	19.208,5	564,9559	10.902.657,9636			
15	34	18.028,44	530,2482	9.595.152,887			
Total	68		547,6021	1.593,8185			
ANOVA							
Source of Variation	*d.f.*	*SS*	*MS*	*F*	*p-level*	*F crit*	*Omega Sqr.*
Between Groups	1	20.478,553	20.478,553	15,6601	0,0002	3,9863	0,1774
Within Groups	66	86.307,2893	1.307,6862				
Total	67	106.785,8423					

Table 4 shows that the analysis of variance (ANOVA) reveals a very significant difference between the mean cutting values depending on the height of the tool in relation to the workpiece. This is confirmed by the value of the significance level (p-level), which in this case is 0.0002, and the significance limit in this case is 0.05. Figure 12 shows a graphical relationship between these two sets of data, as well as a linear function showing that less power is required when cutting with a tool that protrudes 15 mm above the workpiece.

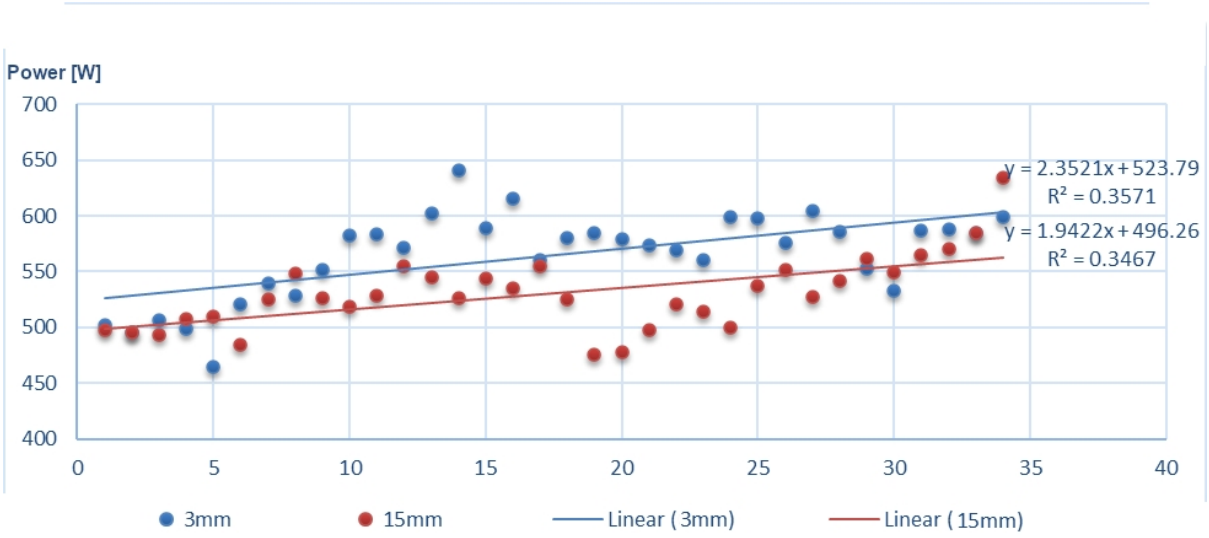

Figure 12. *Distribution graph for mean values of cutting power.*

If you raise the saw in relation to the work object, the mean cutting angle of the fibers changes so that when cutting in the first case, when the saw protrudes 3 mm from the workpiece Φ_m=21.25º, while in the second case, when the saw protrudes 15 mm from the workpiece Φ_m=27.87º. The difference between these two determined mean fiber cutting angles is 6.62°, and the breast angle of the saw used is 20°. This change in the mean cutting angle of the fibers explains the difference in the required cutting performance under the same other conditions.

5. CONCLUSION

Based on the results of this study, it was concluded that the height of the tool influences the cutting performance. There is a significant difference between cutting with a saw that protrudes 3 mm above the workpiece and a saw that protrudes 15 mm above the workpiece. This difference can be explained by the change in the mean cutting angle of the fibers (Φm) and the reduction in performance by increasing this angle.

Future tests should determine which tool height offers more favorable cutting conditions and optimal mean fiber cutting angles should be determined.

REFERENCES

1. M.Mandić (2011): Uticaj toplotne modifikacije i tehnoloških parametara obrade na snage rezanja pri obradi drveta glodanjem, seminarski rad, Beograd
2. Barcík, Š., Kotlínová, M., Pivolusková, E. (2006): Interactive relations at machining of juvenile wood. In: Manufacturing engineering in time of information society (1 Jubilee scientific conference), Gdansk, 43-46.
3. Barcík, Š., Pivolusková, E., Kminiak, R. (2008): Effect of technological parameters and wood properties on cutting power in plane milling of juvenile poplar wood, Drvna Industrija 59 (3), 107-112.
4. Kovač J., Mikleš M. (2010): Research on individual parameters for cutting power of woodworking process by circular saw, Journal of Forest Science, 56 (6), 271-277
5. Đukić, I., Goglia, (2006): Usporedba bruto energetskih normativa jarmača i tračnih pila trupčara, Drvna Industrija 57 (4), 179-182.
6. Iskra, P., Tanaka, C., Ohtani, T. (2005), Energy balance of the orthogonal cutting process, Holz als Roh- und Werkstoff 63: 358–364.
7. Kopecký, Z., Rousek, M. (2005): Determination of cutting forces in cutting wood materials, Drvna Industrija 56 (4), 171-176.
8. Kršljak, B. (1996): Mašine i alati za obradu drveta I, Beograd, 18-23.

9. Lemaster R, Tee L (1985) Monitoring tool wear during wood machining with acoustic emission. Wear 101, 273–282.
10. Šoškić, B., Popović, Z. (2002): Svojstva drveta, Beograd, 275-277.
11. Vazquez-Cooz, I., Meyer, R. (2003): Cutting forces for tension wood and normal wood of maple. In: Proc. of the 12th World Forestry Congress, Quebec City, Canada.
12. Wasielewski, R. (2004): Assessment of radial run-out of circular saw. In Annals of Warsaw Agricultural University, Forestry and Wood Technology. 1. vyd. Warsaw: Warsaw Agricultural University Press, 599-602.
13. Z. Đurišić, G. Danon, M. Furtula, M. Mandić - Tehničko rešenje SRD 1, 2010.
14. G. Danon, M. Furtula, M. Mandić, G. Vučković - Tehničko rešenje SRD 2 , 2010.

THE WATER-VAPOUR PERMEABILITY OF THE COATED MEDIUM DENSITY FIBERBOARD

Tanja Palija[1], Jovica Kojić[1], Igor Džinčić[1]

[1]University of Belgrade, Faculty of Forestry, Serbia
e-mail: tanja.palija@sfb.bg.ac.rs; student.jovicakojic2352002@sfb.bg.ac.rs; igor.dzincic@sfb.bg.ac.rs

ABSTRACT

The use of foil-faced medium density fiberboard (MDF) in wood surface finishing enables a reduction in surface finishing time and an enhancement of specific properties of coated surfaces. The objective of this study was to evaluate the differences in water-vapour permeability between foil-faced MDF and standard MDF panels (without foil), coated with polyurethane (PU) coating. Both types of coated MDF were exposed to water-vapour for a period of 14 days, during which differences in water-vapour absorption and subsequent desorption (for the next 14 days) were examined. The results show that facing the wider face of MDF panels with foil reduced the water-vapour absorption of the coated samples. Considering the results of water-vapour permeability results, the use of MDF double-faced with ground foil prior to finishing show the advantages for the use of furniture components in indoor environments with elevated moisture levels.

Keywords: medium density fiberboard, polyurethane coating, foil-faced, water-vapour permeability.

1. INTRODUCTION

Medium-density fibreboard (MDF) is the second most used wood-based composites in overall furniture production and interior decoration (Akbulut and Ayrilmis 2019). For applications in kitchen and bathroom furniture, especially in doors, MDF represents the primary material engaged today (Kúdela 2020). Compared to particleboard, which has lower density and lower production costs (Akbulut and Ayrilmis 2019), MDF is considered more isotropic. Its compact, voidless structure also provides better surface quality (Lee et al. 2019), which is one of the key parameters for the surface finishing effect. In comparison to natural wood MDF exhibiting higher strength due to its higher density (Sedleckỳ and Gašparík 2017).

Despite these benefits, MDF is highly sensitive to moisture. MDF swelling happens due to water absorption from both liquid water and water-vapour (Kibleur et al. 2022). Prolonged exposure to water causes significant swelling and, in severe cases, material degradation. The irreversible swelling affects the aesthetics and mechanical properties MDF resulting in a reduced service life under moist conditions (Kibleur et al. 2022). Although water-resistant MDF is available on the market, besides higher price this type of MDF can show signs of dimensional and structural changes under long-term moisture exposure.

Exposure to water-vapour of furniture and other products made of MDF in kitchens and bathrooms, can weaken joints, alter dimensions, and lead to material failure. The swelling of MDF is most pronounced at narrow, uncoated edges, such as the bottom of panels or doorframes, where water can most easily penetrate to the material.

MDF can be prefinished (primed) with double-faced foils on the wide surfaces, which prevents the excessive coating absorption that leads to uneven and visually unwanted results. The use of MDF with a coating carrier (ground) foils provides a uniform base for the spreading and levelling of the following coating layer, giving an even and smooth finish. In some cases, the number of coating layers required to achieve through-colored opacity can be reduced, enabling reduction of the overall surface finishing time and costs. The slightly textured surface of the ground foils can promote film coating

adhesion that is particularly important knowing that standard MDF exhibits low surface free energy, which can negatively affect the adhesion of applied film-forming materials (Kúdela 2020).

Since ground foil serves as a physical barrier to coating penetration, the aim of this study was to investigate whether the water-vapour adsorption could be reduce by using prefinished MDF as substrate. This paper investigates the resistance of ground foil-faced (so-called prefinished MDF) and uncoated MDF (so-called raw MDF) to water-vapour.

2. MATERIAL AND METHODS SECTION

Two groups of samples were used: “Group A” - raw MDF samples (manufacturer Kastamonu) and “Group B”- prefinished double-side faced MDF samples with ground foil (manufacturer DDL). Dimension of samples were: 150x70x18 mm. Within each group, 20 samples were tested: 10 control (C) and 10 that were surface finished (F), making the total number of samples 40. All samples were dimensioned on a CNC panel saw-cutting machine (manufacturer SCM, model Sigma Prima 50). The edges of all samples were rounded using a router with a radius of 3 mm to ensure the retention of the coating material on the edges. Sanding of the samples before coating was performed manually with a disc sander (manufacturer Festool). Sanding was performed in two stages using P120 and P180 grit sanding paper.

All of the samples (except the control ones) were surface finished using the following coating system: 1. layer polyurethane (PU) sealer (Milesi LBR21811: Milesi LNB42=2:1), 2. layer white pigmented PU base coating (Milesi LBR102: Milesi LNB42=2:1 +30% Milesi LZC70) and 3. layer white pigmented PU topcoat (Milesi RAL 9016: Milesi LNB623=2:1 +30% Milesi LZC70). All of the used coating materials are based on organic solvents. PU sealer was applied to the entire surface (both the wide and narrow sides) of the raw samples without foil (Group A), while for the prefinished samples (Group B) it was applied only to the narrow sides (Figure 1). The following layers of base and top PU coating were applied to the entire surface of the both groups of samples.

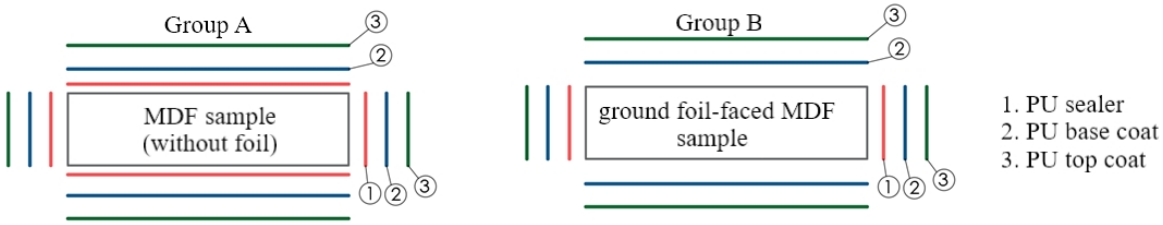

Figure 1. *Layers of coating system applied on wide and narrow sides of: a) raw MDF samples (Group A) and b) ground foil-faced MDF samples (Group B).*

The sealer was applied manually, using brush, and after drying, sanding was performed manually using P240 grit sandpaper. The base coat and topcoat were applied by air spraying in a pressurized spraying booth, using the following parameters of the spraying gun: nozzle diameter 0.6 mm and air pressure 3 bar. The coatings were applied to the wider sides (front and back) in one layer, and in two layers to the narrower sides.

The measurement of the dry film thickness of the coating system was performed using an ultrasonic film thickness gauge (manufactured DeFelsco, model PosiTector 200), in accordance with SRPS EN ISO 2808:2019. Dry film thickness measurement was conducted on all samples surface finished with coatings, on 3 measurement points within each sample. Measurement points were selected randomly on wide side of the coated surface. The total number of measurements per group was 30.

After drying of the base coating in the ambient conditions, the coated samples were manually sanded using P320 grit sandpaper. After the application of the top coating, the samples were dried in the ambient conditions for 24 hours, following by preconditioning and afterwards water-vapour permeability testing (according to EN 927-4:2001). Preconditioning of the samples consisted of several phases: immersing of the samples in water for 24 hours; drying of the samples under ambient conditions for 3 hours; drying of the samples at a temperature of 50 C for 3 hours; drying of the samples under ambient conditions for 18 hours (Figure 2).

a) *b)*

Figure 2. *Preconditioning of the samples: a) immersing of the samples in water for 24 hours and b) drying of the samples at a temperature of 50 °C for 3 hours.*

The testing of the samples was done by placing the samples above water for 14 days, using plastic containers filled with water with grid frame on top (Figure 3). After that, the samples were dried for 14 days at room conditions. The mass of the samples is measured immediately after preconditioning, after exposure to water-vapour, and 14 days after the ending of water-vapour exposure. The mass of samples was measured using an analytical balance (manufacturer CAS, model Kern EW), accuracy 0.01 g. The water-vapour permeability of the samples was expressed by mass gain (after 14. day and after 28. day).

a) *b)*

Figure 3. *Testing the water-vapour permeability: a) containers filled with water with grid frame on top and b) samples placed faced to water by wide side*

3. RESULTS

Table 1 shows the dry film thickness of the coating system of MDF samples with and without ground foil.

Table 1. *Dry film thickness of coated samples.*

	Group AF	**Group BF**
Dry film thickness of system of coatings [µm]	202	153

*Group AF – surface finished raw MDF; Group BF – surface finished ground foil-faced MDF

The difference in dry film thickness between coated MDF samples with and without ground foil is attributed to the imprecision of the measurement method and inclusion of the ground foil thickness in the results of the coating system thickness. The differences in dry film thickness between these two groups were not statistically significant ($t(58) = 2.00$, $p > 0.05$).

The percentage of mass gain during water-vapour absorption and desorption cycle (after 14. and after 28. days the experiment) is given in Table 2.

Table 2. *Mass gain of samples during water-vapour absorption from 1. to 14. day, and during water-vapour desorption from 14. to 28. day.*

Mass gain of samples[%]	**During water-vapour absorption**				**During water-vapour desorption**			
Group of samples	AC	BC	AF	BF	AC	BC	AF	BF
Average value	**10,38**	**7,97**	**0,99**	**0,71**	**6.40**	**4,65**	**0,15**	**-0,06**
Standard deviation	0,06	0,09	0,42	0,24	0,19	0,29	0,03	0,02

* Group AC – control (unfinished) raw MDF; Group BC – control (unfinished) ground foil-faced MDF; Group AF – surface finished raw MDF; Group BF – surface finished ground foil-faced MDF

From Table 2 it can be seen that surface finished samples faced with ground foil (group BF) absorbed less water compared to the samples without foil (group AF) in the period from the 1. to the 14. day of the experiment. This results confirms that foils on MDF surfaces reduces penetration of the liquid and vapour materials into the core of the boards. These findings are in line with implication from previous research that the high density surface layers should be stabilize to achieve dimensional stability of the MDF panels (Candan et al. 2012). The research results of MDF resistance to different cold liquids (Slabejová, Vidholdová, and Iždinský 2023), in which coated samples faced with ground foil had better grade results, in comparison to the samples without foil coated with different coating systems, confirm the role of ground foil as barrier in penetration of liquids and vapours. Even though the difference in mass gain during absorption cycle between group AF and BF was not statistically significant ($t(18) = 0.873$, $p>0.05$), the use of ground-foil faced MDF as substrate can reduce the moisture uptake of the coated panel. A similar trend applies to the control samples that were not surface finished (group AC and BC). The difference between these two groups was statistically not negligible ($t(18) = 0.907$, $p>0.05$).

Regarding water-vapour desorption cycle from day 14. to 28. day of experiment, the mass of all of the samples decreased, as expected. In previous research it was concluded that thickness swelling of MDF panels was higher than thickness shrinkage at any density level (Ganev et al. 2005). While all samples experienced water-vapour desorption, the mass of the uncoated samples (group AC and BC) was higher than the initial mass, indicating that water-vapour was not completely lost from the samples and that the uncoated samples should not be used when panels are expected to be exposed to high humidity during use. However, the slightly lower water–vapour release during desorption cycle of uncoated samples with ground foil was statistically significant ($t(18) = 3.272$, $p<0.05$). The samples double-faced with ground foil before coating, had even showed slight decrease of the mass of the samples (group BF) compared to their mass at the end of absorption time, indicating the higher rate of water- vapour release, which can be important for the use of the product in real conditions. The use

of ground foil significantly enhanced water-vapour desorption of surface finished samples ($t(18) = 18.173$, $p<0.05$)

Table 3 summarize the total mass gain of all groups of samples after 28 days of experiment. In comparison of the initial mass of the samples (1. day of experiment) all of the sample had shown increase of their mass at the end of the experiment.

Table 3. *Mass change of samples after 28 days (absorption cycle: from 1. to 14. day; desorption cycle: 14. to 28.day).*

	Mass gain of samples [%]			
Group of samples	AC	BC	AF	BF
Average value	3,98	3,32	0,84	0,77
Standard deviation	0,10	0,19	0,07	0,06

* Group AC – control (unfinished) raw MDF; Group BC – control (unfinished) ground foil-faced MDF; Group AF – surface finished raw MDF; Group BF – surface finished ground foil-faced MDF

The mass gain (g) of uncoated MDF (group AC and BC) was 4.97 to 4.25 times higher in comparison to coated samples (group AF and BF, respectively). The overall mass gain of double-faced ground foil samples was lower in comparison to raw sample, with and without surface finishing. This result indicates that raw MDF “breathes” more easily compared to MDF with melamine foil. The facing of wide sides of samples with ground foil reduce the water-vapour permeability of MDF. The difference in mass change between samples with and without ground foil, at the end of desorption cycle, was statistically eligible, for uncoated and coated samples (($t(18) = 2.561$, $p<0.05$) and ($t(18) = 6.866$, $p<0.05$), respectively).

Based upon results of water-vapour permeability it makes sense to use MDF double-faced with ground foil prior to finishing for furniture parts in indoor environments with increased moisture.

Along with quantitative differences in resistance to water-vapour permeability between surface finished MDF samples with and without ground foil, qualitative distinction between these two group of samples were noticed. The thickness swelling of the raw samples (without coating) was clearly noticeable, but the change in thickness was followed by the cracks in film coatings in the samples faced with ground foil, Figure 4. Such cracks appeared on the narrow sides, visible to the naked eye. This type of defect of coated surface is not allowed in final products since it can affect strength and durability of the product (if cracks occur near the joining elements). In addition, cracks significantly reduce visual impression and surface quality of the final product. The formation of the cracks can be related to higher mass loss rate of coated samples with ground foil, during desorption cycle, in comparison to coated samples without foil. The faster release of water-vapour through the narrow edges could cause stress and cracking in the coating film.

Figure 4. *Cracks on narrow edges of coated MDF samples double faced with ground foil* **.**

4. CONCLUSIONS

From the results of this study the following can be concluded:

- Surface finishing of MDF with coatings reduces water absorption.
- The ground foil has a significant effect on water absorption, leading to reduced water-vapour uptake in MDF.
- MDF double-faced with ground foil exhibits higher water-vapour desorption resistance, which becomes particularly evident when the surface is surface finished with coatings.
- The use of surface finished MDF faced with ground foil is more suitable in environments with elevated air humidity, although there is a risk of check formation on the narrow edges.

REFERENCES

1. Akbulut, T.; Ayrilmis, N. Some Advantages of Three-Layer Medium-Density Fibreboard as Compared to the Traditional Single-Layer One. J. Wood Sci. 2019, 65, doi:10.1186/s10086-019-1822-4.
2. Kúdela, J. Surface Properties of a Medium Density Fibreboard Evaluated from the Viewpoint of Its Surface Treatment. Acta Fac. Xylologiae Zvolen 2020, 62, 35–45,
3. Sedleckỳ, M.; Gašparík, M. Power Consumption during Edge Milling of Medium-Density Fiberboard and Edge-Glued Panel. BioResources 2017, 12, 7413–7426,.
4. Kibleur, P.; Manigrasso, Z.; Goethals, W.; Aelterman, J.; Boone, M.N.; Van Acker, J.; Van den Bulcke, J. Microscopic Deformations in MDF Swelling: A Unique 4D-CT Characterization. Mater. Struct. Constr. 2022, 55, 1–12,
5. EN 927-4:2000 - Paint and varnishes - Coating materials and coating systems for exterior wood - Part 4: Assessment of the water-vapour permeability.
6. SRPS EN ISO 2808:2019 - Paints and varnishes - Determination of film thickness.
7. Candan, Z.; Akbulut, T.; Wang, S.; Zhang, X.; Faruk Sisci, A. Layer Thickness Swell Characteristics of Medium Density Fibreboard (MDF) Panels Affected by Some Production Parameters. Wood Res. 2012, 57, 441–452.
8. Slabejová, G.; Vidholdová, Z.; Iždinský, J. Evaluation of Resistance Properties of Selected Surface Treatments on Medium Density Fibreboards. *Coatings* **2023**, *13*, 1–15,
9. Ganev, S.; Cloutier, A.; Beauregard, R.; Gendron, G. Linear Expansion and Thickness Swell of MDF as a Function of Panel Density and Sorption State. Wood Fiber Sci. 2005, 37, 327–336

OPTIMIZATION OF SCHOOL CHAIR DESIGN USING FINITE ELEMENT METHOD ANALYSIS

Zoran Spiroski[1], Vladimir Koljozov[2], Zoran Trposki[2], Anastasija Temelkova[2]

[1] Solfins Skopje, e-mail: zoran.spiroski@solfins.com
[2]Ss. Cyril and Methodius University in Skopje, N. Macedonia,
Faculty of Design and Technologies of Furniture and Interior-Skopje,
e-mail: koljozov@fdtme.ukim.edu.mk; trposki@fdtme.ukim.edu.mk; temelkova@fdtme.ukim.edu.mk

ABSTRACT

The aim of the research presented in this paper was to study the possibilities of using the SOLIDWORKS Simulation software application to determine the optimal values of the structural and strength characteristics in the design process of a school chair. By using an optimization analysis module, a simulation of the real loads on a school chair was carried out. Through several iterations with virtual prototypes, the optimal values for the dimensions of the elements were determined from the aspect of durability of static loads.

Keywords: finite element method, Optimization analysis, SOLIDWORKS Simulation, Virtual prototypes.

1. INTRODUCTION

The school chair is a product that is mass-produced and therefore must go through all stages of the design and production process. It is especially important at the beginning of the process to clearly define the design and to make a construction that can meet the required conditions for the chair's use. As part of this work, on a previously submitted and approved design of a school chair, the individual elements were dimensioned and their validation in terms of durability of previously defined loads was performed.

The construction of the school chair consists of a frame, seat and backrest. The frame is an assembly of two tubes bent to a defined shape and welded together with two additional elements into a single unit. The material is plain carbon steel that is protected by painting. The seat and backrest also have a predefined design. The material for the seat and backrest is a beech veneer board. The structure is connected with four rivets, the seat is riveted directly to the tube, while the backrest is attached to additionally welded plates. Elements made of plastic material are added to the legs.

Figure 1. *Design of a school chair.*

2. METHODS

The CAD model of the school chair assembly was created using SOLIDWORKS software, while the SOLIDWORKS Simulation program was used for strength calculations.

The purpose of the calculations is to determine three parameters:

- The distribution of stresses and their maximum values in the structure,
- Deformation and displacements in the structure,
- The lowest value of the factor of safety.

The material chosen for the frame is carbon steel, from the SOLIDWORKS database – Plain Carbon Steel. The tensile strength of the material is 220.6 (N/mm^2).

The material chosen for the seat and backrest is beech plywood (three-layer and five-layer), with a tensile strength of 78 (N/mm^2).

Property	Value	Units
Elastic Modulus	210000	N/mm^2
Poisson's Ratio	0.28	N/A
Shear Modulus	79000	N/mm^2
Mass Density	7800	kg/m^3
Tensile Strength	399.826	N/mm^2
Compressive Strength		N/mm^2
Yield Strength	220.594	N/mm^2
Thermal Expansion Coefficient	1.3e-05	/K
Thermal Conductivity	43	W/(m·K)
Specific Heat	440	J/(kg·K)
Material Damping Ratio		N/A

Figure 2. *Mechanical characteristics of the frame material - carbon steel.*

Property	Value	Units
Elastic Modulus	12500	N/mm^2
Poisson's Ratio	0.35	N/A
Shear Modulus	318.9	N/mm^2
Mass Density	800	kg/m^3
Tensile Strength		N/mm^2
Compressive Strength		N/mm^2
Yield Strength	78	N/mm^2
Thermal Expansion Coefficient		/K
Thermal Conductivity		W/(m·K)
Specific Heat	0	J/(kg·K)
Material Damping Ratio		N/A

Figure 3. *Mechanical characteristics of the seat and backrest material - beech plywood.*

The forces acting on the chair are assumed to be extreme load values. It is assumed that a person with an approximate body mass of 100 kg can sit on the chair, while at the same time the backrest is loaded with a mass of approximately 40 kg.

The simulation is static, the strength calculation was done in SOLIDWORKS Simulation software. Several different simulations of the frame and seat elements were made, with changing parameters and a simulation of an assembled chair with the three elements simultaneously.

The mathematical simulation model defines the supports (surfaces where the part rests on the ground), the location of forces and the value of the forces. In this case, it is the contact between the seat and the frame where a force of 1000 (N) acts and on the backrest plates where a force of 400 (N) acts. Then a finite element mesh is generated.

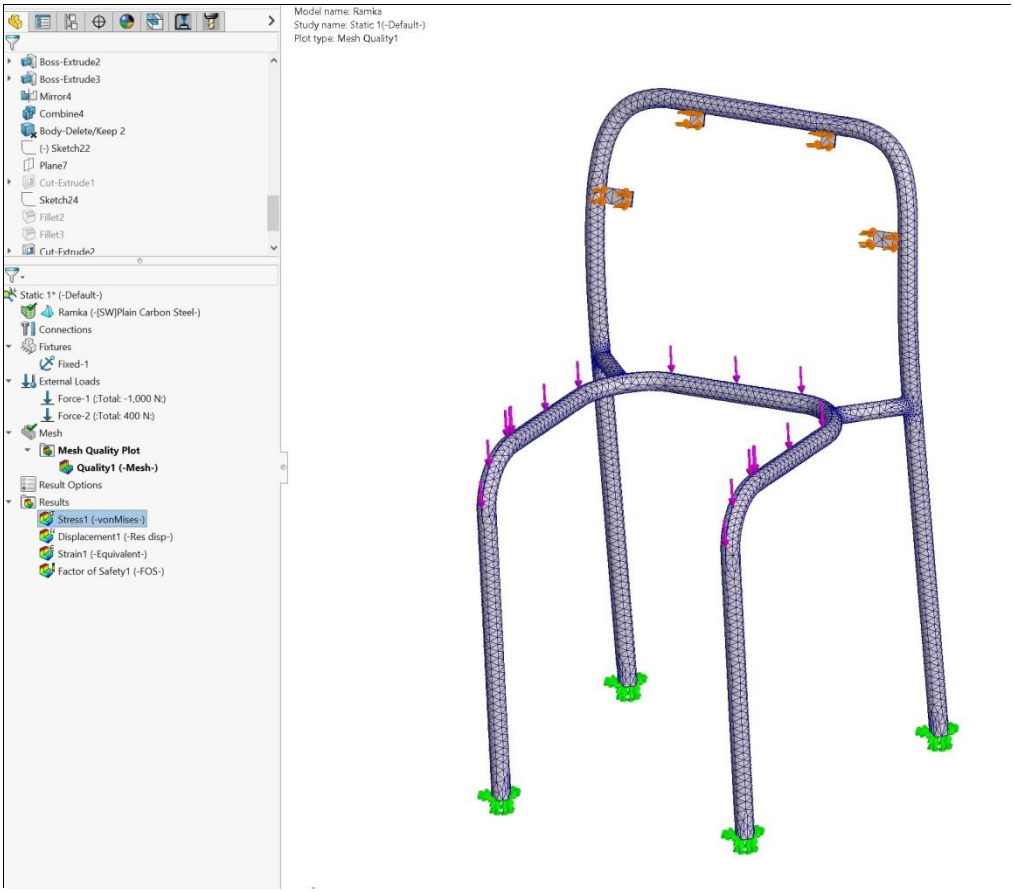

Figure 4. *Mathematical model of the simulation of frame loads.*

3. RESULTS AND DISCUSSION

3.1. Simulation of frame loads

The simulation of the frame loads was done in four iterations, on four different models.

Simulation 1

Frame model 1 - The thickness of the tube is 2 (mm), the thickness of the plates for attaching the backrest is 2 (mm).

By simulating the stresses, the following values were obtained:

- The maximum stress is *Max Stress = 140.9 (N/mm^2)* and it occurs on the support plates
- The maximum deformation is *Displacement = 2.8 (mm)*
- The minimum factor of safety is *FOS = 1.57*

Figure 5. *Model 1 analysis results.*

Simulation 2

Frame model 2 - The thickness of the tube is 2 (mm), the thickness of the plates for attaching the backrest is 2 (mm). A cross-sectional element has been added to this model in order to examine whether it has an impact on the results.

By simulating the stresses, the following values were obtained:

- The maximum stress is *Max Stress = 146.5 (N/mm^2)*
- The maximum deformation is *Displacement = 2.9 (mm)*
- The minimum factor of safety is *FOS = 1.51*

Figure 6. *Model 2 analysis results.*

Simulation 3

Frame model 3 - The thickness of the tube is 2.5 (mm), the thickness of the plates for attaching the backrest is 2 (mm).

By simulating the stresses, the following values were obtained:

- The maximum stress is *Max Stress = 142.2 (N/mm^2)*
- The maximum deformation is *Displacement = 2.5 (mm)*
- The minimum factor of safety is *FOS = 1.52*

Figure 7. *Model 3 analysis results.*

Simulation 4

Frame model 4 - The thickness of the tube is 2 (mm), the thickness of the plates for attaching the backrest is increased to 3 (mm).

By simulating the stresses, the following values were obtained:

- The maximum stress is *Max Stress = 125.9 (N/mm^2)*

- The maximum deformation is *Displacement = 2.9 (mm)*
- The minimum factor of safety is *FOS = 1.75*

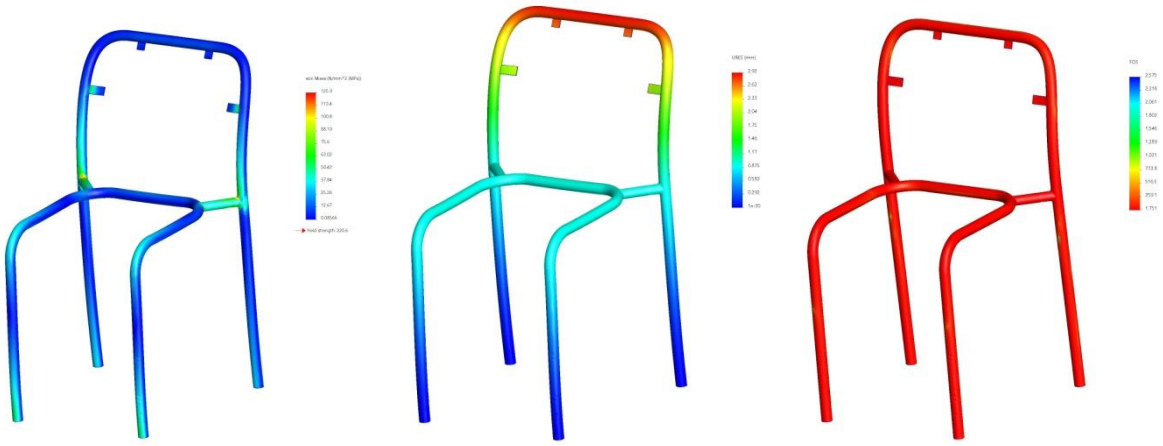

Figure 8. *Model 4 analysis results.*

	Description			Results		
	Tube thickness (mm)	Plates thickness (mm)	Additional frame	Max stress (Mpa)	Displacement (mm)	Min FOS
Model 1	2	2	no	140.9	2.8	1.57
Model 2	2	2	yes	146.5	2.9	1.51
Model 3	2.5	2	no	145.2	2.5	1.52
Model 4	2	3	no	125.9	2.9	1.75

Figure 9. *Table of results from the simulation of the frame models.*

3.2. Simulation of the seat loads

The seat load simulation was performed for two different thicknesses, for values of 6 (mm) and 8 (mm). The support is made at the contact between the seat and the frame and is loaded with a force of 1000 (N) on an area defined in the central part. The material is beech plywood (three-layer and five-layer).

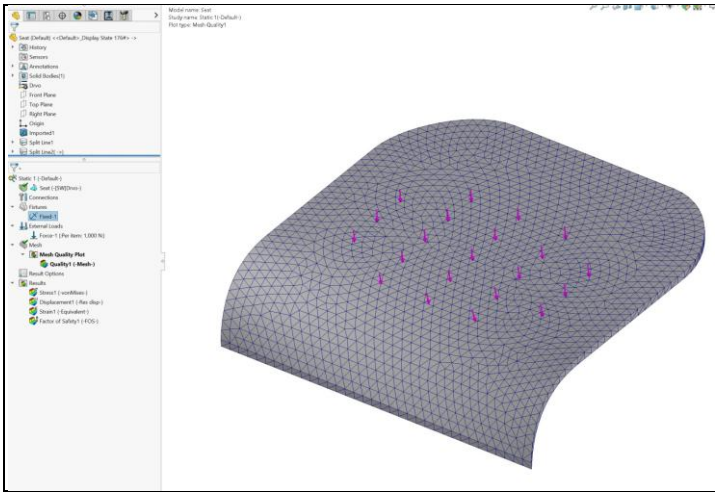

Figure 10. *Mathematical model for seat loads simulation.*

Simulation 5

Obtained values for simulation of a seat with a thickness of 8 (mm):

- The maximum stress is *Max Stress = 31.1 (N/mm^2)*
- The maximum deformation is *Displacement = 0.6 (mm)*
- The minimum factor of safety is *FOS = 2.5*

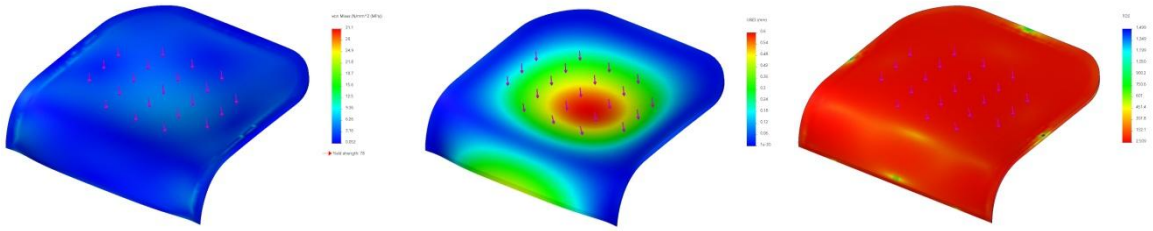

Figure 11. *Results of analysis of a seat with a thickness of 8 (mm).*

Simulation 6

Obtained values for simulation of a seat with a thickness of 6 (mm):

- The maximum stress is *Max Stress = 45.4 (N/mm^2)*
- The maximum deformation is *Displacement = 1.08 (mm)*
- The minimum factor of safety is *FOS = 1.72*

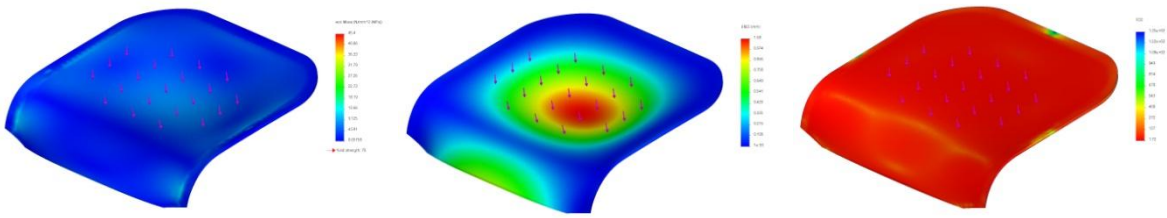

Figure 12. *Results of analysis of a seat with a thickness of 6 (mm).*

Tube thickness (mm)	Max stress (Mpa)	Displacement (mm)	Min FOS
8	31.1	0.6	2.5
6	45.4	1.08	1.72

Figure 13. *Table of results from the seat load simulation.*

3.3. Simulation of the backrest loads

The simulation of the loads on the backrest is made for a situation when all the elements of the chair are assembled. It is made for two different backrest thicknesses, for values of 5 (mm) and 6 (mm). The support is made on the plates added to the frame and is loaded with a force of 400 (N) on an area defined in the central part. The material is beech plywood (three-layer and five-layer), the same as the seat.

Simulation 7

Obtained values for simulation of a backrest with a thickness of 5 (mm):

- The maximum stress is *Max Stress = 157.9 (N/mm^2)*
- The maximum deformation is *Displacement = 4.6 (mm)*
- The minimum factor of safety is *FOS = 1.4*

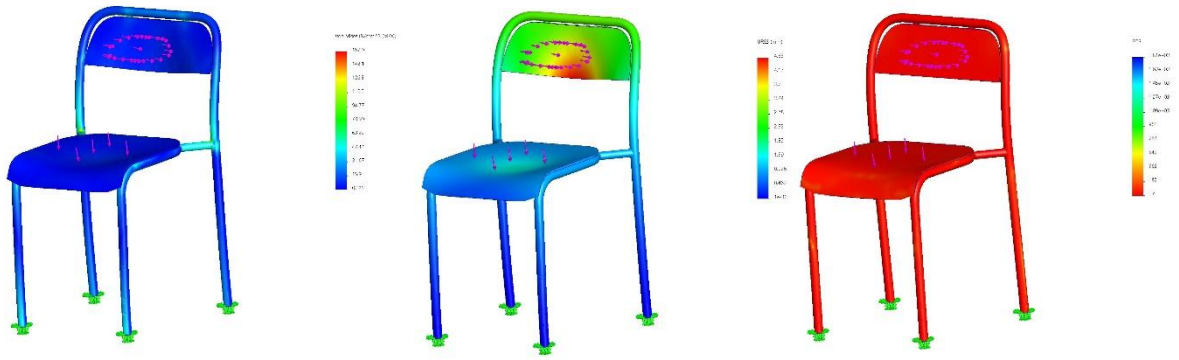

Figure 14. *Results of analysis of a backrest with a thickness of 5 (mm).*

Simulation 8

Obtained values for simulation of a backrest with a thickness of 6 (mm):

- The maximum stress is *Max Stress = 128.4 (N/mm^2)*
- The maximum deformation is *Displacement = 3.7 (mm)*
- The minimum factor of safety is *FOS = 1.72*

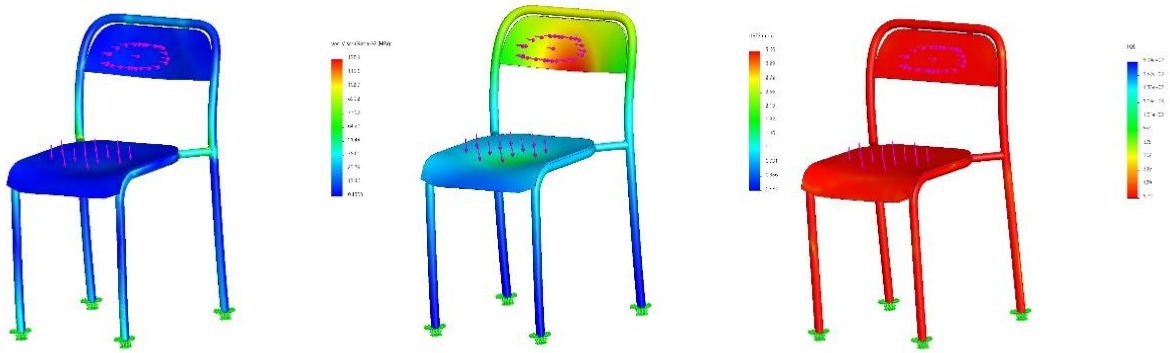

Figure 15. *Results of analysis of a backrest with a thickness of 6 (mm).*

Backrest thickness (mm)	Max stress (Mpa)	Displacement (mm)	Min FOS
5	157.9	4.6	1.4
6	128.4	3.7	1.72

Figure 16. *Table of results from assembly simulation.*

4. CONCLUSIONS

The paper describes the procedure for simulating the stresses on a school chair to determine the optimal design and construction.

Eight different simulations were performed by changing the structural characteristics of the frame material (carbon steel tube) and the seat/backrest material (beech plywood).

According to the results of simulation 2, it can be concluded that the additional cross-section element has no impact on the results and does not need to be added to the structure.

According to the results of simulation 3, it can be concluded that changing the tube thickness to 2.5 (mm) only affects on reducing the deformation.

According to the results of simulation 4, it can be concluded that changing the thickness of the support plates to 3 (mm) has an impact on reducing the maximum stresses and increasing the minimum safety factor.

The maximum stress on the assembly is on the backrest mounting plates, on the metal part. According to the graphic representation in Figure 15, the stresses on the seat and backrest are in the safe zone.

It can be concluded that the school chair can be made of a frame with a tube of 2 (mm) and backrest plates with a thickness of 3 (mm), without the use of additional cross-section elements. The seat and backrest are recommended to be made of beech plywood with a thickness of 6 (mm). The construction defined in this way meets the required conditions for use.

REFERENCE

1. Akin J.E., Finite Element Analysis Concepts via SolidWorks, Rice University, Houston, Texas, USA (2009).
2. Chang T.C., Wysk R.A., Wang H.P., Computer-Aided Manufacturing, Prentice-Hall Inc., N.J. USA (1998).
3. Gustafsson,S.I., Finite element modelling versus reality for birch chairs, Holz als Roh- und Werkstoff (54), Springer – Verlag, (1996).
4. Koljozov V., Dukovski V., Integrating CAD and CAM in woodprocessing industry, 2-nd International conference "Machine-Tool-Workpiece", Technical University of Zvolen, Nitra (1999).
5. Rao P.N., CAD/CAM: Principles and Applications, McGraw-Hill Inc., New York, USA (1991).
6. Shih R.H., Introduction to Finite Element Analysis Using SOLIDWORKS Simulation 2025, SDC Publications, Cansas City, USA (2025)
7. Zeid I., CAD/CAM - Theory and Practice, McGraw-Hill Inc., New York, USA (1991).

The Authors' Address:

Zoran Spiroski, Dr.Sci., Solfins, Skopje, Republic of North Macedonia.

Vladimir Koljozov, Dr.Sci, full professor at Faculty of Design and Technologies of Furniture and Interior-Skopje, Ss. Cyril and Methodius University, 16-ta Makedonska brigada 3, 1000, Skopje, Republic of North Macedonia.

Zoran Trposki, Dr.Sci, full professor at Faculty of Design and Technologies of Furniture and Interior-Skopje, Ss. Cyril and Methodius University, 16-ta Makedonska brigada 3, 1000, Skopje, Republic of North Macedonia.

Anastasija Temelkova, Dr.Sci, assistant at Faculty of Design and Technologies of Furniture and Interior-Skopje, Ss. Cyril and Methodius University, 16-ta Makedonska brigada 3, 1000, Skopje, Republic of North Macedonia.

TREE DYNAMICS: THE MECHANICAL RESPONSE OF A TREE

Barbora Vojáčková[1], Jan Tippner[1]

Mendel University in Brno, Czech Republic,
Faculty of Forestry and Wood Technology,
e-mail: barbora.vojackova@mendelu.cz; jan.tippner@mendelu.cz

ABSTRACT

Mechanical stability is a fundamental criterion in urban tree care and risk management. Despite advancements in research, current assessment practices predominantly rely on static load response analysis without adequate consideration of dynamic performance and response.

To address this, the DYNATREE project was undertaken to characterise the dynamic response of trees and identify key mechanical and structural parameters influencing their behaviour under dynamic loading conditions.

Throughout the project, regular in-situ dynamic measurements were conducted, complemented by detailed investigations at the stem, branch, and root levels. The methodology integrated high-resolution terrestrial laser scanning, three-dimensional geometry reconstruction, advanced numerical modelling, and both laboratory-based and field-based experimental techniques.

The results provided critical insights into non-linear and dynamic mechanical properties of wood, the influence of geometric fidelity of stem and branches on simulation accuracy, and the limitations and precision of laser-based geometry reconstruction. Most importantly, the project contributed to the understanding of tree dynamic response in frequency and time domains, including the tree’s reaction to pruning and the identification of key factors influencing dynamic behaviour.

Keywords: frequency, damping, modal analysis, tree biomechanics.

1. INTRODUCTION

Trees are a fundamental part of our environment; nevertheless, they grow in forests, open landscapes or in urban areas. As well as the economic value, which is mostly defined by sustainable timber production, there are also many other benefits (Pisani et al., 2022). Notably, the ecosystem services provided by trees may hold greater significance in urban settings (Turner-Skoff and Cavender, 2019). Together with the benefits trees bring also a risk caused by their potential failure, especially in frequently visited areas (van Haaften et al., 2021). The increasing intensity and frequency of windstorms, a phenomenon attributable in part to global warming, have also been demonstrated to contribute to an increase in tree failure, given the close interaction between wind and trees (Gardiner, 2021; Gardiner et al., 2016).

Though wind-tree dynamics have been studied for decades (Gardiner et al., 2016; James et al., 2014), a static approach with very simplified mechanical behaviour of a tree prevails (Dahle et al., 2017; Wessolly and Erb, 2016). Trees are structurally complex, heterogeneous cantilever beams influenced by mechanical and physiological drivers (Moulia, 2013; Niklas, 2007; Niklas and Speck, 2001; Read and Stokes, 2006). Their stability arises from the interaction between geometry, material properties, and loading conditions (Brudi and Wassenaer, 2002; Niklas and Spatz, 2012; Wessolly and Erb, 2016). In the context of mechanical analysis, stiffness, as an essential factor for overall stability, is determined by a tree’s geometry and material properties. However, because trees exist in a dynamic environment and respond to time-dependent loading, it is also necessary to consider inertial forces (related to mass) and damping effects (de Langre, 2008; James, 2003), which are particularly influenced by the crown morphology (Moore and Maguire, 2004a; Sellier and Fourcaud, 2009).

Several approaches have been proposed to describe the dynamic response of trees using mechanical models commonly applied in physics, such as pendulum or cantilever beam models. While these simplified representations can aid in the general understanding of tree behaviour, they often fall short in capturing the complexity introduced by tree architecture and crown morphology. Therefore, a

more detailed and nuanced analysis is necessary to accurately reflect the dynamic interactions within the tree structure.

Several approaches have been developed to describe the dynamic response of trees using mechanical models commonly applied in physics, such as pendulum or cantilever beam models (James et al., 2014; Moore and Maguire, 2004b). While these models are useful for gaining a general understanding of tree behaviour (Jackson et al., 2021), they often fail to capture the complexity introduced by tree architecture and crown morphology. As a result, detailed analyses are necessary to accurately reflect tree dynamics. Such analyses typically require advanced numerical methods, with the finite element method (FEM) being the most widely employed (Jackson et al., 2019b; Sellier et al., 2006).

In recent years, more sophisticated studies have emerged that integrate terrain data obtained through terrestrial laser scanning (TLS) with numerical modelling, significantly enhancing our understanding of tree behaviour (Wang et al., 2025; Zanotto et al., 2024a, 2024b). However, these studies remain limited in the number of trees and are often challenging to interpret due to their complexity.

To address these challenges and improve our understanding of the dynamic response of trees to loading, the DYNATREE project was initiated. A central pillar of the project was the development of several validated numerical models, which enabled extensive "what-if" analyses and contributed to a deeper understanding of tree behaviour. To achieve this goal, the project combined efforts in several key areas: the creation of detailed 3D models of trees and their components, mapping of internal defects, analysis of geometric precision, enhancement of material models, and extensive field measurements coupled with numerical validation.

2. MATERIALS AND METHODS

The project DYNATREE focused on describing how trees mechanically respond to loads, as support for tree assessment methods. The aim was to develop experimentally validated, comprehensive physical models of the dynamic response of trees in the frequency and time domains that fully incorporate the following relationships: 1) detailed geometry, 2) material, and 3) realistic loads (Fig. 1). The physical model played a crucial role in the rational definition of parameters influencing the mechanical response of the tree. The inputs of the model and its validation required laboratory experiments and *in-situ* testing. Therefore, work was divided into four interconnected sections covering: 1) Tree morphology, 2) Material properties, 3) Numerical simulations, and 4) *in-situ* testing.

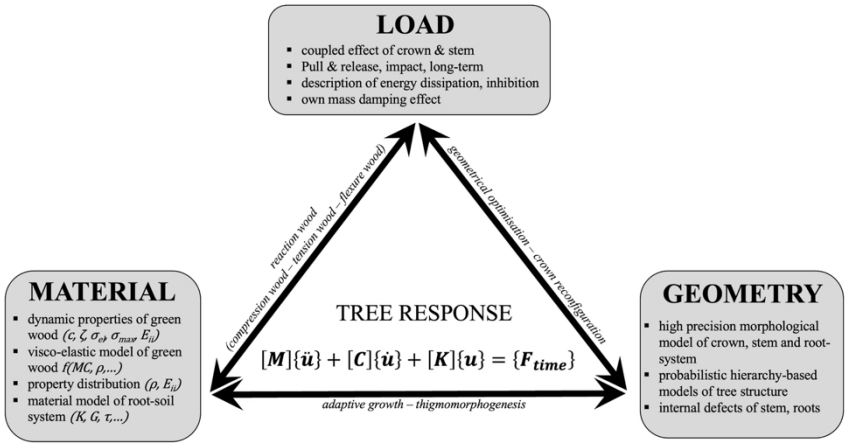

Figure 1. *Concept of interaction between three key aspects which influence the tree's mechanical response in the sense of an advanced dynamic approach.*

2.1. Tree morphology

To capture the external shape of trees and their parts, various laser scanning technologies were employed throughout the project, including 3D Structure Sensor, HandySCAN, LiDAR-equipped iPhones, and terrestrial laser scanners (TLS) from Riegl and Leica. Scanning focused on standing trees with continuous trunks, pronounced root bases, and complex senescent lime trees, where acoustic tomography and resistance drilling were also applied for mapping of internal shape influenced by decay.

TLS were used mainly for whole tree reconstruction by TreeQSM version: 2.4.0 (Åkerblom et al., 2015; Raumonen et al., 2015) in Matlab (R2022b, The MathWorks Inc.). Tree morphology was converted into 3D wireframe models of cylinders, with each cylinder defined by its start and end coordinates and diameter.

Simultaneously, the volumetric models of branches and stems were reconstructed for detailed analysis of geometry precision (Tippner et al., 2022). Scan accuracy was evaluated using MeshLab version 2020.07 and higher, and data processing workflows were standardised for different input types (point clouds, surface meshes), enabling successful import into FEA environments such as ANSYS (2020R2 and later, Ansys Mechanical Research licence, Ansys Inc.) and COMSOL Multiphysics (COMSOL AB, version 5.4 and later, Stockholm, Sweeden).

2.2. Material properties

The extensive mechanical testing was conducted on green wood of beech (*Fagus sylvatica* L.), linden (*Tilia cordata* Mill.), oak (*Quercus robur* L.), and pine (*Pinus sylvestris* L.) wood to determine basic elasticity and strength parameters. For beech and linden, validated elasto-plastic material models were developed. Data for oak and pine were fully evaluated, and material models were optimised. The creation of material models included: 1) sample preparation, 2) material testing of mechanical properties by tension, compression and shear tests in longitudinal, radial and tangential directions by a universal testing machine supplemented by optical measurement and Digital Image Correlation analysis (Fig. 2), 3) statistical evaluation of material properties, 4) optimization of gained 27 material constants to fulfil the computational conditions of FE software (ANSYS) (Fig. 3), and 5) optimization of these constants to obtain reasonable results of bending test. For a detailed description, see references Vand et al. (2025) and Zlámal et al. (2024).

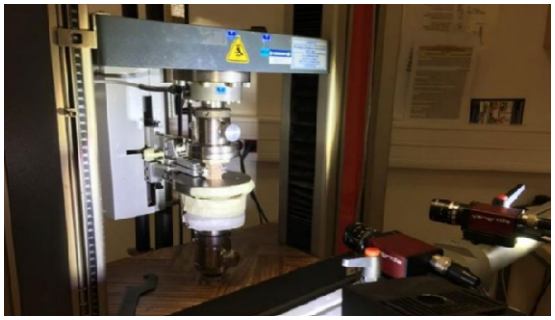

Figure 2. *Testing of mechanical properties in compression with DIC set of stereo cameras and lights (Zlámal et al. 2024).*

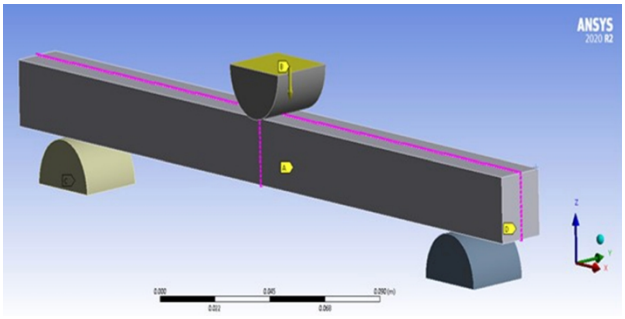

Figure 3. *Numerical model of bending test with boundary conditions (Ansys Mechanical Research licence, 2020R2, Ansys, inc., Vand et al. (2025).*

To validate the portability of properties to a bigger scale, the effect of sample size on the mechanical properties of beech, supporting upscaling to branch and trunk levels, was studied (Zlámal et al., 2025). This was followed by dynamic non-destructive and 3-point destructive bending tests of branches. Combined with 3D scans, these data were used as inputs for dynamic and static branch FE models.

Non-destructive dynamic testing by acoustic wave propagation in longitudinal and transverse directions was also used for field testing of standing trees to obtain elastic material properties. This method was applied as part of each *in-situ* testing.

To consider also the effect of decay, small beech and linden logs were inoculated with *Fomes fomentarius* and *Kretzschmaria deusta*, with weekly monitoring of mechanical properties (Cristini et

al., 2024, 2022). Followed by the experiment focused on the effects of *Ganoderma* spp. (*G. applanatum, G. resinaceum*) on beech wood, with evaluations at one- and two-month post-inoculation.

2.3. Numerical simulations

One of the main objectives of the project was to develop a comprehensive physical model describing the dynamic response of trees to loading. This involved creating and validating a series of numerical models, which were then used for sensitivity analyses.

Initial models featured simplified topologies, including 3D volume representations of stem and root-soil system interactions under static loading. The root-soil component was modelled as a composite, with segmented regions allowing for different material definitions (Vojáčková et al., 2021). This approach was extended to dynamic simulations and used to assess factors such as trunk pre-stress (e.g., from transpiration flow).

For dynamic analysis, also beam-based finite element (FE) models were developed using the parametric language of ANSYS (APDL, Ansys® Academic Research Mechanical, Release 18.1 and later). These models aimed to reconstruct realistic crown architecture while balancing structural accuracy with computational efficiency. The root–soil component was modelled as a composite with segmented sections, using shell elements to represent different materials. The above-ground part of the tree was modelled in three configurations: 1) a simple beam with the crown represented by point masses (Fig. 4a), 2) a complex crown based on field measurements of branch angles and lengths (Fig. 4b, Vojáčková et al., 2020; APDL code available at https://github.com/arborist-mendelu), and 3) a complex crown reconstructed from 3D scan-based wireframe models (Fig. 4c). The simple beam model with added mass, used for modal analysis, enabled a range of sensitivity studies. In contrast, the complex crown models provided more realistic behaviour in both time and frequency domains, capturing the influence of higher-order branches and generating multiple natural frequencies.

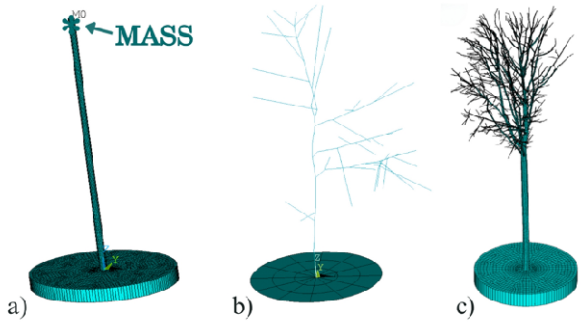

Figure 2. *Tree reconstruction by: a) simple beam and mass point, b) beams based on measured values, c) beams based on 3D scan.*

Partial work was also dedicated to investigating the effects of loading and geometric precision on higher-order branches and the stem. Higher-order branches were modelled using both volumetric scan-based geometry and simplified beam representations, under various loading scenarios (Vojáčková et al., 2023; APDL code available at https://github.com/arborist-mendelu). The next study published by Tippner et al., (2022) focused on the impact of geometric fidelity and material properties on the dynamic response of stems. The stems were modelled using three approaches: 1) beam elements, 2) volumetric primitives, 3) volumetric scan-based geometry. Both dynamic and static moduli of elasticity were applied, and the variations were analysed through modal analysis. The results were compared to assess the influence of the modelling approach and material definition on the dynamic behaviour of the stem.

2.4. In-situ testing

In-situ testing aimed to describe the tree’s response to loading based on measured data and to use this information for validating numerical models (see Numerical Simulations). Three types of measurements were conducted: 1) trees without damage under induced loading, 2) damaged trees under induced loading, 3) tree response under natural wind loading.

The first type involved repeated testing of trees on a reference plot consisting of 13 healthy beeches (*Fagus sylvatica* L.). Trees were tested using both static and dynamic methods, including pulling tests, pull–release tests, and impact excitation. These experiments supported hypotheses related to seasonal variation, climatic effects, pruning, measurement techniques, and changes in natural frequencies and mode shapes.

The second type focused on trees with defects (e.g., decay, large dead branches, complex stem shapes), mostly designated for felling, and was conducted on selected plots across East Bohemia. These tests explored the influence of structural defects and morphological changes on mechanical response.

The third type monitored tree behaviour under wind loading. Sensors were installed for extended periods (e.g., two weeks), including year-round monitoring of a mature beech equipped with anemometers and motion sensors.

Measured data included time-domain amplitude signals, frequency spectra, and damping characteristics. Multiple sensing methods were used: 1) strain and inclination sensors (TreeQinetic set, Fig. 5a), 2) triaxial accelerometers for acceleration (Fig. 5b), 3) optical systems for displacement and deformation via digital image correlation (DIC, Fig. 5c).

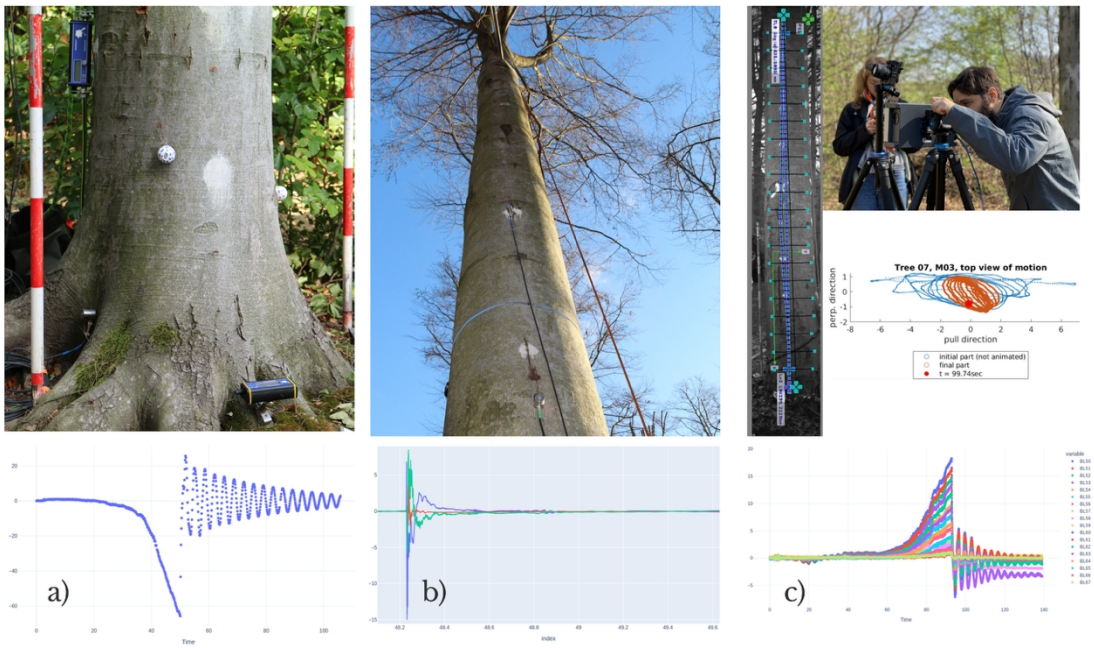

Figure 3. *Mechanical devices and time signal during pull & release test: a) strain and inclination sensors, b) triaxial accelerometer at four high levels, c) optical system (processing in DIC software, camera, displacement in two directions, and displacement along the whole stem in one direction).*

Accelerometers with high sampling rates (5 kHz) captured acceleration in three axes, enabling analysis of natural frequencies, damping, and elastic wave propagation along the trunk. Optical measurements provided displacement data, allowing evaluation of tensile deformation and oscillations perpendicular to the loading direction. Cameras placed parallel and perpendicular to the pull direction enabled reconstruction of bending curves and dynamic motion. This full setup was repeatedly used on the reference plot. For testing damaged trees, simplified setups were applied.

Data processing involved image analysis, data export from devices, format unification, and signal analysis. Several methods were tested for signal processing (Power Spectral Density – PSD, Fast Fourier Transformation – FFT, Tukey and Hanning windows) and damping analysis (amplitude interpolation, Hilbert and wavelet transforms, bandwidth-based methods, and logarithmic decrement). Due to low natural frequencies, short signal durations, and high damping, discrete FFT with a Tukey window proved most effective for spectral analysis. For damping evaluation, the logarithmic decrement method was selected. For static response evaluation, trunk and root system stiffness were obtained from the tangent between the bending moment and measured deformations, and inclinations.

To manage the large and complex dataset, the software tool DynaTree (https://github.com/arborist-mendelu) was developed. Data were converted to binary Parquet format for improved performance, and processing was orchestrated using Snakemake to ensure reproducibility and automation. Time correlation across sensors was performed using an automated algorithm with visual and numerical validation.

3. RESULTS AND DISCUSSION

From the perspective of material properties, the most significant outcomes were the development of optimised elasto-plastic material models for green wood, specifically for beech (Zlámal et al., 2024) and lime (Vand et al., 2025). Although considerable research has already been conducted on the material properties of green wood (Madhoushi and Boskabadi, 2019; Niklas and Spatz, 2010) and elasto-plastic finite element (FE) material models (Milch et al., 2017, 2016; Šebek et al., 2021; Tabiei and Wu, 2000), a comprehensive material model for green wood was still missing. Both studies presented results for 27 measured constants and their optimised values for FE simulations. Zlámal et al. (2024) found no correlation between strength and elastic response in the FE model, nor between elastic modulus and the applied force required to achieve an 8 mm beam deflection. Vand et al. (2025) additionally compared the elasto-plastic properties of lime at two moisture content levels: 40% and 60%.

A secondary objective of the project was to investigate the mechanical properties of decayed wood. Cristini et al., (2024) identified differences in the degradation of mechanical properties between beech and lime, which were also dependent on the fungal species involved (*Fomes fomentarius* and *Kretzschmaria deusta*). A significant difference between these fungi was observed in beech wood, but not in lime. *K. deusta* caused more severe degradation in lime compared to beech, whereas *F. fomentarius* led to greater degradation in beech. These findings are of practical importance, as both fungal species are commonly associated with increased risk of tree failure in urban environments.

Studies focusing on the influence of geometric fidelity in FE modelling revealed that, for stems, scan-based solid models yielded the most reliable results, particularly regarding bending mode frequencies (Tippner et al., 2022). However, for higher-order branches, scan-based geometry did not significantly improve deflection accuracy compared to beam-based models. The reconstruction of smaller branches was affected by the initial scan resolution and subsequent adjustments required for FE software import. The study also demonstrated that single-point loading, commonly used to assess tree stability (Krišāns et al., 2022; Peltola, 2006; Szoradova et al., 2013; Vojáčková et al., 2021), produced a different deflection curve, potentially leading to misinterpretations in advanced risk assessments.

A key component of the research was the numerical and experimental investigation of tree dynamic response. One of the initial steps involved evaluating measurement methodologies and model creation approaches. Vojáčková et al. (2020) in a case study confirmed the suitability of three-axis piezoelectric accelerometers, which provided more precise measurements than vibrometers at higher frequencies. In terms of numerical modelling, the use of beam elements for tree structures combined with shell elements for the root plate was validated. Sensitivity analyses highlighted the critical role of elastic modulus in anchorage stiffness, underscoring the necessity of stepwise validation – beginning with static and followed by dynamic analysis. The importance of conducting all three types of numerical analysis (modal, harmonic, and transient) was also confirmed. Given the large number of modes generated in the modal analysis of complex tree structures (Li et al., 2022; Rodriguez et al., 2012), harmonic analysis is essential to identify the most relevant ones (Fig. 6).

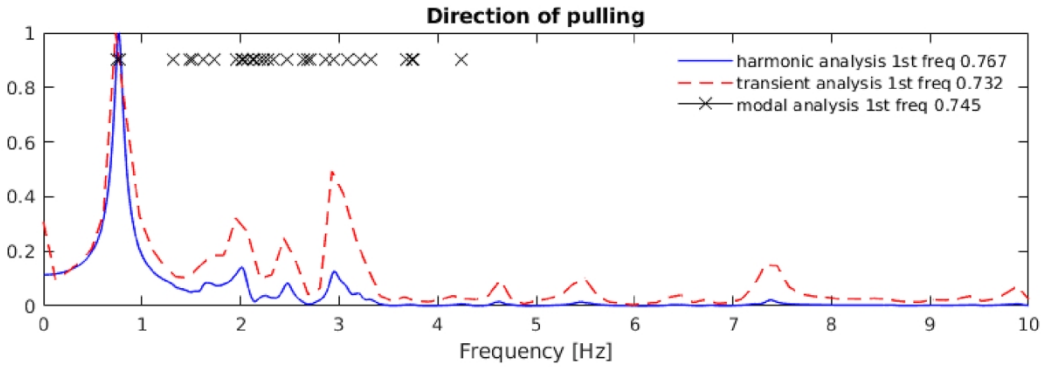

***Figure 4**. Frequency spectrum obtained from modal, harmonic and transient numerical analysis of a tree (Vojáčková et al. 2020).*

Further sensitivity analyses revealed the significance of slenderness (r[1]: 0.75) and centre of gravity (r: -0.8) in determining the first natural frequency of tree structures. Stem stiffness (r: 0.18) and root-plate stiffness (r: 0.57) were also found to be influential, albeit to a lesser extent, aligning with findings from other studies (Jackson et al., 2019b; Yang et al., 2020; Zanotto et al., 2024a). These correlations were further validated through observations of 13 beech trees regularly monitored on a reference plot. Despite the limited sample size, the most significant parameters included slenderness (calculated from centre of gravity and stem base diameter; s[2]: 0.43), mass (s: 0.38), root stiffness (s: 0.51, 0.57), and stem stiffness (s: 0.21).

The relationship between the first natural frequency and combined parameters (models) was also tested, following approaches published by Jackson et al. (2019a) and Moore and Maguire (2004b). Contrary to these studies, for the measured beeches, no significant correlation was found for the pendulum model $\sqrt{1/H}$ or the optimised cantilever beam model DBH/H^2. The strongest correlation (s: 0.47) was observed for the model based on the standard calculation of natural frequency $model\ 3 = \sqrt{EI/m}$.

Two hypotheses regarding crown modification were tested. The first focused on changes in crown architecture through the gradual removal of higher-order branches. Numerical simulations confirmed that such architectural changes significantly affect the tree's dynamic response, consistent with previous findings (James, 2014a; Moore and Maguire, 2004a; Sellier and Fourcaud, 2009). These changes were evident in the frequency spectrum, which became simpler as the number of branches decreased (Fig. 7).

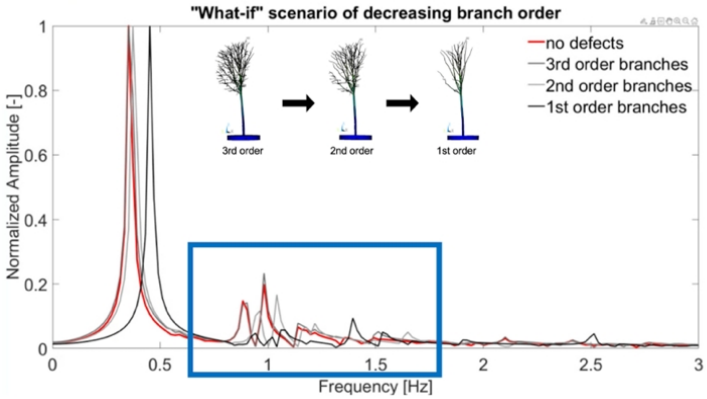

***Figure 5.** Change of frequency spectrum based on removing the higher-order branches.*

The second hypothesis examined peripheral crown reduction (Fig. 8a), which alters crown mass and centre of gravity. This was tested on six beech trees pruned in two successive steps. Results showed that even a 20% reduction affected the first natural frequency, more than seasonal leaf changes

[1] r... Pearson correlation coefficient, α = 0.95
[2] s...Spearman correlation coefficient, α = 0.95

(Fig. 8b). Previous studies have demonstrated the effects of leaves (Bunce et al., 2019), and (Burcham, 2020; Kane, 2018) on natural frequency independently. In correspondence to our observation, Burcham et al. (2020) recommend limiting pruning to small amounts (up to 20%) due to its impact on dynamic response. This finding is particularly relevant for practitioners, as static approaches are commonly used. This means that a more pruned crown is often associated with greater stability due to reduced load area. The same trees were pruned again the following year by an additional 20%, which further increased the first natural frequency, confirming the negative impact of peripheral pruning on mechanical response. Consistent with other studies (James, 2014b; Jonsson et al., 2007; Kane, 2018), damping values were highly variable, with no clear trend observed.

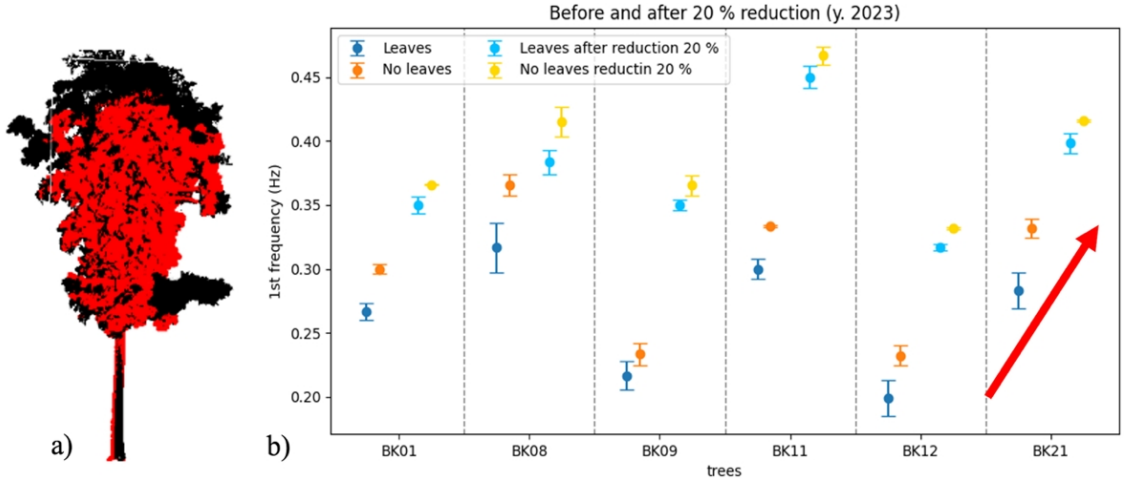

Figure 6. *Change of first natural frequency after crown reduction: a) tree before (black) and after (red) reduction, b) frequency of trees in leaf-on/leaf-off state, and before/after reduction.*

One of the key outputs of the project is the software tool **DynaTree** (https://github.com/arborist-mendelu), which enables efficient data access, processing, and visualisation via a web interface built on the Solara framework. It supports signal visualisation, synchronisation, spectral and damping analysis, and static test evaluation. Summary reports can be generated at various levels (from individual trees to entire datasets), facilitating comprehensive analysis across all measurements. This tool will be used in future research for more advanced analyses of tree dynamic response.

4. CONCLUSION

Among the key findings, the elasto-plastic material characteristics of beech (*Fagus sylvatica* L.) and lime (*Tilia cordata* Mill.) were thoroughly investigated and optimised for use in numerical simulations. It was demonstrated that, in modelling tree behaviour, the precision of stem geometry significantly affects simulation outcomes, whereas higher-order branches can be simplified without substantial loss of accuracy (an insight that enhances computational efficiency).

In terms of tree dynamics, several parameters were identified as significantly influencing the first natural frequency: slenderness, centre of gravity, mass, stem stiffness, and root-plate stiffness. However, the most promising approach appears to be the application of a combined model based on the physical equation $\sqrt{EI/m}$, which integrates both geometric and material properties.

Furthermore, the study confirmed that peripheral crown pruning substantially alters the first natural frequency, more so than seasonal leaf loss. Changes in crown architecture also led to notable shifts in the frequency spectrum. These findings have important implications for arboricultural practice, where pruning is a commonly applied intervention. The mechanical consequences of pruning should be carefully considered, especially in dynamic assessments, to avoid unintended impacts on tree stability.

ACKNOWLEDGEMENT

The work was funded by the Ministry of Education, Youth and Sports in the Czech Republic, project no. LL1909, ERC CZ.

REFERENCES

1. Åkerblom, M., Raumonen, P., Kaasalainen, M., Casella, E. (2015): Analysis of geometric primitives in quantitative structure models of tree stems. Remote Sens (Basel) 7, 4581–4603. https://doi.org/10.3390/rs70404581
2. Brudi, E., Wassenaer, P. Van. (2002): Trees and Statics: Non-Destructive Failure Analysis, in: Smiley, E.T., Coder, K.D. (Eds.), How Trees Stand up and Fall Down Proceedings of the Tree Structure and Mechanics Conference. International Society of Arboriculture, Savannah, pp. 53–70.
3. Bunce, A., Volin, J.C., Miller, D.R., Parent, J., Rudnicki, M. (2019): Determinants of tree sway frequency in temperate deciduous forests of the Northeast United States. Agric For Meteorol 266–267, 87–96. https://doi.org/10.1016/j.agrformet.2018.11.020
4. Burcham, D.C. (2020): The effect of pruning treatments on the vibration properties and wind-induced bending moments of Senegal mahogany (Khaya senegalensis) and rain tree (Samanea saman) in Singapore.
5. Burcham, D.C., Autio, W.R., James, K., Modarres-Sadeghi, Y., Kane, B. (2020):. Effect of pruning type and severity on vibration properties and mass of Senegal mahogany (Khaya senegalensis) and rain tree (Samanea saman). Trees - Structure and Function 34, 213–228. https://doi.org/10.1007/s00468-019-01912-8
6. Cristini, V., Nop, P., Zlámal, J., Tippner, J. (2024): Incipient decay in beech (Fagus sylvatica L.) and linden (Tilia cordata Mill.): An interspecific static and dynamic material analysis. For Ecol Manage 566. https://doi.org/10.1016/j.foreco.2024.122101
7. Cristini, V., Tippner, J., Nop, P., Zlámal, J., Hassan Vand, M., Šeda, V. (2022): Degradation of beech wood by Kretzschmaria deusta: Its heterogeneity and influence on dynamic and static bending properties. Holzforschung 76, 813–824. https://doi.org/10.1515/hf-2022-0039
8. Dahle, G.A., James, K.R., Kane, B., Grabosky, J.C., Detter, A. (2017). A review of factors that affect the static load-bearing capacity of urban trees. Arboric Urban For 43.
9. de Langre, E. (2008): Effects of Wind on Plants. Annu Rev Fluid Mech 40, 141–168. https://doi.org/10.1146/annurev.fluid.40.111406.102135
10.Gardiner, B. (2021): Wind damage to forests and trees: a review with an emphasis on planted and managed forests. Journal of Forest Research 1–19. https://doi.org/10.1080/13416979.2021.1940665
11.Gardiner, B., Berry, P., Moulia, B. (2016):. Review: Wind impacts on plant growth, mechanics and damage. Plant Science. https://doi.org/10.1016/j.plantsci.2016.01.006
12.Jackson, T., Shenkin, A., Moore, J., Bunce, A., Van Emmerik, T., Kane, B., Burcham, D., James, K., Selker, J., Calders, K., Origo, N., Disney, M., Burt, A., Wilkes, P., Raumonen, P., Gonzalez De Tanago Menaca, J., Lau, A., Herold, M., Goodman, R.C., Fourcaud, T., Malhi, Y. (2019a):. An architectural understanding of natural sway frequencies in trees. J R Soc Interface 16. https://doi.org/10.1098/rsif.2019.0116
13.Jackson, T., Shenkin, A., Wellpott, A., Calders, K., Origo, N., Disney, M., Burt, A., Raumonen, P., Gardiner, B., Herold, M., Fourcaud, T., Malhi, Y. (2019b): Finite element analysis of trees in the wind based on terrestrial laser scanning data. Agric For Meteorol 265, 137–144. https://doi.org/10.1016/j.agrformet.2018.11.014
14.Jackson, T.D., Sethi, S., Dellwik, E., Angelou, N., Bunce, A., Van Emmerik, T., Duperat, M., Ruel, J.C., Wellpott, A., Van Bloem, S., Achim, A., Kane, B., Ciruzzi, D.M., Loheide, S.P., James, K., Burcham, D., Moore, J., Schindler, D., Kolbe, S., Wiegmann, K., Rudnicki, M., Lieffers, V.J., Selker, J., Gougherty, A. V., Newson, T., Koeser, A., Miesbauer, J., Samelson, R., Wagner, J., Ambrose, A.R., Detter, A., Rust, S., Coomes, D., Gardiner, B. (2021): The motion of trees in the wind: A data synthesis. Biogeosciences 18, 4059–4072. https://doi.org/10.5194/bg-18-4059-2021

15.James, K. (2014a): A study of branch dynamics on an open-grown tree. Arboric Urban For 40, 125–134.
16.James, K. (2014b): A Dynamic Structural Analysis of Trees Subject to Wind Loading. Doctoral Thesis.
17.James, K. (2003): Dynamic loading of trees 29, 165–171.
18.James, K.R., Dahle, G.A., Grabosky, J., Kane, B., Detter, A. (2014): Tree biomechanics literature review: Dynamics. Arboric Urban For 40, 1–15.
19.Jonsson, M.J., Foetzki, A., Kalberer, M., Lundström, T., Ammann, W., Stöckli, V. (2007): Natural frequencies and damping ratios of Norway spruce (Picea abies (L.) Karst) growing on subalpine forested slopes. Trees - Structure and Function 21, 541–548. https://doi.org/10.1007/s00468-007-0147-x
20.Kane, B. (2018): The effect of simulated trunk splits, pruning, and cabling on sways of quercus rubra L. Trees 32, 985–1000. https://doi.org/10.1007/s00468-018-1690-3
21.Krišāns, O., Čakša, L., Matisons, R., Rust, S., Elferts, D., Seipulis, A., Jansons, Ā. (2022): A Static Pulling Test Is a Suitable Method for Comparison of the Loading Resistance of Silver Birch (Betula pendula Roth.) between Urban and Peri-Urban Forests. Forests 13. https://doi.org/10.3390/f13010127
22.Li, Z., Hao, Y., Kopp, G.A., Wu, C.H. (2022): Identification of Multimodal Dynamic Characteristics of a Decurrent Tree with Application to a Model-Scale Wind Tunnel Study. Applied Sciences (Switzerland) 12. https://doi.org/10.3390/app12157432
23.Madhoushi, M., Boskabadi, Z. (2019): Relationship between the dynamic and static modulus of elasticity in standing trees and sawn lumbers of Paulownia fortune planted in Iran. Maderas: Ciencia y Tecnologia 21, 35–44. https://doi.org/10.4067/S0718-221X2019005000104
24.Milch, J., Brabec, M., Sebera, V., Tippner, J. (2017): Verification of the elastic material characteristics of Norway spruce and European beech in the field of shear behaviour by means of digital image correlation (DiC) for finite element analysis (FEA). Holzforschung 71, 405–414. https://doi.org/10.1515/hf-2016-0170
25.Milch, J., Tippner, J., Sebera, V., Brabec, M. (2016): Determination of the elasto-plastic material characteristics of Norway spruce and European beech wood by experimental and numerical analyses. Holzforschung 70, 1081–1092. https://doi.org/10.1515/hf-2015-0267
26.Moore, J.R., Maguire, D.A. (2004a): Natural sway frequencies and damping ratios of trees: Influence of crown structure. Trees - Structure and Function 18, 195–203. https://doi.org/10.1007/s00468-003-0295-6
27.Moore, J.R., Maguire, D.A. (2004b): Natural sway frequencies and damping ratios of trees: Concepts, review and synthesis of previous studies. Trees - Structure and Function. https://doi.org/10.1007/s00468-003-0295-6
28.Niklas, K.J. (2007): Maximum plant height and the biophysical factors that limit it. Tree Physiol 27, 433–440. https://doi.org/10.1093/treephys/27.3.433
29.Niklas, K.J., Spatz, H.C. (2010): Worldwide correlations of mechanical properties and green wood density. Am J Bot 97, 1587–1594. https://doi.org/10.3732/ajb.1000150
30.Niklas, K.J., Spatz, H.CH. (2012): Plant Physics. University of Chicago Press, Chicago.
31.Niklas, K.J., Speck, T., 2001. Evolutionary trends in safety factors against wind-induced stem failure. Am J Bot 88, 1266–1278. https://doi.org/10.2307/3558338
32.Peltola, H.M. (2006): Mechanical stability of trees under static loads. Am J Bot 93, 1501–1511. https://doi.org/10.3732/ajb.93.10.1501
33.Pisani, D., De Lucia, C., Pazienza, P. (2022): On the investigation of an economic value for forest ecosystem services in the past 30 years: Lessons learnt and future insights from a North–South perspective. Frontiers in Forests and Global Change 5. https://doi.org/10.3389/FFGC.2022.798976/FULL
34.Raumonen, P., Casella, E., Calders, K., Murphy, S., Åkerblom, M., Kaasalainen, M. (2015): Massive-scale tree modelling from TLS data, in: ISPRS Annals of the Photogrammetry, Remote Sensing and Spatial Information Sciences. Copernicus GmbH, pp. 189–196. https://doi.org/10.5194/isprsannals-II-3-W4-189-2015
35.Rodriguez, M., Ploquin, S., Moulia, B., Langre, E. De (2012): The Multimodal Dynamics of a Walnut Tree : Experiments and Models To cite this version. J Appl Mech 79.

36.Šebek, F., Kubík, P., Tippner, J., Brabec, M. (2021): Orthotropic elastic–plastic–damage model of beech wood based on split Hopkinson pressure and tensile bar experiments. Int J Impact Eng 157. https://doi.org/10.1016/j.ijimpeng.2021.103975
37.Sellier, D., Fourcaud, T. (2009): Crown structure and wood properties: Influence on tree sway and response to high winds. Am J Bot 96, 885–896. https://doi.org/10.3732/ajb.0800226
38.Sellier, D., Fourcaud, T., Lac, P. (2006): A finite element model for investigating effects of aerial architecture on tree oscillations. Tree Physiol 26, 799–806. https://doi.org/10.1093/treephys/26.6.799
39.Szoradova, a., Praus, L., Kolarik, J. (2013): Evaluation of the root system resistance against failure of urban trees using principal component analysis. Biosyst Eng 115, 244–249. https://doi.org/10.1016/j.biosystemseng.2013.03.001
40.Tabiei, A., Wu, J. (2000): Three-dimensional nonlinear orthotropic finite element material model for wood. Compos Struct 50, 143–149. https://doi.org/10.1016/S0263-8223(00)00089-1
41.Tippner, J., Vojáčková, B., Zlámal, J., KolařÍk, J., Paulic, V., Group, F., Tippner, J., Zlámal, J. (2022): The role of geometry precision in frequency- resonance method for non-destructive wood assessment – numerical case study on sugar maple destructive wood assessment – numerical case study on sugar maple. Wood Mater Sci Eng 1–9. https://doi.org/10.1080/17480272.2022.2071166
42.Turner-Skoff, J.B., Cavender, N. (2019): The benefits of trees for livable and sustainable communities. Plants People Planet 1, 323–335. https://doi.org/10.1002/ppp3.39
43.van Haaften, M., Liu, Y., Wang, Y., Zhang, Y., Gardebroek, C., Heijman, W., Meuwissen, M. (2021): Understanding tree failure-A systematic review and meta-analysis. PLoS One 16. https://doi.org/10.1371/journal.pone.0246805
44.Vand, H.M., Nop, P., Cristini, V., Zlámal, J., Šeda, V., Tippner, J. (2025): An investigation of mechanical properties of linden green wood. Holzforschung 79, 214–227. https://doi.org/10.1515/hf-2024-0110
45.Vojáčková, B., Tippner, J., Horáček, P., Sebera, V., Praus, L., Mařík, R., Brabec, M. (2021): The effect of stem and root-plate defects on the tree response during static loading—Numerical analysis. Urban For Urban Green 59, 1–13. https://doi.org/10.1016/j.ufug.2021.127002
46.Vojáčková, B., Tippner, J., Mařík, R., Vand, M.H., Constant, T., Dlouhá, J. (2023): Effect of Geometry Precision and Load Distribution on Branch Mechanical Response. Forests 14, 19. https://doi.org/https://doi.org/10.3390/f14050930
47.Vojáčková, B., Tippner, J., Nop, P. (2020): Dynamic Mechanical Response of Beech (Fagus sylvatica L .) - Numerical Analysis, in: Neméth, R., Rademacher, P., Hansman, C., Bak, M., Báder, M. (Eds.), 9th Hardwood Conference 2020 Proceedings, Part I. UNIVERSITY OF SOPRON PRESS, pp. 291–298.
48.Wang, X., Mann, J., Dellwik, E., Angelou, N. (2025): Aerodynamic Admittance and Dynamics of an Open-Grown Tree.
49.Wessolly, L., Erb, M. (2016): Manual of Tree Statics and Tree Inspection, 1st ed. Patzer Verlag, Berlin-Hanover.
50.Yang, M., Défossez, P., Dupont, S. (2020): A root-to-foliage tree dynamic model for gusty winds during windstorm conditions. Agric For Meteorol 287, 107949. https://doi.org/10.1016/j.agrformet.2020.107949
51.Zanotto, F., Grigolato, S., Schindler, D., Marchi, L. (2024a): Identifying wind-tree dynamics with numerical simulations based on experimental modal analysis. For Ecol Manage 569. https://doi.org/10.1016/j.foreco.2024.122188
52.Zanotto, F., Marchi, L., Grigolato, S. (2024b): Wind-tree interaction: Technologies, measurement systems for tree motion studies and future trends. Biosyst Eng 237, 128–141. https://doi.org/10.1016/j.biosystemseng.2023.12.005
53.Zlámal, J., Cristini, V., Nop, P., Šeda, V., Vand, M.H., Tippner, J. (2025): Effect of size on the dynamic and static bending of green wood samples of European beech. International Wood Products Journal 16, 37–47. https://doi.org/10.1177/20426445241312750
54.Zlámal, J., Mařík, R., Vojáčková, B., Cristini, V., Brabec, M., Praus, L., Tippner, J. (2024): Elasto-plastic material model of green beech wood. Journal of Wood Science 70. https://doi.org/10.1186/s10086-024-02140-6

IMPACT OF FEED RATE ON ENERGY CONSUMPTION DURING CUTTING DRY BEECH AND SPRUCE WOOD WITH A CIRCULAR SAW

Anastasija Temelkova[1], Zoran Trposki[1], Vladimir Koljozov[1], Damjan Stanojević[2]

[1] Ss. Cyril and Methodius University in Skopje,
Faculty of Design and Technologies of Furniture and Interior-Skopje
[2] Academy of Technical-Educational Vocational Studies Niš - Vranje Department
email: temelkova@gmail.com; trposki@fdtme.ukim.edu.mk; koljozov@fdtme.ukim.edu.mk; damjan.stanojevic@akademijanis.edu.rs

ABSTRACT

In industrial production, the primary goal is achieving the desired end result; however, it is equally important to ensure that the entire technological process is carried out as cost-effectively as possible. Several key factors influence this efficiency, including the material and geometry of the cutting tool, the properties of the processed wood, and the feed rate. Among these, the feed rate during mechanical wood processing has a particularly strong impact on energy consumption.

This paper focuses on the relationship between feed rate and energy consumption during the cutting process of dry beech and spruce wood using a circular saw. The objective is to identify optimal cutting conditions that minimize energy usage. Three different feed rates were tested: U_1 = 12 m·min $^{-1}$, U_2 = 16 m·min $^{-1}$, and U_3 = 20 m·min $^{-1}$, at a constant cutting height of 15 mm. The tested wood samples (beech and spruce) had a moisture content of W = 10 ± 1%. The experiments were conducted using a circular saw with a cutting tool diameter of D = 250 mm, 40 teeth (Z = 40), and a kerf width of b = 3.2 mm. The number od rounds was n = 5500 min $^{-1}$.

Energy consumption was measured using a clamp ammeter. The results demonstrated a clear, directly proportional relationship between the feed rate and energy consumption.

Keywords: beech wood, spruce wood, circular saw, energy consumption, feed rate.

1. INTRODUCTION

The use of circular saws in the wood industry is widespread. In industrial production, the desired end result is naturally most important, but it is also of special importance that the entire technological process of wood processing be performed with the lowest possible costs. Many different influencing factors determine energy consumption. These include: the material being processed, the material from which the tool is manufactured, tool geometry, the speed of the main motion, the feed speed, and so forth (Stanojević & Stefanović, 2014).

When circular saws of equal diameter and equal peripheral cutting speed are used, the number of teeth actively participating in the cutting process at any instant differs. This has a significant influence on the chip thickness as well as on the loading of the teeth, especially on the rear surface of the cutting edge (Paralidov et al., 2015). In the wood cutting process, cutting force and cutting power are the principal output parameters. Secondary parameters include chip length, chip thickness, feed per tooth, tooth pitch, average kinematic cutting angle, cutting speed, average pressure on the rake face, and the apparent specific pressure on the flank side (Koljozov et al., 2019). The feed speed during mechanical processing of wood is one of the factors that strongly affects energy consumption. A comprehensive insight of the cutting process substantially impacts improved surface quality, machining accuracy, economy, and productivity (Stanojević, 2023).

2. RESEARCH OBJECTIVES

The objective of this research is to determine the dependence of feed speed on energy consumption for beech and spruce during sawing of dry wood with a circular saw, with the intention of defining optimal cutting conditions that minimize energy consumption.

3. MATERIAL AND METHODS

3.1. Material

For the purpose of testing, sawn lumber of beech (*Fagus sylvatica* L.) and fir/spruce (*Picea abies* Karst., *Abies alba*) free of defects was used, with dimensions 1500 × 150 × 15 mm. All sawn lumber was kiln-dried and conditioned. The measured average moisture content of the beech was 9.32 %, and for the spruce was 10.26 %. From the planks, specimens were cut with a constant cutting height of 15 mm.

3.2. Experimental methods

Tests on the specimens were conducted on a format circular saw machine type NIKOLAIDIS TEMA 3800. Three different feed speeds were applied whilst conducting this research: U_1 = 12 m·min $^{-1}$, U_2 = 16 m·min $^{-1}$, and U_3 = 20 m·min $^{-1}$. Measurements were performed with a circular saw of diameter D = 250 mm, number of teeth Z = 40, and kerf width b = 3.2 mm (Figure 1). The spindle rotational speed was n = 5500 min $^{-1}$. The cutting length for each specimen was 1.2 m.

Figure 1. *Circular saw with diameter D = 250 mm, number of teeth Z = 40 and kerf width b = 3.2 mm.*

The measurement of current intensity was performed using a voltage/current clamp (type MASTECH MS 2008B) for each specimen over a length of 1.0 m. The total number of measurements was 50 (Figure 2).

Figure 2. *Voltage/current clamp type MASTECH MS 2008B.*

4. RESULTS AND DISCUSSION

4.1. Measured current intensity values for the beech specimens

Table 1. *Results of the current intensity measurements for beech specimens at various feed speeds (U_1 = 12 m·min^{-1}, U_2 = 16 m·min^{-1}, U_3 = 20 m·min^{-1}).*

Feed speed (U) for number of teeth Z = 40 and diameter D = 250 mm					
U_1 = 12 m·min^{-1}		U_2 = 16 m·min^{-1}		U_3 = 20 m·min^{-1}	
Cutting height [mm]		Cutting height [mm]		Cutting height [mm]	
h = 15mm		h = 15mm		h = 15mm	
Current intensity	[A]	Current intensity	[A]	Current intensity	[A]
Mean value	4.057	Mean value	4.224	Mean value	4.565
Standard deviation	0.2724	Standard deviation	0.2898	Standard deviation	0.3100
Coefficient of variation	6.72	Coefficient of variation	6.86	Coefficient of variation	6.79
Minimum	3.697	Minimum	3.840	Minimum	4.160
Maximum	4.600	Maximum	4.800	Maximum	5.200

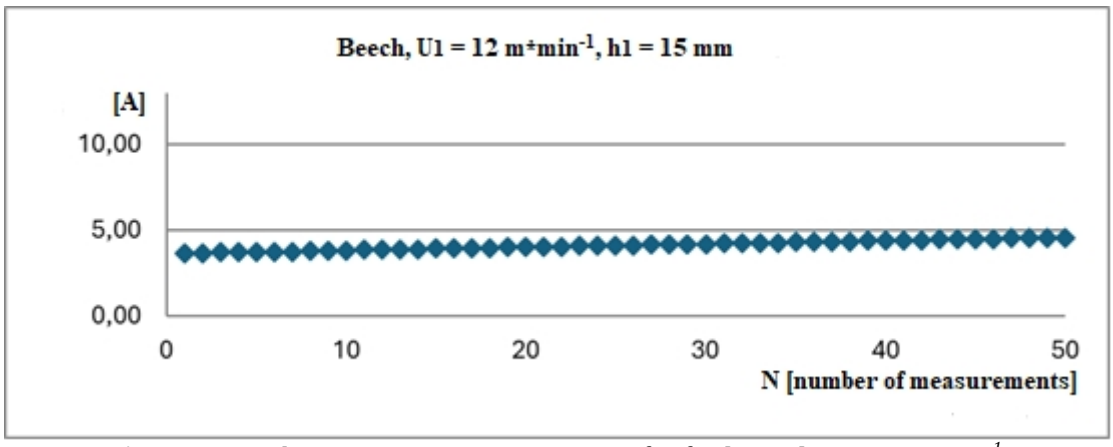

Figure 3. *Beech specimens' current intensity for feed speed U_1 = 12 m·min^{-1}.*

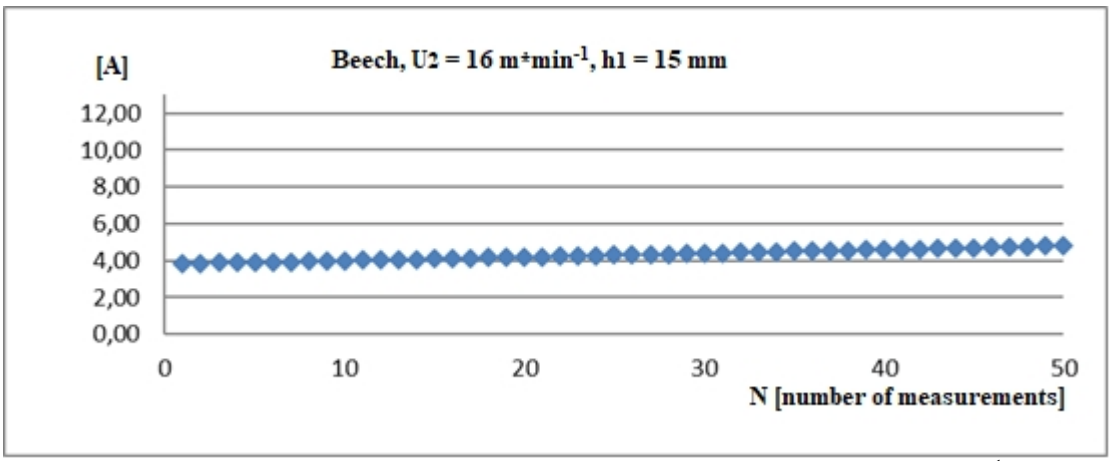

Figure 4. *Beech specimens' current intensity for feed speed U_2 = 16 m·min^{-1}.*

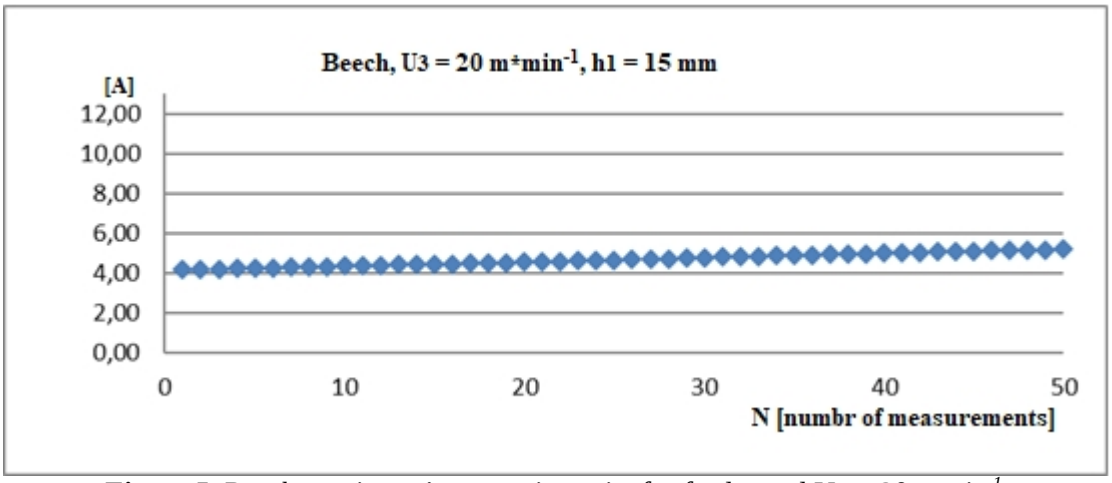

Figure 5. *Beech specimens' current intensity for feed speed U_3 = 20 m·min^{-1}.*

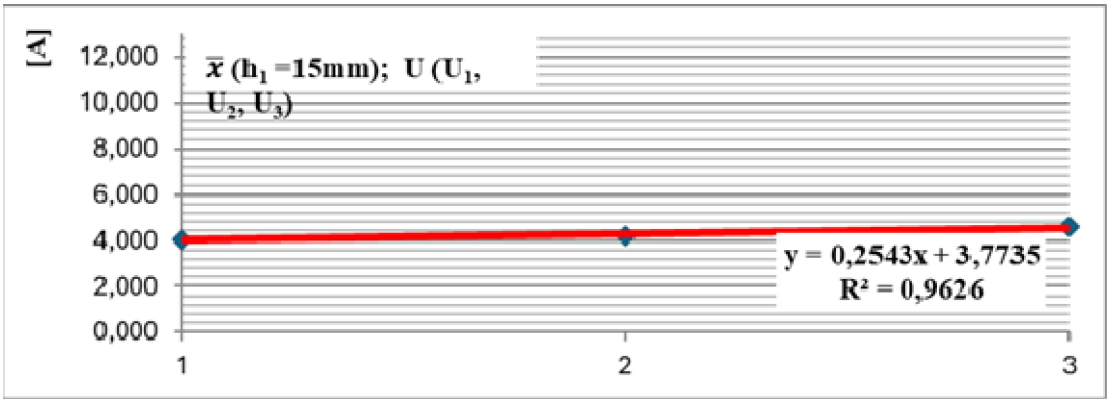

Figure 6. *Regression analysis for mean values of the beech specimens' current intensity with all three feed speeds (U_1=12m·min-1, U_2=16m·min^{-1} and U_3=20m·min^{-1}).*

The measurements indicate a gradual increase in the flow of electric current in all analyzed cases. This observation is can clearly be observed in Figures 3,4, and 5. The mean values from the measurements show an increase corresponding to the increase in feed speed.

Regression analysis of the mean values from the measurements at the different feed speeds (U_1, U_2, and U_3) shows that their dependence is best fitted by the linear equation y = 0.2543x + 3.7735, with a high coefficient of determination R^2 = 0.9626 (Figure 6).

4.2. Measured current intensity values for the spruce specimens

Table 1. *Results of the current intensity measurements for fir/spruce specimens at various feed speeds (U_1 = 12 m·min^{-1}, U_2 = 16 m·min^{-1}, U_3 = 20 m·min^{-1}).*

Feed speed (U) for number of teeth Z = 40 and diameter D = 250 mm					
U_1 = 12 m·min^{-1}		U_2 = 16 m·min^{-1}		U_3 = 20 m·min^{-1}	
Cutting height [mm]		Cutting height [mm]		Cutting height [mm]	
h = 15mm		h = 15mm		h = 15mm	
Current intensity	[A]	Current intensity	[A]	Current intensity	[A]
Mean value	3.638	Mean value	3.974	Mean value	4.051
Standard deviation	0.2485	Standard deviation	0.2730	Standard deviation	0.2727
Coefficient of variation	6.83	Coefficient of variation	6.80	Coefficient of variation	6.73
Minimum	3.300	Minimum	3.600	Minimum	3.680
Maximum	4.130	Maximum	4.504	Maximum	4.602

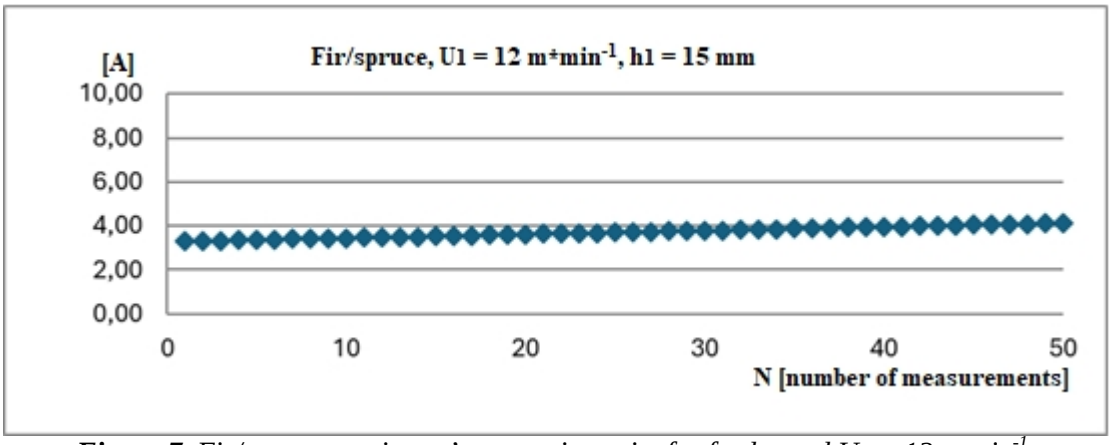

Figure 7. *Fir/spruce specimens' current intensity for feed speed U_1 = 12 m·min^{-1}.*

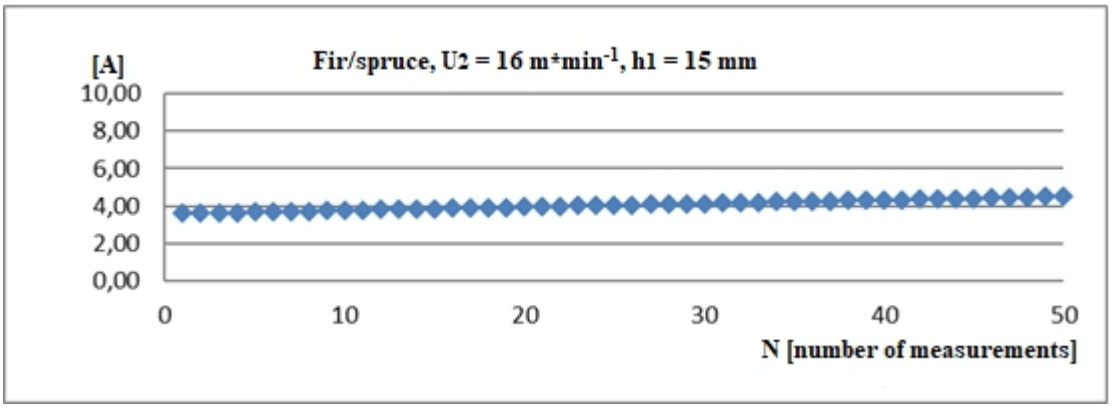

Figure 8. *Fir/spruce specimens' current intensity for feed speed U_2 = 16 m·min^{-1}.*

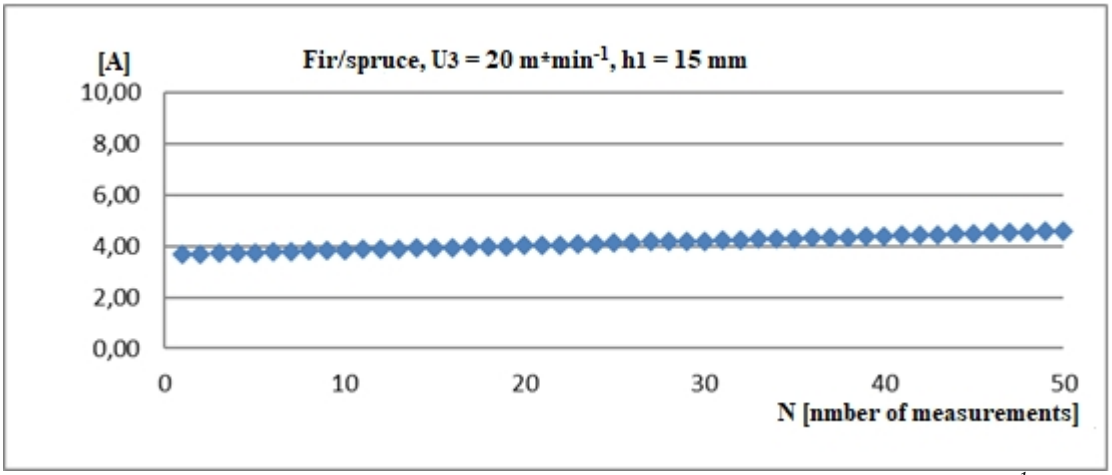

Figure 9. *Fir/spruce specimens' current intensity for feed speed U_2 = 20 m·min^{-1}.*

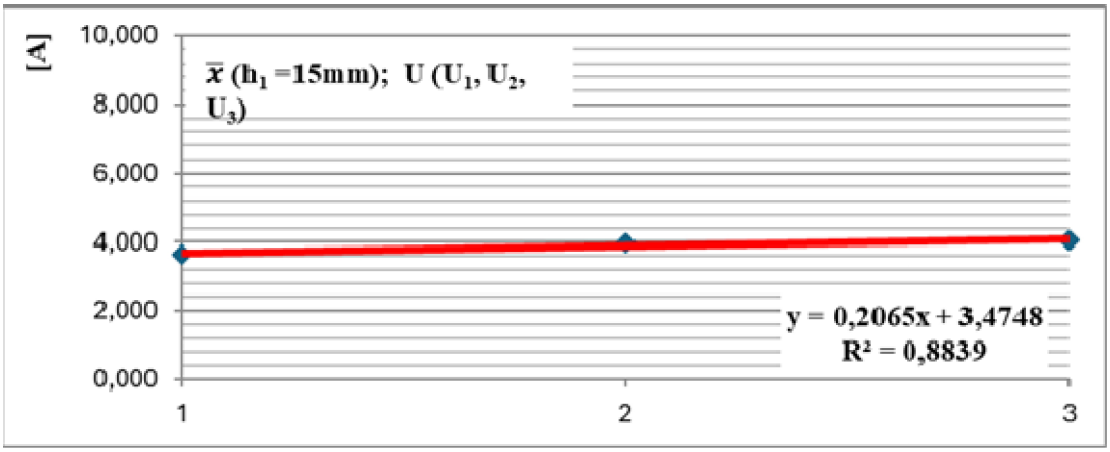

Figure 10. *Regression analysis for mean values of the fir/spruce specimens' current intensity with all three feed speeds (U_1=12m·min-1, U_2=16m·min^{-1} and U_3=20m·min^{-1}).*

The measurements indicate a gradual increase in the flow of electric current in all analyzed cases. This observation is clearly illustrated in Figures 7, 8, and 9. The mean values from the measurements show an increase corresponding to the increase in feed speed.

Regression analysis of the mean values from the measurements at the different feed speeds (U_1, U_2, and U_3) shows that their dependence is best fitted by the linear equation y = 1.2065x + 3.4748, with a high coefficient of determination R^2 = 0.8839 (Figure 10).

5. CONCLUSIONS

The influence of feed speed on energy consumption in the wood cutting process remains a persistent challenge in the field of cutting tools. Mikuláš and Mišura (2006) analyzed experimental measurements of cutting power for the softwood species spruce (*Picea abies*) using two types of circular saws and varying feed speeds. Their results indicated that feed speed is the most influential factor on the energy demands of the cutting process. Experimental research conducted by Svrzić et al. (2021) also demonstrated a strong relationship between feed speed and energy consumption.

From the presented results and the reviewed professional literature, it can be concluded that with an increase in feed speed the current flow (and thus energy consumption) increases. Considering the wood species employed in this research (beech and fir/spruce) there is a noticeable difference in the measured values. Lower energy consumption values were obtained for fir/spruce and higher values for beech, which is attributed to the greater hardness of beech. Quality of the processed surface, machining accuracy, and energy consumption continue to be an ongoing challenge in cutting tool research in order to achieve their optimal balance (Stanojević, 2023). A large number of influencing factors and their interactions are present in every machining process, which renders theoretical determination of optimal parameters with certainty exceedingly difficult.

REFERENCES

1. Koljozov, V., Trposki, Z., Rabadjiski, B., Zlateski, G., & Karanakov, V. (2019). Research on the effects of the cutting speed on cutting force and the cutting power in the process of milling. *Proceedings of the 4th International Scientific Conference "Wood Technology & Product Design"*, pp. 278–283.
2. Mikuláš, S., & Mišura, L. (2006). Investigations of cutting power versus clearance of a circular saw blade over the workpiece and feed speed. *Drvna industrija*, 57(1), pp. 13–17.
3. Paralidov, K., Koljozov, V., Trposki, Z., & Karanakov, V. (2015). Research on kerf number influence on cutting power during wood processing on circular saw. *Proceedings of the 2nd International Scientific Conference "Wood Technology & Product Design"*, pp. 221-225.

4. Stanojević, D. (2023). Investigation of the dependence of cutting power and surface roughness on the processing mode. *Proceedings of the 6th International Scientific Conference "Wood Technology & Product Design"*, pp. 19-26.
5. Stanojević, D., & Stefanović, S. (2014). Influence of physical and mechanic properties of panels on the cutting power. *Technical Science*, pp. 509–516.
6. Svrzić, S., Đurković, M., Danon, G., Furtula, M., & Stanojević, D. (2021). On acoustic emission analysis in circular saw cutting beech wood with respect to power consumption and surface roughness. *BioResources*, 16(4), pp. 8239–8257.

The Authors' Address:

[1] Anastasija Temelkova, PhD, teaching assistant
[1] Zoran Trposki, PhD, full professor
[1] Vladimir Koljozov, PhD, full professor
[2] Damjan Stanojević, PhD, senior lecturer
[1] Ss. Cyril and Methodius University in Skopje, Faculty of Design and Technologies of Furniture and Interior-Skopje 16-ta Makedonska brigada 3, 1000 Skopje, Republic of North Macedonia.
[2] Academy of Technical-Educational Vocational Studies Niš - Vranje Department, Filipa Filipovića 20, 17500 Vranje, Republic of Serbia.

COMPRESSIVE STRENGTH OF PLYWOOD REINFORCED WITH PRE-IMPREGNATED FIBERGLASS FABRICS

Violeta Jakimovska Popovska[1], Borche Iliev[1]

[1] *Ss. Cyril and Methodius University in Skopje, R. of North Macedonia, Faculty of design and technologies of furniture and interior-Skopje*
e-mail:jakimovska@fdtme.ukim.edu.mk, iliev@fdtme.ukim.edu.mk

ABSTRACT

The aim of this research is to study the in-plane compressive strength of eleven-layered beech plywood reinforced with pre-impregnated fiberglass fabrics (fiberglass prepreg).

The reinforcement was made by inserting certain numbers of sheets of fiberglass fabric that was pre-impregnated with methyl alcohol soluble phenol-formaldehyde resin. The same resin was used for veneer bonding. The thickness of the veneers used in plywood structure was 1,5 and 1,85 mm. Four models of plywood were made by changing the position of fiberglass prepreg sheets into the plywood structure. One control model of plywood without reinforcement was made.

In-plane compressive strength of plywood models was tested in five direction: parallel to the face grain, perpendicular to the face grain, at the angles of 22,5°, 45° and 67,5° to the face grain of the plywood panel.

The application of fiberglass prepreg reinforcements in plywood structure has impact on the values of in-plane compressive strength of plywood.

Keywords: plywood, reinforcement, fiberglass fabric, prepreg, pre-impregnated, phenol-formaldehyde resin, compressive strength.

1. INTRODUCTION

Application of non-wood materials in plywood structure can significantly improve the mechanical properties of plywood (Hardeo and Karunasena, 2002; Choi *et al*., 2011, Zīke and Kalniņš, 2011).

There are many studies that explore the possibilities of plywood reinforcement with different types of fibers and matrixes (Xu *et al*., 1996, Xu *et al.*, 1998, Brezović *et al*., 2003, Brezović *et al.*, 2010, Biblis and Carino, 2000, Hrázský and Král, 2007, Maniņš and Zīke, 2011, Saal, K *et. al*., 2024, Cordier and Mai, 2025). Possibilities to reinforce wood with pre-impregnated materials-prepregs were explored by Rowland *et al.* (1986). The application of pre-impregnated glass, carbon and aramid fiber materials results in a significant reduction in deflection and an increase in carrying capacity (Kohl *et al*., 2013).

Application of pre-impregnated fiberglass fabric can increase the plywood bending strength and modulus of elasticity in bending (Jakimovska Popovska and Iliev, 2019).

The results from other research, showed that the application of pre-impregnated cotton fabric in the structure of plywood significantly increases its hardness (Jakimovska Popovska and Iliev, 2021) and in-plane compressive strength of plywood (Jakimovska Popovska and Iliev, 2023).

The aim the research is to study the compressive strength of plywood reinforced with fiberglass fabrics pre-impregnated with methyl alcohol-soluble phenol-formaldehyde resin.

2. EXPERIMENTAL METHODS

For the realization of the research, four experimental reinforced eleven-layered beech plywood were made. The thickness of the veneers was 1,5 mm and 1,85 mm, with moisture content of 9,77 %. The orientation of adjacent veneers in plywood structure was at right angle.

The reinforcement was made through inserting reinforcement sheets of pre-impregnated fiberglass fabric (fiberglass prepreg) in plywood adhesive layers. In three models, each reinforcement layer is

consisted of four sheets of fiberglass prepreg placed one above the other and inserted symmetrically on both sides with respect to its axis of symmetry. In the first model (FP-1), the reinforcements are inserted in the fifth and sixth adhesive layer, while in the second model (FP-2) they are inserted into the third and eighth adhesive layer. In the third model (FP-3), the reinforcements are positioned as surface layers of plywood. The fourth model of plywood (FP-4) has single sheets of fiberglass prepreg inserted in each adhesive layer of the panel. In all of reinforced plywood models, the orientation of the wrap of the fabric is parallel to grain direction of the surface veneers. One control model (C) of plywood without reinforcement was made for comparison of the results.

The fiberglass prepreg was made form fiberglass fabric that was pre-impregnated with methyl alcohol soluble phenol-formaldehyde resin with 51 % dry matters content, in quantity of 140 g/m^2. The same resin was used for veneer bonding, applied on the veneers in quantity of 180 g/m^2. The thickness of the fiberglass fabric before impregnation was 0,173 mm, while the thickness of the fiberglass prepreg was 0,22 mm.

The pattern and cross-section of experimental plywood models, technical characteristics of the fiberglass fabric, the resin characteristics, as well as the impregnation process are given in previous research paper (Jakimovska and Iliev, 2019).

The in-plane compressive strength of plywood was tested according to the national standard MKS D.A8.070/85 on test specimens with dimensions of 50·6d·d (mm). This property is tested in five directions, i.e. parallel to the face grain, perpendicular to the face grain, at the angles of 22,5°, 45° and 67,5° to the face grain of the plywood panel.

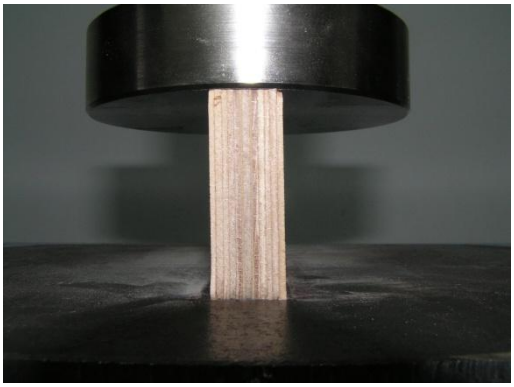

Figure 1. *Test specimen during testing the compressive strength of experimental plywood.*

SPSS Statistic software was used for statistical analysis of the obtained data. One way ANOVA was used to determine the significance of the effect of the fiberglass prepreg reinforcements on plywood in-plane compressive strength. Tukey's test was applied to evaluate the statistical significance between the mean values of compressive strength of plywood with different layouts of reinforcement. The tests were conducted at 0,05 probability level.

3. RESULTS AND DISCUSSION

The obtained results for the in-plane compressive strength of experimental plywood models are shown in table 1 and figure 2.

In all tested directions, models of reinforced plywood have higher values of compressive strength compared to the control model made without reinforcements.

The analysis of variance of the obtained data for compressive strength parallel to the face grain (ANOVA: F (4, 20) = 4,356; p = 0,011) showed that the differences between the mean values of this property of at least two plywood models are statistically significant. The conducted post-hoc Tukey's test for multiple comparison between models showed that there are statistically significant differences in the mean values of compressive strength parallel to the face grain between the control model and all reinforced models. Within the reinforced models, there are no statistically significant differences. The highest mean value of this property is achieved in model FP-2. Compared to this value, the values of models FP-1, FP-3 and FP-4 are lower for 3,22 %, 2,64 % and 2,33 %, respectively.

***Table 1**. Statistical values for compressive strength of experimental plywood.*

Compressive strength	Model	N	Mean (N/mm^2)	Std. Deviation (N/mm^2)	Std. Error (N/mm^2)	95 % Confidence Interval for Mean		Min (N/mm^2)	Max (N/mm^2)
						Lower Bound	Upper Bound		
Paralell to the face grain	**FP-1**	5	68,86[a]	3,29	1,47	64,78	72,94	63,89	72,33
	FP-2	5	71,08[a]	4,83	2,16	65,08	77,09	66,94	78,23
	FP -3	5	69,25[a]	8,01	3,58	59,30	79,20	56,89	76,43
	FP-4	5	69,46[a]	5,39	2,41	62,77	76,16	63,54	77,06
	C	5	59,12[b]	2,10	0,94	56,52	61,72	56,65	61,61
Perpendicular to the face grain	**FP-1**	5	72.99[a]	4,09	1,83	67,90	78,07	66,48	77,82
	FP-2	5	77.11[a,c]	4,20	1,88	71,89	82,33	72,48	82,27
	FP-3	5	64.84[b]	3,94	1,76	59,95	69,74	59,71	70,19
	FP-4	5	81.23[c]	1,99	0,89	78,76	83,70	77,72	82,62
	C	5	58.27[d]	1,75	0,78	56,10	60,44	55,72	60,23
22,5° to the face grain	**FP-1**	5	69.24[a,c]	1,74	0,78	67,08	71,40	66,65	71,34
	FP-2	5	62.39[b]	2,06	0,92	59,83	64,95	60,15	64,95
	FP-3	5	71.35[a]	1,75	0,78	69,17	73,52	68,66	73,55
	FP-4	5	66.76[c]	2,63	1,18	63,50	70,02	64,53	69,84
	C	5	52.39[d]	2,62	1,17	49,15	55,64	48,56	54,44
45° to the face grain	**FP-1**	5	66.17[a]	1,23	0,55	64,64	67,70	64,18	67,33
	FP-2	5	59.77[b]	1,95	0,87	57,35	62,19	57,48	62,12
	FP-3	5	59.20[b]	2,21	0,99	56,45	61,95	57,03	62,50
	FP-4	5	61.71[b]	0,73	0,33	60,80	62,61	60,63	62,51
	C	5	48.06[c]	2,01	0,90	45,57	50,56	45,02	49,86
67,5° to the face grain	**FP-1**	5	70.00[a]	1.58	0.71	68.03	71.96	68.07	72.11
	FP-2	5	64.90[b]	0.72	0.32	64.01	65.79	64.16	65.82
	FP-3	5	60.04[c]	0.87	0.39	58.96	61.12	58.84	60.75
	FP-4	5	70.56[a]	1.21	0.54	69.06	72.06	68.55	71.54
	C	5	53.46[d]	1.65	0.74	51.42	55.51	51.24	55.82

*The mean values with the same letters are not significantly different at 0.05 probability level

The highest mean value of compressive strength perpendicular to the face grain is achieved in model FP-4. The analysis of the variance (ANOVA: F (4, 20) = 37,927; p << 0,001) and post-hoc Tukey's test showed that there is statistically significant differences between the mean value of the control model and mean values of all reinforced models. Compared to the control model C, the mean values of reinforced models are higher for 11,27 % up to 39,40 %. Within the reinforced models, the mean value in model FP-3 statistically differs from the mean values of all other reinforced model.

The analysis of the obtained data for compressive strength at the angle of 22,5° to the face grain showed that the values of all reinforced models statistically differ from the value of the control model without reinforcements. Within the reinforced models, the mean value of model FP-3 is higher for 3,05 %, 14,36 % and 6,87 % compared to the mean values of models FP-1, FP-2 and FP-4, respectively. The application of fiberglass prepreg sheets in plywood structure increase the mean value of this property up to 36,2 % compared to the control model. The analysis of the variance (ANOVA: F (4, 20) = 58,472; p << 0,001) and post-hoc Tukey's test showed that the mean value of model FP-2, as

well as the mean value of model FP-4 statistically differs from the mean values of other reinforced models.

The highest value of compressive strength at the angle of 45° to the face grain of plywood is achieved in model reinforced with prepreg sheets positioned next to the central veneer layer (FP-1).

Compared to the control model without reinforcement, the mean value of model FP-1 is higher for 37,68 %. The mean value of the control model statistically differs from all reinforced models (ANOVA: F (4, 20) = 75,661; p << 0,001). Within the reinforced models, there is no statistically significant differences between the mean values of models FP-2, FP-3 and FP-4.

Compared to the control model, the mean values of compressive strength at the angle of 67,5° to the face grain of reinforced plywood models are higher for 12,3 % up to 32 %. The analysis of the variance (ANOVA: F (4, 20) = 162,104; p << 0,001) and post hoc test showed that the values of all reinforced models statistically differ from the value of the control model. Within the reinforced models, the differences between the mean values of model FP-1 and FP-4 are very small and are not statistically significant.

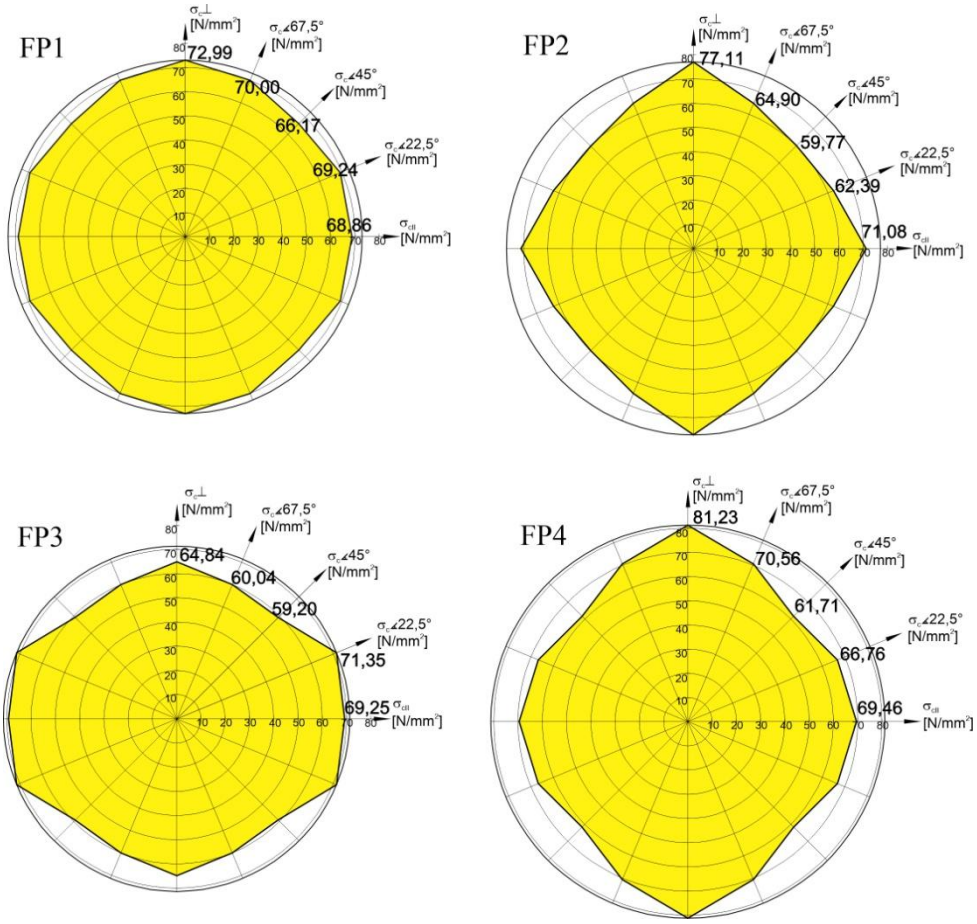

Figure 2. *Polar diagrams of compressive strength of plywood reinforced with fiberglass prepregs.*

With the exception of model FP-3, in all reinforced plywood models the highest value of compressive strength is achieved in direction perpendicular to the face grain, while the lowest value is achieved at the angle of 45° to the face grain of plywood.

The biggest difference between the mean values of the compressive strength parallel and perpendicular to the face grain of plywood occurs in model FP-4 and is 16,94 % ($\sigma\perp>\sigma\parallel$). In other reinforced models, the difference between these values is smaller, whereas in models FP-1 and FP-2, the mean value of the compressive strength perpendicular to the face grain is higher than the mean value of the compressive strength parallel to face grain by 6,00% and 8,48% respectively. In model FP-3, the highest value of the compressive strength was obtained at an angle of 22.5º.

The lowest mean value of compressive strength occurs at the angle of 45º to the face grain of reinforced plywood. The mean value of compressive strength at an angle of 45º is lower than the mean value of compressive strength across the grain direction by 9,34 % for model FP-1, 22,49 % for model FP-2, 8,70 % for model FP-3 and 24,03 % for model FP-4.

The mean values of the compressive strength at an angle of 22,5º and 67,5º to the face grain of reinforced plywood are similar with the exception of the FP-3 model, in which a bigger difference occurs between the values of the compressive strength in these directions (11,31 N/mm^2). In the remaining reinforced models, the difference between these values is 0,76 N/mm^2 in model FP-1, 2,51 N/mm^2 in model FP-2 and 3,8 N/mm^2 in model FP-4.

With the exception of model FP-2, the mean values of the compressive strength parallel to the face grain of all other reinforced models are close to the mean values of the compressive strength at an angle of 22,5º, with the difference between these values being small and amounting to 0,38 N/mm^2 in model FP-1, 2,1 N/mm^2 in model FP-3 and 2,7 N/mm^2 in model FP-4. The difference in the mean values of the compressive strength in these two directions in model FP-2 is 8,69 N/mm^2.

The stress-strain diagrams during testing compressive strength of reinforced plywood models are shown on figures 3, 4, 5, 6 and 7.

The analysis of the stress-strain diagrams of reinforced plywood models showed that in model FP-3 which is overlaid with fiberglass prepreg sheets, the failure of the material happens with bigger plastic deformations compared to other reinforced models.

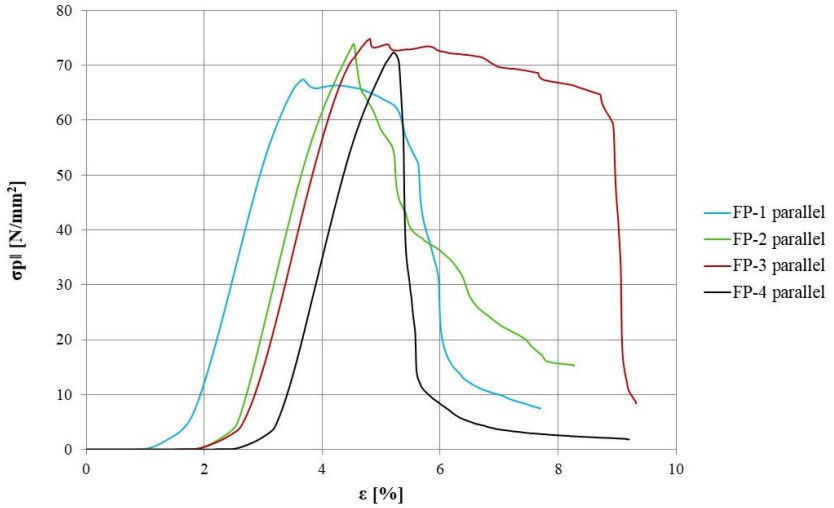

Figure 3. *Stress-strain diagram of compressive strength parallel to the face grain of reinforced models.*

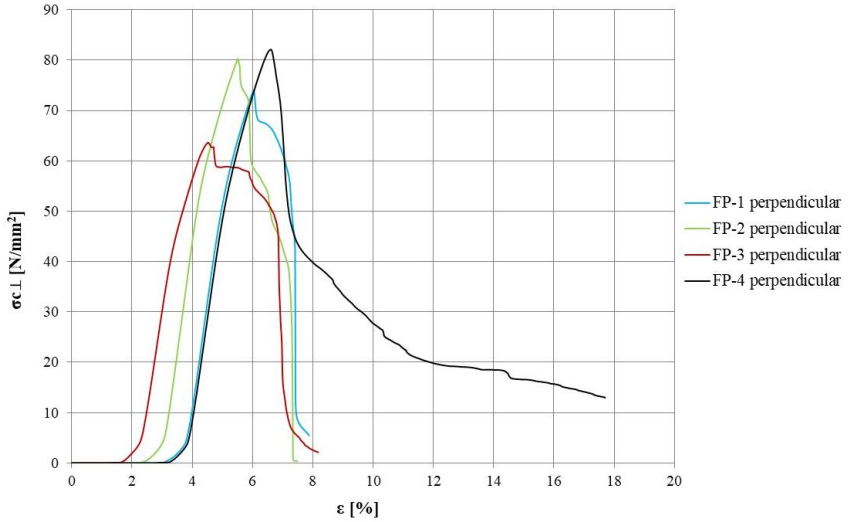

Figure 4. *Stress-strain diagram of compressive strength perpendicular to the face grain of reinforced models.*

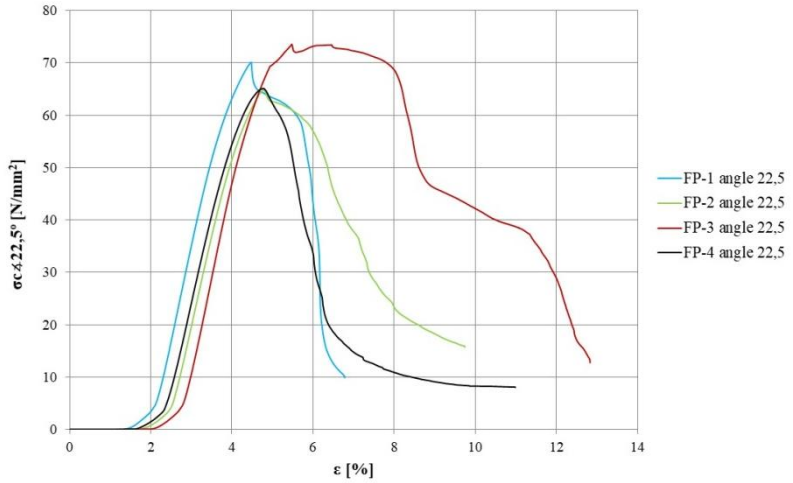

Figure 5. *Stress-strain diagram of compressive strength at the angle of 22,5° to the face grain of reinforced models.*

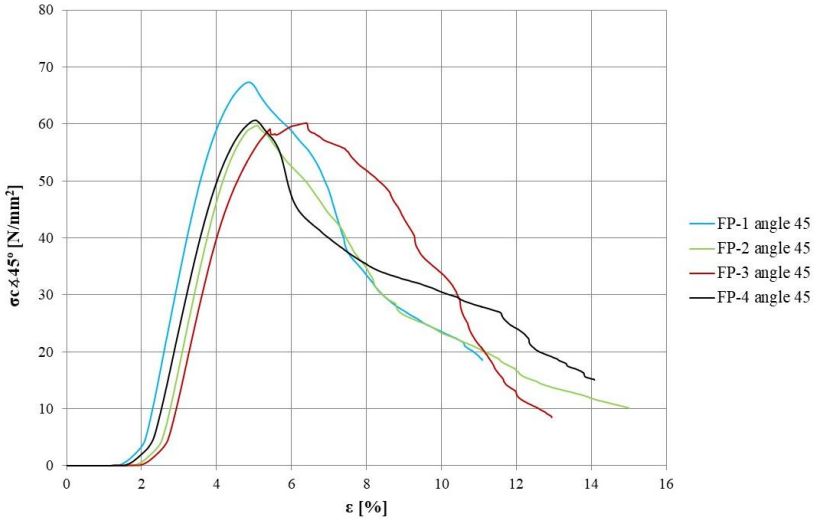

Figure 6. *Stress-strain diagram of compressive strength at the angle of 45° to the face grain of reinforced models.*

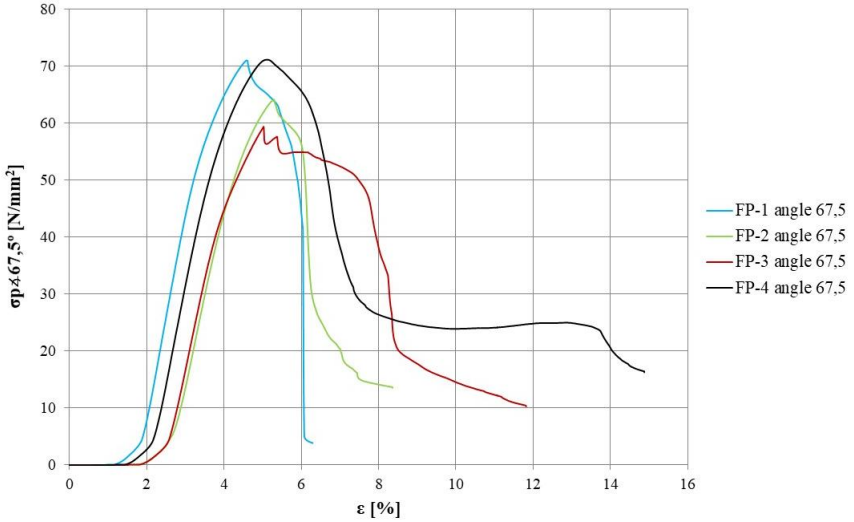

Figure 7. *Stress-strain diagram of compressive strength at the angle of 67,5°*

to the face grain of reinforced models.

Figure 8. *Failure mode of the test specimens of reinforced models during testing the compressive strength parallel to the face grain.*

Figure 9. *Failure mode of the test specimens of reinforced models during testing the compressive strength perpendicular to the face grain.*

All experimental plywood models in all tested direction, exceed the minimal value of compressive strength defined in the national standard MKC D.C5.043 for load-bearing panels for use in construction.

4. CONCLUSIONS

The reinforcement of plywood with fiberglass prepreg significantly increases its compressive strength in all tested directions.

Application of fiberglass prepreg sheets as reinforcement of plywood structure lead to increasing of compressive strength up to 20 % in direction parallel to the face grain, up to 39 % perpendicular to the face grain, up to 36 % at the angle of 22,5° to the face grain, up to 38 % at the angle of 45° and up to 32 % % at the angle of 67,5° to the face grain.

Different position of the fiberglass prepreg sheets in plywood structure has impact on the plywood compressive strength in all panel directions, with the exception of the direction parallel to the face grain where the differences between reinforced models are not statistically significant.

REFERENCES

1. Biblis, E.J.; Carino, H.F., 2000: Flexural properties of southern pine plywood overlaid with fiberglass-reinforced plastic. Forest Prod J., 50 (1): 34-36.
2. Brezović, M.; Jambreković, V.; Pervan, S., 2003: Bending properties of carbon fiber reinforced plywood. Wood Research, 48 (4): 13-24.
3. Brezović, M.; Kljak, J.; Pervan, S.; Antonović, A., 2010: Utjecaj kuta orientacije sintetskih vlakana na savojna svojstva kompozitne furnirske ploče. Drvna ind., 61 (4): 239-243.

4. Choi, S.W.; Rho, W.J.; Son, K.J.; Lee, W.I., 2011: Analysis of buckling load of fiber-reinforced plywood plates for NO 96 CCS. Proceedings of the Twenty-first International Offshore and Polar Engineering Conference, 2011, Maui, Hawaii, USA, pp: 79-83.
5. Cordier, M., Mai, C. 2025. Basalt grid reinforcement of lightweight plywood. Eur. J. Wood Prod. 83, 45 (2025). https://doi.org/10.1007/s00107-024-02196-7.
6. Hardeo, P.; Karunasena, W., 2003: Buckling of fiber-reinforced plywood plates. Proceedings of Second International Conference on Structural Stability and Dynamics, 2002, Singapore, pp. 442-447. https://doi.org/10.1142/9789812776228_0062.
7. Hrázský, J.; Král, P., 2007: A Contribution to the properties of combined plywood materials. J For Sci, 53 (10): 483-490. https://doi.org/10.17221/2087-jfs.
8. Jakimovska Popovska, V., Iliev, B. 2019: Bending Properties of Reinforced Plywood with Fiberglass Pre-Impregnated Fabrics, Proceedings of 30th International Conference on Wood Science and Technology-ICWST and 70th anniversary of Drvna industrija Journal "Implementation of wood science in woodworking sector", 12th -13th December, Zagreb, 2019: 77-85.
9. Jakimovska Popovska, V., Iliev, B. 2021. Janka hardness of plywood reinforced with pre-impregnated cotton fabrics, Proceedings of the 5th International conference „Wood technology and product design", 14-17th September, Ohrid, 2021: 7-14.
10. Jakimovska Popovska, V., Iliev, B. 2023. In-plane compressive strength of plywood reinforced with cotton prepreg, Proceedings of the 6th International conference „Wood technology and product design", 13-15th September, Ohrid, 2023: 111-117.
11. Kohl, D.; Million, M.; Böhm, S., 2013: Adhesive bonded wood-textile-compounds as potentially new eco-friendly and sustainable high-tech materials. Proceedings of the Annual Meeting of the Adhesion Society 2013, Florida, USA, pp: 27-29.
12. Maniņš, M.; Zīke, S., 2011: Textile fabrics reinforced plywood with enhanced mechanical properties. Abstracts of the International Scientific Conference „Civil Engineering'11", 2011, Latvia, pp: 35.
13. Macedonian standards.
14. Rowlands, R.E.; Van Deweghe, R.P.; Launferbeg, T.L.; Krueger, G.P., 1986: Fiber-reinforced wood composites. Wood and Fiber Science, 18 (1): 39-57.
15. Saal, K., Kallakas, H., Tuhkanen, E., Just, A., Rohumaa, A., Kers, J., Kalamees, T., & Lohmus, R. 2024. Fiber-Reinforced Plywood: Increased Performance with Less Raw Material. Materials, 17(13), 3218. https://doi.org/10.3390/ma17133218
16. Xu, H.; Tanaka, C.; Nakao, T.; Nisano Y.; Katayama, H., 1996. Flexural and shear properties of fiber reinforced plywood. Mokuzai Gakkaishi, 42: 376-382.
17. Xu, H., Nakao, T., Tanaka, C., Yoshinobu, M., Katayama, H., 1998: Effects of fiber length orientation on elasticity of fiber-reinforced plywood. Journal of Wood Science, (44): 343-347. https://doi.org/10.1007/bf01130445
18. Zīke S.; Kalniņš K., 2011: Enhanced impact properties of plywood. Proceedings of the 3rd International Conference Civil Engineering'11, 2011, Latvia, pp: 125-130.

IMPACT OF FEED RATE ON ROUGHNESS OF THE CUT SURFACE DURING CUTTING DRY BEECH AND SPRUCE WOOD WITH A CIRCULAR SAW

Anastasija Temelkova[1], Zoran Trposki[1], Vladimir Koljozov[1], Ana Marija Stamenkoska[1]

Ss. Cyril and Methodius University in Skopje,
Faculty of Design and Technologies of Furniture and Interior-Skopje
email: temelkova@gmail.com; trposki@fdtme.ukim.edu.mk;
koljozov@fdtme.ukim.edu.mk; stamenkoska@fdtme.ukim.edu.mk

ABSTRACT

The precision of wood processing and the quality of the machined surface are critical factors in achieving the desired processing outcomes. These factors are influenced by a variety of parameters, among which the feed rate during mechanical processing plays a significant role in determining the surface roughness of the cut. Surface roughness, often caused by tool marks, affects subsequent hydrothermal treatments and other mechanical processes, ultimately reducing the efficiency of wood utilization when it is too high.

For this purpose, in this paper, the dependence of the feed rate on the roughness of beech and spruce wood during cutting of dry wood with a circular saw is investigated, with the intention of determining the optimal cutting conditions for obtaining lower values of the roughness.

In this research, three different feed rates were applied (U_1 = 12 m·min^{-1}, U_2 = 16 m·min^{-1} and U_3 = 20 m·min^{-1}) for a constant cutting height of 15 mm in dry beech and spruce wood with moisture content W = 10 ± 1%. The measurements were made with a circular saw with diameter of cutting tool D = 250 mm, number of teeth Z = 40 and width of the cut b = 3.2 mm. The number of rounds was n = 5500 min^{-1}.

Roughness measurements were taken with a digital comparator, according to the R_{max} criterion. The obtained results showed a pronounced significance, directly proportional dependence of the roughness of the cut surface on the feed rate.

Keywords: beech wood, spruce wood, circular saw, roughness, feed rate.

1. INTRODUCTION

Wood, as a material, is highly suitable for both interior and exterior decoration. It can be shaped easily with relatively low energy consumption. It possesses low acoustic, thermal, and electrical conductivity, along with high resistance to chemical agents (Stanojević, 2016).

Circular saws are among the most widely used tools in the mechanical processing of wood, covering all stages of production. Manufacturers on the market offer various types of saws with different diameters and numbers of teeth. Circular saws are also used for cutting other materials such as plastics, metals, ceramics, and various construction materials (Đurković et al., 2017). In addition to the physical, mechanical, and anatomical properties of wood, the surface quality of components and final products is influenced by numerous factors — such as the cutting direction, the geometry of the tooth and its cutting edge, the thickness of the removed segment, inaccuracies in tool sharpening, and technological parameters (cutting speed, feed speed, etc.) (Richter et al., 1995). The contact surfaces of tools during machining are subjected to high pressures and friction, which leads to tool wear. Tool wear is an important factor in the mechanical processing of wood because it directly affects surface quality, cutting forces, cutting power, and energy consumption (Đurković et al., 2019).

The main criteria that characterize the quality of the processed surface are surface roughness, machining accuracy, and durability. Marks left by vibrations of the machine and the cutting tool, as well as the structure and density of the processed material, are among the causes of surface roughness. In the mechanical processing of wood, feed speed is one of the factors that has a strong influence on the roughness of the sawn surface.

2. RESEARCH OBJECTIVES

The aim of this research is to determine the dependence of feed speed on the roughness of the cut surface in beech and fir/spruce wood when sawing dry wood with a circular saw, in order to define optimal cutting conditions that achieve minimal surface roughness.

3. MATERIAL AND METHODS

3.1. Material

The tests were carried out on defect-free sawn timber of beech (*Fagus sylvatica* L.) and fir/spruce (*Picea abies* Karst., *Abies alba*), with dimensions 1500 × 150 × 15 mm. All samples were kiln-dried and conditioned before testing. The measured average moisture content of beech was 9.32 %, and of fir/spruce 10.26 %. From these planks, specimens were cut with a constant cutting height of 15 mm.

3.2. Experimental methods

The experimental tests were performed on a format circular saw machine type NIKOLAIDIS TEMA 3800. Three feed speeds were applied: U_1 = 12 m·min^{-1}, U_2 = 16 m·min^{-1}, and U_3 = 20 m·min^{-1}. The circular saw blade had a diameter D = 250 mm, number of teeth Z = 40, and kerf width b = 3.2 mm (Figure 1). The spindle rotational speed was n = 5500 min^{-1}. The cutting length for each specimen was 1.2 m.

The surface roughness data were measured using a digital comparator, type SHAHE, according to the R_{max} criterion. For each specimen, 100 measurements were taken over a length of 1.0 m (Figure 2).

***Figure 1**. Circular saw with diameter D = 250 mm, number of teeth Z = 40 and kerf width b = 3.2 mm.*

***Figure 2**. Digital comparator type SHAHE.*

4. RESULTS AND DISCUSSION

4.1. Measured surface roughness values for beech specimens

Table 1. *Results of the surface roughness measurements for beech specimens at various feed speeds (U_1 = 12 m·min⁻¹, U_2 = 16 m·min⁻¹, U_3 = 20 m·min⁻¹), according to the R_{max} criterion.*

Feed speed (U) for number of teeth Z = 40 and diameter D = 250 mm					
U_1 = 12 m·min^{-1}		U_2 = 16 m·min^{-1}		U_3 = 20 m·min^{-1}	
Cutting height [mm]		Cutting height [mm]		Cutting height [mm]	
h = 15mm		h = 15mm		h = 15mm	
Surface roughness	[mm]	Surface roughness	[mm]	Surface roughness	[mm]
Mean value	0.0320	Mean value	0.0491	Mean value	0.0618
Standard deviation	0.0067	Standard deviation	0.0093	Standard deviation	0.0112
Coefficient of variation	20.80	Coefficient of variation	19.05	Coefficient of variation	18.06
Minimum	0.020	Minimum	0.032	Minimum	0.037
Maximum	0.054	Maximum	0.072	Maximum	0.084

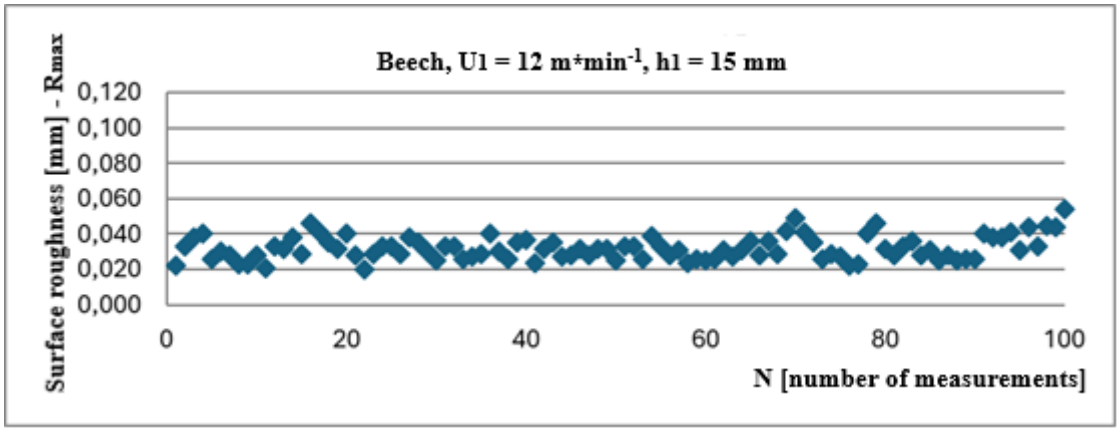

Figure 3. *Beech specimens' surface roughness for feed speed U_1 = 12 m·min^{-1}.*

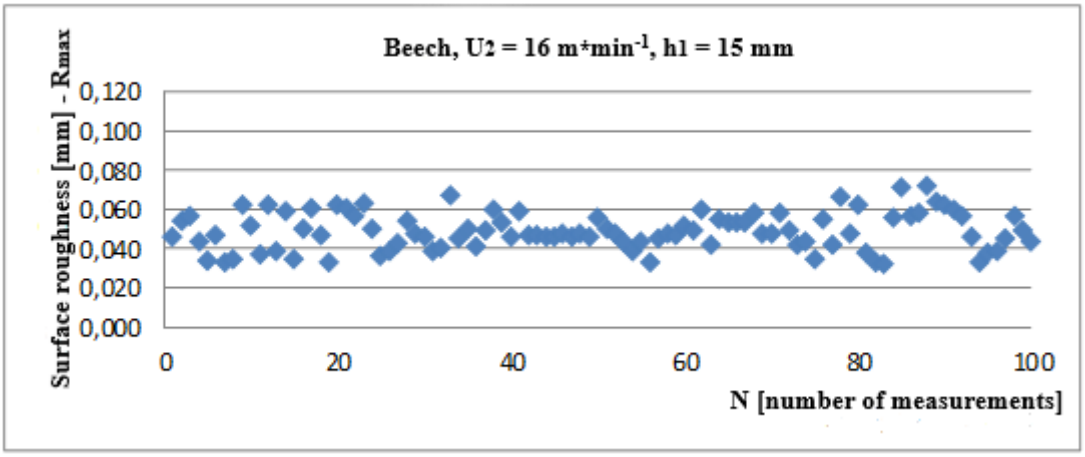

Figure 4. *Beech specimens' surface roughness for feed speed U_2 = 16 m·min^{-1}.*

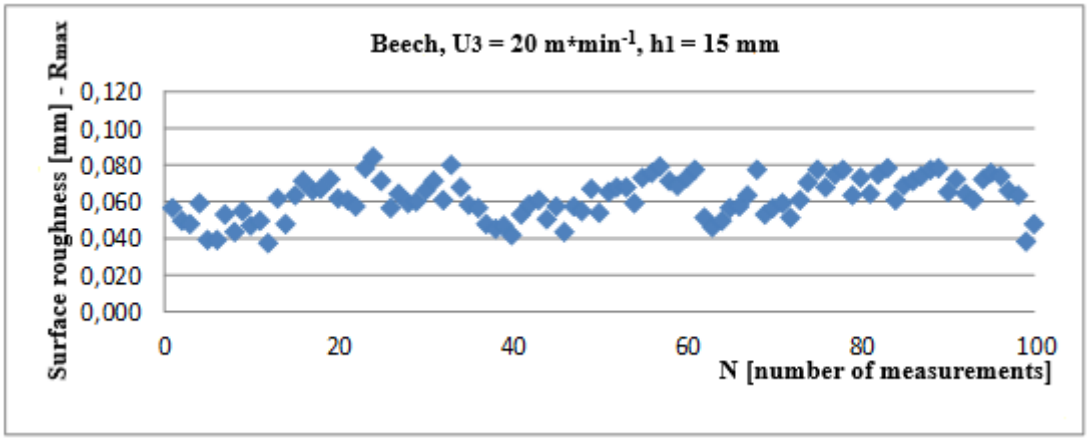

Figure 5. *Beech specimens' surface roughness for feed speed U_3 = 20 m·min^{-1}.*

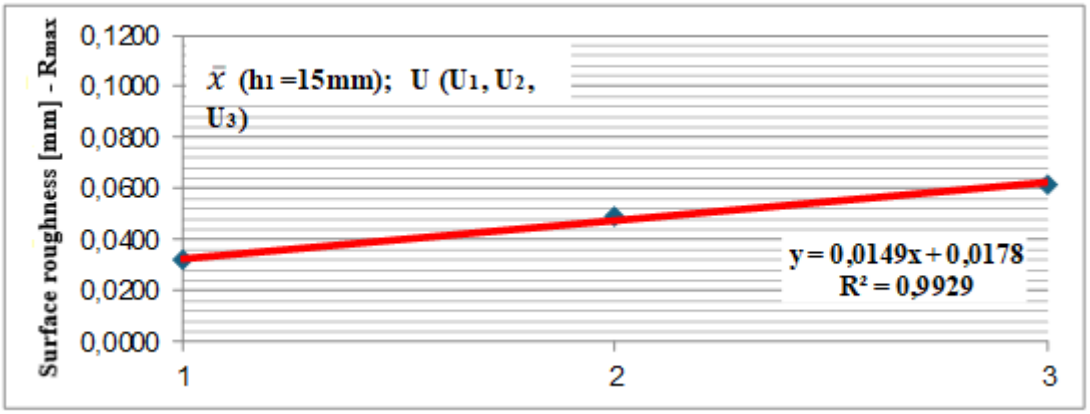

Figure 6. *Regression analysis for mean values of the beech specimens' surface roughness with all three feed speeds (U_1=12m·min-1, U_2=16m·min^{-1} and U_3=20m·min^{-1}).*

From the presented results (Table 1, Figures 3, 4, 5, and 6), it can be concluded that with an increase in feed speed, the roughness of the cut surface increases in direct proportion. The dependence is mathematically expressed by the regression line y = 0.0149x + 0.0178 and the coefficient of determination R^2 = 0.9929. Regression analysis showed that the measurements are best fitted by a linear equation. The correlation coefficient indicates a strong dependence.

4.2. Measured surface roughness values for fir/spruce specimens

T***able 2.*** *Results of the surface roughness measurements for fir/spruce specimens at various feed speeds (U_1 = 12 m·min^{-1}, U_2 = 16 m·min^{-1}, U_3 = 20 m·min^{-1}), according to the R_{max} criterion.*

Feed speed (U) for number of teeth Z = 40 and diameter D = 250 mm					
U_1 = 12 m·min^{-1}		U_2 = 16 m·min^{-1}		U_3 = 20 m·min^{-1}	
Cutting height [mm]		Cutting height [mm]		Cutting height [mm]	
h = 15mm		h = 15mm		h = 15mm	
Surface roughness	[mm]	Surface roughness	[mm]	Surface roughness	[mm]
Mean value	0.0865	Mean value	0.1127	Mean value	0.1733
Standard deviation	0.0077	Standard deviation	0.0095	Standard deviation	0.0123
Coefficient of variation	8.93	Coefficient of variation	8.43	Coefficient of variation	7.09
Minimum	0.040	Minimum	0.099	Minimum	0.131
Maximum	0.115	Maximum	0.139	Maximum	0.201

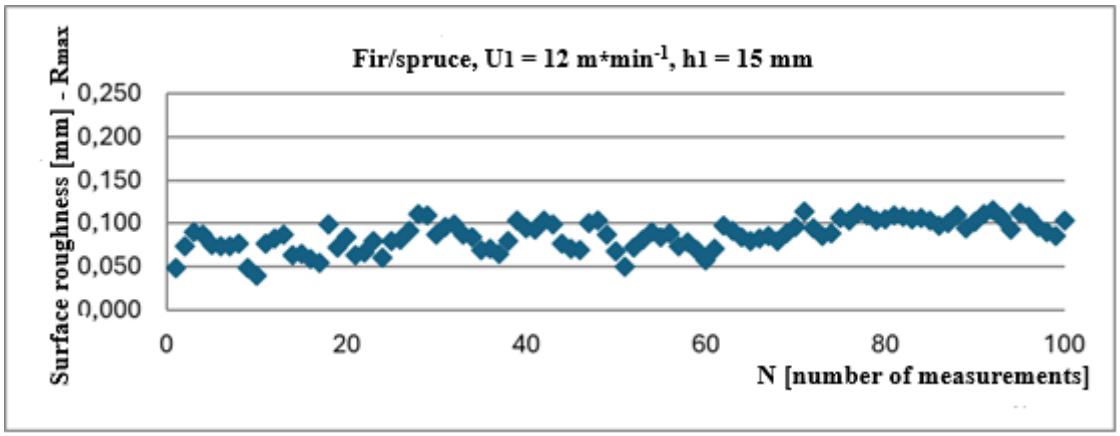

Figure 7. *Fir/spruce specimens' surface roughness for feed speed U_1 = 12 m·min^{-1}.*

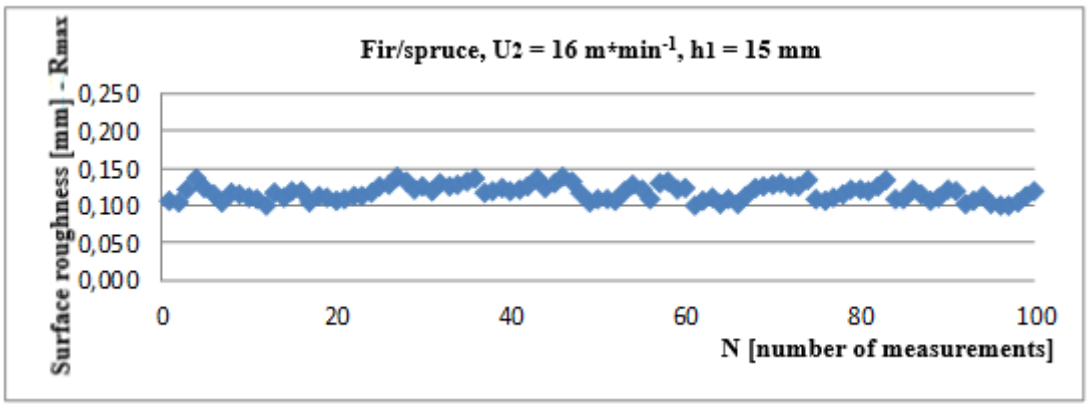

Figure 8. *Fir/spruce specimens' surface roughness for feed speed U_2 = 16 m·min^{-1}.*

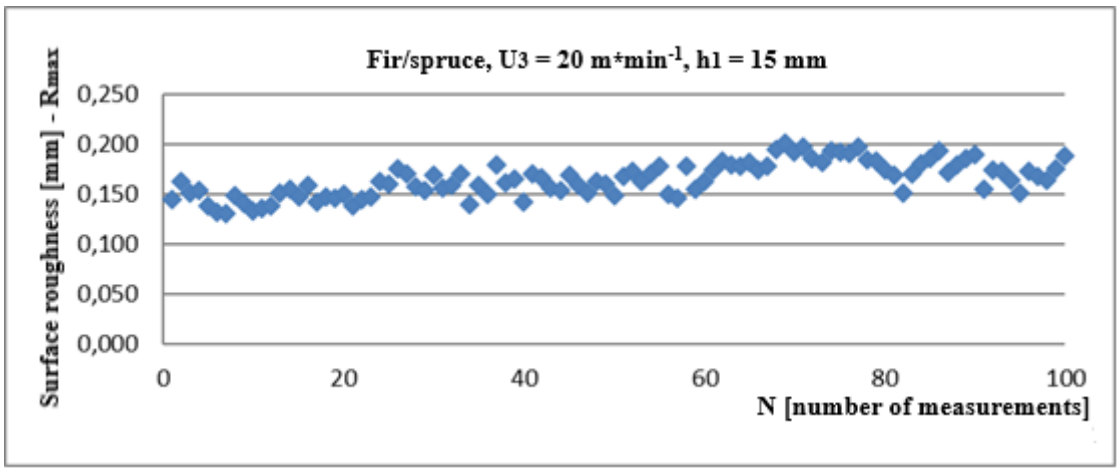

Figure 9. *Fir/spruce specimens' surface roughness for feed speed U_3 = 20 m·min^{-1}.*

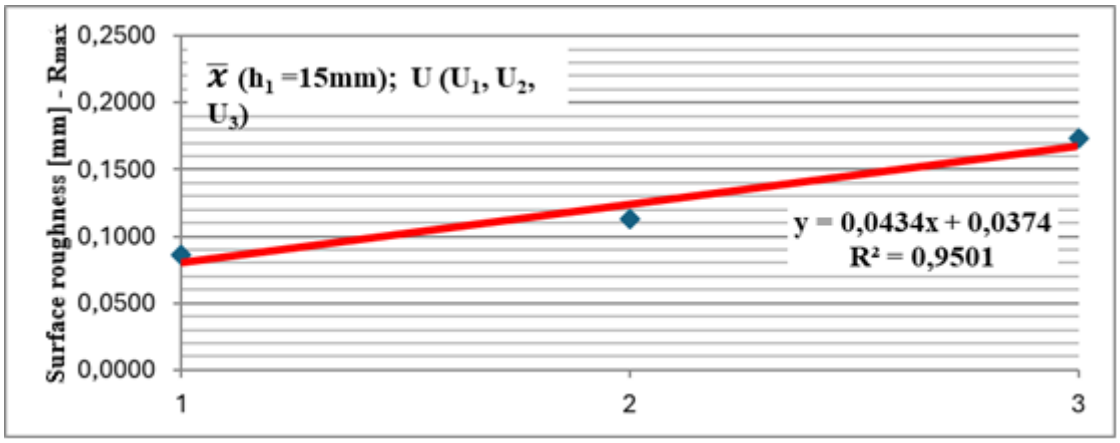

Figure 10. *Regression analysis for mean values of the fir/spruce specimens' surface roughness with all three feed speeds (U_1=12m·min-1, U_2=16m·min^{-1} and U_3=20m·min^{-1}).*

From the presented results (Table 2, Figures 7, 8, 9, and 10), it can be concluded that with an increase in feed speed, the roughness of the cut surface increases in direct proportion. The dependence is mathematically expressed by the regression line y = 0.0434x + 0.0374 and the coefficient of determination R^2 = 0.9501. The correlation coefficient indicates a strong dependence.

5. CONCLUSIONS

The reviewed professional and scientific literature available to us showed that all authors agree in the assertion that an increase in feed speed results in an increase in the roughness of the cut surface, regardless of the type of mechanical processing. The authors Škaljić, Beljo Lučić, Čavlović, and Obućina (2009) examined the surface quality of beech, oak, and spruce wood. The experiment was conducted on a four-sided planer using a tool with two blades at different feed speeds. From the obtained results, they concluded that increasing the feed speed increases the surface roughness. The lowest roughness was recorded in the oak specimens, and the highest in the spruce specimens. In the research conducted by Svrzić, Đurković, Danon, Furtula, and Stanojević (2021), the examination of surface roughness indicated a significant influence of feed speed on the increase of roughness. The results clearly show that the physical and mechanical properties, as well as the anatomical structure of the wood, affect surface roughness. In general, better results in mechanical wood processing are obtained with lower feed speeds. Considering the wood species used in this study as the processing material, beech and fir/spruce, it is possible to observe differences in the obtained values. Namely, lower values for the roughness of the cut surface were obtained for beech, while higher values for the roughness of the cut surface were obtained for spruce, which is due to the anatomical structure of the wood. It is of great importance to determine the optimal feed speed value in order to achieve favorable productivity and surface quality.

REFERENCES

1. Đurković, M., Danon, G., Svrzić, S., Trposki, Z., & Koljozov, V. (2017) A justification of the use of specialized circular saws for wood. *Proceedings of the 3rd International Scientific Conference "Wood Technology & Product Design"*, pp. 61–66.
2. Đurković, M., Milosavljević Mirić, M., Mihailović, V., & Danon, G. (2019). Tool wear impacts on cutting power and surface quality in peripheral wood milling. *Proceedings of the 4th International Scientific Conference "Wood Technology & Product Design"*, pp. 110–118.
3. Richter, K., Feist, W. C., & Knabe, M. T. (1995). The effect of surface roughness on the performance of finishes. Part 1: Roughness characterization and strain performance. *Forest Products Journal, 45*(7/8), pp. 91–97.
4. Škaljić, N., Beljo Lučić, R., Čavlović, A., & Obućina, M. (2009). Effect of feed speed and wood species on roughness of machined surface. *Drvna industrija, 60*(4), pp. 229–234.

5. Stanojević, D. (2016). Basis of maximum qualitative utilized sawing in cutting beech. *Proceedings of the tenth International Scientific Conference "The Power of Knowledge"*, pp. 1205–1212.
6. Svrzić, S., Đurković, M., Danon, G., Furtula, M., & Stanojević, D. (2021). On acoustic emission analysis in circular saw cutting beech wood with respect to power consumption and surface roughness. *BioResources, 16*(4), pp. 8239–8257.

The Authors' Address:

Anastasija Temelkova, PhD, teaching assistant
Zoran Trposki, PhD, full professor
Vladimir Koljozov, PhD, full professor
Ana Marija Stamenkoska, MSc, teaching assistant
Ss. Cyril and Methodius University in Skopje, Faculty of Design and Technologies of Furniture and Interior-Skopje 16-ta Makedonska brigada 3, 1000 Skopje, Republic of North Macedonia.

THE ROLE OF THE INCREASING GEOMETRY PRECISION FOR SAWLOG QUALITY GRADING

Rostislav Berezjuk[1]

[1]*Mendel University in Brno, Czech Republic,*
Faculty of Forestry and Wood Technology,
e-mail: rostislav.berezjuk@mendelu.cz

ABSTRACT

This paper is focused on the possibilities of using geometry obtained by CT scanning to improve the quality assessment of sawlogs. This study is the initial part of the author's research in qualitative log sorting. The selected 60 Norway spruce sawlogs were measured manually according to the valid standards in the Czech Republic and then scanned using a CT.LOG X-ray computed tomography scanner (MiCROTEC, Bressanone, Italy). Based on CT scan reconstruction, the average wood density was determined to be 687.9 kg/m^3 at a moisture content of 60.6%. When comparing methods of manual measurement and computed tomography, a slightly stronger relationship was found between density based on computed tomography and wood moisture content, with a Pearson correlation coefficient of $r = 0.7195$. The tests performed confirmed a statistically significant difference between the volume determined by manual measurement and by computed tomography. Obtained volumes are input in follow-up studies when correcting the parameters received from acoustic non-destructive testing. The results proved the high accuracy of the CT scans, which allows improvement in the quality assessment of sawlogs.

Keywords: CT scanning, non-destructive techniques, acoustic methods, volume reconstruction.

1. INTRODUCTION

Non-destructive methods are an essential tool that allows the prediction of the actual properties of a material without the need to damage its structure. When using wood for construction purposes, it is necessary to know its mechanical properties, which are usually predicted by a number of non-destructive methods, such as visual assessment (Takahashi et al. 2022), acoustic methods (Uzcategui et al. 2023), methods based on computed tomography (Rais et al. 2017), fibre orientation measurements (Olsson et al. 2018), or simulations using the finite element method (Weidenhiller et al. 2023). Each of these options has its advantages and disadvantages, but they all share the principle of indirect measurement of mechanical properties, which are significantly influenced by several factors and the surrounding environment. The properties of final sawn timber can be predicted before processing at the sawlog stage, or later during industrial processing at the sawmill. Since the 20th century, industrial prediction of the mechanical properties of sawn timber has been used primarily before or, more often, after drying, whereby we distinguish between visual and machine grading (Ridley-Ellis et al. 2016). In recent years, however, with the technological development of the above-mentioned non-destructive methods, attempts to predict the properties of sawn timber already at the sawlog stage have begun to appear (Fischer et al. 2015; Krajnc et al. 2019; Simic et al. 2019).

In both cases, information about the geometric properties of wood can play a crucial role in predicting other properties. The geometric model can be used in computer simulations, but it can also refine the calculation of the density of logs, which often have a highly irregular shape. Wood moisture content significantly affects the physical and mechanical properties of wood. In general, the density of wood increases with increasing moisture content (Ross, 2010). A number of studies have also demonstrated the significant influence of moisture content on acoustic properties such as natural frequency or sound velocity (Unterwieser and Schickhofer, 2011). On the contrary, for wood with moisture content above fiber saturation, no significant effect of moisture on the dynamic modulus of elasticity was found when calculations are based on natural frequency (Rais et al. 2020). Determining the moisture content of a log for calculation correction can be technically challenging, as it is often

impossible to take the necessary samples from the log for kiln dry moisture determination method. There is a strong correlation between the density and moisture content of wood, so it can be used to predict real values. Accurate determination of this density is offered by new technologies, where calculations can be based on knowledge of the weight and volume of the trunk, with the volume of the trunk obtained using optical scans or scans taken by computed tomography.

This study is part of a larger project focused on designing models for predicting the mechanical properties of sawn timber based on non-destructive measurements of roundwood. The main objective is to assess the suitability of geometric reconstruction of logs using computed tomography to determine log moisture content. A secondary objective is to compare the results of geometric reconstruction obtained using computed tomography and standard manual measurement.

2. MATERIAL AND METHODS

In total 60 Norway spruce (*Picea abies* L.) sawlogs were processed. Logs came from the University Forest Enterprise Masaryk Forest in Křtiny. After transporting the sawlogs to the measuring area, samples were immediately taken to determine moisture content (Figure 1a). For each sawlog, a piece approximately 5 cm long was taken from the large diameter side of the log to determine the moisture content (Figure 1b). After that all samples were packed and transported to the Josef Ressel Research Centre in Útěchov to determine their moisture content. The weight of the samples was measured with an accuracy of 0.1 g using laboratory scale. The samples were then placed in a drying oven at a drying temperature of (103 ± 2) ˚C. The weight of the samples was measured during drying, with the drying process considered complete when the differences in weight between two consecutive weightings at 2-hour intervals did not differ by more than 0.1 %. The moisture content of the sample was calculated using equation (1). After sampling, all logs were weighed using a BAXTRAN STE 500kg (Giropès SL, Girona, Spain) scale (Figure 1c). The total weight of the sawlog was expressed with an accuracy of 0.1 kg.

$$w = \frac{m_1 - m_0}{m_0} \times 100, \quad (1)$$

where w is moisture content (%); m_1 is weight of test specimen before drying (g); m_0 is weight of test specimen after drying (g).

After sampling and weighing the sawlogs, manual measurements were performed in accordance with the Recommended Rules for Measuring and Grading of Roundwood in the Czech Republic 2008 (Recommended Rules 2007). A calibrated tree caliper and tape measure were used for these measurements. The diameter was measured in the middle of the trunk in two perpendicular directions, with the final thickness expressed as the arithmetic mean of these two measurements. Most of the logs were measured with bark. If bark was missing at the measurement point for a particular log, equation (2) was used to calculate the bark thickness based on the measurement closest to the mid-diameter. The bark thickness was then added to the mid-diameter for the purpose of calculating the volume of roundwood. The nominal length of all logs was 3 m, and the mid-diameter varied between 26.82 and 32.95 cm. Information on the dimensions of the logs based on manual measurements is provided in Table 1.

$$2k = p_0 + p_1 \times d_{sk}^{p_2}, \quad (2)$$

where k is bark thickness (cm); p_0 is 0.57723; p_1 is 0.006897; p_2 is 1.3123; d_{sk} is diameter of the log with bark (cm).

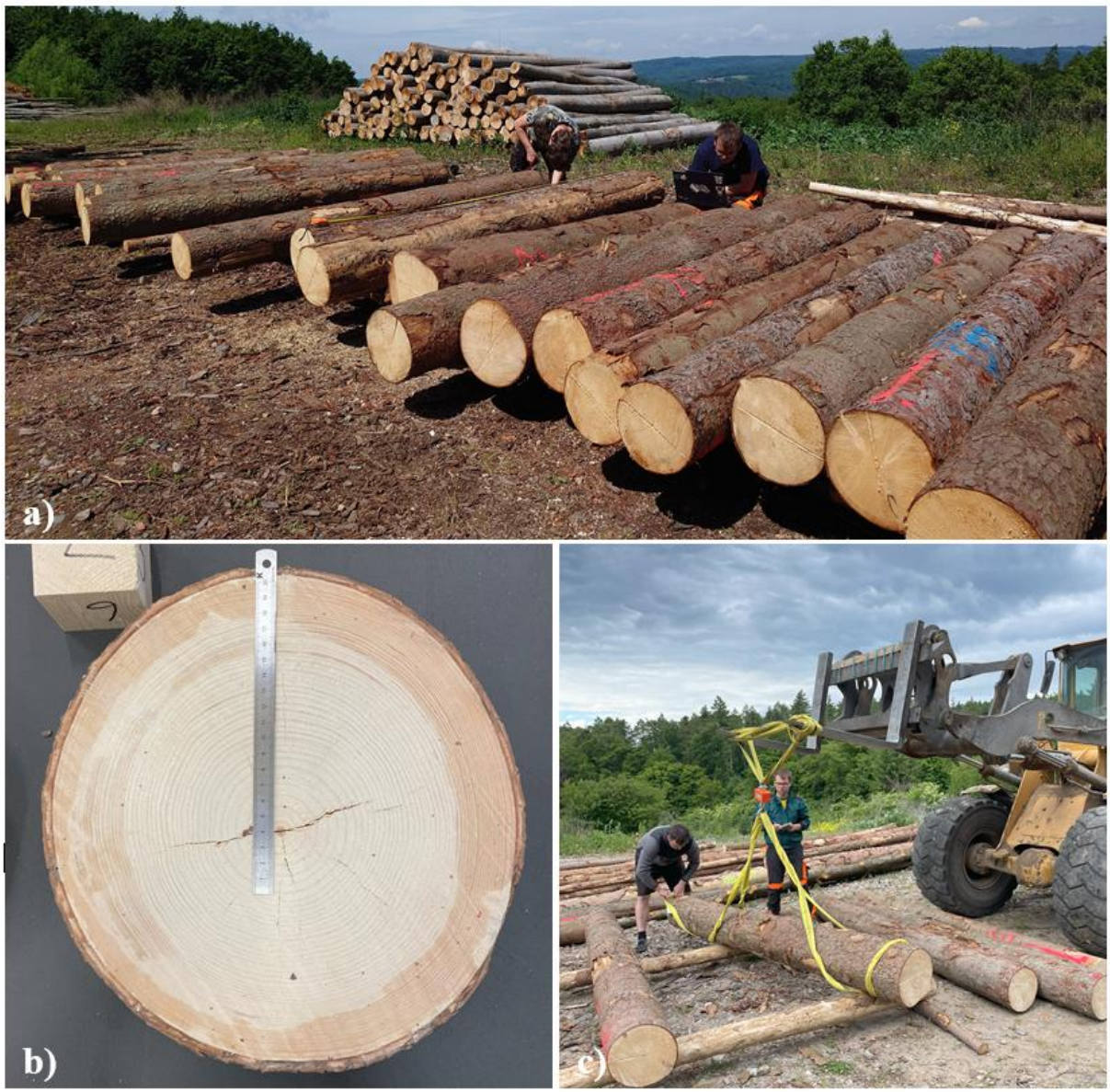

Figure 1. *Measuring area at the Sawmill Olomučany (a); Sample for the determination of the moisture content (b); Weighing of logs (c).*

Table 1.*Basic data of sawlogs according to manual measurement*

	Mean	Minimum	Maximum	St. dev.	CV (%)
Total length (cm)	300.88	299.80	302.30	0.46	0.15
Mid-diameter (cm)	29.30	26.82	32.95	1.57	5.36

St. dev. is Standard Deviation; CV is Coefficient of Variation

The volume of each log was calculated based on manual measurements using the Recommended Rules (2007) and equation (3). All resulting log volumes are based on the average value, including bark thickness.

$$V_{man} = \frac{\pi}{4} \times d_{sk}^2 \times l, \quad (3)$$

where V_{man} is log volume calculated based on the manual measurements (cm^3); l is total length of the log (cm).

After manual measurement was completed, all logs were transported to the National Forest Centre, Zvolen area, where they were scanned using an CT.LOG X-ray computed tomography scanner (MICROTEC, Bressanone, Italy). The CT scanner generated cross-sectional CT images composed of voxels with an in-plane resolution of 1x1 mm, while the images were acquired in longitudinal direction at 10 mm intervals. Results were exported to an image file in TIFF format after scanning. For each scan, TIFF format was transferred by palette for grayscale images in IrfanView (Irfan Skiljan, Jajce, Bosnia and Herzegovina). All scans were then uploaded to the program 3D Slicer (Brigham Women's Hospital, Boston, USA). Subsequently, image spacing was adjusted according to real conditions. For the purpose of volume reconstruction, segmentation was performed using a manually set threshold range. After segmentation was completed, the total volume was exported from all images in cm^3 units (Figure 2). The density of sawlogs based on manual measurement was calculated according to equation (4), while the density of sawlogs based on CT scanning was calculated according to equation (5).

$$\rho_{man} = \frac{m}{V_{man}} \times 10^{-6}, \quad (4)$$

where ρ_{man} is density based on the manual measurements (kg/m^3); m is total mass of the log (kg).

$$\rho_{CT} = \frac{m}{V_{\mathrm{CT}}} \times 10^{-6}, \quad (5)$$

where ρ_{CT} is density based on the computed tomography (kg/m^3);V_{CT} is total volume of the log based on the computed tomography (cm^3).

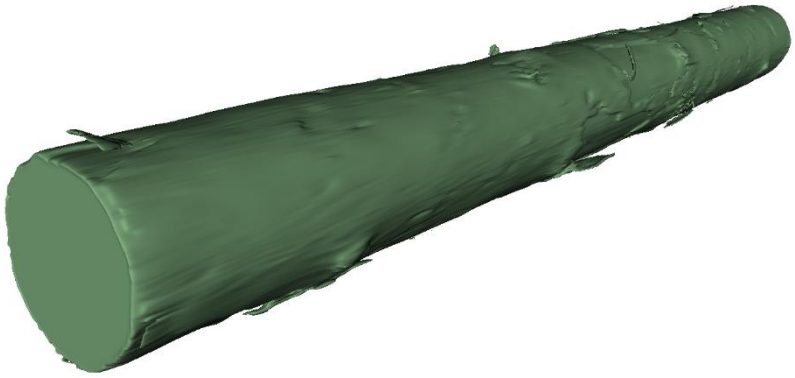

Figure 2. *Reconstructed volume of the log after the segmentation.*

3. RESULTS AND DISCUSSION

The results obtained are presented in Table 2. According to calculations, logs had significant moisture content variability, which can be considered as suitable conditions for assessing the relationship between density and moisture. Only two logs had moisture content lower than the fiber saturation point, with the lowest measured moisture content being nearly 25 %. The average density achieved was 679.8-687.9 kg/m^3 at an average moisture content of 60.6 % is similar to the findings reported by other authors, with Rais et al. (2014) report a spruce logs density 672 kg/m^3 at a moisture content of 58 %, and Unterwieser and Schickhofer (2011) report a density 620 kg/m^3 at a moisture content of 65.7 %. Edlund et al. (2006) generally state green spruce logs density to be 700–1 050 kg/m^3, so it can be concluded from these results that moisture content has a significant effect on wood density. The cause of lower density variability can be explained by the relatively similar dimensions of the logs, resulting in low variability in volume, which is included in the density calculation.

Table 2. *Basic descriptive statistics of the results obtained.*

	Mean	Minimum	Maximum	St. dev.	CV (%)
w (%)	60.6	24.9	115.7	17.9	29.5
m (kg)	138.3	94.5	199.0	22.6	16.3
V_{man} (cm^3)	203 411	169 597	256 410	22 000	10.8
V_{CT} (cm^3)	200 963	166 301	257 700	21 675	10.8
ρ_{man} (kg/m^3)	679.8	491.6	840.6	81.1	11.9
ρ_{CT} (kg/m^3)	687.9	511.4	866.0	80.7	11.7

The relationship between density according to both calculation methods and log moisture content is shown in Figure 3. Both methods of volume determination show a very similar relationship to moisture content, which is expressed by the Pearson correlation coefficient $r = 0.7166$ for manual measurement and $r = 0.7195$ for computed tomography. Unterwieser and Schickhofer (2011) reported a stronger correlation between density and moisture content, but it should be recognized that these experiments were conducted on sawn timber with a much more uniform structure and moisture distribution. Based on our results, it can be clearly confirmed that log density increases with increasing moisture content, however, this moisture content can only be predicted approximately based on density. The prediction can be further improved by including additional log parameters that directly affect wood density but do not significantly affect moisture content. Such parameters include, for example, the presence of compression wood, the proportion of latewood, or the average width of growth rings (Požgaj et al. 1993).

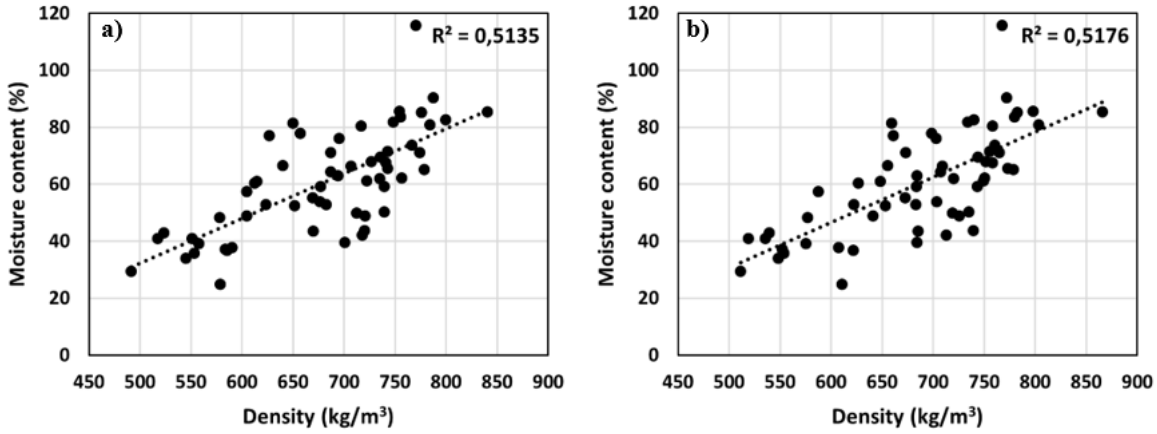

Figure 3.: *Relationship between log moisture content and density determined by manual measurement (a); Relationship between log moisture content and density determined by computed tomography (b).*

The results of determining the volume of roundwood using both methods were compared with the box plot shown in Figure 4. Statistical tests were performed to compare these methods. First, the Shapiro-Wilk test was performed with a significance level of $\alpha = 0.05$. According to the test results, the p-value is 0.0933, which assumes that the data are normally distributed. Based on this, a Paired T-Test was performed with a p-value of 0.0020. Since the p-value is below the set limit of significance level $\alpha = 0.05$, the null hypothesis is rejected – the population means are considered unequal, and a statistically significant difference between the results of the two methods for determining volume was confirmed. The comparison clearly shows that the average log volume determined using computed tomography is higher than the results based on manual measurement. The advantage of computed

tomography is a more accurate reconstruction of the volume and bark over the entire length of the log, whereas manual measurement is based only on the value at a single middle point.

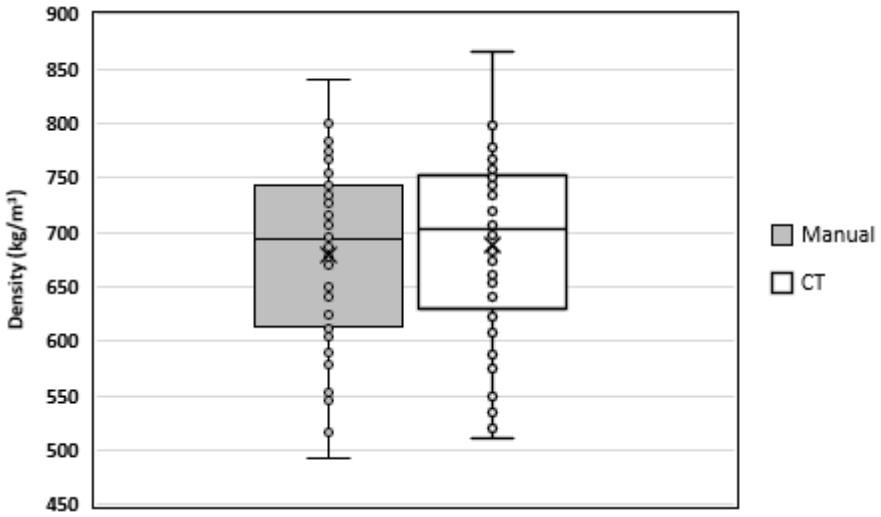

Figure 4. *Box plot for density determined by manual measurement and by computed tomography.*

4. CONCLUSIONS

Computed tomography can be used to easily and accurately reconstruct the volume and create a 3D model of the log, which can serve as input for subsequent analyses and quality assessments. The volume determined using computed tomography is statistically different from the volume determined by manual measurement, with the average log volume being larger according to the results obtained from the processed CT scans. Manual measurement is inaccurate mainly due to the calculation of volume based on thickness at a single point. However, in the case of high-quality roundwood with a uniform shape and surface, the results of manual measurement differ by only 2-3 % compared to 3D reconstruction using computed tomography. When comparing the two volume measurement methods investigated, it can be stated that moisture content correlates slightly better with density determined based on CT scan processing ($r = 0.7195$ against $r = 0.7166$). Predicting log moisture content based on density alone is not very accurate, so it is advisable to include other parameters in the future – for example average width of growth rings.

ACKNOWLEDGEMENTS

This study was funded by internal project agency of Faculty of Forestry and Wood Technology [IGA25-FFWT-IP-022] and cofunded by the European Commission under the LignoSilva project [Grant Agreement #101059552] from the Horizon Europe Teaming for Excellence call within the action of the internal project agency of the National Forestry Center.

REFERENCES

1. Edlund, J., Lindström, H., Nilsson, F., Reale, M. (2006): Modulus of elasticity of Norway spruce saw logs vs. structural lumber grade. Holz als Roh- und Werkstoff 64: 273–279.
2. Fischer, C., Vestøl, G.I., Øvrum, A., Høibø, O.A. (2015): Pre-sorting of Norway spruce structural timber using acoustic measurements combined with site-, tree- and log characteristics. European Journal of Wood and Wood Products 73: 819–828.
3. Krajnc, L., Farrelly, N., Harte, A.M. (2019): Evaluating timber quality in larger-diameter standing trees: rethinking the use of acoustic velocity. Holzforschung 73: 797–806.
4. Ministry of Agriculture of the Czech Republic (2007). The Recommended Rules for Measuring and Grading of Roundwood in the Czech Republic 2008. Lesnická práce s.r.o., Prague, Czech Republic (in Czech).

5. Olsson, A., Pot, G., Viguier, J., Fayidi, Y., Oscarsson, J. (2018): Performance of strength grading methods based on fibre orientation and axial resonance frequency applied to Norway spruce, Douglas fir and European oak. Annals of Forest Science 75: 102.
6. Požgaj, A., Chovanec, D., Kurjatko, S., Babiak, M. (1993): Štruktúra a vlastnosti dreva. Príroda, Bratislava, Slovakia (in Slovak).
7. Rais, A., Pretzsch, H., Kuilen, J.W. (2014): Roundwood pre-grading with longitudinal acoustic waves for production of structural boards. European Journal of Wood and Wood Products 72: 87–98.
8. Rais, A., Pretzsch, H., Kuilen, J.W. (2020): European beech log and lumber grading in wet and dry conditions using longitudinal vibration. Holzforschung 74: 939–947.
9. Rais, A., Ursella, E., Vicario, E., Giudiceandrea, F. (2017): The use of the first industrial Xray CT scanner increases the lumber recovery value: case study on visually strength-graded Douglas-fir timber. Annals of Forest Science 74: 28.
10. Ridley-Ellis, D., Stapel, P., Baño, V. (2016): Strength grading of sawn timber in Europe: an explanation for engineers and researchers. European Journal of Wood and Wood Products 74: 291–306.
11. Ross, R.J. (2010): Wood handbook: wood as an engineering material. Forest Products Laboratory USDA Forest Service, Madison, USA.
12. Simic, K., Gendvilas, V., O´Reilly, C., Harte, A.M. (2019): Predicting structural timber grade-determining properties using acoustic and density measurements on young Sitka spruce trees and logs. Holzforschung 73: 139–149.
13. Takahashi, Y., Ishiguri, F., Nezu, I., Endo, R., Kobayashi, S., Tanabe, J., Otsuka, K., Ohshima, J., Yokota, S. (2022): Sawn-timber quality of six half-sib families of hinoki cypress (Chamaecyparis obtusa (Siebold et Zucc.) Endl.). WOOD MATERIAL SCIENCE & ENGINEERING, 18(4): 1163-1170.
14. Unterwieser, H., Schickhofer, G. (2011): Influence of moisture content of wood on sound velocity and dynamic MOE of natural frequency- and ultrasonic runtime measurement. European Journal of Wood and Wood Products 69: 171–181.
15. Uzcategui, M.G.C., França, F.J.N., Seale, R.D., Senalik, C.A., Ross, R.J. (2023): Nondestructive Evaluation of 2 by 10 Southern Pine Lumber. Forest Products Journal, 73(3): 186–193.
16. Weidenhiller, A., Sandor, B., Simlinger, T., Brüchert, F., Huber, J.A.J. (2023): Prediction of douglas fir sawn timber yield based on log computed tomography. In: Proceedings World Conference on Timber Engineering (WCTE 2023), Oslo, Norway.

NUMERICAL ANALYSIS OF MOISTURE TRANSPORT IN CLT

Jan Tippner[1], Barbora Vojáčková[1], Richard Slávik[1], Pavlína Suchomelová[1]

Mendel University in Brno, Czech Republic,
Faculty of Forestry and Wood Technology,
e-mail: jan.tippner@mendelu.cz; barbora.vojackova@mendelu.cz;
richard.slavik@mendelu.cz; pavlina.suchomelova@mendelu.cz

ABSTRACT

Structural components made from wood and natural fibres are popular due to their favourable mechanical and physical properties, as well as their environmental benefits across the life cycle. However, the use of wood-based structural elements introduces risks, particularly related to increased moisture content and coupled mechanical loading.

The COMET Module project i3Sense aims to develop integrated sensing systems for monitoring key parameters such as moisture content, mechanical strain, and temperature within wood-based composites and structures. One of the project's tasks is the optimisation of the sensor placement in relation to the distribution of physical fields.

To support optimization, a physical analysis based on numerical simulation of moisture transport is being conducted. The modelling approach differentiates moisture behaviour below and above the fibre saturation point by the implementation of diffusion and permeability coefficients. Finite element models are implemented in the COMSOL Multiphysics software.

Keywords: finite element method, moisture diffusion, free water movement, CLT panels.

1. INTRODUCTION

Wood and wood-based composites, particularly cross-laminated timber (CLT), are increasingly used in structural engineering due to their favorable mechanical performance and environmental benefits across the life cycle (Ramage et al., 2017). However, wood's variable, hygroscopic, anisotropic, and heterogeneous nature poses challenges in predicting its long-term structural behavior under varying environmental conditions. Changes in moisture content (MC) strongly influence wood's durability, mechanical properties, dimensional stability, and susceptibility to cracking, particularly when combined with thermal and mechanical loads (Siau, 1995; Hameury, 2005).

Moisture transport in wood involves complex multi-phase interactions between free water, bound water in the cell wall, and water vapor. Below the fiber saturation point (FSP), bound water diffusion dominates, whereas above the FSP, capillary-driven transport and free water movement become critical (Autengruber et al., 2020). This transition introduces nonlinearity and coupling effects that significantly affect the accuracy of predictive models (Trcala, 2012).

Numerical modeling has been employed to describe such transport phenomena. Early approaches were rooted in macroscopic laws, applying Fick's law for mass diffusion and Fourier's law for heat transfer (Babiak, 1995; Sherwood, 1929). Later developments introduced multiphysical frameworks based on irreversible thermodynamics (Luikov, 1966; Whitaker, 1977), enabling the inclusion of coupled hygrothermal effects such as thermo-diffusion (Soret effect) and heat flux induced by water migration (Dufour effect) (Avramidis et al., 1992; Lewis and Ferguson, 1993). While these approaches advanced a modeling approach, they often relied on back-calculated material parameters that lacked clear physical meaning, thereby limiting generalization (Eitelberger and Hofstetter, 2011).

Recent research has introduced significant refinements and applications to wood-based composites. Brandstätter et al. (2024) demonstrated, via two-dimensional simulations, how geographic factors and altitude influence MC distributions in CLT, directly linking moisture gradients to cracking risk and highlighting shortcomings of current standards. Anisotropic hygrothermal modeling by Kalbe et al. (2024) introduced a performance criterion for end-grain moisture safety in CLT, addressing challenges during construction and exposure. Wang et al. (2023) validated hygrothermal models with

field data on CLT end-grain exposure, underscoring the need for precise calibration of moisture storage functions and water absorption coefficients. Beyond pure hygrothermal modeling, coupled moisture–mechanical study (Sun et al., 2025) integrates mechano-sorptive creep and examines long-term deformation of CLT under humidity variations.

The FFG COMET Module project *i3Sense* (I*ntelligent, integrated and impregnated cellulose-based sensors for reliable biobased structures*) aimed to develop integrated sensing systems for monitoring key parameters such as moisture content, mechanical strain, and temperature in wood-based composites. One of the tasks is the optimization of sensor placement in relation to evolving physical fields. To support this, we conduct numerical simulations of moisture transport in CLT using a bifurcated approach, distinguishing between bound-water diffusion below FSP and permeability-driven flow above FSP. Numerical models of moisture transport are implemented using finite-element frameworks in COMSOL Multiphysics.

2. MATERIAL AND METHODS

2.1.Experiment

To investigate moisture transport mechanisms and validate numerical models at the material level, an experiment was conducted using two sets of small spruce (*Picea abies* (L.) H. Karst) and beech (*Fagus silvatica* L.) samples. Each set consisted of four specimens with dimensions of 0.02 × 0.02 × 0.3 m (Fig. 1).

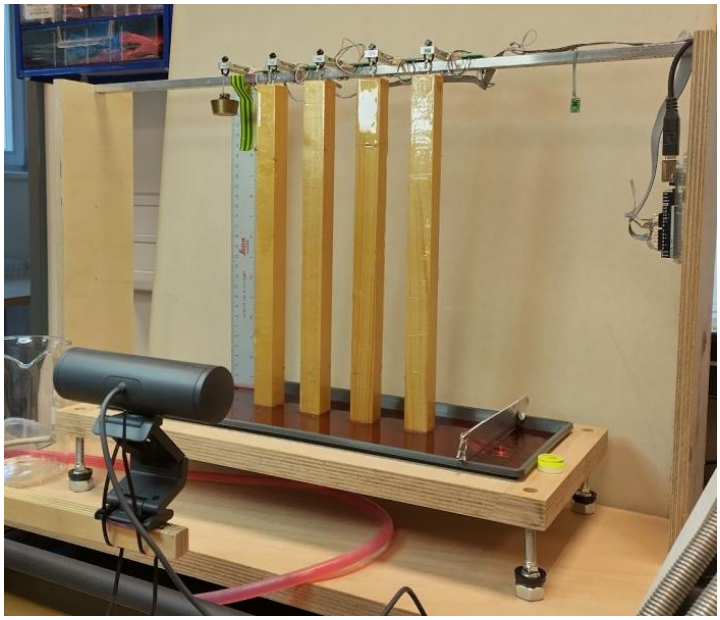

Figure 1. *Experimental set-up for material level validation on small samples.*

The samples were suspended vertically with their lower ends submerged in water. Mass gain of samples and their environmental conditions (temperature and relative humidity) were monitored by a multi-channel board (Atmel328 microcontroller, Microchip Technology Inc, USA) and sensors (SENSIRION SHT21, Mouser Electronics Inc., USA).

The first set of samples had their side walls coated with epoxy resin, restricting the exchange of moisture with the environment. This setup was designed to simulate one-dimensional moisture flow along the longitudinal axis of the wood. The second set remained untreated, with open side walls, allowing for multidirectional moisture exchange. The water level in the soaking container was maintained at a constant height throughout the experiment. The samples were monitored over a period of 27 days.

The experiment provided data for calibrating and validating numerical models aimed at simulating moisture transport in wood, considering its orthotropic nature, the combined effects of moisture diffusion below the FSP, free water movement (above FSP), and moisture exchange with the environment through the surfaces.

To gain an understanding of moisture transport in cross-laminated timber (CLT) panels, two samples (dimensions: 0.9 × 0.2 × 0.1 m) were subjected to a water soaking experiment. Each sample was suspended vertically with its bottom edge submerged in water for a period of 11 days. During this time, ambient air humidity and temperature, and the mass of samples were continuously monitored.

Eight sensors (SENSIRION SHT21, Mouser Electronics Inc., USA) were installed on each sample at three positions (two on the sides and one in the centre) along the panel length (Fig. 2). Two additional sensors were placed in the surrounding environment to monitor ambient conditions. Data acquisition was performed using a multi-channel board (Atmel328 microcontroller, Microchip Technology Inc, USA).

Sample A had open side walls, allowing moisture transfer in all directions and exchange between the air environment and the sample. Sample B had its side walls sealed with aluminium foil, restricting transport to the front and back surfaces only. The water level in the soaking container was maintained at a constant height throughout the experiment.

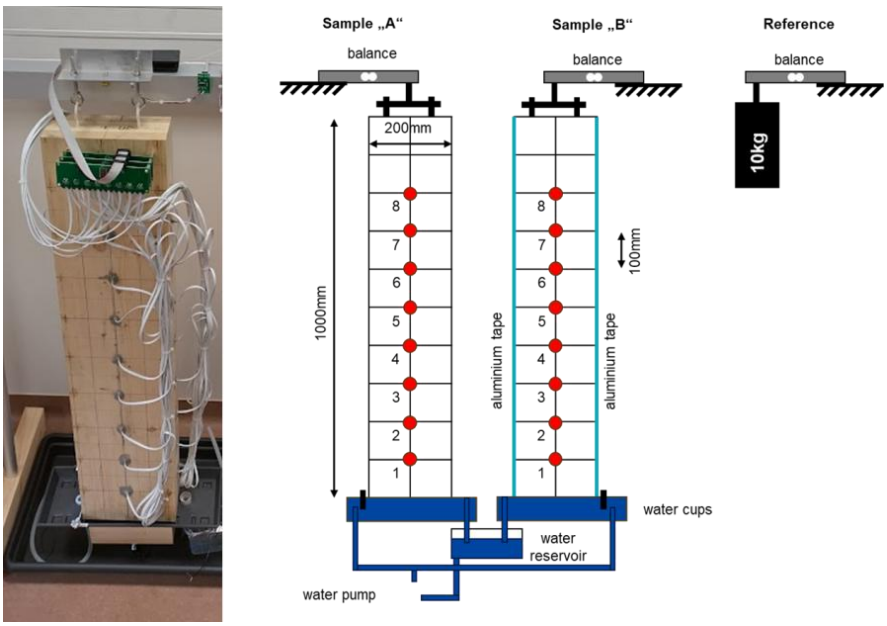

Figure 2. *Set-up for water uptake monitoring of CLT samples.*

2.2. Numerical modelling

A numerical model of coupled moisture transport below and above FSP, using separate diffusion and permeability coefficients for each regime, was developed using COMSOL Multiphysics version 6.2 (COMSOL AB, Sweden), a simulation platform based on the finite element (FE) method.

A three-dimensional (3D) model was built, with governing equations implemented via the Partial Differential Equation (PDE) interface, following a similar approach to that described by Suchomelová et al. (2019). Moisture transport was modelled as a combined process, integrating both moisture diffusion and free-water movement. Moisture diffusion (M_d), driven by concentration gradient and described by Fick's law, uses diffusion coefficients (D, eq. 1). For the movement of free-water (M_f), driven by pressure gradients, the equation based on Darcy's law uses the permeability coefficients (P, eq. 2).

$$\frac{\partial M_d}{\partial t} - \nabla(D\nabla M_d) = 0 \qquad (1),$$

$$\frac{\partial M_f}{\partial t} - \nabla\left(P\nabla M_f\right) = 0 \qquad (2),$$

The diffusion coefficients were defined as a function of MC and calculated to the FSP (set at 28% MC), following Suchomelová et al. (2019). The permeability coefficients are also moisture-dependent up to full saturation. The mathematical derivation of permeability coefficients was based on Autengruber et al. (2020); the permeability coefficients for longitudinal, radial, and tangential (L, R, T) directions were determined using the following equation:

$$P = K\left(-0.61\left(12400\left(\frac{M_d}{f_{lum}\rho_{H2O}}\right)^{-0.61}\right)\right)\frac{1}{M_d} \quad (3),$$

where K is the absolute permeability defined by Autengruber et al. (2020); f_{lum} volume proportion of the cell lumen depending on the bound water concentration.

The geometry of the model was represented by a solid block with dimensions corresponding to the experiment (0.02 × 0.02 × 0.3 m), Fig. 3. The geometrical axes corresponded to anatomical directions (L= Z, R = Y, T = X). The maximum element size was set to 0.005 m, and the overall number of domain, boundary, and edge elements was 1180.

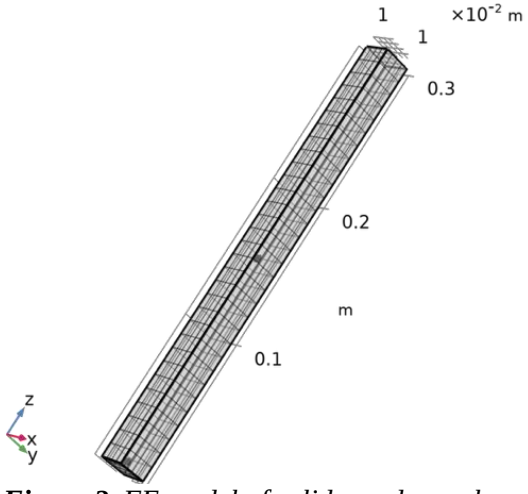

Figure 3. *FE model of solid wood sample.*

The initial conditions (MC = 1%) were assumed to be uniform throughout the entire volume. MC value for the diffusion component of moisture transfer was set below the FSP, in accordance with experimental observations, while the free-water component was initialized at the FSP.

Boundary conditions, applied on all open walls except the bottom one (intake), were implemented using the predefined flux/source equations in COMSOL Multiphysics. Based on Suchomelová et al. (2019) the adsorption/impedance term was defined by the moisture transfer coefficient (α_M), and the flux/source term was defined as α_M multiplied by potential equilibrium moisture content (EMC) corresponding to the ambient environment conditions (temperature, humidity) during the experiment. The Dirichlet boundary conditions were applied on the bottom wall (intake). The solution was a time-dependent nonlinear, with a time step 600 s, and the integrated solver MUMPS was used.

Default range of selected basic physical parameters for the testing of material models of spruce and beech were: oven-dry density: 516 / 705 kg.m^{-3}; moisture transfer coefficient (α_M): 5.10^{-6} - 5.10^{-9} m^{-1}; longitudinal diffusion coefficient (D_L): 2.10^{-8} - 2.10^{-9} (-); transversal diffusion coefficient (D_T): 1.10^{-9} - 1.10^{-11} (-); longitudinal permeability coefficient (P_L): 2.10^{-2} - 2.10^{-6} g.m^{-9}; transversal permeability coefficients (P_T): 2.10^{-2} - 2.10^{-6} g.m^{-9}. However, full orthotropy with MC-dependency was definde.

The equation-based prescription of MC dependencies for all material and boundary conditions parameters was used in the COMSOL Multiphysics environment. The calibrated and validated physical model of solid wood response was adopted for a 3D model of CLT panel sample with the dimensions, boundary conditions, and initial conditions corresponding to the experiment. The geometry of the model was represented by an interacting three solid-block layers with overall dimensions corresponding to the experimental CLT sample (0.9 × 0.2 × 0.1 m), Fig. 4. The geometrical axes corresponded to anatomical directions of layers (L= Z, R = Y, T = X for two outer surface layers; L= X, R = Z, T = Y for inner layer). The interaction between layers (bond line) was simplified to fully coupled regions (shared FE nodes), and the complex influence of the bond line was simplified and represented by calibrated material parameters of wood. The maximum element size was set to 0.01 m, and the overall number of domain, boundary and edge elements was 7992. The solution

was realized as a time-dependent nonlinear (12 days in total), with a time step of 20 minutes, and the integrated solver MUMPS was used.

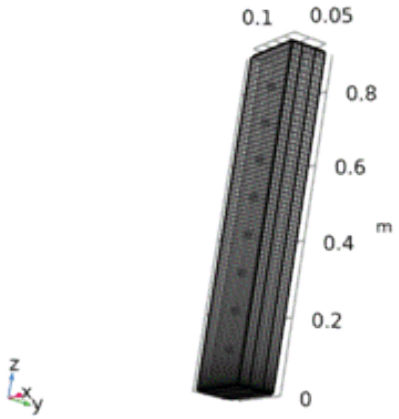

Figure 4. *FE model of CLT sample.*

3. RESULTS AND DISCUSSION

The experimental evaluation was based on mass recording. The change of MC was calculated in principle of the gravimetric method and represented by time-history plots. Typical postprocessing outputs from FE simulation consist of a) nodal contour plots of MC distribution, and b) time-history listing of MC values – local (nodal) values and average values calculated for selected regions. These outputs were used for experimental validation.

3.1. Small sample model validation

Fig. 5 illustrates the development of MC distribution in 3 time steps, where the region with higher values of MC, even in later periods, shows evident distribution restrictions to the area close to the intake of water.

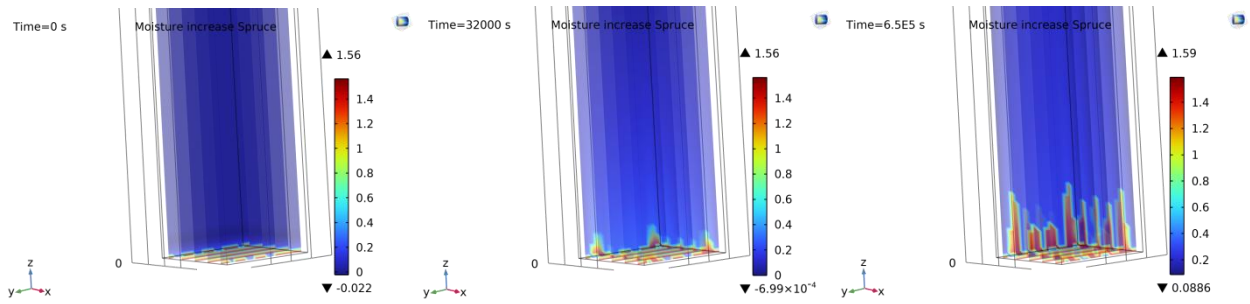

Figure 5. *Nodal solution of MC in 0 seconds, 9 hours, and 7.5 days.*

Fig. 6 shows behaviour of small-sample models for beech and spruce under different initial conditions and boundary conditions. The time-history of a) bound water - increasing MC from 5% to 15%, b) bound water - decreasing MC from 15% to 5%, c) mixed free and bound water - increasing MC from 5% to 18%, shows a physically consistent response in drying, wetting, and soaking water. In next, d) comparison of MC development on the surface and inside the sample verifies the consistency transversal distribution of MC in transient tasks too.

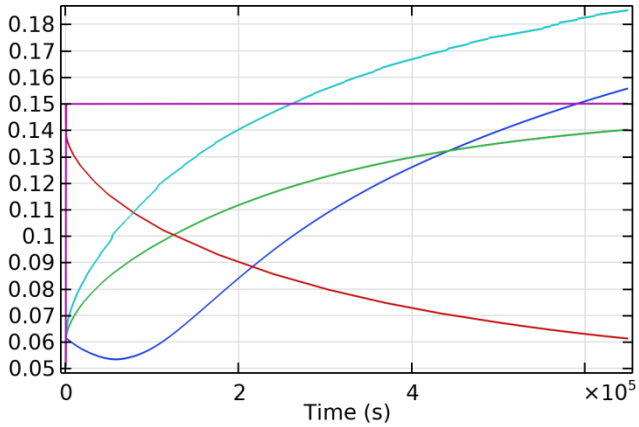

Figure 6. *Verification of small-sample model with different initial and boundary conditions. Average MC (-) for spruce; red curve - drying, green - wetting, cyan - wetting + soaking (for which the violet is from the surface, blue from the middle of the sample).*

The influence of moisture exchange with environment, represented by α_M was tested on the responses of FE models by closing lateral walls. The insulation also has an impact on the anisotropy of water transport in solid (3D to one-directional). For the insulated case, an increase of moisture uptake, at 7.5 days, is about 31% higher for beech and 48% for spruce (Fig. 7).

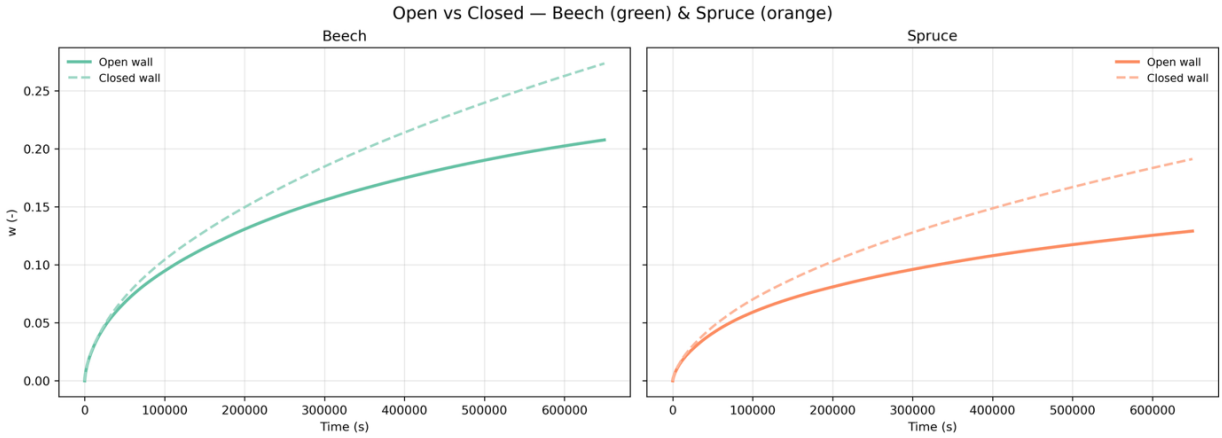

Figure 7. *Verification of the influence of boundary conditions for beech (green) and spruce (orange). Solid lines – open wall with transfer to air environment, dashed line – closed wall (insulated by resin).*

The experimentally observed MC increase for spruce with open walls (not treated with resin) over 7.5 days was 13%, with very low variability. For beech, there was a 20% MC increase, but with higher variability among the samples (Fig. 8). Two samples showed an increase in MC similar to spruce (11% and 13% MC change), while two others exhibited much higher values (27% and 43%). This variability in moisture uptake is particularly interesting because the variability in density of the small samples was low (coefficient of variation: 5% for spruce, and only 2% for beech). Moreover, the samples were high quality (defect-free, of regular structure) and visually similar (fibre orientation, annual ring thicknesses), suggesting that microscopic or chemical factors may play an influential role.

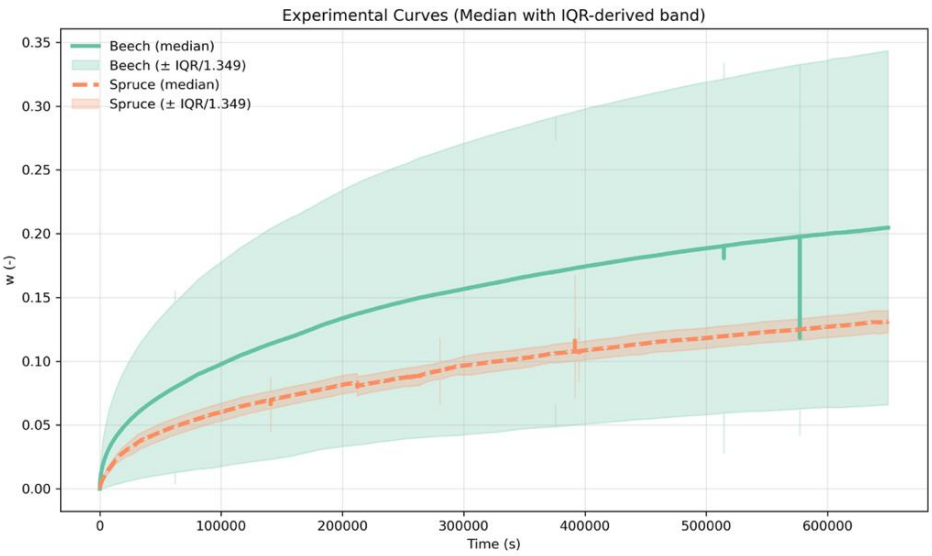

Figure 8. *Experimental validation - time-history of MC for spruce (orange) and beech (green) with corresponding intervals of variability.*

The FE model of the MC increase in spruce required calibration. This was achieved through a sensitivity analysis (500 loop computations for testing of input parameters, Fig. 8), in which the optimized values of parameters included the moisture transfer coefficient (α_M), permeability coefficients (P_L, P_R, P_T), and diffusion coefficients (D_L, D_R, D_T), all in the longitudinal, radial, and tangential directions. The parameters with significant influence were α_M, P_L, and D_L. The best-fit model yielded an α_M of 5×10^{-9} m^{-1}, a P_L ranging from 0.0014×10^5 and exponentially decreasing to 0.0001×10^5, and a D_L exponentially increasing from 2.06×10^{-9} to 2.18×10^{-9} .

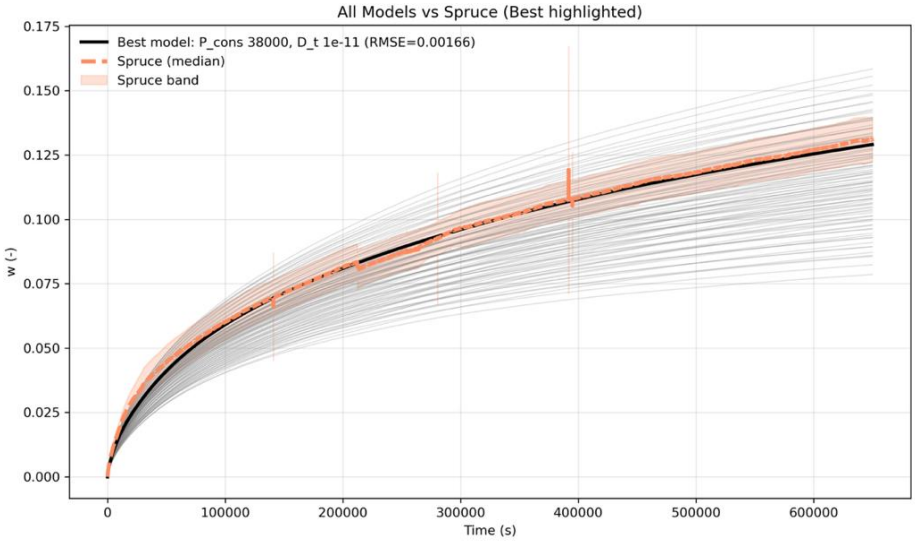

Figure 9. *Sensitivity analysis for spruce small samples – the range of FE models' responses compared to experimental records of MC.*

For beech (Fig. 9) the calibration was mainly concentrated on the properties which differ from spruce, and the sensitivity analysis contains only 20 computations. P_L, D_L *and* D_R with D_T were calibrated. P_L ranging from 0.0055 and exponentially decreasing to 0.0004, and a D_L exponentially increasing from 2.06×10^{-8} to 2.18×10^{-8}, and D_R 4.2×10^{-10} to 5.8×10^{-10}.

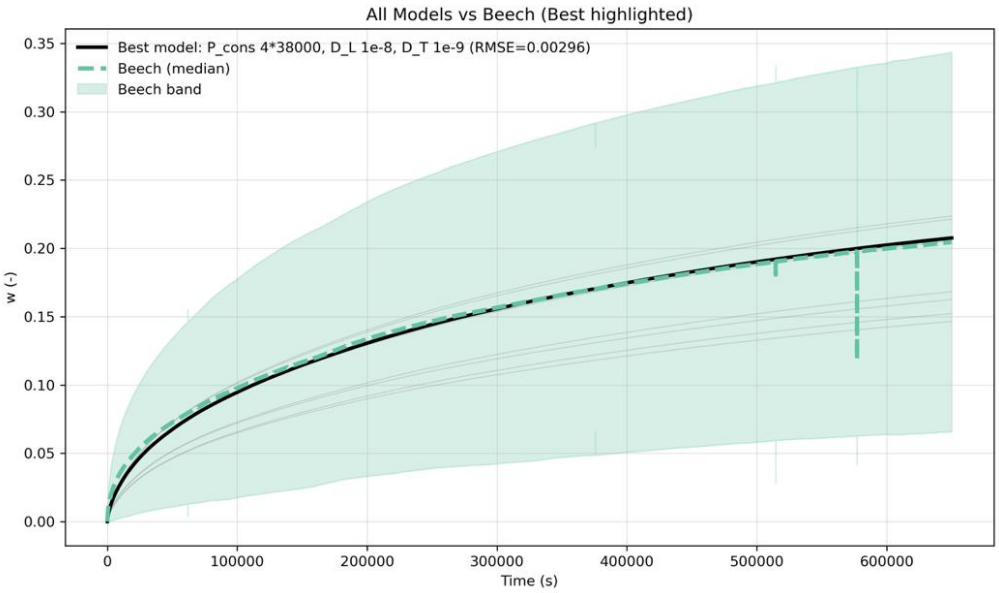

Figure 10. *Sensitivity analysis for beech small samples – the range of FE models' responses compared to experimental records of MC.*

3.2. CLT-sample model validation

Fig. 11 illustrates experimentally evaluated distributions of MC in CLT samples for case studies with different boundary conditions (open or closed by non-permeable insulation on lateral sides). The highly variable original data were filtered, the smooth MC distributions show: 1) comparable MC values between lateral sensors, 2) differences between centre and lateral sensors, 3) consistent increase of MC of all sensors in time. The closed samples show 1) higher values of MC in central sensors in comparison to the closed sample, 2) higher MC values measured by central sensors in comparison to the lateral one, 3) higher velocity of MC increase in time for the central part in comparison to less-intensive MC increase in insulated regions.

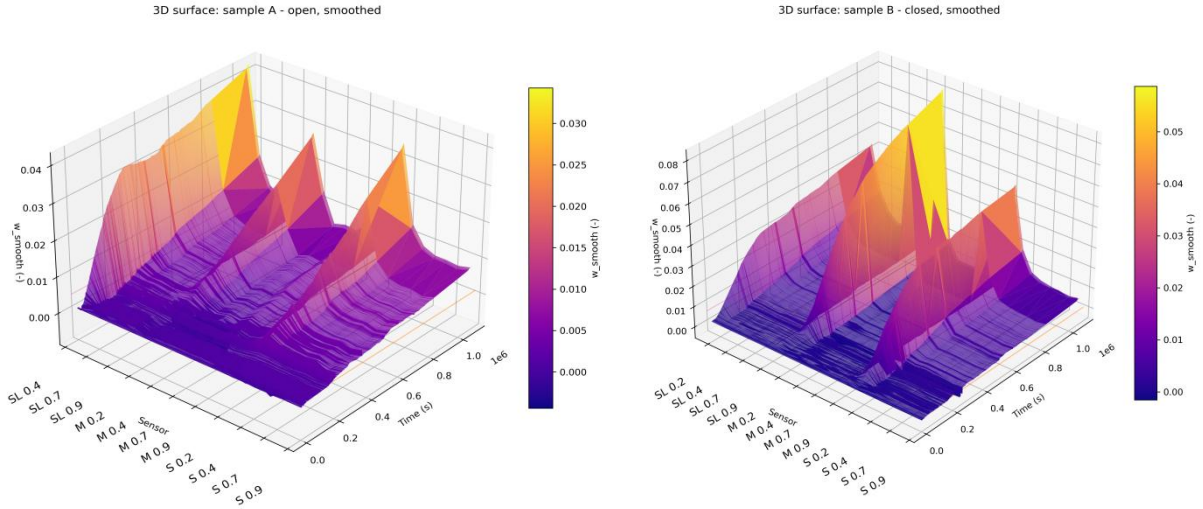

Figure 11. *Experimentally evaluated MC distribution in CLT sample– sensor values in time for open vs. closed lateral walls.*

The outputs of the numerical study of CLT samples are shown on the Fig. 12 with a contour plot of the nodal solution of MC. The distribution points to a low-lying region with higher MC values,

followed by a large region with MC corresponding to a common range of EMC during use of CLT construction. The sharp MC distribution with the highest gradient of MC in the region up to approx. 0.1 m is supported by a trend of experimental data (Fig. 11). A satisfactory agreement of experimental and simulation data in the time domain at initial part of process is illustrated on Fig. 13 too.

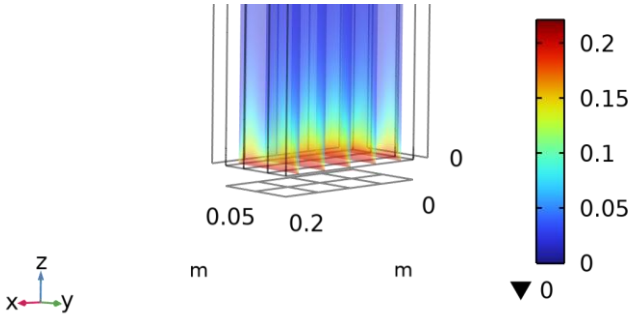

Figure 12. *Nodal solution of MC in CLT sample, detailed distribution of the bottom of the sample in steady state (at terminating time).*

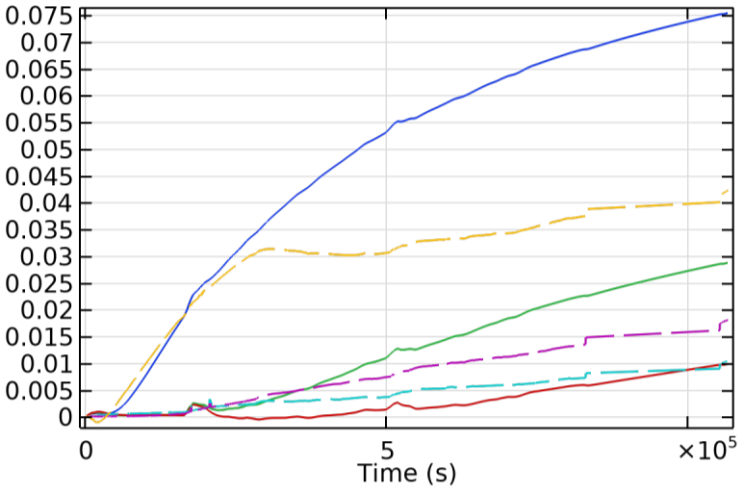

Figure 13. *Time-history plots of MC (-) in 0.1, 0.2, 0.3 m height positions (dashed line – experimental values, solid line – FE model).*

4. CONCLUSIONS

The FE transient simulation in COMSOL Multiphysics software successfully predicted moisture transport in wood, considering its orthotropic nature, coupled effects of moisture diffusion below FSP, free-water movement above FSP, and moisture exchange between the surface and the air environment.

The process of model building based on material validation on small-scale solid wood samples, and up-scaling to real-scale CLT models was successfully applied.

The physical consistency of the model was verified by testing alternating scenarios 1) with/without water intake (moisture movement above/below FSP), and 2) different initial conditions (MC) and boundary conditions (air humidity and temperature), inducing an increase or decrease of EMC.

The verified model with consistent physical response under different scenarios was calibrated and experimentally validated for 2 materials (spruce and beech solid wood). The experiment of longitudinal water soaking of small solid wood samples (0.02 × 0.02 × 0.3 m) was used for the validation.

A material model was applied to a case study of a 3-layered CLT. The numerical model of the CLT sample (0.9 × 0.2 × 0.1 m) water soaking was experimentally validated at 2 scenarios of

environment boundary conditions (open or closed lateral sides). Validated model of CLT brought a time-dependent 3D description of MC distribution. Results show a high gradient of MC in the bottom region of the sample (close to contact with the water level) and a relatively homogeneous response in regions above the 0.1 m level. This behaviour should be respected in the design of sensors and their placement, and data interpretations during CLT construction monitoring, as well.

The FE model of CLT was used for what-if scenarios covering changes of material parameters (parameters' variability, anisotropy ratios), initial conditions (MC) and boundary conditions (air humidity). The response was highly influenced by the alteration of transfer coefficients (αM), longitudinal dinal diffusion coefficient (D_L) and longitudinal permeability coefficient (P_L).

Based on MC outputs, the several types of regions relevant to sensor placement can be recognized: bottom region (below 0.05 - 0.1 m) with MC above FSP, the region about FSP, the region with increased MC (easily detectable by sensors), large region (above approx. 0.3 m) with MC vary in common range corresponds naturally to oscillations during year, where the detection can be complicated.

Next research aims to 1) add geometry-defined glue-line regions, 2) add full structure composition (wall layers and connections), 3) involve in-situ environment parameters in long-term life cycle, 4) use probabilistic approach dealing with variability of materials and conditions, 5) application of models for in-practice monitoring during water-hazard incidents.

ACKNOWLEDGMENT

This work has been supported by COMET module project "i3sense" (Intelligent, integrated and impregnated cellulose-based sensors for reliable biobased structures, project number: FO999888361) funded by the Austrian ministries BMK, BMAW, and the federal states of Upper Austria, Lower Austria, and Carinthia, operated by the FFG.

REFERENCES

1. Autengruber, M., Lukacevic, M., Füssl, J. (2020): Finite-element-based moisture transport model for wood including free water above the fiber saturation point. International Journal of Heat and Mass Transfer, 161:120228.
2. Avramidis, S., Englezos, P., Papathanasiou, T. (1992): Dynamic Nonisothermal Transport in Hygroscopic Porous Media: Moisture Diffusion in Wood. American Institute of Chemical Engineers, 38:1279–1287.
3. Babiak, M. (1995): Is Fick's law valid for the adsorption of water by wood?, Wood Science and Technology, 29:227–229.
4. Brandstätter, F., Autengruber, M., Lukacevic, M., Füssl, J. (2024): The influence of geographical location on moisture distribution in wood cross sections: a numerical simulation study using Austria as an example. Journal of Wood Science 70(1):35.
5. Kalbe, K., Kalamees, T., Kukk, V., Ruus, A., Annuk, A. (2022): Wetting circumstances, expected moisture content, and drying performance of CLT end-grain edges based on field measurements and laboratory analysis, Building and Environment, 221:109245.
6. Eitelberger, J., Hofstetter, K. (2011): A comprehensive model for transient moisture transport in wood below the fiber saturation point: Physical background, implementation and experimental validation. International Journal of Thermal Sciences, 50(10):1861–1866.
7. Hameury, S. (2005): Moisture buffering capacity of heavy timber structures directly exposed to an indoor climate: A numerical study. Building Environment 40(10):1400–1412.
8. Lewis, R.W., Ferguson, W.J. (1993): A partially nonlinear finite element analysis of heat and mass transfer in a capillary-porous body under the influence of a pressure gradient. Applied Mathematical Modelling, 17(1):15-24.
9. Luikov, A.V. (1966): HEAT AND MASS TRANSFER IN CAPILLARY-POROUS BODIES, in: Heat and Mass Transfer in Capillary-Porous Bodies. Elsevier, pp. 233–303.
10. Ramage, M.H., Burridge, H., Busse-Wicher, M., Fereday, G., Reynolds, T., Shah, D.U., Wu, G., Yu, L., Fleming, P., Densley-Tingley, D., Allwood, J., Dupree, P., Linden, P.F., Scherman, O. (2017): The wood from the trees: The use of timber in construction. Renewable and Sustainable Energy Reviews, 68(1):333-359.

11. Sherwood, T.K. (1929): The Drying of Solids-I. Industrial & Engineering Chemistry, 21(1):12–16.
12. Siau, J.F. (1995): Wood: Influence of Moisture on Physical Properties. Virginia Poly Institute and State University, Blacksburg.
13. Suchomelová, P., Trcala, M., Tippner, J. (2019): Numerical simulations of coupled moisture and heat transfer in wood during kiln drying: Influence of material nonlinearity. Bioresources, 14(4):9786–9805.
14. Sun, X., He, M., Li, Z., Ou, J., Zheng, X., Wei, M. (2025): Experimental study on the long-term creep behavior of cross-laminated timber under axial compression used for mass timber structural systems, Engineering Structures 338:120644.
15. Trcala, M. (2012): A 3D transient nonlinear modelling of coupled heat, mass and deformation fields in anisotropic material. International Journal of Heat and Mass Transfer, 55(17–18):4588-4596.
16. Wang, L, Ge, H., Wang, J. (2023): Model validation and 2-D hygrothermal simulations of wetting and drying behavior of cross-laminated timber. Journal of Building Physics. 46(6):737-761.
17. Hitaker, S. (1977): Simultaneous Heat, Mass, and Momentum Transfer in Porous Media: A Theory of Drying, 13:119–203.

A REVIEW OF THE DEVELOPMENT OF SYSTEMS AND STANDARDS FOR TOLERANCES AND FITS IN WOODWORKING

Nikola Mihajlovski[1], Gjorgi Gruevski[1]

[1]Ss. Cyril and Methodius University in Skopje, Macedonia,
Faculty of Design and Technologies of Furniture and Interior-Skopje,
e-mail: mihajlovski@fdtme.ukim.edu.mk;gruevski@fdtme.ukim.edu.mk

ABSTRACT

In the production of final products, variations in part dimensions can occur due to errors related to machines, tools, operators, and material properties. Therefore, it is important to set limits within which these variations can take place. The acceptable deviation is determined by dimension tolerances while ensuring the interchangeability of parts, as well as the quality and functionality of the product.

Initially, standards established for the mechanical engineering sector were utilized. The first standard applicable to tolerances and fits in wood processing is the Russian national standard GOST 6449. This was followed by the introduction of German standards DIN 68100 and DIN 68101, which also account for moisture correction in wood. Both of these standards have undergone multiple revisions and remain effective today.

Recent trends in standardization indicate a need to align woodworking standards with the GPS (Geometrical Product Specifications) system, which encompasses all geometric characteristics of parts, including dimensions, form, orientation, location, and surface quality.

Keywords: tolerances and fits, systems, standards.

1. INTRODUCTION

In the wood industry, particularly in the production of final products, manufacturing is typically done in series that often consist of over a hundred pieces. It is essential that these components are interchangeable during assembly. This implies that any piece from the series can fit into the product without requiring additional processing or adjustments. However, during the production of final products, variations in measurements can occur due to machine and tool imperfections, labour factors, and material properties. Consequently, it is necessary to establish limits within which these deviations can occur. The allowable deviation is defined by measurement tolerances, which are crucial for maintaining the interchangeability of parts, as well as the overall quality and functionality of the product (Potrebic, 1984).

The need to measure and record dimensions has been present since the inception of manufacturing. The initial written documents for dimensional control emerged alongside industrialization (Pfeifer, 2015). Tolerances and fits in woodworking began to be developed and applied in the 1930s, particularly for products that required high precision in part and assembly manufacturing. The tolerance and fit systems and standards that originated in woodworking and are still in use today were established by national standardization organizations such as GOST, DIN, and ISO.

This review aims to analyse the development of tolerance and fit systems and to investigate the current status and emerging trends in the standardization of these systems in woodworking.

2. DEVELOPMENT OF A TOLERANCE SYSTEM ACCORDING TO RUSSIAN NATIONAL STANDARDS - GOST

Initially, 4 to 7 accuracy classes were applied in woodworking, based on guidelines from metalworking accuracy documents, which represented the early stages of ISO standards. Due to the unique properties of wood, there was a need to establish a dedicated system. In 1934, the (Tsentralnyj nauchno-issledovatelskij institut mehanicheskoj obrabotki drevesiny - TSNIIMOD) conducted a study

on tolerances for wood joints in furniture and construction carpentry. The common slot system was used as a foundation, with the strength of the joint serving as the main criterion for fit selection, influenced by the gap or overlap present. For mortise and tenon joints, it was established that the maximum overlap should generally not exceed 0.3 mm, while the maximum gap should not exceed 0.2 mm.

In 1948, several institutes put forward their own solutions to the issue. The first, the (Lesotehnicheskaja Akademija - LTA), proposed a system of tolerances and fits specifically for wood processing. This system was developed with consideration of the level of accuracy achievable during normal machine operation. The calculation for the standard tolerance factor was based on the size of the hole and was determined using the following equation:

$$i = 0.05 + 0.04\sqrt{D} \quad (1)$$

i = standard tolerance factor (mm)
D = nominal size (mm)

According to this system, there are two classes of accuracy and three types of fit: clearance, interference, and transition fit. The second class of accuracy incorporates changes in dimensions due to variations in wood moisture. An analysis of this system revealed that tolerances are only applicable for dimensions up to 500 mm. In the same year, the (Institut aviamaterialov - VIAM) published a system of tolerances and fits designed for special final products. This system included two measurements —one for a hole and one for a shaft. It also considered dimensional changes resulting from variations in wood moisture and provided three classes of accuracy and three types of fit: clearance, interference, and transition fit. However, this system had several shortcomings. That year, the (Tsentralnyj nauchno-issledovatelskij institut mehanicheskoj obrabotki drevesiny – TSNIIMOD) proposed a revised system of tolerances and fits, using the hole size as the basic measurement and utilizing an equation to calculate the standard tolerance factor.

$$i = 0.1\sqrt[3]{D + 25} \quad (2)$$

i = standard tolerance factor (mm)
D = nominal size (mm)

This system did not account for changes in dimensions resulting from variations in wood moisture content, which typically happen during storage prior to assembly. Such changes also lead to increased tolerances and diminished control over machining accuracy by machines. The system incorporates two classes of accuracy, deviations of free dimensions, and four types of fits: clearance, interference, transition, and sliding fit. Subsequently, in 1952, the researcher (Manzhos, 1957) introduced a new equation for the same system to calculate the tolerance unit:

$$i = 0.1\sqrt[3]{D + 20} \quad (3)$$

i = standard tolerance factor (mm)
D = nominal size (mm)

In the same year, the (Institut aviamaterialov - VIAM) introduced its second system of tolerances and fits. The significant distinction from the original system lies in the modification of the equation for calculating the unit tolerance, which uses Manzhos's equation for both the first and second accuracy classes.

Each of the systems has its own limitations, highlighting the growing demand for a cohesive Russian system of tolerances and fits in the final processing of wood.

In 1953, the (Tsentralnyj nauchno-issledovatelskij institut mehanicheskoj obrabotki drevesiny - TSNIIMOD), in collaboration with the (Moskovskija lesotehnicheski institut – MLTI), (Lesotehnicheskaja akademija – LTA) and (Institut aviamaterialov – VIAM), developed the national standard GOST 6449-53, titled “Dopuski i posadki v derevoobrabotke” (Mihajlov, 1957). This standard represents the first official guideline for tolerances and fits in wood processing, based on a

common hole size system. It specifies nominal measurements ranging from 1 to 3150mm. The standard includes three accuracy classes, four classes of tolerances for free dimensions, and seven types of fits. The equation provided (2) is utilized to calculate the standard tolerance factor. To determine the tolerance factor, the result from this formula is multiplied by a coefficient k, which can be 0.5, 1.0, or 2.0, based on the applicable accuracy class.

This standard was revised in 1976 and replaced by GOST 6449 – 76. The new standard was developed based on ST SEV 144-75, which is harmonized with ISO/R 286:1962. According to (Koolikov et al. 1977), the main changes in this standard include the alignment of terminology for tolerances and fits with international standards and the expansion of nominal sizes ranging from 1 to 10000 mm, divided into nine accuracy classes.

The standard was revised again in 1982 and is divided into five parts: GOST 6449-1-82 covers tolerances for dimensions, GOST 6449-2-82 addresses tolerances for angles, GOST 6449-3-82 focuses on tolerances for form and surfaces, GOST 6449-4-82 pertains to tolerances for position and symmetry, and GOST 6449-5-82 relates to tolerances for non specified limiting dimensions. The range of nominal dimensions is categorized from 1 to 500 mm and from 500 to 10000 mm, divided into nine quality classes. This is the latest revision of the standard, and it remains valid today.

3. DEVELOPMENT OF A TOLERANCE SYSTEM ACCORDING TO GERMAN NATIONAL STANDARDS DIN

The initial literature on the development of tolerance and fit systems in Germany dates back to 1935, as noted by researcher (Blankenstein, 1956). He introduced a system of tolerances and fits applicable to both sliding and fixed components. This system included three accuracy classes and three types of fit: a tight glued joint, a movable joint that does not glue, and a loose movable joint that does not glue. A drawback of this tolerance system is the lack of consistency in tolerances relative to nominal measures, meaning the same tolerance was applied across different measurements. In 1938 (Schlutter, 1938) developed an improved system of tolerances and fits specifically for woodworking. In this system, the size of the tolerance was determined based on the dimensions of the part, with the standard tolerance factor calculated according to a specific equation:

$$i = 0.03\sqrt[3]{D} + 0.001D \quad (4)$$

i = standard tolerance factor (mm)
D = nominal size (mm)

The common hole size system served as the foundation for the calculation. It included three accuracy classes and three types of fits: tight, sliding, and loose fit. While this system appeared suitable, it later became unacceptable because of the small tolerance unit defined in the three accuracy classes.

In 1977, the German National Institute for Standardization introduced the first standard for tolerances in woodworking, DIN 68100:1977-02, which addressed tolerances for linear and angular dimensions in the woodworking and wood-processing sector.

In 1984, the standard was revised to DIN 68100:1984-12, focusing on the tolerance system for woodworking and wood processing, including concepts, series of tolerances, shrinkage, and swelling. This revision introduced the impact of moisture changes on the dimensional properties of wood. The same year, a new standard for joint fits was established: DIN 68101:1984-12, which specified fundamental deviations and tolerance zones in woodworking and wood processing.

In 2010, the standard was again revised, now designated as DIN 68100:2010-07, which continued to address the tolerance system for woodworking and wood processing, refining concepts, series of tolerances, shrinkage, and swelling. This version aligned terms and units of tolerance with ISO 286-1:2010. It also included tolerances for angles, flatness, and parallelism of sides. Additionally, more wood species were incorporated, detailing the dimensional changes related to moisture variations. Three new classes for machining accuracy were introduced, specifically for smaller parts, alongside the existing ten.

In 2012, the standard for fits was updated to DIN 68101:2012-02, which covered fundamental deviations and tolerance zones for woodworking and wood processing. The main changes in this

revision centered on harmonizing terms and fits in accordance with the international standard ISO 286-2:2010.

4. DEVELOPMENT OF A TOLERANCE SYSTEM ACCORDING TO INTERNATIONAL NATIONAL STANDARDS ISO

The earliest documented rules for tolerances can be found in the Draft Final Report of ISA Committee 3 from December 1935. Subsequently, the first standard was issued in 1941 under the title "The ISA Tolerance System," published in ISA Bulletin 25. Following this, a new standard titled ISO/R 286:1962 - ISO system of limits and fits, Part I: General, tolerances, and deviations was released in 1962, which included new tables and accuracy classes.

In 1988, this existing standard was replaced by two new standards, ISO 286-1:1988 and ISO 286-2:1988, which enhanced the standard's international applicability. A revision of these standards occurred in 2010, leading to their integration into the GPS - Geometrical product specifications system of standards. This system facilitates the use of a common hole and a common shaft, providing twenty-one combinations of tolerance fields for openings and closures. The standard encompasses nominal measurements ranging from 1 to 3150 mm, divided into eleven classes for machining accuracy.

While these standards are primarily designed for the mechanical engineering industry, their application in woodworking is limited, particularly with very small or very large dimensions (Tkalec and Prekrat, 2000).

5. NEW TRENDS IN THE USE OF TOLERANCES AND FITS IN PRODUCTION

The advancement of CAD/CAM technology has increased the demand for quality control and precision in processing. In 1996, the Technical Committee for International Standardization (ISI/TC 213) introduced a series of standards known as GPS (Geometrical Product Specifications). This system includes standards for drawings, markings, symbols, measuring tools, measurement principles, tolerances, and more. Within the GPS framework, the ISO 14638:2015 standard provides a matrix that encompasses all characteristics of an element, including dimensions, shape, direction, position, angles, and surface quality.

Currently, there is limited data in the literature regarding the use of the GPS system in the wood industry. The first to discuss this topic is (Riegel, 2018), who highlights the importance of applying the GPS system in the furniture sector. He suggests that this system is particularly relevant for the production of panel furniture, which involves numerous holes for fittings, dowels, and joints, necessitating precise hole positioning. Warmefjord et al. (2019) also note the potential for using GPS in the context of tolerances within ready-to-assembly furniture production. Additional authors, including (Turbanski et al. 2021) and (Sydor et al. 2021), further acknowledge the relevance of the GPS system in furniture manufacturing. Collectively, these authors point out that the standard for tolerances in the wood industry, DIN 68100, does not align with the GPS system.

The determination and control of tolerances and fits for wood products should be guided by the ISO 14638:2015 framework, considering the complexity of functional and durability requirements. This approach encompasses all geometric characteristics of the element, including dimensions, form, orientation, position, angles, and surface quality.

6. CONCLUSION

The analysis of existing literature indicates that the development of the system of tolerances and fits in final wood processing considers multiple factors, which are reflected in tolerance unit calculations. Initially, standards sustems for the mechanical industry were utilized. The primary standard for tolerances and fits in wood processing is the Russian national standard GOST 6449. Subsequently, the German standards DIN 68100 and DIN 68101 were introduced, which also account for moisture correction in wood. Both national standard systems have undergone several revisions and remain in effect today. Recent trends in standardization suggest the need to harmonize wood

processing standards with the GPS system, which aims to encompass all geometric characteristics of products, including dimensions, shape, direction, position, and the quality of surfaces.

REFERENCES

1. Blankenstein C. (1956): Holztechnische Taschenbuch. Hanser Verlag, Munchen 1956.
2. DIN 68100:1977-02: Tolerances for linear measure and angular dimensions in the wood-working and wood-processing industry
3. DIN 68100:1984-12: Tolerance system for wood working and wood processing; concepts, series of tolerances, shrinkage and swelling
4. DIN 68101:1984-12: Fundamental deviations and tolerance zones for wood working and wood processing
5. DIN 68100:2010-07: Tolerance system for wood working and wood processing - Concepts, series of tolerances, shrinkage and swelling
6. DIN 68101:2012-02: Fundamental deviations and tolerance zones for wood working and wood processing
7. GOST 6449-53: Dopuski i posadki v derevoobrabotke
8. GOST 6449-76: Product of woods and wooden materials. Limits and fits
9. GOST 6449.1-82: Products of wood and wooden materials. Tolerance zones for linear dimensions and recommended fits
10. GOST 6449.2-82: Products of wood and wooden materials. Tolerances of angles
11. GOST 6449.3-82: Products of wood and wooden materials. Tolerances of form and arrangement of surfaces
12. GOST 6449.4-82: Products of wood and wooden materials. Tolerances of arragement of hole axis for fixing details
13. GOST 6449.5-82: Products of wood and wooden materials. Non-specified limiting deviations and tolerances
14. International federation of the national standardizing associations (1941): The ISA Tolerance System, ISA Bulletin 25, January, 1941
15. ISO/R 286:1962 - ISO system of limits and fits, Part I : General, tolerances and deviations
16. ISO 286-1:1988 - ISO system of limits and fits, Part 1: Bases of tolerances, deviations and fits
17. ISO 286-2:1988 - ISO system of limits and fits, Part 2: Tables of standard tolerance grades and limit deviations for holes and shafts
18. ISO 286-1:2010 - Geometrical product specifications (GPS) — ISO code system for tolerances on linear sizes, Part 1: Basis of tolerances, deviations and fits
19. ISO 286-2:2010 - Geometrical product specifications (GPS) — ISO code system for tolerances on linear sizes, Part 2: Tables of standard tolerance classes and limit deviations for holes and shafts
20. ISO 14638:2015 - Geometrical product specifications (GPS) — Matrix model
21. Kolikov V. A., Stovpju F . S., Kirova S. M., Fomochkin N. I., (1977): O novom GOSTe na dopuski i posadki v derevoobrabotke, Derevoobrabatyvajuschaja promyshlennost, 1977/2
22. Manzhos, F. M. (1957): Tochnost mehanicheskoj obrabotki drevesiny, Goslesbumizdat, Moskva 1959. - 264 s.
23. Mihajlov V.N. (1957): Tehnologija derevoobrabatyvajuschih proizvodstv, M. Lesnaja promyshlennost, 402 str.
24. Pfeifer T. (2015): Production metrology. Walter de Gruyter GmbH & Co KG.
25. Potrebić, M. I. (1984): Drvne konstrukcije. 1, Opšti principi konstruisanja (p. 438). Institut za preradu drveta Šumarskog fakulteta.
26. Riegel, A., "Geometric tolerancing of furniture", (2018): Proc. 8th International conference on Production Engineering and Management (PEM), F.-J. Villmer, and E. Padoano, eds., Hochschule Ostwestfalen-Lippe.
27. Sydor, M., Majka, J., and Langová, N. (2021): "Effective diameters of drilled holes in pinewood in response changes in relative humidity," BioResources 16(3), 5407-5421, DOI: 10.15376/biores.16.3.5407-5421

28. Schlüter, R. (1938): Toleranzen und Passystem in der Holzbearbeitung. *Holz als Roh-und Werkstoff* **1**, 131–139. https://doi.org/10.1007/BF02612285
29. ST SEV 144-75 Edinaja sistema dopuskov i posadok SEV. Polja dopuskov i rekomenduemye posadki
30. Tkalec S., Prekrat S. (2000): Konstrukcije proizvoda od drva 1 Osnove drvnih konstrukcija, Šumarski fakultet Sveučilišta, Zagreb
31. Turbański, W., Sydor, M., Matwiej, Ł., & Wiaderek, K. (2021): Moisture swelling and shrinkage of pine wood versus susceptibility to robotic assembly of furniture elements. *Annals of WULS, Forestry and Wood Technology*, DOI:10.5604/01.3001.0015.5274
32. Wärmefjord, K, Söderberg, R, Lindkvist, L, & Dagman, A. (2019): "Non-Rigid Variation Simulation for Ready-to-Assemble Furniture." *Proceedings of the ASME 2019 International Mechanical Engineering Congress and Exposition. Volume 2B: Advanced Manufacturing.* Salt Lake City, Utah, USA.

EPHEMERITY IN PUBLIC ARCHITECTURE AND INTERIORS: THE RETAIL DESIGN IN THE REPUBLIC OF NORTH MACEDONIA

Edona Arifi Sadiku[1], Elena Nikoljski Panevski[2],

[1]PhD candidate, Faculty of Design and Technologies of Furniture and Interior, Ss. Cyril and Methodius University in Skopje
[2]Professor, Faculty of Design and Technologies of Furniture and Interior, Ss. Cyril and Methodius University in Skopje

ABSTRACT

The Republic of North Macedonia during this last half of a century has undergone major internal and external influences that have affected architecture and design. When it comes to public interiors, in addition to architecture, it keeps pace with the times and is constantly changing. Changes in retail design occur in the architectural basis, in the way of functioning, interior design, type of furniture including materialization, form, location and appearance. Shops have also changed the external appearance of the facade, shop window and format.

The changes are a consequence of major economic, political and sociological changes in the country. However, in recent decades, globalism and world trends have had a greater impact. After the terrible earthquake in Skopje and the reconstruction of the city, the transition to capitalism is even more emphasized and applied. There is also a stronger exchange of trade with Europe, which results in new influences in the architecture and retail design (design for commercial premises). Consequently, the direction of changes in architecture and interior design is oriented from the 2WW style through modernism until today's contemporary retail design style.

This research will use the qualitative method, field research, measurement and drawing, the method of comparison and the method of simulation. Through comparative and qualitative tables, it will be concluded that there are changes in the atmosphere of shops in the Republic of North Macedonia, which indicate rapid transitions from one type to another - this gives us a direction towards defining retail interiors in the Republic of North Macedonia as ephemeral - often changing, short-lived and transient.

Keywords: public architecture, public interior, retail design, ephemeral architecture.

1.0 INTRODUCTION

The topic of this paper is precisely the architectural, more specifically, interior public changes, which have occurred in a short time due to various internal and external influences, which in turn have created changes in the culture of consumption.

In addition to the theoretical part - from a philosophical and ontological aspect for analyzing the phenomena with their occurrence and movement, the factual social and economic aspects of the Republic of North Macedonia are also researched, from 1963 to 2024. The manifestations that jointly acted to make public interiors undergo four different periods of development are investigated: *Period 1* - occupies the time frame 1963-1970, the period with domestic shops with artisanal service and sales activities, in the process of restructuring the interiors towards the West after the earthquake and the Western influence of the architecture of Kenzo Tange, which reinforces the already begun modernism; *Period 2* - with a time frame 1971-1991, when modern architecture is intensively developed and interior design is especially cherished, a period when Yugoslav brands are spreading in addition to older shops; *Period 3* – with a time frame of 1991-2004, explores and explains the shops after the independence of the state and privatization, when citizens approach to public interior with their own private possibilities and knowledge. In this period, the effort of designing public interiors is obvious; *Period 4* – with a time frame of 2005-2024, a period when changes occur in the standard of buying and consumption, when modern standards of consumption and contemporary architecture and interior design emerge from globalism.

The research relies on an analysis of existing stores from P1 – P4, analyzing planimetry, area, functional and zonal division of use for furniture, for seller and for buyer, type of furniture with materialization, floor and ceiling with lighting elements.

From a phenomenological perspective, it is concluded that there have been rapid changes in retail design in stores from 1963 to the present, moving from one type of store to another, with changes in location, type of shopping center, style of interior decoration, and the introduction of new content in retail public design.

1.1 RESEARCH PURPOSE

The purpose of this research is to reveal and confirm the obvious association of public interiors that have emerged as ephemeral. Ephemerality is a phenomenon of short duration, which in architecture defines rapid architecture for a specific purpose and disappearance from the place after the completion of that purpose. Contemporary developments in public design – specifically retail design, confirm rapid changes, in order to realize aesthetically luxurious ambiances in retail interiors, managed in parallel with the products for sale and the brand. The holistic approach to store interiors contributes to them creating maximum attraction for the mass at the same time and purchasing, in order to increase financial benefits. In this case, the interior is constantly changing, with the acquisition of new retail formats, different in each period. Since each phenomenological appearance is different in each city, the emergence of ephemeral design is a consequence of various manifestations taking place in Skopje, over a short period of time 1963-2024. The demonstrations encompass economic stagnation, political state changes, social issues, transition, internal and external trade, and globalism.

1.2 RESEARCH METHODS

The dual nature of architecture, technical and artistic, encompasses several research methods, among the main ones being the theoretical method and the analytical method. The theoretical method investigates domestic and foreign literature on phenomenal manifestations, with the specific focus on the phenomenon of ephemerality. In doing so, it investigates formats for the appearance of ephemerality in architecture and interiors.

To confirm the appearance of ephemeral architecture and interiors in public stores in our country in the period 1963-2024, the analytical research method is used. Through case study analyses in existing public functional stores, through measurements and images in real stores, it is concluded that there have been changes in public design over time. Architectural planimetry, characteristic furniture, shop windows and signs are analyzed. The obtained data are compared in qualitative tables, to conclude changes in design. Changes in design indicate short-lived, changeability and transience - ephemeral public interiors.

2.0 IMPACT FACTORS FOR INITIATING CHANGE

Research on a phenomenological basis is the understanding of the way in which events occur spontaneously, in terms of description, based on real evidence. The process encompasses a wide range of theoretical and applied factors that influence the occurrence of phenomena. Phenomena occurring in one place may be similar to phenomena in another place, but each city/state experiences and processes them differently, from that society.

The research so far verifies changes in the internal affairs of the state, with parallel external indications and problems. The table below shows the factors that influenced the occurrence of phenomena in public interiors. The table helps in identifying the events that contributed to public retail interiors changing in a short period of time. At the same time, the events in the table define time divisions of changes in public interiors. These time divisions will help confirm the identification of real retail interiors with their style, furniture, window displays, signage, and formats in our region.

Table 1. *Qualitative table of events in the region of Macedonia from 1963-2024.*

YEAR	INTERNAL EVENTS	EXTERNAL INFLUENCES	TIME PERIODS
Before 1963	People's Republic of Macedonia	Industrialism Transition	Post World War II architecture
1963-1991	1963-1991 Socialist Republic of Macedonia Earthquake and reconstruction under modernism	Europeanization Trade with countries in Europe	Post World War II architecture – **P1** (1963-1970)
			Modern architecture and interior – **P2** (1971-1991)
1991-2019	Republic of Macedonia	World standards of trade, globalization	Postmodern architecture and interiors – **P3** (1992-2004)
2019-2024	Republic of North Macedonia	Modern world standards of trade, globalization, digitalization	Modern architecture and interiors – P4 (2005-2024)

The table shows the events in the country that affect changes in the development of public interiors. In field research, the differences point to four periods, which contribute to the formation of different formats of shopping centers and stores in our country.

In addition to the main influencing factors, the development of the economy plays a key role. The development of the economy, in addition to internal affairs, also depends on world trends. Today's world economy aims at international consumerism and consumption with global standards. In addition to the above-mentioned changes in Macedonia, the economy is based on constant stagnation. Industrialism and transition are processes that are experienced in Macedonia under inappropriate circumstances and conditions of development. Frequent major changes have created chaotic situations in the country, which pass incompletely developed, disrupting the stability of the standard of living.
Economic growth was observed between 1968 and 1989, especially in the area of trade. This growth was halted by the division of the SFRY, especially in Macedonia. The privatization process, the Greek embargo in 1992, the interethnic conflict in 2001, and the constant inappropriate policies contributed to the Republic of Macedonia being the poorest country in the SFRY.

After independence, despite the very low economic development, citizens devoted themselves to independent ways of survival, including opening private shops throughout the cities. This is confirmed by Table 2, when from 1989-1996 the number of opened shops grew from 9957 to 23101 shops.

Table 2. *Number of stores, sales area, warehouse space and number of employees.*

Т-01: Број на продавници, продажен простор, приракен магацин и број на работници

T-01: Number of stores, sales area, at-hand storage space and number of employees

	Број на продавници Number of stores	Продажен простор во м² Sales area in m²	Приракен магацин во м² At-hand storage space in m²	Број на вработени во продавницата Number of employees in stores	Просечен продажен простор во м² Average sales area in m²		Просечен број на работници во продавницата Average number of employees per store
					по продавница per store	по продавач per seller	
1 976	6 173	464 573	114 726	17 814	75	26	3
1 978	6 861	511 350	125 363	20 400	74	25	3
1 980	6 986	552 107	149 169	21 093	79	26	3
1 982	7 364	603 702	194 356	23 740	82	25	3
1 984	7 505	670 590	181 729	24 467	89	27	3
1 986	7 995	697 111	181 906	26 532	87	26	3
1 989	9 957	764 874	191 891	27 806	77	28	3
1 996	23 101	893 179	131 384	30 839	38	28	1
2 003	24 276	1 233 505	159 066	32 537	51	38	1
2 008	22332*	1 367 063	188 364	32 021	61	43	1
2 016	18 250	1 213 895	243 166	41 057	67	30	2

* не се вклучени аптеките

* excluding pharmacies

Despite the low economic development, the number of stores is increasing. After 2000, the country emphasized foreign investments as a way of developing the economy. In this case, the number of stores is decreasing but the sales area is increasing. This data shows changes in the formats of stores, i.e. reaching stores with world standards in our country.

2.1 DEVELOPMENT STAGES

The development stages, in addition to external and internal indicators, initiate changes in public design. As a consequence of different processes and phases of development, there are divisions that are directly related to changes in public retail interiors. In Table 1, as a result of the comprehensive changes in the country, a direct indication of initiating changes in internal retail interiors is observed. Based on field research, the following is a classification of types and formats of interiors, divided into four typologies, based on time, location and current events:

- **Period 1 (1963-1970) -** As part of Yugoslavia, at this time shopping was organized at green markets and old bazaars. Bazaars as urban structures with Ottoman origins and centuries-old existence, showed the traditional side of buying and selling in every city, especially Skopje, Bitola, Tetovo, etc. The shops in the old bazaars, in addition to the urban structure and application of craftsmanship, preserve the historical spirit and craftsmanship, although in a much lower percentage. At this time, in addition to the former small private shops with craftsmanship, services and sales, Yugoslav brands began to appear, active in department stores and old bazaars. Modern architecture expanded intensively with rapid dynamics after the earthquake in Skopje (1963).
- **Period 2 (1971-1991)** – In this period, modern buildings are emphasized, especially with the construction of the City Shopping Center. In addition to the old bazaars, shops are spread throughout public buildings on the ground floor and department stores. Industrialism is expanding, new shops are opened for sale only in addition to the artisan shops in the bazaar, while Yugoslav brands are presented with newly decorated interior stores. Yugoslav brands with their stores are spreading throughout the new shopping centers and in the old bazaars.
- **Period 3 (1992-2004)** – The period after the independence of the Republic of Macedonia, despite the severe economic and political stagnation and prohibited trade routes, the embargo from Greece, new open shopping centers are being built in several cities of the country. The difficult conditions encourage citizens to orient themselves towards opening various stores, everywhere in the cities without planning. Expert support is noted in the composition of public postmodern interiors. Foreign investments, which were necessary for improving the economy in Macedonia, bring the modern format of closed shopping centers or "shopping malls".
- **Period 4 (2005-2024) –** this period marks a modern global architecture of commercial buildings with world standards – large enclosed volumes, with internal galleries and halls and shops with windows facing the halls. The interior of the shops is modern and holistic, a consequence of global companies, spread through chain stores.

The above-mentioned divisions in the period indicate comprehensive changes and phases of development. By defining indicators of change, the development of retail interiors is also defined. This research also shows ways in which state development and global indications acts in the formation of retail interiors.

3.0 EPHEMERAL ARCHITECTURE AND INTERIOR

After industrial expansion and globalism, ephemeral architecture has gained great attention in the applied world. Technological development and digitalization, the global economy and massive industry have created rapid and dynamic changes. Changes in architecture are explained by the phenomenon of ephemerality, which gives architecture an additional dimension, that of transience, which is traditionally not desirable. Long-lasting objects have always been reliable and desirable by people. Modern trends and the development of technology always bring architecture into temptation: trying innovations and keeping up with novelties and needs.

The term ephemera comes from the Greek language, which when translated means “lasting only one day”, that is, “epi” – upon, over and “hemera” – day [Chappel 2004:11]. In a book written under deep analysis, Chappell talks about the impermanence or impermanence side of architecture, evidence

of a phenomenon in architecture based on time. Otherwise, according to him, the definition would be: "-A type of object designed to be distinguished by its impermanence and its physical departure from the location." [Chappel 2004:4].

After Robert Kronenburg and the books on ephemeral types of objects [Kronenburg 1998, 2003, 2006], there are also authors who have explored a wide spectrum of uses of the term ephemerality in architecture and design. Galia Boustani investigates the new short-lived so-called pop-up stores, which are built for a short existence/sale and quickly depart from the site after completing their purpose [Boustani 2020, Boustani 2023]. Consequently, the ephemeral phenomenon describes attributes in architecture and design such as: transience, changeability, and transience.

3.1 THE PHENOMENON OF EPHEMERITY AND RETAIL DESIGN

Public buildings are spaces for work and socialization, aesthetically arranged and prone to frequent changes. Due to the wide industrial expansion, massive production, and easy distribution, the culture of retailing is changing very quickly and the number of stores is increasing. The dynamics also affect the types of stores, with a great evolution – changes in the organization and frequent reorganization of stores. Ways to document the rapid development specifically in public interiors are framed by defining the constituent elements of retail interiors.

The consequence of the rapid development of interiors, in addition to the above-mentioned changes in the internal affairs of the country, are also the external indicators, shown in Table 1. The private economic benefits of large industrial companies for sales and their competition, contributed in this hyper-consumer world (Baudrillard) to interiors being at a high level aesthetically decorated and resembling a theatrical performance. From the shopping centers themselves, shop windows and interior decoration, the interiors are carefully decorated with unique furniture and materialization, in addition to management and brand, for greater attraction of people and increase in shopping under the euphoria of aesthetics in the space.

The great effort to create beautiful retail interiors introduces a separate discipline in design – retail design. The term "science of shopping" was used by the author Underhill in 1997, who explained the ways of shopping and the environment in which shopping is done, by listing characteristics and clarifications [Underhill 2009: 4]. Among the wide range of researchers, Christiaans and other authors describe retail design as "experience design" or "experience design" [Christiaans at al 2012: 1893-1902].

The strategic thinking and management of large retail companies, with the aspiration for greater economic benefits, have initiated frequent changes in retail interiors. In addition to the fact that the phenomenon of ephemerality possesses the attributes of short-termity, transience and changeability, in addition to the ephemeral architecture of objects with a short-term purpose, this paper analyzes the attributes of ephemerality in retail interiors in more depth and specifically.

Author Lynn, in a book on defining retail design, identifies the constituent elements of this type of design, with the following elements:

- "Store brand or identity;
- Retail sector: food (catering), fashion (wardrobe), home sector, leisure and recreation;
- Store location (department store, high street retail, shopping malls, peripheral retail content, showrooms and retail parks, additional content in transport facilities, virtual shopping);
- Sales environment/environment (sustainable retail, materialization, lighting, climate and sounds);
- Methods and organization of space (principles of store organization, advertising, service and auxiliary space);
- Design details (store facade, interior architecture or interior, fixed and freestanding elements)" [Lynne, 2020].

In scientific articles and books, several authors have defined the constituent elements of shopping malls and retail design [Boustani, 2020: 44], [Juan et al, 2021], [Daucé, Rieunier 2020]. Based on these data and research in a real applied dimension, the elements of interior retail design would be as follows as in the table 3[1]:

[1] Table 3 is taken from a doctoral dissertation in progress, author.

Table 3. *Elements of interior retail design.*

FRONT FACADE	Fully or partially glazed
DISPLAY WINDOW	Completely separated (enclosed) from the store space, furniture separated from the store, not separated from the store
ZONALLY DIVISIONED SPACES BY DESIGN	Window display space, product display space (wall-mounted, freestanding sales furniture, cash register), salesperson space (cashier, warehouse), customer space (paths)
SALE FURNITURE AND ORGANIZATION	Sales furniture is divided into: G shelves, flex systems, smart systems, pole systems and freestanding systems.
PATHS (movement)	Free space for customer communication
MARKETING AND BRAND MANAGEMENT	Brand creation, brand advertising
MUSIC AND SMELL	Thematic selection of music and presence of scent
CONTENT AND CHANGES	Thematic change of product content, seasonal, holidays, trendy, organized events
INTERIOR ARRANGEMENT	Style, interior design (furniture, walls, materialization, lighting)

Defining the elements reveals the components of retail interiors. When defining them, a case study analysis follows, in which, through the analysis of the component elements of the interior, a comparison and changes in public interiors in P1, P2, P3 and P4 are concluded.

4.0 CASE STUDY - SHOPS IN P1

The constituent elements of a retail store help define changes in public design over the given time period 1963-2024. This research describes a given number of real functional stores, opened at times designated as P1, P2, P3 or P4. The following table shows two example stores opened in P1.

Table 4. *Example shops P1.*

Descriptive characteristics of shops for example in P1:

- Smaller shops in terms of square footage, in addition to selling in the shops, handicrafts are also practiced;
- Different layouts of the shops as a result of the centuries-old morphological changes of the old bazaar. Over time, shops have opened in different parts of the buildings in the old bazaar, which have expanded or merged with the buildings/shops next to them;

- In addition to sales in the shops, handicraft activities are carried out, where the owners produce the products they sell. The activities of the handicrafts are carried out in the shop space and in other private locations;
- The shops taken as an example in P1 have the same layout from the 60s and are functional today with the same purpose;
- Public sales furniture is created based on the basic needs of the seller, most often produced by local craftsmen vernacular materialization. The interior for work and sales was realized by the seller, under their taste, possibilities and conditions;
- The Ottoman origin of the bazaar, although upgraded under the spirit of the Western style of the last century, is clearly noticeable in the interiors and in the front facade. Materials such as wood, glass and metal were used: wooden shelves, small chests of drawers, walls covered with wooden paneling, wooden work and sales tables. Usually glass for the need for display space. The ceilings are with white painted ribbed sheet metal, with paneling, etc. The floor is made of wooden planks, ceramic tiles, made earlier or more recently. Ambient lighting with neon follows;
- The long existence of the shops has influenced the furniture to be constantly added and changed, a lack of uniformity is noticeable;
- The facades and shop windows are similar, from the materialization of wood and transparency with glass.

4.1 WINDOW DISPLAYS AND SIGN IN STORES FROM P1

Throughout the field research and in the sample stores from P1, three typologies of window displays are observed:
- in a flat window display,
- a window display pulled outwards and
- a window display pulled inwards.

The front facade is derived from the Ottoman style, structured in wood and glass. It is found on protectors from excessive solar radiation or security protection at night on glass surfaces: metal blinds that lower down, metal mesh or sheet metal, "wooden shutters", fabric blinds that lower and gather above the window, etc.

The sign aims to inform customers about the type of store and the services provided. In the two stores mentioned, for example, the sign informing about the services in the store is difficult to see for the consumer. It is presented through cut letters from foil and glued to the glass surface of the window or door.

4.2 SHOPS IN P2

The sample stores in P2 cover the period 1971-1991. During this period, public design changed drastically, characterized by a rapid transition from small, service shops without decorated interiors to a serious tendency towards decorated public interiors in the spirit of modernism. The major differences are observed in the bazaars, which as the oldest trading locations, due to the rapid changes resulting from industrialism, are beginning to change their interiors to modernism.
The following is a table of two example stores opened in P2.

***Table 5**. Example shops P2.*

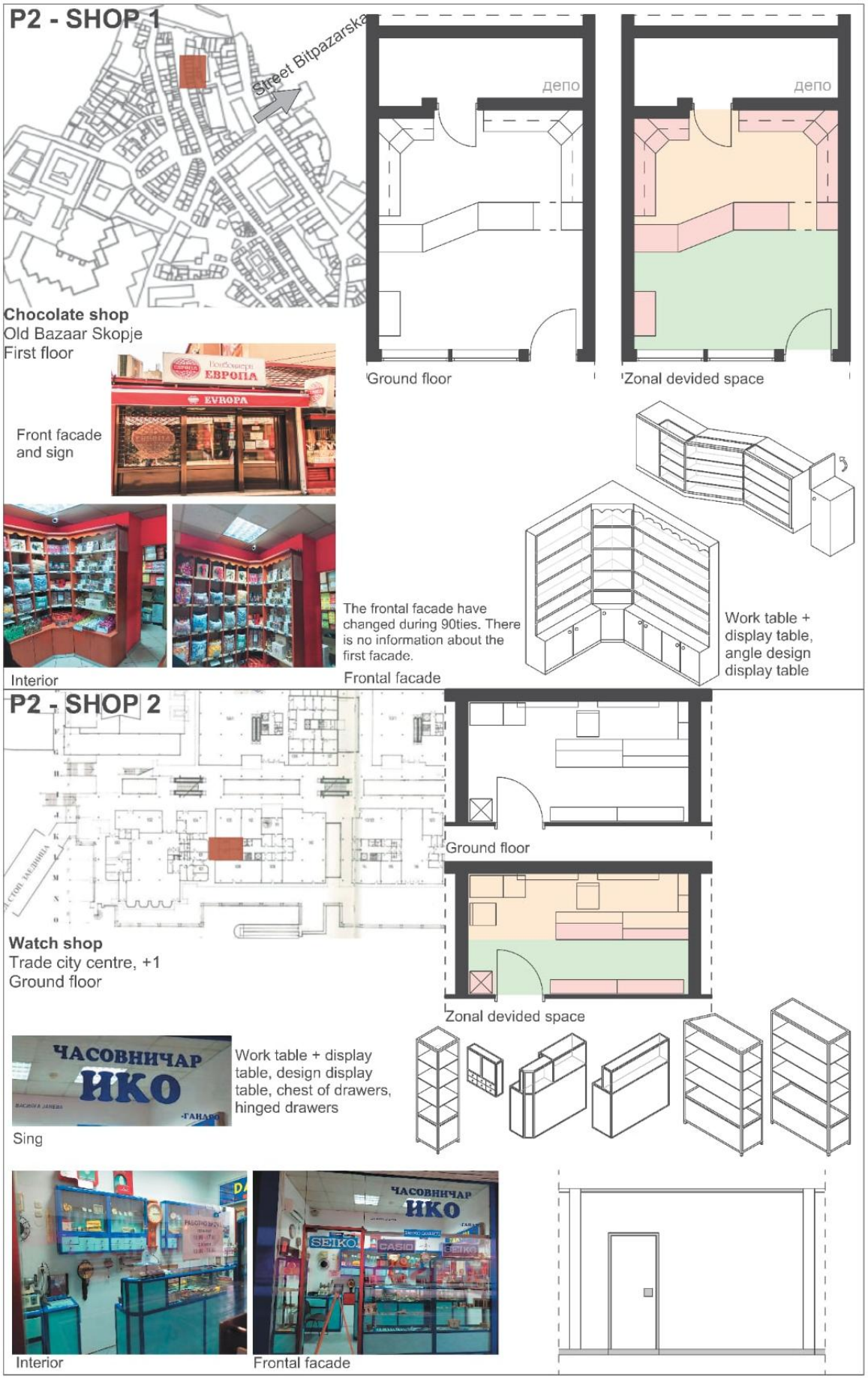
P2 - SHOP 1
Street Bitpazarska
депо
депо
Chocolate shop
Old Bazaar Skopje
First floor
Ground floor
Zonal devided space
ЕВРОПА
EVROPA
Front facade and sign
Interior
The frontal facade have changed during 90ties. There is no information about the first facade.
Frontal facade
Work table + display table, angle design display table
P2 - SHOP 2
Ground floor
Zonal devided space
Watch shop
Trade city centre, +1
Ground floor
ЧАСОВНИЧАР
ИКО
Work table + display table, design display table, chest of drawers, hinged drawers
Sing
ЧАСОВНИЧАР
ИКО
SEIKO
CASIO
SEIKO
Interior
Frontal facade

Descriptive characteristics of sample stores in P2:
- The interior of the sample stores was influenced by modern architecture, despite the fact that they are located in the Old Bazaar and the City Shopping Center in Skopje;
- In the stores of this period, craftsmanship begins to decline. In the sample stores, one store has only a sales function, the second also has a service activity – watch repair.
- Appropriate public furniture has been implemented, according to the needs of the store and the dimensions of the space. The furniture is pre-conceived and designed in accordance with the function, operation, needs and dimensions of the space;
- The materialization of the furniture used is made of wood, metal (iron, aluminum) and ordinary 4mm glass, built over wooden frames in tables that display small products. Wooden furniture often appears painted with paint (in example 2 painted with blue paint) and painted with transparent varnish (example 2).
- The window in store 1 has been changed, although the location is in the Old Skopje Bazaar, the window has been changed from an old bazaar window with wood and glass to a flat window made of aluminum and glass. Store 2 in the City Shopping Center is completely transparent with 6mm glass, the glass door hangs in a metal aluminum frame with mechanical opening.
- The furniture is made by local craftsmen, durable and functional to this day.

Store number 2 still exists with the same function, while store 1, immediately after field measurements, research and analysis, completely changes its interior, while still being functionally active.

4.2.1 WINDOW AND SIGN IN SHOPPING SPACE FROM P2

The sign in shops, for example, is a simple sign for informing about the type of shop and its name. It is noticeable in the form of glued foil letters in the window, above the glass surface. In rare shops, a special logo and sign design is noticeable in P2.

At this time, a chain of Yugoslav stores is also observed, in which a logo and a special sign of the company are noticeable. Through this type of stores, the advertisement and brand of a store begins to appear. A similar case is the domestic chain store example 1.

The front facades of both examples are flat, while the shop window is realized from the inside with special display cases, similar to the furniture of the entire store. A clear tendency towards holism is observed in public interiors.

4.3 SHOPS IN P3

The independence of the Republic of Macedonia brought difficult economic conditions and a chaotic situation in the country. During this period, a large number of private shops were opened, as one of the simple ways of survival. Private shops were opened everywhere in the cities without any provision or planning from the state. Unlike in 1989 when there were 9957 shops (excluding pharmacies) with an area of 764,874 m2 + warehouse space, in 1996 a total of 23101 shops (excluding pharmacies) with an area of 893,179 m2 + warehouse space were registered (see table 2).

The wide expansion of stores contributes positively to public interiors. Professional progress is seen in the development of public retail interiors. However, interiors are divided into interiorwith higher investment and interiors with lower investment.

The following is a table of two example stores from P3.

Table 6. *Example shops P3.*


P3 - SHOP 1
Sewing equipment store
Kumanovo
Ground floor
Ground floor
Sign
Display table with drawers + cash register, display shelves, high dsplay shelves, chest of drawers, chair
Интериор
Изглед
P3 - SHOP 2
Gold store
City trade centre, Ground floor
Ground floor
Ground floor
Zonal devided space
Display table with drawers + cash registre, display shelves
Знак
Interior
Frontal facade

Descriptive characteristics of example stores in P3:
- Of the above-mentioned stores, one is located in the city center, adapted in an old building with a former function as a house in the center, while the second store is in a shopping center.
- In these stores, mainly sales are small services.
- In a store in a shopping center, the primary function is sales, in which case the furniture is made for a specific purpose, in a space with a primary function for sales. The furniture in a store with a former other function is interesting: the furniture is excellently designed for public sales purposes and has a serious tendency towards holism.
- The style of interior decoration in the stores is, for example, postmodernism neoclassicism. The interior decoration is realized by an appropriate professional person. The furniture is mainly made of wood, in lacquer color, with a glazed part in the tables where products are displayed. Wall covering with wood is also found. The same texture and color of wood used in furniture and walls. Wall covering is sometimes for leveling old walls, sometimes as a detail for aesthetics.
- The storefront in the city center has a smaller glazed area, the other remaining part is with a wall, where the storefront has a door and a window. The other example is completely transparent in a shopping mall.
- The ceiling is usually lowered, the floor is with ceramic tiles or laminate.
- The lighting in both example stores is ambient with neon. There is a tendency to harmonize the lighting elements with the overall interior design.
- The example stores have kept their interior, realized in the 90s, which represents a unique public sales design, durable, realized by domestic craftsmen.
- Both stores are functional today. The second store has changed certain elements of the interior several times, but with the same materials and spirit of the interior.

4.3.1 WINDOW AND SIGN IN STORE FROM P3

The effort to design the name and logo of the store is obvious. The work done by an expert in logo design is noticeable.

The signs are presented to us in various forms: glued foil letters in the glass surface of the facade, a plastic volume element with the logo and name of the store and built-in lighting, metal letters engraved in a marble slab, a flat metal plate with a gold color and the name of the store, established in the interior, etc.

The graphic design shows the presence of awareness of the sellers about the importance of advertising in sales.

4.4 STORES IN P4

Stores in P4 represent a modern type of store. Modern stores are a consequence of globalism, the international culture of buying and selling that has undoubtedly expanded massively in the Republic of Macedonia in the last decade.

Contemporary retail design encompasses multiple disciplines: physical store, retail store design (transdisciplinary design), functional layout, aesthetics, appropriate atmosphere, lighting and visual marketing [Quartier, 2016]. Modern store formats represent an international dimension, surviving as a consequence of industrial massive expansion, digitalization and consumerism.
The following are two examples of modern stores.

Table 7. *Example shops P4.*


P4 - SHOP 1
Store for men
Trade centre „Mavrovka“
Skopje, Ground floor
Ground floor
Ground floor planimetry
Zonal devided space
BEG
Sign
Furniture
Interior and facades
F1
F2 Facade
P4 - Shop 2
RESERVED
CENTRAL BOULEVARD
CENTRAL SQUARE
H&M
ZARA
LC Waikiki
NEW YORKER
DeFacto
Store for gold jewellery
Sjopping centre „East Gate“
Skopje, Ground floor
Ground floor
Ground floor planimetry
SMARAGD
Image and sign
Furniture
Elevation
Zonal devided space
Elevation

Descriptive characteristics of example stores in P4:
- The stores represent modern formats of trade, located in an older format of a shopping center and a new format of a closed shopping center, opened after 2020.
- The sellers in these stores perform exclusively sales activities.
- There is a noticeable difference in the level of investment in interior design. All interiors have attributes of minimalism, industrialism, holism, maximum transparency, luxurious aesthetics.
- The furniture in modern stores is intended exclusively for sales. Designing specific furniture for specific products. All types of products have a specific place for display, in a special type of public furniture.
- The windows are glazed and transparent.
- The atmosphere in the stores is comprehensively designed to be holistic. There are stores designed by professionals and stores designed by the store owners.
- Materialization used in the interiors: different types of glass, wood and wood products (chipboard, MDF), granite, marble, metal (iron, aluminum), decorative elements, greenery.
- Interiors are often changeable, innovative, for greater attraction. For each holiday, season, new collections, discounts, there is a change in the position of the furniture, changing the furniture, introducing new products, new advertisements and discounts, to achieve greater sales.
- A special arrangement of the window is noted, with special lighting elements to emphasize the new collections presented in the window.
- The above examples of stores are actively functioning; one is a private store while the other is a chain store.

4.4.1 WINDOW AND SIGNS IN STORES P4

The main attribute and the same in most modern stores is maximum transparency. In a smaller part of stores, a decorated wall and framing of glass surfaces appear.
In modern stores, the front facade with the main entrance and window represents the first impression of the store and its brand, at the same time a delicate and main detail of a store. In addition to fully or partially transparent front facades, the window is designed inside, which is integrated into the front facade at its parapets or is a separate part of the front facade.

As a separate part, it is presented in separate showcases or in closed additional rooms where the window is treated independently, or is completely transparent and part of the store, where the shelves of the window serve as a comprehensive regular part of displaying the products of the store. In P4, all variants of shop windows are found, specifically in stores, for example, separate dressers or display cases for the shop window are found (example 2 P4), and non-separated dressers that can be seen from the outside and inside (example 1 P4).

5.0 CONGLOMERATE OF RESULTS

This research takes into account the analysis of 8 sample stores, their layout, zoning, area, interior, window, front facade and online sales.

The qualitative table shows the data of all sample stores, opened in four different periods. The table shows the differences and development of stores in the time period 1963-2024.

Table 8. *Qualitative table of changes and developments in sample stores 1963-2024.*

P1	Area (net) m^2	Display window	Furniture	Materialization	Floor	Ceiling	Lighting	Music	Scent	sign	Online sale
1	5.7 $м^2$	flat	Table, shelves, chair	Wood, metal	Ceramic plates	White facade	General lighting, neon	no	no	yes	no
2	8.7 $м^2$	Pulled out	Table, chair, chest of	Wood, glass	Ceramic plates	White facade	General lighting, neon	no	no	yes	no

			drawers								
P2	**Area (net) m^2**	**Display window**	**Furniture**	**Materialization**	**Floor**	**Ceiling**	**Lighting**	**Music**	**Scent**	**sign**	**Online sale**
1	15.8 $м^2$	Flat glass and aluminum	Cupboards with open and closed shelves, table	Wood (plywood), glass	White Ceramic plates	Lowered ceiling	General lighting, neon, light panels	no	no	yes	No Yes for a website
2	8.8 $м^2$	Flat glass and aluminum	Tables, chests of drawers, hanging closed shelves	Wood, glass, metal	Ceramic plates	Lowered ceiling	General lighting, light panels, neon in the shop window	no	no	yes	no
P3	**Area (net) m^2**	**Display window**	**Furniture**	**Materialization**	**Floor**	**Ceiling**	**Lighting**	**Music**	**Scent**	**sign**	**Online sale**
1	14.6 $м^2$	Wall, door and window with parapet	Walls with a white facade. Designed furniture with a large L table and shelves on three sides. Tendency towards holism.	Wood, glass, metal reinforcement.	Ceramic plates.	A lowered wooden element with built-in neon lighting matches the interior.	Neon hanging.	no	**no**	yes	no
2	15.7 $м^2$	Fully glazed / transparent with aluminum door frame	Designed interior, wooden and glass shelves. Same look and table with	Wood, glass.	Ceramic plates	Lowered designed ceiling.	neon and spot. ambient and accent lighting.	yes	no	yes	Social networks.

			glass display section. Partially wood-clad walls.								
P4	**Area (net) m^2**	**Display window**	**Furniture**	**Materialization**	**Floor**	**Ceiling**	**Lighting**	**Music**	**Scent**	**sign**	**Он Online sale**
1	23.1 $м^2$	Partially glazed, decorated with arcades, special dressers for the window display from the inside.	Wooden chests of drawers rounded with marble, finished with glass. White and black marble in furniture	White painted wood, white marble, black marble, mirrors.	Decorated floor, marble and white ceramic tiles.	Lowered ceiling with unevenness. Hanging chandelier and spotlight.	Lowered ceiling with a chandelier in the middle and spotlights throughout the store and in the window.	yes	yes	yes	Website, online ordering, social media.
2	16.5 $м^2$	Fully glazed facade, with a small aluminum door frame.	The window is transparent. Metal shelves and hangers for goods, a wardrobe in the corner. A wooden cash register with drawers, a stool.	Wood, metal, glass.	Laminate	The ceiling is made of black painted sheet metal.	Spot above the shop window. Ambient and accent lighting.	yes	no	yes	Social networks

The above table shows the growth of the area of the stores. The growth of the depots is also shown (table 2). The interiors are changing, from necessary furniture for the basic purpose and function in a store, a transition to modernism, then neoclassicism and today the contemporary style. The shop windows from not completely transparent and Ottoman style, pass into a modernist style completely glazed. The materialization in the furniture expands the palette, newly made types of glass are used, more types of metal and wood, marble and granite are added. The interiors have a strong effort towards holism. The floors are increasingly materialized with ceramic glossy tiles, with large dimensions and maximum reflection. The ceiling is lowered or arranged, with various lighting elements, which are ambient at the beginning and then moderate and emphasize the shop windows. Special lighting is also added in the shop window.

The use of websites for marketing is observed even in stores at P2, which is expanded in P3 by using social networks for advertising and sales. Modern stores massively use social networks and their own websites for online sales. The time of the Covid-19 pandemic has initiated online sales all over the world.

Industrial expansion is clearly increasing consumerism, changing the culture of retail, the style of architecture and the interiors of retail spaces, and under the indications of globalism, introducing a special discipline in retail design.

5.1 CHANGES IN RETAIL PUBLIC INTERIORS

Based on the above examples, it is concluded that there are dynamic changes in public retail interiors. For a concise explanation, the following are the constituent components and descriptive clarification.

Historical and traditional component in addition to public design – the old bazaars, especially the Old Skopje Bazaar, are among the oldest trading locations, where buying and selling has been carried out for centuries, in addition to Skopje citizens and many people from other cities and countries. The crafts developed in this region were irreplaceable at the state level. The old guilds were known for their trading skills and appreciated by the citizens. In addition to this indication, the shops have a smaller area, concentrated with frontal facades facing the streets. They were made of wood and glass, similar to each other, in the Ottoman style. The interiors are concentrated on the purpose of the shop and the crafts, without special attention and investment in aesthetics. Due to the small area, there were also few opportunities for special interior decoration. The largest material used in the interiors is wood, which is concluded from vernacular architecture. Walls covered with wood, floor with wooden boards, later replaced with ceramic tiles. The tables were wooden, with a work area, drawers and in some shops a space for displaying products, glazed with ordinary glass. The ceiling is again with wooden boards or with white painted sheet metal. Old archaeological decoration is noticeable, most often Ottoman, to show the ancient value of the bazaar itself. Decoration with religious content is also noticeable. The interior decoration shows a realistic picture of the people who worked and lived in this region, multiethnic and traditional.

Political and economic component in addition to public design – the Macedonian region, due to frequent political changes, is experiencing destabilization and stagnation, which is most reflected in economic development. The transition from a Yugoslav state to an independent state, name change, interethnic conflicts have created enormous economic stagnation and social trauma [Petkovska 2019:64]. Despite the weak economic development, retail stores are developing dynamically. Factors of change occur quickly, although under chaotic conditions, retail interiors reflect and change with every internal and external indication. Under the influence of Ottoman architecture in the bazaars, the Ottoman style is also evident in the interiors of retail stores. During modernization, especially after the earthquake, architecture transitions to modern commercial buildings and stores with maximum transparency. Yugoslav chain stores emphasize modernism in the interiors, when stores appear aesthetically decorated in a modern style and retro style. In the 1990s, independent private efforts by sellers towards the arrangement of public interiors appeared in private shops. Classicism, neoclassicism and postmodern styles of interior decoration were observed. Again, the interiors differed in greater and lesser investment in the arrangement. During this period, advertising of shops on television channels also began. Modern shop formats are international standards, which also reached Macedonia in the form of foreign investors, who completely changed the culture of buying and selling.

Architectural component in addition to public design – acts in an appropriate function. In the example of the shops, the basics of space utilization by buyers, sellers and furniture are analyzed – green color with a defined space for buyers, orange color for a defined space for sellers and pink color with a defined space for furniture (tables 4, 5, 6 and 7). In P1, the space is used more by the seller, despite the fact that the shops at that time also performed a service activity. With a space divided in half for buyers and sellers, it is seen in P2, while the space begins to be used more for furniture and for buyers in P3 and especially P4. The space used for the seller is minimal, while for additional goods there is a depot in the back of the shop. Otherwise, the shops are aesthetically arranged with a larger number and types of furniture for displaying the products for sale.

Brand and store management in addition to public design - the modern format of stores, i.e. retail design as a separate discipline, does not exist without brand and store management by professionals, especially chain stores. The brand is a unique name of an industrial company, which in cooperation with the sales manager and the interior architect fits a special store. The great proliferation of industries and similar stores, acts in creating a brand and uniqueness of stores, to achieve greater sales.

The architect, the brand and the store manager are missing in P1. They appear in some stores in P2, mainly Yugoslav chain stores. In P3, advertising of the service begins on television channels in some stores, otherwise larger stores begin to implement it on websites. During this period, in stores with a larger investment, an architect appears who designs special furniture for a particular store, which furniture is made by home craftsmen.

The modern stores in P4, originating from global chain stores, are the same everywhere in the world, with their products and physical appearance of the store. The furniture in these stores is designed by foreign architects, which furniture is re-assembled under the same regulations for each store around the world. Domestic chain stores and private stores make a great effort to follow the same global steps, which create new trends and are necessarily followed. Experts are involved in the process.

The component of aesthetics, technology and digitalization in addition to public design – from industrialism and the great global spread, massive competition is reached. In addition to the brand that insists on identification and unification, the marketing that affects informing and impressing citizens, aesthetics in architecture is among the most important dimensions in the creation of "theatrical" stores.

Aesthetics in retail design, which can also be interpreted as hyperrealism, is treated by several authors. Baudrillard describes hyperrealism as a process of "disnification", which can be understood as culture being transformed into economic capital, especially emphasized in tourism and retail design [Harris, 2004] [Baudrillard, 2020]. In addition to nostalgia, young people are deeply immersed in the digital world as opposed to real socialization. The English language and digital platforms are rapidly spreading new trends, creating addictions among the younger generations and a desire to follow them.
The development of technology acts to increase the real aesthetics in stores. It allows for the creation of a hierarchy of furniture, elements and products in the store. Possibilities of processing with different techniques of materials, is closely linked to the processing of excellent furniture, with well-processed materials and techniques. The wide possibilities act in diversity, creating greater aesthetics and attraction to people, in addition to the architectural functional component. The improvement of the type of glass acts in a wider application of glass in addition to the massive window and in furniture, creating high transparency. The use of metal in minimal dimensions, allows for beautiful minimalism.

The shiny surfaces of the furniture and the floor, increase the reflection and shine. In particular, the use of several types of lighting elements, separate above each exhibited piece of furniture, contributes to a luxurious aesthetic.

5.2 EPHEMERAL RETAIL INTERIORS

The phenomenon of ephemerality explains the dynamic nature of architecture in the face of global changes, characterizing it with attributes of changeability, transience and short-termism. Interior design over a period of six decades shows transformations in design, chaotic changes without proper processes, interrupted ongoing processes. From a social perspective, by reviewing state authors and comparing with world literature, it can be concluded that RSM is passing into cultural backwardness

(the theory of William Ogburn) [Ogburn, 1964], when material conditions (economy, technology) change faster than cultural beliefs or social institutions, creating tensions and instability. Consequently, Western development with its media, consumerism, liberal politics are implemented before the state with its institutions and cultural identity is ready to absorb them. The natural evolution in our country occurs with constant problems that interrupt the appropriate direction of movement [2].
Public interiors have gone through several development phases over six decades; these phases, along with architecture and interior design, are closely related. The following is a table showing the development of public interiors over the period 1963-2024, showing indicators and results.

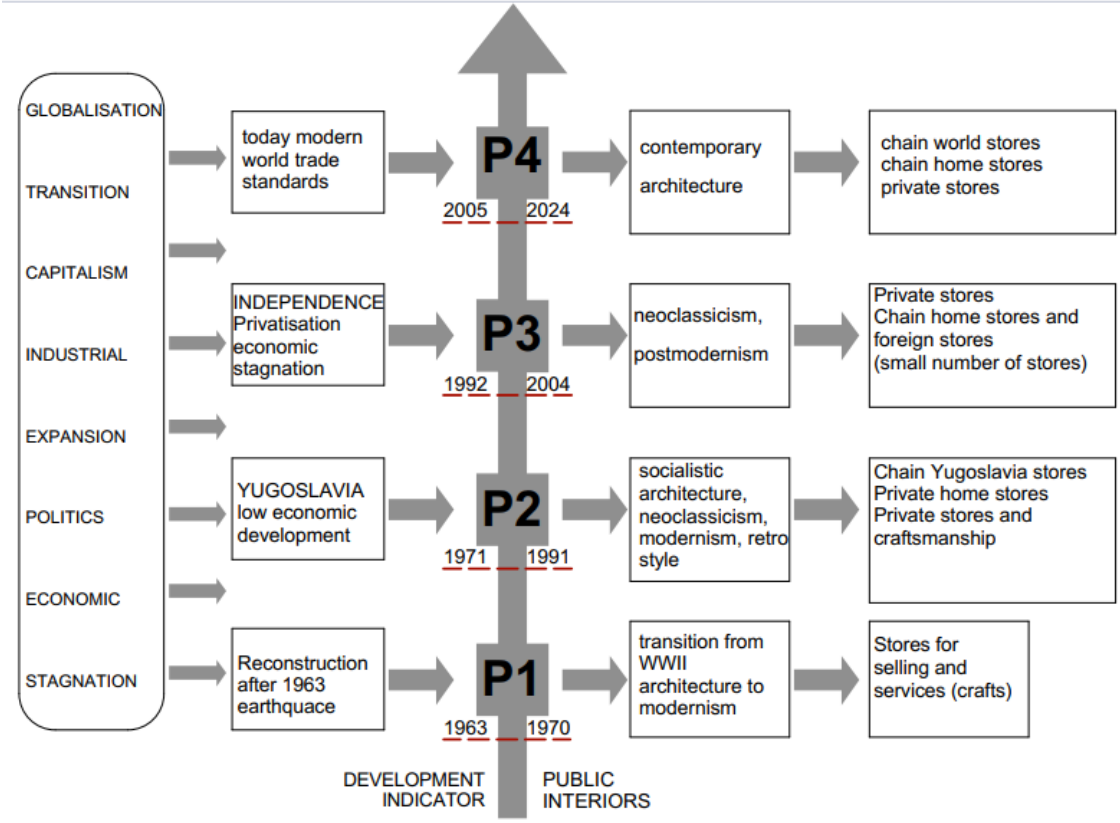

Table 9. *Final results of research.*

9. KEY INDICATIONS OF DEVELOPMENT AND CHANGE IN PUBLIC INTERIORS 1963-2024.

Table 9 shows the final results of the research. The table, viewed from left to right, shows the comprehensive indicators that contribute to major changing events in the country, which events manifest themselves in the styles of architecture and interior design and the emergence of new formats of public interiors.

The process of change is obvious and leads to the manifestation of phenomena. The phenomenon of ephemerality in architecture, which implies short-termity, changeability and transience, in the public context of interior design proves rapid transitions in different architectural styles, changes in types of stores along with their interior and window displays, changes in the process of buying and selling, changes in the level of investment, changes in technological processing, the introduction of new standards in store management and branding and digitalization.

[2] The parallel idea is confirmed by Petrovska [Petkovska 2019:64], when interpreting Macedonian culture as a social cultural trauma.

6.0 CONCLUSION

This paper aims to define the development of public retail interiors in the region of the Republic of Macedonia, in the time frame 1963-2024. The method of researching development and changes is phenomenological, by defining public retail interiors as ephemeral, due to the great rapid changes.
From the above, it is concluded on the impact factors that contributed to public interiors being very dynamic. It is concluded on the specific reasons for the occurrence of rapid, imposed changes, to keep up with comprehensive global trends.

In addition to historical, economic and social analyses and defining development processes, 8 specific stores are investigated, opened in different periods. The stores experienced changes in area, public furniture, manner of interior decoration, architectural style and bringing new trendy contents.
By analyzing the type of furniture, style, materialization and real application, the conclusion is real and tangible. Despite the phenomenological research method and the qualitative method of comparison, it is concluded that rapid imposed changes in public retail design are insufficiently experienced, analyzed and developed. Retail design has experienced several unfinished processes in our region. In the modern and contemporary world, when consumerism in the period of digitalization moves uncontrollably, retail design inevitably changes, with short-term changes and accepts new challenges of the trend. The short-term nature of public retail, often changing and innovative formats, leads to ephemeral design.

Research based on the occurrence of phenomena contributes to the disclosure of manifestations and understanding of the directions of development. The paper aims to define the process of changes in public architecture and interior design, with concretion in retail premises, existing in the RNM, and also to define the rapid applications in public interiors as ephemeral. Further desirable studies in this area would be the consequences of the uncontrolled construction of a large number of shopping centers in our region, their function in the absence of sufficient demand, as well as the endless uncontrolled global consumption.

REFERENCES

1. Петковска, Антоанела (2019): *Консумеризмот во уметноста во услови на културна траума.* Списанието „Културата на распродажба – консумеризмот и комерцијализацијата на културните продукти“.
2. Baudrillard, Jean. (2020): *Shoqëria e Konsumit. Mitet dhe strukturat e saj*. Logos A. Shkup.
3. Chappel, Bryan (2004): *Ephemeral Architecture – towards definition 3*.
4. Petermans, Ann & Anthony, Kent (2017): *Retail Design. Theoretical Perspectives*. Routledge. New York.
5. Boustani, Ghalia (2020): *Ephemeral retailing. Pop-up stores in postmodern consumption era.*Routledge Taylor and Francis Group. New York, USA.
6. Boustani, Ghalia (2021): *Pop-up Retail..The evolution, application and future of ephemeral stores*. Routledge Taylor and Francis Group. New York, USA.
7. Underhill, Paco (2009): *Why we buy – the science of shopping.* Simon & Schuster Paperbacks New York.
8. Kronenburg, Robert (1997): *Transportable Environments: Theory, Context, Design and Technology*. Taylor and Francis. Routledge. London.
9. Kronenburg, Robert; Lim, Joseph; Chii Yunn, Wong (2003): *Transportable Environments 2: Theory, Context, Design and Technology*. Spoon Press, London.
10. Robert, Kronenburg (2003): *Portable Architecture*. Oxford. Elsevier/Architectural Press.
11. Kronenburg, Robert (2008): *Portable Architecture: Design and Technology*. Birkhauser Verlag, Germany.
12. Rieunier, Sophie; Jallais, J. (2013): *Marketing sensoriel du point de vente: Créer et gérer l'ambiance des lieux commerciaux*. Paris: Dunod.
13. Mesher, Lynne (2010): *Basics interior design*. Retail design. AVA Publishing. Canada.
14. Quartier, Katelijn (2016): *Retail design, a discipline in its own right*. Hasselt University.
15. Ogburn, F. William; Nimkoff, Francis Meyer (1964): A handbook of sociology. Routledge and K. Paul. California University Press.

16. Harris, D. (2004). *Key Concepts in Leisure Studies*. Sage, London.
17. Yuan, Ye., Gang, L., Dang, R., Lau, S.S.Y., Qu, G.(2021): *Architectural Design and consumer experience: an investigation of shopping malls throughout the desing process*. Asia Pacific Journal of Marketing and Logistics. China.
18. H. Christiaans and R. A. Almendra (2012): *Retail Design: A new discipline.* International Design Conference – Design. Dubrovnik – Croatia, 1893-1902.

DESIGNING AN URBAN FURNITURE PLAN: URBAN ANALYSIS OF TETOVO

Umnije Aziri[1], Elena Nikoljski Panevski[2], Zejnelabedin Aziri[3]

[1]Phd candidate, Faculty of Design and Technologies of Furniture and Interior, Ss. Cyril and Methodius University in Skopje
[2]Professor, Faculty of Design and Technologies of Furniture and Interior, Ss. Cyril and Methodius University in Skopje
[3]Assistant Professor, Faculty of Technological Sciences at "Mother Teresa" University in Skopje
e-mail: umnije.aziri@gmail.com

ABSTRACT

In this study, we explore the essential elements and guiding principles necessary for the development of a comprehensive urban furniture plan specifically tailored for the city of Tetovo, North Macedonia. The paper draws upon contextual analysis, site assessments, and a review of existing infrastructure and demographic trends to propose strategic improvements in public space design. We evaluate various urban typologies such as parks, plazas, and transit hubs, and consider socio-cultural dynamics and environmental sustainability as integral parts of the design process. This interdisciplinary approach combines urban planning, architecture, and community engagement to deliver targeted recommendations for urban furniture interventions. Our goal is to create inclusive, resilient, and multifunctional public spaces that reflect Tetovo's unique identity while addressing its challenges related to rapid urban growth and limited green infrastructure.

Keywords: urban furniture, space analysis, public space typology, urban planning, Tetovo.

1. INTRODUCTION

Urban public spaces are essential components of city life, serving not only as places of transit and leisure but also as platforms for social interaction, cultural expression, and civic engagement. In contemporary urban planning, the design and integration of urban furniture—elements such as benches, lighting, signage, waste bins, and shelters—play a fundamental role in shaping the experience, accessibility, and inclusivity of these spaces (Gehl, 2011; Carmona et al., 2010). Far beyond their practical functions, urban furniture pieces serve as markers of identity and quality of life, reflecting the values, needs, and aspirations of the communities they serve (Barbaux, 2011).

Urban furniture planning is not an isolated design task; it is embedded in the broader framework of urban programming, land use planning, and place-making strategies. Effective furniture planning requires a deep understanding of spatial typologies—parks, plazas, streetscapes, transit hubs—as well as of the diverse behaviors, expectations, and rhythms of the urban population (Moughtin et al., 2003). Questions such as who will use the space, at what time of day, for what activities, and under what environmental conditions must guide every planning and design decision (Francis, 2003). These micro-scale considerations must also align with macro-scale objectives, such as improving walkability, fostering environmental resilience, and enhancing social cohesion (Carmona, 2014).

In the case of Tetovo, a city in North Macedonia known for its multicultural population and historical significance, urban furniture planning presents both challenges and opportunities. The city is experiencing rapid urban growth, which, while signaling economic potential, has also led to fragmented development and a marked deficit in public infrastructure and green spaces (State Statistical Office, 2023). Many existing public areas lack adequate amenities, are poorly maintained, or are simply not designed to accommodate the needs of a diverse and growing population. As a result, citizens often find themselves disconnected from public life, lacking spaces where they can comfortably gather, relax, or engage with their surroundings.

This study positions urban furniture as a strategic design tool capable of enhancing the quality, functionality, and inclusivity of public spaces in Tetovo. Through a mixed-methods approach that

includes literature review, spatial analysis, and stakeholder assessment, the research explores the potential for designing a comprehensive and context-sensitive urban furniture plan. The goal is not only to improve physical infrastructure but also to foster a more socially cohesive, environmentally sustainable, and culturally vibrant urban landscape (Calkins, 2009; Bill & Gail, 2010).

By examining the unique characteristics of Tetovo's urban environment, and by proposing targeted interventions rooted in best practices and local realities, this paper seeks to contribute to the growing body of knowledge on human-centered urban planning. It highlights the importance of designing with intention—where every bench, lamp post, or trash bin is seen not merely as an object, but as an opportunity to make the city more livable, equitable, and inclusive for all (Gehl, 2011).

2. MATERIALS AND METHODS

This study employed a mixed-methods approach to ensure a comprehensive analysis of urban furniture planning in Tetovo. A thorough literature review was conducted, drawing on academic sources related to urban furniture design, public space theory, and urban sociology. Site analysis was carried out through field observations across various public spaces in Tetovo, with particular attention to spatial typologies, user behavior, and the placement of existing urban furniture. In addition, GIS mapping and urban data were utilized to assess factors such as population density, accessibility, and the availability of green spaces, using both municipal and national datasets. Finally, Stakeholder insights were incorporated through a qualitative review of existing municipal planning documents, urban development strategies, and community reports published by the Municipality of Tetovo. While primary survey data was not collected for this study, secondary data provided by local authorities and national statistics offered a window into the socio-economic and demographic makeup of Tetovo's urban population. Additionally, indirect stakeholder perspectives were inferred from documented citizen feedback in local urban development initiatives, online public forums, and published interviews with municipal officials. These sources allowed for a nuanced understanding of the diverse user groups who interact with Tetovo's public spaces ranging from families with children and elderly residents to students, business owners, and commuters.

Field observations were also used as a tool for user behavior analysis, identifying usage patterns, spatial conflicts, and accessibility barriers. Together, these indirect methods provided a grounded view of the interests and needs of key stakeholders affected by urban furniture planning decisions.

3. PLANNING FRAMEWORK FOR URBAN FURNITURE

An effective urban furniture plan begins with programming and identifying the space's intended users. Each location must be studied to understand who will use it, what they will do there, and what environmental factors may affect its use. The design process should be rooted in empathy and the needs of different users, including children, elderly individuals, people with disabilities, and professionals.

By applying design thinking—empathy, ideation, prototyping—urban planners can ensure spaces are user-centered. Incorporating universal design principles guarantees accessibility for everyone, regardless of ability. This section explores how temporal, spatial, and functional considerations shape the design of urban furniture.

4. SOCIAL, CULTURAL, AND HISTORICAL CONTEXT OF TETOVO

Tetovo is characterized by a multiethnic population, comprising Albanians, Macedonians, and Turks, among others. These diverse cultural and religious groups use public spaces differently, necessitating culturally sensitive designs. Historical layers from the Ottoman period through to modern times influence the aesthetics and usage of space, with many areas retaining historical monuments and architectural elements.

Public space design must accommodate gender-specific expectations, intergenerational interactions, and communal memory. Furniture, signage, and even colors must align with local traditions and social norms while remaining inclusive and modern.

5. URBAN SPACE TYPOLOGIES AND FURNITURE NEEDS

The design and selection of urban furniture must be carefully adapted to the specific characteristics of each public space. Different types of environments, whether plazas, parks, or transit areas—serve distinct functions and user groups, and therefore demand tailored furniture and amenity strategies. Factors such as the configuration of the space, its location within the city, and the patterns of activity it supports all play a critical role in determining the most appropriate interventions.

Urban plazas, typically located near commercial or governmental hubs, are high-density spaces where people gather, rest, meet, or pass through. As such, they require robust and weather-resistant furniture solutions, including durable seating, ample lighting, accessible water fountains, and efficient waste disposal systems. The layout should promote social interaction while maintaining clear circulation paths to accommodate high foot traffic.

Urban parks, in contrast, prioritize natural aesthetics and relaxation. These spaces often feature soft landscaping elements like grass, trees, and water features. Furniture in parks should support varied activities—quiet reading, social gatherings, child play, or fitness—and include benches, picnic tables, shaded shelters, drinking fountains, and possibly public restrooms. Dispersed furniture placement can preserve open green vistas while providing moments of rest and comfort.

Transit stops focus on efficiency, safety, and comfort during short waiting periods. Here, furniture must prioritize shelter from weather, clear sightlines, and accessibility. Common elements include covered seating, real-time information displays, tactile flooring for the visually impaired, lighting for security, and clear signage. The quality of furniture at these nodes directly affects the perception of public transport systems.

Emerging trends in urban design now emphasize **smart furniture solutions** that integrate technology with sustainability. These include solar-powered lighting, public benches with USB charging ports, Wi-Fi access, and sensor-activated lighting systems. However, not all innovations succeed; poorly contextualized designs—such as unshaded metal benches in hot climates or overly rigid installations—often go unused or become barriers rather than assets. This underscores the importance of **context-sensitive design**, where climate, culture, user diversity, and behavioral patterns are all taken into account.

Ultimately, urban furniture should not be treated as static objects but as tools for shaping behavior, enabling inclusion, and enhancing the character and usability of public spaces. A one-size-fits-all approach risks alienating users and undermining the potential of urban space to support vibrant community life.

6. URBAN CONTEXT AND ANALYSIS OF TETOVO

Municipality of Tetovo is located in the Northwestern part of the Republic of North Macedonia, on the slopes of Sharr Mountain as well as in the lower parts of the Polog valley. The municipality extends from the northwest to the south-east. To the north, north-west and west it borders the municipalities of Dragash and Prizren in the Republic of Kosovo; to the east and south-east with the municipalities of Tearce, Jegunovce and Zhelino and to the south with the municipalities of Bogovinje and Brvenica (see Figure 1).

Tetovo is located an average of 824 meters above sea level and has a moderate continental climate with an average annual temperature of 11.6°C. Of the total area, 47.262 ha is utilized agricultural land,6.837 ha is covered with forests, 7.047 ha is arable land, 9.726 ha is pastures, 2.197 ha is meadows, 2 ha is vineyards, and 2.197 is orchards.

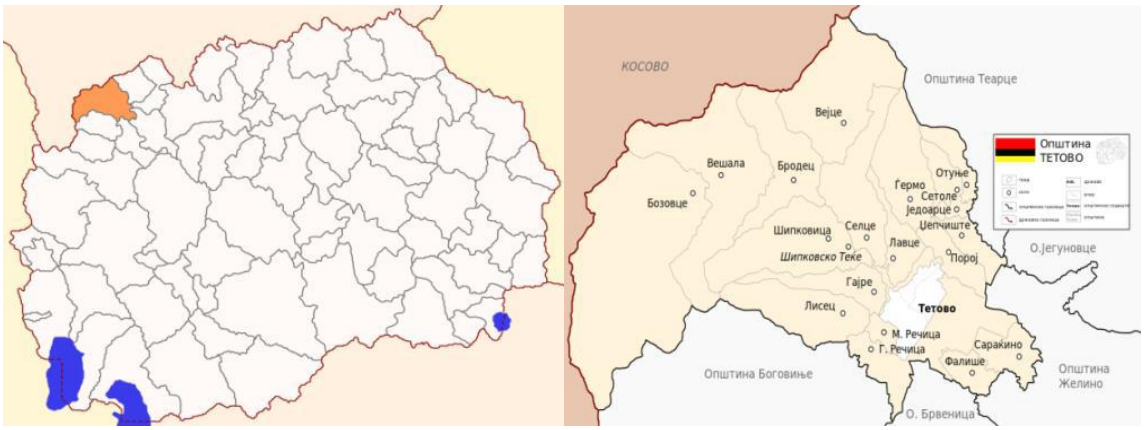

Figure 1. *Geographic position of Tetovo (Source: Archivo:Map of Tetovo Municipality.svg - Wikipedia, la enciclopedia libre).*

The municipality covers an area of 261.89 km2 and has a total of 84,770 inhabitants according to the 2021 census. The municipality consists of 20 settlements: 10 lowlands, 6 hillside and 4 mountainous.

The demographic composition of Tetovo reveals a critical understanding that highlight the need for strategic investment in public greenery and urban furniture. The population is fairly balanced by gender, with women representing a slight majority. This balanced distribution highlights the importance of designing public spaces that are inclusive, safe, and comfortable for all users, particularly women and children, who are often underserved in urban infrastructure. The age structure further emphasizes the city's diverse needs: while a significant 68% of residents fall within the working-age population (15–64), there is also a substantial presence of both youth (20% aged 0–14) and elderly citizens (12% aged 65 and above). Such diversity calls for multifunctional spaces that cater to different life stages—playgrounds and safe recreational zones for children, accessible seating and shaded rest areas for older adults, and dynamic public plazas or green corridors for the active adult population. Moreover, with approximately 72% of the population living in urban areas, Tetovo is experiencing high pressure on its existing infrastructure. This urban concentration intensifies the consequences of the city's lack of green space and pedestrian areas, which have been systematically reduced over recent decades due to uncontrolled development. In this context, the restoration and expansion of urban greenery, along with the thoughtful integration of urban furniture, are not simply aesthetic or recreational concerns, they are public health imperatives and a matter of environmental resilience. Well-designed, inclusive public spaces can serve as vital urban infrastructure, improving air quality, reducing urban heat, supporting mental and physical well-being, and fostering a sense of community among a diverse and densely concentrated population.

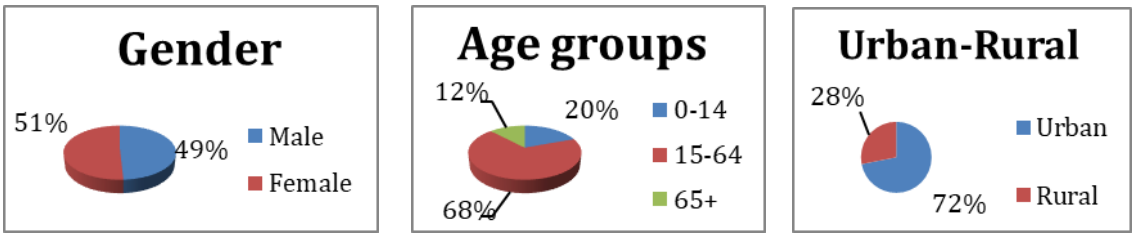

Graph 1. *Population distribution of Tetovo by gender, age and urban -rural relationship, 2021. Source: State Statistical Office of the Republic of North Macedonia.*

Tetovo's strategic location at the foot of the Šar Mountains and its connection via major highways and rail lines contribute to its urban development. However, rapid urbanization has outpaced planning, resulting in a lack of green spaces and public infrastructure. Population growth and construction encroach on agricultural land, and there is a visible shortage of recreational areas.

Despite its geographic advantages and cultural significance, the city struggles with traffic congestion, limited pedestrian pathways, and insufficient urban furniture. A SWOT analysis highlights

strengths in location and diversity, weaknesses in infrastructure, opportunities in tourism, and threats from unregulated expansion.

The cadastral maps in the figure 2. shows the substantial and radical changes in urbanism and architecture, especially in public spaces in ten years. Most often, these changes come at the expense of urban green areas. The construction dynamics in Tetovo have created a noticeable absence of green areas as public spaces where people can gather. It is very visible how the city is growing uncontrollably towards agricultural areas.

Table 1. *Comparative representation of built surface and population of Tetovo between 2002 and 2022.*

Year	Built surface (xa)	Population
2002	131.32	52,915
2021	167.83	63,176

Figure 2. *Cadastral maps of Tetovo city from 2002 (left) and 2021 (right).*

7. URBAN GREEN SPACES AND CHALLENGES

Tetovo was once considered one of the greenest cities in North Macedonia, with tree-lined streets, small parks, and numerous public green areas. However, over the past few decades, this green character has eroded significantly. Widespread and often unregulated construction has replaced green spaces with concrete developments, resulting in the loss of urban trees, small parks, and even informal recreational areas. Tetovo hasn’t managed to prepare a comprehensive urban plan since 2002, leaving the city to grow without vision or spatial coherence. This neglect has transformed Tetovo from a once-lush urban environment into a dense, traffic-congested landscape with polluted air and a near-total absence of large public parks.

Despite having a population of over 60,000 in its urban core, Tetovo does not meet the legal definition of a park under the Law on Urban Greenery, which requires a minimum size of one hectare. The city has just 0.2 m² of green space per capita—far below the World Health Organization’s recommendation of 9 m². The only notable green spaces, such as the Park of the Woman Fighter (0.85 ha) and the park near the Colorful Mosque (0.40 ha), fall short of both legal and functional standards. Furthermore, laws like the Denationalization Law and the Legalization of Illegal Constructions have been misused, allowing previously public plots—such as sports fields and parking lots—to be privatized or converted into oversized buildings, exacerbating infrastructure pressure.

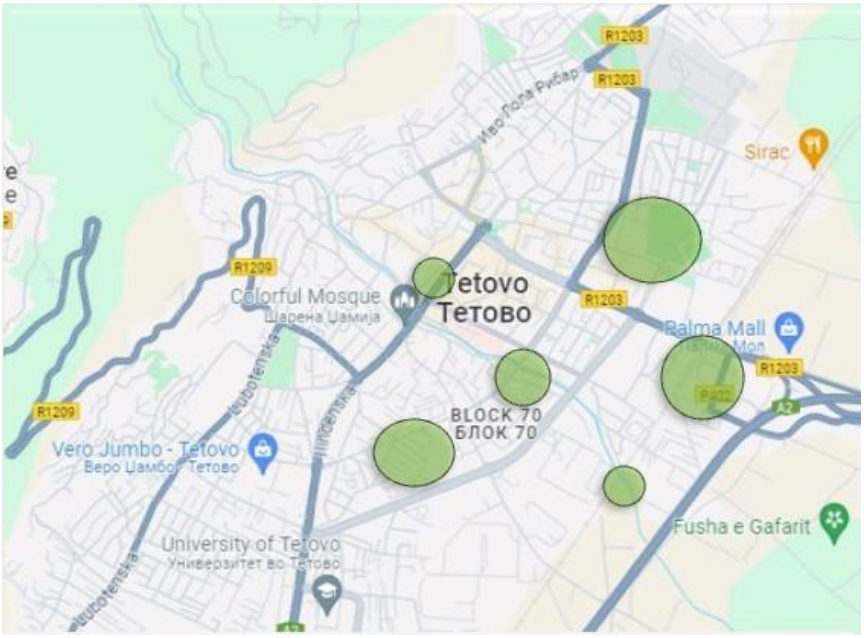

Figure 3. *Conceptual map showing the distribution of parks in the city of Tetovo.*

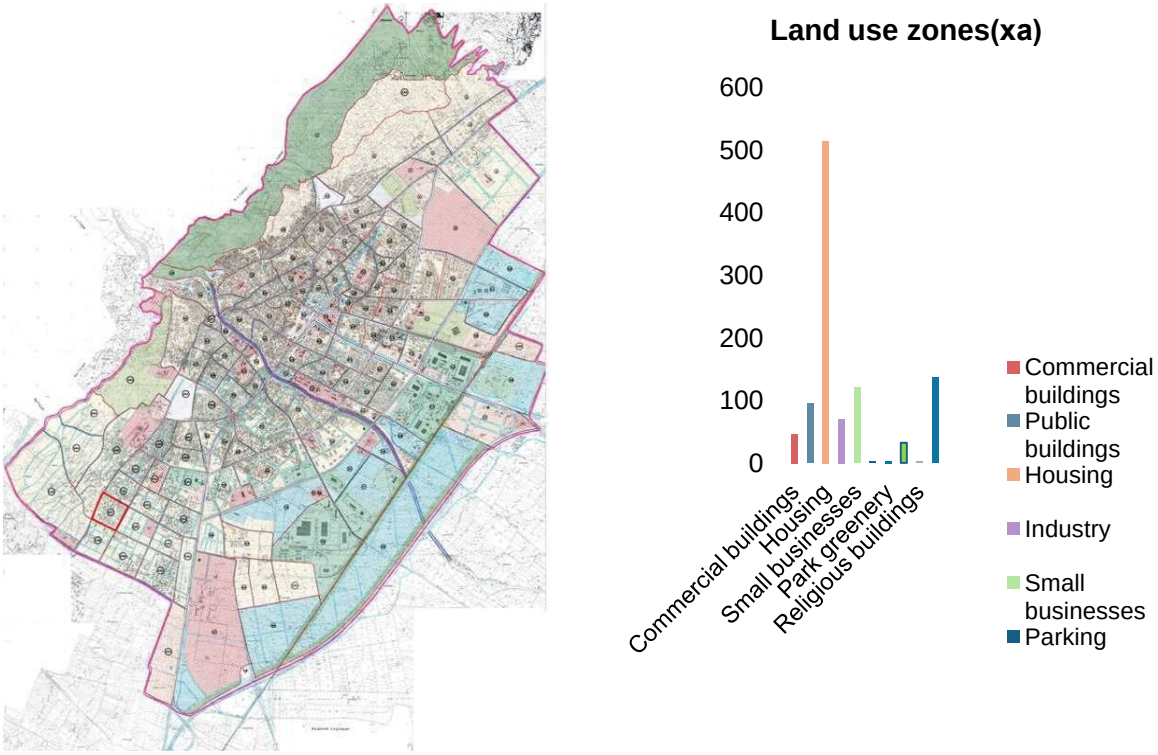

Figure 4. *Graphical representation of the distribution of land use zones in Tetovo in 2022. Source: Municipality of Tetovo.*

The land use distribution in Tetovo (fig. 4) clearly illustrates a significant imbalance in how urban space has been allocated. Residential areas overwhelmingly dominate the urban fabric, occupying the majority of the city’s surface. In contrast, zones designated for commercial use and small businesses are far more limited, reflecting a constrained economic diversification in spatial planning. Most

concerning, however, is the minimal allocation for urban greenery, which is almost negligible when compared to other land use categories. This stark underrepresentation of green areas highlights the lack of prioritization for environmental quality and public well-being in Tetovo's urban development.

The current land use pattern points to a city shaped by housing demands and construction pressures, with insufficient attention paid to creating healthy, livable, and balanced urban environments.

8. PROPOSED INTERVENTIONS AND DESIGN RECOMMENDATIONS

To address Tetovo's public space deficiencies and use its urban potential, several targeted interventions are proposed. These recommendations aim to enhance the functionality, inclusivity, and cultural relevance of public spaces across the city.

One key intervention is the revitalization of the Dva Bresta Park. Currently, the park is underutilized, lacking cohesive design, sufficient seating, and programming for public activities. The proposed solution involves redesigning the area as a flexible, multifunctional space capable of hosting markets, performances, and gatherings. Elements such as retractable shading structures, movable seating, interactive art installations, and embedded lighting would make the plaza vibrant and usable both day and night. Strategic paving patterns can help define activity zones without creating physical barriers, maintaining the openness of the space.

To support active mobility and better integrate existing green spaces into Tetovo's urban fabric, this study proposes a Green Mobility Corridor connecting the Park of the Woman Fighter, located near the central bus station, with the main urban plaza. This corridor will serve as both a physical and symbolic artery, prioritizing pedestrian and cyclist movement while improving environmental and aesthetic conditions in the city's core. The corridor would include widened sidewalks, separated cycling lanes, shaded tree-lined paths, and regular resting areas equipped with benches, water fountains, and solar-powered lightting. The route should be designed with universal accessibility in mind, incorporating tactile surfaces and resting zones for elderly and disabled users.

The river corridor, particularly along the River Pena, represents a largely untapped civic asset. Although it flows through the city, it remains disconnected from daily urban life. The proposed activation would transform the riverbanks into a scenic promenade for pedestrians and cyclists. Enhancements include wooden decks, outdoor fitness zones, fishing spots, and small cafés or kiosks, all complemented by native vegetation to aid ecological restoration and stormwater management. This would position the river as both a leisure destination and a social connector.

In the city's dense residential neighborhoods, the absence of green space calls for the creation of community-designed micro parks. These would utilize vacant lots or underused public land, transformed through participatory planning. Each pocket park would include age-inclusive furniture—such as benches for seniors and play areas for children—alongside pollinator gardens and sustainable features like rainwater harvesting systems.

To bring coherence to the city's fragmented urban furniture landscape, integrated urban furniture modules are proposed. These modular units would combine seating, lighting, greenery, and waste management into a single form, designed to reflect local culture while allowing easy maintenance and upgrades.

Lastly, to increase engagement in public spaces, the introduction of seasonal and temporary installations is recommended. Modular furniture and pop-up structures—such as book-sharing kiosks or small community stages—can be deployed during festivals, weekends, or summer events. These temporary features not only activate public space but also serve as a low-risk way to test ideas before permanent implementation.

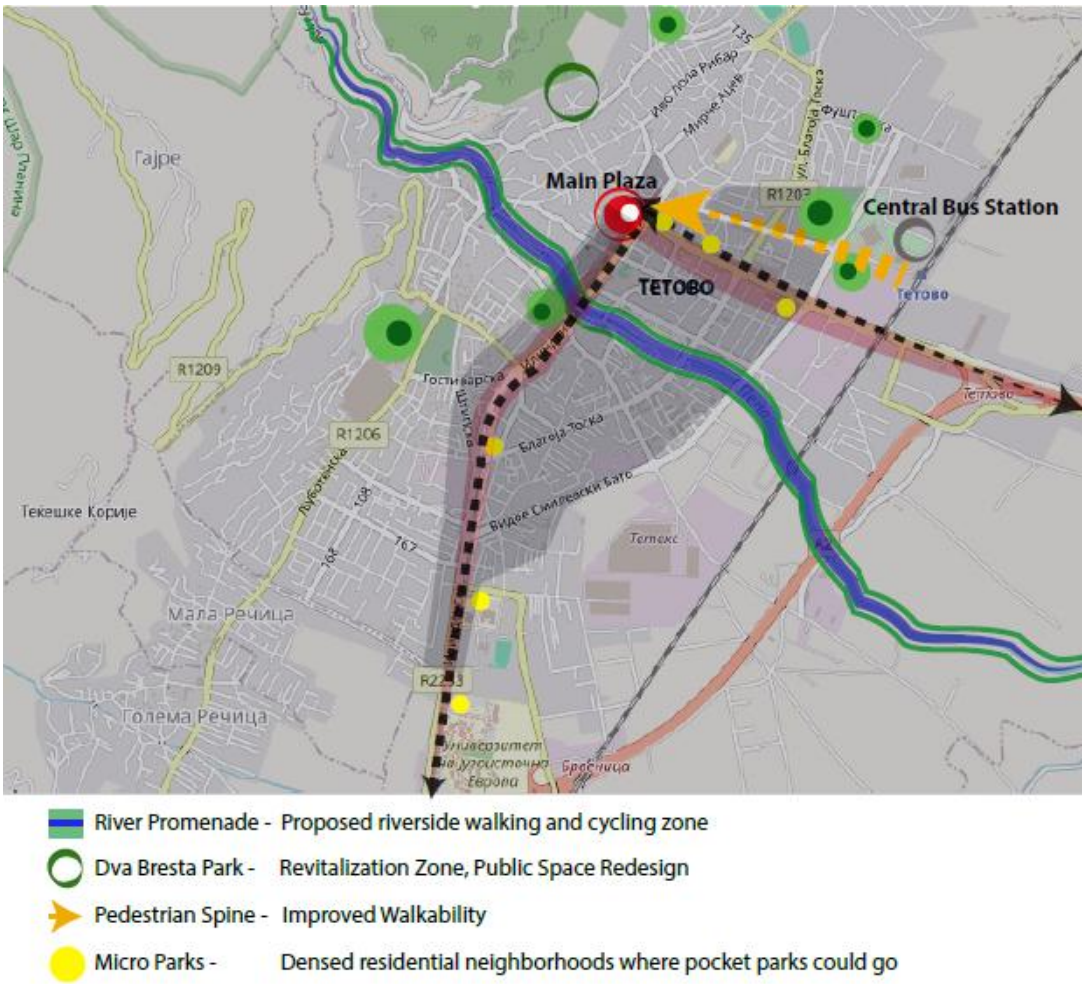

Figure 5. *Conceptual Map with the proposed interventions in Tetovo.*

9. CONCLUSION

Urban furniture is a critical interface between people and public space, playing a central role in how citizens interact with their environment. In the case of Tetovo—a city marked by rapid urbanization, rich cultural diversity, and underutilized public infrastructure—strategically designed urban furniture has the potential to catalyze significant improvements in both the functionality and inclusivity of public areas.

This paper demonstrated that urban furniture is not merely a matter of aesthetic enhancement or utility but a multidisciplinary design challenge that integrates architecture, urban planning, environmental sustainability, and social equity. Through a careful analysis of Tetovo's spatial dynamics, historical context, and social needs, we identified a set of interventions that are both realistic and transformative. The proposed actions, from revitalizing key public plazas and green corridors to activating the riverbanks and improving pedestrian connections, aim to reshape the city's public realm into a network of vibrant, accessible, and resilient spaces.

An important conclusion drawn from this research is the necessity of contextual sensitivity. Furniture solutions must be tailored to reflect the unique socio-cultural makeup of Tetovo's population, accommodating diverse groups with differing needs—families, elderly residents, children, office workers, and people with disabilities. Urban spaces must also serve as platforms for cultural expression, civic engagement, and environmental stewardship, which means the design and placement of furniture must encourage interaction, inclusivity, and sustainability.

Moreover, successful implementation of these interventions requires collaborative planning involving local government, urban designers, community stakeholders, and citizens themselves. Community engagement should not be an afterthought; rather, it must guide the planning and design process from inception to execution. Participatory design approaches can ensure that the proposed

furniture and public space interventions are embraced by the community and serve real, rather than perceived, needs.

Finally, this study emphasizes that urban furniture should not be seen as isolated objects but as part of an integrated urban system that contributes to the long-term resilience and adaptability of the city. As Tetovo continues to evolve, its ability to deliver public spaces that are inclusive, inviting, and adaptable will be a key indicator of its social and urban progress.

REFERENCES

1. Barbaux, S. (2011). *Urban Furniture: A New City Life*. Design Media Publishing.
2. Bill, M., & Gail, G. H. (2010). *Site Furnishings: A Complete Guide to the Planning, Selection and Use of Landscape Furniture and Amenities*. Wiley & Sons.
3. Calkins, M. (2009). *Materials for Sustainable Sites*. John Wiley & Sons.
4. Carmona, M. (2014). *The Place-shaping Continuum: A Theory of Urban Design Process*. Journal of Urban Design, 19(1), 2-36.
5. Carmona, M., Heath, T., Oc, T., & Tiesdell, S. (2010). *Public Places, Urban Spaces: The Dimensions of Urban Design*. Routledge.
6. Francis, M. (2003). *Urban Open Space: Designing for User Needs*. Island Press.
7. Gehl, J. (2011). *Life Between Buildings: Using Public Space*. Island Press.
8. Moughtin, C., Cuesta, R., Sarris, C., & Signoretta, P. (2003). *Urban Design: Method and Techniques*. Routledge.
9. State Statistical Office of the Republic of North Macedonia. (2023). https://www.stat.gov.mk
10. Stefanovski Z. & Pavlovski J. (1969). Tetovo (monografija). Nova Makedonija, Skopje
11. Svetozarevik B. (1999). Tetovski Spomenar (1919–1941). Napredok, Tetovo.
12. Target Communications DOOEL Skopje. Guide for investments in Polog Planning Region.
13. Municipality of Tetovo. http://www.tetova.gov.mk/en/b/31/

DEVELOPMENT OF A STARCH-BASED BINDER FOR BIODEGRADABLE PARTICLEBOARD COMPOSITES

Jan Weiss[1]

[1]*Mendel University in Brno, Czech Republic,*
Faculty of Forestry and Wood Technology,
e-mail: jan.weiss@mendelu.cz

ABSTRACT

The thesis focuses on the development of a biocomposite using bioplastic as a binder. The aim is not to fully replace petroleum-based adhesives, such as urea-formaldehyde, but rather to explore more environmentally friendly and biodegradable alternatives. The bioplastic was prepared from water, starch, vinegar, and glycerol, with potato starch selected as the most suitable source based on a literature review. Several variables were tested, including water content, application method, pressing temperature, and pressing time. The best results were obtained at a pressing temperature of 180 °C and a water content of 14.4%. The produced panels were subsequently tested for their physical and mechanical properties, where the maximum values reached were MOR = 13.8 MPa, MOE = 3060 MPa, and IB = 2.2 MPa.

1.INTRODUCTION

According to Mohanty (2002), sustainability, industrial ecology, eco-efficiency, and green chemistry play a key role in shaping a new generation of materials, products, and processes. The development of innovative bio-based products and technologies that are not dependent on fossil fuels is of fundamental importance. For long-term sustainability, particular attention must be given to biological materials that are wholly or partially derived from biomass (Weiss et al. 2012).
Globally, the most widely used adhesives in the production of wood-based composites are thermosetting resins derived from formaldehyde, valued primarily for their properties and low cost. In the United States alone, more than one billion pounds of such adhesives are consumed annually in the production of particleboards, oriented strand boards, and plywood (Imam et al. 2001). These adhesives are synthesized from non-renewable petroleum-based resources, and an additional concern is their formaldehyde content. In residential environments, formaldehyde is most often associated with wood-based panels, but it can also be found in water-based paints and cleaning agents. The most common adhesives used in particleboard production are urea–formaldehyde (UF) resins, which often reach near- limit values for formaldehyde emissions. Formaldehyde is classified by the European Chemicals Bureau in Category 3, indicating a risk of permanent health damage, while the International Agency for Research on Cancer (IARC) lists it in Group 2A – probably carcinogenic to humans (Böhm, 2005).
In response to these issues, natural alternatives based on tannins and lignins, or their combinations, have been investigated (Ballerini et al. 2005). Another representative of bio-based adhesives, in use for centuries, are starch-based adhesives (Tester et al. 2004). However, the main drawback of these biodegradable adhesives remains their poor water resistance, which limits their widespread commercial application.

2. MATERIAL AND METHODS

Preparation of wood particles

Wood particles were prepared from low-grade coniferous lumber. The material consisted of lumber classified according to EN 1611-1 in category G 2–4 and undersized short pieces of lumber . The lumber was first cut with a circular saw into segments with a maximum length of 3 cm and subsequently disintegrated using a RETCH SM300 laboratory mill. For the preparation of the medium particle fraction (Middle), a sieve with a mesh size of 2 × 2 mm was used, while a sieve with a mesh size of 4 × 4 mm was applied for the coarse fraction (Big). The finest fraction (Small) was represented

by sawdust generated during the initial cutting process, ensuring full utilization of the wood material. The mill speed was set to 1800 rpm for both fractions. Different particle sizes were prepared in order to assess their influence on the physical and mechanical properties of the produced composites.
Preparation of bioplastic

The bioplastic was prepared according to a custom formulation consisting of four components: distilled water (H_2O), potato starch (purchased from Belbake, Germany), glycerol 99.5% (purchased from Fichema, Czech Republic), and 8% spirit vinegar (purchased from Burg, Czech Republic). All components were weighed on laboratory scales with an accuracy of two decimal places. The mixture was prepared in glass laboratory beakers and subsequently heated to the gelatinization temperature, which in this case was approximately 70 °C. A water bath was used to maintain and control the temperature, ensuring a homogeneous consistency of the final mixture. This procedure prevented clogging of the air nozzle during application with the coating device. A total of four types of bioplastic were prepared with water contents of 16.5%, 14.4%, 12.9%, and 10.6%.

Application method

Manual method (M)

The wood particles together with the bioplastic were placed into a plastic container. Mixing was carried out using a spiral mixer attached to a Makita drill. The mixing lasted for 5 minutes, after which the quality of blending was checked.

Drum applicator (D)

For blending the wood particles with the bioplastic, a drum applicator was used. The bioplastic was sprayed into the wood mixture using a pneumatic nozzle. The amount of sprayed bioplastic was monitored using laboratory scales with an accuracy of 0.01 g.

Figure 1. *a – drum applicator, b – laboratory scale used for monitoring the application of bioplastic.*

Board production

Weighing procedure

All weighing was carried out using laboratory scales with an accuracy of two decimal places. In the initial phase of the experiment, each board was prepared from a different combination of self-produced wood particles. Three particle-size fractions were used: small, middle, and big. For the subsequent testing, a commercial particleboard mixture supplied by Kronospan was used, eliminating the need for further fraction blending. The target density of the produced boards was 800 kg/m³.
Moisture content of the particles was determined using a Radwag MAC210 moisture analyzer. The device heats the particles at 120 °C and continuously records the weight loss over time. Once the

change in mass falls below 0.001 g, the measurement is automatically terminated and the final moisture content is calculated. The instrument determines moisture content according to the standard gravimetric principle

$$M_c = \frac{M_H - M_0}{M_0} \times 100$$

M_c – Moisture content of wood particles (%),
M_H - mass of the particles before drying (g) ,
M_0 - mass of the oven-dried particles (g).

The moisture content of the self-produced wood particles was 15.35%, while the moisture content of the particles purchased from Kronospan was 3.43%. For pressing, molds with dimensions of 300 × 300 mm were used. In order to evaluate the applicability to larger board formats, molds with dimensions of 600 × 600 mm were also employed. The prepared mixture was gradually layered into the molds to ensure uniform density distribution and a random orientation of the particles.

Pressing process

The boards were pressed using an HL 400 hydraulic press, 12 mm thick boards were pressed. Various combinations of pressing time and temperature were tested, with pressing times of 1200 s and 800 s, and pressing temperatures of 150 °C and 180 °C. A constant pressing pressure of 3.5 MPa was applied. In some boards, insufficient evaporation of water was observed immediately after pressing, which resulted in delamination in the core layer. In total, 35 boards were produced for the purpose of testing.

Physical properties of the samples

The physical properties of the samples, including density, thickness swelling (TS), and water absorption (WA), were evaluated according to the relevant EN standards. Density was determined in accordance with EN 323. TS and WA were tested according to EN 317; however, the conditions were modified by reducing the immersion time in distilled water to 0.5 h.

Thickness swelling (TS)

The TS test was performed according to EN 317 for particleboards. Due to the poor water resistance of the material, the immersion time was reduced from the standard 2 h to 30 min. The dimensions of the test specimens were prepared in accordance with the standard, using square samples with a side length of 50 ± 1 mm.

$$T_s = \frac{t_2 - t_1}{t_1} \times 100$$

T_s- thickness swelling (%),
t_1 – thickness of the specimen before immersion (mm),
t_2 – thickness of the specimen after immersion (mm)

Water absorption (WA)

Water absorption (WA, %) expresses the amount of water absorbed by the tested specimen after complete immersion in water. It was calculated according to the following equation:

$$W_A = \frac{m_2 - m_1}{m_1} \times 100$$

W_A – Water absorption (%),
m_1 – mass of the specimen before immersion (g),
m_2 – mass of the specimen after immersion (g).

Density

Prior to testing, the specimens were conditioned for one week at a relative humidity of 65 ± 5% and a temperature of 20 ± 2 °C. All samples were weighed using a balance with an accuracy of 0.01 g. Thickness was measured at the intersection of the diagonals with an accuracy of 0.05 mm. The length and width were measured at two points parallel to the edges, with an accuracy of 0.1 mm.
The density (ρ, kg/m³) was calculated according to the following equation:

$$\rho = \frac{m}{a \times b \times t} \times 10^6$$

ρ- Density (kg/m3),
m- mass of the specimen (g),
a- length (mm),
b- width (mm),
t – thickness (mm)

Mechanical Properties of the Samples

Internal bond (IB)

Internal bond (IB) strength is commonly used as a measure of the cohesion between particles and fibers within the core layer (Liiri et al. 1980). It is determined by a tensile test carried out perpendicular to the plane of the board. The test was performed in accordance with EN 319, while specimen preparation followed EN 326-1. The specimens were square with side dimensions of 50 ± 1 mm. The loading rate of the testing machine was set to 2 mm/min.

$$IB = \frac{F_{max}}{a \times b}$$

IB - Internal bond (MPa),
F_{max} – maximum tensile force at failure (N),
ab - cross-sectional area of the specimen (mm²)

Modulus of elasticity (MOE) and modulus of rupture (MOR)

The modulus of elasticity (MOE) and modulus of rupture (MOR) were determined by a three-point bending test. The tests were carried out using a ZWICK 050 universal testing machine. From each panel, specimens were cut in accordance with EN 326-1, with dimensions of 290 × 50 mm, and subsequently tested. The loading rate of the testing machine was 10 mm/min.

$$MOR = \frac{3 \times F_{max} \times l_1}{2 \times b \times t^2}$$

F_{max} - load at failure (N)

$$MOE = \frac{l_1^3 \times (F_2 - F_1)}{4 \times b \times t^3 \times (a_2 - a_1)}$$

l_1-distance between the centers of the supports (mm), b-width of the specimen (mm), t-thickness of the specimen (mm), $F_2 - F_1$-increment of load within the linear portion of the load–deflection curve (N), $a_2 - a_1$- increment of deflection at the midpoint of the specimen (mm)

Vertical density profile (VDP)

The vertical density profile was determined using an Imal device, model DPX300-LTE. This equipment allows the density distribution across the thickness of the board to be measured with a step resolution of 0.05 mm. Specimens with dimensions of 50 × 50 mm were placed into the sample holder, and after the measurement was initiated, the density profile was displayed on the computer screen.

2. RESULTS AND DISCUSSION

Effect of particle size fractions on board properties

Table 1. *Board composition and overview of measured density and mechanical properties.*

Number	Pressing temperature (°C)	Pressing time (s)	Water content (%)	Small (g)	Middle (g)	Big (g)	Application method	Density (kg/m³)	MOE (MPa)	MOR (MPa)
1	150	900	23,4	250	200	100	M	375	87	0,3
2	150	900	33,1	300	200	0	M	325	130	0,2
3	150	1000	26	300	450	0	M	485	462	1,3
4	150	1000	19,4	350	250	125	M	435	241	0,7
5	150	1500	20	65	200	350	M	397	482	0,3
6	150	1200	23,1	0	120	380	M	454	182	0,5
7	150	1200	22,1	400	450	100	M	629	1 286	3,7
8	150	1400	20,6	400	550	100	M	700	1 787	5,7

The table 1. provides a summary of pressing conditions, water content, the proportion of individual particle fractions, the application method (manual method), and the resulting values of density, modulus of elasticity (MOE), and modulus of rupture (MOR). The results indicate that the overall board density itself is not the decisive factor for mechanical properties.

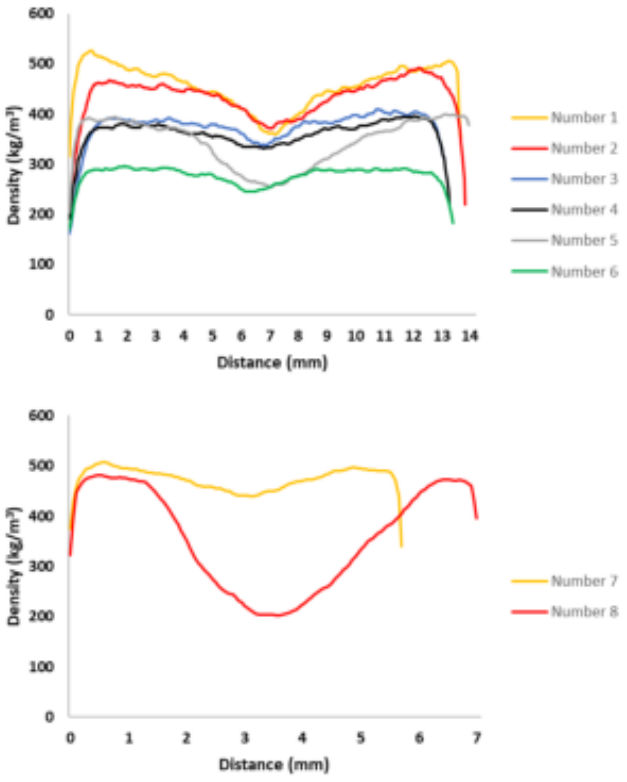

Figure 2. *Density profile of the manufactured boards.*

The measured results show that the individual boards exhibited markedly different vertical density profiles, which directly affected their mechanical behavior. For example, Board No. 8 reached very high values of modulus of elasticity (1 787 MPa) and modulus of rupture (5.7 MPa), indicating the formation of distinctly densified surface layers. These findings confirm that achieving higher strength depends not only on the overall density, but above all on the shape of the density profile and its distribution across the board thickness.

Boards with more uniform or only slightly differentiated profiles showed lower mechanical parameters, whereas boards with a pronounced contrast between the surface and the core (the so-called U-shaped profile) demonstrated superior performance. This trend is consistent with the literature, which states that the majority of bending loads are carried by the surface layers, and therefore their densification leads to significant improvements in strength and modulus of elasticity (Böhm et al. 2012).

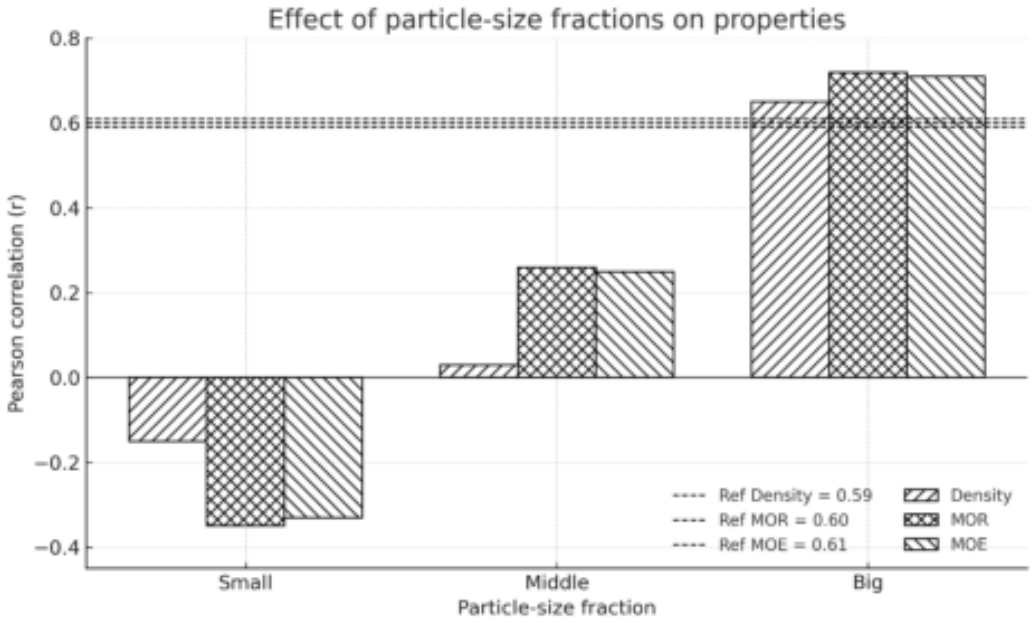

Figure 3. *Assessment of the effect of particle size fractions on density and mechanical properties.*

Figure 3 illustrates the effect of particle-size distribution on the properties of the produced panels. Small particles showed negative correlations with density (r = –0.15), modulus of rupture (MOR, r = –0.35), and modulus of elasticity (MOE, r = –0.33), indicating that an increased proportion of fines reduced overall panel strength and stiffness.

In contrast, middle-sized particles were positively correlated with MOR (r = 0.26) and MOE (r = 0.25), suggesting that a balanced presence of longer wood particles can enhance load transfer and bending resistance. The effect was most pronounced for big particles, which exhibited strong positive correlations with density (r = 0.65), MOR (r = 0.72), and MOE (r = 0.71). These results confirm that a higher proportion of coarse particles significantly improves the mechanical performance of particleboards.

This trend is consistent with previous findings (Jathungeye, 2007; Heebink, 1972), which reported that larger wood particles in the surface layers contribute to greater stiffness and bending strength. However, an excessive proportion of big particles may compromise surface smoothness and dimensional stability, indicating the need for an optimized particle-size distribution to balance mechanical strength and panel quality.

Effect of water content on board properties

Table 2. *Water content and overview of measured density and mechanical properties.*

Number	Pressing temperature (°C)	Pressing time (s)	Water content (%)	Application method	Density (kg/m³)	MOE (MPa)	MOR (MPa)	IB (MPa)	TS (%)	WA (%)
A	150	1200	16,5	M	663	1 791	6,7	1	97,5	127,6
B	150	1200	14,4	M	680	1 904	7,6	1,13	92,7	126,3
C	150	1200	12,9	M	678	1 829	7,5	1,15	98,1	119,6
D	150	1200	10,6	M	659	1 318	4,9	0,75	100,4	119,8

The table 2. provides a summary of pressing conditions, water content, the application method (manual method), and the resulting values of density, modulus of elasticity (MOE), modulus of rupture (MOR), internal bond (IB), thickness swelling (TS), and water absorption (WA). The results show that although the density of the boards remained relatively consistent (659–680 kg/m³), there were clear differences in mechanical and physical properties. Boards B and C, with water contents of 14.4% and 12.9%, reached the highest values of MOE (1 904 and 1 829 MPa) and MOR (7.6 and 7.5 MPa), as well as satisfactory IB. In contrast, Board D with the lowest water content (10.6%) exhibited significantly lower mechanical performance (MOE 1318 MPa, MOR 4.9 MPa, IB 0.75 MPa). These findings confirm that the water content during pressing is a decisive factor influencing both the mechanical strength and dimensional stability of the boards.

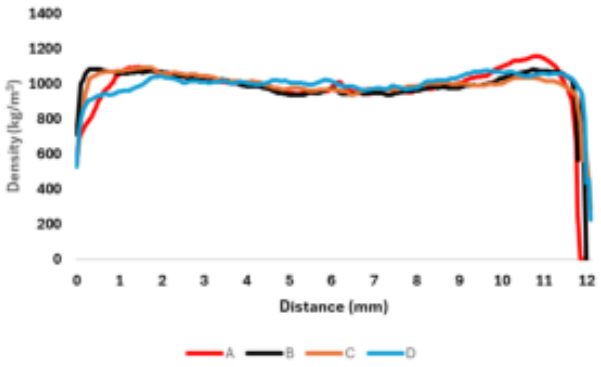

Figure 4. *Density profile of the manufactured board.*
Water content: A-16,5%, B-14,4%, C 12,9%, D-10,6%.

Figure 4. The density profiles of all four boards (A–D) show a similar pattern without significant deviations. The highest densification is observed in the surface layers, where the density exceeds 1100 kg/m³, while in the core layers it remains around 950–1000 kg/m³. Differences between individual boards are minimal.

Table 3. *ANOVA – Effect of water content on board properties.*

Variable	df_between	df_within	F	p-value
Density	3	36	2,222	0,1024
MOR	3	36	20,341	0,0001***
MOE	3	36	22,641	0,0001***
BI	3	36	3,58	0,0231*
TS	3	25	0,774	0,5196
WA	3	18	0,465	0,7103

* p<0.05, ** p<0.01, *** p<0.001

Table 4. *Tukeys range test – Effect of water content on board properties.*

Comparison	Density	MOR	MOE	BI	TS	WA
A–B	0,341	0,123	0,494	0,771	0,715	0,998
A–C	0,433	0,173	0,963	0,678	1	0,797
A–D	0,981	0,0001***	0,0001***	0,295	0,952	0,81
B–C	0,998	0,998	0,782	0,998	0,767	0,869
B–D	0,18	0,0001***	0,0001***	0,044*	0,517	0,88
C–D	0,243	0,0001***	0,0001***	0,03*	0,982	1

* p<0.05, ** p<0.01, *** p<0.001

The results demonstrate a significant influence of water content on the mechanical properties of particleboards bonded with bioplastic. While density remained statistically unaffected by the variation in water content ($p = 0.1024$), both MOR and MOE showed highly significant differences ($p < 0.001$). The highest flexural strength (7.6 MPa) and modulus of elasticity (1 904 MPa) were obtained at a water content of 14.4% (sample B), whereas a further reduction to 10.6% (sample D) led to a substantial decline in mechanical performance (MOR 4.9 MPa, MOE 1 318 MPa). Internal bond strength was also significantly reduced at the lowest water content, with Tukey's test confirming the difference between D and B/C groups ($p < 0.05$). In contrast, thickness swelling and water absorption did not show significant variation across treatments, indicating that dimensional stability was not affected by the initial moisture content of particles. These findings highlight the critical role of optimal water content in achieving sufficient adhesion and mechanical integrity, with 14–16% moisture appearing most favorable under the tested conditions.

Effect of application method on board properties

Table 5. *application method and overview of measured density and mechanical properties.*

Number	Pressing temperature (°C)	Pressing time (s)	Water content (%)	Application method	Density (kg/m³)	MOE (MPa)	MOR (MPa)	IB (MPa)	TS (%)	WA (%)
A	150	1200	14,4	M	673	1 833	7,1	1,1	90,1	120,3
B	150	1200	14,4	D	706	2 153	7,9	0,8	151	157

The table 5. provides a comparison of pressing conditions, water content, the application method (manual vs. drum applicator), and the resulting values of density, modulus of elasticity (MOE), modulus of rupture (MOR), internal bond (IB), thickness swelling (TS), and water absorption (WA). Both variants were produced under identical pressing parameters (150 °C, 1200 s, 14,4% water content). The results demonstrate that the drum applicator (Board B) yielded higher density (706 kg/m³) and superior bending properties (MOE 2153 MPa; MOR 7.9 MPa) compared to the manual method (Board A). However, this improvement in bending strength was accompanied by a reduction in internal bond strength (0.8 vs. 1.1 MPa) and a significant increase in thickness swelling (151% vs. 90,1%) and water absorption (157% vs. 120,3%).

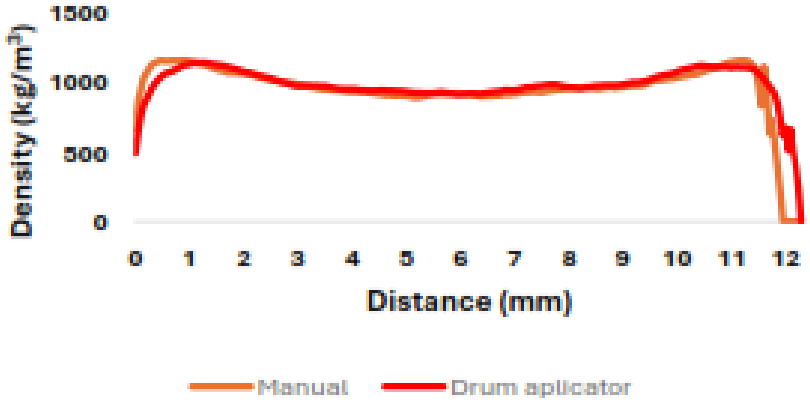

Figure 5. *Density profile of the manufactured boards.*

Figure 4. The density profiles of the boards produced using the manual method and the drum applicator show a very similar course, with no significant differences observed between them. In both cases, the highest densification occurs in the surface layers, where the density reaches values of around 1200 kg/m³. This profile shape is typical for board materials and has a positive effect on mechanical properties, as the surface layers carry the largest share of the load under bending.

Table 6. *ANOVA – Effect of application method on board properties.*

Variable	df_between	df_within	F	p-value
Density	2	12	6,263	0,0137*
MOR	2	12	16,974	0,0003***
MOE	2	12	12,036	0,0014**
IB	2	12	3,236	0,0752
TS	2	15	35,025	0,0001***
WA	2	15	8,001	0,0043**

* p<0.05, ** p<0.01, *** p<0.001

Table 7. *Tukeys range test – Effect of application method on board properties.*

Comparison	Density	MOR	MOE	IB	TS	WA
A–B	0.284	0.314	0.0235*	0.066	0.0000***	0.0032**
A–C	0.171	0.0038**	0.226	0.278	0.0032**	0.083
B–C	0.0106*	0.0003***	0.0011**	0.652	0.0015**	0.255

* p<0.05, ** p<0.01, *** p<0.001

The results demonstrate that the method of adhesive application had a statistically significant influence on most of the evaluated properties. While density showed only moderately significant differences ($p = 0.0137$), mechanical parameters were clearly affected. The highest values of modulus of rupture (MOR 7.9 MPa) and modulus of elasticity (MOE 2 153 MPa) were achieved with mechanical application (sample B), representing a significant improvement compared to manual application ($p < 0.01$). Internal bond strength (IB) did not differ significantly between variants ($p = 0.0752$); however, mean values ranged from 0.8 to 1.1 MPa, which exceeds the minimum requirement specified in EN 312.

Physical properties exhibited more pronounced differences depending on the application method. Thickness swelling (TS) and water absorption (WA) were significantly higher in the case of mechanical application (151% and 157%, respectively), as confirmed by ANOVA (TS: $p < 0.001$; WA:

p = 0.0043). This unexpected result can be attributed to insufficient mixing when using the applicator.

While manual mixing was sufficient with an input batch size of 2.5 kg, in the case of the applicator a substantial proportion of the material adhered to the inner drum surface, leading to incomplete homogenization of the mixture. Consequently, poor distribution of the bioplastic adhesive resulted in higher water uptake, greater swelling, and reduced delamination resistance. Although mechanical applicators are described in the literature as a standard industrial approach (Bohm, 2005), and were therefore expected to yield superior results, the insufficient batch size clearly limited their efficiency. This problem was successfully solved in a later stage of the experiment by increasing the batch size to 7 kg, which allowed proper homogenization and improved dimensional stability.

Effect of pressing temperature and time on board properties

Table 8. *pressing temperature and time and overview of measured density and mechanical properties.*

Number	Pressing temperature (°C)	Pressing time (s)	Water content (%)	Application method	Density (kg/m^3)	MOE (MPa)	MOR (MPa)	IB (MPa)	TS (%)	WA (%)
A	150	1200	14,4	D	736	2 701	12,3	2,13	38,3	74,2
B	150	800	14,4	D	677			1,58	79,8	133,8
C	180	1200	14,4	D	745	2 932	12,9	2,01	41,4	75,1
D	180	800	14,4	D	749	2 912	13,1	2,12	54,4	87,2

Table 8 summarizes the influence of pressing temperature (150 °C and 180 °C) and pressing time (1200 s and 800 s) under identical water content (14.4%) and application method (drum applicator). The results show that boards pressed for longer times (A and C) achieved better mechanical performance compared to boards with shorter pressing times (B and D). For example, Boards A and C reached MOR values of 12.3 and 12.9 MPa and MOE values of 2701 and 2932 MPa, respectively, while Board B, pressed at 150 °C for only 800 s, could not be fully tested due to delamination in the core layer caused by insufficient consolidation.

Comparable research on starch-based bioplastics was conducted by Hellmayr et al. (2022), who identified 150 °C and 320 s as the most suitable pressing combination, while Monteiro (2020) recommended a pressing time of 240 s. However, both studies worked with boards only 5 mm thick, which explains the use of significantly shorter pressing times. A more relevant comparison can be found in the study by Moubarik et al. (2009), who tested 14 mm thick boards and recommended pressing at 170 °C for 1020 s. These conditions are much closer to those applied in the present study, where 12 mm thick boards were pressed, and they support the use of longer pressing times for thicker boards.

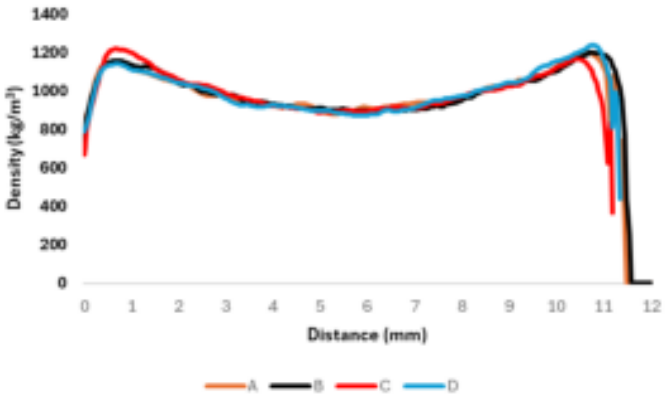

Figure 6. *Density profile of the manufactured boards.*

The Figure 6. density profiles of boards A–D show a very similar course with a characteristic U-shaped pattern. The highest density values, exceeding 1200 kg/m³, are located in the surface layers, while in the core the density remains around 900–950 kg/m³. Differences between the individual boards are minimal, indicating that variations in pressing parameters did not significantly affect the overall shape of the density profile.

Table 9. *ANOVA – Effect of pressing temperature and time on board properties.*

Variable	df_between	df_within	F	p-value
Density	3	39	0,563	0,574
MOR	3	39	0,762	0,474
MOE	3	39	2,039	0,144
IB	3	52	13,647	0,0001***
TS	3	71	36,730	0,0001***
WA	3	71	31,354	0,0001***

* p<0.05, ** p<0.01, *** p<0.001

Table 10. *Tukeys range test – Effect of pressing temperature and time on board properties.*

Comparison	Density	MOE	MOR	IB	TS	WA
A-B				0,0001***	0,0001***	0,0001***
A-C	0,763	0,175	0,635	0,628	0,875	0,999
A-D	0,557	0,232	0,474	1,000	0,0009***	0,180
B-C				0,0004***	0,0001***	0,0001***
B-D				0,0001***	0,0001***	0,0001***
C-D	0,940	0,986	0,963	0,680	0,0096**	0,239

* p<0.05, ** p<0.01, *** p<0.001

The results indicate that pressing temperature and pressing time did not have a statistically significant effect on density ($p = 0.574$), modulus of rupture (MOR, $p = 0.474$), or modulus of elasticity (MOE, $p= 0.144$). MOR values (12.3–13.1 MPa) and MOE values (2701–2932 MPa) were comparable across all testable variants without significant differences, suggesting that the investigated range of conditions (150–180 °C, 800–1200 s) was sufficient to achieve stable mechanical properties.
A notable exception was variant B (150 °C, 800 s), where MOR and MOE could not be determined. Under these conditions, delamination occurred in the core layer of the board, making bending tests impossible. This result demonstrates that the combination of lower temperature and shorter pressing time does not provide sufficient adhesive activation and leads to inadequate bonding in the core.
Statistically significant differences were observed for internal bond strength (IB) and physical properties. IB ranged from 1.58 to 2.13 MPa and differed highly significantly between treatments ($p < 0.001$), with the lowest value recorded in the problematic variant B. Similarly, thickness swelling (TS) and water absorption (WA) varied significantly ($p < 0.001$). The lowest values of TS (38.3–41.4%) and WA (74.2–75.1%) were achieved at longer pressing times (1200 s, samples A and C), whereas shorter pressing times (800 s, samples B and D) led to markedly poorer dimensional stability (TS up to 79.8%, WA up to 133.8%).

When compared to EN 312 requirements, all testable variants (A, C, D) met the minimum standard for bending strength in P2 type boards (MOR ≥ 11.0 MPa) and MOE values exceeded the required minimum (≥ 1600 MPa). Internal bond strength also surpassed the standard (IB ≥ 0.40 MPa) in all cases. The only exception was variant B, where pressing conditions were insufficient to produce a cohesive board.

Correlation analysis

Table 11. *Correlation analysis.*

Variable	Density	MOR	MOE	IB	TS	WA
Density	x	0,88	0,89	0,82	-0,72	-0,78
MOR		x	0,95	0,94	-0,84	-0,83
MOE			x	0,91	-0,79	-0,79
IB				x	-0,88	-0,76
TS					x	0,91
Wa						x

In table 11. the strongest positive correlation was observed between modulus of rupture (MOR) and modulus of elasticity (MOE), with a coefficient of r = 0.95. This finding is consistent with Jathungeye (2007), who reported that an increase in bending strength is typically accompanied by an increase in modulus of elasticity.

Significant correlations were also found between density and all of the evaluated properties. The highest coefficients were recorded for the relationship between density and MOE (r = 0.89), followed by density and MOR (r = 0.88). These results are in agreement with Istek and Siradag (2013), who stated that density positively affects all mechanical properties. Similarly, Vital et al. (1974) also reported that density has a positive influence on mechanical performance.

However, Vital et al. (1974) further indicated that higher density is generally associated with increased thickness swelling. This contrasts with the results of the present study, which revealed a negative correlation between density and thickness swelling (r = –0.72). These findings therefore suggest that increasing density leads to reduced swelling. According to Hrázský and Král (2000), this phenomenon may be explained by the lower penetration of moisture through the surface layers of denser boards. A similar conclusion—that swelling decreases with increasing density—was also reported by Rachtanapun et al. (2012) and Istek and Siradag (2013).

Overall, the results of this study demonstrate a negative correlation between thickness swelling and water absorption with key mechanical parameters, such as density, bending strength, modulus of elasticity, and internal bond.

3. CONCLUSIONS

This study demonstrated the potential of starch-based bioplastic as a binder for the production of biodegradable particleboard composites. The results confirmed that several factors significantly influence the mechanical and physical properties of the produced boards, including the particle-size composition, water content, adhesive application method, and pressing conditions.

The optimal combination was achieved with 14.4% water content, drum applicator application, and pressing at 180 °C for 1200 s, which resulted in maximum measured values of MOR = 13.8 MPa, MOE = 3060 MPa, and IB = 2.2 MPa. Boards with a pronounced U-shaped vertical density profile showed superior mechanical performance, confirming that densification of surface layers is essential for enhancing bending strength and stiffness.

Although starch-based binders still show limited water resistance, this work confirms their potential as a more environmentally friendly alternative to conventional petroleum-based adhesives. Further research should focus on improving water resistance and optimizing the production process for industrial-scale applications.

REFERENCES

1. Ballerini, A., Despres, A., & Pizzi, A. (2005). Non-toxic, zero emission tannin-glyoxal adhesives for wood panels. European Journal of Wood and Wood Products, 63(6), 477–478.

2. Böhm, M. (2005). Technology of wood-based composite materials. Prague: Czech University of Life Sciences, 97 p.
3. Böhm, M., Reisner, J., & Bomba, J. (2012). Wood-based materials. Prague: Czech University of Life Sciences, 2012.
4. Heebink, B. G. (1972). Reducing particleboard pressing time: Exploratory study. Forest Products Laboratory, Madison, USA. 13 p.
5. Hellmayr, R., Šernek, M., Myna, R., Reichenbach, S., Kromoser, B., Liebner, F., & Wimmer, R. (2022). Heat bonding of wood with starch–lignin mixtures creates new recycling opportunities. Materials Today Sustainability, 19, 100194.
6. Hrázský, J., & Král, P. (2000). Technology of wood-based composite materials. Brno: Mendel University of Agriculture and Forestry, 218 p. ISBN 80-7157-428-7.
7. Imam, S. H., Gordon, S. H., Mao, L., & Chen, L. (2001). Environmentally friendly wood adhesive from a renewable plant polymer: characteristics and optimization. Polymer Degradation and Stability, 73(3), 529–533.
8. İstek, A., & Siradag, H. (2013). The effect of density on particleboard properties. In Proceedings of the International Caucasian Forestry Symposium (pp. 932–938). Artvin, Turkey.
9. Jathungeye, N. U. (2007). Economical particleboard production using hardwood sawmill residues (Doctoral thesis). RMIT University, Melbourne, Australia. 260 p.
10. Liiri, O., Kivistö, A., Tuominen, M., & Aho, M. (1980). Determination of the internal bond of particleboard and fibreboard. Holz als Roh- und Werkstoff, 38, 185–193.
11. Mohanty, A. K., Misra, M., & Drzal, T. (2002). Sustainable bio-composites from renewable resources: Opportunities and challenges in the green materials world. Journal of Polymers and the Environment, 10(1), 19–26.
12. Monteiro, S. C. C. (2020). Development of low-density particleboards bonded with starch-based adhesive (Doctoral thesis). University of Porto, Porto, Portugal. 183 p.
13. Moubarik, A., Charrier, B., Allal, A., Charrier, F., & Pizzi, A. (2009). Development and optimization of a new formaldehyde-free cornstarch and tannin wood adhesive. European Journal of Wood and Wood Products, 68(2), 167–177.
14. Rachtanapun, P., Sattayarak, T., & Ketsamak, N. (2012). Correlation of density and properties of particleboard from coffee waste with urea–formaldehyde and polymeric methylene diphenyl diisocyanates. Journal of Composite Materials, 46(15), 1839–1850.
15. Tester, R. F., Karkalas, J., & Qi, X. (2004). Starch composition, fine structure and architecture. Journal of Cereal Science, 39(2), 151–165.
16. Vital, B. R., Lehmann, W. F., & Boone, R. S. (1974). How species and board densities affect properties of exotic hardwood particleboards. Forest Products Journal, 24(12), 37–45.
17. Weiss, M., Haufe, J., Carus, M., Brandão, M., Bringezu, S., Hermann, B., & Patel, M. K. (2012). A review of the environmental impacts of biobased materials. Journal of Industrial Ecology, 16(1), 169– 181.

YIELD COMPARISON OF BEECH (*Fagus sylvatica* L.) AND FIR/SPRUCE (*Abies alba* Mill/*Picea abies* L.) LOGS IN THE SAWMILL PROCESSING INDUSTRY

Ana Marija Stamenkoska[1], Goran Zlateski[1], Branko Rabadjiski[1], Anastasija Temelkova[1]

Ss. Cyril and Methodius University in Skopje, Macedonia,
Faculty of Design and Technologies of Furniture and Interior-Skopje,
email: stamenkoska@gmail.com; zlateski@fdtme.ukim.edu.mk;
rabadziski@fdtme.ukim.edu.mk; temelkova@fdtme.ukim.edu.mk

ABSTRACT

Sawmilling technology in Macedonia is primarily characterized by small to medium-capacity sawmills, many of which operate with mixed species and variable equipment configurations. These sawmills typically process between 1500 and 5000 m³ of roundwood annually and play a crucial role in the domestic wood industry. The technology employed often includes vertical band saws for primary sawing and simple layouts for material flow. Beech *(Fagus sylvatica* L.) and fir/spruce (*Abies alba* Mill./*Picea abies* L.) are among the most commonly processed species, representing a significant share of the raw material input due to their abundance, accessibility, and economic relevance. Beech is predominantly used in furniture production, while fir/spruce is more common in construction and structural applications.

This paper presents a focused comparative analysis of raw material yield efficiency between beech and fir/spruce logs in a primary processing setting. The study was conducted at the MARKISTO sawmill in Leskoec, Ohrid, a representative facility within the North Macedonian context, operating with a capacity of 2,500–3,000 m³ per year. A total of 160 logs were analyzed—80 from each species—across I, II, and III quality classes and two standardized lengths (4.0 m and 5.0 m). The objective was to quantify and compare the percentage yield of sawn timber relative to log volume, under real production conditions, without altering existing workflows. Key influencing factors such as log diameter, taper, and wood defects were recorded and assessed.

Results indicated that fir/spruce logs generally achieved higher yield rates than beech, particularly in the higher quality classes. For instance, Class I fir/spruce logs yielded up to 10–15% more usable lumber compared to Class I beech logs, mainly due to more uniform structure and lower waste values. In contrast, beech logs, especially from lower quality classes, were more affected by natural defects like heart checks and curvature, reducing the quantitative yield despite similar or larger diameters. The study confirms that both species and log quality significantly affect sawmill efficiency and that careful log selection and classification are essential for optimizing material recovery.

Keywords: beech, fir/spruce, quality class, sawmills, yield, efficiency.

1. INTRODUCTION

The ultimate objective of the primary processing of wood is the production of final products, characterized by appropriate dimensions, shape, and quality. In order for such products to be manufactured, a sequence of technological operations is required, whereby the initial system that begins with the natural form of the raw material (roundwood) is referred to as primary wood processing. The process of log conversion begins on the primary machines through sawing with various cutting tools, such as band saws, frame saws, or circular saws. In addition, combined methods in processing may also be employed, such as sawing-milling, among others. The log sawing process may be determined in several ways and it depends on the wood species, the dimensions and quality of the logs, the dimensions of assortments, the assortment structure of the sawn products, their intended purpose, the quality class, and so forth.

The efficiency of sawmilling capacities is closely associated with the method of log sawing. The performance of operations is influenced by multiple factors, such as: sawlogs yield, the species of wood being processed, the level of equipment of the sawmill, the sawing method, etc. Among these

factors, sawlogs yield is directly linked to the economic profitability of a sawmilling capacity. Yield is defined as the degree of utilization in the form of sawn lumber or as the quantity of sawn assortments obtained as the result of log processing. In addition to sawn assortments, the processing of logs yields other products, such as parquet blanks, wooden elements, laths, and other products. Yield can be examined from the perspectives of quantitative, qualitative, and value-based point. The notion of maximal quantitative yield refers to the quantity of sawn assortments obtained from the processing of a single log or a greater number of sawmill logs. Qualitative yield is a complex concept that implies obtaining assortments of the highest quality, while value-based yield is closely connected to both quantitative and qualitative yield. The focus of this paper will be directed toward quantitative yield, as the principal indicator of the rational use of sawlogs.

The rational use of sawlogs is significant from the perspective of planned exploitation of forest potentials and the ecological aspect of the environment. Through rational use of sawlogs, the quantity of waste generated in the process of log processing is reduced, thereby decreasing unnecessary tree felling within forest resources. For rational raw material utilization, it is essential to prepare a sawing plan in advance, to be aware of sawlogs quality, dimensions, and the final dimensions of the sawn assortments. The sawing plan or the sawing pattern, denotes the arrangement of cuts on the transverse section of the log. Through proper selection of the sawing pattern, the unnecessary number of cuts is reduced, the formation of unnecessary both fine and coarse waste is avoided, and thereby also reducing consumption of electrical energy required for powering sawing machinery.

In practice, the maximal quantitative yield of logs depends upon numerous factors, such as: log diameter, assortment dimensions, thickness allowance of assortments, kerf width, and many other factors. The listed factors define the geometry of maximal quantitative yield. The geometry of maximal quantitative yield is reduced to the assumption that the log at its thin end is circular in shape, while the coverage of the circle's surface is by assortments in the form of quadrilaterals – prism model (Rabadjiski 2019). Under practical conditions, the formation of sawing patterns is not limited solely to the transverse section of the log. When forming these patterns, the dimensions of assortments (width and thickness), as well as shrinkage allowance, must be taken into consideration. For these reasons, in theory, apart from the geometry of maximal quantitative yield, optimization methods are also devised when forming sawing patterns (Nikolić 2010). Knežević (1968) provides a method for creating sawing patterns of logs by means of the coefficient method, wherein the thickness of assortments is reduced to the nearest thickness of boards or planks in accordance with the prescribed standard. This method represents a mathematical model, but its shortcoming lois in the approximate thickness of assortments or the inability to obtain an exact value. Considering such factors, Knežević (1955) established a method for forming sawing patternss, whereby the process begins with the thinnest assortment on the lateral sides of the transverse section, with the thickness of assortments increasing toward the central portion of the log. According to this method, assortments of greatest thickness are positioned in the middle of the cross-section.

Each wood species is distinguished by different anatomical characteristics. Consequently, these characteristics includethe form of the stem, its length, and cross-section. Quantitative yield is predetermined also by the geometry of the logs. In the formation of patterns, diameter taper is also taken into account. Taper denotes the gradual reduction of diameter from the thin toward the thick end of the log, which represents a deviation from the cylindrical form. Within sawmilling capacities, both coniferous and deciduous logs are processed, possessing various diameters, lengths, and quality classes. Consequently, the percentage of quantitative yield also varies. Under production-exploitation working conditions, according to Rabadjiski (2019), the percentage of quantitative yield ranges within rather wide limits, averaging between 48.0 and 70.0%. In the processing of beech logs of I/II quality class, with diameters from 26.0 to 58.0 cm on a band saw, quantitative yield ranges from 46.0 to 57.0% (Rabadjiski 1991). In the processing of logs with identical characteristics on a vertical frame saw, the author states that yield falls within the limits of 46.0 to 57.0%. Šoškić and Popović (2004), in processing beech logs of quality class I, report that yield ranges from 47.0 to 62.0%, averaging 60.0%; for quality class II, 54.0%; and for the third class, 49.0%. According to Чернаев (1960), in the processing of coniferous logs, yield ranges from 53.0 to 64.0%. Brežnjak (2000) reports that the average quantitative yield for fir/spruce logs amounts to 65.0%. Based on the mentioned research, it may be concluded that coniferous wood species yield a higher quantitative percentage . Apart from the

sawing pattern, important factors influencing yield include the quality class and the applied sawing technology.

The paper presents data derived from conducted research under production-exploitation working conditions. A comparative analysis has been carried out of the quantitative yield in beech logs and fir/spruce logs of equal lengths and quality class.

2. MATERIALS AND METHODS

The subject of research in this paper are sawlogs of beech (*Fagus sylvatica* L.) and fir/spruce (*Abies alba* Mill./*Picea abies* L.) of I, II, and III quality class. As the research facility, the sawmill MARKISTO, located in the village of Leskoec, Ohrid, was selected. The raw material used in the company MARKISTO is supplied from the Public Enterprise Macedonian Forests. Within the chosen sawmilling capacity, logs of both deciduous and coniferous origin are processed. Among the deciduous species, beech wood predominates in processing. Additionally, logs of walnut (*Juglans regia* L.) are included in small quantities. The coniferous logs are from fir/spruce (*Abies alba* Mill./*Picea abies* L.).

It may be concluded, from the general data, that beech represents the dominant deciduous species in primary processing in the Republic of North Macedonia. The territory of the state abounds in this wood species, and the industry utilizes what is most readily available. Sawn lumber from beech is predominantly employed in the furniture industry, particularly in the production of tables and chairs.

Fir and spruce are marketed as a single wood species, commonly known as čam. They are classified as one species owing to their similar anatomical structure and technical properties. This wood is primarily applied in construction. It demonstrates exceptionally favorable load-bearing properties, and it is likewise utilized for roofing and flooring structures. For flooring and roofing structures, wooden laths are commonly employed.

The selection of wood species was made based on the availability of these species in the sawmilling capacity at the time of data collection. For the analysis, a dominant deciduous species (beech) and a coniferous species (fir/spruce) were chosen, with the aim of conducting a comparison of the percentage of maximal quantitative yield between deciduous and coniferous species.

The research presented in this paper was carried out through the application of methodology appropriate for this type of study. The investigations were conducted in two phases:

1. determination of maximal quantitative yield of beech sawlogs, and
2. determination of maximal quantitative yield of fir/spruce sawlogs.

The factors that primarily influence the maximal quantitative yield of sawlogs may be of both technological and economic nature. The technological factors that significantly affect the yield of wood mass are:

- selection of raw material;
- selection of saw thickness;
- selection of sawing pattern;
- determination of shrinkage allowance;
- determination of the degree of processing of sawn timber;
- determination of the quantity of coarse waste;
- determination of wood moisture content;
- selection of the concept of sawmilling technology.

The sawlogs were processed on a band saw. The method of processing was appropriate for the wood species and their characteristics. After processing, sawmill assortments with appropriate dimensions were produced from the sawlogs.

The research was performed under production-exploitation working conditions. No interventions were made upon the working and sawing conditions. These conditions were merely observed, as were the results. Measurements were taken of the logs' length, the diameter of the thin end, and the diameter of the thick end of the log. Classification of the logs was conducted in accordance with Macedonian standards MKS EN D.B4.028/1:1990, MKS EN D.C1.022, and MKS EN 1316-1:2013.

The method of work consisted of:

- measurement of logs (length, diameter of the thin end, and diameter of the thick end);
- calculation of:

a) mean diameter,
b) volume of the log,
c) diameter taper,
d) maximal quantitative yield;
- processing of the data from measurements and calculations using statistical methods.

The measurement of the logs was performed in the log yard. For the measurement of the required dimensions of the logs, a wooden caliper (Figure 1) and a steel tape were used. The wooden caliper was employed for measuring the diameters of the logs intended for processing. The scale of the caliper is graduated in centimeters. The steel tape has a length of 10 meters, divided into meters, centimeters, and decimeters, with the first meter divided into millimeters. The steel tape was used for measuring the length of the logs. All measured parameters were recorded in pre-prepared tables for documentation.

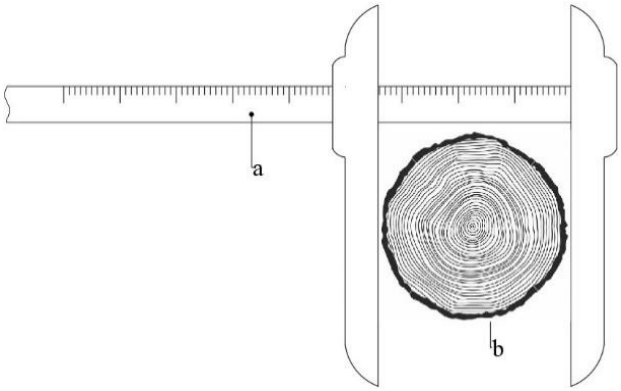

Figure 1. *Wooden caliper,*
a – caliper, b – sawlog.

In total, 40 beech logs with a length of 4.0 m were analyzed. The total volume of these logs amounts to 25.929 m³. The logs are grouped into 6 thickness classes, according to their mean diameter, with an interval of 5 cm between each group. The analyzed logs belong to the I, II, and III quality class. The diameter of the thin end (d_1) ranges from 31.0 to 56.0 cm; the diameter of the thick end (d_2) ranges from 33.0 to 60.0 cm; while the mean diameter (d_{sr}) ranges from 52.0 to 58.0 cm. The taper (S), as an important indicator for the maximum quantitative yield of the logs, varies from 0.25 to 2.75 cm/m. The beech logs are presented in Figure 2. With a length of 5.0 m, a total of 40 logs were analyzed, belonging to the I, II, and III quality class. The total volume of these logs amounts to 32.169 m³. The classification was carried out into 6 groups, according to the mean diameter, with a difference of 5 cm between the groups. The diameter of the thin end (d_1) ranges from 28.0 to 56.0 cm; the diameter of the thick end (d_2) ranges from 31.0 to 56.0 cm; while the mean diameter (d_{sr}) ranges from 30.0 to 59.0 cm. The taper (S) ranges from 0.40 to 2.20 cm/m.

Figure 2. *Beech sawlogs*
(Fagus sylvatica L.*)1.*

Figure 3. *Fir/spruce sawlogs*
(Abies alba Mill*/Picea abies* L.*).*

A total of 40 fir/spruce logs were analyzed, which belong to the I, II, and III quality class. The total volume amounts to 25.562 m³. The diameter of the thin end (d_1) ranges from 29.0 to 56.0 cm; the diameter of the thick end (d_2) ranges from 32.0 to 60.0 cm; while the mean diameter (d_{sr}) is from 30.0 to 58.0 cm. The taper (S) is from 0.50 to 2.75 cm/m. With a length of 5.0 m, a total of 40 logs were analyzed, distributed across 6 thickness groups. Their total volume amounts to 32.444 m³. The logs belong to the I, II, and III quality class. The diameter of the thin end (d_1) is from 28.0 to 56.0 cm; the diameter of the thick end (d_2) is from 33.0 to 60.0 cm; while the mean diameter (d_{sr}) ranges from 30.0 to 58.0 cm. The taper (S) is within the range of 0.20 to 1.60 cm/m. The fir/spruce logs are presented in Figure 3.

The logs are sawn with specialized sawing (their final intention is known in advance), with predetermined dimensions of assortments. The assortments are intended for furniture production, while the large waste is utilized for parquet blanks. The wooden elements are intended for the production of tables and chairs. Boards are commonly used for the manufacture of solid furniture. The logs are most frequently sawn according to the live sawing pattern (Figure 4). The sawing of fir/spruce logs is also specialized. The timber is used for construction purposes. From the peripheral zone of the log, boards and planks are obtained, while from the central zone of the log, beams, scantlings, and laths are produced. These logs are sawn by live sawing pattern (Figure 5), since it is considered that by this method the yield is higher. In this method of sawing, the percentage of fine waste increases, and in some cases, it can equal the percentage of coarse waste. This is characteristic in the sawing of laths.

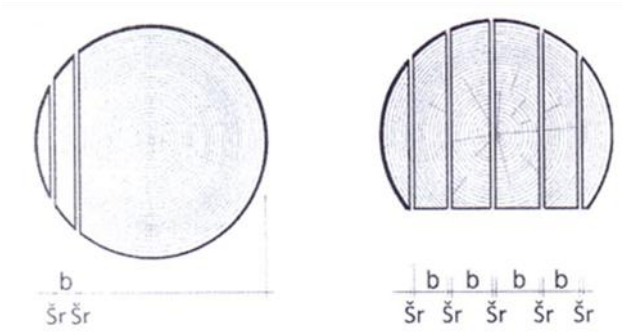

Figure 4. *Sawing pattern for the beech sawlogs,*
b – assortments thickness(mm), $š_r$ – kerf width of the bandsaw.

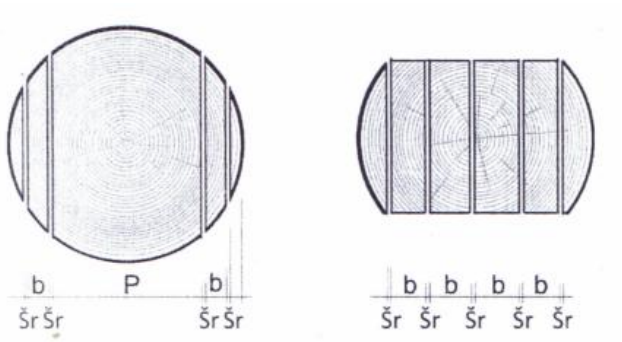

Figure 5*. Sawing pattern for fir/spruce sawlogs,*
b – assortments thickness (mm), $š_r$ – kerf width.

For the purposes of statistical processing of the data from this research, descriptive statistics and regression analysis were used. The data analysis was performed in relative values (the values are expressed in %). To investigate the interrelations between two occurrences, the methods of simple (linear or curvilinear) regression and correlation analysis are applied, while for multiple occurrences the methods of multiple (linear and curvilinear) regression and correlation analysis are used. The data processing was conducted in the software Microsoft Excel.

3. RESULTS AND DISCUSSION

The analysis of the maximum quantitative yield in beech sawlogs was carried out separately for logs with lengths of 4.0 m and 5.0 m. According to the results obtained for both lengths, a comparative analysis was performed between the yields. With the purpose of comparing the yield of beech logs and certain parameters that influence the yield, an analysis was conducted for both log lengths. The analysis was carried out depending on the length and thickness group. The objective of the analysis was to investigate the effect of length and thickness group on the percentage of maximum quantitative yield. For the analysis, descriptive statistics and regression analysis were employed. Table 1 presents the statistical values of the quantitative yield of beech logs with lengths of 4.0 m and 5.0 m.

Table 1. *Statistical values of the quantitative yield of beech (Fagus sylvatica* L.*) logs with lengths of 4.0 m and 5.0 m.*

Thickness group	Lenght	Mean value	Standard deviation	Standard error	95% confidence interval		Minimum	Maximum
					Lower bound	Upper bound		
[cm]	[m]	[%]	[%]	[%]	[%]	[%]	[%]	[%]
1	2	3	4	5	6	7	8	9
1. 30.0 - 34.0	4.0	46.62	2.85	1.16	43.63	49.61	43.79	51.67
	5.0	46.10	1.96	0.80	44.04	48.16	43.28	48.47
2. 35.0 - 39.0	4.0	41.16	5.04	1.90	36.50	45.82	35.91	48.39
	5.0	51.24	5.56	2.10	46.10	56.38	44.21	59.54
3. 40.0 - 44.0	4.0	46.09	3.91	1.48	42.48	49.70	40.29	51.52
	5.0	52.84	2.35	0.89	50.66	55.02	50.22	56.39
4. 45.0 - 49.0	4.0	49.08	2.95	1.50	45.99	52.17	45.54	53.08
	5.0	53.60	2.66	1.08	50.81	56.39	50.73	57.93
5. 50.0 - 54.0	4.0	49.57	4.23	1.60	45.66	53.48	43.37	56.41
	5.0	56.48	2.78	1.05	53.91	59.05	53.28	60.08
6. 55.0 - 59.0	4.0	52.07	4.01	1.51	48.36	55.78	45.38	56.29
	5.0	59.52	3.24	1.22	56.52	62.52	54.88	64.69

According to Table 1, it may be concluded that the highest yield is achieved in the sixth thickness group, for both lengths. The first thickness group exhibits approximate values of quantitative yield, and this trend continues across all thickness groups, except in the second group, where the difference amounts to about 10.00%. The lowest value of yield was recorded in the second thickness group (35.91%) for the length of 4.0 m, while the highest value was recorded in the sixth thickness group (54.88%) for the length of 5.0 m. It can therefore be concluded that with an increase in both the diameter and the length of the log, the percentage of quantitative yield also increases. Based on the data presented in the table, it may be inferred that with a difference of 1.0 m in length, at the same mean diameter, the yield may increase by as much as 10.00%. When drawing conclusions regarding the increased percentage of yield, other factors must also be taken into consideration, such as anatomical defects, taper, curvature of the log, and quality class. The percentage of maximum quantitative yield is a complex concept, particularly in the case of beech. The complexity is due to the specific anatomical structure, namely the presence of false heartwood in this wood species, which can significantly reduce the yield percentage. In designing the sawing patterns, efforts are made to incorporate the heartwood into as few assortments as possible. The assortments obtained from the central zone, which contain this defect, represent a challenge during the process of artificial drying. In order to increase yield in beech, parquet blanks are manufactured from coarse waste and lower-quality

log zones. For better visualization of the data from the table, a graph has been created illustrating the relationship between the thickness group of beech sawlogs and the percentage of quantitative yield, for both analyzed lengths, presented in Figure 6.

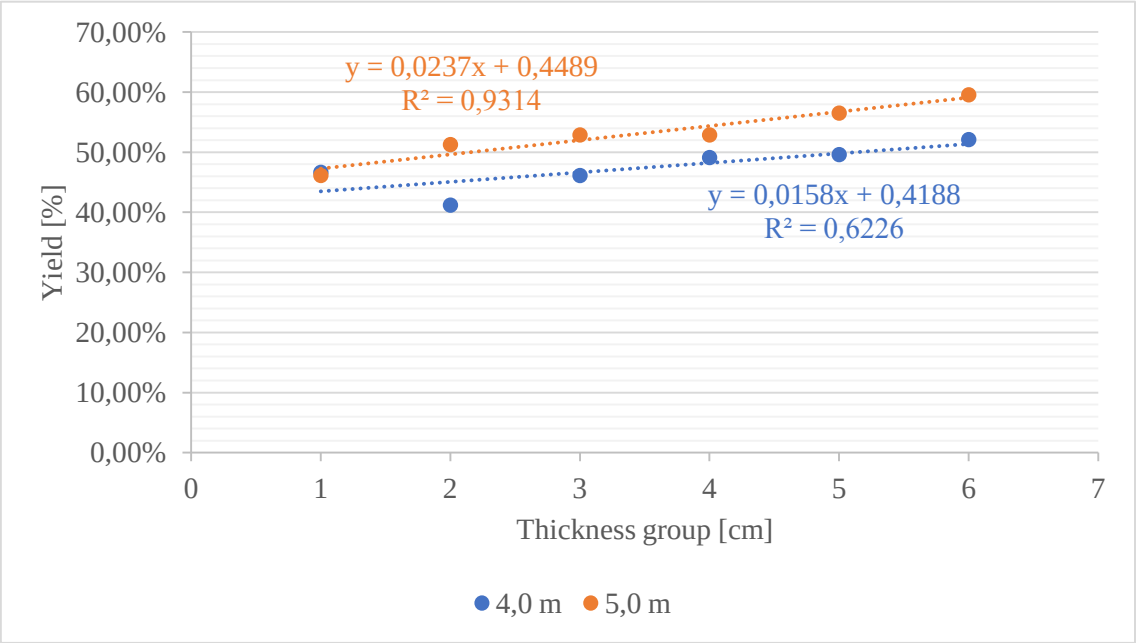

Figure 6. *Relationship between thickness group and quantitative yield of beech (Fagus sylvatica* L.*) sawlogs.*

According to the correlation coefficient (R), it may be concluded that for beech sawlogs of 4.0 m length, with an increase in mean diameter, the percentage of quantitative yield also increases. The value of coefficient R for sawlogs of 5.0 m length indicates a weaker correlation. In other words, in these sawlogs, the percentage of quantitative yield is influenced by certain other factors.

Table 2 displays the statistical values for the quantitative yield of fir/spruce sawlogs with lengths of 4.0 m and 5.0 m. According to Table 2, it can be concluded that in fir/spruce logs of 4.0 m length, yield increases with increasing diameter. For logs of 4.0 m length, the lowest percentage of yield was recorded in the first thickness group, amounting to 50.33%, while the highest percentage was recorded in the sixth thickness group, amounting to 74.78%. Smaller-diameter logs were processed into beams and scantlings, while larger-diameter logs yielded boards, planks, and laths. The sawmill products from fir/spruce are intended for the needs of the construction industry.

For logs of 5.0 m length, a slight deviation from the linear increase of yield may be observed. The second thickness group demonstrates a higher percentage of yield than the third, while the fourth has a higher percentage than the fifth. This is due to the lower quality of the logs being sawn, given that the majority of the processed sawlogs belonged to the third quality class. The deviation from linear increase, however, is minor and does not exceed 3.00%. The lowest yield among the 5.0 m logs was observed in the third thickness group, amounting to 59.99%, while the highest yield was in the sixth thickness group, amounting to 75.70%. It can be concluded that in fir/spruce sawlogs, as the mean diameter increases, the yield also increases. With an increase in length by one meter, at the same mean diameter, the yield increases from 1.32% to 11.32%, with an average increase of 6.04%. The increase in yield percentage with growth in length is particularly pronounced in smaller diameters. The high percentages of yield in fir/spruce sawlogs are due to the reduced presence of anatomical defects, owing to their simple anatomical structure, the small taper, and the minimal curvature of the logs. Since the lumber is intended for construction, when sawing beams, a greater portion of the cross-section is utilized, fewer cuts are required, and consequently the proportion of both fine and coarse residues is waste. The high percentage of yield is attributed primarily to the small taper.

Table 2. *Statistical values of the quantitative yield of fir/spruce (Abies alba* Mill*/Picea abies* L.*) logs with lengths of 4.0 m and 5.0 m.*

Thickness group	Lenght	Mean value	Standard deviation	Standard error	95% confidence interval		Minimum	Maximum
					Lower bound	Upper bound		
[cm]	[m]	[%]	[%]	[%]	[%]	[%]	[%]	[%]
1	2	3	4	5	6	7	8	9
1. 30.0 - 34.0	4.0	52.68	1.65	0.67	50.95	54.41	50.33	54.71
	5.0	63.49	2.65	1.08	60.71	66.27	60.09	66.62
2. 35.0 - 39.0	4.0	54.74	3.16	1.20	51.82	57.66	50.86	60.08
	5.0	66.06	2.01	0.76	64.20	67.92	63.25	68.85
3. 40.0 - 44.0	4.0	62.20	3.09	1.17	59.35	65.05	57.03	66.68
	5.0	64.84	4.77	1.80	60.43	69.25	59.99	70.90
4. 45.0 - 49.0	4.0	64.96	4.01	1.64	60.75	69.17	58.85	69.52
	5.0	71.12	2.23	0.91	68.78	73.46	67.84	74.37
5. 50.0 - 54.0	4.0	66.48	4.97	1.88	62.42	70.54	60.63	72.48
	5.0	70.76	2.09	0.79	68.83	68.83	68.25	73.25
6. 55.0 - 59.0	4.0	71.67	3.63	1.37	68.31	75.03	65.31	74.78
	5.0	72.99	2.66	1.01	70.53	75.45	69.27	75.70

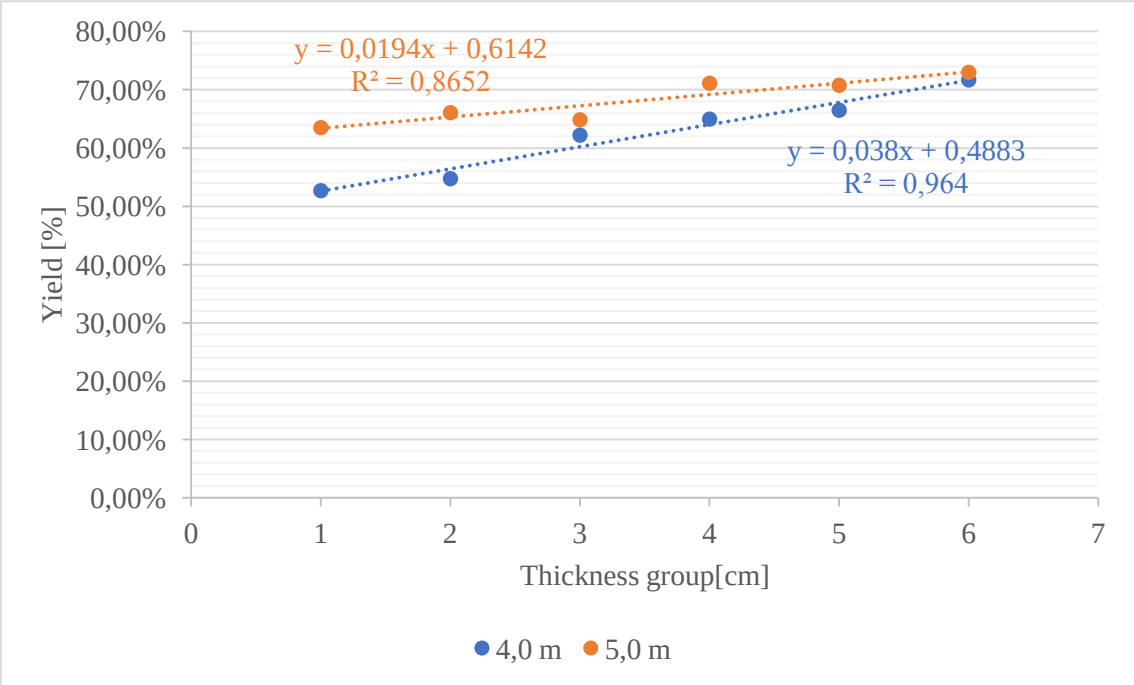

Figure 7. *Relationship between thickness group and quantitative yield in sawlogs of fir/spruce (Abies alba* Mill*/Picea abies* L.*).*

According to Table 2, for a clearer overview of the data, a regression analysis has been performed, presented in Figure 7. Based on the correlation coefficient R, for both the 4.0 m and the 5.0 m logs it may be concluded that with the increase of the mean diameter, the percentage of quantitative yield also increases. In logs of 5.0 m length, the correlation is somewhat weaker than in those of 4.0 m. In

these logs, a slight decline in yield can be observed in the third thickness group, as well as a deviation from the linear increase of yield. This is due to the lower quality of the 4.0 m logs and the greater taper, as one of the main factors influencing the percentage of quantitative yield. With the increase of log length, the taper also increases, which explains the reduction of quantitative yield in the third thickness group of logs with a length of 5.0 m. In the logs with a length of 5.0 m, the correlation coefficient R demonstrates a strong correlation. In can be concluded, that for these logs with the increase of the mean diameter, the percentage of quantitative yield increases.

The research begins from the observation available in the literature that deciduous wood species have a lower percentage of yield compared to coniferous species. In order to examine this hypothesis, identical lengths of sawlogs were selected for both analyzed wood species. The logs were divided into six identical thickness groups, based on their mean diameter. The comparison of quantitative yield in beech and fir/spruce is presented in Table 3 and Figure 8.

Table 3. *Comparison of yield in logs of beech (Fagus sylvatica L.) and fir/spruce (Abies alba* Mill*/Picea abies* L.*).*

Thickness group (cm)	Wood species	Diameter taper (cm/m)	Quantitative yield (%)	Coarse waste (%)	Fine waste (%)	Shrinking allowance (%)	Total waste (%)
1	2	3	4	5	6	7	8
1. 30.0 - 34.0	beech	0.87	**46.36**	31.48	13.91	8.11	53.50
	fir/spruce	0.99	**57.83**	20.47	14.15	6.80	41.42
2. 35.0 - 39.0	beech	1.34	**45.92**	30.59	16.00	8.04	54.63
	fir/spruce	0.98	**60.13**	16.36	14.90	7.07	38.33
3. 40.0 - 44.0	beech	1.55	**49.35**	26.89	14.62	8.64	50.16
	fir/spruce	1.14	**63.51**	15.26	14.93	7.46	37.65
4. 45.0 - 49.0	beech	0.98	**51.29**	24.52	14.96	8.98	48.46
	fir/spruce	0.89	**67.97**	9.71	14.10	7.94	31.74
5. 50.0 - 54.0	beech	1.31	**52.91**	23.91	13.49	9.26	46.66
	fir/spruce	1.06	**68.59**	8.38	14.10	8.05	16.44
6. 55.0 - 59.0	beech	1.18	**55.67**	20.10	13.15	9.74	43.00
	fir/spruce	1.09	**72.33**	5.97	13.08	8.49	27.54

From the data presented, it may be concluded that the percentage of yield in fir/spruce sawlogs is significantly higher in all thickness groups. The difference between the yield of fir/spruce and beech, for each thickness group, ranges from 11.47% to 16.66%. This difference is considerable, and is clearly observable through the volume of sawn products. The comparison between yields is relevant since the same thickness groups and identical sawlog lengths are being considered. The percentage of coarse waste is significantly lower in fir/spruce than in beech. In terms of fine waste, the values are approximately equal, with small, negligible differences. The percentage of coarse and fine waste depends primarily on the sawing pattern and the presence of defects. The taper largely dictates the percentage of coarse waste. It is important to note that in sawing both wood species, the objective is to achieve the maximum quantitative yield, and therefore the coarse waste are additionally utilized. From the coarse waste of beech sawlogs, parquet blanks are produced. The coarse waste of fir/spruce sawlogs are minimized as much as possible through the sawing of laths. Concerning fine waste, it is important to emphasize that the kerf width in the primary sawing machine for beech sawlogs amounts to 3.5 mm, whereas in fir/spruce sawlogs it amounts to 4.0 mm. The shrinkage allowance is more favorable in fir/spruce sawlogs, due to the physical-mechanical properties of this wood species and its

low volumetric shrinkage. In beech, volumetric shrinkage amounts to 17.5%, whereas in fir/spruce it amounts to 11.8%, for each sawn product individually. With regard to taper, although the general observation holds that coniferous logs exhibit smaller taper, we were nevertheless unable to establish a relevant relationship for either of the two wood species.

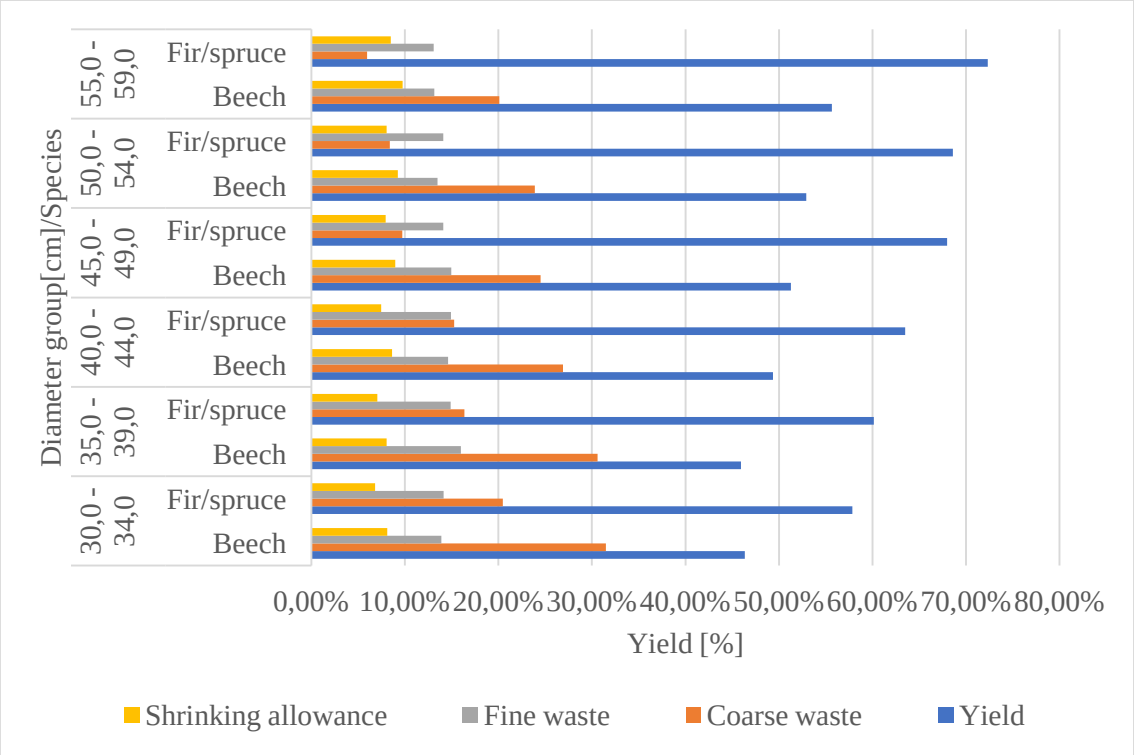

Figure 8. *Comparison of yield in logs of beech (Fagus sylvatica* L.*) and fir/spruce (Abies alba* Mill/*Picea abies* L.*).*

4. CONCLUSIONS

The quantitative yield of sawmilling raw material constitutes a broad and complex domain which exerts a direct influence upon the economic performance of a sawmilling facility. Beyond economic performance, yield also represents an important concept for the ecology of sawmilling processes and the planned exploitation of forest resources. Several factors affect the percentage of quantitative yield, among which the most significant are: the type of raw material and its properties, the characteristics of the processing technology, and the choice of sawing pattern. An inadequately arranged sawing pattern leads to increased amounts of waste and unplanned use of sawlogs, resulting in economic losses.

In the research, an attempt was made to compare the yield of sawlogs of beech and fir/spruce. Beech was selected as a characteristic and dominant deciduous species in domestic sawmilling facilities, while fir/spruce was chosen as a dominant species of coniferous origin. The selection of wood species was also made based on their availability within the analyzed research facility. A total of 160 logs were analyzed, 80 from each wood species. The logs were grouped according to length (4.0 and 5.0 m) and according to mean diameter. The grouping according to mean diameter was carried out in six diameter classes, with an interval of 5.0 cm between each class. The cutting was performed on identical primary and secondary machines.

Based on the available collected data, it can be concluded that the yield of fir/spruce sawlogs is significantly higher than that of beech sawlogs, which also confirms the general statement, widely available in the literature, that coniferous species provide a higher percentage of quantitative yield compared to deciduous species. For the beech logs, the results correspond with those of Rabadjiski (1991) and Šoškić and Popović (2004), with the note that in some groups the percentages are lower (especially for Class II and smaller diameters), yet still within the range of 46.0–57.0%. For fir/spruce logs, the results are higher than those of Чернаев (1960) (53–64%) and close to, or even above, those

of Brežnjak (2000) (average 65.0%), with maximum values reaching up to 75.0%, which confirms the tendency that conifers yield significantly better percentages.

Acknowledgments

This work was financially supported by the Ss. Cyril and Methodius University in Skopje. Project No: NIP.UKIM.23-24.9.

REFERENCES

1. Bežnjak, M. (2000). *Pilanska tehnologija drva, II dio, udzbenik.* Zagreb: Šumarski fakultet Sveućilista u Zagrebu.
2. Brežnjak, M. (1963). *Analiza elemenata koji utječu na iskorištenje pilanskih trupaca, interna studija.* Šumarski fakultet Sveućilista u Zagrebu, Zagreb.
3. Brežnjak, M. (1967). Iskorisćenje bukovih pilanskih trupaca kod piljenja na traćnoj pili i jarmaći. *Drvna industrija, 18*(2), 3-21.
4. Kolin, B. (2000). *Hidrotermička obrada drveta* (Vol. 2). Šumarski fakultet Univerzitet u Beogradu.
5. Rabadziski, B., Zlateski, G., Stamenkoska, A. M., & Krstev, M. (14 - 17 September, 2021). Analysis of the Influence of Beech Sawmill Logs on Maximum Quantity Exploitation. *Wood, Technology & Product Design*, (pp. 187-198). Ohrid.
6. Šoskič, B., & Popovič, Z. (2004). Uticaj kvaliteta bukove oblovine na strukturu glavnih i sporednih proizvoda u pilanskoj preradi. *Prerada drveta, 20*(1).
7. Михајлов, И. (1968). *Дендометрија.* Скопје: Земјоделско - шумарски факултет.
8. МКС EN 1312:2010.
9. МКС EN 1313-2:2010.
10. МКС EN 1316-1:2013.
11. Рабациски, Б. (1991). *Квантитативно и квалитативно искористување на букови пилански трупци при бичење на гатер и лентовидна пила-трупчарка, Магистерски труд.* Скопје: Шумаски факултет, Универзитет ,,Св. Кирил и Методиј".
12. Рабациски, Б. (2000). Квантитативно искористување на технички облици од буково дрво при бичење на лентовидни пили. *Јубилеен годишен зборник*.
13. Рабациски, Б. (2019). *Пилanска технологија на дрвото.* Скопје: Факултет за дизајн и технологии на мебел и ентериер.

Authors' address:

[1]Ana Marija Stamenkoska, MSc, teaching assistant; [1]Prof. Goran Zlateski, PhD, full professor;
[1]Prof. Branko Rabadjiski, PhD, retired full professor; [2]Anastasija Temelkova, PhD, teaching assistant
[1]Department of primary wood processing
[2] Department of machines, energy and transport
Faculty of Design and Technologies of Furniture and Interior-Skopje, Ss. Cyril and Methodius University in Skopje, Republic of North Macedonia
16-ta Makedonska brigada 3, PO box 223, 1000, Skopje.

STRENGTH OF THE CORNER JOINTS OF THE WINDOW FRAME

Elena Jevtoska[1], Gjorgi Gruevski[1], Nikola Mihajlovski[1]

Ss. Cyril and Methodius University in Skopje, Macedonia,
Faculty of Design and Technologies of Furniture and Interior-Skopje
e-mail: jevtoska@fdtme.ukim.edu.mk; gruevski@fdtme.ukim.edu.mk;
mihajlovski@fdtme.ukim.edu.mk

ABSTRACT

The window as a product used in construction aims to provide natural light and the possibility for ventilation in the building where it is placed but at the same time to protect the room from external influences such as wind and rain and to prevent uncontrolled cooling or heating of the building in which it is built-in. Given the purpose, a quality window is one that protects against air permeability, water permeability and provide wind resistance. The window is a complex product that is composed of different parts that can be made of different materials. This research is focused on the area of frame joining and joint strength. This research will cover windows made from the same PVC profile but manufactured in different production facilities. The windows will be measured for air permeability, water permeability and wind resistance, and corner samples will be taken after wards. The samples are prepared according to the standard EN 514:2018 Plastics - Poly(vinyl chloride) (PVC) based profiles - Determination of the strength of welded corners and T-joints.

Keywords: construction carpentry, window, air permeability, water permeability, wind resistance, PVC profiles.

1. INTRODUCTION

Today's windows are elements of construction carpentry that are composed of movable and immovable parts. Depending on the function that the windows of the building have to achieve, it is chosen from which materials they will be made and which attributes have to be met by the materials for constructing a window. If the windows are to provide only daylight in the space, they are constructed as fixed, in other words, they have only a stationary part, and if, in addition to light, they are to provide ventilation of the space, the windows are constructed with a fixed, specifically immovable case and a movable sash that, according to needs, has the possibility to opens. In order to choose the most appropriate combination of materials for the construction of a quality window that will satisfy all the required functions, it is necessary to know the attributes of the built-in materials and how they affect the quality of the window.

The window as a product is a complex composition of different materials and parts. As different parts of the window, the basic structural elements, filling elements, fittings, additional accessories are distinguished. Basic structural elements of the window are the supporting frame, that is case and the window sash.

- The supporting frame – case. The supporting frame is a fixed structural element, attached to the sides of the communication opening. This case bears the window sash (Kyuchukov)
- The window sash is the moving part of the basic structural elements. Depending on the need, it can rotate along a horizontal or vertical axis, slide laterally, but also a combination of several directions of rotation.

The research will be performed on cuts from joints, specifically casing and sash angles taken from 10 windows. The examination will be on 80 samples divided into 2 groups. A group of 40 case specimens and a group of 40 sash specimens. The samples are prepared according to the standard EN 514:2018 Plastics – Poly (vinyl chloride) (PVC) based profiles - Determination of the strength of welded corners and T-joints [109]. The results of the test will give us data on the strength of the welded corners made from the same profile and how much it differs between the sash and the case.

2. MATERIALS AND METHODS

Windows from different manufacturers were taken as samples for research, using different types of hardware, but made of identical frame and sash profiles. The windows will be tested for quality. In order to obtain a sufficient number of results that can be compared, the test will be carried out on ten windows made by different manufacturers. The selection of samples is that all ten samples will be made of PVC profile from the ALUPLAST brand, model IDEAL 4000.

The selected windows were initially tested for air permeability. After testing these methods, 8 samples were taken from each window, or a total of 80 samples, which were divided in two groups of 40 samples each. The first group refers to the frame samples, and the second group refers to the sash samples.

The samples were placed on a universal machine and a compressive force F was applied to them. At the moment of failure of the joint, the applied force was recorded

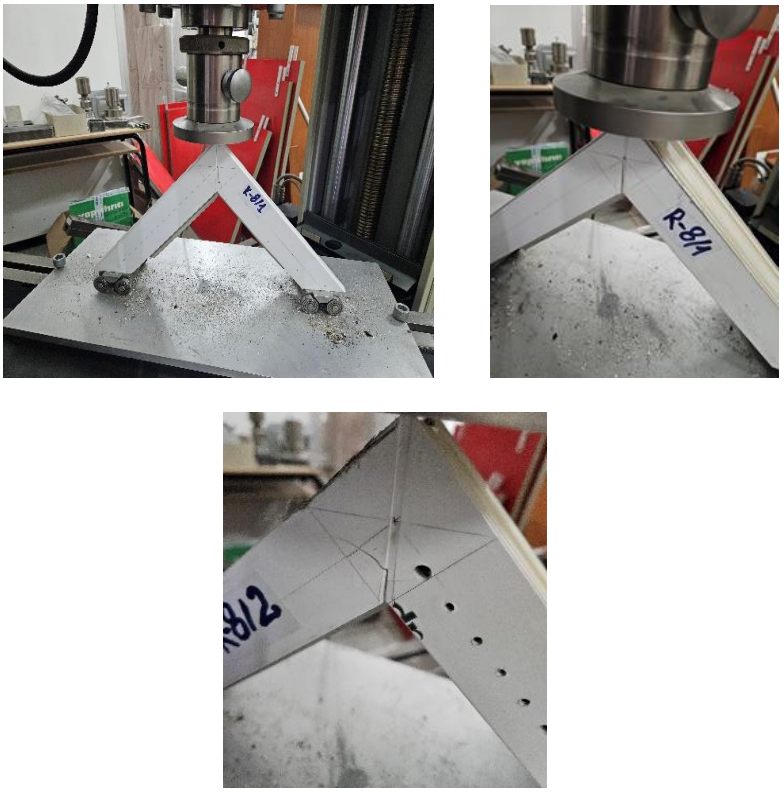

Figure 1. *Force action on samples from a frame group.*

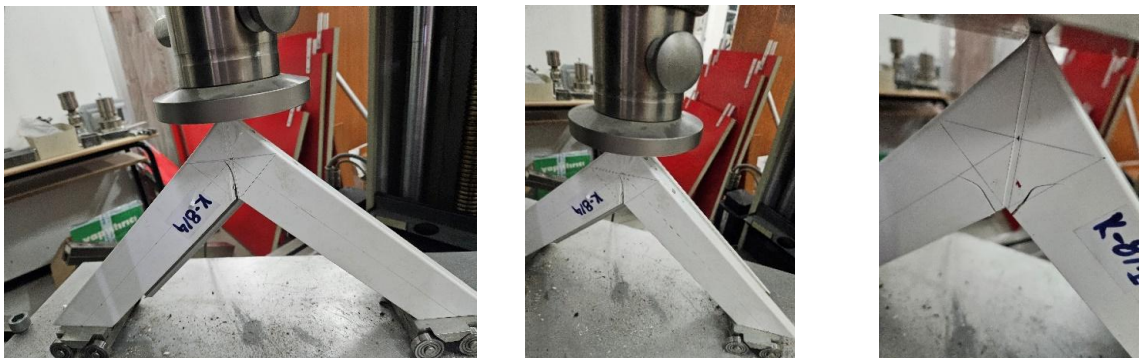

Figure 2. *Force action on samples from a sash group.*

3. RESULTS AND DISCUSSION

3.1.Results of the air permeability

3.1.1. Results – air permeability

Table 1. *Sample 1 – air permeability.*

P_a normal		50	100	150	200	250	300	450	600	
P_a actual		49	100	150	200	250	302	453	600	
Air permeability	m^3/h	15,88	24,81	33,03	42,15	52,42	64,59	113,69	175,56	General class
Perimeter	$m^3/(h/m)$	2,74	4,28	5,69	7,27	9,04	11,14	19,60	30,27	
Class		2	2	2	2	2	2	0	0	2
Window surface	$m^3/(h/m^2)$	8,49	13,27	17,66	22,54	28,03	34,54	60,79	93,98	
Class		2	2	2	2	2	2	0	0	2
										2

Table 2. *Sample 2 – air permeability.*

P_a normal		50	100	150	200	250	300	450	600	
P_a actual		49	102	150	201	251	303	451	596	
Air permeability	m^3/h	14,18	23,37	30,97	38,14	45,32	52,43	75,07	100,15	General class
Perimeter	$m^3/(h/m)$	2,26	3,59	4,71	5,80	6,90	7,98	11,43	15,24	
Class		2	2	2	2	2	2	0	0	2
Window surface	$m^3/(h/m^2)$	7,57	11,92	15,80	19,46	23,12	26,75	38,30	51,10	
Class		2	2	2	2	2	2	0	0	2
										2

Table 3. *Sample 3 – air permeability.*

P_a normal		50	100	150	200	250	300	450	600	
P_a actual		51	101	149	201	251	300	451	598	
Air permeability	m^3/h	14,82	23,20	30,78	38,14	45,33	52,45	75,30	100,38	General class
Perimeter	$m^3/(h/m)$	2,24	3,53	4,73	5,80	6,90	7,97	11,46	15,29	
Class		2	2	2	2	2	2	0	0	2
Window surface	$m^3/(h/m^2)$	7,55	11,90	15,78	19,46	23,12	26,76	38,33	51,13	
Class		2	2	2	2	2	2	0	0	2
										2

Table 4. *Sample 4 – air permeability.*

P_a normal		50	100	150	200	250	300	450	600	
P_a actual		50	100	150	201	251	301	454	604	
Air permeability	m^3/h	2,07	3,22	4,13	4,93	5,60	6,20	7,86	9,38	General class
Perimeter	$m^3/(h/m)$	0,50	0,79	1,01	1,20	1,36	1,51	1,92	2,29	
Class		3	3	3	3	4	4	4	4	3
Window surface	$m^3/(h/m^2)$	1,82	2,82	3,62	4,32	4,91	5,44	6,89	8,23	
Class		4	4	4	4	4	4	4	4	4
										4

Table 5. *Sample 5 – air permeability.*

P_a normal		50	100	150	200	250	300	450	600	
P_a actual		50	101	150	200	251	301	452	604	
Air permeability	m^3/h	7,23	10,77	14,09	16,66	18,92	21,00	26,25	30,97	General class
Perimeter	$m^3/(h/m)$	1,29	1,93	2,52	2,99	3,39	3,76	4,70	5,55	
Class		3	3	3	3	3	3	3	3	3
Window surface	$m^3/(h/m^2)$	5,56	8,28	10,84	12,81	14,55	16,16	20,19	23,82	
Class		3	3	3	3	3	3	3	3	3
										3

Table 6. *Sample 6 – air permeability.*

P_a normal		50	100	150	200	250	300	450	600	
P_a actual		52	102	150	202	251	302	451	604	
Air permeability	m^3/h	1,31	2,10	2,78	3,41	4,00	4,55	6,20	7,87	General class
Perimeter	$m^3/(h/m)$	0,36	0,57	0,76	0,93	,09	1,24	1,70	2,15	
Class		4	4	4	4	4	4	4	4	4
Window surface	$m^3/(h/m^2)$	1,37	2,19	2,90	3,55	4,17	4,74	6,46	8,19	
Class		4	4	4	4	4	4	4	4	4
										4

Table 7. *Sample 7 – air permeability.*

P_a normal		50	100	150	200	250	300	450	600	General class
P_a actual		50	100	150	201	251	300	453	601	
Air permeability	m^3/h	3,15	4,93	6,51	8,56	10,76	13,46	26,25	43,81	
Perimeter	$m^3/(h/m)$	0,86	1,34	1,77	2,33	2,93	3,67	7,15	11,94	
Class		3	3	3	3	3	3	0	0	2
Window surface	$m^3/(h/m^2)$	3,28	5,13	6,78	8,91	11,21	14,02	27,34	45,63	
Class		3	3	3	3	3	3	0	0	2
										2

Table 8. *Sample 8 – air permeability.*

P_a normal		50	100	150	200	250	300	450	600	General class
P_a actual		50	100	150	202	251	302	453	603	
Air permeability	m^3/h	0,88	1,65	2,20	2,66	3,07	3,47	4,58	5,93	
Perimeter	$m^3/(h/m)$	0,22	0,41	0,54	0,66	0,76	0,86	1,13	1,46	
Class		4	4	4	4	4	4	4	4	4
Window surface	$m^3/(h/m^2)$	0,78	1,47	1,96	2,37	2,74	3,10	4,09	5,30	
Class		4	4	4	4	4	4	4	4	4
										4

Table 9. *Sample 9 – air permeability.*

P_a normal		50	100	150	200	250	300	450	600	General class
P_a actual		51	100	151	201	251	303	451	603	
Air permeability	m^3/h	2,20	3,42	4,41	5,20	5,92	6,55	7,96	8,84	
Perimeter	$m^3/(h/m)$	0,78	1,20	1,55	1,83	2,08	2,31	2,80	3,11	
Class		3	3	3	3	3	3	3	3	3
Window surface	$m^3/(h/m^2)$	3,49	5,42	6,99	8,26	9,39	10,40	12,64	14,04	
Class		3	3	3	3	3	3	3	3	3
										3

Table 10. *Sample 10 – air permeability.*

P_a normal		50	100	150	200	250	300	450	600	General class
P_a actual		50	100	150	200	250	301	451	603	
Air permeability	m³/h	1,45	2,40	3,14	3,80	4,39	4,95	6,72	9,02	
Perimeter	m³/(h/m)	0,38	0,63	0,82	1,00	1,15	1,30	1,74	2,37	
Class		4	4	4	4	4	4	4	4	4
Window surface	m³/(h/m²)	1,30	2,14	2,80	3,39	3,92	4,42	6,00	8,06	
Class		4	4	4	4	4	4	4	4	4
										4

3.2. Results from windows made from the same identical profile, determining the strength of the corner joints of the frame (sash, frame)

3.2.1. Results from a group of sash tests

Window number	Simple number	F (N)	Mean Value – F (N)
1	**1**	5279 N	F_1 = 5180 N
	2	5121 N	
	3	5278 N	
	4	5042 N	
2	**1**	4305 N	F_2 = 4255 N
	2	4284 N	
	3	4118 N	
	4	4311 N	
3	**1**	4825 N	F_3 = 4863 N
	2	4903 N	
	3	4911 N	
	4	4813 N	
4	**1**	5744 N	F_4 = 5727 N
	2	5707 N	
	3	5709 N	
	4	5748 N	
5	**1**	5413 N	F_5 = 5408 N
	2	5419 N	
	3	5395 N	
	4	5403 N	
6	**1**	5863 N	F_6 = 5672 N
	2	5312 N	
	3	5780 N	
	4	5733 N	
7	**1**	4388 N	F_7 = 4362 N
	2	4361 N	
	3	4313 N	

	4	4387 N	
8	**1**	5713 N	F_8 = 5616 N
	2	5648 N	
	3	5511 N	
	4	5593 N	
9	**1**	4813 N	F_9 = 4870 N
	2	4915 N	
	3	4889 N	
	4	4864 N	
10	**1**	5763 N	F_{10} = 5743 N
	2	5711 N	
	3	5784 N	
	4	5717 N	

3.2.2. Results from a group of frame tests

Window number	**Simple number**	**F (N)**	**Mean Value – F (N)**
1	**1**	4796 N	F_1 = 4891 N
	2	4851 N	
	3	4013 N	
	4	4904 N	
2	**1**	4881 N	F_2 = 4894 N
	2	4903N	
	3	4874 N	
	4	4918 N	
3	**1**	4987 N	F_3 = 4935 N
	2	4913 N	
	3	4893 N	
	4	4948 N	
4	**1**	5250 N	F_4 = 5151 N
	2	5098 N	
	3	5112 N	
	4	5144 N	
5	**1**	5010 N	F_5 = 5050 N
	2	5108 N	
	3	5970 N	
	4	5112 N	
6	**1**	4980 N	F_6 = 5388 N
	2	5725 N	
	3	5041 N	
	4	5804 N	
7	**1**	4613 N	F_7 = 4819 N
	2	4985 N	
	3	4913 N	

	4	4764 N	
8	**1**	5290 N	F_8 = 5293 N
	2	5311 N	
	3	5301 N	
	4	5270 N	
9	**1**	4968 N	F_9 = 4946 N
	2	4915 N	
	3	4977 N	
	4	4815 N	
10	**1**	5014 N	F_{10} = 5119 N
	2	5096 N	
	3	5312 N	
	4	5054 N	

4. CONCLUSION

In this research obtained results were used for comparison with the results – air permeability obtained from the strength of the joints of the case and the sash.

The profile that is used for making windows has a minimal influence on the air permeability of the window.

The construction of the window has a significantly large influence on the frontal deviations during the wind load.

The same profile assembled in a different production capacity gives different joint strength results.

The strength of the joint and the frame has an impact on the air permeability of the window. The corner joint of the frame and the sash is one part of the window construction that affects the final quality of the window.

REFERENCES

1. Кучуков, Г., Конструиране на мебели, врати и прозорци, 2009, Матком, София.
2. Postowa, P., (2017), Strength analysis of welded corners of PVC window profiles, IOP Conference Seres: Materials and Engineering.
3. EN 1026:2016 "Windows and doors - Air permeability - Test method" standard.
4. EN 1027:2016 "Windows and doors - Water tightness - Test method" standard.
5. EN 12211:2016 "Windows and doors - Resistance to wind load - Test method" standard.
6. EN 514:2018 Plastics - Poly(vinyl chloride) (PVC) based profiles - Determination of the strength of welded corners and T-joints.
7. https://www.aluplast.net/eng-int/produkte/fenster/ideal/ideal-4000/ пристапено на 14-04-2025 год.
8. Gruevski,T., Simakoski, N. (2002): Elementi na drvnite konstrukcii, Skopje: UKIM Shumarski fakultet.
9. Gruevski,T., Simakoski, N. (2003): Konstruiranje na mebel, Skopje: UKIM Shumarski fakultet.
10. Zakon za energetska efikasnost (2020): Sluzben vesnik na Republika Makedonija, br.32/2020 od 09-02-2020 god.
11. Zakon za gradezni proizvodi (2015): Sluzben vesnik na Republika Makedonija, br.104/2015 od 24-06-2020 god.
12. Ibrahimovic, E., Kljuno, H.A. Window frame materials and window size: parametesrs that influence enegy efficiency in buildings. Technics technologies education management.

THE INFLUENCE OF THE NUMBER OF CABINET CONNECTOR FITTINGS ON THE DURABILITY OF CABINET FURNITURE – A CASE STUDY

Igor Džinčić[1], Ivan Simić[1]

University of Belgrade, Faculty of Forestry,
Department of Wood Science and Technology
e-mail: igor.dzincic@sfb.bg.ac.rs; ivan.simic@sfb.bg.ac.rs

ABSTRACT

This paper shows the influence of the quality of the chipboard on the number of fittings (cabinet connectors) per connection line. In order to reduce transportation costs, cabinet furniture is in most cases made as knock-down furniture by applaying excenter connecting fitting. The number of fittings per connection line in most cases depends on the depth of the cabinet, as well as on the quality of the chipboard. The strength of the board against delamination is the main property of the board that will affect the number of connection elements. The test was carried out on cabinets taken from regular production, which belong to the lowest price group of cabinet furniture. The static analysis showed that there is a significant influence of the number of fittings on the rigidity and durability of cabinet furniture. Variation in the number of fittings leads to changes in the rigidity and durability of the tested furniture.

The results of this research proved that during the prosess of constructing furniture from the lowest price group, the construction rules should be take with caution into consideration. The paper gives recommendations regarding the number of connection elements per connection line.

Keywords: wood-based panels, joints, knock down furniture, durability.

1. INTRODUCTION

The idea for this work was created on the basis of years of monitoring the results of controlling the case furniture within the Bureaufor Control of Furniture Faculty of Forestry Faculty, Belgrade University. Analysis of the results of controlling the case furniture from the lowest price range, which was controlled according to EN 16122: 2012, large variations were observed regarding the number of furniture fittings, as well as damage caused during testing. This analysis covered only products of the lowest price ranking of medium and large production systems, which are forced to produce knock down case furniture in order to decrease storage costs. Due to the small purchasing power of the population, this group of case furniture is also the most widespread type of case furniture.

As with all types of products, the production price is made up of material costs and the price of work (the time consumed for product production). Type of the boards does not affect the time required for the production, so the workout time will not be analyzed here. In the case furniture, the cost of the material will depend on the price of the basic material (panel), the prices of the fittings needed to connect products and packaging costs.

All tests performed by other researchers, are made on the boards of higher quality classes, so that the recommendations regarding the number and types of fittings cannot be used directly in real production conditions. With such available data, the engineers are referred to their own experiences and data they receive from the service complaints.

Examining the strength of the corner joints, as well as factors that affect the strength was performed a large number of times. From the prehodd survey, it is known that the joints are a critical point of each product (EFE and Kasal, 2000; Smardzewski and beautiful, 2002; Kasal et al., 2006; Abdulkadir et al., 2013, Abdulkadir et al., 2014). Based on the results of previous research, it can be easily noticed that joints represent critical points in the construction, as well as stiffness and durability of case furniture in direct correlation with the type and number of applied fittings. In addition to the type and number of joints per connection line, stiffness and durability of the case furniture will also depend on the ways of placing the back and quality of the panel. In knock down furniture, the back

can be placed in the slot or can be attached with some fitting. Installation of the back in the slot is the financially the cheapest solution because there is no fittings that would increase the price of the basic material.

Koreny, A. and Simek, M. (2011) analyzed the influence of the distance of the dry dowels from the fittings. The basis of the distance of dry dowels from the axis of the fittings was 40, 80, 120 and 155mm. The recommendation to which they came based on the results obtained, is that the largest stiffness are achieved when the distance from the dry dowels and the fittings are 120 or 155mm. Within the very extensive research conducted by Abdulcadir with his associates (Abdulkadir et al., 2013 and 2014) the impact of the number and type of fittings on the strength of the joints, as well as the number and position of dry dowels, was analyzed. In no of these papers, there are no variable properties of basic material. Namely, within certain papers, the properties of the boards was tested, but the experiment was not made on the material of different starting characteristics.

Based on examined literature, there may be concluded that there are a number of papers in this area that provide valuable information to the scientific and professional public. However, by reviewing the available works, there was no guideline on the impact of the quality of the basic material to the number of joints per connection line. The aim of this paper is to examine the impact of the quality of the boards and the number of fittings on the stiffness and durability of the case furniture with a special emphasis on the approach of the scientific experiment to the real requirements of practical application.

2. MATERIALS AND METHODS

In accordance with the aim of the work, six groups of samples (cases) were made, Table1. The dimensions of the samples were 2000x900x540mm (height, width, depth). The structural elements of the case were connected using eccentric fittings and wooden dry dowels. In all groups of samples, the back was placed in a groove. In order to avoid additional stiffening and to obtain stiffness results that depend exclusively on corner joints, the cases did not have a plinth, nor shelves.

The samples of the first three groups were made of melamine-coated chipboard taken from regular production, while the remaining three groups of samples were made of higher quality chipboard that was purchased specifically for the purposes of the experiment.

Table 1. *Groups of samples.*

sample group label	chipboard type	number of connection elements per connection line	number of samples
1	type 1	3	3
2		4	3
3		5	3
4	type 2	3	3
5		4	3
6		5	3

Before the samples were made, the general physical and mechanical properties of the particleboard panels were selected and tested. When choosing the materials, the criterion was respected to select materials that are used in real production conditions so that the results obtained could be applied to improve production. In accordance with the above, for the purposes of the experiment in this work, chipboard panels with melamine foil on both sides, with a nominal thickness of 18 mm, were selected. In order to determine the characteristics of the chipboard that are important for this work, the following properties were selected and tested: Moisture content according to standard EN 322:2010; Board density according to standard EN 323:2010; Resistance to delamination according to standard EN 319:2010; Modulus of elasticity in flatwise bending and bending strength of wood-based panels according to standard EN 310:2016.

These tests were carried out at the Faculty of Forestry, University of Belgrade, in the Laboratory for wood-based panels According to the plan for testing the properties of the boards, a scheme for cutting the boards was created in order to obtain test pieces, Figure 1.

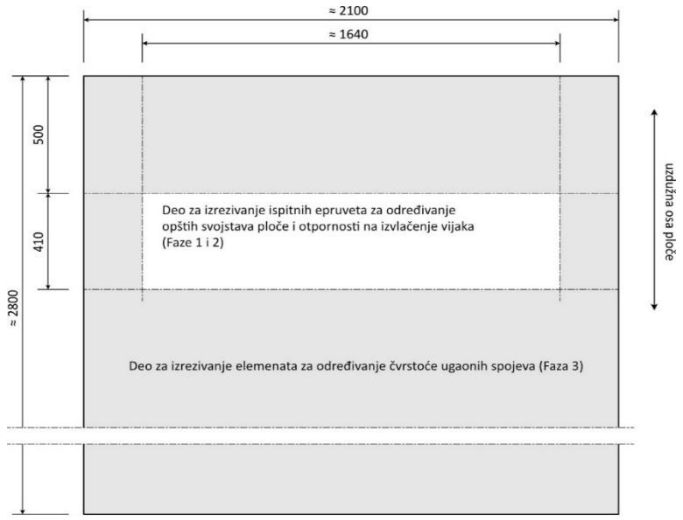

Figure 1. *Plan for cutting a section of chipboard.*

From the selected section, according to the cutting plan (Figure 2), test pieces were cut to determine the general properties of the chipboard.

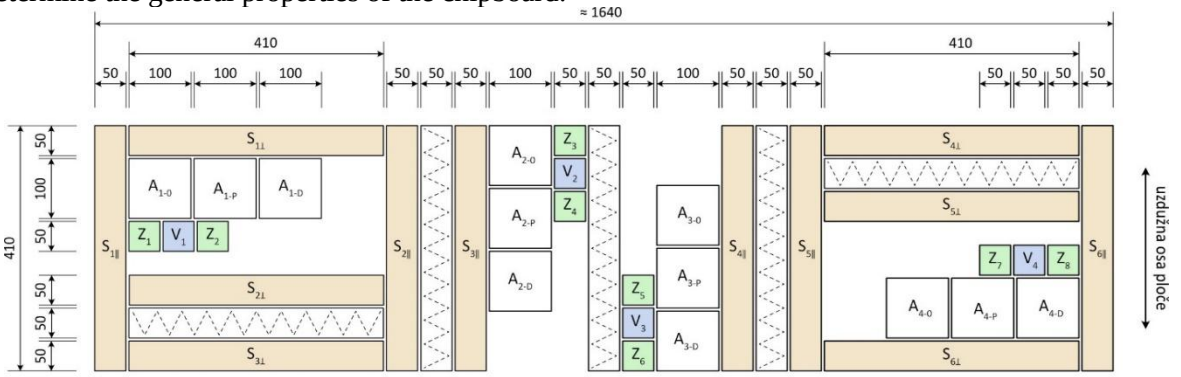

Figure 2. *The cutting plan.*

Test pieces markings:

• V - test pieces for controlling moisture content, dimensions 50 x 50 mm;

• Z - test pieces for testing tensile strength perpendicular to the plane of the plate (debonding): dimensions 50 x 50 mm;

• S - test pieces for testing tensile strength, dimensions 410 x 50 mm, support distance lo= 360 mm ($S_{x⊥}$ parallel and $S_{x∥}$ perpendicular to the plate axis);

The samples were conected using an fitting from Häfele, model “Minifix”. This type of fitting is the most commonly used connecting device for assembly-disassembly furniture, which is constructed from chipboard panels. The dry dowel with dimensions of 8•30mm was made of beech. All samples were made on a numerical machine. Before joining the samples, the accuracy of the production was controlled with a digital movable caliper with an accuracy of ±0.01mm. The dry dowels were selected so as to achieve an overlap fit with an overlap size of 0.1 mm. Before testing, all samples were conditioned in accordance with EN16122:2012, chapter 4.1. As part of the cabinet testing, only the strength and stiffness of the cabinet furniture were checked according to EN 16122:2012, chapter 6.4. Figure 3 shows the directions of force action.

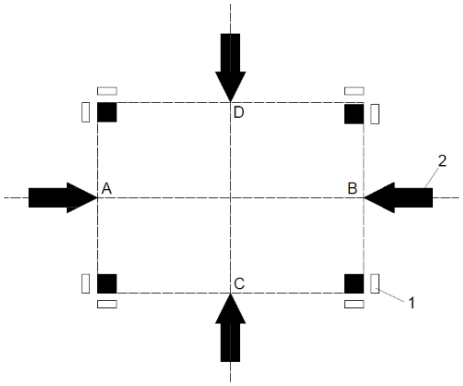

Figure 3. *Directions of force action.*

3. RESULTS AND DISCUSSION

The first part of this chapters presents the results of testing the properties of the boards from which samples were later made.

The moisture content was tested according to EN 322:2010. The measurement results and the average moisture value of the chipboards (type 1 and type 2) are shown in Table 2.

Table 2. *Moisture content results (W) of chipboards.*

chipboard - type 1			
Test pieces N^o	m_{VL} [g]	m_0 [g]	W [%]
1.1	28.57	26.86	6.37
1.2	28.31	26.59	6.47
1.3	28.03	26.36	6.34
1.4	28.58	26.89	6.28
Moisture content – average value			**6.4**
Standard deviation			**0.08**
chipboard - type 2			
Test pieces N^o	m_{VL} [g]	m_0 [g]	W [%]
2.1	28.78	27.01	6.55
2.2	28.99	27.19	6.22
2.3	29.01	27.26	6.41
2.4	28.81	26.89	7.14
Moisture content – average value			**6.68**
Standard deviation			**0.1**

The values obtained from the tests, for both samples groups, are within the prescribed limits according to the EN 322 standard, as well as according to the values which the manufacturer refers to. The permissible moisture range for chipboard panels, according to the standards, ranges from 4 to 13%.

Density, as a physical property, has a major impact on other physical, mechanical and technological properties of wood based panels. The density of chipboard was determined according to the EN 323, and the results obtained are shown in Table 3.

Table 3. *The density of chipboard.*

chipboard - type 1			**chipboard - type 2**		
Test pieces N°	$m\,[g]$	$\rho\ [kg/m^3]$	Test pieces N°	$m\,[g]$	$\rho\ [kg/m^3]$
1.1	28.46	635.1	2.1	28.55	634.4
1.2	28.38	632.6	2.2	28.81	640.2
1.3	28.25	631.0	2.3	28.88	641.7
1.4	28.19	633.3	2.4	28.72	638.2
1.5	28.16	630.1	2.5	28.69	637.5
1.6	28.67	642.6	2.6	28.99	644.2
1.7	28.12	631.3	2.7	29.44	654.2
1.8	28.35	635.5	2.8	28.02	622.6
average value		**633.9**	average value		**639.1**
Standard deviation		**4.00**	Standard deviation		**2.49**

Both types of boards meet the density tolerance within the board (± 10%), prescribed by the EN 312 standard, as well as the average density (≤ 640 kg/m3) given in the manufacturer's technical specification. Based on the results obtained, it can be noted that the board from the second manufacturer has a slightly higher average density value.

Due to the lower density and weaker adhesion of the chips, delamination of the chipboard usually occurs in the middle layer. Considering the fact that the connection elements rest with their largest surface precisely on the middle layer, it was of great importance to test the delamination strength. In fixed connections using glue, delamination strength is not a decisive factor in the durability of cabinet furniture, Abdulkadir et all (2013). The reason for this improvement should be sought in the fact that the glue used to connect the connecting element (dowel or bisvit) penetrates the porous structure and additionally connects the chipboard chips. However, in the case of assembly-disassembly fittings, delamination strength is an important factor. The results of testing the resistance of the chipboard to delamination are given in Table 4.

Table 4. *The results of testing the resistance of the chipboard to delamination.*

chipboard - type 1			**chipboard - type 2**		
Test pieces N°	$F_{max}\,[N]$	$\sigma_S\ [N/mm^2]$	Test pieces N°	$F_{max}\,[N]$	$\sigma_S\ [N/mm^2]$
1.1	724.06	0.289	2.1	936.5	0.3746
1.2	829.55	0.330	2.2	912.7	0.36508
1.3	743.85	0.297	2.3	845.9	0.33836
1.4	783.36	0.314	2.4	831.2	0.33248
1.5	636.91	0.255	2.5	967.4	0.38696
1.6	810.80	0.325	2.6	867.5	0.347
1.7	805.35	0.323	2.7	989.1	0.39564
1.8	761.2	0.304	2.8	922.3	0.36892
average value		**0.30**	average value		**0.36**
Standard deviation		**0.027**	Standard deviation		**0.028**

When it comes to delamination strength (Internal bond), the European particle board manufacturer refers to the standard method EN 319, which is also listed in the technical specification standard for chipboards EN 312. According to the specifications for chipboards with a thickness of 13 to 20 mm, the delamination strength should be at least 0.35 N/mm2. From the attached results, it can be concluded that the delamination strength value of the first tested chipboard is slightly lower than the value specified in the EN 312 standard. However, the tested value of the second group of samples is within the recommended limit. Based on the obtained values, it can be expected that when testing the body stiffness, the samples of the second group will show better results.

Given the use of chipboards panels as supported elements in furniture constructions, bending strengths present the most significant mechanical properties. When bending the sample of the highest

stress (pressure and tightening) occur in the outer layers of the board. This means that the quality of external layers has the greatest impact on this mechanical property.

Bending strength was tested according to EN 310 for both directions - parallel ($\sigma_s^{\parallel}$), and scross ($\sigma_s^{\perp}$) compared to the longitudinal axis of the boards. The obtained results are shown in Table 5.

Table 5. *The results of the bending strength.*

bending strength **(N/mm^2)**	**chipboard - type 1**	**chipboard - type 2**
$\sigma_s^{\parallel}$	17,29	20.52
Standard deviation	1,12	1.92
$\sigma_s^{\perp}$	20,12	23.35
Standard deviation	1,88	2.39

From the obtained results, it can be concluded that the bending strength has slightly higher values on the longitudinal axis, which can be connected to the technology of board production (with the preferential orientation of the chips in the longitudinal direction of the formation of the board). Although the mean value of a bending strength parallel to the axis 17,29 N/mm^2) shoved average lower values of bending strength perpendicular to the borads axis (20.12 N / mm2), it still meets the requirements of EN 312 standards, for P2 class boards types, of thickness from 13 to 20 mm (> 11 N / mm2). From the presented results, it can also be noted that the type 2 panel samples have shown larger values of bending strength in both directions. The obtained values are in line with higher obtained values of delamination resistance.

By comparing the obtained results with the values received by Popović 2005 (Table 6), it can be concluded that there are certain deviations in the values obtained. Since the tested material was not taken from the same manufacturer, registered differences are understandable. Although certain differences in the values obtained are observed, they are within the framework of allowed deviations and in accordance with the values prescribed by the standards and factory recommendations of the manufacturer.

Table 6. *Comparison of results.*

Type of test	**chipboard - type 1**	**chipboard - type 2**	**Popović 2005**
Moisture content [*%*]	6,4	6.68	6,95
The density of chipboard [*kg/m^3*]	633,9	639.1	709
resistance to the delamination [*N/mm^2*]	0,3	0.36	0,36
bending strength–longitudinal [*N/mm^2*]	17,29	20.52	17,5
bending strength–perpendicular [*N/mm^2*]	20,12	23.35	15,1

Samples of all groups were tested according to EN 16122:2012, point 6.4 (Strength of the structure). The test involves applying force to specific points ten times. The sample is then inspected to determine any damage that may have occurred during testing. In order to determine the quality of the quality of the construction and impact of the main material (chipboard), a modified test was applied within the testing, where the number of cycles was increased until the sample was damaged or until 12,500 cycles were reached (which corresponds to the number of cycles according to the withdrawn national standard SRPS D.E2.105/1 1990). In addition to the increased number of cycles, deflection was also monitored. The deflection was controlled at the beginning of the control, and after 100, 500, 2500 and 12500 cycles, according to SRPS D.E2.105/1 1990. Due to the very large number of measuring points, samples and positions, only an extract from the measurement is shown in Table 7. Table 7 shows the average values of the case deflection, expressed as the deflection size in mm. All versions of the samples reached the number of cycles of 12500 repetitions, without damage occurring.

Table 7. *Average values of the case deflection.*

sample group label	chipboard	number of connection elements per connection line	Directions of force action A-B		Directions of force action C-D	
			deflection (mm)	Standard deviation	deflection (mm)	Standard deviation
1	type 1	3	18.4	2.67	7.8	4.12
2		4	14.3	6.22	7.4	3.89
3		5	13.2	5.12	7.1	4.01
4	type 2	3	14.8	2.67	7.5	3.75
5		4	12.6	4.01	7.3	2.59
6		5	11.5	2.99	7.1	5.11

Given that equality of variances was established (Levine's test F (6,28) = 0.660 for p = 0.682), the prerequisite for analysis of variance was met, which showed that there was a statistically significant difference in the stiffness results of individual sample groups (F (6,28) = 5.265 for p = 0.001). To determine which sample groups had a statistically significant difference, the Tukey HSD post-hoc test was used, which is recommended when there is equality of variances.

The results of the analysis show that the value of the deflection along the width of the samples (direction A-B) is significantly higher than the deflection measured along the depth (direction C-D). This difference can be explained by the orientation of the connection elements. If we look only at the deflection measured along the depth of the samples, it can be seen that there is no statistically significant difference between the groups. Based on the measurements, we can conclude that the type of particle board and the number of connection elements do not have a significant effect on the stiffness along the depth of the case.

The results of the analysis show that the stiffness of samples 4th, 5th and 6th group (chipboard type 2) is statistically significantly higher than the values of samples 1st, 2nd and 3rd group (chipboard type 1). The registered difference can be explained by the difference in the quality of the base material. Namely, the chipboard type 2 showed a higher delamination strength by 16% and higher values of bending strength in both directions by about 15%. The delamination strength is a more significant data, because the largest part of the connecting fittings is located in the middle layer, which is the thickest layer of the three-layer particle board. If the values obtained in this work are compared with the values obtained by other researchers (Abdulkadir et all 2013, Abdulkadir et all 2014), it can be seen that these values are higher by about 10% in total. The reason for these discrepancies should be sought in the quality of the base material. Similar conclusions have been reached by other researchers (Vassiliou and Barboutis, 2006 and 2009; Zhang and Eckelman, 1992). Direct comparison is not possible to achieve due to the origin of the base material and difference in number and type of the connecting hardware, as the dimensions of the samples.

By analyzing the values of standard deviations between groups, it can be observed that samples made of chipboard type 1 show a slightly higher dispersion of results. These deviations can be explained by the slightly lower quality of the chipboard observed through the values of delamination strength. By observing the influence of the number of connecting elements per depth of the case, it can be observed that in both types of boards, with an increase in the number of connecting elements, the deflection value decreases, i.e. the stiffness of the structure increases. Similar conclusions have been reached by other researchers (Efe, H., Kasal, A., (2000), Kasal, A., et al(2006), Koreny, A., et al (2013), Smardzewski, J., Prekrat, S. (2002), Tankut, A.N., Tankut, N. (2009)). Direct comparison of results is difficult to achieve given the different dimensions of the samples, the type of bonding elements used, and the quality of the particleboard for which there is generally no data on physical and mechanical properties.

4. CONSLUSIONS

The paper presents the results of testing the influence of the quality of the chipboard and the number of assembly fittings on the rigidity and durability of cabinet furniture, with a special emphasis on bringing the scientific experiment closer to the real requirements of practical application. The test was carried out on two groups of samples using chipboard from different manufacturers and of different quality. The samples were joined using an eccentric joint from the company Häfele, model "Minifix". According to the Institute for Furniture Quality Control, this type of fitting is the most commonly used connecting device for knock-down furniture, which is constructed from chipboard in our area.

The tested physical and mechanical properties of the particleboard are within the permitted range of values prescribed by EN standards. This leads to the conclusion that the chipboard on which the tests were performed is within the limits of permitted values.

Based on the analyzed experimental results, as well as on the comparison of the obtained values with the values obtained by other researchers, it can be concluded that the number of assembly fittings in the knock-down furniture contributes to increasing the rigidity of cabinet furniture.

By analyzing the registered deflection values, it can be concluded that the type of chipboard and the number of connection elements do not have a significant impact on the stiffness along the depth of the case. However, inspection of the case stiffness by the width of the samples, give a different picture. The results of the analysis show that the stiffness of the samples made of chipboard that showed higher values of delamination strength is statistically significantly higher compared to the values of the samples made of lower quality board. The key property of the chipboard that influenced the increase in stiffness is the delamination strength.

REFERENCES

1. Abdulkadir, M., Nurdan Ç.Y., Fevzi L.C. (2013): Effects on number and distance between dowels on ready to assemble furniture on bending moment resistance of corner joints, Wood Research 58 (4):671-680
2. Abdulkadir, M., Nurdan Ç.Y., Surku, O. (2014): Evaluation and optimization of bending moment capacity of corner joints with diferent boring plans in cabinet construction, Wood Research 59 (1):201-216
3. Efe, H., Kasal, A., (2000): Tension strength of case construction with and without demountable corner joints. Industrial Architecture Journal of Faculty of Education Ankara, 8(8): 61-74
4. Kasal, A., Sener, S., belgin, C.M., Efe, H. (2006): Bending Strength of Screwed Corner Joints with Different Materials, G.U. Journal of Science 19(3): 155-161
5. Koreny, A., Simek, M., Eckelman, C.A., Haviarova,E. (2013): Mechanical Properties of Knock-down Joints in Honeycomb Panels, Bio Resources 8(4), 4873-4882
6. Koreny, A., Simek, M. (2011): Experimental testing of cam fittings, Forestry and Wood Technology 73: 51-59
7. Поповић М. (2005): Утицај неких физичких и механичких својстава OSB и конвенционалне плоче иверице, Магистарски рад, Шумарски факултете, Београд.
8. Smardzewski, J., Prekrat, S. (2002): Stress Distribution in Disconected Furniture Joints, Electronic Journal of Polish Agricultural Universities, Wood technology, Volume 5, Issue 2, Series
9. Tankut, A.N., Tankut, N. (2009): Evaluation the effects of edge banding type and thickness on the strength of corner joints in case-type furniture, Materials and Design 31: 2956-2963
10. Vassiliou, V., Barboutis, I. (2006): Expression Problems of Screw Withdrawal Capacity Used in Furniture Eccentric Joints, Nabytok conference, Technical University in Zvolen
11. Vassiliou, V., Barboutis, I. (2009): Improvements in holding strength of cam fittings used in eccentric joints Bending, Forestry and Wood Technology 67: 268-274
12. Zhang, J.,Eckelman, C.A. (1992): Rational design of multi dowel corner joints in case furniture, Forest Product Journal 43 (11/12), 52-58
13. EN 16122:2012

14. SRPS D.E2.105/1 1990
15. EN 322:2010;
16. EN 323:2010
17. EN 319:2010
18. EN 310:2016
19. EN 312:2010

Acknowledgments

The study was supported by Republic of Serbia, Ministry of Science, Technological Development and Innovation, Scientific Research Project no. 451-03-137/2025-03/ 200169

CIP - Каталогизација во публикација
Национална и универзитетска библиотека "Св. Климент Охридски", Скопје

674-045.431(062)
684.4(062)

INTERNATIONAL scientific conference (7 ; 2025 ; Ohrid)
Wood technology & product design : proceedings / 4th International scientific conference, 17-20 September, 2025, University congress centre - Ohrid. - Skopje : Faculty of design and technologies of furniture and interior, 2025. - 312 стр. : граф. прикази ; 30 см

Текст на англ. јазик. - Библиографија кон трудовите

ISBN 978-608-4723-06-6